

Mechanisms and Machine Science

Natalya Barmina
Evgenii Trubachev *Editors*

Gears in Design, Production and Education


A Tribute to Prof. Veniamin Goldfarb

 Springer

Mechanisms and Machine Science

Volume 101

Series Editor

Marco Ceccarelli , Department of Industrial Engineering, University of Rome Tor Vergata, Roma, Italy

Advisory Editors

Sunil K. Agrawal, Department of Mechanical Engineering, Columbia University, New York, USA

Burkhard Corves, RWTH Aachen University, Aachen, Germany

Victor Glazunov, Mechanical Engineering Research Institute, Moscow, Russia

Alfonso Hernández, University of the Basque Country, Bilbao, Spain

Tian Huang, Tianjin University, Tianjin, China

Juan Carlos Jauregui Correa, Universidad Autonoma de Queretaro, Queretaro, Mexico

Yukio Takeda, Tokyo Institute of Technology, Tokyo, Japan

This book series establishes a well-defined forum for monographs, edited Books, and proceedings on mechanical engineering with particular emphasis on MMS (Mechanism and Machine Science). The final goal is the publication of research that shows the development of mechanical engineering and particularly MMS in all technical aspects, even in very recent assessments. Published works share an approach by which technical details and formulation are discussed, and discuss modern formalisms with the aim to circulate research and technical achievements for use in professional, research, academic, and teaching activities.

This technical approach is an essential characteristic of the series. By discussing technical details and formulations in terms of modern formalisms, the possibility is created not only to show technical developments but also to explain achievements for technical teaching and research activity today and for the future.

The book series is intended to collect technical views on developments of the broad field of MMS in a unique frame that can be seen in its totality as an Encyclopaedia of MMS but with the additional purpose of archiving and teaching MMS achievements. Therefore, the book series will be of use not only for researchers and teachers in Mechanical Engineering but also for professionals and students for their formation and future work.

The series is promoted under the auspices of International Federation for the Promotion of Mechanism and Machine Science (IFTOMM).

Prospective authors and editors can contact Mr. Pierpaolo Riva (publishing editor, Springer) at: pierpaolo.riva@springer.com

Indexed by SCOPUS and Google Scholar.

More information about this series at <http://www.springer.com/series/8779>


Natalya Barmina · Evgenii Trubachev
Editors


Gears in Design, Production and Education

A Tribute to Prof. Veniamin Goldfarb

 Springer

Editors

Natalya Barmina 
Institute of Mechanics
Kalashnikov Izhevsk State Technical
University
Izhevsk, Russia

Evgenii Trubachev 
Institute of Mechanics
Kalashnikov Izhevsk State Technical
University
Izhevsk, Russia

ISSN 2211-0984

ISSN 2211-0992 (electronic)

Mechanisms and Machine Science

ISBN 978-3-030-73021-5

ISBN 978-3-030-73022-2 (eBook)

<https://doi.org/10.1007/978-3-030-73022-2>

© The Editor(s) (if applicable) and The Author(s), under exclusive license to Springer Nature Switzerland AG 2021

This work is subject to copyright. All rights are solely and exclusively licensed by the Publisher, whether the whole or part of the material is concerned, specifically the rights of translation, reprinting, reuse of illustrations, recitation, broadcasting, reproduction on microfilms or in any other physical way, and transmission or information storage and retrieval, electronic adaptation, computer software, or by similar or dissimilar methodology now known or hereafter developed.

The use of general descriptive names, registered names, trademarks, service marks, etc. in this publication does not imply, even in the absence of a specific statement, that such names are exempt from the relevant protective laws and regulations and therefore free for general use.

The publisher, the authors and the editors are safe to assume that the advice and information in this book are believed to be true and accurate at the date of publication. Neither the publisher nor the authors or the editors give a warranty, expressed or implied, with respect to the material contained herein or for any errors or omissions that may have been made. The publisher remains neutral with regard to jurisdictional claims in published maps and institutional affiliations.

This Springer imprint is published by the registered company Springer Nature Switzerland AG
The registered company address is: Gewerbestrasse 11, 6330 Cham, Switzerland

Foreword

This book deals with the technology of gearing systems by looking at theory, research, and practice with recent updates and results from activity within the IFToMM (the International Federation for the Promotion of Mechanism and Machine Science) community with the special aim of being in memory and honor of the late Prof. Veniamin I. Goldfarb (February 1, 1941–November 12, 2019).

Professor Veniamin I. Goldfarb has been a great IFToMMist and a distinguished MMS (Mechanism and Machine Science) scientist figure with a gentleman dynamic attitude in his ideas and activities. He has been a very prolific MMS scientist with a great reputation worldwide not only within the IFToMM community.

Professor Veniamin I. Goldfarb got his Master's and Ph.D. degrees in Mechanical Engineering in Izhevsk Mechanical Institute in 1962 and in 1969. In 1988, he became a professor at the same Institute of Izhevsk State Technical University, where he served with dedication throughout all his life with successful activity in teaching, research, and technological transfers. He was a member of the Russian Academy of Natural Sciences among many honors received worldwide for his significant contributions in engineering. He served IFToMM as Chairman of the Technical Committee for Gears from 1998 to 2005, member of the Executive Council from 2007 to 2011, and Vice President from 2011 to 2015. Moreover, he proposed and started the organization of the IFToMM student Olympiad (SIOMMS) with the first event in 2011 in Izhevsk, and today the fifth one is planned again in Izhevsk in 2021 in conjunction with the International Forum on MMS. His reputed leadership in Gear Technology led him also to start the IFToMM bilingual (English–Russian) journal “Gearing and Transmissions” in 1991.

The main scientific achievements of Prof. Goldfarb can be highlighted in classification and design of spatial gears with special attention to spiroid gears and a non-differential design method for envelope profiles, with also practical implementation in industrial production for pipeline valve applications. As a gentleman he was a colleague and friend always available to support and help for the progress of technology toward peace and benefits in the society. During my 2009–2011 IFToMM presidency I could appreciate his true IFToMM spirit and friendship in collaboration and share of initiatives and achievements in the whole MMS for the benefits of the

world community with impressive strength and open-mind attitudes even in a combination with his other interests, like the jazz music, to aggregate people in common challenging subjects.

The gearing systems are important elements with an important interest in MMS both for design and performance of machines, even in the most sophisticated solutions with modern mechatronic structures.

This volume is organized within a series to collect surveys, updates, and achievements by experts within the communities of several IFToMM member organizations from all over the world. The content of the book ranges from historical surveys to technical overviews of current challenges in further developments for design and manufacturing processes of gears and geared systems. Research issues are also addressed as per visionary trends in the field.

Therefore, I am sure that readers will find interesting discussions and research updates that can reinforce and indeed stimulate their attention and activity in the field of gearing systems for both research and applications.

I congratulate the editors for the successful result of their efforts and time they have spent in coordinating and preparing this volume as well as connected to a memorial celebration of Professor Goldfarb. I thank the authors for their valuable contributions that show clearly that gearing systems are of current fundamental importance in further developing mechanical and mechatronic systems. This volume can be also considered as a source of inspiration for still better consideration of gearing systems also within challenges of modern developments of science and technology within the activity for teaching, professional activity, design, and research.

Rome, Italy
February 2021

Marco Ceccarelli
IFToMM Past President
ASME Fellow
Doctor Honoris Causa
Editor-in-Chief of MMS Book Series

Preface

We present the fourth contributed volume on the theory and practice of gearing within the MMS series. This book traditionally unites publications of gear scientists from Russia, China, USA, Japan, Italy, Germany, Canada, Bulgaria, Belarus, Kazakhstan, Slovenia, and other countries. As time has shown, this gearing series with such a vast geography contributes to the popularization of both the mechanisms and machine science, in general, and its component gearing science, in particular.

We dedicate this collection to the memory of the organizer of this series of books on gears, Prof. Veniamin Goldfarb, who, to our deep regret, left us in 2019. This series was his last important international scientific project among his other numerous scientific, educational, organizational, and industrial achievements.

Of course, we focus the opening manuscripts of this volume on Prof. Veniamin Goldfarb, in particular, his biography and bibliography, one of his most essential publications largely summarizing the approaches to the enveloping process, and memories about Veniamin from his longtime friends and colleagues.

Behind all the efforts for the multifaceted improvement of gears and their technology, we should not forget about the educational component of our activities. In this respect, we welcome the review made by Prof. M. Ceccarelli, which should certainly be interesting and useful both for the leading gear experts and for their followers, the detailed work on the classification of gears, and the manuscript on the role of gears in the MMS university course. It is symbolic that these publications are present in the contributed volume in memory of Prof. V. I. Goldfarb. We all know how much importance he paid to the discussed issues and to pass on the scientific and practical experience to the younger generation within his various activities.

The reader familiar with the previous books on gears [1–3] will find relevant themes that, in essence, continue the work previously done by the authors of the contributed volumes to follow and assess their further achieved development.

We would like to specify new issues discussed in the present book related to cylindrical gears with arched teeth, their history, capabilities, and current trends in their development and to the organization of chamfering and rounding operations, although seemingly unimportant, very relevant in view of modern requirements and possibilities.

We are grateful to all the authors for their efforts and participation in this contributed volume, and we hope that together we will be able to maintain its high level and the interest of its readers in the future.

By tradition, we want to express our deep gratitude to Springer publishers, especially to the chief editor of the MMS series Prof. Marco Ceccarelli for the constant support of this series of books and also to Dr. Eng. Ph.D. Sergey Lagutin for his sustained assistance and advice in gear terminology issues.

Izhevsk, Russia

Natalya Barmina
Evgenii Trubachev

References

1. Goldfarb, V., Barmina N. (eds.): Theory and Practice of Gearing and Transmissions: In Honor of Professor Faydor L. Litvin, vol. 34, p. 450. Springer International Publishing AG Switzerland (2016). ISBN 978-3-319-19739-5, <https://doi.org/10.1007/978-3-319-19740-1>. <https://www.springer.com/gp/book/9783319197395>
2. Goldfarb, V., Trubachev, E., Barmina, N. (eds.): Advanced Gear Engineering, vol. 51, p. 497. Springer International Publishing AG Switzerland (2018). ISBN 978-3-319-60398-8, <https://doi.org/10.1007/978-3-319-60399-5>. <https://www.springer.com/gp/book/9783319603988>
3. Goldfarb, V., Trubachev, E., Barmina, N. (eds.): New Approaches to Gear Design and Production, vol. 81, Springer International Publishing AG Switzerland (2020). ISBN 978-3-030-34944-8, <https://doi.org/10.1007/978-3-030-34945-5>. <https://www.springer.com/gp/book/9783030349448>

Contents

Professor V. I. Goldfarb: Life Activity and Contribution to Gearing Science	1
Evgenii S. Trubachev, Nataya A. Barmina, and Olga V. Malina	
Some Exercises with Equations of Meshing: Review of Fundamental Manuscript	61
Veniamin Goldfarb	
Challenges of Mechanical Engineering and in IFToMM: Yesterday and Tomorrow	69
Marco Ceccarelli	
Classification of Gear Pairs with Fixed Axes. Review	85
V. E. Starzhinsky, S. V. Shil'ko, E. V. Shalobaev, A. L. Kapelevich, V. B. Algin, and E. M. Petrokovets	
Virtual Metrology of Helical Gears Reconstructed from Point Clouds	107
Ignacio Gonzalez-Perez, Pedro L. Guirao-Saura, and Alfonso Fuentes-Aznar	
Cylindrical Arc Gears: History, Achievements, and Problems	131
Vladimir N. Syzrantsev	
Gear Tooth Edge Deburring and Chamfering in 5Axis CnC Manufacturing	153
Claude Gosselin	
Worm-Type Gear with Steel Gearwheel	185
Evgenii S. Trubachev	
Parametric Synthesis of Technological Systems for Gear Finishing	203
M. Storchak	
Gears in Russian University Courses on Mechanism and Machine Science	225
Eduard G. Krylov and Natalya A. Barmina	

Geared Designs from the Past for Today Inspiration	243
Marco Ceccarelli and Fernando Viadero Rueda	
Theory of Adaptive Transmission	255
Konstantin Ivanov	
Load State of Low-Speed Spiroid Gears	279
Andrey Kuznetsov and Alexander Sannikov	
Uncertainties in Modeling the Lifetime-and-Functional Properties of Gear Trains and Transmissions and Ways to Reduce Them	305
V. B. Algin, M. A. Kananovich, S. M. Paddubka, U. M. Sarachan, S. V. Shil'ko, and V. E. Starzhinsky	
Minimization of Contact Pressure in the Straight Bevel Gear with Saving of Its Size	325
A. E. Volkov, S. S. Biryukov, and S. A. Lagutin	
Conic Linear Helicoids: Part 1. Synthesis and Analysis of the Basic Geometric Characteristics	339
Valentin Abadjiev and Emilia Abadjieva	
Conic Linear Helicoids: Part 2. Applications in the Synthesis and Design of Spatial Motions Transformers	361
Emilia Abadjieva and Valentin Abadjiev	
Automation of Engineering Design and Configuration of Medium Complexity Products by Example of Spiroid Gearboxes	389
Olga V. Malina	
Meshing Limit Line of Normal Arc-Toothed Cylindrical Worm Drive	403
Qingxiang Meng, Yaping Zhao, and Gongfa Li	
Improving the Efficiency of Gear Milling of Cylindrical Gears with Worm Cutters When Using Pulse Feed	417
M. M. Kane	
Advanced Lifetime Tests of Plastic Gears with E- and S-Geometry	427
Gorazd Hlebanja, Matija Hriberšek, Miha Erjavec, and Simon Kulovec	

Professor V. I. Goldfarb: Life Activity and Contribution to Gearing Science



Evgenii S. Trubachev, Nataya A. Barmina, and Olga V. Malina

Abstract The life and professional scientific way of Prof. V. I. Goldfarb is considered. The manuscript touches upon the main milestones of development and main achievements of the Izhevsk school in the field of gears and, in particular, spiroid ones and methods of their analysis. The main scientific achievements obtained personally by Prof. V. I. Goldfarb and scientific problems solved under his supervision are noted. The section devoted to organizing scientific activity of Professor Goldfarb describes the development of the Institute of Mechanics, Small Innovative Enterprise “Mechanic”, new scientific direction—gears and gearboxes for pipeline valves control, traditional Izhevsk scientific and technical forums “Theory and practice of gears and gearbox engineering”, publishing activities, and activities in national scientific communities and IFToMM where Prof. Goldfarb chaired the Gearing Technical Committee for many years and became Vice-President.

Keywords Professor V. I. Goldfarb · Spiroid gears · Institute of mechanics of Kalashnikov ISTU · IFToMM

1 Ancestry

The future professor Veniamin Iosifovich Goldfarb (Fig. 1) was born on February 01, 1941 in Izhevsk in the family of a professor of medicine—Iosif Veniaminovich Goldfarb. Professor I. V. Goldfarb was a famous doctor, but he became a doctor almost by accident: being mobilized for the First World War, he was attached as an assistant to a military paramedic, proved himself well there, and this, in fact, determined his

E. S. Trubachev · N. A. Barmina (✉) · O. V. Malina
Scientific Department “Institute of Mechanics named after Professor V. I. Goldfarb”, Kalashnikov
Izhevsk State Technical University, Izhevsk, Russia
e-mail: barmina-nat@mail.ru

E. S. Trubachev
e-mail: truba@istu.ru

O. V. Malina
e-mail: malina_0705@mail.ru



Fig. 1 Professor Veniamin Goldfarb

entire destiny. His beloved wife, Veniamin’s mother, was also a doctor. His son, our teacher Professor V. I. Goldfarb, remembered his father with great warmth, and it is not said just for effect. Whenever V. I. spoke of him, it was a word of affection for the man who had been with him all his life, and only a bitter regret that he, the son, had not been able or had not had time to do something for his father, only it gave away the fact that the latter was no longer with us.

He often cited his father: “If you want to have an interesting and colorful life, study sciences”. His parents’ influence was so strong that already being a Ph.D. in Engineering and a well-known scientist in Russia, the future professor V. I. Goldfarb at the age of 34 was seriously going to leave the engineering profession and... enter the medical institute to study medical cybernetics. Knowing his teacher, we have no doubt that he would have risen to eminence in medicine, but... fortunately for us, it did not happen. However, the subject of medicine turned out to be not at all closed for Professor Veniamin Goldfarb; both his children—daughters Olga and Irina—studied medicine and achieved success in it.

2 Becoming a Scientist

By the time he graduated from Izhevsk Mechanical Institute—IMI (now Kalashnikov Izhevsk State Technical University—ISTU), V. I. Goldfarb was one of the most promising excellent students of the class of 1962. He graduated from the Department of Instrument Design where he was transferred when it opened in 1960. The issues of instruments and everything connected with them, including computers and their programming were not just popular, but super popular that time. We can say that through the development and widespread introduction of this technology, the mankind was looking for new opportunities to organize their lives (and, judging by

the last decades, found them), and the competition for admission to these specialties of universities was off the scale. One can imagine that the best pupils went there. And the future professor V. I. Goldfarb was one of the best and most notable in this community. It should be said that even then he was distinguished not only by his intellect and quick wit—his charisma and leadership qualities were evident to everybody. Just look at the celebratory procession in honor of the first flight of Yuri Gagarin into space (1961) which was spontaneously organized by V. I. Goldfarb! We emphasize that it was not the Soviet power which used to organize everything and everyone at the time and did not welcome any activity outside official structures, but the student himself!

Getting off the chronology, we should note that multifaceted talents of Professor Goldfarb's personality, his leadership and unifying qualities, were not limited to professional activities. Colleagues (and many people in the world) knew him as a brilliant musician, an indispensable member of IMI/ISTU jazz ensemble, a satirical student theater of miniatures, and one of the main activists of the IMI/ISTU sports camp in Galevo on the bank of the Kama River.

One of the lucky cases for us was that the talented student attracted the attention of the already known by that time gearing scientist (specialized in planetary gears), the soon-to-be Doctor of Engineering Science and Professor V. M. Yastrebov. He proposed to make a large series of computer calculations of coordinates of points of ordinary involutes of circumferences. Nowadays this task seems trivial, but at that time the issue was so actual for industry (mainly, for gear control purposes) that a book with the results of the calculations was published by a central Moscow publishing house. For those days it was a great achievement, especially for a student. So, "he was caught", and the graduate of the Instrument Design Department found gearing calculations so interesting and promising that he went to Prof. Faydor L. Litvin, the most famous at that time (we can now confidently say—one of the leading researchers in the whole history of the theory of gearing). Veniamin was welcomed by him and in response to the question "what can you already do, young man?" he answered with confidence: "I solved the contact problem!" When learning the details of the involute calculations, Professor F. L. Litvin smirked and said that the contact problem was "somewhat" different and much more complicated... Prof. V. I. Goldfarb himself liked to recall this case with a smile. We cannot say now what went wrong to the postgraduate course of Prof. Litvin, but there is no doubt that this case and this conversation were memorable for Professor Goldfarb, and probably one of the most important events.

That period of 1950–1980s was called by our senior colleague Ph.D. Sergey Lagutin the period of "*Sturm und Drang*" in the Soviet gearing science. At that time an avalanche-like formation of the solid foundation for the beautiful building of the theory of gearing took place within 30 years; several scientific schools appeared in Moscow, Leningrad (now Saint-Petersburg), Saratov, Kiev, Odessa, Kharkov, Minsk, Khabarovsk, Kurgan, Novocherkassk, and other cities of the USSR—which gave both outstanding scientists and engineers, and multifaceted studies of gears. However, this is a topic for a separate discussion; different aspect of this process are considered, for example, in [1–3]. The city of Izhevsk, where one of the largest



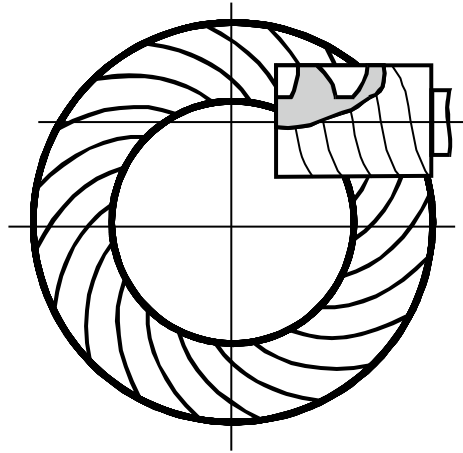
Fig. 2 Spiroid gears. General view

gearbox engineering enterprises in Europe was organized, was also not left out. A famous professor N. V. Vorobyov moved there from the largest technical university of the country—Moscow State Technical University named after N. E. Bauman, and a promising graduate of IMI, who had already become interested in calculations of gears, Veniamin Goldfarb, was admitted to his postgraduate course.

But what does this have to do with spiroid gears (Fig. 2) which later became the forte of Professor V. I. Goldfarb and which were invented very shortly before that (in 1954) by the American citizen of Finnish origin Oliver Saari [4, 5]? This is because almost immediately after their invention the data about them came from American scientific and technical journals to IMI in Izhevsk. One could say that the powerful wind of that very “storm” blew it over. How many modern innovations can we name in the period of global and instantly spreading information, which had not just fallen into the hands of engineers at the other end of the planet, but were thoroughly studied within 4–5 years since their appearance? By the time V. I. Goldfarb was enrolled to the post-graduate course, there were at least two studies made by Izhevsk experts—B. D. Zotov and N. S. Golubkov. They confirmed the American opinion that the spiroid gear had a number of objective advantages over its analogs—worm and hypoid ones [4–7].

Under the supervision of Prof. N. V. Vorobyov, a group of spiroid gears was created at IMI under the guidance of A. K. Georgiev, a young scientist, soon-to-be Ph.D. in Engineering, a leader of the Izhevsk gearing school, a teacher and longtime supervisor of Veniamin Goldfarb. The group soon became a scientific department of IMI—the Spiroid Gear Laboratory (SGL). The talented and active V. I. Goldfarb, avidly grasping the wisdom of the geometrical theory of gears and programming of complicated calculations, practically immediately became the right hand of the head, the main gearing theorist and calculating engineer in the SGL. His Ph.D. thesis presented in 1969 was mainly devoted to the study of a new variety of spiroid gears—with a concave right and convex left flank profile of worm threads (Fig. 3). The gear was patented in several countries and, in general, corresponded to the general trend of searching for optimal tooth profiles—it is enough to remember the gears by E. Wildhaber—Novikov [8, 9], Niemann and Litvin [10, 11], Korostelev and Lagutin [12]. The studied gear gave some effect in the load-carrying capacity (up to 10–15%), but, as usual, it was not free: its manufacture was associated with additional technological difficulties. Apparently, it was the reason to postpone (perhaps, temporarily) the common implementation of this technical solution. However, the study of the complicated gear made scientists look for new methods and techniques for solving

Fig. 3 Spiroid gear with convex-concave worm profile

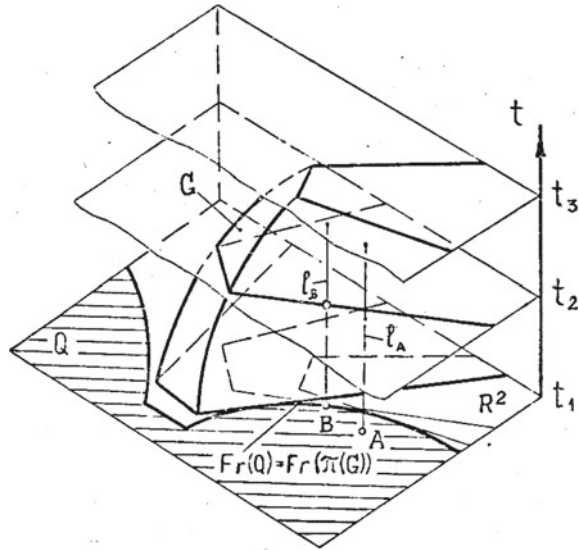


various problems—searching for contact lines, evaluation of undercutting, geometrical and kinematic parameters of meshing, calculating the complex geometry of teeth. The work undoubtedly contributed to the growth of the scientific skill and scientific outlook of our teacher. The mathematical and software developed by him became the calculation basis for many Ph.D. theses presented by the Izhevsk gearing school, which, it can be said, experienced its own “*Sturm und Drang*” period in the 1970s.

3 Beginning of Individual Scientific School

By the end of the 1970s Ph.D. Veniamin Goldfarb had obviously outgrown his teacher, developed as a scientist so much that he had the potential and motivation for independent work, and in 1980 he began to form his own scientific school at his Instrument Design Department. Perhaps, one of findings of that time was the form of organization of this school—as a Student Design Bureau of the Instrument Design Department. It was named “Student Design Bureau of Gears” first among the students and then officially; many promising students got “scientific trial by fire” there. Hundreds of students’ term and graduation projects and scientific research works, carried out under the supervision of V. I. Goldfarb, made it possible to polish both his methods of work with students and his own new methods of calculation. The basis for their proposal and development was the experience of solving complex geometrical problems obtained in the 1960s and 1970s. Among these methods, the “non-differential method” of calculating the generated and meshing surfaces proposed jointly with Eng. Nesmelov [13] is of a special importance (Fig. 4). The method is based on application of R-functions apparatus, proposed by the Soviet scientist Rvachev [14]; it is oriented to computer-aided design and provides reliable search, automatically excluding cases of secondary solutions and physically impossible contact from inside

Fig. 4 Scheme of “non-differential method” (fragment from Doctor of Science Thesis by V. I. Goldfarb)



the solid of an enveloping (generating) element, which can arise and require special diagnosis when using the classical apparatus of the differential geometry and common kinematic method. This development was in the general course of aspirations of many specialists in creation of universal methods of gear calculation. For example, Prof. G. I. Sheveleva proposed the “method of enveloping surfaces” a little earlier [15], and traditional differential methods were summarized for generating surfaces and their edges by Babichev [16]. Prof. V. I. Goldfarb himself made the most interesting theoretical generalization of the methods in his later manuscript “Some exercises with the equation of meshing” [17].

The second major part of V. I. Goldfarb’s research in the early 1980s was related to studies of spatial gearing schemes and aimed at predicting the principal properties of gears at the early stage of design: dimensions and shape of elements, direction and character of tooth contact (internal or external). The following general solutions for arbitrary arrangement of axes and shapes of elements were obtained:

- condition for contact of initial surfaces;
- areas of gear scheme existence;
- conditions for determining the type of contact—internal or external;
- condition for choosing a preferred ratio of directions for rotation of elements.

These works were also in tune with the works of other scientists, who were looking for generalizations: for example, M. L. Erikhov, who classified the schemes of machine-tool gearing [18], L. V. Korostelev and his students, who generalized the properties of worm type gearing [19], at last, the Bulgarian researcher K. Minkov, who classified schemes of spatial gears almost simultaneously with Goldfarb [20]. Prof. V. I. Goldfarb’s classification (Fig. 5) included gears with:

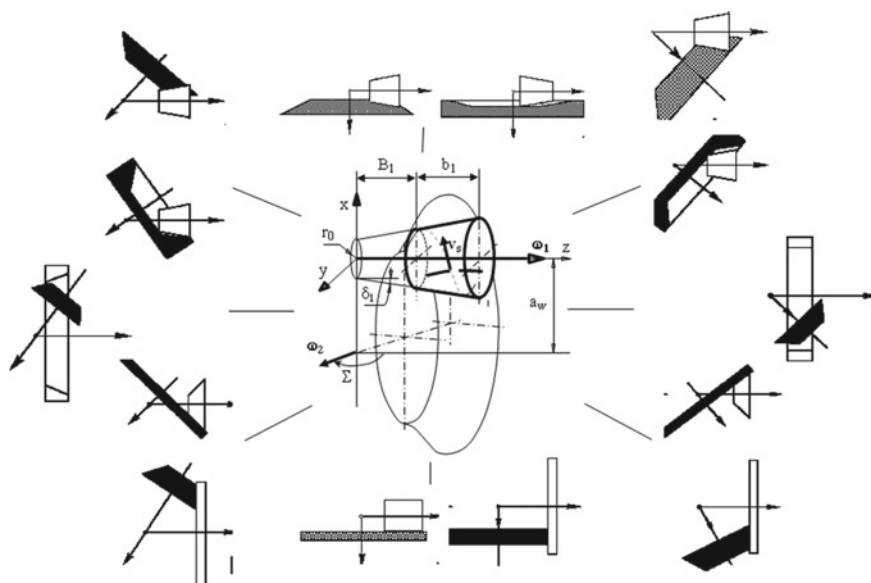


Fig. 5 Scheme of spatial gear by V. I. Goldfarb and fragment of his classification of single-stage gears

- bevel and inverse conical elements;
- one flat element;
- one cylindrical element;
- internal meshing with respect to each of the elements.

The number of variants turns out to be one order greater in schemes of two-stage gears [21].

Here are other interesting schematic solutions obtained by V. I. Goldfarb (of course, this is only a small part of the proposed solutions):

- gear with ideal-constant helical parameter (axial pitch) of a pinion (worm) [22],
- gear with rotaprint lubrication [23] (self-lubricating gear—in co-authorship with Prof. V. N. Anferov)—Fig. 6,
- worm type gear with internal meshing relative to the worm [24]—Fig. 7,
- non-orthogonal gear with two meshing zones [25]—Fig. 8.

The third important scientific problem solved by V. I. Goldfarb in 1980s was the generalization of the approach to computer-aided design of the conjugate worm-type gear. The main result is a reasonable decomposition of this process [26] into stages:

1. Selection of the gear scheme.
2. Calculation of tooth flank geometry.

Fig. 6 Spiroid gear with rotaprint lubrication of meshing (the lubricating gearwheel is above the worm, the operating one is below)

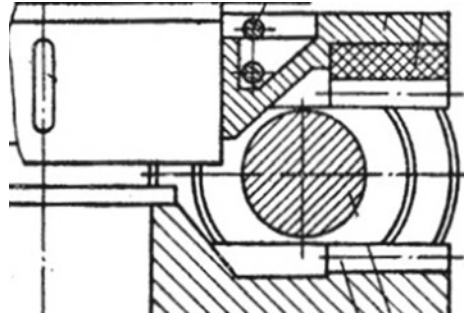


Fig. 7 Gear with internal meshing relative to the worm [17]

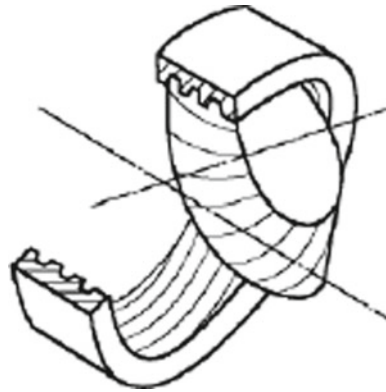
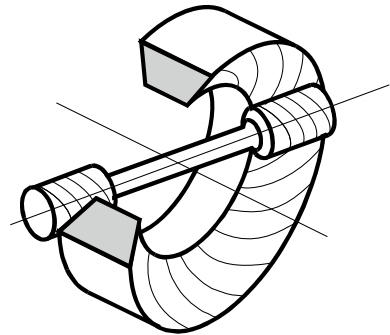


Fig. 8 Non-orthogonal gear with two meshing zones [18]



3. Calculation of geometrical and kinematic contact parameters (sliding velocities, length and arrangement of lines/points of the conjugate contact, reduced radii of curvature, velocities of movement of contact points on the tooth flanks).
4. Evaluation of forces acting in the meshing, efficiency, load-carrying capacity of the gear in accordance with various criteria.

This sequence aims to streamline the automated design process, to make it more meaningful for the designer by leading the process “from simple to complex”, giving the designer an opportunity to consistently narrow down the multi-dimensional space of parameters and the number of possible and acceptable solutions, to obtain fast gear estimates at early stages, and it allows a designing engineer to rationally arrange the computational procedures and data structures. The sequence was implemented in the first CAD-program for spiroid gears “SPDIAL” developed by Eng. I. P. Nesmelov under the guidance of Goldfarb 1980s [27]. The calculation in this program was focused on designing a theoretically accurate conjugate spiroid gear. Later on, the sequence was developed taking into account the problems of real manufacturing and real operation of gears, and it was extended to the cases of worm and bevel gears by V. I. Goldfarb and his pupil, one of the authors of this manuscript, E. S. Trubachev, who implemented it together with his pupils in the new software complex CAD system “SPDIAL+” in the period from 1996 to the present [28, 29].

The mentioned three parts of V. I. Goldfarb’s scientific developments became the basis for his D.Sc. Thesis “Fundamentals of the theory of automated geometrical analysis and synthesis of general type worm gears”, which was presented in 1986.

4 “Sturm Und Drang-2”. Institute of Mechanics

Soon after that “Perestroika” came down in the USSR which ended, as we know, with the destruction of the USSR and, more importantly for our story, with a complete change in the economic order of our country. It had a disastrous effect on the traditional sources of funding and on the traditional order of Russian university science. Professor V. I. Goldfarb turned out to be one of the best in scientific organization having found the practical implementation of his scientific developments and obtained the practical basis for new ones as well as for new growth of his students at new conditions. In 1990 and his pupils moved at, one might say, the most productive department of IMI/ISTU—“Technology of Robotics Production” Department (somewhat earlier it was “Technology of Mechanical Engineering”, now it is “Design and Manufacturing Preparation of Mechanical Engineering Production”). Since 1994 the former head of this department, Professor I. K. Pichugin persuaded Professor V. I. Goldfarb to head this department and on February 1, 1994, at the initiative and with the blessing of ISTU Rector Professor I. V. Abramov a scientific department “Institute of Mechanics” was founded (now—“Institute of Mechanics named after Professor V. I. Goldfarb”) where 20...25 employees worked in different years, both experienced and having scientific degrees, and young ones, eager to acquire them (Fig. 9). The Institute of Mechanics became an innovative solution, a new form of organization of science, when it became integrated in one complex with the educational department of the University and commercial production—Small Innovative Enterprise “Mechanic” (SEI “Mechanic”), which was established soon after formation of the Institute of Mechanics and became not only a place of approbation for scientific ideas, but also the founder of new scientific and manufacturing tasks. According to Prof.



Fig. 9 Scientific department “Institute of mechanics”, 2011

V. I. Goldfarb himself, “The main purpose of its organization was to create conditions for combining scientific research and production of science-intensive products, in particular, gears and gearboxes, with the educational process and problems of training qualified engineering and scientific personnel. Such a combination harmoniously unites the need for personnel in scientific research and the need to maintain the educational process at a high scientific level”.

The period from 1995 to 2004 was, in fact, the second wave of the “Sturm und Drang” in the Izhevsk school—now under the leadership of Professor V. I. Goldfarb. During this period, 13 Ph.D. theses and 5 D.Sc. theses were presented (that is, on average, almost 2 theses per year). Their topics covered a broad range of problems related to the theory of gearing, studying the specific gear types, gearboxes and their properties, and software tools for their design:

N. V. Isakova, 1994 (Ph.D.)—spiroid gears with the ideal worm pitch;

O. V. Malina, 1995 (Ph.D.), 2002 (D.Sc.)—invariant methods of computer-aided design of complex objects and processes;

A. I. Abramov, 1996 (Ph.D.)—accuracy and vibration activity of spiroid gears;

D. V. Glavatskikh, 1997 (Ph.D.), 2002 (D.Sc.)—implementation of the “non-differential method” in studies of helical surfaces;

A. G. Russkikh, 1997 (Ph.D.)—computer-aided synthesis of gear schemes;

E. S. Trubachev, 1999 (Ph.D.), 2004 (D.Sc.)—non-orthogonal spiroid gears, methods of design of spiroid gears taking into account real manufacturing and operating conditions;

D. F. Plekhanov, 1999 (Ph.D.)—non-traditional planetary 3 K gears;

R. V. Voznyuk, 1999 (Ph.D.)—software implementation of the “non-differential method”;

D. V. Koshkin, 1999 (Ph.D.)—accuracy of spiroid gears with the localized contact;

A. A. Tkachev, 1999 (Ph.D.)—computer-aided design of spur and helical involute gears by means of Dynamic Blocking Contours;

S. V. Lunin, 2000 (Ph.D.)—computer-aided solid-state modeling of meshing gears;

A. S. Kuniver, 2001 (D.Sc.)—spiroid gears with the localized contact;

V. N. Anferov, 2002 (Ph.D.)—wear of spiroid gears;

N. A. Barmina, 2002 (Ph.D.)—double-stage cylindrical-spiroid and spiroid-cylindrical gearboxes;

E. I. Popova, 2004 (Ph.D.)—study of spiroid gears with plastic gearwheels.

5 Manufacturing Gears and Gearboxes

The individual manufacturing activity organized at the scientific school of Professor V. I. Goldfarb is a phenomenon unique in its own way. The enterprise, in fact, emerged “out of nothing”, relying almost entirely on the activity, energy and qualification of V. I. Goldfarb himself and his subordinated associates at the Institute of Mechanics. At first, the old machine-tools available at the department’s training workshop were used (in many respects, restored and “revived”). During the first fifteen years (approximately by 2010) the company acquired its own machinery for the comprehensive support of the production process, its staff increased from 15...20 people to 70...80.

Applications for gears are as varied as they are traditional. Not only technical solutions, but also specific suppliers and manufacturers are often long-present. It is difficult for consumers to abandon them in favor of new ones. However, the situation in the 1990s, with the actual rejection of Soviet methods, bankruptcy of many enterprises, opening of the foreign market and foreign supplies of more advanced gear equipment on the one hand, and the galloping exchange rate of the foreign currency on the other, promoted the search for new solutions for both consumers and new manufacturers. Actuators for pipeline valves were a great finding for the team of Professor V. I. Goldfarb. Contrary to the general trend, production of the latter was constantly growing, first because of Russia’s well-known specialization in the production and supply of hydrocarbons and then due to a rather rapid recovery of many other things in the production sphere. In the mid 1990s on the initiative of Cameronvolgomash enterprise (now Samaravolgomash) there was a meeting in Izhevsk with gear manufacturers with the issue of creating analogues to foreign products. The gear manufacturers said “definitely”: “No. We do not have such design and production methods”. And it was Professor V. I. Goldfarb invited to the meeting who uttered the famous Lenin’s phrase in the USSR: “We have such a party!” The point here was not so much in V. I. Goldfarb’s determination and vigor, as in his deep understanding of gears—worm gears, used in analogs, and spiroid ones, which have a number of favorable properties for the successful application in conditions, typical for valve control—at low speeds, rare actuating and high overload torques. From that moment a multifaceted work on research, creation of methods and means for design, organization of pilot and then serial production of gearboxes for pipeline valves control began (Figs. 10 and 11). The work started with experimental testing of future effective solutions. Several prototypes, differing in design, were broken during the tests. The result of the work (we dare to think, not final at all) was... let me quote our colleague and a long-time friend Prof. V. I. Goldfarb Dr. S. A. Lagutin: “A small innovative enterprise “Mechanic” cooperated with the Institute of Mechanics is producing now up to 1000 gearboxes per month (!), providing almost

a**b**

Fig. 10 **a** Small Innovative Enterprise “Mechanic” (machining site). **b** Small Innovative Enterprise “Mechanic” (testing site)

all pipeline valves in Russia with its production. As a manufacturer and supervisor of the gearbox workshop at Elektrostal Heavy Engineering Plant, I can only be envious of such results”. This is the most important practical result of Prof. V. I. Goldfarb’s initiative, which provided and continues to provide interesting work for dozens of specialists, for whom it became a great school. No less important scientific and manufacturing results that became possible due to it are as follows:

- theory of design of heavy-loaded spiroid and worm gears and gearboxes adapted to production and operating conditions [29, 30];
- invariant methods and software tools for synthesis of complex objects and processes [31];
- new types of gears [32–34];
- improved methods of gear cutting [35–38].

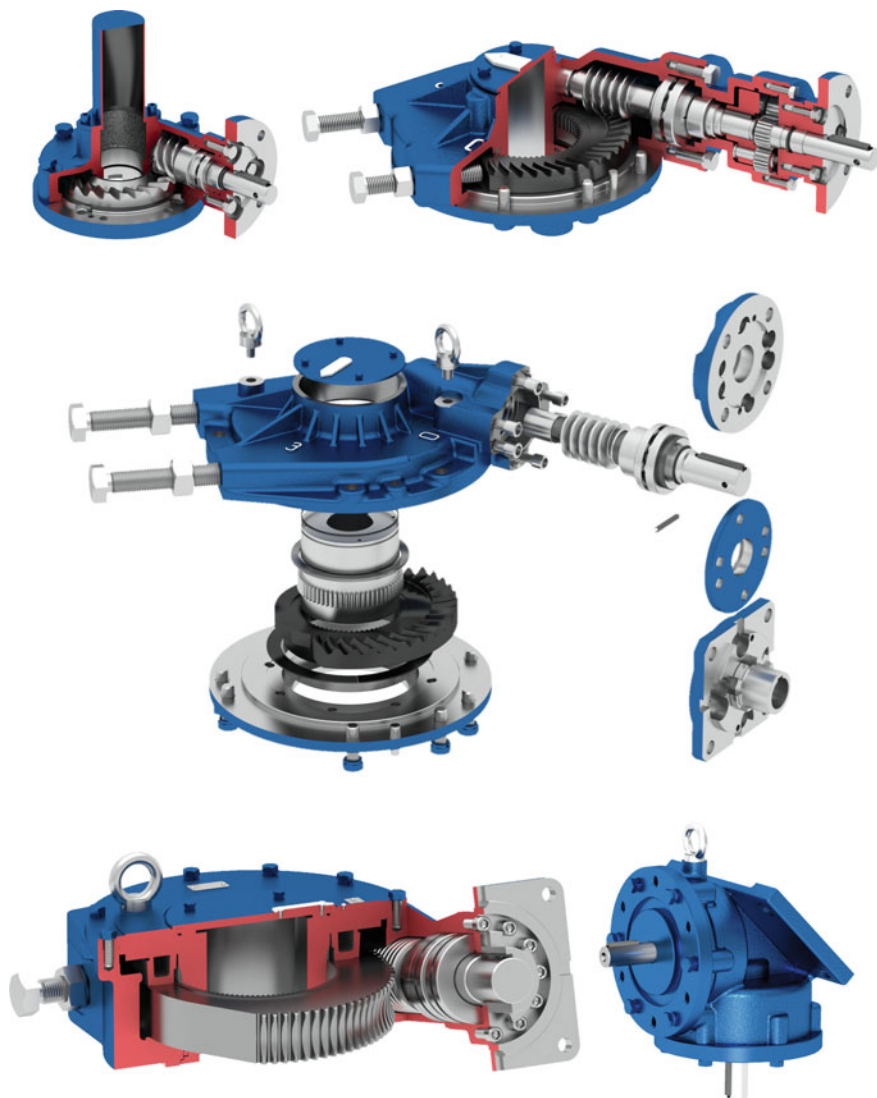


Fig. 11 Gearboxes produced by SIE “Mechanic”

To summarize, we must say: thanks to this, the scientific school of Professor V. I. Goldfarb became in many respects self-sufficient, well-motivated, capable of stating, discussing and solving important, useful and interesting problems in the field of gears and gearbox engineering.

6 Professor V. I. Goldfarb—Organizer and Leader of Russian and International Scientific Community

During different periods of his scientific activity V. I. Goldfarb was an active participant of scientific communities. In particular, he was a member of Technical Committee TC-258 for Machine Parts and Gears of the Russian State Standardization Committee; he was the Vice-President of Udmurt Association of Scientists, and he was the initiator and Vice-President of Russian non-profit partnership “Association of Mechanical Transmission Engineers”.

In difficult economic transition conditions in the 1990s, Russian scientific schools in the field of gears and gearbox engineering found themselves in an extremely difficult financial situation. In these conditions, from 1991 to 2004, Professor V. I. Goldfarb initiated the joint participation of leading Russian scientific schools of 14 Russian technical universities in target programs of Russian state and interstate financing.

This allowed to soften the blow of shock reforms to a great extent, to preserve personnel and intellectual potential of Russian technical science. One aspect of these integration efforts of Prof. V. I. Goldfarb was the organization of scientific and technical conferences. The first of them were held in Izhevsk in the 1980s. These conferences and symposia acquired a national and international status in the 1990s. At the same time, they were traditionally called “Theory and practice of gears and gearbox engineering” (Fig. 12) and Institute of Mechanics of Kalashnikov ISTU became de facto the leading Russian center in this field, welcoming leading gear experts from Russia and other countries. For example, the International Symposium “Theory and practice of gearing” in 2014 brought together over 100 participants from 12 countries.

Until the late 1980s, Izhevsk was a so-called partially closed industrial city with a large share of defense industry, which dramatically complicated international contacts; such communication was possible, at best, with scientists from Eastern European countries. Therefore, it is not surprising that Goldfarb’s first publication was in Europe, published in the Proceedings of the 15th National Seminar in Varna, Bulgaria [39]. At that time, it became obvious that a certain level of foreign language proficiency was necessary to initiate international scientific and educational cooperation. Having learnt German at school and university, which remained unclaimed, Veniamin Iosifovich started to study English independently at the age of 50 and succeeded in it. Within a few years, first with the support of teachers from English department of ISTU, then with the help of students of the specialty “Interpreter in the sphere of professional communication”, he began to prepare scientific manuscripts in English, and then to make presentations independently and speak at English-language scientific events of the highest level. His organizational talent very quickly manifested itself in the diverse international cooperation between universities and scientific schools of different countries. The first foreign guests who came to Izhevsk to ISTU were precisely gear experts from Great Britain, Czech Republic, Poland, and Slovakia. Every year the geography of contacts and the number of new joint projects



Fig. 12 Conferences “Theory and practice of gearing”, 2004, 2008

were expanding rapidly. The first agreements on international cooperation at ISTU with the universities of Slovakia (Bratislava, Trnava), Czech Republic (Brno), Poland (Warsaw), Bulgaria (Sofia), England (Nottingham), and USA (Los Angeles) were signed on the initiative of Prof. V. I. Goldfarb.

Later on, Professor V. I. Goldfarb became a member of the Technical Committee for gears of the International Standardization Organization (ISO TC 60), member of editorial boards of international journals “Mechanism and Machine Theory”, “Machine Design” and others. He was a frequent chairman and member of scientific program and organizational committees of international conferences on gears and transmissions: “Power Transmissions” (Greece, 2009), “Power Gears and Transmissions” (Japan, 2009), “Fundamentals of Machine Design” (Bulgaria, 2009), “Gears” (Germany, 2010), “Terminology in Mechanisms and Machines Science” (Belarus, 2010), “Development and Study of Mechanical Components and Systems” (Serbia, 2011) and a member of program committees of IFToMM World Congresses on MMS (Finland-1999, China-2004, France-2007, Mexico-2011, Taiwan-2015).

The International Federation for the Promotion of Mechanism and Machine Science (IFTToMM) was established in 1969 by the initiative of the famous Soviet scientist, Academician I. I. Artobolevsky. Today the Federation has national MMS committees in more than 50 countries, and its governing bodies are elected at the General Assembly. The structure of IFTToMM includes 14 Technical Committees and 4 Permanent Commissions. One of the most authoritative is the Technical Committees for Gearing and Transmissions (TC for Gearing and Transmissions), established in 1976. Since 1994, Russia has been represented in the TC by Prof. E. L. Airapetov (Moscow) and Prof. V. I. Goldfarb (Izhevsk). In 1998, Prof. V. I. Goldfarb was elected Chairman of the Committee, and in 2001, after the report meeting of the Committee, his chair term was extended for 4 more years. The main tasks of the Technical Committee were to establish contacts between scientists and engineers of different countries in the field of gears and transmissions, development of databases and joint solution of actual technical problems, promotion of information exchange, etc. The general concept of its activity within the framework of the International Federation on MMS, its main objectives, tasks, priorities were published in two languages in the international journal "Gearing and Transmissions", No.1, 1998. Prof. Goldfarb's active work in this Technical Committee was appreciated by the Executive Council of the Federation and since 2008 he became one of three Russians in the history of the Federation who was a member of IFTToMM.

In 2010, due to poor reporting of the next Chairman of the Gearing TC (he did not submit on time annual reports on the activities of the Committee, although the active work in the Technical Committee continued), the management of the Federation decided to abolish this TC and merge it with the TC for Cams and Linkages and call the new Committee "Mechanical Transmissions". The appropriate changes were made in the IFTToMM Constitution. Prof. Goldfarb did not agree with this decision, which was taken without thorough discussion with members of the Gearing TC and leading experts from various countries. He organized this communication and found support of many colleagues, including Prof. D. Su (Great Britain), Prof. A. Kubo (Japan), IFTToMM President Prof. M. Ceccarelli (Italy) and others. One year later, the Gearing TC resumed its work as a separate committee with its own specific theoretical approaches and practical tasks (Fig. 13).

In 2011, Professor Goldfarb was elected the Chairman of the Permanent Commission for Communications, Publications and Archiving (IFTToMM PC CPA). The crowning achievement of Prof. V. I. Goldfarb's international activities was his election as Vice-President of this prestigious organization from 2011 to 2015. Unfortunately, he did not have time to complete some of the projects he initiated as IFTToMM Vice-President, but they may be of interest to future generations of experts:

- An appeal to UNESCO to hold together with IFTToMM a series of international conferences "Mechanisms and Humans", "Mechanisms in Medicine", etc.
- Integration of IFTToMM website into various social networks.
- Creation of a forum of young scientists on IFTToMM website with the purpose of their uniting and discussing urgent issues.
- Cooperation of IFTToMM with industry.



Fig. 13 IFToMM World Congress, Poland, 2019

We should tell separately about the first-ever international student subject Olympiad on MMS, which was held in ISTU on April 19–21, 2011 (Fig. 14). The idea to organize the Student International Olympiad on MMS (SIOMMS) was proposed by V. I. Goldfarb in 2009 in Mexico at the IFToMM conference. IFToMM Executive Council decided to organize the International Student Olympiad (SIOMMS) in 2011 in Izhevsk State Technical University, Izhevsk, Russia. SIOMMS-2011 was held on April 19–21, 2011 [40]. 17 student teams from 8 countries took part in this competition. This Olympiad initiated regular Students International Olympiads on MMS which were held every two or three years in different parts of the world: 2011 (Izhevsk, Russia), 2013 (Shanghai, China), 2016 (Madrid, Spain) and 2018 (Lima, Peru).

Understanding the importance of publications in scientific communication, promotion of interesting ideas, in the growth of young scientific personnel, Prof. V. I. Goldfarb initiated scientific and technical publications, and contributed volumes. The earliest of them was the abstracts of the scientific and technical conference “Development and Implementation of Computer-Aided Design Systems”, Izhevsk, 1981, later such volumes became an integral part of all scientific events.

The journal “Gearing and Transmissions” took a special place among all publications. Now it has become history, but it was the first and only bilingual journal of its kind, where the results of scientific research in the field of gears and transmissions performed by foreign scientists and scientists from Russia were published. All the manuscripts were published both in Russian and in English, which in itself was a pioneering decision and served as a powerful impetus to international communication and cooperation among the scientists involved in gears around the world. It was thanks to the initiative and efforts of Prof. V.I. Goldfarb, that the acquaintance of Russian gear scientists with the works of their foreign colleagues began, and also

a**b**

Fig. 14 **a** Organizers and special guests of SIOMMS-2011, Izhevsk, Russia. **b** Participants of SIOMMS-2011, Izhevsk, Russia

the international gear scientific community and manufacturers could get acquainted with the works of Soviet and Russian scientists, who had not published their works in English before.

In 1991, Prof. Goldfarb initiated its publication first as the edition of the Association of Mechanical Transmission Engineers (AMT) and then, with the election



Fig. 15 Journals “Gearing and Transmissions”

in 1994 of Prof. Goldfarb as the Russian representative in the IFToMM Technical Committee on Gearing and Transmissions, it became a permanent publication under the auspices of IFToMM. Between 1991 and 2004, it was published once, twice, or three times a year by the Institute of Mechanics, supported by the Association of Mechanical Transmission Engineers (AMT), Technical University of Brno (Slovakia), Slovak Technical University of Bratislava, and Technical University of Nottingham (UK). It was sent to dozens of Russian and foreign universities and enterprises, and in 1994 became the official journal of IFToMM (Fig. 15).

In 2014, by the initiative of IFToMM Vice-President, Professor M. Ceccarelli (Italy), Prof. Goldfarb started a new project—regular publication of books on gears in the series “Mechanisms and Machine Science” in the largest European publishing house “Springer”. As editor-in-chief of these books, he united manuscripts of the leading gear scientists from Russia, China, the United States, Japan, Italy, Germany, Canada, Bulgaria, Belarus, and other countries. Three contributed volumes have already been published to date in 2016, 2018, 2020 [41–43].

7 Conclusion

So, it was the scientific life journey and main achievements of Professor Veniamin Iosifovich Goldfarb. Of course, the scope of the manuscript in a scientific and technical book does not allow us to fully reflect what this outstanding man left for us and

what he was for us. He did not just open up the world of gear science to us, including people of different nations, generations, and activities—he was, in fact, creating that world (with many other outstanding people). We thank Providence for the gift of being close to Prof. Goldfarb, of being his students, and, finally, of having the “*la richesse des relations humaines*” with him.

Professor Veniamin Goldfarb was a brilliant teacher and instructor, his lectures were unique, he generously shared his knowledge with his students, and, with his ability to build up a scientific work and clearly express its essence, he gave help and support to many Russian scientists. In 2020 the Scientific Department “Institute of Mechanics” of Kalashnikov ISTU was renamed into “Institute of Mechanics named after professor V. I. Goldfarb”.

Appendix 1: Memories of Friends, Relatives and Gear Colleagues—A Tribute to Professor Veniamin Goldfarb

It is impossible to describe all the love, recognition and respect to Prof. Goldfarb among his friends and colleagues, the coryphaei of the gearing science. His talent, irrepressible energy, scientific and organizational abilities were always the subject of admiration and sincere envy.

Sergey Abramovich Lagutin, Ph.D. in Engineering, Senior Researcher, Leading Gearbox Designing Engineer, Elektrostal Heavy Machine Building Plant JSC (Elektrostal, Russia):

Dear Veniamin Iosifovich, I remember how in 1993 you shared with me the idea of establishing the Institute of Mechanics. I always appreciated your scientific talent, energy, and organizational abilities which allowed you to establish the laboratory of spiroid gears in Izhevsk, which by that time had already become a recognized leader in our country and abroad in research, development, and implementation in various fields of spiroid gears and gearboxes. I was amazed that you managed to implement such bold and ambitious projects as the organization of the Russian Association of Mechanical Transmission Engineers and the publication of the International bilingual journal “Gearing and Transmissions” in Izhevsk.

However... 1993 was the year, when the collapse of science and industry in the country occurred, plants were shut down, technical universities were rebuilt for training managers and economists, young specialists were largely searching for jobs abroad. In such an atmosphere, the idea of creating a new scientific Institute, frankly speaking, seemed to me like utopia.

And yet you managed to implement this idea. Institute of Mechanics was created and has been successfully working for over 25 years. The subjects of its scientific research went far beyond the initial framework of the study of spiroid gears. The Institute has become a scientific school of multi-purpose research of various types of gears, unfortunately, today, practically the only such school in Russia.

The Small Innovative Enterprise “Mechanic” co-operated with the Institute produces up to 1000 gearboxes per month (!), providing practically all the pipeline valves in Russia with its products. As a manufacturer and supervisor of the gearbox production site at EZTM, I can only envy such results.

The institute successfully trains scientific personnel, suffice it to say that many of its employees have already prepared and presents D.Sc. theses.

Institute of Mechanics regularly holds conferences and symposiums on the theory and practice of gears, where Russian specialists can meet each other, exchange experiences, and publish their results in the rated scientific proceedings. Under your editorship, three contributed volumes of Springer were also published, in which the latest achievements of Russian and international gearing science are collected and presented to numerous readers. I wish the Institute of Mechanics new creative successes for the next 25 years. And I hope for further fruitful cooperation with your Institute.

Glazunov Viktor Arkadievich, D.Sc. in Engineering, Professor, Director of Institute of Mechanical Engineering of Russian Academy of Sciences (Moscow, Russia):

Dear friends, I would like to say a few words about our precious person—Veniamin Iosifovich Goldfarb, with whom I was fortunate to communicate quite closely during the World Congress on the Theory of Mechanisms and Machines in 2011 in Guanohuato (Mexico). Veniamin Iosifovich showed himself to be a very friendly, sincere and charming person. We talked a lot with him about literature, art, and played music together. He played the piano very well and, what is especially important to me, he could improvise in a jazz style. It seems to me very valuable that a creative man—Veniamin Iosifovich—manifested his creative nature in many hypostases.

Andrey Erikovich Volkov, D.Sc. in Engineering, Professor, Federal State Budgetary Educational Institution of Higher Professional Education “Stankin” (Moscow, Russia):

V. I. Goldfarb was a leading gear expert in Russia and one of the most authoritative gear specialists in the world. He combined, with remarkable ease, scientific work in the field of the gearing theory, management of production and implementation of spiroid gears and gearboxes, organization of international conferences, representing our country at the international level for a long time, including his work as Vice-President of IFToMM. His main lifetime project was the founding of the Institute of Mechanics in ISTU, which he led for more than a quarter of a century. Today, his scientific school is the leading one in the field of gears in Russia and one of the leading ones in the world.

For many years, Veniamin Iosifovich kept in touch with the Department of Theoretical Mechanics of “Stankin”. We were united by a common interest in the development of the theory of generating by cutting. Cooperation and scientific competition between two scientific schools—of Prof. Sheveleva G. I. and Prof. Goldfarb V. I.—was expressed in the development of the theory of generating by means of developing non-differential methods of analyzing generation processes using software packages. This made it possible to solve many complex problems set by our industry.

It is difficult to overestimate the contribution of V. I. Goldfarb to the theory and practice of gearing. His name has been forever inscribed in the history of Russian mechanical engineering.

Alexander Kapelevich, Ph.D., AKGears, LLC (USA):

My friendship with Veniamin was, unfortunately, rather short. Although we met back in the 1980s at one of the seminars in Moscow organized by Professor Vulgakov, our real communication began in 2007 at the ASME conference in Las Vegas, USA. He took the time to listen to my presentation on asymmetrical gears and offered me to write a joint paper combining two approaches to optimal gear design, his Dynamic Blocking Contours method and my Direct Gear Design. This manuscript, written in co-authorship with Ph.D. Alexander Tkachev, was published in August 2008 in Gear Solutions magazine, USA. Later there were unforgettable meetings at conferences in 2009 in Matsushita (Japan), in 2011 in Xian (China) and in 2013 in Munich (Germany). In addition to these meetings, there was constant electronic communication and Skype communication. During the last 3–4 years, when his health condition noticeably deteriorated, we continued to meet by Skype about once a month. He was interested in literally everything, not just research and projects, but also my family, travel, sports, and more. These, sometimes serious, sometimes fun conversations were essential for both of us, and our Skype communication continued until his death. Back in September 2019, when our mutual good friend Dr. Franz Joachim was looking for opportunities and experts to calculate, design and manufacture spiroid gears, Veniamin was interested and involved in finding solutions to these issues.

Fyodor Ivanovich Plekhanov, D.Sc. in Engineering, Professor, Kalashnikov ISTU (Izhevsk, Russia):

Being engaged in the scientific work in 1990s, I didn't think about writing the D.Sc. thesis, I considered that the results of my scientific activity did not correspond to the level required for such degree. But once I made a presentation at an international scientific conference organized by V. I. Goldfarb. After that, Veniamin Iosifovich invited me to his office and told me that the results of my research could be the basis for my D.Sc. thesis, and he was ready to assist me as a scientific supervisor. To do this, he asked me to show him all my publications. Having brought my published manuscripts and patents for inventions into the system, I gave them to Professor Goldfarb, and after a while he answered: "The material you have presented is a D.Sc. thesis, you only need to edit some of its sections and go out to present it". After about a year I became a D.Sc. in Engineering.

Valery Nikolaevich Anferov, D.Sc. in Engineering, Professor, Siberian State University of Railway Transport (Novosibirsk, Russia):

In 1972, I was sent to Izhevsk to assess the possibility of using spiroid gears in our designs of special hoisting devices. At first I introduced myself to Vice-Rector for scientific work Mironov—he described me the course of work and then I worked in the laboratory of spiroid gears (headed by Georgiev A. K.). The businessstrip lasted a week, so I got acquainted with the main laboratory staff: Goldfarb V. I., Ezerskaya

S. V., Shibanov E. K., Modzelevsky V. A., Manshin S. D., Kuniver A.S., Ivaykin V. A. and others. The first impression is the most profound and vivid. It became clear to me, as a design engineer, that the practical realization of the developments is “like walking on foot to the Moon”, so after arrival home in Sverdlovsk, I honestly outlined the situation to my chiefs and proposed to sign a business contract with IMI on the application of spiroid gears in the nuclear industry with the development of methodological recommendations. I was entrusted to supervise the business contract, to design the structures, to master the technology in SverdNIikhimmash, to conduct research on the evaluation of gear durability.

Veniamin Iosifovich Goldfarb stood out from all the employees, he was already a Ph.D. in Engineering, the rest were ordinary laboratory employees. It was clear—he was a highly educated, intellectual leader, not arrogant, respectful of everyone, at the same time being at a certain distance and knowing his own worth. I thought then—I would like to work in science with such a bright man!

Dreams do come true! A conference was held in Sverdlovsk on the application of gears in industry, and Veniamin Iosifovich and Svetlana Yezerzkaya came there to deliver lectures. Here we had a good talk and got to know each other better. That was when I made Veniamin Iosifovich a proposal for cooperation. Later this cooperation grew into a true man’s friendship until the last days. This is my best friend and authority in life. Veniamin Iosifovich was the scientific advisor of my two scientific Ph.D. and D.Sc. works.

Unfortunately, not all plans for joint work were implemented, but I hope that cooperation and research with the Institute of Mechanics of ISTU will be continued, because Veniamin Iosifovich left a good groundwork for the future. I wish all the staff of the Institute of Mechanics successful work in the future, good health, personal happiness, and new scientific achievements.

Mark Moiseevich Kane, D.Sc. in Engineering, Professor, Belarusian National Technical University (Minsk, Belarus):

We met about 1975, when we happened to stay in the same hotel room during a scientific conference in Kharkov. From the first minutes of our meeting I was impressed by his charm, intelligence, various interests and hobbies, cheerfulness, open and friendly character. We became friends and later I always felt his support. The more I got to know him, the more I understood the scale of his personality, his ability to unite people, to formulate and solve large problems. He acted in accordance with a well-known Japanese proverb “think globally, act locally”—he was not only generating ideas, but also showing ways to implement them. In doing so he almost never used administrative resources, acted with soft power, i.e., persuasion. He was highly respected and acknowledged by all his colleagues and friends, and many were simply in love with him. His home was filled with hospitality, warmth, and love.

I will not talk about the professional achievements of Veniamin Iosifovich. His former employees will probably speak about this. A few words about his human qualities. Veniamin Iosifovich had a wonderful gift of always being the soul of any company or meeting, making them warm and charming. At the same time, everyone enjoyed the event, enjoyed each other’s company, and remembered it for a long

time. I remember the “gearing” conferences at ISTU, the get-togethers after each meeting, the joy of communicating with colleagues and friends. These conferences, for which Veniamin Iosifovich spent much effort and money, made it possible to turn ISTU into the International Gearing Center, a ground for information exchange between researchers of many countries. Thanks to Veniamin Iosifovich many of his colleagues became friends and will always cherish the memory of him, a remarkable, bright man, who could still do so much for everyone, but passed away so early and tragically.

Maxim Nikolayevich Karakulov, D.Sc. in Engineering, Professor, Kalashnikov ISTU (Izhevsk, Russia):

My first meeting with Veniamin Iosifovich took place only in 2006, when I was preparing my Ph.D. The first thing that surprised me was his openness to a dialogue with a complete stranger, which I was at that moment. I was also surprised by his ability to instantly grasp the essence of the processes described by dry scientific data, as if he could see the problem from the inside, leading me with his reasoning to its solution. Therefore, my decision to ask him for scientific supervision for my D.Sc. thesis was predetermined. Those years of working together from 2007 to 2012 were and still are the happiest and most fruitful in my working activity. During these years, Veniamin Iosifovich taught me a lot: dedication in promoting my scientific ideas, openness to new approaches, and respect for opinions of my opponents. All this now forms the basis of my activity, and I am sincerely grateful to him for this.

Dmitry Tikhonovich Babichev (1940–2020), Tyumen Industrial University (Tyumen, Russia):

Veniamin Iosifovich Goldfarb was and still is a great man, teacher, outstanding scientist, skillful leader and organizer. He did more than anyone else for the retaining and development of the theory of gearing and practice of gear production in Russia. For me, for almost 50 years he was not only an authoritative expert and a many-sided decent HUMAN, but also a close friend.

Tesker Yefim Iosifovich (1941–2020), Volgograd State University (Volgograd, Russia):

Professor Goldfarb was a very cheerful person. I will tell you about one case that Venya told his colleagues during our meetings. He and I were at a conference in England in 1998. Due to limited funds, Venya and I asked for a double room. The organizers were beyond amazed. Two men in one room. After a rather long pause, we were given a room (Mr. Goldfarb and Mrs. Tesker). These documents were used in reporting documents, and an explanation was required on all stages of the reporting on coming back.

Elena Ivanovna Popova, Ph.D. in Engineering, Associate Professor, Kalashnikov ISTU (Izhevsk, Russia):

Veniamin Iosifovich Goldfarb was the head of the department when I was a student, then my academic supervisor and my direct chief. In my memoirs, Veniamin Goldfarb

easily climbs the steps of the porch of the Building number 4 of ISTU. It seemed that everything was easy for him! Any work, no matter what he undertook, he turned out to be a virtuoso. He always radiated enthusiasm. The main thing I learned from Benjamin Goldfarb was a responsible attitude to his work. He was always busy, but the door of his office was open almost all the time. One could come in with any question. He was distracted from his important matters, ready to help, to advise, and to solve any problem.

Victor Evgenyevich Starzhinskiy, Institute of Mechanics of Metal-Polymer Systems, National Academy of Sciences of Belarus (Gomel, Belarus):

We met in Kharkov at one of the numerous All-Union conferences that were held in the USSR. I don't remember the year. I remember only my feeling of a certain rise when four unknown, in my opinion, ambitious people pretending to leadership—V. I. Goldfarb (Izhevsk), M. M. Kane (Minsk), V. E. Starzhinsky (Gomel), and E. V. Shalobaev (Leningrad), talked to each other ironically and with girls who joined them. This meeting then grew into a benevolent mutually respectful creative relationship. I consider Veniamin Iosifovich as one of my teachers and supporters, along with the principal academician of the BSSR Academy of Sciences, Vladimir Alexeyevich Belyi, my supervisor. He promoted me into the IFToMM Technical Committee for Gearing and Transmissions, which he chaired at the time, and organized my participation in the work of the IFToMM Permanent Commission for Terminology. I felt constant support and, one might say, care. We often met at scientific conferences and meetings of the mentioned Committee in Izhevsk, Sevastopol, Moscow, Bratislava, Paris, Zlatibor. Together with Professor Eduard Leonovich Airapetov we prepared the edition of the four-language dictionary on gears, for which in 1997 the three of us visited the Moscow Center “Science and Technology”, where we made an agreement with the chief scientific editor of the International Engineering Encyclopedia Professor V. Ya. Karshenbaum about the edition of the dictionary. Later this initiative was realized by writing the Chap. 12 “Gearing” within the framework of the IFToMM Permanent Commission for Standardization of Terminology in the Field of Mechanism and Machine Science. Thanks to Veniamin Iosifovich there were no problems with publication of manuscripts in his journal “Gearing and Transmissions”.

I also remember the meetings of the All-Russian Association of Mechanical Transmission Engineers (AMT) in Moscow, Moscow Region and Izhevsk, the successful functioning of which was mainly due to Prof. E. L. Airapetov and Prof. V. I. Goldfarb. The headquarters of the Association was naturally located in Izhevsk.

In the year of the 60th anniversary of Professor Goldfarb in 2001, when the Belarusian delegation headed by the director of the Institute of Reliability and Durability of Machines of the National Academy of Sciences of Belarus came to congratulate him, the greeting poem lines were sounded, inspired by the iconic picture on the cover of his journal “Gearing and Transmissions”—a dwarf (in his place we put Goldfarb) rotating the globe with the help of the gear transmission:

Like Archimedes but not with a lever,
But with one foot, one left.

Sixty years and without a day off,
 With gears and transmissions
 Different kinds, including spiroid ones
 You are not only spinning the globe of the Earth
 But all around thou axis alone,
 Our good friend
 Chairman
 And editor-in-chief
 Son of Iosif
 Veniamin!

I cannot pass by mentioning in this context my unrealized dream, which Veniamin Iosifovich managed to realize—the implementation of his scientific developments into production by organizing a chain “scientific developments-design office-pilot production” with necessary manufacturing equipment and control and measuring instruments. He organized and headed the Institute of Mechanics with the pilot production as a part of ISTU! Bravo!

I am eternally grateful to Providence, which granted me the pleasure of communicating with this outstanding man!

The master has gone. But there is a school. Grateful students are left behind. Life goes on!

Evgeny Lukin, Ph.D. in Engineering, Head of Advanced Engineering Department, “Concern Kalashnikov JSC” (Izhevsk, Russia):

What distinguishes endlessly talented people? Erudition, tremendous energy, keen intellect, speed of decision-making and, of course, humor. Veniamin Iosifovich certainly had it all. His authority was absolute, since it was based on sincere and deep respect. Every day he taught and fed us with his energy. And when I or my friends-colleagues were at a standstill or ran out of energy to work on their theses, they would say: “Go to Goldfarb (Chief) he will help and inspire...”. Separately, I would like to recall our discussions not only on scientific and engineering topics, but also on history and everyday topics, which sometimes lasted more than one hour and involved everyone around us. Wonderful stories connected with Veniamin Iosifovich can be recalled endlessly! There are people, in addition to your parents, who completely shape your world view and world outlook, remaining in your memory and heart for life. For me Veniamin Iosifovich Goldfarb was and remains such a man, a great man and teacher.

I was the last lucky person to have Veniamin Goldfarb as a Ph.D. supervisor.

Olga Veniaminovna Efimova-Goldfarb (Salt Lake City, USA):

Kate (granddaughter of Veniamin Iosifovich) was about 10 years old, she and her grandfather were sitting in his study and grandfather was showing her his awards and medal and giving explanations.

One such badge was “Inventor of the USSR”. Seeing this badge, Katya shouted in delight: “Grandfather, so it was you who invented the USSR!”

Ludwig Slusky, Ph.D., Professor of Information Systems, California State University (Los Angeles, USA):

I cannot think about my uncle Vena (a nickname for Veniamin Goldfarb) without deep sorrow. He will be remembered as a wonderful human being, dear relative, close friend, talented scientist, and gifted business person... Yet, he cannot be reached for sharing, brainstorming ideas and projects, doing them together, just laughing and seeing each other.

In the turbulent 90 s and after, he mastered his professional life seeing no limits but only opportunities. Professor then an academician and later the founder of the Institute of Mechanics and its gearing production branch, a growing business person—he held a steady course and achieved his lifelong success, as the saying goes, old fashion way by earning it. With the recognition of his achievements reaching its heights domestically and internationally, he was awarded as “Honored Scientist of Russia” and Vice-President of IFToMM.

Veniamin’s intelligence and abundance of energy were the magnets attracting to him his friends, colleagues, and first-time acquaintances. Above that, his kind eyes and a charming smile projected that powerful, irresistible sympathy that opened many peoples’ hearts.

His talent’s rarity was in being multifaceted, which does not happen too often among gifted people. There were many ways in life open to him, and on each of them, he would find success. Had he chosen to become a politician, musician, doctor, stage performer ... his talent would become immediately evident, and he would celebrate success in any of them. He was so lucky to have such remarkable gifts from his parents.

Sometimes in our lives, we are fortunate to meet someone who was (or is) the soul of many. Veniamin was such a person. First and foremost, his soul flourished in his loving and devoted family, for which he was the undisputable leader and a shining example. He cherished his two beautiful daughters, who inherited and carry forward many of his remarkable qualities with admiration.

Veniamin’s presence had also notably affected the lives of many others. His numerous followers—students and colleagues—will remember him as a leader and contributor, compassionate friend, or just a great person connected to in life.

But there are a few for whom not having him around is an irreplaceable and painful loss. I am one of them.

Now looking back at those years, I see the steadily rising unique individual with captivating charm and an enormous capacity for science, music, kindness.

Irina Veniaminovna Krikova-Goldfarb (Salt Lake City, USA):

Dad, music, and me

Music is one of the biggest things I associate with my dad, it’s the thing, which has largely helped make me into who I am today....

... for example let me paint you a picture: I am 3, I am sitting on his knees, dad is sitting at the piano and is playing something, and I poke at the keys with the utmost seriousness...

... I also remember how I used to play a game with my dad—play the song “Kuznechik” from any key, I think back then my dad was trying to my musical ear.

The meaning of “playing by ear”, “jazz” and “Gershwin” was fully inherited by me.

For me it was always important to share with my dad any song that I liked. My dad immediately sat at the piano and played his own “jazzy” version. We argued fiercely! Dad never tried to “lay it down softly.” If he didn’t like something, then he talked firmly and harshly. But I always knew—he would support it! He would play it!

And he would tell everyone how amazing Olga and I are! When I became a mom, I understood how important it is for a daughter to hear that from her dad!

My dad loved people and people loved him. He really liked it when we had company over at our house, with much thanks to my supportive mom who would always happily take in guests.

It was always loud in our house when there were meetings and his friends—the “gear heads”—would come over. Oh but the birthday of the mechanical institute—that was exceptionally pleasant! After the ceremonial concert, always people would come over and gather around the table! At a certain moment dad would sit at the piano... and everyone sang! All of his school songs we could recall from memory.

He adored and cherished his students. I think that he worried about them no less than he did about Olga and I. For him they were also his kids!

... returning back to music...

Dad was an improviser on a cosmic level. It was meaningless to explain to him when to step in and how to play a part. Imagine, our performance is starting and suddenly before the start of the first song my dad asks “Irina, what key are we playing in?” Covered in cold sweat I angrily whisper to him the key we’re playing in and what do you think happens next?! He plays everything perfectly!!! Then we look at each other and he lays down a magnificent solo.

Now this is a memory from his famous orchestra at the mechanical institute, when during a practice Mr. Slava Chernoskutov angrily said “what are you playing?!”

Dad: “what, am I not playing in the right key?” Turns out, there was a 16 measure rest for the piano. In all truth the concerts of the mechanical institute were grandiose events. And performances of their legendary orchestra were always sold out. The first time, when dad took me to perform with them, was definitely a feeling of delight and pride! From then it was certain. No matter where we were in life, I knew that performing was something we were going to do! That’s how in Salt Lake City came about a trio, and then the band “Phonograph Blue.” Even when dad was already sick, we still managed to pull off performing in a large city festival.

Dad isn’t here anymore... I want to believe that he’s with mom somewhere there, in the other world... Dad always said, about his parents, that he feels, knows, they are next to him, looking after and celebrating his successes...

Well dad, let’s play? C Major?

Appendix 2: List of Awards and Honorary Titles of Professor Veniamin Iosifovich Goldfarb

- Dedicated Service Award of International Federation for the Pro motion of Mechanism and Machine Science (IFTToMM) (2017)
- Acknowledgment of the Head of Udmurt Republic (2016)
- Order of Honor (2011)
- Laureate of the State Prize of Udmurt Republic in the field of science and technology (2008)
- Acknowledgment of the President of Udmurt Republic (2011)
- Academician Vernadsky Medal, 2nd degree (2001)
- Medal of Academician Kapitsa “To the Author of Scientific Invention” (2001)
- Honorary Worker of Higher Professional Education of Russian Federation (2000)
- Veteran of Labor of the USSR (1988)
- Honored Scientist of Udmurt Republic (1993)
- Honored Scientist of Russian Federation (1997)
- Honorary Professor of Izhevsk State Technical University (1994)
- Inventor of the USSR
- St. George Cross of the Russian Academy of Natural Sciences for merit to economics and science
- Academician of International Academy of Informatization, Russian Academy of Natural Sciences, New York Academy of Sciences
- Honorary member of the Slovak Union of Mechanical Engineers
- Honorary member of the Bulgarian Union of Mechanical Engineers

Appendix 3: Full Bibliography List of Professor Veniamin Goldfarb for the Period of 1964–2019

Monographs in Russian

1. Goldfarb, V.I., Tkachev, A.A.: Design of involute spur gears. New approach. ISTU, Izhevsk (2004).
2. Goldfarb, V.I., Glavatskikh, D.V., Trubachev, E.S., Kuznetsov, A.S., Lukin, E.V., Ivanov, D.E., Puzanov, V. Yu.: Spiroid gears for pipeline valves, Moscow, Veche (2011).
3. Starzhinsky, V.E., Antonyuk, V.E., Goldfarb, V.I., Kane, M.M., Shilko, S.V., Goman, A.M., Reichman, G.N., Soliterman, Yu.L., Shalobaev, E.V.: Reference dictionary on gears: Russian-English-German-French. 5th edn, Gomel, IMMS NASB (2011).
4. Antonyuk, V.E., Basinyuk, V.L., Grazhdanny, V.M., Goldfarb, V.I., Kapelevich, A.L., Mardosevich, E.I., Starzhinsky, V.E., Tkachev, A.A. et al.: Elements of

the device drive. Calculation, design, technology. Ed. by Pleskachevskiy Yu. M. Minsk: Belarusian science (2012).

5. Goldfarb, V.I., Anferov, V.N., Glavatskikh, D.V., Trubachev, E.S.: Spiroid gear-boxes for operation in extreme conditions. Edited by Goldfarb V. I. Izhevsk, ISTU, ISBN 978-5-7526-0650-2 (2014).
6. Georgiev, A.K., Goldfarb, V.I., Rud, L.V.: Russian State Standard GOST 22850–77. Spiroid gears. Terms, definitions and designations (1977).

Monographs in English

1. Goldfarb, V.I., Lunin, S.V., Trubachev, E.S.: Direct digital simulation for gears. Vol. 1, Izhevsk, ISTU (2004).
2. Theory and practice of gearing and transmissions: in honor of professor Faydor L. Litvin. Springer International Publishing AG Switzerland, V. Goldfarb, N. Barmina Eds., Vol. 34, ISBN 978-3-319-19739-5, <https://doi.org/10.1007/978-3-319-19740-1>, <https://www.springer.com/gpbook9783319197395> (2016).
3. Advanced gear engineering. Springer International Publishing AG Switzerland, V. Goldfarb, E. Trubachev, N. Barmina Eds., Vol. 51, ISBN 978-3-319-60398-8, <https://doi.org/10.1007/978-3-319-60399-5>, <https://www.springer.com/gpbook9783319603988> (2018).
4. New approaches to gear design and production. Springer International Publishing AG Switzerland, V. Goldfarb, E. Trubachev, N. Barmina Eds., Vol. 81, ISBN 978-3-030-34944-8, <https://doi.org/10.1007/978-3-030-34945-5>, <https://www.springer.com/gpbook9783030349448> (2020).

Patents and Inventor Certificates

1. Goldfarb, V.I., Georgiev, A.K.: Gear with intersecting axes. Author's certificate №208396 dated 16.10.67.
2. Goldfarb, V.I., Georgiev, A.K.: Ortogonal skew axis gearing. Patent of England №1359550 dated 16.12.71.
3. Goldfarb, V.I., Georgiev, A.K.: Ingranaggio ortogonale con assi incrociati. Patent of Italy №949487 dated 20.01.72.
4. Goldfarb, V.I., Georgiev, A.K.: Transmissio ortogonale an engrénage a axec entrecroises. Patent of France N2166643 dated 23.08.73.
5. Goldfarb, V.I., Georgiev, A.K.: Orthogonal skew-axis gearing. Patent of the USA №3768326 dated 30.10.73.
6. Goldfarb, V.I., Georgiev, A.K.: Orthogonale nonintersecting axis gearing.— Patent of Canada №954340 dated 10.09.74.
7. Goldfarb, V.I., Georgiev, A.K.: Ortogonal skew axis gearing. Planskruvvaxel. Swedish Patent №361346 dated 7.02.74.
8. Goldfarb, V.I., Georgiev, A.K.: Orthogonales Radgetriebe. Patent of Germany №2161666 dated 7.08.75.
9. Goldfarb, V.I., Georgiev, A.K.: Orthogonale nonintersecting axis gearing. Orthogonale skew-axis gearing. Patent of Japan №5125894 dated 3.08.76.

10. Goldfarb, V.I., Nikitin, A.S., Nesmelov, I.P.: Double-stage gearbox. Author's certificate №875133 dated 23.10.81, bul. N39.
11. Goldfarb, V.I., Nesmelov, I.P.: Non-orthogonal gear transmission with intersecting axes. Author's certificate №806935, dated 23.02.81, bul. №7.
12. Goldfarb, V.I., Nesmelov, I.P., Chistyakov, D.E.: Double-stage gearbox. Author's certificate №973973 dated 15.11.82, bul. N42.
13. Goldfarb, V.I., Nesmelov, I.P., Teterin, A.N.: Double-rim gear with intersecting axes. Author's certificate №1059325 dated 7.12.83, bul. N45.
14. Goldfarb, V.I., Solovyov, B.M., Savin, M.N., Gilfanov, R.M.: Device for the precise displacement of the machine-tool working part.—Author's certificate №1199461 dated 23.12.85, bul. N47.
15. Goldfarb, V.I., Chekalkin, G.T., Lagutin, S.A., Borilo, A.M., Galkin, N.I.: Device for control of longitudinal line of gearwheel teeth. Author's certificate №1237896 dated 15.06.86, bul. N22.
16. Goldfarb, V.I., Lagutin, S.A., Kovtushenko, A.A., Verkhovsky, A.V.: Method of cutting the worm cylindrical gearwheel teeth. Author's certificate N1231717 dated 15.01.86.
17. Goldfarb, V.I., Mardanov, I.I.: Non-orthogonal tooth gear with intersecting axes. Author's certificate №1421912 dated 7.09.88, bul. №33.
18. Goldfarb, V.I., Kuniver, A.S., Chekalkin, G.T.: Assembled gear wheel. Author's certificate №1744351 dated 30.06.92, bul. №24.
19. Goldfarb, V.I., Kuniver, A.S.: Cylindrical spiroid hob. Patent of Russia №2095204 dated 10.10.97.
20. Goldfarb, V.I., Osetrov, V.G., Mokretsov, V.N., Kuniver, A.S.: Ball worm gear. Patent of Russia №2092726 dated 10.10.97.
21. Goldfarb, V.I., Plekhanov, F.I., Mokretsov, V.N., Spiridonov, V.M.: Planetary gear. Patent of Russia №2092727 dated 10.10.97.
22. Goldfarb, V.I., Russkikh, A.G., Trubachev, E.S.: Internal gear with intersecting axes. Patent of Russia №2101582 dated 10.01.98.
23. Goldfarb, V.I., Makarov, V.V., Gromov, D.P., Trubachev, E.S., Kuznetsov, A.S., Fedin, S.A., Shanaurin, A.L.: Drive for stop and regulating valves. Patent of Russia N46066 U1 dated 10.06.2006.
24. Anferov, V.N., Goldfarb, V.I., Kovalkov, A.A.: Spiroid gear with rotaprint gear lubrication. Patent of Russia №2306465 C2 dated 20.09.2007.
25. Goldfarb, V.I., Gromov, D.P., Trubachev, E.S., Kuznetsov, A.S., Makarov, V.V., Shanaurin, A.L.: Double-speed manual drive for pipeline valves. Patent of Russia №2343329 C2 dated 10.01.2009.
26. Goldfarb, V.I., Gromov, D.P., Trubachev, E.S., Kuznetsov, A.S., Makarov, V.V.: Double-speed manual drive for pipeline valves. Patent of Russia N2454590 C2 dated 27.06.2012.
27. Plekhanov, F.I., Goldfarb, V.I.: Planetary gear. Patent of Russia N2460916 C1 dated 10.09.2012.

Ph.D. and Dr. Sc. theses made under the scientific supervision of Professor Veniamin Goldfarb**D.Sc. in Engineering**

1. Kuniver, A.S.: Theoretical fundamental of the meshing synthesis for modified spiroid cylindrical gears (2001).
2. Anferov, V.N.: Development of hoisting-and-transport machine drives based on spiroid gears (2002).
3. Malina, O.V.: Theory and practice of automation of the structural synthesis of the objects and processes using the characterization analysis methods (2002).
4. Trubachev, E.S.: Fundamental of analysis and synthesis of the real spiroid gears (2004).
5. Karakulov, M.N.: Scientific fundamentals of plunger gear design (2012).

Ph.D. in Engineering

1. Anferov, V.N.: Development of a method for calculating the wear lifetime of cylindrical spiroid gears (1988).
2. Kulemin, V.Yu.: Development and study of dynamics of the test bench for rotating rotors with large disbalance (1994).
3. Isakova, E.V.: Development and research of the spiroid gear with ideal helical parameter of the worm (1995).
4. Malina, O.V.: Development of software and mathematical support for computer-aided design of mechanical engineering products (by example of the spiroid gearbox) (1995).
5. Glavatskikh, D.V.: Computer-aided modeling of generating helical surfaces of mechanical engineering products (1997).
6. Abramov, A.I.: Theoretical and experimental research of kinematic accuracy and vibration activity of spiroid gears (1996).
7. Russkikh, A.G.: Computer-aided synthesis of gear schemes with intersecting axes (1997).
8. Trubachev, E.S.: Research of the parameters space for non-orthogonal spiroid gears (1999).
9. Plekhanov, D.F.: Research of geometry and main quality parameters of the unconventional gear with involute-epitrochoid meshing (1999).
10. Vozniuk, R.V.: Instrumental system of modeling the enveloping process (1999).
11. Koshkin, D.V.: Error influence research and geometrical modeling of localized contact in the spiroid gear (1999).
12. Tkachev, A.A.: Development of the dialogue design system for involute cylindrical gears (1999).
13. Lunin, S.V.: Development and research of the computer-aided system of solid-state modeling of gears (2000).
14. Barmina, N.A.: Structural and parametric synthesis of double-stage gearboxes with spiroid and cylindrical gears (2002).

15. Popova, E.I.: Development of tools and technology of generating the metal polymeric spiroid gearwheels (2004).
16. Lukin, E.V.: Theoretical fundamentals of designing low-speed heavy-loaded spiroid gearboxes (2013).

Other publications of Professor Veniamin Goldfarb for the period of 1964–2019

1. Goldfarb, V., Trubachev, E., Barmina, N.: Innovations in design and production of spiroid gears in the XXI century. In: MATEC Web of Conferences 287, 01002, <https://doi.org/10.1051/mateconf201928701002> (2019).
2. Goldfarb, V., Trubachev, E., Pushkareva, T., Savelyeva, T.: Comparative investigation of worm and spiroid gears with cylindrical worms. In: Uhl T. (eds) Advances in Mechanism and Machine Science. IFToMM WC 2019. Mechanisms and Machine Science, vol 73, pp. 925–935, Springer, Cham, <https://doi.org/10.1007/978-3-030-20131-9-92> (2019).
3. Goldfarb, V.I., Trubachev, E.S., Bogdanov, K.V. et al.: Prospects of manufacturing spiroid gears with small gear ratios. In: Forsch Ingenieurwes 83: 781, <https://doi.org/10.1007/s10010-019-00343-8> (2019).
4. Plekhanov, F.I., Goldfarb, V.I.: Geometry and strength index of internal gearing of planetary transmission wheels cut with a non standard tool. In: Journal of machinery manufacture and reliability, v. 48, N5, pp. 379–384 (2019).
5. Goldfarb, V., Krylov, E., Perminova, O., Barmina, N., Vasiliev, L.: Aspects of teaching “Advanced gears” for future mechanical engineers within “Bachelor of Sciences” program in technical universities. In: Advanced Gear Engineering. Mechanisms and Machine Science 51, pp. 271–288. Springer International Publishing AG Switzerland, ISBN: 978-3-319-60398-8, <https://doi.org/10.1007/978-3-319-60399-5> (2018).
6. Plekhanov, F., Goldfarb, V., Vychuzhanina, E.: Load distribution in meshing of planetary gearwheels and its influence on the technical and economic performance of the mechanism. In: Advanced Gear Engineering. Mechanisms and Machine Science 51, pp. 117–138. Springer International Publishing AG Switzerland, ISBN: 978-3-319-60398-8, <https://doi.org/10.1007/978-3-319-60399-5> (2018).
7. Goldfarb, V.I.: Innovative way of development of producing spiroid gears and gearboxes at a higher education institution. In: Innovations, N2 (220), pp. 6–9 (2017).
8. Goldfarb, V.I., Trubachev, E.S., Kharanzhevsky, E.V., Ipatov, A.G., Bogdanov, K.V., Matveeva, Yu. Yu.: New technology for laser modification of flanks of low-speed heavy-loaded sliding supports. In: Bulletin of Kalashnikov ISTU, N2(20), pp. 112–117. ISTU Publishing House, Izhevsk (2017).
9. Goldfarb, V.I.: Innovative way of development of producing spiroid gears and gearboxes. In: Intelligent systems in manufacturing, vol. 15, N1, pp. 9–12. ISTU Publishing House, Izhevsk (2017).

10. Starzhinsky, V.E., Goldfarb, V.I., Shilko, S.V., Shalobaev, E.V., Tesker, E.I.: Terminology development in the field of gears and transmissions. Part 1. Development of terminology in the field of gears and transmissions by the Permanent Commission of IFToMM “Standardization of TMM terminology”. In: Intelligent systems in manufacturing, vol. 15, N1, pp. 30–36. ISTU Publishing House, Izhevsk (2017).
11. Starzhinsky, V.E., Goldfarb, V.I., Shilko, S.V., Shalobaev, E.V., Tesker, E.I.: Terminology development in the field of gears and transmissions. Part 2. Compilation of the dictionary and reference book for gears. In: Intelligent systems in manufacturing, vol. 15, N2, pp. 60–66. ISTU Publishing House, Izhevsk (2017).
12. Starzhinsky, V.E., Goldfarb, V.I., Shilko, S.V., Shalobaev, E.V., Tesker, E.I.: Terminology development in the field of gears and transmissions. Part 3. Identification of concepts by types of gearwheel damages. In: Intelligent systems in manufacturing, vol. 15, N3, pp. 51–61. ISTU Publishing House, Izhevsk (2017).
13. Starzhinsky, V.E., Shalobaev, E.V., Kane, M.M., Goldfarb, V.I.: Activities of Russian-speaking scientists in development of MMS terminology, mechanisms and machine science. In: Kluwer Academic Publishers, vol. 46, pp. 209–216, <https://doi.org/10.1007/978-3-319-45450-4-21> (2017).
14. Goldfarb, V., Malina, O., Trubachev, E.: New concept of the process of designing gearboxes and gear systems. In: Theory and Practice of Gearing and Transmissions. Mechanisms and Machine Science, vol. 34, pp. 405–424. Springer, Springer International Publishing AG Switzerland, ISBN 978-3-319-19740-1 (2016).
15. Goldfarb, V.: Development of the theory and practice of spiroid gears. In: Theory and Practice of Gearing and Transmissions. Mechanisms and Machine Science, vol. 34, pp. 55–66. Springer, Springer International Publishing AG Switzerland, ISBN 978-3-319-19740-1 (2016).
16. Plekhanov, F., Goldfarb, V.: Rational Designs of Planetary Transmissions, Geometry of Gearing and Strength Parameters. In: Theory and Practice of Gearing and Transmissions. Mechanisms and Machine Science, vol. 34, pp. 285–300. Springer, Springer International Publishing AG Switzerland, ISBN 978-3-319-19740-1 (2016).
17. Goldfarb, V.I., Krylov, E.G., Serova, T.S.: IFToMM contribution to attracting youth to MMS development and promotion. In: Mechanism and Machine Theory, pp. iii–vii. Elsevier Science Publishing Company Inc., <https://doi.org/10.1016/j.mechmachtheory.2016.02.008> (2016).
18. Goldfarb, V.I., Trubachev, E.S., Kuznetsov, A.S. Comparative analysis of generations of the spiroid gearboxes for pipeline valves drives. In: Armaturstroenie, N1 (94), pp. 80–87, ISSN: 2411–1155 (2015).
19. Goldfarb, V.I., Trubachev, E.S., Kuznetsov, A.S.: Possibilities and problems of import substitution at the market of pipeline valve gearboxes. In: Armaturstroenie, N2 (95), pp. 80–87, ISSN: 2411–1155 (2015).

20. Goldfarb, V.I., Reshetnikov, S.M., Trubachev, E.S., Kharanzhevsky, E.V., Kuznetsov, A.S., Kornilov, A.A., Petrova, O.V., Kurlykova, D.Yu.: Experimental research of gearwheel sliding supports materials and lubricants in low-speed heavy-loaded spiroid gearboxes. In: *Vestnik mashinostroeniya*, N5, pp. 35–39. Innovative Mechanical Engineering Publishing House, Moscow, ISSN: 0042-6333 (2015).
21. Goldfarb, V.I.: Innovative development of theory and practice of spiroid gears and gearboxes. In: *Innovations*, N4 (198), pp. 115–120, ISSN: 2071-3010 (2015).
22. Goldfarb, V.I., Reshetnikov, S.M., Trubachev, E.S., Kuznetsov, A.S., Kornilov, A.A.: Slip bearings and lubricants in low-speed heavy-duty spiroid gears. In: *Russian Engineering Research*, vol. 35, 8, pp. 584–588. Allerton Press, Inc., New York, ISSN: 1068-798X, eISSN: 1934-8088, <https://doi.org/10.3103/S1068798X15080055> (2015).
23. Goldfarb, V.I., Trubachev, E.S., Kuznetsov, A.S., Kornilov, A.A.: Experimental studies of the low-speed heavy-loaded spiroid gearboxes. In: *Intelligent systems in manufacturing*, N1, pp. 31–41. ISTU Publishing House, Izhevsk (2014).
24. Goldfarb, V.I.: Development of the theory and practice of spiroid gears. In: *Proceedings of the International Symposium “Theory and Practice of Gears”*, pp. 31–41. ISTU Publishing House, Izhevsk (2014).
25. Goldfarb, V.I., Anferov, V.N., Tkachuk, A.P., Sergeeva, I.V.: Physical modelling of spiroid gearing for estimation of antifricition properties of lubricating oils. In: *Proceedings of the International Symposium “Theory and Practice of Gears”*, pp. 258–262. ISTU Publishing House, Izhevsk (2014).
26. Plekhanov, F.I., Goldfarb, V.I.: Development and research of high-loaded planetary gears with roller mechanism for motion removal from satellites. In: *Proceedings of the International Symposium “Theory and Practice of Gears”*, pp. 330–337. ISTU Publishing House, Izhevsk (2014).
27. Starzhinsky, V.E., Goldfarb, V.I., Algin, V.B., Shalobaev, E.V., Kane, M.M.: Participation of scientists from USSR and CIS countries in IFToMM activities. In: *Theory of Mechanisms and Machines*, vol. 12, N2 (24), pp. 81–102. Springer (2014).
28. Goldfarb, V.I.: Scientific school of Institute of mechanics in the field of development of the theory and practice of spiroid gears. In: *Intelligent systems in manufacturing*, N2 (24), pp. 31–35. ISTU Publishing House, Izhevsk (2014).
29. Goldfarb, V.I., Poskrebyshev, S.A., Tkachev, A.A.: Enhancement of strength calculation of gears based on the concept of a dynamic blocking contour. In: *Intelligent systems in manufacturing*, N1, pp. 69–73. ISTU Publishing House, Izhevsk (2013).
30. Goldfarb, V.I.: Spiroid gears and their application. In: *International Journal “Planetary Science and Technology”*, vol. 5, 1, pp. 101–108. Global Sciencetech (2013).
31. Goldfarb, V., Krylov, E., Elenski, A.: The First Student International Olimpiad on Mechanism and Machine Science—The Challenge in MMS Education. In:

- Journal of Mechanical Engineering and Automation, Vol. 3, N3, pp. 152–158 (2013).
32. Goldfarb, V.I., Trubachev, E.S., Kuznetsov, A.S., Kornilov, A.A., Pushkarev, D.S.: Experimental investigations of low-speed heavy-loaded spiroid gearboxes. In: Proc. International Conference on Gears, Munich, Germany (2013).
 33. Goldfarb, V.I.: Report of the annual activity of the Vice-President and Chair of the Permanent Commission for Communications, Publications, and Archiving (PC CPA) of the International Federation of the Theory of Mechanism and Machines (IFTToMM) for the period. Hsin-Chu, Taiwan (2013).
 34. Goldfarb, V.I., Barmina, N.A.: Internet-forum of young scientists as a means of development of general cultural and foreign-language professional competences for MMS students. In: Bulletin of Kalashnikov ISTU, N4, pp. 188–191. ISTU Publishing House, Izhevsk (2013).
 35. Goldfarb, V., Anferov, V.: Spiroid gears with rotaprint lubrication of engagement. In: Proceedings of the 7th International Symposium “Machine and Industrial Design in Mechanical Engineering” KOD 2012, 24–26 May, 2012, Balatonfüred, Hungary, pp. 17–20 (2012).
 36. Tkachev, A., Goldfarb, V., Terekhov, A., Poskrebyshev, S.: Computer-Aided Design System “Contour” for Involute Spur and Helical Gears. In: Proceedings of the 7th International Symposium “Machine and Industrial Design in Mechanical Engineering” KOD 2012, 24–26 May, 2012, Balatonfüred, Hungary, pp. 321–326 (2012).
 37. Koroleva, E.V., Puzanov, Yu.V., Goldfarb, V.I.: Pre-processing of initial data for formation of the competence model of the curriculum. In: Technical universities: integration with European and world education systems: materials of V International conf., V3, vol. 1, pp. 407–410. ISTU Publishing House, Izhevsk (2012).
 38. Goldfarb, V., Krylov, E., Elensky, A.: The First Student International Olympiad on Mechanism and Machine Science—the challenge in MMS education. In: Proceedings of the 2nd IFTToMM Asian Conference on Mechanism and Machine Science, November 7–10, 2012, Tokyo, Japan (2012).
 39. Goldfarb, V.: Spiroidal gears and applications. In: International Journal of Terraspace Science and Engineering, vol. 5, iss. 2, November, 2012, pp. 93–100. Global Scientech (2012).
 40. Goldfarb, V I., Trubachev, E.S., Glavatskikh, D.V., Kuznetsov, A.S.: Spiroid gearboxes for actuators of pipeline valves. In: Proceedings of the 7th International Scientific Conference “Research and development of mechanical elements and systems”, Zlatibor, Serbia, pp. VII-XII (2011).
 41. Goldfarb, V.I., Tkachev, A.A.: Optimization approach to computer-aided design of spur and helical gears. In: Proceedings of the 13th World Congress in Mechanism and Machine Science, Guanajuato, México (2011).

42. Goldfarb, V.I.: Theory and practice of gearing in machines and mechanisms science. In: *Technology Developments: the Role of Mechanisms and Machine Science and IFToMM*, pp. 133–139. Springer (2011).
43. Goldfarb, V.I., Glavatskikh, D.V., Trubachev, E.S., Kuznetsov, A.S.: State of design and production of spiroid gearboxes for pipeline valves. In: *Proceedings of the International Conference on Power Transmissions*, Xi'an, China, October 25–29 (2011).
44. Goldfarb, V.I., Anferov, V.N., Sergeeva, I.V.: Variants of designs of spiroid gearboxes with rotaprint lubrication of gearing. In: *Intelligent systems in manufacturing*, N2 (18), pp. 100–107. ISTU Publishing House, Izhevsk (2011).
45. Goldfarb, V.I.: Theory and practice of gears in the theory of machines and mechanisms. In: *Intelligent systems in manufacturing*, N2 (18), pp. 95–100. ISTU Publishing House, Izhevsk (2011).
46. Goldfarb, V.I., Trubachev, E.S., Kuznetsov, A.S.: Prospects and practice of application of spiroid gears in pipeline valve drives. In: *Izvestia TulSU, Technical sciences*, TulSU Publishing House, Tula (2011).
47. Makarov, V.V., Goldfarb, V.I., Glavatskikh, D.V.: Innovative prospects of development of pipeline valve and drive production. In: *Proceedings of the Conference "Innovative Development of CIS Countries"*, pp. 372–377. Saratov (2010).
48. Goldfarb, V.I., Trubachev, E.S.: What to Do and What Not to Do when Choosing and Designing Gearboxes for pipeline valves. In: *Armaturostroenie*, No 1, pp. 52–57 (2010).
49. Goldfarb, V.I., Trubachev, E.S., Glavatskikh, D.V.: Spiroid gears with small gear ratios. Some problems of design and production. In: *Proceedings of the International Conference on Gears*, Munich, Germany, pp. 429–442 (2010).
50. Goldfarb, V.I.: To the problem of classifying of gearing. In: *Proceedings of the Scientific Conference "Terminology for the Mechanism and Machine Science"*, pp. 69–78, Gomel, Belarus (2010).
51. Goldfarb, V.I.: Complicated science about "inevitable evil". In: *Armaturostroenie*, N3, pp. 44–47 (2010).
52. Goldfarb, V.I., Karakulov, M.N.: Design of Plunger Gears. In: *Vestnik Mashinostroeniya*, N9, pp. 8–12 (2010).
53. Goldfarb, V.I., Karakulov, M.N.: Design of piston transmission. In: *Russian Engineering Research*, vol. 30, N9, pp. 856–861 (2010).
54. Goldfarb, V.I., Trubachev, E.S., Kuznetsov, A.S.: Load capacity of the heavily-loaded low-speed spiroid gears. In: *Proceedings of the International Conference on Power Transmissions and Transmissions of the Japanese Community of Mechanical Engineers*, Sendai, Japan, pp. 380–385 (2009).
55. Tkachev, A., Goldfarb, V.: Development of the concept of optimized design of cylindrical gears. In: *Proceedings of the International Conference on power transmissions and transmissions of the Japanese Community of Mechanical Engineers*, Sendai, Japan, pp. 6–9 (2009).

56. Goldfarb, V.I., Trubachev, E.S., Puzanov, V.Yu.: New possibilities of non-orthogonal worm gears. In: Proceedings of the 3rd International Conference “Power Transmissions-09”, Chalkidiki, Greece, pp. 139–144 (2009).
57. Tkachev, A.A., Goldfarb, V.I.: Concept of optimization design of cylindrical gears. In: Proceedings of the 3rd International Conference “Power Transmissions-09”, Chalkidiki, Greece (2009).
58. Goldfarb, V.I., Yakimovich, B.A., Glavatskikh, D.V.: Some tendencies of development of the theory and practice of gears. In: Proceedings of the International Conference “General Machine Design”, Bulgaria (2009).
59. Goldfarb, V.I., Glavatskikh, D.V.: Innovation activity of Institute of Mechanics of ISTU. In: Proceedings of the conf. “Innovative way of development of economy: strategies and prospects”, Saratov, pp. 143–152 (2009).
60. Goldfarb, V.I., Trubachev, E.S., Kuznetsov, A.S.: To selection of a gearbox for the electric drive of pipeline valves. In: *Armaturostroenie*, N2, p. 25 (2009).
61. Goldfarb, V.I., Trubachev, E.S., Kuznetsov, A.S.: To selection of the gearbox module of electric drives for pipeline valves. In: *Armaturostroenie*, N2, p. 41 (2009).
62. Goldfarb, V.I., Kapelevich, A.L., Tkachev, A.A.: An advanced approach to optimal gear design. In: *Gear Solutions*, August 6 (2008).
63. Goldfarb, V.I., Makarov, V.V., Trubachev, E.S., Kuznetsov, A.S., Maratkanov, A.M.: Features of design of the low-speed spiroid gearboxes for pipeline valve drives. In: Works of the All-Russian Scientific and Technical Conference “Machine science and machine parts”, Moscow State Technical University named after Bauman, pp. 162–165 (2008).
64. Goldfarb, V.I., Tkachev, A.A.: New possibilities of computer-aided design of involute cylindrical gears by means of the blocking contours. In: *Machine science and machine parts*, Moscow State Technical University named after Bauman, pp. 136–138 (2008).
65. Goldfarb, V.I., Trubachev, E.S., Kuniver, A.S., Kuznetsov, A.S.: Reliability and durability tests of special spiroid gearboxes. In: Works of the All-Russian Scientific and Technical Conference “Machine science and machine parts”, Moscow State Technical University named after Bauman, pp. 158–159 (2008).
66. Goldfarb, V.I.: State of the gear industry. In: *Armaturostroenie*, N5, pp. 66–69 (2008).
67. Goldfarb, V.I., Trubachev, E.S.: Development of high-efficiency gearboxes for pipeline valve drives. In: Proceedings of the 1st International Scientific and Technical Conference “Pipeline valves of the 21st century: science, engineering, innovative technologies”, Kurgan, pp. 68–76 (2008).
68. Goldfarb, V.I.: Some aspects of the modern theory and practice of the gears. In: Proceedings of scientific and technical conference “Theory and practice of gears and gear gearbox construction”, pp. 8–15. ISTU Publishing House, Izhevsk (2008).

69. Goldfarb, V.I., Glavatskikh, D.V., Gromov, D.P., Makarov, V.V., Maratkanov, A.M., Trubachev, E.S.: Mastering of production of spiroid gearboxes for pipeline valve drives. In: Proceedings of scientific and technical conference "Theory and practice of gears and gear gearbox construction", pp. 227–232. ISTU Publishing House, Izhevsk (2008).
70. Goldfarb, V.I., Trubachev, E.S., Lunin, S.V.: System of hob unification for cutting of the worm-type gearwheels. In: Proceedings of the International Conference IDETC' 07 of the American Society of Mechanical Engineers, Las Vegas, USA, NV, pp. 807–811 (2008).
71. Goldfarb, V.I., Trubachev, E.S.: Algorithm of designing worm type gears with the localized contact formed by the unified tool, In: Information mathematics, N1, pp. 157–167 (2007).
72. Goldfarb, V.I., Tkachev, A.A.: Concept of optimal computer-aided design of involute cylindrical gears. In: Informational mathematics, N1, pp. 168–173 (2007).
73. Goldfarb, V.I., Makarov, V.V., Trubachev, E.S., Kuznetsov, A.S.: New progressive applications of spiroid gears. In: Proceedings of the 12th World Congress on TMM, Bezanson, France (2007).
74. Goldfarb, V.I., Pichugin, I.K.: 50th anniversary of the "Robotized production technology" department. In: Bulletin of Kalashnikov ISTU, N1, pp. 131–133. ISTU Publishing House, Izhevsk (2007).
75. Goldfarb, V.I., Puzanov, Y.V., Isakova, N.V., Koroleva, E.V., Popova, Z.E.: Enhancement of educational process at "Technology of robotized production" department due to transition to the two-level system of education. In: Bulletin of Kalashnikov ISTU, N1, pp. 133–134. ISTU Publishing House, Izhevsk (2007).
76. Goldfarb, V.I., Trubachev, E.S., Kuznetsov, A.S.: Load distribution in statically loaded spiroid gear. In: Proceedings of the International Conference "Power Transmissions 06", Novi Sad, Serbia, pp. 369–376 (2006).
77. Popova, E.I., Goldfarb, V.I.: Investigation of spiroid gears with plastic gearwheels. In: Proceedings of the International Conference "Power Transmissions 06", Novi Sad, Serbia, pp. 365–368 (2006).
78. Goldfarb, V.I.: What do we know about spiroid gears. In: Proceedings of the International Conference on Mechanical Transmissions, China, Vol. 1, pp. 19–26. Science Press (2006).
79. Goldfarb, V.I., Trubachev, E.S., Kuznetsov, A.S., Makarov, V.V.: Development and manufacturing of spiroid gear drives for pipeline valves. In: Proceedings of the International Conference on Mechanical Transmissions, China, vol. 1, pp. 220–223. Science Press (2006).
80. Goldfarb, V.I., Tkachev, A.A.: Forecasting design of spur and helical gears. In: Proceedings of the International Conference on Mechanical Transmissions, China, vol. 1, pp. 245–249. Science Press (2006).
81. Goldfarb, V.I., Pichugin, I.K.: 50th anniversary of the "Robotized production technology" department. In: Proceedings "Modern technologies", pp. 3–6. ISTU Publishing House, Izhevsk (2006).

82. Goldfarb, V.I., Puzanov, Yu.V., Isakova, N.V., Koroleva, E.V., Popova, Z.E.: Enhancement of educational process at “Technology of robotized production” department due to transition to the two-level system of education. In: Proceedings “Modern technologies”, pp. 7–9. ISTU Publishing House, Izhevsk (2006).
83. Goldfarb, V.I., Trubachev, E.S., Makarov, V.V.: A new generation of drives for pipeline valves. In: Valve World, vol. 11, iss. 6, pp. 32–36 (2006).
84. Goldfarb, V.I., Trubachev, E.S., Popova, E.I.: Algorithms of designing the tool for generating spiroid plastic gearwhels teeth. In: Journal “Information mathematics”, Moscow, N1, pp. 106–113 (2005).
85. Goldfarb, V.I., Makarov, V.V., Maslov, V.M.: Prospects of development of drive technology for pipeline valves. In: *Armaturstroenie*”, N5, pp. 43–45 (2005).
86. Goldfarb, V.I., Makarov, V. V.: Enhancement of drive technology for pipeline valves. In: Journal “Technologies of Fuel and Energy Complex”, N4, pp. 42–44. Moscow (2005).
87. Goldfarb, V.I., Tkachev, A.A.: Non-traditional approach to design of involute cylindrical gears with extreme properties. In: Proceedings of the International Conference on Gears, Munich, Germany, pp. 1749–1753 (2005).
88. Goldfarb, V.I., Trubachev, E.S., Savelieva, T.V.: Unification of the hobs in spiroid gears. VDI Berichte, Unification of spiroid gears. In: Proceedings of the International Conference on Transmissions, Munich, Germany, pp. 1755–1759 (2005).
89. Goldfarb, V.I.: Progressive gears. In: *Innovations*, N6 (83), pp. 89–91 (2005).
90. Goldfarb, V.I., Tkachev, A.A.: New approach to computerized design of spur and helical gears. In: *Gear Technology*, vol. 22, N1, pp. 26–32 (2005).
91. Goldfarb, V.I., Lunin, S.V.: Modeling in Gear Design. In: The 11th World Congress in Mechanism and Machine Science, Tianjin, China, pp. 723–727 (2004).
92. Goldfarb, V.I., Trubachev, E.S.: Manufacturing Synthesis of Spiroid Gearing. In: The 11th World Congress in Mechanism and Machine Science, Tianjin, China, pp. 901–905 (2004).
93. Herzenstein, S.Ya., Goldfarb, V.I., Suvorov, A.V.: 40th anniversary of the scientific school on the theory of characterization analysis. In: Journal “Informational Mathematics”, Moscow, N1, pp. 4–6 (2004).
94. Goldfarb, V.I., Nekrasov, V.I., Shirmanova, L.A.: Tendencies of development of gear production and consumption market. In: Proceedings of scientific and technical conference with international participation “Theory and practice of gears”, pp. 5–9. ISTU Publishing House, Izhevsk (2004).
95. Goldfarb, V.I., Lunin, S.V., Trubachev, E.S.: New approach to development of universal gears CAD systems. In: Proceedings of scientific and technical conference with international participation “Theory and practice of gears”, pp. 269–277. ISTU Publishing House, Izhevsk (2004).

96. Goldfarb, V.I., Lunin, S.V., Trubachev, E.S.: Advanced computer modeling technique in gear engineering. In: ASME IDETC-2003, 9th International Conference "Power Transmissions and Gearing", Chicago, USA (2003).
97. Goldfarb, V.I., Tkachev, A.A.: New approach to computerized design of spur and helical gears. In: ASME IDETC-2003, 9th International Conference "Power Transmissions and Gearing", Chicago, USA (2003).
98. Goldfarb, V.I., Lunin, S.V., Trubachev, E.S.: Modern approach to development of means of computer-aided modeling of gears. In: Journal "Information mathematics", N1, pp. 103–109 (2003).
99. Goldfarb, V.I., Kuniver, A.S.: Features of design and profiling of a mill for modification of teeth of spiroid wheels. In: Journal "Mashinostroitel", N3, pp. 29–31 (2003).
100. Goldfarb, V.I., Barmina, N.A.: Structural and parametric synthesis of the combined gearboxes with spiroid and cylindrical. In: Proceedings "Progressive gears", Novouralsk, pp. 99–109 (2003).
101. Goldfarb, V.I., Popova, E.I.: Research of spiroid gears with plastic gear-wheels. In: Proceedings "Progressive gear drives", Novouralsk, pp. 35–39 (2003).
102. Goldfarb, V.I.: Activity of International and National Organizations in the Field of Gears and Gearbox Engineering. In: Proceedings of the All-Russian Scientific and Practical Conference with International Participation "Gearbox Engineering in Russia: state, problems, prospects", St. Petersburg, pp. 15–18 (2002).
103. Goldfarb, V.I., Spiridonov, V.M., Koshkin, D.V., Barmina, N.A.: Creation of perspective models of the combined spiroid gearboxes and motor-gearboxes. In: Proceedings of the All-Russian scientifically-practical conference with international participation "Gearbox Engineering in Russia: state, problems, prospects", St. Petersburg, pp. 31–32 (2002).
104. Goldfarb, V.I., Trubachev, E.S.: Model of spiroid gearing under the action of errors. In: Proceedings of the International Conference on Gears, Munich, Germany, vol. 1, pp. 197–209 (2002).
105. Goldfarb, V.I., Trubachev, E.S.: Development and application of computer-aided design and tooth contact analysis of spiral-type gears with cylindrical worms. In: Technical Paper for AGMA FTM, USA, pp. 17–21 (2002).
106. Goldfarb, V.I.: Some exercises with equations of gearing. In: Gearing and Transmissions, N1, pp. 14–20 (2001).
107. Goldfarb, V.I.: Development, research, production of spiroid gears—the main scientific direction of the Institute of mechanics of ISTU. In: Proceedings of reports of the international scientific seminar "Modern information technologies. Problems of gear research, design and production", ISTU Publishing House, Izhevsk (2001).
108. Goldfarb, V.I., Spiridonov, V.M., Golubkov, N.S.: Development of heavily-loaded low-speed spiroid gearmotors. In: Proceedings of reports of the international scientific seminar "Modern information technologies. Problems of

- gear research, design and production”, pp. 50–55. ISTU Publishing House, Izhevsk (2001).
109. Trubachev, E.S., Goldfarb, V.I.: About the meshing axes in a spiroid gear. Meshing space. In: Proceedings of reports of the scientific seminar of the educational and scientific center of gears and gearbox engineering, pp. 71–76. ISTU Publishing House, Izhevsk-Elektrostal (2001).
 110. Goldfarb, V.I., Trubachev, E.S.: Forecasting of the contact quality in a spiroid gear at the action of errors. In: Materials of the international conference “Reliability of machines and technical systems”, vol. 2, Minsk, p. 68 (2001).
 111. Goldfarb, V.I., Trubachev, E.S.: Spiroid wheel tooth hobbing process Improvement. In: Proceedings of the International Conference on Mechanical Transmissions, Chongqiung, China, pp. 96–98 (2001).
 112. Goldfarb, V.I.: Development of research and production of progressive gears. In: Bulletin of Kalashnikov ISTU, pp. 4–9. ISTU Publishing House, Izhevsk (2001).
 113. Goldfarb, V.I.: What kind of skew-axis gearing do you prefer. In: Proceedings of the International Conference on Mechanical Transmissions, Chongqing, pp. 612–616 (2001).
 114. Goldfarb, V.I.: The word about the scientist. To the 65th anniversary of Professor E. L. Airapetov. In: Proceedings “Problems of improving transmissions by hooking”, Izhevsk-Moscow, pp. 7–18 (2000).
 115. Goldfarb, V.I., Airapetov, E.L.: Creation of the educational-scientific centre of gears and gearbox engineering. In: Proceedings “Problems of improvement of gears by gearing”, Izhevsk-Moscow, pp. 43–48 (2000).
 116. Goldfarb, V.I., Plekhanov, F.I., Plekhanov, D.F.: Geometry of internal quasi-involuted gearing of the satellite of coaxial planetary gear. In: Proceedings “Problems of Improvement of Gears by Meshing”, Izhevsk-Moscow, pp. 72–81 (2000).
 117. Goldfarb, V.I., Anferov, V. N.: Results of investigation of friction coefficients in meshing of a cylindrical spiroid gear. In: Proceedings “Problems of improvement of gears by gearing”, Izhevsk-Moscow, pp. 144–148 (2000).
 118. Goldfarb, V. I.: Design and application of spiroid gears, gearboxes and gear-motors. In: Proceedings of the 5th International Conference “Dynamics of Machine Aggregates”, Gabcikovo, Slovakia, pp. 3–9 (2000).
 119. Goldfarb, V.I., Airapetov, E.L., Mudrik, J., Kral, S., Kratochvil, T.: Organization of the international scientific educational center “Gears and transmissions”. In: Proceedings of the 5th International Conference “Dynamics of Machine Aggregates”, Gabcikovo, Slovakia, pp. 73–79 (2000).
 120. Goldfarb, V.I.: Directions in gear research—contribution and function of IFToMM technical committee on gearing. In: Proceedings of the International Conference on Gearing, Transmissions and Mechanical Systems, Nottingham, London, pp. 3–9 (2000).

121. Goldfarb, V.I., Kuniver, A.S., Koshkin, D.V.: Investigation of spiroid gear tooth tangency under action of errors. In: Proceedings of the International Conference on Gearing, Transmissions and Mechanical Systems, Nottingham, London, pp. 65–73 (2000).
122. Goldfarb, V.I., Voznyuk, R.V.: Computerized Simulation of Enveloping Process for Different Application. In: Proceedings of 26th Design Automation Conference, ASME Design Engineering Technical Conference, Baltimore, USA (2000).
123. Goldfarb, V.I., Trubatchev, Ye.S.: Predesign Investigations of Non-Orthogonal Spiroid Gears. In: Proceedings of 8th Power Transmissions and Gearing Conference, ASME Design Engineering Technical Conference, Baltimore, USA (2000).
124. Goldfarb, V.I., Spiridonov, V.M., Golubkov, N.S.: Development of High-Loaded, Low-Speed Spiroid Gearboxes. In: Proceedings of 8th Power Transmissions and Gearing Conference, ASME Design Engineering Technical Conference, Baltimore, USA (2000).
125. Goldfarb, V.I., Budenkov, G.A., Nedsvetskaya, O.V.: Development of the acoustic emission wave radiation model for gear damage diagnostics. In: Proceedings of the 4th World Congress on Gearing and Power Transmissions, vol. 3, pp. 2337–2345. Paris (1999).
126. Goldfarb, V.I., Trubatchev, Ye.S., Kuniver, A.S., Monakov, A.V.: Computer-aided design and some results of spiroid gears and gearboxes investigation. In: Proceedings of the 4th World Congress on Gearing and Power Transmissions, vol. 1, Paris (1999).
127. Goldfarb, V.I., Malina, O.V.: Skew axis gearing scheme classifier building technique. In: Proceedings of the 10th World Congress on TMM, vol. 6, Oulu, Finland, June 20–24, pp. 2227–2232 (1999).
128. Goldfarb, V.I., Tkachev, A.A.: Some theoretical and practical aspects of developing CAD-system for spur and helical gears design. In: Proceedings of the 10th World Congress on TMM, vol. 6, Oulu, Finland, June 20–24, pp. 2276–2280 (1999).
129. Goldfarb, V.I., Airapetov, E.L., Novoselov, V.Yu.: Analytical and experimental assessment of spiroid gear tooth deflection. In: Proceedings of the 10th World Congress on TMM, vol. 6, Oulu, Finland, June 20–24, pp. 2257–2262 (1999).
130. Goldfarb, V.I.: Trends of gearing theory development. In: Proceedings of the 10th World Congress on TMM, vol. 6, Oulu, Finland, June 20–24, pp. 24–29 (1999).
131. Goldfarb, V.I., Glavatskikh, D.V., Su, D.: Computer-aided design of surfaces of engineering products. In: Academic proceedings of scientific works “Problems of characterization analysis and logical control”, pp. 75–80. Moscow (1999).
132. Goldfarb, V. I., Malina, O. V.: The method of creation of a classifier of a class of material objects by an example of gear schemes with intersecting axes. In:

- In: Academic proceedings of scientific works “Problems of characterization analysis and logical control”, pp. 80–90. Moscow (1999).
133. Goldfarb, V. I., Anferov, V. N.: To the choice of parameters and the scheme of a friction unit of the roller stand at modelling of gearing of spiroid cylindrical gears. In: Proceedings of the international conference “Strojne inžinierstvo—99”, pp. 201–204. Bratislava (1999).
 134. Goldfarb, V. I., Koshkin, D. V.: Numerical modelling of the localized contact of the modified spiroid gearing. In: CO-MAT-TECH’99, 7th International Conference, STU, pp. 318–324. Trnava (1999).
 135. Goldfarb, V. I.: Russian program “Progressive gears”. In: Gearing and Transmissions, N2, pp. 30–41 (1998).
 136. Goldfarb, V. I.: Scientific directions of Institute of Mechanics of ISTU. Problems of design of mechanical engineering products. In: Proceedings of researchers of the research center for gearboxes and gearboxes engineering of the Institute of Mechanics of ISTU, pp. 3–8. Izhevsk (1998).
 137. Goldfarb, V. I.: Spiroid gearboxes and gearmotors: design and application experience. In: Proceedings of the International Conference “Mechanics in Design”, Nottingham, pp. 36–43. UK (1998).
 138. Goldfarb, V.I., Tkachev, A.A., Sobakin, V.L.: CAD for the choice of shift coefficients in designing spur and helical gears. In: Proceedings of the International Conference “Mechanics in Design”, Nottingham, pp. 71–78. UK (1998).
 139. Goldfarb, V.I., Voznyuk R.V. Development of a CAD tool for enveloping modeling. In: Proceedings of the International Conference “Mechanics in Design”, Nottingham, pp. 471–478. UK (1998).
 140. Goldfarb, V.I., Mokretsov, V.N.: Organization of a testing laboratory for certification of gears and gearboxes. In: Abstracts of the conference “Quality, safety and energy saving”, pp. 15–17. Samara, SamSTU (1998).
 141. Goldfarb, V.I., Airapetov, E.L.: Integration of academic and university science in the field of gears. In: Dynamics of machine aggregates. Proceedings of 4th International Conference. Gabcikovo, pp. 48–53. Slovak Republic (1998).
 142. Goldfarb, V.I., Abramov, A.I., Koshkin, D.V.: Influence of manufacturing and assembly errors of the spiroid gear on the clearance field in meshing. In: Proceedings of International Conference “Strojne inžinierstvo”. Part 1, pp. 245–250. Bratislava, STU (1998).
 143. Goldfarb, V.I., Kuniver, A.S., Koshkin, D.V.: Analysis of methods for contact localization in spiroid gears. In: Proceedings of International Conference “Strojne inžinierstvo”. Part 1, pp. 251–254. Bratislava, STU (1998).
 144. Goldfarb, V.I.: Problems of organization of the Russian educational and research center of gears and gearbox engineering (FTP “Integration”, stage 1997). In: Bulletin of ISTU, N1, pp. 9–11. ISTU Publishing House, Izhevsk (1998)

145. Goldfarb, V.I., Abramov, I.V.: Russian program "Progressive gears and prospects of its development". In: Proceedings of the International Conference "Theory and Practice of Gearing", pp. 31–44. ISTU Publishing House, Izhevsk (1998).
146. Goldfarb, V.I., Mokretsov, V.N., Spiridonov, V.M., Golubkov, N.S.: Development of a new generation of spiroid gearboxes and gearmotors. In: Proceedings of the International Conference "Theory and Practice of Gearing", pp. 316–320. ISTU Publishing House, Izhevsk (1998).
147. Goldfarb, V.I., Makarov, N.G., Plekhanov, D.F.: New designs of carrierless planetary gears. In: Proceedings of the International Conference "Theory and Practice of Gearing", pp. 324–330. ISTU Publishing House, Izhevsk (1998).
148. Goldfarb, V.I., Airapetov, E.L., Aparkhov, V.I.: Ways to reduce vibrations and noise in gears. In: Proceedings of the International Conference "Theory and Practice of Gearing", pp. 101–107. ISTU Publishing House, Izhevsk (1998).
149. Goldfarb, V.I.: Concept of activity of IFToMM Technical Committee for Gearing and Transmissions. In: Gearing and Transmissions, N1, pp. 53–65 (1998).
150. Goldfarb, V.I., Slusky, L., Yampolsky, V.Z., Partow, P., Dubina, G.: Pilot project in international electronic distance education in Russia. In: Journal Technological Horizons in Education, vol. 24, N6, pp. 61–66 (1997).
151. Goldfarb, V.I.: Russian participation in scientific and economic cooperation. In: Proceedings of the international seminar "Attraction of extra-budgetary funds for the effective development of university science and educational services, p. 66–70. St. Petersburg (1997).
152. Goldfarb, V.I., Trubatchev, Ye.S.: Peculiarities of nonorthogonal spiroid gearing parametric synthesis. In: Proceedings of International Conference on Mechanical Transmissions and Mechanisms (MTM'97), Tiajin, pp. 613–616. China (1997).
153. Goldfarb, V.I., Abramov, A. I.: Vibration and accuracy of spiroid gears. In: Proceedings of the International Conference on Mechanical Transmissions and Mechanisms (MTM'97). Tiajin, pp. 617–619. China (1997).
154. Goldfarb, V.I.: Development and improvement of the progressive spiroid gears—the main scientific direction of the Institute of Mechanics of ISTU. In: proceedings: Selected Scientific Notes, vol. 1, pp. 45–50. ISTU Publishing House, Izhevsk (1997).
155. Goldfarb, V.I., Airapetov, E.L., Novoselov, V.Yu.: Calculated model of bending deformation of a spiroid gearwheel tooth. In: Proceedings of the XXXVIII International Machine Parts Department Conference, pp. 26–29. Slovakia, Bratislava (1997).
156. Goldfarb, V.I., Tkachev, A.A.: Computer-aided system for design of cylindrical gears. In: Proceedings of the XXXVIII International Machine Parts Department Conference, pp. 55–57. Slovakia, Bratislava (1997).
157. Goldfarb, V.I., Majercak, P., Kral, S., Antala, J.: Use perspectives of spiroid gears in practice. In: Proceedings of the XXXVIII International Machine Parts Department Conference, pp. 101–104. Slovakia, Bratislava (1997).

158. Goldfarb, V.I., Korolyova, Ye.V., Legutko, S.: Przeslanki optimalizacji stuktury zautomatizowanego systemu projektowania przekladni spiroidalnych. In: VIII Miedzunarodowa Konferencja naukowo—techniczna. Sekcja II, Projektowanie wspolbiezne, pp. 37–42. Zilona Gora, Polska (1997).
159. Goldfarb, V.I., Spiridonov, V.M.: Development of microdrives with spiroid gear. In: Mechatronika-97, III Konferencja Naukovo-Techniczna, Tom II, pp. 485–487. Warszawa (1997).
160. Goldfarb, V.I., Mokretsov, V.N., Spiridonov, V.M., Ivaykin, V.A., Matveev, V.I.: Spiroid gearboxes and gearmotors: experience in development and production. In: Drive technique, N4, pp. 36–38 (1997).
161. Goldfarb, V.I., Kuniver, A.S., Koshkin, D.V.: To the question on contact localization in spiroid gears. In: Proceedings of the VIth International Symposium “Theory of real gearing”, Part 1, pp. 29–31. Kurgan (1997).
162. Goldfarb, V.I., Russkikh, A.G.: Classification and Computer database of gears with Intersecting Axes. In: Proceedings of the VIth International Symposium “Theory of real gearing”, Part 1, pp. 41–44. Kurgan (1997).
163. Goldfarb, V.I., Spiridonov, V.M.: Design of the two-stage spiroid gear units and gear-motors. In: Proceedings of the International Conference on Gears, pp. 579–586. VDI, Dresden (1996).
164. Goldfarb, V.I., Kuniver, A.S., Trubachev, Ye.S.: Peculiarities of spiroid gear wheel hobbing. In: Proceedings of the IXth International Conference of Tools, pp. 441–444. Hungary, Miskolc (1996).
165. Goldfarb, V.I., Glavatskikh, D.V.: The simulation of the screw surface formation on the basis of nondifferential method. In: Proceedings of the IXth International Conference of Tools, pp. 469–474. Hungary, Miskolc (1996).
166. Goldfarb, V.I., Mudrik, Y., Kral, S., Oleksiuk, V.: Some results of joint research on international scientific program “Mechanical drives of new generation”. In: Proceedings of the International Seminar “Problems of the dynamics aggregates”, p. 7. Trnava, Slovakia (1996).
167. Goldfarb, V.I., Mudrik, Y.: Contribution of aggregate dynamics to the theory of machines and mechanisms. In: Proceedings of the International Seminar “Problems of the dynamics aggregates”, p. 9. Trnava, Slovakia (1996).
168. Goldfarb, V.I., Abramov, A.I.: Research of influence of primary errors on kinematic accuracy of a spiroid gear. In: Proceedings of the International Seminar “Problems of the dynamics aggregates”, p. 19. Trnava, Slovakia (1996).
169. Goldfarb, V.I.: International and Russian programs for improvement of gears and gearboxes. In: Proceedings of the International Conference “Theory and Practice of Gearing”, pp. 13–23. ISTU Publishing House, Izhevsk (1996).
170. Goldfarb, V.I., Abramov, A.I.: Research of vibroacoustic properties of a spiroid gear. In: Proceedings of the International Conference “Theory and Practice of Gearing”, pp. 135–140. ISTU Publishing House, Izhevsk (1996).
171. Goldfarb, V.I., Mokretsov, V.N., Spiridonov, V.M., Ivaykin, V.A., Matveev, V.I.: Experience of development and manufacture of spiroid gearboxes and

- garmotors. In: Proceedings of the International Conference “Theory and Practice of Gearing”, pp. 213–218. ISTU Publishing House, Izhevsk (1996).
172. Goldfarb, V.I., Glavatskikh, D.V., Vozniuk, R.V.: Instrumental system for modeling of the enveloping process In: Proceedings of the International Conference “Theory and Practice of Gearing”, pp. 481–484. ISTU Publishing House, Izhevsk (1996).
173. Goldfarb, V.I.: Theory of design and practice of development of spiroid gearing. In: Proceedings of the XXXVI Conference of the Department of Machine Parts and Machine Design, vol. 1, pp. 115–120. Technical University of Brno (1995).
174. Goldfarb, V.I., Golubkov, N.S., Bazhin, A.G.: Peculiarities of design of bearing units for the spiroid gearbox worm shaft. In: Proceedings of the XXXVI Conference of Department of Machine Parts and Machine Design, vol. 1, pp. 121–124. Technical University of Brno (1995).
175. Goldfarb, V.I., Spiridonov, V.M., Malina, O.V.: Spiroid gearbox designs. In: Proceedings of the XXXVI Conference of Department of Machine Parts and Machine Design, vol. 1, pp. 125–128. Technical University of Brno (1995).
176. Goldfarb, V.I., Mudrik, J., Muran, M., Kral, S., Majercak, P.: Dynamic properties of machine aggregate with gearing. In: Proceedings of the XXXVI Conference of the Department of Machine Parts and Machine Design, vol. 2, pp. 41–44. Technical University of Brno (1995).
177. Goldfarb, V.I., Mudrik, J., Kral, S., Majercak, P.: Modelovanie a analyza dynamickyh vlastnosti strojoveho agregatu s ozubenym prevodom. In: Engineering Mechanics’95. National Conference, vol. 2, pp. 363–366. Svratka, Czech Rep. (1995).
178. Goldfarb, V.I., Isakova, N.V.: Variants of spiroid gearing from pitch realization point of view. In: Gearing and Transmissions, N1, pp. 25–34 (1995).
179. Goldfarb, V.I.: The nondifferential method of the geometrical modeling of the enveloping process. In: Proceedings of the 9th World Congress on the Theory of Machines and Mechanisms, vol. 1, pp. 424–427. Milano (1995).
180. Goldfarb, V.I.: Theory of design and practice of developing spiroid gearing. In: Proceedings of the International Congress of Gear Transmissions, vol. 2, pp. 1–5. Sofia (1995).
181. Goldfarb, V.I.: Computer-aided design of gearboxes. New approaches. In: Proceedings of the International Congress of Gear Transmissions, vol. 2, pp. 128–131. Sofia (1995).
182. Goldfarb, V.I., Granberg, A.G., Safronov, E.I.: Participation of Russia in Pacific economic cooperation. In: Proceedings of the International Congress on Informatization, pp. 11–15. ISTU Publishing House, Izhevsk (1995).
183. Goldfarb, V.I., Abramov, I.V., Mudrik, Y., Moravchik, O., Kratochvil, C., Grois, M.: Experience of integration of educational and scientific programs of technical universities of Izhevsk, Trnava, Brno. In: Proceedings of the International Congress on Informatization, pp. 32–33. ISTU Publishing House, Izhevsk (1995).

184. Goldfarb, V.I., Golubkov, N.S., Kuniver, A.S., Mokretsov, V.N., Spiridonov, V.M.: Development of a number of spiroid gearboxes and gearmotors for general mechanical engineering application. In: Progressive gears. Reports of the International Symposium, pp. 156–161. ISTU Publishing House, Izhevsk (1994).
185. Goldfarb, V.I., Spiridonov, V.M., Mokretsov, V.N., Ivaykin, V.A.: Problems of creation of spiroid drives for stop and regulating valves. In: Progressive gears. Reports of the International Symposium, pp. 149–156. ISTU Publishing House, Izhevsk (1994).
186. Goldfarb, V.I., Chervik, V., Oleksiuk, V.: Installation for measurement of kinematic accuracy of a spiroid gearbox. In: Progressive gears. Reports of the International Symposium, Izhevsk, pp. 60–65. ISTU Publishing House, Izhevsk (1994).
187. Goldfarb, V.I., Isakova, N.V.: Possibilities of reproducing a helical surface with variable pitch. In: Progressive gears. Reports of the International Symposium, Izhevsk, pp. 174–178. ISTU Publishing House, Izhevsk (1994).
188. Goldfarb, V.I.: The synthesis of nontraditional kind of skew axis gearing. In: International Gearing Conference, BGA transmission technology, Newcastle, MEP, London, pp. 513–516 (1994).
189. Goldfarb, V.I., Oleksiuk, W., Czerwec, W.: Badania spiroidalnej przekladni zebatej. In: Mechatronika 94, Prace naukowe konferencje, Z.3, s. 215–218. Warszawa (1994)
190. Goldfarb, V.I., Mardanov, I.I.: Creation of a range of new spiroid geared motors and reduction gear units. In: Russian Engineering Research, vol. 70, N. 12, pp. 54–57. Allerton Press Inc (1994).
191. Goldfarb, V.I., Abramov, A.I.: Spiroid gearing as an element of mechatronic system. In: Euro-mech 318. Stability and vibration of mechatronic system, p. 5. Prague (1994).
192. Goldfarb, V.I., Isakova, N.V., Ivajkin, V.A.: Reproducing method of tool-helicoid surface with variable pitch. In: Gepguarta technologia, 9–10, pp. 379–381. Budapest (1994).
193. Goldfarb, V.I., Malina, O.V., Ivaikin, V.A.: Automatized design of hobbing cutter. In: Gepguarta technologia, 9–10, pp. 421–422. Budapest (1994).
194. Goldfarb, V.I., Spiridonov, V.M.: Application of progressive spiroid gears for creation of new generation of drives for stop and regulating valves. In: Proceedings of the scientific and technical conference “Scientists of Izhevsk State Technical University to Production”, p. 23. ISTU Publishing House, Izhevsk (1994).
195. Goldfarb, V.I., Koryakin, N.A.: Application of stamping by rolling in manufacture of spiroid gearboxes. In: Proceedings of the scientific and technical conference “Scientists of Izhevsk State Technical University to Production”, p. 50. ISTU Publishing House, Izhevsk (1994).
196. Goldfarb, V.I., Airapetov, E.L., Mudrik, Y., Kral, Sh., Kratokhvil, C., Groys, M., Parushev, P., Abadzhiev, V., Oleksiuk, V., Slutskiy, L.: Some results and prospects of development of the international program “Mechanical

- drives of new generation". In: Problems of dynamics of machine aggregates. Medzinarodny seminar, pp. 1–2. Bratislava, Slovakia (1994).
197. Goldfarb, V.I., Kuniver, A.S., Mokretsov, V.N.: Development of progressive technology of manufacturing of spiroid gearwheels for gearboxes. In: Proceedings "Transfer technologies, complexes and equipment in mechanical engineering. Small series and low tonnage high technology products", pp. 40–41. Saratov (1994).
 198. Goldfarb, V.I., Kuniver, A.S., Mokretsov, V.N.: Development of regulation documents for preparation of spiroid gearbox production. In: Proceedings "Transfer technologies, complexes and equipment in mechanical engineering. Small series and low tonnage high technology products", pp. 41–42. Saratov (1994).
 199. Goldfarb, V.I., Isakova, N. V.: Approach to synthesis of mechanisms for reproduction of a helical surface with the variable pitch. In: *Mechanika na mashinite*, Book 1, pp. 78–80. Varna, VMEI ed. (1994).
 200. Goldfarb, V.I.: Possibilities of computer-aided synthesis of hyperboloid gear schemes. In: *Mechanika na mashinite*, Book 1, pp. 80–83. Varna, VMEI ed. (1994).
 201. Goldfarb, V.I., Airapetov, E. L., Abramov, A. I., Akhatov, R. R.: Prospects of application of spiroid gears in mechanisms with the reduced vibroactivity. In: *Mezinarodni seminar "Dinamicka a pevnostni analiza pohonyich systemu"*, pp. 18–21. Svatka, Czech Republic (1993).
 202. Goldfarb, V.I., Kuniver, A.S.: Approach to estimation of load capacity of spiroid gears. In: *Mezinarodni seminar "Dinamicka a pevnostni analiza pohonyich systemu"*, pp. 75–82. Svatka, Czech Republic (1993).
 203. Goldfarb, V.I., Malina, O.V., Bazhin, A.G.: Modular synthesis of spiroid gearbox design. In: *XVI Sympzion Podstaw Konstrukcji Maszyn, Referaty*, pp. 102–109. Warszawa (1993).
 204. Goldfarb, V.I.: Spiroid gearboxes. Designs and possibilities. In: *XVI Sympzion Podstaw Konstrukcji Maszyn, Referaty*, pp. 94–101. Warszawa (1993).
 205. Goldfarb, V.I.: Results of complex development of spiroid gears and gearboxes. In: *Proceedings of the International Symposium "Development of Geometric Theory of Gearing"*, pp. 9–12. ISTU Publishing House, Izhevsk (1993).
 206. Goldfarb, V.I., Isakova, N.V.: Geometry of meshing of spiroid gears with worms of variable pitch. In: *Proceedings of the International Symposium "Development of Geometric Theory of Gearing"*, pp. 37–38. ISTU Publishing House, Izhevsk (1993).
 207. Goldfarb, V.I., Oleksiuk, V.: Geometric modeling of tooth flanks. In: *Proceedings of the International Symposium "Development of Geometric Theory of Gearing"*, pp. 24–25. ISTU Publishing House, Izhevsk (1993).
 208. Goldfarb, V.I., Kuniver, A.S., Mokretsov, V.N.: Methodology and results of estimation of load capacity of spiroid gears. In: *Proceedings of the*

- Vth Internatinal Symposium “Theory of Real Gearing”, pp. 20–21. Kurgan (1993).
209. Goldfarb, V.I., Mudrik, I., Parushev, P., Kosorin, D.: Experimental investigation of dynamics of a machine unit with a gearmotor. In: Proceedings of the International Symposium “Development of Geometric Theory of Gearing”, pp. 61–62. ISTU Publishing House, Izhevsk (1993).
 210. Goldfarb, V.I.: Integration of CAD systems for spiroid gears and gearboxes. In: Proceedings of the Vth Internatinal Symposium “Theory of Real Gearing”, p. 7. Kurgan (1993).
 211. Goldfarb, V.I., Malina, O.V.: Intelligence of the computer-aided design of mechanical engineering products. In: ITS-93 World Congress “Information Communications, Networks, Systems and Technologies”, pp. 169–174. Moscow (1993).
 212. Goldfarb, V.I., Kuniver, A.S., Mokretsov, V.N.: Rational choice of parameters of a spiroid gear by strength condition. In: Theses of reports of scientific and technical conference “Problems of Gears and Gearbox Engineering”, p. 35. Kharkov (1993).
 213. Goldfarb, V.I., Mokretsov, V.N., Kuniver, A.S.: Development, mastering and production of highly demanded gear mechanisms with spiroid gears. In: Transfer technologies. Complexes and equipment in mechanical engineering. Theses of reports, pp. 63–64. Saratov (1993).
 214. Goldfarb, V.I., Koryakin, V.N.: Prospects of stamping by rolling in manufacture of spiroid gearboxes. In: Perspective processes of metal forming with locally movable spot of plastic deformation. Theses of Reports of the All-Russian Seminar, pp. 9–10. ISTU Publishing House, Izhevsk (1993).
 215. Goldfarb, V.I., Koryakin, N.A.: New series of spiroid reducers and motor-reduces. Design and manufacturing. In: The 3rd World Congress on Gearing and Power Transmission, pp. 281–287. Paris (1992).
 216. Goldfarb, V.I., Russkikh, A.G.: Computer-aided synthesis of gear structure at arbitrary axes arrangement. In: International Conference on the Theory of Machines and Mechanisms, September, pp. 65–71. Liberec, Czechoslovakia (1992).
 217. Goldfarb, V.I., Anferov, V.N.: Features of choosing meshing zones in spiroid gears with rotaprint method of lubrication. In: Proceedings of the 5th International younht summer school. Application of mechanics and biomechanics in mechatronics, pp. 76–81. Varna, Bulgaria (1992).
 218. Goldfarb, V.I., Isakova, N.V.: Alternative Approaches to Choice of helical Parameter Value at Design of Spiroid Gears. In: Proceedings of the 5th International younht summer school. Application of Mechanics and biomechanics in mechatronics, pp. 96–105. Varna, Bulgaria (1992).
 219. Goldfarb, V.I.: Industry aspects of development of CAD systems for gearboxes. In: “Quality problems of the mechanical transmissions and gearboxes. Accuracy and Control of Gearwheels and Gears”, pp. 64–65. Leningrad (1991).

220. Goldfarb, V.I., Kuniver, A.S., Chekalkin, G.T.: Gearwheel of the spiroid gear subjected to wear tests. In: Information bulletin #66–91, part 55, p. 4. Udmurt CNTI (1991).
221. Goldfarb, V.I.: Aspects of the problem of automation of gears and gearbox design. In: Gearing and Transmissions, N1, pp. 20–24. Izhevsk (1991).
222. Goldfarb, V.I.: Marketing aspects of development of CAD systems for gears and gearboxes. In: Computer-aided Design of Mechanical Transmissions. Materials of the International Seminar, pp. 3–4. Izhevsk (1991).
223. Goldfarb, V.I., Muntyan, V.V., Yatsin, Yu.L.: Computer-aided calculation of a spiroid-cylindrical gearbox. In: Computer-aided Design of Mechanical Transmissions. Materials of the International Seminar, pp. 41–43. ISTU Publishing House, Izhevsk (1991).
224. Goldfarb, V.I.; Malina, O.V.: Automation of the modular design of spiroid gearboxes. In: Computer-aided Design of Mechanical Transmissions. Materials of the International Seminar, pp. 44–46. ISTU Publishing House, Izhevsk (1991).
225. Goldfarb, V.I., Russkikh, A.G.: Skew axis gearing scheme synthesis. In: MPT'91 JSME International Conference on Motion and Power Transmissions, Nov. 23–26, pp. 649–653. Hiroshima, Japan (1991).
226. Goldfarb, V.I.: Organization of design and production of new types of gearboxes and gearmotors. In: 4th International School “Application on Mechanics and Biomechanics in Robotics”, pp. 15–18. Varna (1991).
227. Goldfarb, V.I., Russkikh, A.G.: Computer-aided synthesis of the worm type gear schemes. In: *Mechanika*, z.27. XV Sympozjon podstaw konstrukcji maszyn, cz.II, Komunikaty, pp. 101–103. Rzeszow, Polska (1991).
228. Goldfarb, V.I., Golubkov, N.S., Malina, O.V.: Design of a spiroid gearmotor from the automation point of view. In: *Mechanika*, z.27, XV Sympozjon podstaw konstrukcji maszyn, cz.II, Komunikaty, pp. 105–107. Rzeszow, Polska (1991).
229. Goldfarb, V.I., Malina, O.V.: Structural approach to the computer-aided design by the example of a gearbox. In: “Logic control with the use of computer”. XIII All-Union Symposium, pp. 71–72. Moscow, Scientific Council of the USSR Academy of Sciences on the problem of “Cybernetics” (1990).
230. Goldfarb, V.I., Kulemin, V.Yu.: Algorithm of a control stand for testing of fast rotors with disbalance. In: “Logic control with the use of computer”. XIII All-Union Symposium, pp. 111–112. Moscow, Scientific Council of the USSR Academy of Sciences on the problem of “Cybernetics” (1990).
231. Goldfarb, V.I.: Precise drives based on spiroid gearing. State and prospects. In: 13 Internationales Kolloquium der Feinwerktechnik. p. 3. Kopenhagen (1990).
232. Goldfarb, V.I.: Koroleva, E.V.: Information support of the computer-aided design of spiroid gearmotors. In: Development and introduction of CAD and ASTP in mechanical engineering”. Materials of scientific and technical conference, pp. 118–119. ISTU Publishing House, Izhevsk (1990).

233. Goldfarb, V.I., Kulemin, V.Yu.: Dynamic test bench for the fast rotors with big unbalance. In: Dynamics on mechanics systems. Reports 15 national seminar, vol. 1, pp. 176–178, Varna (1990).
234. Goldfarb, V.I., Mardanov, I.I.: Creation of a range of new spiroid gearmotors and gearboxes. In: Vestnik mashinostroeniya, N12, pp. 54–57 (1990).
235. Goldfarb, V.I., Mardanov, I.I.: Creation of a range of new spiroid gearmotors and gearboxes. In: Gears: state of the art and progress. Theses of reports of All-Union Scientific and Technical Conference, pp. 22–23. Odessa (1990).
236. Goldfarb, V.I.: Gear quality assurance at a design stage with the use of CAD. In: Problems of quality improvement, reliability and durability of machines. Theses of reports of All-Union Scientific and Technical Conference, p. 13. Bryansk (1990).
237. Goldfarb, V.I., Mardanov, I.I., Chekalkin, G.T.: Standardization of parameters and unification of design of spiroid gearmotors and gearboxes. In: Standardization and unification in the field of gears. Theses of reports of the scientific and technical conference, pp. 34–36. Kharkov (1990).
238. Goldfarb, V.I., Koroleva E.V.: Problems of optimal design of spiroid type gears. In: “Integrated Computer-Aided Design Systems”, pp. 91–93. Moscow (1989).
239. Goldfarb, V.I., Koroleva, E.V., Russkikh, A.G., Savinov, O.Yu.: Commercial system for consumers of spiroid gears, gearboxes and gearmotors. In: Computer-Aided Design of Gears and Gearboxes. Materials of scientific and technical seminar, pp. 73–75. Izhevsk (1989).
240. Goldfarb, V.I.: Features in approaches to development and implementation of CAD systems for gears and gearboxes. In: Computer-Aided Design of Gears and Gearboxes. Materials of scientific and technical seminar, pp. 3–5. Izhevsk (1989).
241. Goldfarb, V.I., Kupreev, N.I., Koroleva, E.V.: About the position of CAD products in “calculation-object-information” space. In: Computer-Aided Design of Gears and Gears. Materials of scientific and technical seminar, pp. 25–26. Izhevsk (1989).
242. Goldfarb, V.I., Moskvina, N.N., Voloshin, Yu.I.: Theoretical and experimental investigation of spiroid gearmotor wear at the variable mode of rotation. In: “Ways of Intensification of Agricultural Production in Farms of the Pskov Region”, pp. 105–107. V. Luki (1989).
243. Chekalkin, G.T., Goldfarb, V.I., Mardanov, I.I., Pichugin, A.I., Tanygin, S.V.: Choice of initial contour for spiroid cylindrical gears. In: “Development of Gear Design and Production”, pp. 68–69. Sverdlovsk (1989).
244. Goldfarb, V.I., Golubkov, N.S., Mardanov, I.I., Koroleva, E.V.: Development of a dimensional parametric series of spiroid gearmotors. In: “Development of Gear Design and Production”, pp. 69–70. Sverdlovsk (1989).
245. Goldfarb, V.I.: Succession at computerization of general mechanical engineering disciplines. In: Complex Computerization of the Educational Process in Higher School. Theses of Reports of the All-Union Scientific and Methodological Conference, pp. 31–32. Leningrad (1989).

246. Goldfarb, V.I.: Peculiarities of the approach to development and introduction of CAD systems for gears and gearboxes. In: CAD of gears and gearboxes. Abstracts of reports of scientific and technical seminar, p. 3. Izhevsk (1989).
247. Goldfarb, V.I., Vavro, V.N., Russkikh, A.G.: Information model of the gear scheme with intersecting axes. In: Mathematical and software support of integrated CAD-FMS. Theses of reports of the coordination meeting. Ustinov (1987).
248. Goldfarb, V.I.: Trends of development of CAD systems for gears. In: Computer-aided design of gear elements. Izhevsk (1987).
249. Goldfarb, V.I.: Fundamentals of the theory of computer-aided geometrical analysis and synthesis of general type worm gears: Thesis of Doctor of Technical Sciences (Dr. Sc. in Engineering). Ustinov (1985).
250. Goldfarb, V.I., Trubitsyn, O.A.: Geometrical modeling of the gear scheme with application of the machine graphics programs. In: Mathematical support of systems with machine graphics. Materials of the third scientific and technical seminar, pp. 73–75. Ustinov (1985).
251. Goldfarb, V.I.: Methodological fundamentals of the computer-aided synthesis of general type worm gears. In: “Computer-aided design in mechanical engineering”, Theses of reports of scientific and technical conference, p. 57, Ustinov (1985).
252. Goldfarb, V.I., Zlatkin, V.M.: Target training of system engineers in the field of creation of computer-aided mechanic electronic systems. In: “Computer-aided design in mechanical engineering”, abstracts of reports of scientific and technical conference, Ustinov (1985).
253. Goldfarb, V.I., Zenzinov, V.V., Glavatskikh, D.V.: Computer-aided calculation of geometry and parameters for control of cylindrical worms. In: “Mathematical support of CAD and FMS in mechanical engineering”, materials of coordination meeting, pp. 88–90, Izhevsk (1984).
254. Goldfarb, V.I.: Synthesis of schemes of two-stage spiroid gearboxes. In: Theses of reports of the scientific-technical conference “Reduction of metal intensity of gears and gearboxes”, p. 15. Sverdlovsk (1984).
255. Goldfarb, V.I., Nesselov, I.P.: Definition of the areas of preferable values for spiroid gear parameters. In: Theses of reports of scientific and technical conference “Reduction of metal intensity of gears and gearboxes”, p. 40. Sverdlovsk (1984).
256. Goldfarb, V.I., Nesselov, I.P., Gilfarnov, R.M.: Choice of parameters of spiroid gears from the condition of the increased load capacity. In: Theses of reports of the republican scientific and technical conference “Increase of reliability and decrease in metal intensity of gears and gearboxes of the general mechanical engineering purpose. p. 86. Sevastopol (1983).
257. Goldfarb, V.I.: Experience of spiroid gear design by the dialogue CAD system. In: “Development and introduction of the automated design systems in mechanical engineering”, pp. 78–79. Izhevsk (1983).

258. Goldfarb, V.I., Nesmelov, I.P.: Computer-aided modelling of generation by enveloping method. In: M. Dep. in NNIIMASH No.17 MSh-D83, Bibl index VINITI, vol. 6, p. 6 (1983).
259. Goldfarb, V.I., Nesmelov, I.P., Glavatskikh, D.V.: Computer-aided modeling of Surface generation by enveloping method. In: Application of the computer-aided design of structures in mechanical engineering. Theses of reports of All-Union Scientific and Technical Symposium, pp. 75–77. Moscow (1983).
260. Nesmelov, I.P., Goldfarb, V.I.: Non-differential approach to the solution of the enveloping problem. In: “Mechanics of Machines”, N 61, pp. 3–10. Moscow, Nauka (1983).
261. Goldfarb, V.I., Nesmelov, I.P.: Dialogue system for the computer-aided design of spiroid gears. In: “Automated Design of Mechanical Transmissions”, Abstracts of the scientific and technical conference, pp. 5–7. Izhevsk (1982).
262. Goldfarb, V.I., Nesmelov, I.P.: Principles of development of the computer-aided system for spiroid gears. In: Theses of reports of the second All-Union Congress on the theory of machines and mechanisms, Part 1, p. 113. Kiev, Naukova Dumka (1982).
263. Goldfarb, V.I., Long, V.A.: Program for profile calculation and choice of tool setting parameters for machining cylindrical spiroid worms. In: “Computer-aided Design of Mechanical Transmissions”, Abstracts of the scientific and technical conference, p. 36. Izhevsk (1982).
264. Goldfarb, V.I., Nesmelov, I.P., Glavatskikh, D.V.: Modeling of helical surface generation by bevel tools. In: “Computer-aided Design of Mechanical Transmissions”, Theses of reports of scientific and technical conference, p. 38. Izhevsk (1982).
265. Goldfarb, V.I., Nesmelov, I.P.: Choice of non-orthogonal gear schemes with intersecting axes. In: Izvestia of higher educational institutions. Mechanical Engineering, N10, pp. 31–35 (1982).
266. Goldfarb, V.I., Anikin, L.A.: Computer-aided search design of the gear scheme with intersecting axes. In: Development and implementation of computer-aided design systems. Theses of reports of scientific and technical conference. Izhevsk (1981).
267. Goldfarb, V.I., Nesmelov, I.P.: Choice of geometrical parameters for the non-orthogonal spiroid gear. In: “Izvestiya vysshikh uchebnykh zavedeniy”, N8, pp. 48–51 (1981).
268. Goldfarb, V.I., Nesmelov, I.P.: Calculation method of the size required at the control of cylindrical spiroid worms by means of balls. In: Izvestiya vuzov. Mashinostroyenie, N2, pp. 158–160 (1980).
269. Goldfarb, V.I., Nesmelov, I.P.: Formalization of contact condition for physical bodies with reference to the solution of the problem of spiroid worm control by means of balls and rollers. In: “Prospects of development and application of spiroid gears and gearboxes”, reports of All-Union Scientific Meeting, pp. 57–62. Izhevsk (1979).
270. Goldfarb, V.I., Nesmelov, I.P.: Problems of synthesis of the scheme of a non-orthogonal hyperboloid third class gear. In: Theses of reports of the third

- all-Union symposium “Theory and geometry of spatial gears”, pp. 22–23. Kurgan (1979).
271. Georgiev, A.K., Goldfarb, V.I.: Preferable combination of rotation directions for elements of the non-orthogonal hyperboloid gear. In: *Izvestiya vuzov. Stroitelstvo i arkhitektura*, pp. 34–37 (1978).
 272. Georgiev, A.K., Goldfarb, V.I., Matveev, V.I., Shibanov, E.K.: Definition of a profile and setting parameters of a two-row cutter head. In: *Izvestia vuzov. Mashinostroenie*, N5, pp. 155–158 (1978).
 273. Goldfarb, V.I., Nesmelov, I.P.: Application of interpolation methods at research of spiroid gearwheel flanks. In: “Mechanical transmissions”, Interuniversity proceedings, issue 2, pp. 28–33. Izhevsk (1977).
 274. Goldfarb, V.I.: Comparative study of the curvature of mutually enveloping surfaces in spiroid cylindrical gears with the worms of ideal variable and constant pitch. In: *Mechanical transmissions*, N2, pp. 34–39 (1977).
 275. Georgiev, A.K., Goldfarb, V.I., Ezerskaya, S.V., Manshin, S.D.: Spiroid gears with cylindrical worms. Geometry calculation. Recommendations under the editorship of I.N. Frankel. VNIINMASH (1976).
 276. Nesmelov, I.P., Goldfarb, V.I.: Algorithm for determination of points of the enveloping element surface. In: *Improvement of Metal Processing by Cutting*, Issue 1, pp. 92–95. Izhevsk, IMI (1976).
 277. Goldfarb, V.I.: Construction of the longitudinal lines of gearwheel teeth for the orthogonal spiroid gear with a cylindrical worm having threads with the ideal variable pitch. In: *Mechanical transmissions*, Issue 1, pp. 9–12, Izhevsk (1976).
 278. Goldfarb, V.I., Georgiev, A.K., Ardashev, B.N.: Calculation of caliber for controlling the gearwheel tooth profile for the orthogonal spiroid gear with the cylindrical worm having threads of a convex-concave profile. In: *Mechanical transmissions*, Issue 1, p. 20 Izhevsk (1976).
 279. Goldfarb, V.I.: The form of an ideal initial surface of the worm of the orthogonal spiroid gear. In: *Izvestia vuzov. Mashinostroenie*, N11, pp. 38–41 (1976).
 280. Goldfarb, V.I.: The equation of an ideal initial surface of the worm. In: *Izvestia vuzov. Mashinostroenie*, N3, pp. 52–55 (1976).
 281. Georgiev, A.K., Goldfarb, V.I., Kuniver, A.S.: Determination of longitudinal lines and tooth pointing of an orthogonal spiroid gear with a cylindrical worm of a convex-concave profile. In: *Mechanical transmissions*, Issue 7, pp. 3–7. Izhevsk (1975)
 282. Georgiev, A.K., Goldfarb, V.I.: New variety of the orthogonal spiroid gear with the cylindrical worm. In: *Mechanical transmissions*, Issue 7, pp. 8–17. Izhevsk (1975).
 283. Goldfarb, V.I., Pasinskiy, V.S., Nesmelov, I.P.: Research and automated processing of calculation results by means of the computer at the analysis of meshing conditions in spiroid gears. In: *Mechanical transmissions*, Issue 7. Izhevsk (1975).

284. Goldfarb, V.I., Ezerskaya, S.I.: To the question of choosing the size of a helical parameter in the orthogonal spiroid gear with a cylindrical worm. In: *Izvestia vuzov. Mashinostroenie*, N2, pp. 184–186 (1975).
285. Georgiev, A.K., Goldfarb, V.I.: To investigation of an orthogonal spiroid gear with a cylindrical worm having threads of an ideal variable pitch. In: *Proceedings of the USSR Academy of Sciences. Department of Technical Sciences. Mechanics and Engineering*, N45, pp. 91–99 (1974).
286. Georgiev, A.K., Goldfarb, V.I., Shibarov, E.K.: Some issues of thread generation for cylindrical spiroid worms having the convex-concave profile when machining by the disk tool. In: *Researches in the field of equipment technology for external and internal threads, thread-forming tools and methods of thread control*, pp. 166–172. Tula, TPI (1974).
287. Georgiev, A.K., Goldfarb, V.I.: To the question of schemes for machining by a cutter and profile shapes of cylindrical ruled-surface worms of spiroid (hypoid worm) gears. In: *“Mechanical transmissions”*, p. 47. Izhevsk (1972).
288. Georgiev, A.K., Goldfarb, V.I.: To research of load capacity of a spiroid gearbox with the unground steel cylindrical worm and bronze gearwheel. In: *“Mechanical transmissions”*, p. 76. Izhevsk (1972).
289. Goldfarb, V.I.: About undercutting in an orthogonal spiroid gear with a cylindrical worm. In: *“Mechanical transmissions”*, pp. 97–103. Izhevsk (1972).
290. Goldfarb, V.I.: Some results of investigation of the curvature of mutually enveloping surfaces in hypoid worm (spiroid) gears with cylindrical ruled-surface worms. In: *Proceedings of the scientific and technical conference of Ural universities on mechanical engineering “Mechanical transmissions”*, pp. 135–140. Izhevsk (1971).
291. Goldfarb, V.I., Georgiev, A.K.: Aspects of geometrical theory and research results for spiroid gears with cylindrical worms. In: *“Mechanics of machines”*, Issue 31, pp. 70–80. Moscow, Nauka (1971).
292. Goldfarb, V.I.: Research of a variety of the orthogonal hypoid worm (spiroid) gear with a cylindrical worm: Thesis of Candidate of Technical Sciences (Ph.D. in Engineering). Izhevsk (1969).
293. Goldfarb, V.I.: Calculation of a disk tool profile for machining the convex helical surface. In: *“Improvement of cutting processes and accuracy increase in metal-cutting machines”*, Issue 2, pp. 87–97. Izhevsk (1968).
294. Goldfarb, V.I., Georgiev, A.K.: To the choice of the wheel diameter at grinding of worms having threads with concave profile by the method of F. L. Litvin. In: *“Accuracy of machine tools and ways of expanding their manufacturing possibilities”*. Izhevsk (1967).
295. Yastrebov, V.M., Goldfarb, V.I.: Tables of coordinates of curvature radii and radii-vectors of involute points for gearwheels with tooth numbers from 12 to 120. Moscow, Mashinostroyenie (1964).

References

1. Litvin, F.L.: Development of Gear Technology and Theory of Gearing, NASA (1997)
2. Babichev, D.T., Lagutin, S.A., Barmina, N.A.: Russian school in the theory and geometry of gearing. Part 1. Its origins and Golden period of 1935–1975. Jnl “Frontiers of Mechanical Engineering”, FME-15028-MA, <https://doi.org/10.1007/s11465-015-0360-z>, N11(1), pp. 44–59 (2016)
3. Babichev, D.T., Lagutin, S.A., Barmina, N.A.: Russian School of the Theory and Geometry of Gearing. Part 2. Development of the Classical Theory of Gearing and Establishment of the Theory of Real Gearing in 1976–2000. New approaches to gear design and production. Springer International Publishing AG Switzerland, V. Goldfarb, E. Trubachev, N. Barmina Eds., Vol. 81, pp. 1–46 (2020)
4. Saari, O.: Speed-Reduction Gearing. Patent USA №2696125
5. Saari, O.: Skew-Axis Gearing. Patent USA №2954704
6. Goldfarb, V.I.: What do we know about spiroid gears. In: Proceedings of the International Conference on Mechanical Transmissions, China, Vol. 1, pp. 19–26. Science Press (2006)
7. Goldfarb, V., Trubachev, E., Pushkareva, T., Savelyeva, T.: Comparative investigation of worm and spiroid gears with cylindrical worms. In: Uhl, T. (eds) Advances in Mechanism and Machine Science. IFToMM WC 2019. Mechanisms and Machine Science, v. 73, pp. 925–935. Springer, Cham (2019)
8. Wildhaber, E.: Helical gearing. US Patent No 1,601,750 (1926)
9. Novikov, M.L.: Gears with new meshing. Published by Zhukovsky Aviation Institute (1958)
10. Niemann, G., Heyer, E.: Untersuchungen an Schneckengetrieben. Germany: VDI, N6. S. 147–157 (1953)
11. Litvin, F.L.: New types of cylindrical gears. Mashgiz, Moscow (1962)
12. Korostelev, L.V., Lagutin, S.A.: Synthesis of gears with closed line of contact. *Machinovedeniye* **N6**, 44–50 (1969)
13. Nesmelov, I.P., Goldfarb, V.I.: Non-differential approach to the solution of the enveloping problem. In: “Mechanics of Machines”, N 61, pp. 3–10. Moscow, Nauka (1983)
14. Rvachev, V.L.: The theory of R-functions and some of its applications. Nauk. Dumka, Kiev (1982)
15. Sheveleva, G.I.: Algorithm of numerical calculation of a machined surface. *Stanki i instrument* **N8**, 17–20 (1969)
16. Babichev, D.T.: Prospects of applying a system of updated geometrical primitives in the study of real gearing. In: Proceedings of The international Conference “Theory and Practice of Gearing”, pp. 531–536. Izhevsk (1998)
17. Goldfarb, V.I.: Some exercises with equations of gearing. *Gearing Trans* **N1**, 14–20 (2001)
18. Erikhov, M.L.: Geometric and kinematic diagrams of machine-tool gearing and principles of their classification. In: Abstracts of reports of the third All-Union symposium “Theory and geometry of spatial gears”. Kurgan, pp. 7–9 (1979)
19. Korostelev, L.V., Baltadzhi, S.A., Lagutin, S.A.: Conjugate meshing lines of a general type worm gear. *Mach Learn: Moscow* **N5**, 49–56 (1978)
20. Minkov, K.: Basic theory and classification of hyperboloid gears. In: Abstracts of international symposium “Development of geometrical theory of gears”, Izhevsk, p. 8 (1993)
21. Goldfarb, V.I., Malina, O.V.: Skew axis gearing scheme classifier building technique. In: Proceedings of the 10th World Congress on MMS, vol. 6, Oulu, Finland, June 20–24, pp. 2227–2232 (1999)
22. Goldfarb, V.I.: The form of an ideal initial surface of the worm of the orthogonal spiroid gear. *Izvestia vuzov. Mashinostroenie* **N11**, 38–41 (1976)

23. Goldfarb, V.I., Anferov, V.N.: Features of choosing meshing zones in spiroid gears with rotaprint method of lubrication. In: Proceedings of the 5th International youngth summer school. Application of mechanics and biomechanics in mechatronics, pp. 76–81. Varna, Bulgaria (1992)
24. Goldfarb, V.I., Russkikh, A.G., Trubachev, E.S.: Internal gear with intersecting axes. Patent of Russia №2101582 dated 10.01.98
25. Goldfarb, V.I., Nesmelov, I.P.: Non-orthogonal gear transmission with intersecting axes. Author's certificate №806935, dated 23.02.81, bul. №7
26. Goldfarb, V.I.: Aspects of the problem of automation of gears and gearbox design. In: Gearing and Transmissions, N1, pp. 20–24. Izhevsk (1991)
27. Goldfarb, V.I., Nesmelov, I.P.: Dialogue system for the computer-aided design of spiroid gears. In: "Automated Design of Mechanical Transmissions", Abstracts of the scientific and technical conference, pp. 5–7. Izhevsk (1982)
28. Trubachev, E., Oreshin, A.: CAD system for spiroif gears. In: Jnl Informational mathematics, N1(3). Izdatelstvo physic-matematicheskoy literatury: Moscow, pp. 1590165 (2003)
29. Goldfarb, V.I., Trubachev, E.S.: Development and application of computer-aided design and tooth contact analysis of spiral-type gears with cylindrical worms. In: Technical Paper for AGMA FTM, USA, pp. 17–21 (2002)
30. Goldfarb, V.I., Glavatskikh, D.V., Trubachev, E.S., Kuznetsov, A.S., Lukin, E.V., Ivanov, D.E., Puzanov, V.Yu.: Spiroid Gears for Pipeline Valves. Veche, Moscow (2011)
31. Goldfarb, V., Malina, O., Trubachev, E.: New concept of the process of designing gearboxes and gear systems. In: Theory and practice of gearing and transmissions: in honor of professor Faydor L. Litvin. Springer International Publishing AG Switzerland, V. Goldfarb, N. Barmina Eds., Vol. 34, pp. 405–424 (2016)
32. Goldfarb, V. I., Trubachev, E. S., Puzanov, V. Yu.: New possibilities of non-orthogonal worm gears. In: Proceedings of the 3rd International Conference "Power Transmissions-09", Chalkidiki, Greece, pp. 139–144 (2009)
33. Trubachev, E., Mogilnikov, A.: Planetary mechanisms based on worm and spiroid gears. In: Advances in Mechanism and Machine Science: Proceedings of the 15th IFToMM World Congress on Mechanism and Machine Science, pp 915–924 (2019)
34. Trubachev, E.: Worm-type gear with steel gearwheel. In this volume
35. Goldfarb, V.I., Trubachev, E.S., Savelieva, T.V.: Unification of the hobs in spiroid gears. VDI Berichte, Unification of spiroid gears. In: Proceedings of the International Conference on Transmissions, Munich, Germany, pp. 1755–1759 (2005)
36. Trubachev, E., Loginov, S., Bogdanov, K., Khvatov, D., Shutkina A.: Efficient schemes and methods for gear machining of spiroid gearwheels and worms. In: Advanced Gear Engineering, Springer International Publishing AG Switzerland, V. Goldfarb, E. Trubachev, N. Barmina Eds., Vol. 51, pp. 465–480 (2018)
37. Trubachev, E.: On possibility of cutting bevel gearwheels by hobs, new approaches to gear design and production. In: New approaches to gear design and production, Springer International Publishing AG Switzerland, V. Goldfarb, E. Trubachev, N. Barmina Eds., Vol. 51, pp. 273–294 (2020)
38. Trubachev, E.: New possibilities of tooth cutting by running cutter heads. In: New approaches to gear design and production, Mechanisms and Machine Science 81, Springer International Publishing AG Switzerland, pp. 295–310 (2020)
39. Goldfarb, V.I., Kulemin, V.Yu.: Dynamic test bench for the fast rotors with big unbalance. In: Dynamics on mechanics systems. Reports 15 National Seminar, vol. 1, pp. 176–178, Varna (1990)
40. Goldfarb, V., Krylov, E., Elenski, A.: the first student international olimpiad on mechanism and machine science—the challenge in mms education. J. Mech. Eng. Autom. 3(3), 152–158 (2013)
41. Theory and practice of gearing and transmissions: in honor of professor Faydor L. Litvin. Springer International Publishing AG Switzerland, V. Goldfarb, N. Barmina Eds., Vol. 34, ISBN 978–3-319-19739-5, <https://doi.org/10.1007/978-3-319-19740-1> (2016)

42. Advanced gear engineering. Springer International Publishing AG Switzerland, V. Goldfarb, E. Trubachev, N. Barmina Eds., Vol. 51, ISBN 978-3-319-60398-8, <https://doi.org/10.1007/978-3-319-60399-5> (2018)
43. New approaches to gear design and production. Springer International Publishing AG Switzerland, V. Goldfarb, E. Trubachev, N. Barmina Eds., Vol. 81, ISBN 978-3-030-34944-8, <https://doi.org/10.1007/978-3-030-34945-5> (2020)

Some Exercises with Equations of Meshing: Review of Fundamental Manuscript



Veniamin Goldfarb

Abstract The manuscript by Professor V. I. Goldfarb discusses approaches to obtaining the equation of the enveloping surface for a one-parameter family of surfaces, which is usually called in the theory of gearing “the equation of meshing”. Professor V. I. Goldfarb shows, through relatively simple transformations (exercises in the author’s terms), the generality of this condition and the internal relation between the concepts and techniques used, obtained and used by different authors, who worked in different eras and in different fields of science—differential geometry, higher geometry, theory of gearing and theory of generating. The manuscript is of both fundamental and educational importance and serves to form a general concept of the processes of meshing and generating and to better understand these processes.

Keywords Equation of meshing · Theory of enveloping surfaces

1 Editors’ Comments

Dear readers, we offer to your attention a relatively small, but, in our opinion, interesting manuscript by Prof. V. I. Goldfarb, which was published in the journal “Gearing and Transmissions” 1, 2001 (Izhevsk, ISTU Publishing house). This edition had a very limited number, and not everybody had a chance to read it. Dr. Eng. Sergey Lagutin suggested to review it and reprint in this volume for a wider audience with this comment. This manuscript briefly describes the history of solving one of the fundamental questions in the theory of gearing—the question about the search for generated and meshing surfaces of teeth, the question about the “equation of meshing”, different versions of its representation and their application for solving the problems of gear analysis and synthesis are considered. V. I. Goldfarb is one of the founders of the currently prevailing non-differential methods for studying gears (see, in particular, the classical work by Neshmelov I. P. and Goldfarb V. I. Non-differential approach to solving the enveloping problem. *Mechanics of Machines* 61. Moscow,

V. Goldfarb (✉)

Scientific Department “Institute of Mechanics Named After Professor V. I. Goldfarb”,
Kalashnikov Izhevsk State Technical University, Izhevsk, Russia
e-mail: truba@istu.ru

Nauka, pp. 3–10 (1983) or a more recent paper by Goldfarb V. I. The non-differential method of the geometrical modeling of the enveloping process. In: Proceedings of 9th World Congress on the Theory of Machines and Mechanisms, vol. 1, pp. 424–427, Milano (1995). And it is therefore more interesting for the reader to get acquainted with his evaluation of analytical methods of gearing research. Besides, in our opinion, the importance of this work is to summarize the efforts of the scientists who worked on the methods of searching for enveloping surfaces in different fields—basically higher and differential geometry (to which the question goes back), theory of gearing, theory of generating, and theory of cutting tools. Although the question of fundamental methods for calculating the meshing surfaces in the modern theory of gearing and theory of generating is, as we see it, solved with the exhaustive completeness for common applications, the generalization made by Prof. Goldfarb, finding general theoretical assumptions, concepts and regularities, in our opinion, serves to better modern understanding of this issue. We also see the great educational value of the published manuscript; it is of fundamental importance and allows the contemporaries who apply and improve numerical methods of simulation not to lose sight of the very essence of the meshing process. Let us also pay attention to the fact that although Prof. V. I. Goldfarb stipulated the case of meshing of two gear elements rotating relative to their stationary axes at the very beginning, in principle the approach and all calculations are easily extended to more general cases of meshing and generating, including processes with other motions and multiple coordinate transformations—to those cases which are reduced to the enveloping process of one-parameter families of surfaces.

2 Introduction

The role of the equation of meshing in the theory of gearing is well known [1, 2, 3 and many others]. This is the fundamental equation used for solving both the basic problem of enveloping—the problem of finding coordinates of enveloping surface points (the enveloping process is of fundamental importance for the theory and practice of gearing)—and many other problems associated with determination of geometric and kinematic parameters of meshing for practically all types of gears. Quite a few modifications of this equation are known; they are based on different approaches to the equation derivation [1–7 and others]. These modifications made possible detecting certain properties of lines which take part in generation (the term ‘generation’ implies here first of all the derivation of the equation in the first place) of enveloping surfaces.

This paper shows certain transformations of the equation of meshing made by the author on the basis of the classical differential approach, which show opportunities of different ways to derive and analyze this equation. In author’s opinion, results described below are mainly of theoretical interest, since in modern practice numerical methods for solution of the above-mentioned enveloping problem are usually used, which in some cases (and, maybe, more often) simulate the enveloping process

in a more adequate manner, than the classical differential approach with all its modifications. Nevertheless, classical analytical techniques are, first of all, of fundamental importance, and, second, sometimes they can be much more efficient, resultant, and precise than numerical ones (examples of such cases the author learned from a fruitful discussion with the well-known gear scientist S. A. Lagutin).

3 Classical Differential Approach

Let $F_1(x_1, y_1, z_1) = 0$ be the equation of the enveloped surface in the coordinate system S_1 related to this surface; $F_2(x_2, y_2, z_2, \varphi_1, u_{12}) = 0$ is the equation of a family of surfaces F_1 in the system S_2 related to the enveloping surface; φ_1 is the parameter of enveloping—for gears it is the angle of rotation of S_1 along with F_1 with respect to some fixed system S ; $u_{12} = \varphi_1/\varphi_2$ is the gear ratio of a gear, φ_2 is the angle of rotation of S_2 with respect to S . Therefore, points which belong to the enveloping surface are located within the set of solutions of the system [8, 9]

$$F_2(x_2, y_2, z_2, \varphi_1) = 0, \quad \partial F_2(x_2, y_2, z_2, \varphi_1)/\partial \varphi_1 = 0 \quad (1)$$

The second equation of this system which is called the condition of attachment [6] or—in theory of gearing—the equation of meshing, can be represented as

$$\frac{\partial F_2}{\partial x_2} \cdot \frac{\partial x_2}{\partial \varphi_1} + \frac{\partial F_2}{\partial y_2} \cdot \frac{\partial y_2}{\partial \varphi_1} + \frac{\partial F_2}{\partial z_2} \cdot \frac{\partial z_2}{\partial \varphi_1} = 0 \quad (2)$$

Here, at the point of contact of the enveloped and enveloping surfaces, the function F_2 must be differentiable and its partial derivatives $\partial F_2/\partial x_2$, $\partial F_2/\partial y_2$, $\partial F_2/\partial z_2$ must not turn to zero simultaneously.

At the fixed value of the enveloping parameter φ_1 Eq. (1) determine the line of contact of the enveloped and enveloping surfaces. And elimination of φ_1 from the Eq. (1) will determine the enveloping surface in S_2 . In order to find coordinates of points of the contact line in S_1 or in the fixed system S , with respect to which the arrangement of fixed systems S_1 and S_2 is assigned, it is necessary to use formulae of transition from S_2 to S_1 and S , correspondingly.

The described classical approach appeared in the analysis [8], and it is commonly applied in the differential geometry [9, etc.].

Improvement of the classical approach proposed by Gochman [1] allows for deriving the equation of meshing in any coordinate system, and exactly in the system in which it is preferred to obtain the equation of contact lines (as a rule, in the fixed system S or S_1 with which the initial (enveloped) surface is related). For this purpose, Kh. I. Gokhman applied formulae of transformation of coordinates and differential relations derived by differentiating these formulae over the enveloping parameter, which is the angle of the driving link rotation φ_1 . The obtained set of equations is equivalent to the system (1) in its mathematical sense, but application of the former

simplifies determination of lines of contact of mutually enveloped surfaces and the enveloping surface.

For instance, if we need to obtain the equation of contact lines in S_1 , then the system (1) should be rewritten in the form

$$\begin{aligned} F_1(x_1, y_1, z_1) = 0, \text{ a),} \\ \frac{\partial F_1}{\partial x_1} \cdot \frac{\partial x_1}{\partial \varphi_1} + \frac{\partial F_1}{\partial y_1} \cdot \frac{\partial y_1}{\partial \varphi_1} + \frac{\partial F_1}{\partial z_1} \cdot \frac{\partial z_1}{\partial \varphi_1} = 0, \text{ b),} \end{aligned} \quad (3)$$

where $\bar{r}_1 = \bar{r}_1(x_2, y_2, z_2, \varphi_1, u_{12})$, \bar{r}_1 is the position vector of the point in S_1 , determined by coordinates x_1, y_1, z_1 . u_{12} is the gear ratio relating φ_1 and φ_2 . And in order to replace x_2, y_2, z_2 by x_1, y_1, z_1 in partial derivatives $\partial \bar{r}_1 / \partial \varphi_1$, one must use reverse formulae of coordinate transformation $\bar{r}_2 = \bar{r}_2(x_1, y_1, z_1, \varphi_1, u_{12})$.

The method of Ch. I. Gochman was developed and widely applied by Kolchin [2, 4] for analysis of numerous types of specific gearing.

The method that gained an extensive application in the theory of gearing was developed by Shishkov [10], Davydov [11], and Litvin [3]; this method was called ‘kinematic method’ [3]. According to this method, contact points of mutually enveloped surfaces can be determined by the following equation of meshing

$$\bar{n}_1 \cdot \bar{V}_{S1} = n_{x_1} \cdot V_{Sx_1} + n_{y_1} \cdot V_{Sy_1} + n_{z_1} \cdot V_{Sz_1} = 0, \quad (4)$$

and which states analytically the fact that in the mentioned contact points the relative velocity vector \bar{V}_{S1} lies in the common plane which is tangent to common surfaces. Here \bar{n}_1 is the vector of the normal line to the enveloped surface in S_1 .

It is easy to see that (4) is identical to (3b). Indeed, derivatives $\partial F_1 / \partial x_1, \partial F_1 / \partial y_1, \partial F_1 / \partial z_1$ are proportional to direction cosines of the normal line to the surface F_1 in the system S_1 , and $\partial x_1 / \partial \varphi_1, \partial y_1 / \partial \varphi_1, \partial z_1 / \partial \varphi_1$ are projections of the relative velocity vector in this system.

The equation of meshing can be derived in any coordinate system by writing projections of vectors \bar{n}_1 and \bar{V}_{S1} . In a fixed coordinate system this equation has the form $\bar{n} \cdot \bar{V}_S = 0$, and in S_2 it is $\bar{n}_2 \cdot \bar{V}_{S2} = 0$.

4 Exercises with the Equation of Meshing

Let us consider another form of representation of the equation of meshing by writing the transition from S_1 to S_2 as

$$\bar{r}_2 = \mathbf{M}\bar{r}_1 + \bar{A}, \quad (5)$$

where \mathbf{M} is the matrix whose elements are cosines of angles between axes S_1 and S_2 :

$$\mathbf{M} = \begin{pmatrix} c_{11} & c_{12} & c_{13} \\ c_{21} & c_{22} & c_{23} \\ c_{31} & c_{32} & c_{33} \end{pmatrix}, \quad (6)$$

\bar{A} is the position vector of the origin of the system S_1 in S_2 :

$$\bar{A} = \begin{pmatrix} A_{x_1} \\ A_{y_1} \\ A_{z_1} \end{pmatrix}. \quad (7)$$

Let us differentiate (5) with respect to φ_1 :

$$\frac{\partial \bar{r}_2}{\partial \varphi_1} = \frac{\partial \mathbf{M}}{\partial \varphi_1} \cdot \bar{r}_1 + \frac{\partial \bar{A}}{\partial \varphi_1}. \quad (8)$$

Let us multiply (8) by the transposed matrix \mathbf{M}^T and then scalarwise multiply the product by \bar{n}_1 . Thus we will obtain

$$\begin{aligned} \mathbf{M}^T \cdot \frac{\partial \bar{r}_2}{\partial \varphi_1} &= \mathbf{M}^T \cdot \frac{\partial \mathbf{M}}{\partial \varphi_1} \cdot \bar{r}_1 + \mathbf{M}^T \cdot \frac{\partial \bar{A}}{\partial \varphi_1}, \\ \bar{n}_1 \cdot \left(\mathbf{M}^T \cdot \frac{\partial \bar{r}_2}{\partial \varphi_1} \right) &= \bar{n}_1 \cdot \left(\mathbf{M}^T \cdot \frac{\partial \mathbf{M}}{\partial \varphi_1} \cdot \bar{r}_1 + \mathbf{M}^T \cdot \frac{\partial \bar{A}}{\partial \varphi_1} \right) \end{aligned} \quad (9)$$

Since $\bar{n}_1 \cdot \left(\mathbf{M}^T \cdot \frac{\partial \bar{r}_2}{\partial \varphi_1} \right) = (\mathbf{M} \cdot \bar{n}_1) \cdot \frac{\partial \bar{r}_2}{\partial \varphi_1} = \bar{n}_2 \cdot \frac{\partial \bar{r}_2}{\partial \varphi_1}$ and $\bar{n}_2 \cdot \frac{\partial \bar{r}_2}{\partial \varphi_1} = 0$ according to (2), then the equation of meshing will take the form

$$\bar{n}_1 \cdot (\mathbf{M}^* \cdot \bar{r}_1 + \bar{A}^*) = 0, \quad (10)$$

where $\mathbf{M}^* = \mathbf{M}^T \cdot \frac{\partial \mathbf{M}}{\partial \varphi_1}$ is skew-symmetric matrix of the form

$$\mathbf{M}^* = \begin{pmatrix} 0 & -R & Q \\ R & 0 & -P \\ -Q & P & 0 \end{pmatrix}$$

whose elements Q, R, P are, in accordance with [12], as follows:

$$\left. \begin{aligned} Q &= c_{11} \cdot \frac{\partial c_{13}}{\partial \varphi_1} + c_{21} \cdot \frac{\partial c_{23}}{\partial \varphi_1} + c_{31} \cdot \frac{\partial c_{33}}{\partial \varphi_1}, \\ R &= c_{12} \cdot \frac{\partial c_{11}}{\partial \varphi_1} + c_{22} \cdot \frac{\partial c_{21}}{\partial \varphi_1} + c_{32} \cdot \frac{\partial c_{31}}{\partial \varphi_1}, \\ P &= c_{13} \cdot \frac{\partial c_{12}}{\partial \varphi_1} + c_{23} \cdot \frac{\partial c_{22}}{\partial \varphi_1} + c_{33} \cdot \frac{\partial c_{32}}{\partial \varphi_1} \end{aligned} \right\} \quad (11)$$

and the vector \bar{A}^* has the form

$$\bar{A}^* = \frac{\partial \bar{A}}{\partial \varphi_1} \cdot \mathbf{M}^T = \begin{pmatrix} \xi \\ \eta \\ \zeta \end{pmatrix} = \begin{pmatrix} c_{11} \cdot \frac{\partial A_{x_1}}{\partial \varphi_1} + c_{21} \cdot \frac{\partial A_{y_1}}{\partial \varphi_1} + c_{31} \cdot \frac{\partial A_{z_1}}{\partial \varphi_1} \\ c_{12} \cdot \frac{\partial A_{x_1}}{\partial \varphi_1} + c_{22} \cdot \frac{\partial A_{y_1}}{\partial \varphi_1} + c_{32} \cdot \frac{\partial A_{z_1}}{\partial \varphi_1} \\ c_{13} \cdot \frac{\partial A_{x_1}}{\partial \varphi_1} + c_{23} \cdot \frac{\partial A_{y_1}}{\partial \varphi_1} + c_{33} \cdot \frac{\partial A_{z_1}}{\partial \varphi_1} \end{pmatrix}. \quad (12)$$

After substituting \mathbf{M}^* and \mathbf{A}^* in (10) and simple transformations, the equation of meshing will be derived in the form

$$n_{1x_1}(-Ry_1 + Qz_1) + n_{1y_1}(Rx_1 - Pz_1) + n_{1z_1}(-Qx_1 + Py_1) + n_{1x_1} \cdot \xi + n_{1y_1} \cdot \eta + n_{1z_1} \cdot \zeta = 0, \quad (13)$$

or, finally,

$$\begin{vmatrix} n_{1x_1} & n_{1y_1} & n_{1z_1} \\ P & Q & R \\ x_1 & y_1 & z_1 \end{vmatrix} + n_{1x_1} \cdot \xi + n_{1y_1} \cdot \eta + n_{1z_1} \cdot \zeta = 0. \quad (14)$$

The equation of meshing in the form (14) is derived in [12, 13] in a somewhat different way, while Yegorov [12] states this equation to be the condition of identifying the family of lines (characteristics, contact lines) on the enveloped surface which ‘allow distribution’.

Equations (10), (13), (14) (the first one is in the vector form, the others are in the coordinate form) are equations of the linear set of normal lines. This can be shown, in particular, as follows.

Six components of the Eq. (14)

$$\begin{vmatrix} n_{1y_1} & n_{1z_1} \\ y_1 & z_1 \end{vmatrix}, \begin{vmatrix} n_{1z_1} & n_{1x_1} \\ z_1 & x_1 \end{vmatrix}, \begin{vmatrix} n_{1x_1} & n_{1y_1} \\ x_1 & y_1 \end{vmatrix}, n_{1x_1}, n_{1y_1}, n_{1z_1}$$

are six Pluecker coordinates [12] of the normal line to the initial surface. Since values $P, Q, R, \xi, \eta, \zeta$ in [14] depend only on φ_1 , when $\varphi_1 = const$ these values are constant, and the above-mentioned Pluecker coordinates determine a certain family of normal lines called the linear complex [14], which varies with variation of φ_1 .

We can see then that normal lines \bar{n}_1 belonging to the above-mentioned linear set coincide with beams of the instantaneous screw of relative movement. To do so, let us rewrite the Eq. (1) assuming that the initial surface is defined in the explicit form $z_1 = z_1(x_1, y_1)$, in the following manner:

$$\begin{aligned} \frac{\partial z_1}{\partial x_1} \cdot (-Ry_1 + Qz_1) + \frac{\partial z_1}{\partial y_1} \cdot (Rx_1 - Pz_1) + (Qx_1 - Py_1) \\ + \frac{\partial z_1}{\partial x_1} \cdot \xi + \frac{\partial z_1}{\partial y_1} \cdot \eta - \zeta = 0 \end{aligned}$$

or, after grouping:

$$\frac{\partial z_1}{\partial x_1} \cdot (-Ry_1 + Qz_1 + \xi) + \frac{\partial z_1}{\partial y_1} \cdot (Rx_1 - Pz_1 + \eta) = (-Qx_1 + Py_1 + \zeta) \quad (15)$$

The Eq. (15) is the equation of a helicoid [15] whose axis coincides with the axis of the instantaneous screw of relative movement, and the screw parameter [14]

$$P_M = \frac{P\xi + Q\eta + R\zeta}{P^2 + Q^2 + R^2}$$

coincides with that of the instantaneous screw of the relative movement.

This property of normal lines shown in a different way was commonly used in papers by Altmann [16], Nikolayev [17], Pismanik [18], Zlatopolsky [19] and other authors to determine the points of contact lines.

Another property can be found, if one compares the Eq. (13) with the equation of the so called ‘zero-system’ [14]. It can be shown, that normal lines n_l belonging to the zero-system defined by (13) must intersect certain lines—conjugate polar lines [14] whose role in the theory of gearing is played by axes of meshing [3, etc.].

Analysis of equations of meshing written in different forms allows for revealing of other interesting properties [20] that can be used to develop different methods of determining points of contact lines and enveloping surfaces. The described methods can be considered as the development of the classical differential approach to solution of the enveloping problem.

References

1. Gochman, Ch.I.: Theory of Gearing, Generalized and Developed by Analysis. Odessa (1886)
2. Kolchin, N.I.: Analytical Investigation of Planar and Spatial Gearing. Mashgiz, Moscow (1949)
3. Litvin, F.L.: Theory of Gearing, 2nd edn. Nauka, Moscow (1968)
4. Kolchin, N.I.: Method of the screw complex in the theory of spatial gearing. In: Proceedings of the 3rd Meeting on Basic Problems of MSS. Theory of Gears in Machines, pp. 7–18. Moscow, Mashgiz (1963)
5. Sheveleva, G.I.: Solution for one problem of the enveloping theory. Mashinovedeniye **6**, 48–53 (1976)
6. Zalgaller, V.A.: Theory of Envelopes Moscow, Nauka (1976)
7. Lagutin, S.A.: Envelope singularities and tooth undercutting in rack and worm gearing. In: Proceedings of International Conference on Gearing, Transmissions and Mechanical Systems, pp. 99–108. Nottingham (2000)
8. Monge, G.: Application of Analysis to Geometry. ONTI, Moscow (1936)
9. Rashevsky, P.K.: Course of Differential Geometry. Moscow-Leningrad, GONTI (1938)
10. Shishkov, V.A.: Formation of Surfaces by Cutting by Means of Running-in. Mashgiz, Moscow (1951)
11. Davydov, Ya.S.: Non-involute Gearing. Moscow, Mashgiz (1950)
12. Egorov, D.F.: Works on Differential Geometry. Nauka, Moscow (1970)

13. Zamoruev, G.B.: Two algorithmic forms of the equation of meshing. *Izvestiya Vuzov. Eng.* **10**, 64–68 (1977)
14. Klein, F.: *Higher geometry*. Moscow-Leningrad, GONTI (1939)
15. Kamke, E.: *Reference book on differential equations with the first order partial derivative*. Fizmatgiz, Moscow (1966)
16. Altmann, F.: *Bestimmung des Zahnflankeneingriffs bei allgemeinen Schrauben-getrieben*. Forschung aus dem Gebiete des Ingenieurwesens, Sept.-Okt. (1937).
17. Nikolayev, A. F.: *Screw diagram and its application to determining conjugate linear surfaces with linear contact*. In: *Proc. of the seminar on MMS*, vol. X, 37, 52–106. Publishing House of the Academy of Sciences of the USSR (1950).
18. Pismanik, K.M.: *Hypoid gears*. Machine Engineering, Moscow (1964)
19. Zlatopolsky, M. D.: *Fundamentals of the conjugation theory and new methods of research and design of spatial gearing*. In: *Works of the Leningrad Technological Institute named by Lensovet*, Iss. 32 (1955).
20. Lyukshin, V. S.: *On some issues of the enveloping theory and its application in the tool theory*. In: *Works of First All-Union Geometrical Conference*, 69–70. Kiev (1962).

Challenges of Mechanical Engineering and in IFToMM: Yesterday and Tomorrow



Marco Ceccarelli 

Abstract Will mechanical engineering and mechanical systems have an important role in the technological development of society in the past? Yes, Of course! Analyzing the past one can understand future trends, with motivations, situations, solutions, characters and experiences that have determined the past success of mechanical engineering as the first engine of society's development. This lecture paper illustrates examples of machines with their inventors and developments not only to emphasize the past role and impact of mechanical engineering, but to motivate the future role of mechanics in an ever more IT-based world. The characteristics of future machines are discussed (with less mechanical elements, but more essential ones) and the requirements that mechanical engineering must address (with always more integrated disciplines) for innovative and / or updated solutions with attention to the environment, efficiency, reduced size, affordable cost and attractive forms, inside and outside of a scientific and professional community in continuous evolution (even with a fragmentation of identities). An outline of History of IFToMM is presented on how IFToMM have been evolved and affected also from non-technical aspects including community and social developments. This paper gives main information on main milestones in IFToMM History, including a memory of prof Veniamin Goldfarb with his activity and significant role in IFToMM.

Keywords History of mechanical engineering · History of machines · TMM · MMS · IFToMM · History of IFToMM

1 Introduction

Challenges in Mechanical Engineering are usually considered in terms of novel achievements both for knowledge for science developments and solutions for practical applications to improve production activities and welfare of diary life, as pointed out for example in [1]. It is well recognized the impact that modern engineering can

M. Ceccarelli (✉)

Laboratory of Robot Mechatronics, Department of Industrial Engineering, University of Rome Tor Vergata, 00133 Rome, Italy

e-mail: marco.ceccarelli@uniroma2.it

have in more and more areas of human activities with novel solutions and user/cost-oriented systems with communities that continuously enlarge the horizons of activity goals. Novelty is considered a primary target in challenging new achievements and this addresses a great attention to Innovation as related to protection of intellectual property, technological transfer, and successful application.

Those challenges for Mechanical Engineering can be considered from several viewpoints, such as technical or financial ones as reported in a rich literature that is available even from each aspect of the innovation activity referring to surveys and trends, since the early days of modern engineering. But also, aspects and impact in social life are determinant to motivate activities and future plans in engineering. Particularly, mechanical engineering can be considered of primary interest as related to mechanical aspects that impact and help the human behavior and life. References are included in this paper as per its character as mainly based on a personal experience of the author as in the reference list, although surveys and trends are discussed by other many authors also from different perspectives.

In this paper a discussion is focused on aspects that are related to the mechanical structure of modern systems as key design issue both in structure and operation with human-like capabilities and interactions when considering that assigned tasks are aimed at either substituting or helping human operators with tele-operated/supervision modes or fully intelligent autonomous work. The paper gives accounts on aspects of the role of mechanism design in system developments as based on the fact that the operation of modern systems performing their tasks, either in coordination or not with human operators, is yet of mechanical nature due to motion and force transmission goals of the operation aims. The challenges of mechanism design of systems are presented both in terms of technical solutions and community activity, since each other depends, impacts, and generates the other. Specific attention is reported on community aggregation as result and source of technical- scientific activities with a special eye to the IFToMM community, with a vision of still strong significance for the future.

2 Mechanism Design in Mechatronic Systems for Innovation

Today, Innovation is stressed as a multidisciplinary activity to produce technological developments for practical implementations for benefits both of their producers and users within society improvements. In the last decades Science achievements have made possible new engineering developments (and vice versa!) in many fields with evolutions that have been much faster than in the past, as noted for example in [1, 2]. Aspects and trends of multidisciplinary activity are today discussed and solicited from many viewpoints towards Innovation sometimes with overestimation of specific experience and expertise of the innovation actors.

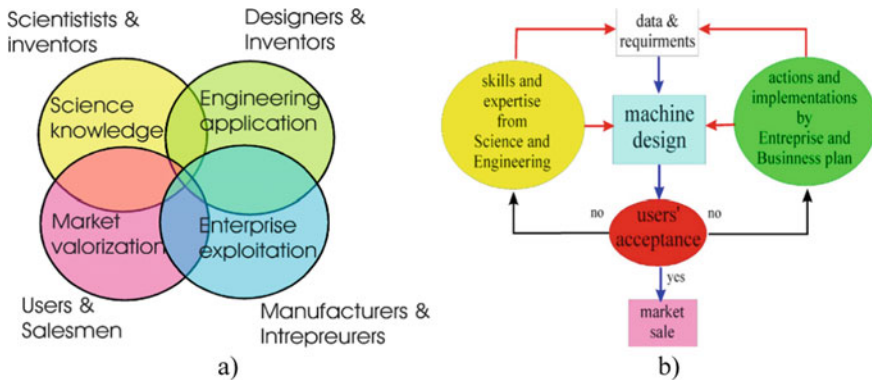


Fig. 1 Scheme of activity for: **a** Innovation; **b** synergic design of mechanical systems

Figure 1a summarizes concepts related to innovation as produced and exploited by individual actors within a multidisciplinary frame of several different areas. Indeed, the success of innovation requires that all these aspects will concur synergically to a final definition and implementation of an innovative product/idea for the usage by a large community or public. It is to note the innovation is strongly based on technical ideas/achievements, but its success can be achieved only thanks other non-technical factors, as pointed out in [1–3].

Innovation in modern mechanical systems can be recognized in developments for Science knowledge and novel solutions both with mechatronic systems and their operations in new areas and public fruition at proper level of complexity and cost by complementing technical issues with the other aspects and needs coming from the other disciplines per innovation activities, as summarized in the scheme in Fig. 1b.

3 Examples of Past Designs with Modern Contents

Innovative solutions of machines and mechanisms can also be inspired by solutions from the past as well as from the first century BC. the Roman engineer Frontinus commented with the observation ‘there is nothing new except what has been forgotten’. Few cases are reported as examples of a rich background in past and recent solutions, as for example discussed in [4, 5] on practical design and theoretical developments.

Figures 2 and 3 show emblematic examples of this aspect as related to conceptual solutions that can be identified in past machine designs and solutions as a source of inspiration for future developments as well as rigorous recognition of the state of the art in the design of specific systems. In particular, Fig. 2a shows an automatic wood sawing machine reported by Villard de Honnecourt in the thirteen century with a mechanism used to guide the saw with a solution that can be interpreted as

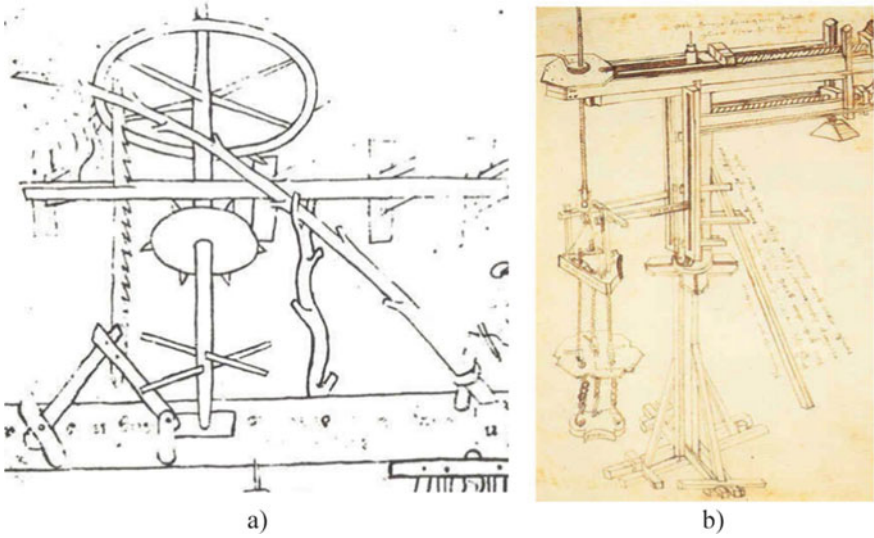


Fig. 2 Examples of modern-like mechanism design form the past: **a** automatic wood sawing machine of thirteenth century with a four-bar or five-bar mechanism coupler guiding the saw; **b** a crane design of 14th century with belt system as cable parallel manipulator for load handling

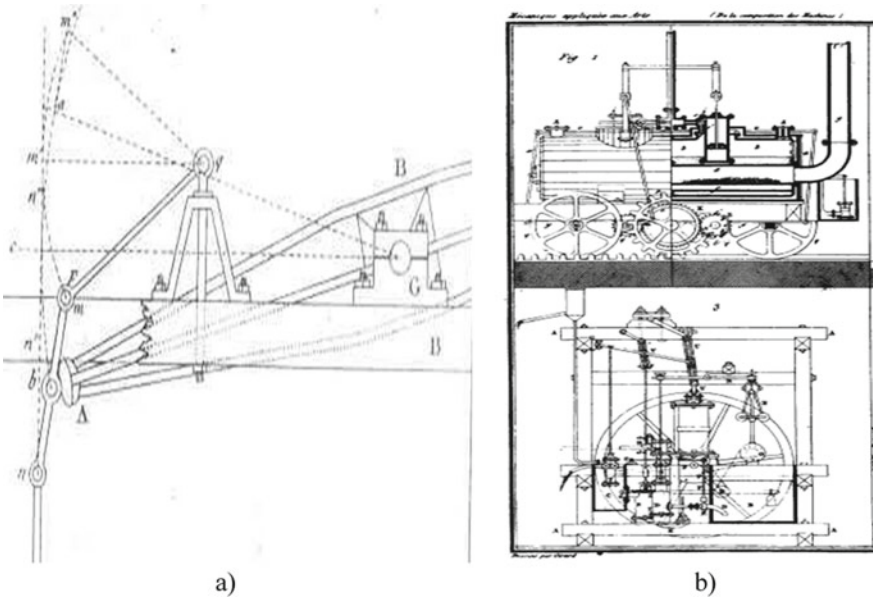


Fig. 3 An example of innovation by a four-bar mechanism: **a** the Watt mechanism design for linear guiding of steam engine piston; **b** application of the steam engine with Watt mechanism in locomotive at the beginning of Industrial Revolution

a quadrilateral or a five-bar linkage with its coupler curve usage, well before the innovation attributed to James Watt. Figure 2b shows a surprising drawing of a crane design by Filippo Brunelleschi crane in the fourteen century for the construction of the Duomo of Florence in which the characteristics of a parallel manipulator can be recognized with the purpose of controlling the pendular movement and increase of the load capacity, with a functionality believed to be developed only a few decades ago.

In the past, as today, innovation can be determined by innovative solutions but also by innovative uses of existing mechanisms as reported in the example of Fig. 3 that is related to the famous Watt mechanism. It should be noted that the mechanisms were well known and used extensively but not always used and exploited for all their capabilities, as well as being often not considered existing analogous solutions (see for example Fig. 2a). Figure 3a shows the original design of the Watt mechanism which uses a connecting coupler point to guide the head of a piston of a steam engine, determining an innovative solution that has increased the efficiency of the engine with immense repercussions during the industrial revolution. An example of this technological impact with effects also in the social frames is shown in Fig. 3b where the Watt mechanism is used with the steam engine to give power to a locomotive vehicle.

4 Examples of Modern Mechanism Designs for Robotics

Mechanism design can be considered an important item in design procedures for new robot systems when considering the mechanical nature of the structure and task to be achieved in application and usage of robots.

Figure 4 summarizes main concepts and activities of the design process of robot systems considering a central role for mechanism design as related to the challenges for Innovation expectations from a perspective giving a key role to the mechanical design for matching operation and design issues in robot features, as also outlined for example in [1, 3]. Although the scheme shows a sequential order of the activities, the design process can be considered iterative or even with (reiterative) implications from one aspect to another. The technical aspects in the first step can be considered completed with intellectual achievements to be protected either with patents or publications in order to ensure a technological transfer as well as dissemination and cultural share with new formation outcomes. Those aspects can be also developed during the next phase of production exploit with involvement of entrepreneurs and manufacturing frames. An innovation character is definitively identified when a market valorization of the well-directed service solution is achieved successfully with large/proper sales of the innovative product after or because the users' acceptance and satisfaction for a large public fruition. This last aspect refers to the impact of a proposed innovation both from social and financial viewpoints for an expected long duration.

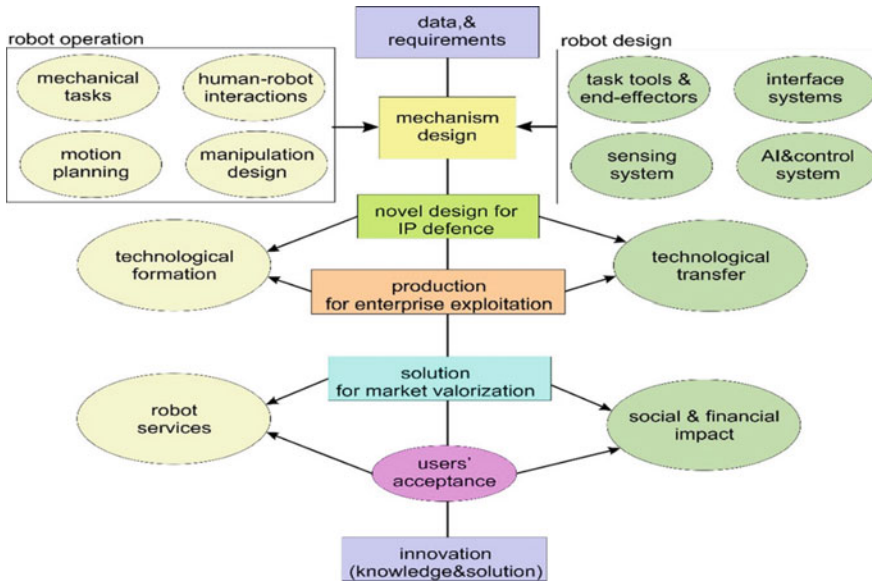


Fig. 4 A flowchart for mechanism design for robots with aspects for innovation aims in Fig. 2

Figures 5, 6, 7 and 8 illustrate examples of how mechanisms play a central role in the design and functionality of robotic systems for various applications. In particular, Fig. 5 refers to an emblematic example in which the structure of a deployable mechanism plays a central role in the robotic structure of systems for various applications. It should be noted that the innovation proceeding from a solution developed in mathematical fields with an initial innovative result in the toys of Fig. 5a

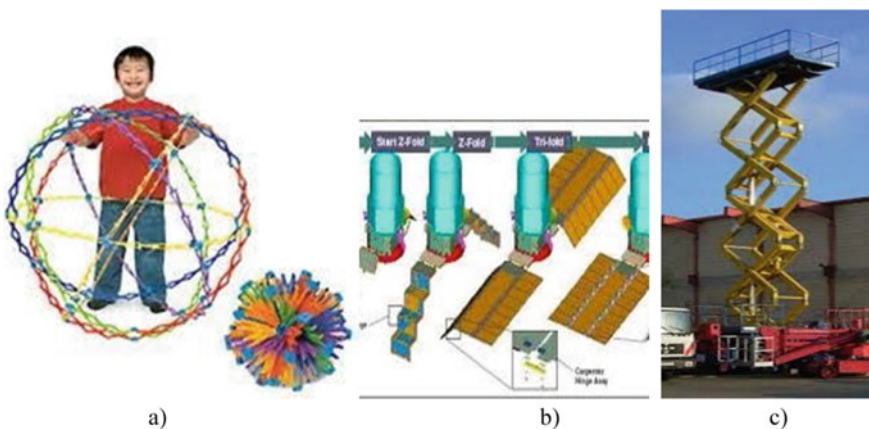


Fig. 5 An example of a deployable mechanism source for innovation: **a** in toy design; **b** antenna package for space satellites; **c** for load lifting machines

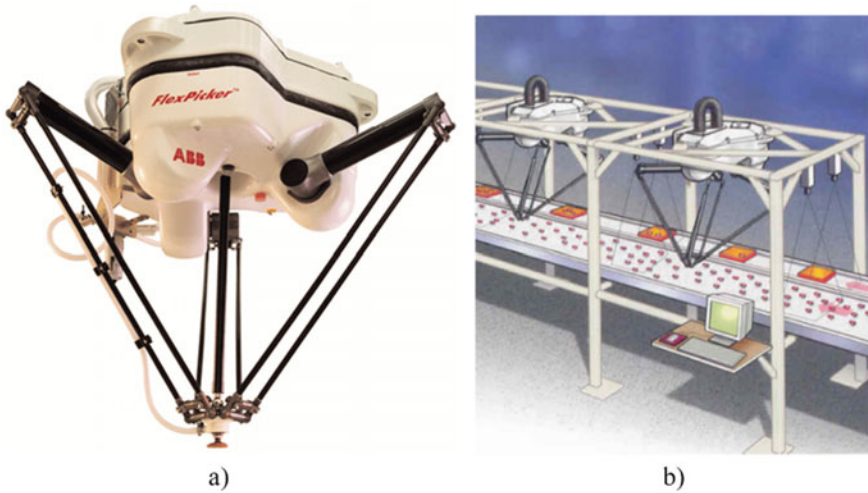


Fig. 6 An example of modern linkage mechanism in robots: **a** DELTA robot; **b** its usage in fast pick-place application in food industry

and subsequently with the concept of general deployable mechanisms also had an impact in structures of different application areas as represented in the Fig. 5b, c. Figure 6 shows an example of an innovative application of the articulated structure of mechanisms in an innovative robot solution such as that of the DELTA robot, which was conceived and designed by Raymond Clavel in 1988 with immediate effects in successful applications in industrial fields. and not, like the one shown in Fig. 6b for the food industry.

Figures 7 and 8 refer to direct experiences of the author, who developed innovative robot solutions by centering the structural design on the use and conception of mechanisms suitable for the application purposes. In particular, Fig. 7 refers to a humanoid robot structure such as LARMbot [6–8], that is based on structures with parallel architecture both for the legs and for the torso thus giving the possibility to the robot high payload capacities and remarkable stiffness in operation. It should be noted in this innovative solution of robot humanoid the role not only of the structure but also functionality of the parallel architecture mechanisms is used with innovative purposes by adapting already well-known structures of parallel manipulators. Figure 8 shows the design and application experience of cable mechanisms [9–11], with still parallel structure as per the current hot interest in the development of a motion assistance exoskeletons as it has been applied in solutions for the elbow and ankle. The conceptual solution in Fig. 8a emphasizes the essential role of the mechanism both in the structure of the medical device and in its motion assistance functionality.

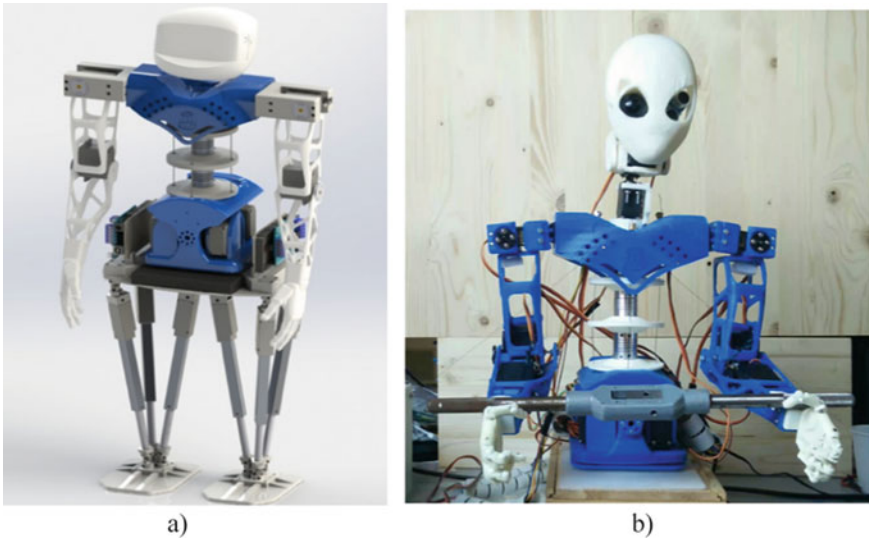


Fig. 7 An example of modern linkage mechanism in robots by author’s experience: **a** LARMbot humanoid robot design; **b** the trunk design with serial-parallel mechanism

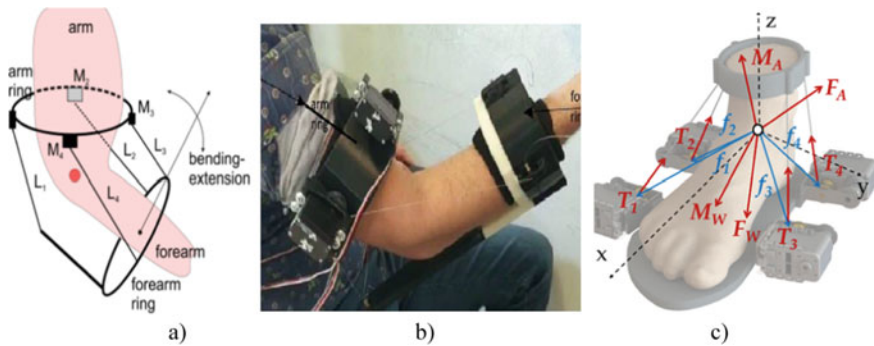


Fig. 8 An example of modern linkage mechanism in medical devices by author’s experience: **a** design scheme for cable-driven mechanism; **b** CADEL prototype; **c** CableAnkle design

5 Impact and Fame of Inventors: Past Lights and Modern Limits

A peculiar aspect of innovation activities is linked to the personality and recognition of this personality of inventors and designers, who today are not duly celebrated and repaid for the intellectual, human and financial efforts in their activities. The examples of Figs. 9 and 10 want to summarize a historical development and a current state of aspect for which in the past the merit of inventors and designers



Fig. 9 An example of impact and fame in the past: **a** Dorando Petri, a sport man; **b** Franz Reuleaux, mechanism designer figure

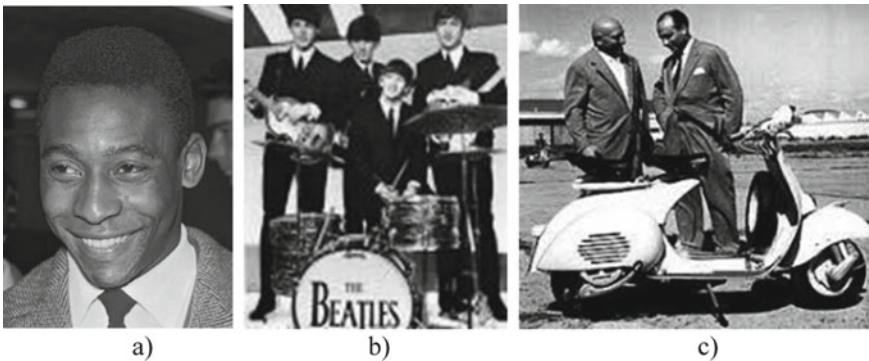


Fig. 10 An example of today impact and fame: **a** Pelè, soccer player; **b** the Beatles, music players; **c** Corradino D'Ascanio, designer of Vespa scooter

was widely and dutifully recognized much more than is done today with respect to social-media impacting figures, such as sportsmen and musicians considering that the formers produce well-doing and lasting benefits for individuals and society while the latters, nowadays over well paid and celebrated, are capable of producing only limited moments of personal satisfaction. Figure 9 shows how at the end of the nineteenth century Professor Franz Releuax, inventor and mechanical engineering scientist, was much better known and celebrated than the sportsman Dorando Petri even though he was the winner of the first modern Olympics. In Fig. 10 that is related to our days in the modern era, the ephemeral merits of cocker player like Pelè and musicians like the Beatles are much more recognized, who still produce ephemeral results without producing lasting and structured well-being for an improvement in

society and lifestyles as they can in reality to achieve the products of a technical-scientific innovation by inventors and scientists such as the one shown in the figure for the Vespa scooter of planetary success by the engineer of D'ascanio.

Figure 10 actually poses a crucial question and addresses considerations especially in the context of a large public and of the new generations for which the figures of inventors and scientists are of lesser importance and less attractive than those social-media impacting figures such as those cited by soccer player and musicians. What actions can be planned, and even which consequences of scientific technological innovation can re-establish a correct evaluation of merits and therefore attract the best forces of society for the improvement of society itself?

6 Aggregation in Societies and IFToMM Role

Innovations is produced by inventors both coming from a community and producing community. Significance of innovation is produced and supported by a corresponding community and particularly significant example can be considered the history and role of IFToMM in Robotics and MMS at large, as outlined for example in [2, 3].

Processes of aggregation in communities of people with specific interests and needs are motivated by being able to have a greater visibility and impact in the recognition of results and in their influence on the aspects in which the community works. Aggregation is also an index of how significant the corresponding activity is both numerically and socially and therefore it is also a reason and at the same time a source of innovation. Unfortunately, recently it must be noted that the new generations do not fully understand the benefits and potential of a community aggregation also considering that today's (internet) communication technology allows a virtual aggregation, even temporal, which seems to satisfy the new generations without the need for a legalized and lasting forms of aggregation. In the field of mechanical engineering, however, the aggregation is significant and of important reference in national and international societies in specific and even broad-ranging technical-scientific fields for which IFToMM can be indicated as an important example.

The structure of IFToMM worldwide federation is summarized in Fig. 11a in terms of IFToMM bodies (www.iftomm.net) with mission to provide leadership for cooperation and development of modern results in MMS at international levels with technological transfers for the benefit of the society with clear aims toward innovation. The bodies of IFToMM are the General Assembly (GA), Executive Council, GA Committees on Constitution, Nominating, and Honours, Technical Committees (TCs), and Permanent Commissions (PCs). The structure and activities of PCs and TCs are aimed at promoting and improving specific MMS fields with researchers and practitioners, including young individuals as outlined in Fig. 11b.

IFToMM itself can be considered an innovation result (as founded in 1969) when it is recognized as a product of new attention to a community working for developments of MMS. Significant examples of contributions of IFToMM with innovation contents can be summarized both in community aggregation and identification for research

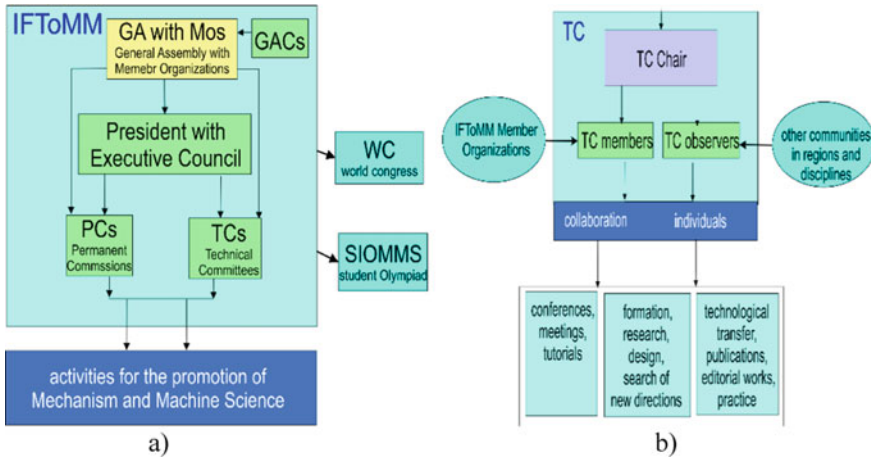


Fig. 11 A scheme of IFToMM: **a** bodies in the federation structure; **b** TC organization and activity

trends of large interest, new forums and publication frames, with new formation characters in research and profession. Specifically, in Robotics, the TC of Robotics and Mechatronics is the innovative community result that since the early days of IFToMM searches for new horizons looking at main mechanical implications of the mechatronic design and operation of robots.

Figure 12 aims to summarize the impact and source of innovation as related to publication frames of technical-scientific activities in the context of specific communities. In particular, an indication of the proceedings of the first congress in robotics in 1972 is shown in Fig. 12a and the success of a specific series on the specific topic of the Mechanism Design for robots in Fig. 12b referring to the MEDER conferences as an example of role and source of innovation of a scientific-technical community in terms of publications.

6.1 A Short Presentation of Late Prof Veniamin I. Goldfarb

Prof. Veniamin Iosifovich Goldfarb (1 February 1940–12 November 2019), Fig. 13a, was a worldwide reputed scientist of gearing systems with a successful activity of technological transfer also with a production of industrial products, at Institute of Mechanics of Kalashnikov Izhevsk State Technical University. He was also a leader in IFToMM as being member of Executive Council (2008–11), Vice-President (2012–15) and Chair of Technical Committee for Gears (1998–005) with several international activities among which it is to note that in 2011 he was the initiator of SIOMMS, the IFToMM Student Olympiad on MMS [12], Fig. 14.

He has been a great IFToMMist as a distinguished MMS scientist figure with a gentleman dynamic attitude in his ideas and proposals, as in Fig. 13b. He has been

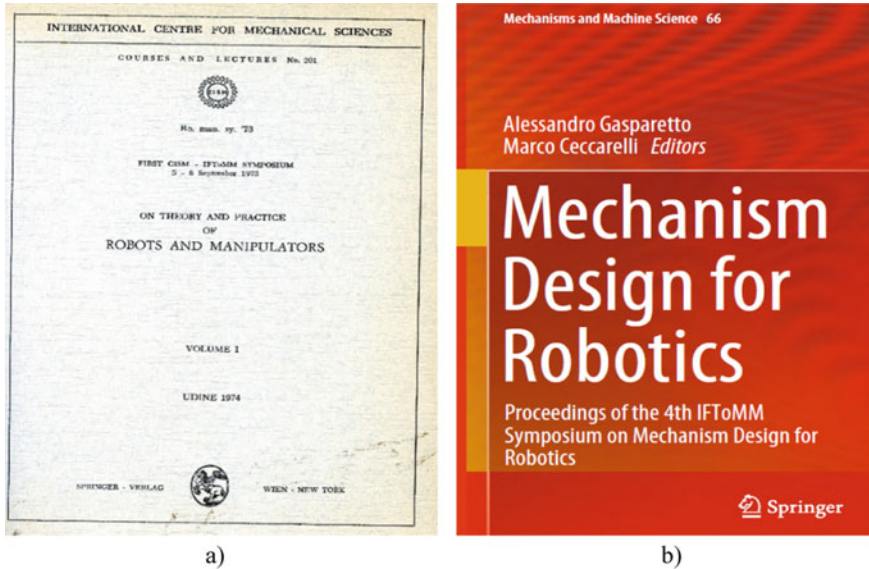


Fig. 12 Example of community results in terms of publications in Robotics as specific published proceedings of: **a** Romansy, the first conference in 1972; **b** MEDER a new conference series on mechanism design for robots with last event in 2018

a very prolific MMS scientist with a great reputation worldwide not only within the IFTOMM community. He has been awarded with several honors by local, national and international institutions, among which it may be heighthed the membership in the Russian Academy of Natural Sciences. He has been member of several scientific committees for international conferences and journals as result of his reputation of an intense scientific activity that is documents by papers, books (for teaching and with research results) as those in Fig. 15, and patents.

The main scientific achievements of Prof. Goldfarb can be recognized in a classification and design of spatial gears with special attention to spiroid gears and a non-differential design method for envelope profiles, with also practical implementation in an industrial production for pipeline valve applications by even starting and directing a company for an industrial production, Fig. 16.

Prof. Veniamin Goldfarb has been a prestigious figure, who has been admired worldwide also for his unique attitude to combine friendships and scientific activity in working the true spirit of IFTOMM for collaboration, sharing, and improving the technology for the benefit of the society in the welfare of human beings.



Fig. 13 Prof. Veniamin Goldfarb (1940–2019): **a** portrait; **b** playing music during a social break during 2010 EC meeting; **c** at the 2011 EC meeting in Guanajuato Mexico



Fig. 14 SIOMMS 2011, the first IFToMM Student Olympiad on MMS: **a** the poster; **b** cover page of the book with problems and solutions



Fig. 15 Title pages of the Springer published books by Prof. Veniamin Goldfarb: **a** In 2016; **b** in 2018



Fig. 16 A technological transfer activity by prof. Veniamin Goldfarb: **a** the international Journal on Gearing and Transmissions; **b** a catalog of product by Izhevsk company

7 Conclusions

In this paper, the various aspects of innovation activities have been illustrated, especially in the field of the Mechanism Design for Robotics, also considering a particular attention to social aspects in the technical-scientific community. The role Mechanism Design is presented with successful results since the past also discussing the outcome of inventions in terms of figures and their fame for recognition in society at large. It is noted that today, although the role of Mechanism Design in the development of mechatronic and robotic systems is still decisive, adequate recognition is not properly given not only to the corresponding technical-scientific communities but even to individual inventors and designers. It is hoped that a better activity of the technical-scientific communities also in communication and dissemination to a large public will be able to recover such a recognition and central role of the technical-scientific aspects for a healthy development of society itself.

References

1. Ceccarelli, M.: Innovation challenges for mechanism design. *Mech. Mach. Theory* **125**, 94–100 (2018). <https://doi.org/10.1016/j.mechmachtheory.2017.11.026>
2. Ceccarelli, M.: A short account of history of IFToMM and its role in MMS. *Mech. Mach. Theory* **89**, 75–91 (2015). <https://doi.org/10.1016/j.mechmachtheory.2014.09.007>
3. Ceccarelli, M.: Challenges for mechanism design in robotics, ROMANSY 22—robot design, dynamics and control. In: Arakelyan, V., Wenger, P. (Eds), pp. 1–9. Springer, Cham (2019). http://doi.org/https://doi.org/10.1007/978-3-319-78963-7_1.
4. Ceccarelli, M.: Renaissance of machines in Italy: from Brunelleschi to Galilei through Francesco di Giorgio and Leonardo. *Mech. Mach. Theory* **43**, 1530–1542 (2008). <https://doi.org/10.1016/j.mechmachtheory.2008.01.001>
5. Ceccarelli, M., Cafolla, D., Russo, M., Carbone, G.: LARMBot humanoid design towards a prototype. *Appl. Bionics Biomech.* **1**(2), 08 (2017) <https://doi.org/10.15406/mojabb.2017.01.00008>
6. Russo, M., Cafolla, D., Ceccarelli, M.: Design and experiments of a novel humanoid robot with parallel architectures. *Robotics* **7**(4), 79 (2018). <https://doi.org/10.3390/robotics7040079>
7. Ceccarelli, M., Russo, M., Morales-Cruz, C.: Parallel architectures for humanoid robots. *Robotics* **9**, 75 (2020). <https://doi.org/10.3390/robotics9040075>
8. Ceccarelli, M., Ferrara, L., Petuya, V.: Design of a cable-driven device for elbow rehabilitation and exercise. In: *Interdisciplinary Applications of Kinematics*, pp. 61–68. Springer, Cham (2019) https://doi.org/https://doi.org/10.1007/978-3-030-16423-2_6
9. Kozisek, A., Ceccarelli, M., Laribi, M.A., Ferrara, L.: Experimental characterization of a cable-driven device for elbow motion assistance, new trends in medical and service robotics—MESROB 2020. Springer AG **2021**, 71–78 (2021). https://doi.org/10.1007/978-3-030-58104-6_9
10. Zuccon, G., Bottin, M., Ceccarelli, M., Rosati, G.: Design and performance of an elbow assisting mechanism. *Machines* **8**, 68 (2020). <https://doi.org/10.3390/machines8040068>
11. Russo, M., Ceccarelli, M.: Analysis of a wearable robotic system for ankle rehabilitation. *Machines* **8**(3), 48 (2020). <https://doi.org/10.3390/machines8030048>
12. Krylov, E., Egorova, O., Gubert, A., Devyaterikov, S.: SIOMMS: evolution and development. *Mech. Mach. Theory* **153**, 104029 (2020)

Classification of Gear Pairs with Fixed Axes. Review



V. E. Starzhinsky, S. V. Shil'ko, E. V. Shalobaev, A. L. Kapelevich,
V. B. Algin, and E. M. Petrokovets

Abstract A review of sources regarding classification of the gear trains with toothed wheels on fixed axes is given. A variety of classification systems and criteria are under consideration, which relate to the type of gears and gear pairs, meshing systems, axes position, etc. These specific characteristics overtake the variations in the type of initial surface and the angle of inclination of the tooth at the designed point; in the form of initial body on which tooth surface should be formed; by the relative position of initial bodies; according to the tooth shape and the types of tooth profile (involute, cycloid, epy- or hypocycloid, complete of circle arcs and straight lines), accordingly with relative positions of the axes. Gear pairs with the flat gear wheels are distinguished in the shape-generated surfaces. Involute gears are classified by the virtual number of teeth, different for spur, helical, crossed helical, straight bevel, etc. Hyperboloid gears are differentiated by the number of meshing zones and location of them relatively to the line of centers, as well as in according to the shape of initial surfaces of the conjugate links and type of meshing. Orthogonal worm gear pairs are classified in the form of the original body of the worm—cylindrical worm, globoid worm, flat worm gear pairs—with flat worm, with shifted axes; hypoid gear pairs; spiroid gear pairs—properly spiroid one and cylindrical spiroid gear pair—helicon.

Keywords Classification systems and criteria · Gearing · Shape-Generating surfaces · Meshing zone · Conjugate links

V. E. Starzhinsky · S. V. Shil'ko (✉) · E. M. Petrokovets
The State Scientific Institution “V.A. Belyi Metal-Polymer Research Institute of National Academy of Sciences of Belarus”, Gomel, Belarus
e-mail: shilko_mpri@mail.ru

E. V. Shalobaev
National Research University of Information Technologies, Mechanics and Optics, ITMO University, St. Petersburg, Russia

A. L. Kapelevich
AK GEARS, New York, USA

V. B. Algin
The State Scientific Institution “The Joint Institute of Mechanical Engineering of the National Academy of Sciences of Belarus”, Minsk, Belarus

1 Introduction

As is known, three-link toothed mechanisms are represented three-link kinematic chain (KCH), where two toothed links, generating the higher pair of kinematic elements (HKP), are jointed with third, another link, by lower kinematic pair. The last ones could be either both of rotational, or one of them—rotational one, whereas another—progressive (translational) one. For the formation of mechanism from the HKP, it is necessary due one of the few of links convert to the fixed member (FM). If by way of FM to use a non-tooth link, then we obtain the mechanism with the immovable axis of rotation of gear wheels, which is named of simple three-links toothed mechanism (STM). At intended axis location and gear ratio translation of motion could be per-formed by external or internal meshing. In the external meshing both gear wheels have external teeth, in the internal—one of gear wheel has external teeth, other—internal ones.

2 Classification of Gears on the Kind of Pitch Surfaces and Helix Angle in the Center of the Action

Along the criterion of the helical angle of longitudinal line in the center of the action and form of pitch surfaces it is distinguished the gear wheels with the helix angle $\beta = 0^\circ$, with inclined teeth $\beta_0 > |\beta| > 0$ and worms $\pi/2 > |\beta| \geq \beta_0$, where β_0 is a conventional boundary value of helix angle, which is divided essentially gear wheels against the worms, which have helix angle more $\beta_0 = 80 \dots 85^\circ$. Charts of gear wheels of external and internal meshing are presented in Figs. 1 and 2 correspondingly, where on the conventional gear figures the location of the center of the action and direction of the

		Type of reference surface			
		Flatness	Cylinder	Cone	Torus
Helix angle in center of action	$\beta = 0$				
	$\beta_0 > \beta > 0$				
	$\frac{\pi}{2} > \beta > \beta_0$				

Fig. 1 Classification of gears with external teeth on the kind of pitch surface and the helix angle in center of action in accordance with [1]

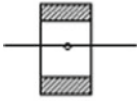
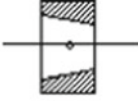
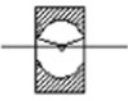
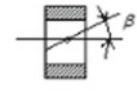
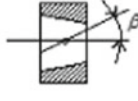


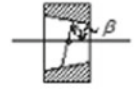
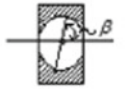
		Type of reference surface			
		Flatness	Cylinder	Cone	Torus
Helix angle in center of action	$\beta = 0$				
	$\beta_0 > \beta > 0$				
	$\frac{\pi}{2} > \beta > \beta_0$				

Fig. 2 Classification of gears with internal teeth on the kind of pitch surface and the helix angle in center of action in accordance with [1]

tangent to the tooth line at that point. Gear wheels, for which pitch surface is flatness carried off to gears with external teeth only [1].

In the frame of idem classification, it is possible further specification. So, along with the form of the longitudinal line, the gears with spur (right), bevel (spiral), screw, circular, arch, and herringbone teeth are distinguished. Along with the form of tooth flank the involute, cycloid (epicycloid and hypocycloid) pin-gear tooth form, approximately epicycloidal tooth form, circumscribe of circular arc, etc. are distinguished.

3 Generalized Classification of Toothed Mechanisms Along the Form of Initial Bodies, on the Surface of Which the Teeth Are Shaped

In accordance with [2], the main problem of geometrical synthesis of the surfaces of non-orthogonal gearing is the selection of forms most compliant to requirements and calculation of optimal sizes. Because of the most widely used surfaces (discus, cylinder, cone, and toroid), it is offered generalized classification for external (Table 1) and internal (Table 2) gearing. To the exclusion from the common data array the similar variants (2 and 5, 3 and 9, etc.) from Table 1 and analogous ones from Table 2, we have 9 variants of external gears and 5 of internal ones.

Table 1 The generalized classification of external gearing along the form of initial bodies [2]

The first gear type	The second gear type			
	Disk	Cylinder	Cone	Toroid
Disk	1	2	3	4
Cylinder	5	6	7	8
Cone	9	10	11	12
Toroid	13	14	15	16

Table 2 The generalized classification of internal gearing along the form of initial bodies [2]

The first gear type	The second gear type			
	Disk	Cylinder	Cone	Toroid
Disk	1	2	3	4
Cylinder	5	6	7	8
Cone	9	10	11	12
Toroid	13	14	15	16

4 Classification of Contrate (Flat Bevel, Flat Cylindrical) Gears

In this section the classification of gears according to the source [3] is presented, where above gears named collectively as a facial one (in standard [4] gears of this type it is conferred term flat bevel gears).

For the facial gears the terminology, covering geometrical elements and parameters of gears and gear wheels, terms and definitions of techniques and means of face teeth, classification of gearing and gears, are developed in [5–11].

In accordance with [3] toothed links and mechanisms consisted of these links can be di-vided on the criterion of form shape-generating surfaces on three classes: surface, flatness, and flatness-surface. The notion flatness tooth mechanism is introduced with toothed links, located on the flatness, and flat tooth mechanism, conjugated links of which take part in the parallel-plane motion, parallel certain motionless flatness.

Class flatness mechanisms are consisted of cylindrical and bevel gears, gearing (meshing), gear trains; class flat mechanisms consist of flat toothed and worm trains, toothed belts, spiroid gears, flat wave mechanisms. The main types of such toothed mechanisms are presented in Fig. 3 and Table 3.

Let us note that considered type of meshing opens the multifold possibilities for arrangement of gear units with undirected (whereas sometimes impossible for

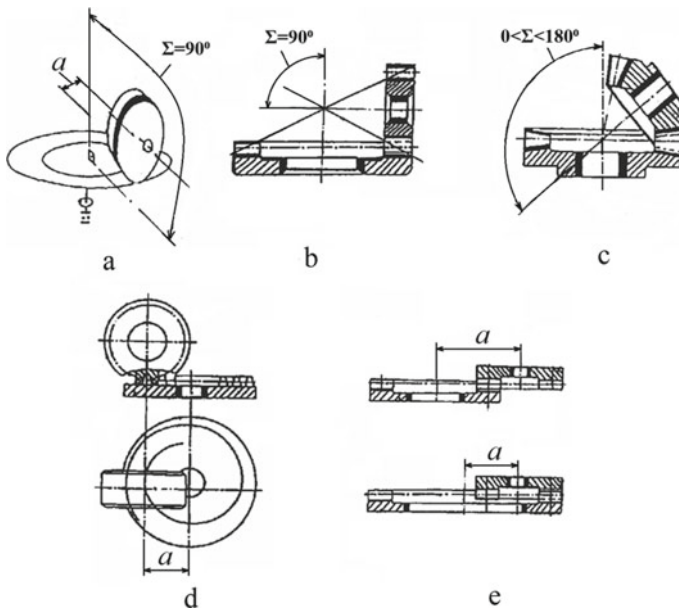


Fig. 3 The main types of flat gear pairs: a—flat-hypoid, b—flat-cylindrical, c—flat-conical, d—flat worm, e—flat external and internal gearing [3]

Table 3 Classification of cylindrical-bevel and flat-cylindrical gears [3]

Relative location of axes	Parameters of relative location of axes		Type of meshing	Type of pinion/gear wheel	Reference surface/pitch	Axoid surface
	Center distance a	Shaft angle Σ				
Train with parallel axes	$a > 0$	$\Sigma = 0$	Facial Figure 3, e	Facial/Facial	Facial/Facial	Circular cylinder
Train with intersecting axes	$a = 0$	$\Sigma = 90^\circ$	Facial cylindrical Figure 3, b	Cylindrical/Facial	Cylindrical/Facial	Circular cone
	$a = 0$	$0 < \Sigma < 180^\circ$	Facial bevel Figure 3, c	Bevel/Facial	Bevel/Facial	–
Cross axed gear train	$a > 0$	$\Sigma = 90^\circ$	Hypoid facial cylindrical Figure 3, a	Facial/Cylindrical	Cylindrical/Facial	Single-space rotation hyperboloid
			Facial-worm Figure 3, d	Gear wheel—cylindrical/Worm—facial	Cylindrical/Facial	Cylindrical/Facial

cylindrical and worm reducers) relative location of input and output axles. Universal technology, providing on the unified principles of manifold arrangements of gear pairs with cylindrical pinion and, accordingly, cylindrical, bevel and face gear wheels is proposed by corporation Crown Gear B.V. under proprietary trade name Cylkro Gears® [12, 13].

Developers of Cylkro Gears System [12, 13], based on the early proposed [14, 15] basic principles of geometry and technology of flat-cylindrical gear trains, create mathematical methods and computer-aided software for the complex design of such trains, included computation of their geometrical and kinematic parameters, evaluation of load capacity, special cutting tool and manufacturing equipment, optimization of production parameters, as well as measuring means for the inspecting cutting instrument and finished products.

Cylkro Gears® geometry is determined with pinion geometry (spur or helical one), a relative location of the pinion and gear wheel axes (trains with parallel or intersecting axes), and gear ratio. In this system, the pressure angle varied along the gear width, smaller at the inner diameter and greater at the outer one. The details of the arrangement of gear units of the Cylkro Gears® System can become acquainted according to reference [16].

5 Classification of Gears on the Criterion of Virtual Tooth Number

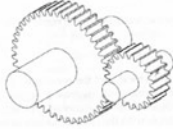
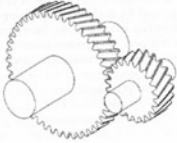

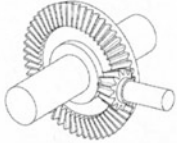
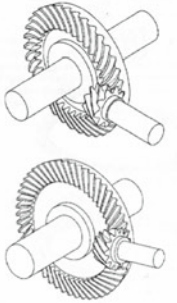
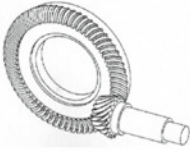
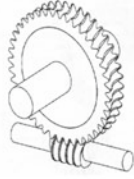
Authors suppose that one of the criteria of the classification of involute gears it is possible to take the virtual tooth numbers. As is known, tooth profile any involute gear can be considered as a tooth profile of the virtual spur gear. Virtual numbers of teeth are usually real numbers with the decimal parts and along with this parameter one may to classify involute gears with sufficient accuracy. Types of gears and formulae for calculation tooth numbers of virtual spur gear with tooth profile identical to the tooth profile in the normal plane different types of involute gears are shown in Table 4 [17].

6 Classification of Simple Three-Links Toothed Mechanisms on the Relative Axis Location

On the kind and location of lower kinematic pairs STM are divided to the following groups:


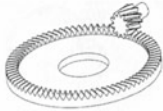

- (1) Mechanisms with parallel axes of gear rotation.
- (2) Mechanisms with crossing axes of gear rotation.
- (3) Mechanisms with skew (non-crossing) axes of gear rotation (cross axed gear pairs).

Table 4 Classification of gears on virtual tooth numbers of spur gear [17]

Type of gear		Number of teeth of virtual spur gears
Spur		$Z_{1,2v} = Z_{1,2}$
Helical		$Z_{1,2v} = \frac{Z_{1,2}}{\cos(\beta)^3}$
Crossed helical		$Z_{1,2v} = \frac{Z_{1,2}}{\cos(\beta_{1,2})^3}$
Straight bevel		$Z_{1,2v} = \frac{Z_{1,2}}{\cos(\gamma_{1,2})}$
Spiral and skewed bevel		$Z_{1,2v} = \frac{Z_{1,2}}{\cos(\gamma_{1,2}) \cos(\beta)^3}$
Hypoid		$Z_{1,2v} = \frac{Z_{1,2}}{\cos(\gamma_{1,2}) \cos(\beta_{1,2})^3}$
Worm		$Z_{wv} = Z_w / \cos(\pi/2 - \beta)^3$ $Z_{wgv} = Z_{wg} / \cos(\beta)^3$ $Z_{wv} = \infty$ $Z_{wgv} = Z_w$

(continued)

Table 4 (continued)

Type of gear		Number of teeth of virtual spur gears
Face spur		$Z_{1v} = Z_1$ $Z_{2v} = \infty$
Face helical		$Z_{1v} = \frac{Z_1}{\cos(\beta)^3}$ $Z_{2v} = \infty$
Face spiral		$Z_{1v} = \frac{Z_1}{\cos(\beta_1)^3}$ $Z_{2v} = \infty$

Note $z_{1,2}$ —number of teeth of the real pinion and gear; $z_{1v, 2v}$ —number of teeth of virtual spur pinion and gear; z_w and z_{wg} —number of starts of real worm and number of teeth of real worm gear; z_{wv} and z_{wgv} —number of teeth of virtual gears that replace real worm and worm gear; β —helix angle of helical or worm gears and spiral angle of spiral bevel gears; γ —pitch angle of bevel gears

- (4) Rack-and-pinion gear pairs, where one of lower kinematic pair is rotating one, whereas other link is translation one—toothed rack.

The relative position of gear rotation axes for the first group of mechanisms is determined with center distance a , for the second one—shaft angle Σ , for the third one—with both of indicated parameters.

Let us consider more detailed above classification, following [18]. Denote that division “Variety of Gears” from the [18] was reproduced without alterations in [19], then was announced in Russian-English version in [20] and was included, with some amendments, in monograph [21].

6.1 Gears with Parallel Axes

Gears with parallel axes (Fig. 4)—cylindrical, which in turn are distinguished from each other:

- As was mentioned earlier, by the shape of initial (original) bodies where teeth are formed: cylindrical (Fig. 4a), bevel (Fig. 4b), toroidal (Fig. 4c), flat (Fig. 4d).
- By the relative arrangement of bodies: external (Fig. 4) and internal (Fig. 5).

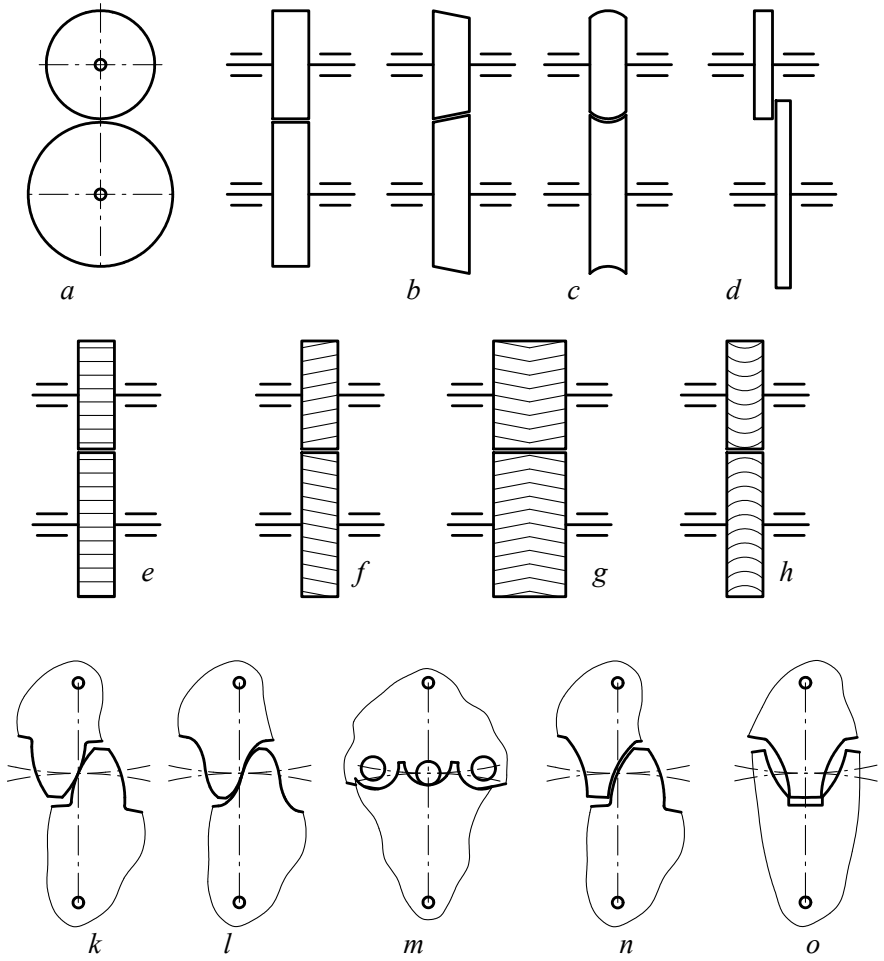


Fig. 4 External gears with parallel axes [18]

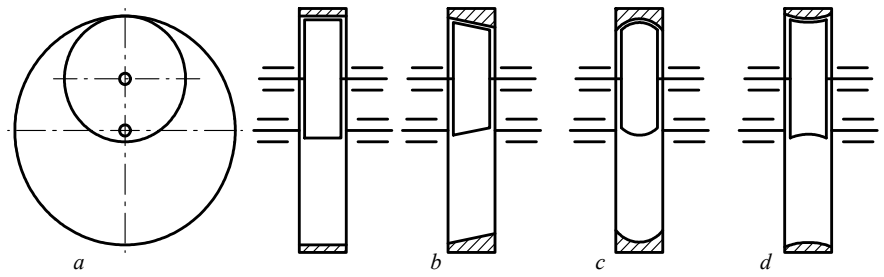


Fig. 5 Internal gears with parallel axes [18]

- By tooth shape, according to which gearwheels are called: spur (Fig. 4f); helical (Fig. 4g)—tooth line is screw here; herring-bone (Fig. 4h); with arch teeth (Fig. 4k)—here several types of gears with arch teeth are known depending on the way of tooth cutting and the type of cutting tool (in particular, four variety of arch cylindrical gearing and technological processes of their tooth forming are studied and proposed by Sidorenko [22]). Correspondingly, tooth form of internal gears, as well as external ones, may be cylindrical, spur or helical (Fig. 5a), straight bevel (Fig. 5b) or arched (Fig. 5c, d).
- By the tooth profile.

The last feature should be especially commented since the subset of gears distinguished according to this characteristic is very numerous. The involute gears which have the involute as the tooth profile (Fig. 4e) got the widest application.

Originally the involute gearing was preceded by cycloid one (Fig. 4m) whose profile is enveloped by different types of cycloid curves. The classic cycloid gearing (Fig. 4m) has an epicycloid profile of the addendum and hypocycloid profile of the dedendum. One of its varieties is a pin gear (Fig. 4n), one of its gearwheels has a circular tooth profile and the tooth itself is a cylinder.

In this context, it is pertinent to note the matter of the relative location of the right and left tooth profiles in the asymmetric involute meshing. It is proposed [23] to call the drive side of tooth profile the Basic Side and the coast side one the Adjacent Side. For manufacturing terminology authors [23] propose to use term Flat side for drive profile and term Abrupt (Bluff) Side for the coast one. Along the profile basic side (with greater pressure angle) the basic calculation is carried out, location of profile adjacent side can be changed according to rules due to improving gear pair quality parameters [23, 24].

Gears with the so-called Novikov meshing are well known and very popular. In some cases, this gearing is called Novikov-Wildhaber and sometimes—Wildhaber-Novikov. Both authors, who are outstanding experts in the field of gears, suggested in various times to profile teeth with segments of circular arcs of different diameters. The curvature sign of meshing profiles should be the same here, that is, one profile is convex and the other is concave.

Gearwheel tooth profiling with circle arches is interesting so that the contact zone could be closed (gears with closed-loop contact lines). Implementation of this idea allows to increase the carrying capacity of the lubrication layer within the contact zone and to increase the loading capacity of the gear. One of the representatives of this gear is shown in Fig. 4n [25].

We did not exhaust the manifold of cylindrical gears distinguished by the tooth profile. Perspective evolution ideas also arise nowadays. We showed only the most popular examples.

Fall back on Novikov gears let us noted that their load capacity significantly determined with the basic rack tooth profile parameters. Upon appearance in the middle of 50th of manifold basic rack tooth profiles are elaborated, varying with form and parameters, and pursued the aim to increase the load capacity of that sort

of gear trains. The fullest analysis of the references in this field of investigations is fulfilled by V.I. Korotkin with coauthors (refer to the issue of the 2007 year [26]).

According to [26] authors made the attempt to give a classification of Novikov gears along different criteria.

6.2 Novikov Gearing Classification

1. Classification on the number of line of action criterion:
 - Novikov gear pair—with one line of action (OLA);
 - Novikov gear pair—with two line of action (TLA);
 - Basic rack tooth profiles TLA, where active arc sections of addendum of tooth and dedendum one is connected by rectilinear transition sections [26];
 - Basic rack tooth profiles TLA, where mentioned transition section is fulfilled of concave in consequence of shifting active profiles of addendum and dedendum relative of tooth axis [26].
2. Novikov gear TLA on the criterion of tooth height are classified on the following ones [27]:
 - Height ones $h = (2 \div 3) m_n$;
 - Middle ones $h = (1.7 \div 2) m_n$;
 - Small ones $h = (1.35 \div 1.7) m_n$.
3. Novikov gears on the location of centers of fillet arcs on the reference line are classified on [28]:
 - Novikov gear of the first kind ($\rho_a < 0.5\pi m_n$);
 - Novikov gear of the second kind ($\rho_a > 0.5\pi m_n$), where ρ_a is radius of active section of tooth addendum.
4. Novikov gears on the criterion of arrangement of fillet arcs on relative to axis of symmetry of tooth space are classified on [27]:
 - Normal ones ($l_a = 0$);
 - Positive corrected ones ($l_a > 0$);
 - Negative corrected ones ($l_a < 0$),

where l_a is distance from the center of the arc of the active section of the tooth addendum of radius ρ_a to the axis of symmetry of the tooth.
5. Novikov gears OLA and TLA on the form of basic rack profile are classified on [28]:
 - With equally divided one;
 - With unequally divided one.

6. Cylindrical Novikov gears are classified on [26]:
 - With rectified teeth (gears with reduced axial force);
 - With herringbone teeth (variety of gears with rectified teeth).
7. On the criterion of Novikov gears contact type are classified on [26]:
 - Novikov gears with linear contact;
 - Novikov gears with close to linear contact.

6.3 Gears with Crossing Axes

Gears with crossing axes (Fig. 6)—bevel gears. The number of varieties of bevel gears is greater than of cylindrical ones. This is caused by the following: the change of angles between axes (these angles are equal to 0 for cylindrical gears) leads to the change of the shape of initial surfaces. Particularly, when the initial surface shape of one component is predetermined as bevel, the initial surface can be bevel (Fig. 6a, d), cylindrical (Fig. 6b) and flat (Fig. 6c) for external (Fig. 6a–d) and internal (Fig. 6e–g) meshing. A bevel gear is practicable with the flat first component and the cylindrical second one (Fig. 6h). This gear is called a face gear drive. When the initial bodies are torus (Fig. 6k, l), the following gears are known: either one torus is convex and the other is concave (Fig. 6k) or both torus are convex (Fig. 6l). In the last case, the performance is possible which allows some variation of the angle between axes during the operation process. These gears are known as Beveloid ones [29].

Another characteristic—tooth shape depends on the way method of bevel gears cutting and on the type of cutting tool. Gears are possible with the following types of gearwheel teeth: spur (Fig. 6m), helical (Fig. 6n), circular (Fig. 6o), and spiral (Fig. 6p). The last ones may be different depending on the cutting tool type and its motion during tooth cutting. The so-called Zerol bevel gears are also known which have curvilinear teeth with zero slope angle at the mean value (Fig. 6r).

Evidently, the tooth profile of a bevel gear wheel is also an important feature distinguishing bevel gears from each other. Let us take an example of a bevel gear with straight teeth and a circular-arc form, i.e., Rivacycle [4]. Notice that in a general case the bevel gear teeth may be of any regular curvilinear form, for example, involute or cycloid ones. The bevel gear pairs are distinguished by the form of their tooth flank, in particular, so-called half-generated bevel gear pair Formeit or Helixform is known, having the main tooth flank surfaces either flat, conical, spherical or helicoidal [4].

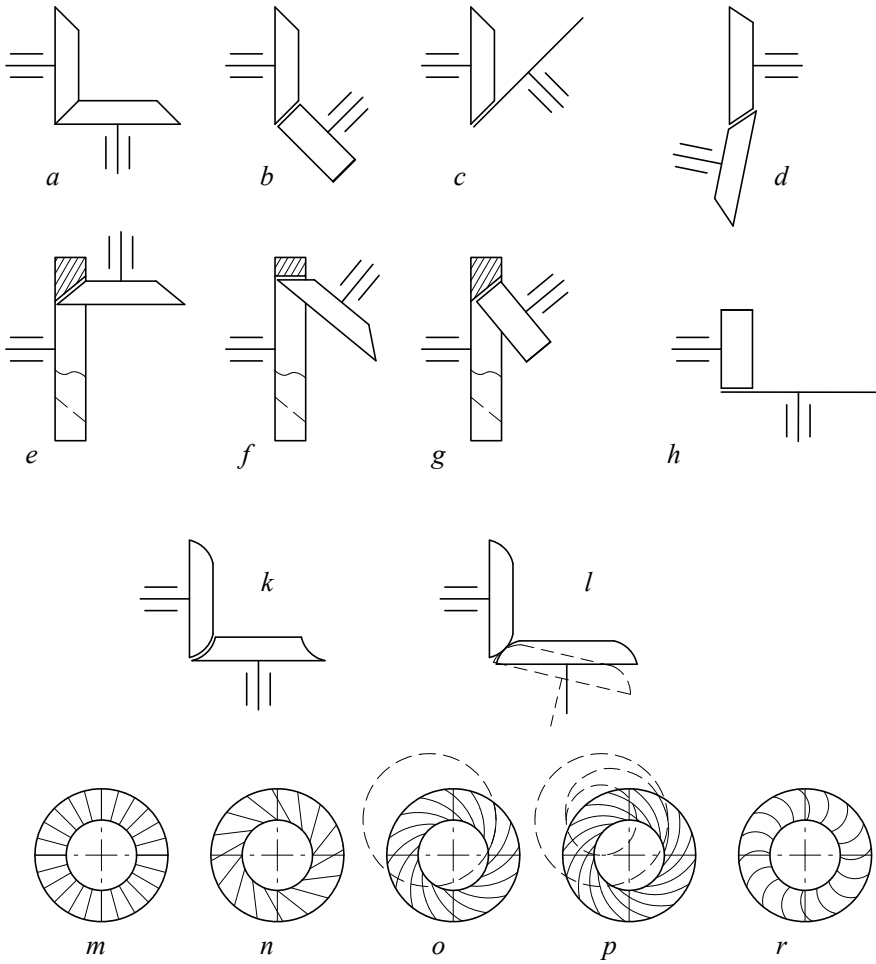


Fig. 6 Gears with crossing axes [18]

6.4 Gears with Skew (Non-crossing) Axes (Cross Axed Gear Pairs)

Gears with skew (non-crossing) axes—hyperboloid gears. They got the last name according to the shape of so-called axoid surfaces which are hyperboloids of rotation [30, 31].

The opportunity to vary two mounting dimensions—the distance a_w and the angle Σ between axes in combination with the arrangement of components with respect to each other and to the common interaxial line of a gear increases tenfold the number of varieties of hyperboloid gears compared with bevel and cylindrical gears.

Figure 7 shows the main varieties of hyperboloid gears: screw (Fig. 7a); cylindrical worm (Fig. 7b); globoid worm (Fig. 7c) which has several names—double enveloping worm gear, hourglass worm gear, cone drive (cone is the name of the engineer who proposed this gear); worm gear with flat worm (Fig. 7d); hypoid gear (Fig. 7e); face gear with shifted axes (offset face gear) (Fig. 7f); spiroid gear (Fig. 7g); helicon—cylindrical spiroid gear (Fig. 7h).

Several types of hyperboloid gears classification are known. In accordance with one of them [32], hyperboloid gears are distinguished depending on the location of the meshing zone with respect to the gear center line O_1O_2 (Fig. 8). In compliance with this feature the pointed gears are divided into three classes:

- 1 class—the meshing zone intersects the line O_1O_2 —screw, worm, cylindrical worm and globoid worm gears (Fig. 7a–c);
- 2 class—the meshing zone is shifted relative to the line O_1O_2 along the axis of one of the components—worm gear with flat worm (Fig. 7d);
- 3 class—the meshing zone is shifted relative to the line O_1O_2 along the axes of both components—hypoid, spiroid, face gears (Fig. 7e–h) and their varieties.

In [33] orthogonal worm gears are classified in three groups (Fig. 9) depending on the shape of the worm body:

- 1 group (Fig. 9a)—the initial body of the worm is bounded by a bevel surface (worm gears themselves);
- 2 group (Fig. 9b)—the initial body of the worm is bounded by the concave toroid surface (toroid worm gears);
- 3 group (Fig. 9c)—the initial body of the worm is bounded by the convex toroid surface (toroid worm gears).

Classification of certain kinds of worm gear general view on the relative location of axes, type of worm (on the form of the reference surface and the form of generating

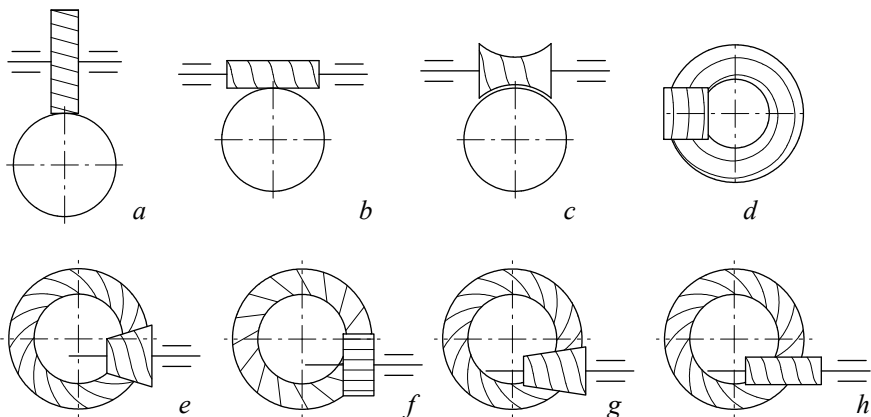


Fig. 7 Main types of hyperboloid gears [18]

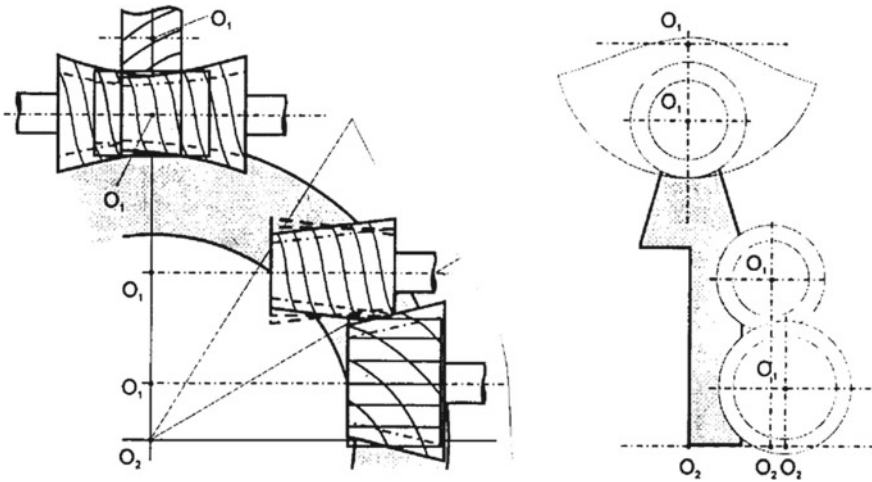


Fig. 8 Classification of hyperboloid gears depending on the location of meshing zone [32]

element), arrangement and characteristics of contact are reporting in [34], standard [35] designates 4 certain kinds of worm gear drive, 4 types of the worm gears and 43 variety of worms. In international standard [36] all together 6 positions, relative to kinds of worm gear drives, are reported.

A detailed description of the kinds of spiroid drives, the variety quantity of which, in accordance with [37], compile 29 types (varieties of spiroid gears—3, cylindrical spiroid worms—15, bevel and reverse-bevel spiroid worms—11) is reported in [38].

In that context, it is pertinent to know to the presence in dictionary [20] terms on spiroid drives on French and German.

Without commenting here the possibility of practical implementation of enumerated gears (generally speaking, this requires special studies), note, that the variation of the angle Σ between axes, at the first, increases the number of varieties of hyperboloid gears, and firstly second, makes this pointed possibility of practical implementation real.

Figures 10 and 11 shows the fragment of classification [39, 40] of hyperboloid gears of the 3rd class with auxiliary (including orthogonal) arrangement of components axes.

The features distinguishing one gear from others are:

- the shape of initial surfaces of components—cylindrical, bevel, flat (others are possible, for example, toroid);
- the meshing type—external (Fig. 10a), internal (Fig. 10b, c), flat (Fig. 10d, e); the internal meshing can be of two types—the pinion is inside the gearwheel (Fig. 10b); the gearwheel is inside the pinion (Fig. 10c); the flat meshing can also be of two types—the pinion is flat (Fig. 11, d) or the gearwheel is flat (Fig. 10, e);
- the relative arrangement of components which determines the value of the sliding speed in the meshing zone [40];

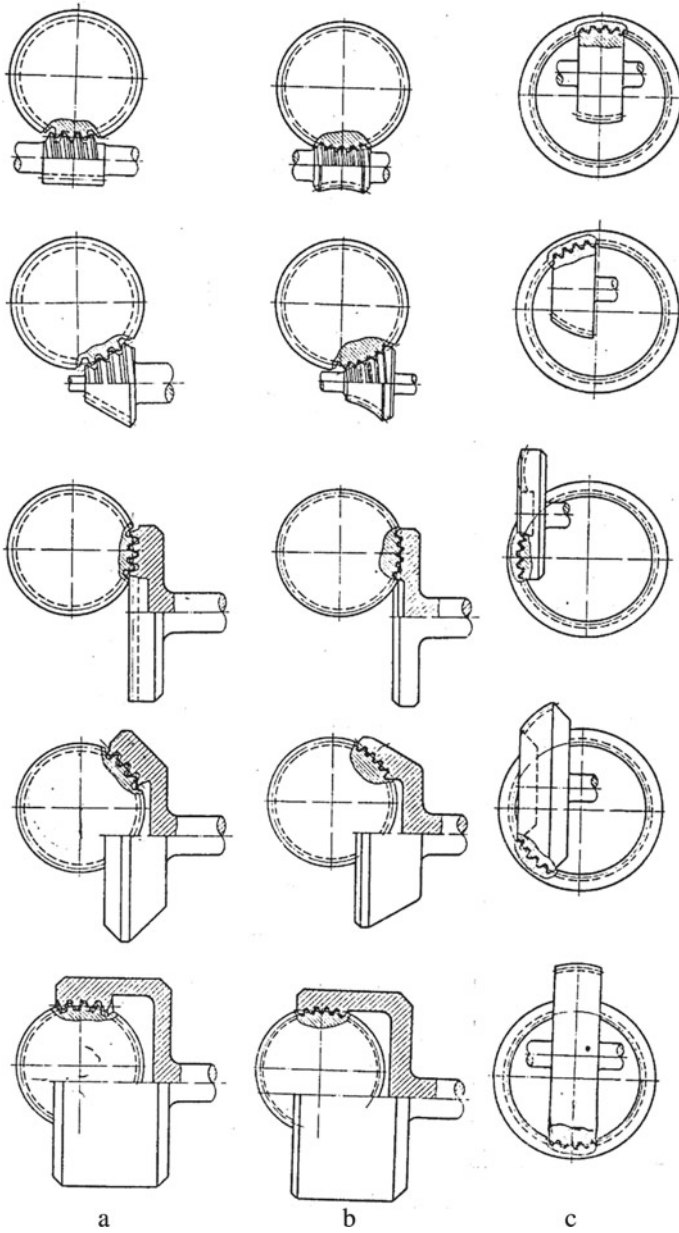


Fig. 9 Types of worm gears according to [33]

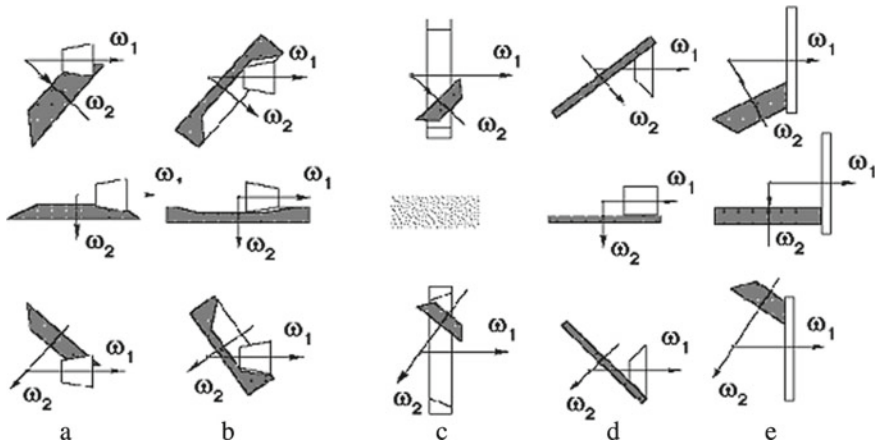


Fig. 10 Hyperboloid gears of the 3rd class with one meshing zone [39, 40]

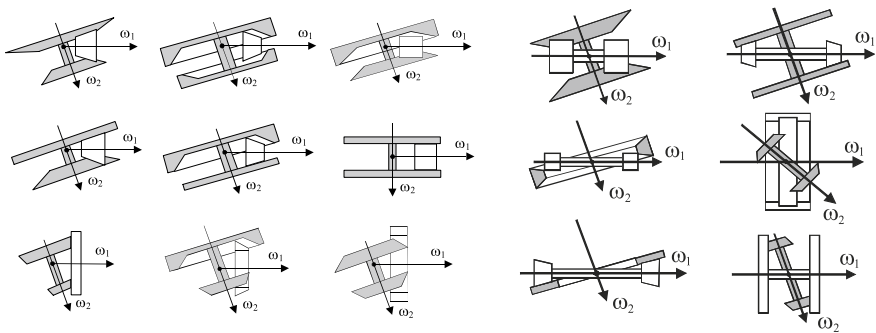


Fig. 11 Hyperboloid gears of the 3rd class with two meshing zones [39, 40]

- the number of meshing zone—Fig. 10 presents gears with one meshing zone, Fig. 11—gears with two meshing zones.

The given enumeration of hyperboloid gears is already enough to show their multitude. This multitude will many times increase if the opportunities are added connected with the variation of tooth profile or method of gear manufacturing.

The described above gears are intended to convert rotational motion into a rotational one. There are gears, which are called a rack, which convert rotational motion into translation one (or otherwise, the translation motion into rotational one). Some of them are shown in Fig. 12.

There is another interesting feature, which distinguishes one gear from the other—constancy or variability of gear ratio—the ratio i_{12} of angular velocities ω_1 of the driving ω_2 and driven components. All the gears described above are gears with a constant value of i_{12} . There are gears, which have a constant value of ω_1 and variable

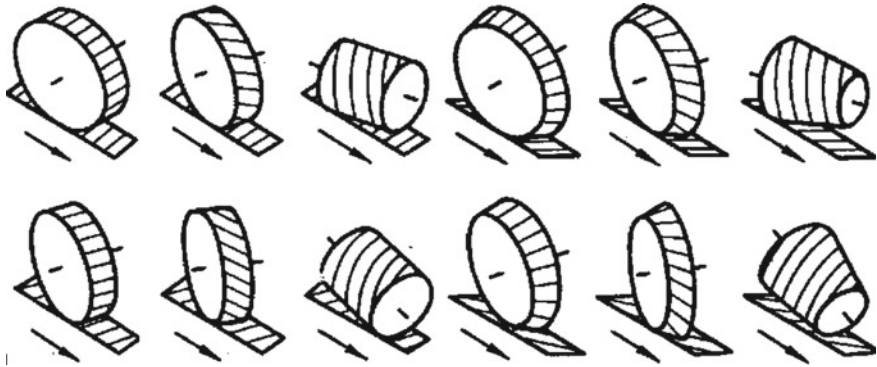


Fig. 12 Some types of rack gears [18]

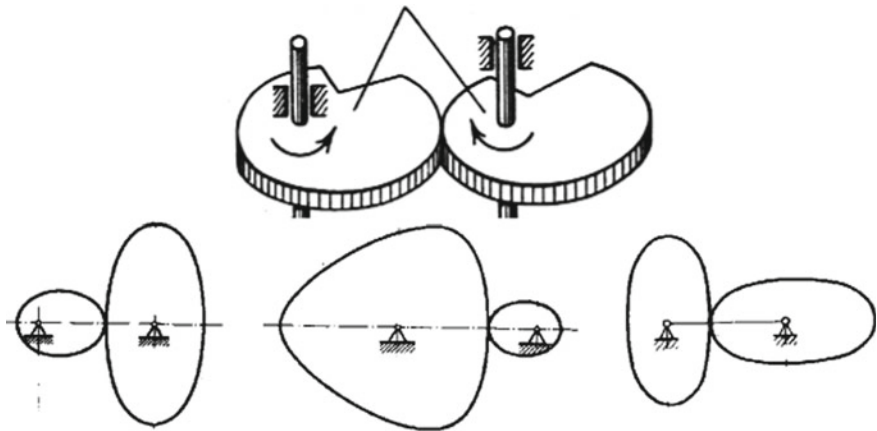


Fig. 13 Examples of gears with non-circular wheels [18]

value of ω_2 . They are called gears with non-circular wheels (Fig. 13). All the features described above can also be applied to them.

The review of different systems and criteria of gear mechanism classification is given. It is shown that one can get almost any configuration of the gear meshing, satisfying the operating conditions by varying the shape of the surfaces of conjugated links (cylindrical, conical, toroidal, flat) on which the teeth are formed, and meshing parameters (shaft angle; variable along the tooth length, pressure angle; helical angle).

7 Conclusions

The review of different systems and criteria of gear mechanism classification is given. It is shown that one can get almost any configuration of the gear meshing,

satisfying the operating conditions by varying the shape of the surfaces of conjugated links (cylindrical, conical, toroidal, flat) on which the teeth are formed, and meshing parameters (shaft angle; variable along the tooth length, pressure angle; helical angle).

Acknowledgements The authors are deeply grateful to all the gear specialists (experts) whose achievements are used in this review. Special thanks to the outstanding gear scientist Veniamin Iosifovich Goldfarb, who throughout all periods of interaction from the mid-80 s of the last century helped the authors to promote their ideas and projects, including the field of the subject under consideration. He has approved the proposal to publish the section “Variety of Gears” from [18] in Proceedings of the Scientific Seminar of the 23rd Working Meeting of the IFToMM Permanent Commission on MMS Terminology [19]. He has supported the idea of including this section in English and Russian into the reference dictionary [20] and praised the extended description of the classification in [41], where the stages of formation of this dictionary have been considered.

The authors are also grateful to the students and followers of V.I. Goldfarb—Evgeny Semenovich Trubachev and Natalya Aleksandrovna Barmina for constant assistance in publishing the results of the authors’ research in publications edited by V.I. Goldfarb, E.S. Trubachev, and N.A. Barmina.

This work was supported by the Belarusian Republican Foundation for Fundamental Research (Project T20R-223).

References

1. Vul’fson, I.I., Erikhov, M.L., Kolovskii, M.Z., Peisakh, E.E., Semenov, Yu.A., Sloushch, A.V., Smirnov, G.A., Timofeev, B.P.: *Mechanics of machines*. Smirnov, G.A. (Eds.). Vysshaya Shkola, Moscow (1996). (in Russian)
2. Minkof, K.A.: New approach to basic geometry and classification of non-orthogonal GEARING. In: Proceedings of the 1989 International Power Transmission and Gearing Conference, vol. 2, pp. 893–598. The American Society of Mechanical Engineering, Chicago, Illinois, USA (1989)
3. Raikhman, G.: Terminology and classification of facial toothed joints and gearings. In: Proceedings of the International Conference on Gearing, Transmissions and Mechanical Systems, pp. 31–39. Professional Engineering Publishing, St. Edmunds and London (2000)
4. GOST 19325–73. Bevel Gear Pairs. Terms, Definitions and Symbols. (Has been introduced from 01.01.1975) Moscow. Publishing House of Standards (1987) (in Russian)
5. Raikhman, G.: Facial toothed joints and gearings. In: Proceedings of the 27th Israel Conference on Mechanical Engineering, pp. 463–469. Haifa, Israel (1998)
6. Raikhman, G.: Terminology of facial toothed joints and gearings. In: Proceedings of the 10th World Congress on the Theory of Machines and Mechanisms, vol. 6, pp. 2251–2256. Oulu, Finland (1999)
7. Raikhman, G.: Terminology of facial toothed joints and gearings. In: Proceedings of the 11th World Congress in Mechanism and Machine Science, vol. 2, pp. 882–887. Tianjin, China (2004a)
8. Raikhman, G.: Classification of facial toothed joints and gearings. In: Proceedings of the 11th World Congress in Mechanism and Machine Science, vol. 2, pp. 867–871. Tianjin, China (2004b)
9. Raikhman, G., Starzhinsky, V.: Terminology and classification of principal methods and modes of facial gears processing. In: Proceedings of the 2nd International Conference “Power Transmissions–06”, pp. 331–338. Faculty of Technical Science, Novi Sad, Serbia & Montenegro (2006)

10. Bartov, M., Raikhman, G.: Principal terms and definitions of geometrical components and parameters of facial gears, joints and gearings. In: Proceedings of the 2nd International Conference “Power Transmissions–06”, pp. 245–252. Faculty of Technical Science, Novi Sad, Serbia & Montenegro (2006)
11. Raikhman, G.N., Bartov, M., Starzhinsky, V.E.: Terminology and classification of geometrical parameters of facial gears, their processing methods and regimes. In: Proceedings of the 12th IFToMM World Congress, 6 p. Besancon, France (2007)
12. Basstein, G., Sijstra, A.: New developments in design manufacturing and applications of cylkro—(face) gears. AGMA. Technical paper, 93FTM7, 12 p. (1993)
13. Basstein, G.: Technology behind Cylkro®_Gears and their applications. In: Proceedings of the International Conference on Gearing, Transmissions and Mechanical Systems, pp. 41–54. Professional Engineering Publishing, St. Edmunds and London (2000)
14. Bloomfield, B.: Designing face gears. *Machine Design* **19**(4), 129–134 (1947)
15. Martin, L.D.: Face gear geometry. *Mach. Design* **28**(10) (1956)
16. Basstein, G., Sijstra, A.: Neue Entwicklungen bei Auslegung und Fertigung von Kronenrädern. *Antriebstechnik* **32**(11), 53–60 (1993)
17. Kapelevich, A.L.: *Asymmetric gearing*. CRS Press, Taylor and Francis Group (2019)
18. Goldfarb, V.I., Lunin, S.V., Trubachov, E.S.: Direct digital simulation for gears. IzhTU, Izhevsk (2004)
19. Goldfarb, V.I.: Variety types of gear drives. In: Proceedings of the Scientific Seminar “Terminology for the Mechanism and Machine Science”. The 23rd Working Meeting of the IFToMM Permanent Commission for Standardization of Terminology for MMS, pp. 69–76. BelGISS, Minsk (2010)
20. Starzhinsky, V.E., Antonyuk, V.E., Goldfarb, V.I., Kane, M.M., Shil’ko, S.V., Goman, A.M., Shalobaev, E.V.: Reference-dictionary book on gearing. Rus.-Eng.-German-French. Starzhinsky, V.E. (ed.). MPRI NAS B, Gomel (2011)
21. Starzhinsky, V.E., Shalobaev, E.V., Shil’ko, S.V., Antonyuk, V.E., Basinuyk, V.L., Blagodarny, V.M., Goldfarb, V.I., Kapelevich, A.L., Mardosevich, E.I., Timofeev, B.P., Tkachyov, A.A.: Elements of instrument drives. Pleskachevsky, Yu.M. (eds). *Belaruskaya navuka*, Minsk (2012). (in Russian)
22. Sidorenko, A.K.: High performance arched gear trains. Geometrical design and technological technics. Part 1. Kolonna (1996). (in Russian)
23. Novikov, A., Golovanov, V., Dorofeyev, D., Dorofeyev, V.: Terminology and design of asymmetrical gears for aircraft. In: Theory and practice of gearing and transmissions. In: Honor of Prof. Faydor L. Litvin. Goldfarb, V., Barmina, N. (eds.). *Mechanism and Machine Science*, vol. 34, pp. 381–392. Springer (2016)
24. Dorofeev, V.L., Arnaudov, K.B., Dorofeev, D.V.: Assignment of basic rack tooth profile parameters of involute gears with asymmetric teeth. In: Bulletin of National Technical University “KhPI” **29**, 53–60 (2011). (in Russian)
25. Roano, A.: Zahnradpaare für umsteuerbare zahnradgetriebe mit parallelen oder leicht gegeneinander geneigten achsen. Patentschrift Nr. 940194 Bunderrepublik Deutschland (1956)
26. Korotkin, V.I., Onishkov, N.P., Kharitonov, YuD: Novikov gear trains. Achievements and developments. *Mashinostroenie*, Moscow (2007). (in Russian)
27. Burov, Yu.F.: Breaking and wearing of the teeth of the pre-pole gears of Novikov with different basic rack tooth profiles. In: Abstracts of Scientific and Technical Conference “Results of Investigation and Practical Application of Novikov Gear Trains”. Kharkov, pp. 108–112 (1971) (in Russian)
28. Belyi, V.A., Sviridyonok, A.I., Starzhinsky, V.E.: Basic rack tooth profiles for metal-polymer Novikov gear trains. In: Reports, Acceptable to All-Soviet Union Scientific and Technical Conference “Gear Trains with Novikov Meshing”. issue 1, pp. 211–219. Central Institute of Scientific and Technical Information on Automation and Mechanical Engineering, Moscow (1964). (in Russian)
29. Beam, A.S.: Beveloid gearing. *Mach. Design* **26**(12), 220–238 (1954)
30. Gavrilenko, V.A.: Gears in Mechanical Engineering. Mashgiz, Moscow (1962). (in Russian)

31. Minkov, K.: About structure and geometry of non-orthogonal hyperbolic crossed axes gearing. In: Proceedings of the 10th World Congress on TMM in Oulu, Finland, 1999. Mechanics of Machines, Bulgaria, No. 25, 199, pp. 39–44 (1999)
32. Goldfarb, V.I.: What kind of skew-axis gearing do you prefer? In: Proceedings of the International Conference on Mechanical Transmissions, pp. 612–616. Chongqing, China (2001)
33. Zak, P.S.: Various types of worm gears and methods for their manufacture. Progressive gear production methods and their adaptability, pp. 198–239. Mashgiz, Moscow (1962) (in Russian)
34. Sandler, A.I., Lagutin, S.A., Verkhovskii, A.V.: Production of Worm Gear Trains. Mashinostroenie, Moscow (2008). (in Russian)
35. GOST 18498-89. Worm Gear Pairs. Terms, Definitions and Symbols. (Has been introduced from 01.01.90). Publishing House of Standards, Moscow (1990). (in Russian)
36. ISO/DIS 1122-2. Vocabulary of Gear Terms. Part 2: Definitions Related to Worm Gear Geometry
37. GOST 22850-77. Spiroid Gear Pairs. Terms, Definitions and Symbols. (Has been introduced from 01.01.1979). Publishing House of Standards, Moscow (1978). (in Russian)
38. Goldfarb, V.I., Anferov, V.N., Glavatskikh, D.V., Trubachev, E.S.: Spiroid Reducers for Work in Extreme Conditions. Publishing House of IzhSTU named after M.T. Kalashnikov, Izhevsk (2014). (in Russian)
39. Goldfarb, V.I., Malina, O.V.: Skew axis gearing scheme classifier building technique. In: Proceedings of the 10th World Congress on TMM in Oulu, Finland, vol. 6, pp. 2227–2232 (1999)
40. Goldfarb, V.I.: The synthesis of non-traditional kind of skew axis gearing. In: International Gearing Conference, BGA Transmission Technology, pp. 513–516. Newcastle, MEP, London (1994)
41. Starzhinsky, V.E., Goldfarb, V.I., Shil'ko, S.V., Shalobaev, E.V., Tesker, E.I.: Development of terminology in the field of gears and transmissions. Part 2. Compilation of a dictionary on gears. Intell. Syst. Product. **15**(2) 60–66 (2017). (in Russian)

Virtual Metrology of Helical Gears Reconstructed from Point Clouds



Ignacio Gonzalez-Perez, Pedro L. Guirao-Saura, and Alfonso Fuentes-Aznar

Abstract Application of non-contact metrology constitutes a promising technique that may complement the application of contact metrology for gear inspection. Point clouds with the coordinates of the gear tooth surfaces can be generated as a rate of millions of points per second. These point clouds obtained from non-contact metrology machines in combination with computational procedures to regenerate the gear tooth surfaces permit the determination of the most relevant tooth flank deviations to assess the flank tolerance classification according to the ISO Standard 1328-1:2013. Computational procedures to predict each type of deviation for reconstructed helical gears from point clouds are presented and applied for inspection of two apparently similar helical gears measured and regenerated from their corresponding point clouds. The influence of application of a guided 3D point cloud filtering algorithm on the results of tooth contact analysis and class classification assessment of the reconstructed gears from point clouds is also revealed. Results show that filtering the point clouds is necessary for a better estimation of the contact pattern and function of transmission errors of the reconstructed gears from point clouds when in mesh with a master gear. However, the assessment of the gear class classification number might be influenced by the filtering process yielding to lower class classification numbers or lower tolerances.

I. Gonzalez-Perez (✉) · P. L. Guirao-Saura
Universidad Politécnica de Cartagena (UPCT), Cartagena, Spain
e-mail: ignacio.gonzalez@upct.es

P. L. Guirao-Saura
e-mail: pedro.guirao@upct.es

A. Fuentes-Aznar
Rochester Institute of Technology (RIT), Rochester, NY, USA
e-mail: afeme@rit.edu

1 Introduction

The application of non-contact metrology for gear inspection constitutes a promising technique that could complement the actual process based on contact metrology. Non-contact metrology allows gear tooth surfaces to be quickly measured and yields a wealth of data to determine the pitch, profile, helix, and tooth thickness deviations as well as the runout of the to-be-inspected gear.

The actual machines for non-contact metrology of gear drives are based on laser technology that allows a fast measurement of gear tooth surfaces with high precision. As a result, point clouds with the coordinates of the gear tooth surfaces are generated. Based on them, the gear tooth surfaces can be regenerated computationally and tooth surface deviations determined.

The first known attempt to regenerate gear tooth surfaces from point clouds was presented in [1] to reconstruct a helical gear. The point clouds of just one tooth were considered and the need of application of a filtering process was revealed. In [2], the point clouds of all the teeth were considered for the whole reconstruction of a helical gear that enabled tooth contact analysis and stress analysis when in mesh with a master gear to be performed. The need of application of a filtering approach was also revealed in this work. Later, in [3], the reconstruction of a whole spiral bevel gear was performed from the points clouds corresponding to one tooth and a bilateral filter was applied to the point clouds for a more accurate determination of the contact pattern and function of transmission errors.

In this work, the application of point clouds obtained from non-contact metrology machines in combination with computational procedures to regenerate the gear tooth surfaces will permit the reconstruction of all tooth surfaces of a helical gear and the determination of the most relevant deviations of the gear tooth surfaces to assess the flank tolerance classification according to ISO Standard 1328-1:2013 [4]. The tooth surface deviations to be determined prior to obtaining the flank tolerance classification are:

- The pitch deviations given by the single pitch deviation f_p , the individual cumulative pitch deviation F_{pi} , and total cumulative pitch deviation F_p .
- The profile deviations given by the profile form deviation $f_{f\alpha}$, the profile slope deviation $f_{H\alpha}$, and the total profile deviation F_α .
- The helix deviations given by the helix form deviation $f_{f\beta}$, the helix slope deviation $f_{H\beta}$, and the total helix deviation F_β .
- The runout of the gear.

After reconstruction of all the gear tooth surfaces, the tooth thickness deviations can also be determined. For contact-based metrology, thickness deviations can be obtained through a chordal measurement, a measurement over pins, or the span measurement of the gear teeth. For non-contact metrology, thickness deviations can be derived through a computational procedure to predict the normal tooth thickness at each reconstructed tooth. Therefore, the tooth thickness allowance and tolerance according to the Standard DIN 3967 can also be determined.

Presented in the following sections are several computational procedures to predict each type of deviation for reconstructed helical gears from point clouds. The results will show the effect of filtering the point clouds prior to the computation of the deviations and tolerance classification of the reconstructed gears.

2 Regeneration of Gear Tooth Surfaces

Regeneration of helical gear tooth surfaces from points clouds obtained with non-contact metrology machines is performed following the ideas exposed in [1, 2]. Each tooth is regenerated from the point clouds provided for its left and right sides. The regeneration is based on the application of NURBS (Non-Uniform Rational B-Spline) surfaces [5] that are built from a grid of points that belong to each point cloud. Previously, each point cloud may be filtered as explained in detail in [3] for the case of a reconstructed spiral bevel gear. Here, a bilateral filter is considered. The points of the filtered point cloud are selected using a K-D tree algorithm [6] to determine the closest points whose radial projections are the nearest to those of a preestablished structured grid.

Figure 1 shows a regenerated gear model comprising twenty teeth and their corresponding forty point clouds (two for each tooth). The fillets were obtained using Hermite curves as proposed in [1] to adjust the regenerated fillet geometry to some points selected from the point cloud presented in the fillet area.

3 Determination of Pitch Deviations

For each tooth of a total of N teeth, single pitch deviations $f_{pi}, i = \{0, \dots, N - 1\}$, are obtained for each tooth side through the application of the following steps (see Fig. 2):

1. Coordinate system S_g fixed to the gear will be considered with origin in the point of intersection of the axis of rotation with the middle transverse section along the face width of the gear. Points P_i are obtained at the intersection of the pitch circle defined at the transverse plane with $z_g = 0$ and the regenerated gear tooth surfaces Σ_i of each tooth side (left or right). Assuming that the gear tooth surfaces are determined in coordinate system S_g by position vector $r_g(u, v)$, surface parameters (u_i, v_i) of point P_i can be derived considering the following system of two equations with two unknowns, u_i and v_i :

$$f_1(u_i, v_i) = z_g(u_i, v_i) = 0 \quad (1)$$

$$f_2(u_i, v_i) = x_g^2(u_i, v_i) + y_g^2(u_i, v_i) - r_p^2 = 0 \quad (2)$$

where r_p is the pitch radius of the reconstructed gear.

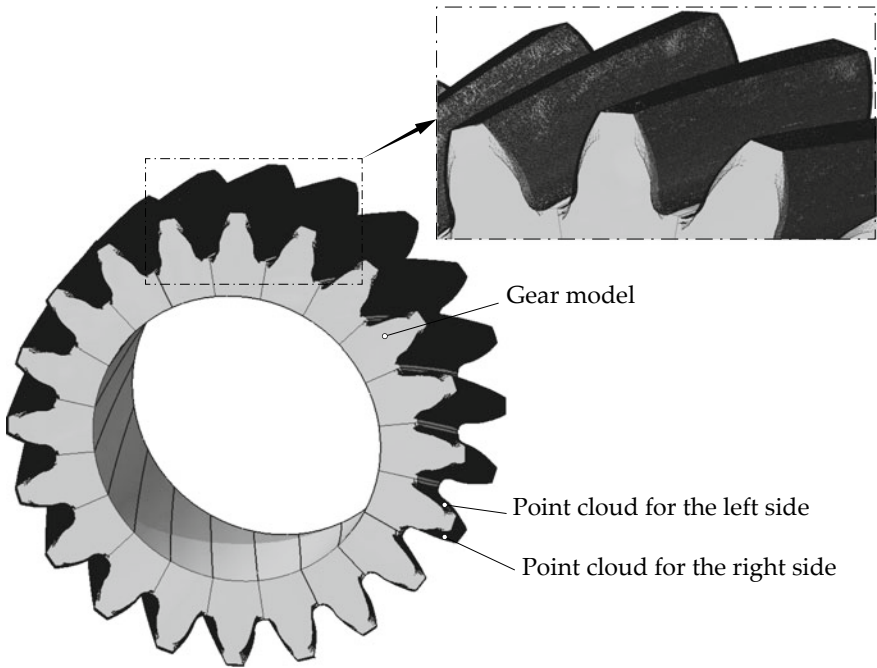
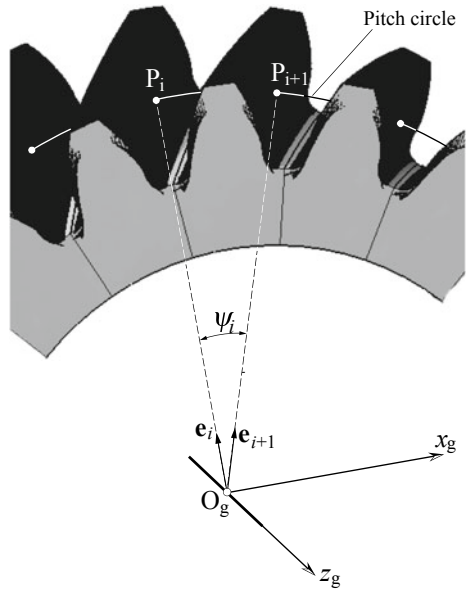


Fig. 1 Point clouds for each tooth and gear model obtained from the regenerated gear tooth surfaces

Fig. 2 Towards derivation of pitch deviations at right side



2. Unit vectors $\mathbf{e}_i, i = \{0, \dots, N - 1\}$, directed from the origin of coordinate system S_g to each point P_i , are derived as

$$\mathbf{e}_i = \frac{\overrightarrow{O_g P_i}}{|\overrightarrow{O_g P_i}|} \quad (3)$$

3. Based on unit vectors \mathbf{e}_i , the pitch angle ψ_i is determined as

$$\psi_i = \arccos(\mathbf{e}_i \cdot \mathbf{e}_{i+1}), \quad i = \{0, \dots, N - 2\} \quad (4)$$

$$\psi_{N-1} = \arccos(\mathbf{e}_{N-1} \cdot \mathbf{e}_0) \quad (5)$$

4. The pitch deviation for each tooth is determined by

$$f_{pi} = r_p \psi_i - \frac{\pi m}{\cos \beta}, \quad i = \{0, \dots, N - 1\} \quad (6)$$

Here, m is the normal module and β is the helix angle of the reconstructed gear. The single pitch deviation is obtained as the maximum absolute value of all the individual single pitch deviations

$$f_p = \max(|f_{pi}|) \quad (7)$$

The individual cumulative pitch deviations $F_{pi}, i = \{0, \dots, N - 1\}$, are determined as

$$F_{pi} = \sum_0^i f_{pi} \quad (8)$$

The total cumulative pitch deviation, F_p , is determined as

$$F_p = \max(F_{pi}) - \min(F_{pi}) \quad (9)$$

According to Standard ISO 1328-1:2013, the flank tolerance class due to the single pitch deviation, A_{f_p} , is assessed as

$$A_{f_p} = \frac{2 \log \left(\frac{f_p}{0.001d + 0.4m + 5} \right)}{\log 2} + 5 \quad (10)$$

Here, d is the pitch diameter. Furthermore, the flank tolerance class due to the total cumulative pitch deviation, A_{F_p} , is assessed as

$$A_{F_p} = \frac{2 \log \left(\frac{F_p}{0.002d + 0.55\sqrt{d} + 0.7m + 12} \right)}{\log 2} + 5 \quad (11)$$

Finally, the flank tolerance class due to the pitch deviations will be determined as

$$A_{pitch} = \max \{ A_{f_p,l}, A_{f_p,r}, A_{F_p,l}, A_{F_p,r} \} \tag{12}$$

Here, subindex l is applied to the left sides of the teeth and subindex r is applied to the right sides of the teeth.

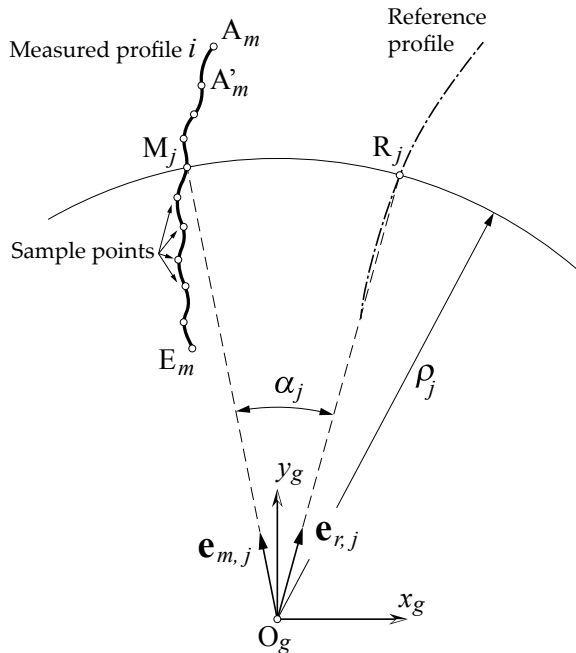
4 Determination of Profile Deviations

Profile deviations consist of the total profile deviation, F_α , the profile form deviation, $f_{f\alpha}$, and the slope form deviation, $F_{H\alpha}$. Algorithms to determine these profile deviations are presented below.

4.1 Determination of Total Profile Deviation

The total profile deviation, F_α , is determined through the application of the following algorithm (see Fig. 3):

Fig. 3 Towards derivation of total profile deviation



1. Each measured profile $i, i = \{0, 1, \dots, N - 1\}$, is determined as the intersection of each regenerated gear tooth surface, $r_g(u, v)$, with the transverse plane $z_g = 0$.
2. The reference profile will be an involute curve. The algorithm is independent of the location of the reference profile in coordinate system S_g where the regenerated gear tooth surface is obtained.
3. The start point of the measured profile, E_m , belongs to the regenerated active profile, and provides the following roll path length

$$L_{E_m} = \sqrt{\rho_{E_m}^2 - r_b^2} \quad (13)$$

Here, r_b is the base radius of the regenerated helical gear in the transverse section.

4. Considering as given the roll path length of the profile evaluation range, L_α , the radius of the end point of the measured profile for evaluation, point A'_m , is determined as

$$\rho_{A'_m} = \sqrt{(L_{E_m} + L_\alpha)^2 + r_b^2} \quad (14)$$

The ISO Standard 1328-1:2013 recommends a value of 0.95 times the tip form radius for $\rho_{A'_m}$. Instead of the tip form radius, the radius of the end point of the measured profile, point A_m , will be considered.

5. A set of sample points between point E_m and point A'_m is defined in the measured profile considering as input data a profile form filter cutoff length λ_α (see [4]) in order to avoid consideration of deviations with a short period as those due to surface roughness. The ISO Standard 1328-1:2013 recommends $\lambda_\alpha = L_\alpha/30$ but not less than 0.25 mm. Then, the number of sample points is obtained by

$$n_j = \text{Int}\left(\frac{L_\alpha}{\lambda_\alpha}\right) + 1 \quad (15)$$

Here, $\text{Int}()$ is a function that provides an integer number by trimming all decimals of a real number.

6. For each sample point $M_j, j = \{0, 1, \dots, n_j - 1\}$, its counterpart R_j in the reference profile is found. Unit vectors $\mathbf{e}_{m,j}$ and $\mathbf{e}_{r,j}, j = \{0, \dots, n_j - 1\}$, are derived as follows

$$\mathbf{e}_{m,j} = \frac{\overrightarrow{O_g M_j}}{|\overrightarrow{O_g M_j}|} \quad (16)$$

$$\mathbf{e}_{r,j} = \frac{\overrightarrow{O_g R_j}}{|\overrightarrow{O_g R_j}|} \quad (17)$$

7. Phase angles $\alpha_j, j = \{0, 1, \dots, n_j - 1\}$, are determined as

$$\alpha_j = \arccos(\mathbf{e}_{m,j} \cdot \mathbf{e}_{r,j}), \quad j = \{0, \dots, n_j - 1\} \quad (18)$$

8. The maximum and minimum values of the phase angles α_j are determined for each measured profile i

$$\alpha_{\max,i} = \max(\alpha_j) \quad (19)$$

$$\alpha_{\min,i} = \min(\alpha_j) \quad (20)$$

9. The total profile deviation for each measured profile i , $i = \{0, 1, \dots, N - 1\}$, is obtained as

$$F_{\alpha_i} = (\alpha_{\max,i} - \alpha_{\min,i})r_b \quad (21)$$

10. The total profile deviation is given by

$$F_\alpha = \max(F_{\alpha,0}, F_{\alpha,1}, \dots, F_{\alpha,N-1}) \quad (22)$$

and its mean value will be obtained as

$$F_{\alpha,m} = \frac{\sum_0^{N-1} F_{\alpha_i}}{N} \quad (23)$$

The flank tolerance class due to the total profile deviation, A_{F_α} , is assessed as (see [4])

$$A_{F_\alpha} = \frac{\log \left(\frac{F_\alpha^2}{(0.4m + 0.001d + 4)^2 + (0.55m + 5)^2} \right)}{\log 2} + 5 \quad (24)$$

4.2 Determination of Profile Form Deviation

Once the profile deviations respect to the reference profile are determined, a function of profile deviations D_m can be provided for the *measured* profile as the one represented in Fig. 4.

$$D_m(\alpha_j) = k[\alpha_j - \min(\alpha_j)]r_b \quad j = \{0, 1, \dots, n_j - 1\} \quad (25)$$

where each value of α_j (determined as described in the previous subsection) corresponds to a known value of radius ρ_j (see Fig. 3) and therefore to a known value of roll path length L_{α_j} through the relation $L_{\alpha_j} = \sqrt{\rho_j^2 - r_b^2}$. Here, $k = +1.0$ if the deviation of the measured profile respect to the reference profile represents an increment in material and $k = -1.0$ if it represents a removal of material.

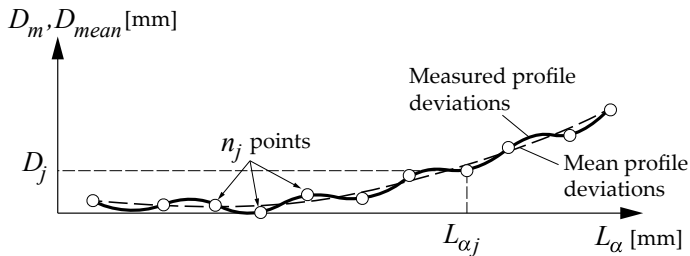


Fig. 4 Towards derivation of profile form deviation

Factor k is determined after rotation of the reference profile through the angle $\min(\alpha_j)$ to get the measured and the reference profiles in touch. Then, if component z of vector $\mathbf{e}_{m,j} \times \mathbf{e}_{r,j}$ is positive, $k = -1.0$ for the left side and $k = +1.0$ for the right side.

In order to determine the profile form deviation of the measured profile, the objective is to obtain first the function of deviations of a mean profile respect to the reference profile. Figure 4 shows the function of the mean profile deviations, which can be expressed as a second order function

$$D_{\text{mean}} = c_0 + c_1 L_\alpha + c_2 L_\alpha^2 \quad (26)$$

that relates deviations D_{mean} to rolling path length L_α .

An optimization process can be set up to find the variable vector $\mathbf{x} = [c_0, c_1, c_2]^T$ that minimizes the function

$$f(\mathbf{x}) = \sum_{j=0}^{n_j-1} [D_m(\alpha_j) - D_{\text{mean}}(\mathbf{x}, L_{\alpha_j})]^2 \quad (27)$$

Once $\mathbf{x} = [c_0, c_1, c_2]^T$ is known, the profile form deviations are obtained through the function

$$f_{f\alpha,j} = D_m(\alpha_j) - D_{\text{mean}}(L_{\alpha_j}) \quad (28)$$

The profile form deviation is then obtained as

$$f_{f\alpha} = \max(f_{f\alpha,j}) - \min(f_{f\alpha,j}) \quad (29)$$

The corresponding flank tolerance class due to the profile form deviation, $A_{f\alpha}$, is assessed as (see [4])

$$A_{f\alpha} = \frac{2 \log \left(\frac{f_{f\alpha}}{0.55\text{m} + 5} \right)}{\log 2} + 5 \quad (30)$$

This flank tolerance is obtained for each profile $i, i = \{0, 1, \dots, N - 1\}$, and for both tooth sides.

4.3 Determination of Slope Form Deviation

The slope form deviation $f_{H\alpha}$ is determined as the distance between two copies of the reference profile intersecting the extrapolated mean profile at the radii of the start point E_m and the tip point A_a (see Fig. 5). Since the deviations of the extrapolated mean profile line respect to the reference profile at such locations are given by

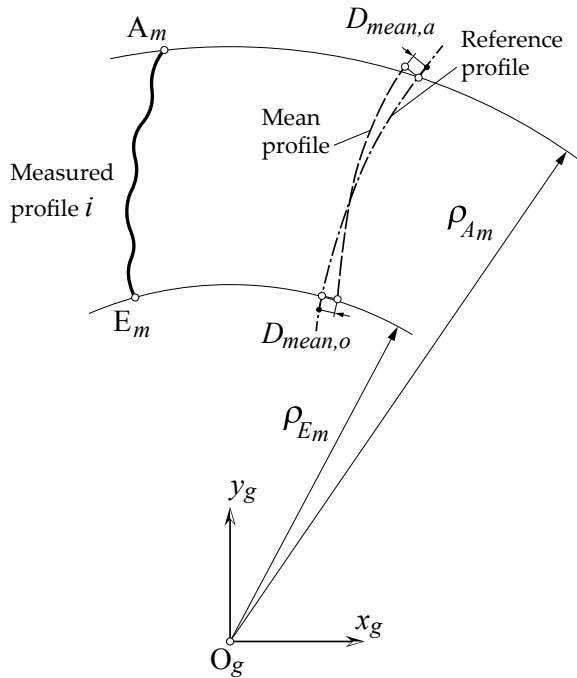
$$D_{\text{mean},o} = c_0 + c_1 L_{\alpha,o} + c_2 L_{\alpha,o}^2 \quad L_{\alpha,o} = \sqrt{\rho_{E_m}^2 - r_b^2} \quad (31)$$

$$D_{\text{mean},a} = c_0 + c_1 L_{\alpha,a} + c_2 L_{\alpha,a}^2 \quad L_{\alpha,a} = \sqrt{\rho_{A_m}^2 - r_b^2} \quad (32)$$

the slope form deviation $f_{H\alpha}$ is given by

$$f_{H\alpha} = D_{\text{mean},a} - D_{\text{mean},o} \quad (33)$$

Fig. 5 Towards derivation of slope form deviation



The corresponding flank tolerance class due to the slope form deviation is assessed as (see [4])

$$A_{f_{H\alpha}} = \frac{2 \log \left(\frac{f_{H\alpha}}{0.4m + 0.001d + 4} \right)}{\log 2} + 5 \quad (34)$$

This flank tolerance is obtained for each profile i , $i = \{0, 1, \dots, N - 1\}$, and for both tooth sides.

5 Determination of Helix Deviations

Determination of total helix deviations, helix form deviations, and helix slope deviations follow computational procedures that are similar to those related to profile deviations. The measured helix for each tooth surface is determined as the intersection of the corresponding regenerated gear tooth surface, $r_g(u, v)$, with the pitch cylinder with radius r_p . The helix evaluation range cover a flank area shortened in axial direction at each end by the smaller of 5% of the face width or a length equal to one module (see [4]). A helix form filter cutoff length λ_β allows the number of sample points in the measured helix to be determined as

$$n_j = \text{Int} \left(\frac{L_\beta}{\lambda_\beta} \right) + 1 \quad (35)$$

where L_β is the length of the helix evaluation range.

Relations similar to (16), (17), (18), (19), (20) are applied here for each point M_j of the measured helix and its counterpart point, R_j , in the reference helix, allowing determination of total helix deviation $F_{\beta,i}$, $i = \{0, 1, \dots, N - 1\}$, as

$$F_{\beta,i} = (\alpha_{\max,i} - \alpha_{\min,i})r_p \quad (36)$$

where r_p is the pitch radius.

The total helix deviation is given by

$$F_\beta = \max(F_{\beta,0}, F_{\beta,1}, \dots, F_{\beta,N-1}) \quad (37)$$

and its mean value determined as

$$F_{\beta,m} = \frac{\sum_0^{N-1} F_{\beta,i}}{N} \quad (38)$$

The flank tolerance class due to the total helix deviation is assessed by the following formula (see [4])

$$A_{F_\beta} = \frac{\log \left(\frac{F_\beta^2}{(0.07\sqrt{d} + 0.45\sqrt{b} + 4)^2 + (0.05\sqrt{d} + 0.35\sqrt{b} + 4)^2} \right)}{\log 2} + 5 \quad (39)$$

where d is the pitch diameter and b is the face width. Furthermore, a function of helix deviations can be provided for the measured helix as

$$D_m(\alpha_j) = k[\alpha_j - \min(\alpha_j)]r_p \quad j = \{0, 1, \dots, n_j - 1\} \quad (40)$$

where factor $k = +1$ when the deviation makes the absolute value of the helix angle of the measured helix larger than that of the reference helix and $k = -1$ when it makes such absolute value smaller. Prior to the determination of factor k , it is required the reference helix to be rotated the angle $\min(\alpha_j)$ to touch the measured helix. A procedure similar to that applied to determine the profile form deviations is applied here to obtain the helix form deviation $f_{f\beta}$ considering a second order function of the mean helix deviations

$$D_{\text{mean}} = c_0 + c_1 L_\beta + c_2 L_\beta^2 \quad (41)$$

where L_β is the length along the axial direction with its origin at the middle of the face width.

The corresponding flank tolerance class due to the helix form deviation is assessed by (see [4])

$$A_{f_{f\beta}} = \frac{2 \log \left(\frac{f_{f\beta}}{0.07\sqrt{d} + 0.45\sqrt{b} + 4} \right)}{\log 2} + 5 \quad (42)$$

This flank tolerance is obtained for each profile i , $i = \{0, 1, \dots, N - 1\}$, and for both tooth sides.

The slope helix deviation $f_{H\beta}$ is determined as the distance between two copies of the reference helix intersecting the extrapolated mean helix at both face ends. Since the deviations of the extrapolated mean helix line respect to the reference helix at such locations are given by

$$D_{\text{mean},I} = c_0 + c_1(0.5b) + c_2(0.5b)^2 \quad (43)$$

$$D_{\text{mean},II} = c_0 + c_1(-0.5b) + c_2(-0.5b)^2 \quad (44)$$

the deviation $f_{H\beta}$ can be determined as

$$f_{H\beta} = D_{\text{mean},II} - D_{\text{mean},I} \quad (45)$$

The corresponding flank tolerance class due to the slope helix deviation is assessed by (see [4])

$$A_{f_{H\beta}} = \frac{2 \log \left(\frac{f_{H\beta}}{0.05\sqrt{d} + 0.35\sqrt{b} + 4} \right)}{\log 2} + 5 \quad (46)$$

This flank tolerance is obtained for each profile i , $i = \{0, 1, \dots, N - 1\}$, and for both tooth sides.

6 Determination of Radial Runout

Radial runout is the maximum difference on radial direction around the gear of the measurement over balls or rollers that are assembled into the tooth space near the pitch circle. It accounts for pitch errors, profile errors, tooth thickness deviations, out of roundness and eccentricity errors. The radial runout of the to-be-inspected gear can be determined using the radial distances ρ_i , $i = \{0, 1, \dots, N - 1\}$ (see Fig. 6), from the gear axis to the center of a ball of radius ρ_b . The following algorithm is proposed:

1. Each tooth i , $i = \{0, 1, \dots, N - 1\}$, provides two measured profiles, the left side profile and the right side profile, that are determined as the intersection of the regenerated gear tooth surfaces with the transverse plane $z_g = 0$.
2. A ball is located in the space between the right side profile of tooth i , $i = \{0, 1, \dots, N - 1\}$, and the left side profile of tooth $i + 1$. The right side profile of tooth $i = N - 1$, will be considered with the left side profile of tooth 0.
3. Profile parameters u_{RS} and u_{LS} of points P_{RS} and P_{LS} (see Fig. 6) are considered as unknowns in the proposed algorithm.
4. The tangent vectors to the measured profiles at points P_{RS} and P_{LS} are derived as

$$\mathbf{t}_{RS} = \left. \frac{\partial \mathbf{r}_g^{(RS)}}{\partial u} \right|_{u=u_{RS}} \quad (47)$$

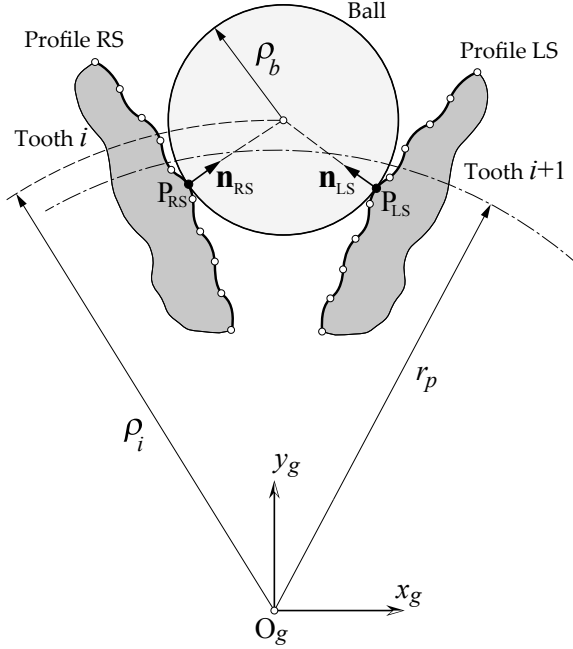
$$\mathbf{t}_{LS} = \left. \frac{\partial \mathbf{r}_g^{(LS)}}{\partial u} \right|_{u=u_{LS}} \quad (48)$$

5. The normal vectors to the measured profiles at points P_{RS} and P_{LS} are derived as

$$\mathbf{n}_{RS} = \frac{\mathbf{t}_{RS}}{|\mathbf{t}_{RS}|} \times \mathbf{k} \quad (49)$$

$$\mathbf{n}_{LS} = \mathbf{k} \times \frac{\mathbf{t}_{LS}}{|\mathbf{t}_{LS}|} \quad (50)$$

Fig. 6 Towards derivation of the gear runout



6. The Newton-Raphson algorithm is applied to determine u_{RS} and u_{LS} considering the following two equations

$$f_1(u_{RS}, u_{LS}) = r_{g,x}^{(P_{RS})} + r_b \cdot n_{RS,x}^{(P_{RS})} - r_{g,x}^{(P_{LS})} - \rho_b \cdot n_{LS,x}^{(P_{LS})} = 0 \quad (51)$$

$$f_2(u_{RS}, u_{LS}) = r_{g,y}^{(P_{RS})} + r_b \cdot n_{RS,y}^{(P_{RS})} - r_{g,y}^{(P_{LS})} - \rho_b \cdot n_{LS,y}^{(P_{LS})} = 0 \quad (52)$$

7. Radii $\rho_i, i = \{0, 1, \dots, N - 1\}$ are determined as

$$\rho_i = \sqrt{\left(r_{g,x}^{(P_{RS})} + \rho_b \cdot n_{RS,x}^{(P_{RS})}\right)^2 + \left(r_{g,y}^{(P_{RS})} + \rho_b \cdot n_{RS,y}^{(P_{RS})}\right)^2} \quad (53)$$

8. The runout is then computed as

$$F_r = \max(\rho_i) - \min(\rho_i) \quad (54)$$

9. The corresponding flank tolerance class due to the runout is assessed by (see [4])

$$A_{F_r} = \frac{2 \log \left(\frac{F_r}{0.9(0.002d + 0.55\sqrt{d} + 0.7m + 12)} \right)}{\log 2} + 5 \quad (55)$$

7 Determination of Tooth Thickness Deviations

The transverse and normal tooth thicknesses are determined using the following algorithm (see Fig. 7):

1. Each tooth i , $i = \{0, 1, \dots, N - 1\}$, provides two measured profiles, the left side profile and the right side profile, that are determined as the intersection of the regenerating gear tooth surfaces with the transverse plane $z_g = 0$.
2. Profile parameters u_{LS} and u_{RS} of points P_{LS} and P_{RS} are determined through the applicator of the Newton-Raphson algorithm that requires the following equations to be satisfied

$$f_{LS}(u_{LS}) = (r_{g,x}^{(P_{LS})})^2 + (r_{g,y}^{(P_{LS})})^2 - r_p^2 = 0 \quad (56)$$

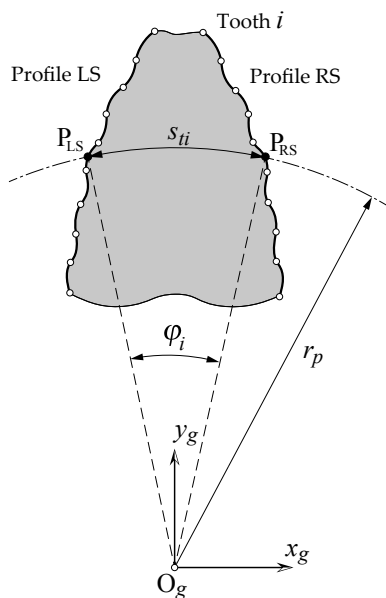
$$f_{RS}(u_{RS}) = (r_{g,x}^{(P_{RS})})^2 + (r_{g,y}^{(P_{RS})})^2 - r_p^2 = 0 \quad (57)$$

where r_p is the pitch radius.

3. Angle φ_i , $i = \{0, 1, \dots, N - 1\}$, is determined as

$$\varphi_i = \arccos \left(\frac{\overrightarrow{OgP_{LS}} \cdot \overrightarrow{OgP_{RS}}}{|\overrightarrow{OgP_{LS}}| \cdot |\overrightarrow{OgP_{RS}}|} \right) \quad (58)$$

Fig. 7 For derivation of tooth thickness deviations



4. The transverse tooth thickness, s_{ti} , for the tooth i , $i = \{0, 1, \dots, N - 1\}$, is obtained by

$$s_{ti} = \varphi_i r_p \quad (59)$$

5. The normal tooth thickness s_{ni} , for the tooth i , $i = \{0, 1, \dots, N - 1\}$, is given by

$$s_{ni} = s_{ti} \cos \beta \quad (60)$$

where β is the helix angle of the regenerated gear.

6. The expected upper and lower allowances for the normal tooth thickness of the to-be-inspected gear are determined as

$$E_{sns} = \max(s_{ni}) - \frac{\pi m}{2} - 2\chi_1 m \tan \alpha_n \quad (61)$$

$$E_{sni} = \min(s_{ni}) - \frac{\pi m}{2} - 2\chi_1 m \tan \alpha_n \quad (62)$$

Here, m is the normal module, χ_1 is the profile shift coefficient and α_n is the normal pressure angle of the to-be-inspected gear.

7. The expected tolerance for the normal tooth thickness of the to-be-inspected gear is determined as $T_n = E_{sns} - E_{sni}$.

8 Numerical Examples

Two apparently similar gears referred to henceforth as Gear A and Gear B are inspected based on their corresponding point clouds obtained by a non-contact metrology machine. Unfortunately, the gear quality was not known and no further information about the gears apart from the point clouds was provided for this work. Application of reverse engineering allows the main parameters of the gears (see Table 1) to be determined (see [1]).

A guided 3D point cloud filtering algorithm has been applied to the point clouds corresponding to each tooth of a total of twenty teeth for gears A and B. A detailed description of this filtering algorithm can be found in [7]. The following two parameters are required for the application of this filtering algorithm, namely a sphere radius, r , and a parameter to control the filtered effects, ϵ . To choose appropriate values of these parameters, tooth contact analysis (TCA) of the regenerated gear in mesh with a master gear is carried out following the directions given in [2]. Master gear refers to a theoretically generated virtual gear. This process of TCA can be considered as part of the gear inspection process that complements the results of tooth surface deviations (see [4]). The master gear is based on the same basic parameters of the to-be-inspected gears, but with 29 teeth and a left helix hand. The gears will be mounted at the nominal center distance.

Table 1 Results of reverse engineering applied to gears A and B [1]

Gear parameter	Value
Tooth number	20
Module [mm]	3.0
Normal pressure angle [°]	20.0
Helix angle [°]	20.0
Helix hand	Right
Face width [mm]	26.845
Profile shift coefficient	0.055
Addendum coefficient	0.915
Dedendum coefficient	1.398

Figure 8 shows the contact patterns obtained for gear A in mesh with the master gear, considering the regenerated gear tooth surfaces from non-filtered point clouds and filtered point clouds using a sphere radius $r = 50.0 \mu\text{m}$ and a filter control parameter $\epsilon = 0.45$. When considering these parameters for the filtering algorithm, the contact pattern is spread over the active tooth surface of the inspected gear without the isolated areas that the contact pattern obtained without application of the filtering algorithm shows (see Fig. 8a). Furthermore, the function of transmission errors shows a reduced level of peak-to-peak transmission errors compared to the function of transmission errors obtained without application of the filtering algorithm. Similarly, Fig. 9 shows the results obtained for gear B. A virtual making compound thickness of 0.0065 mm is considered for representation of the contact patterns on

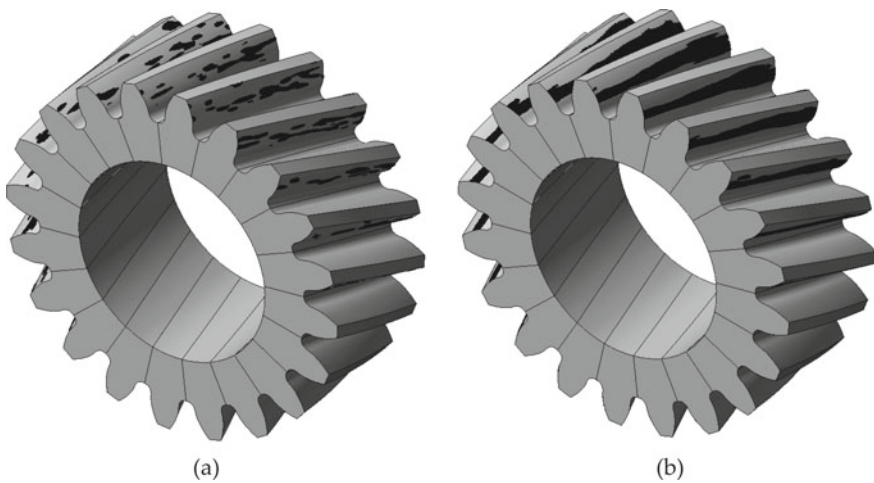


Fig. 8 Contact patterns of the to-be-inspected gear A in mesh with a master gear in case of: **a** no-filtered point clouds and **b** filtered point clouds with $r = 50.0 \mu\text{m}$ and $\epsilon = 0.45$

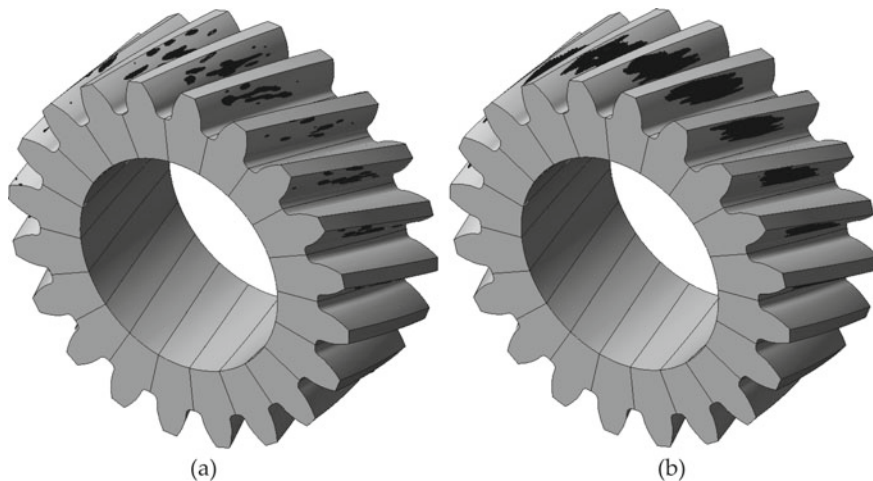


Fig. 9 Contact patterns of the to-be-inspected gear B in mesh with a master gear in case of: **a** no-filtered point clouds and **b** filtered point clouds with $r = 50.0 \mu\text{m}$ and $\epsilon = 0.45$

the gear tooth surfaces, being this value the one that is commonly used for TCA of perfect (theoretical) gears.

Figures 10 and 11 show the comparison of the unloaded functions of transmission errors for a whole revolution of the to-be-inspected gear A and gear B, respectively, in mesh with the master gear.

The contact pattern obtained for the regenerated gear A with filtered point clouds (Fig. 8b) seems to correspond to the case when profile crowning is applied to one of the gears of the gear set, in this case the to-be-inspected gear. The contact pattern obtained for gear B with filtered point clouds seems to correspond to the case when longitudinal crowning is provided. Although the intended modifications can be visualized, the exact amount of crowning is not easy to be verified.

Application of the developed algorithms for determination of tooth surface deviations and flank tolerance classification for gears A and B regenerated from non-filtered and filtered point clouds provides the following results. Table 2 summarizes de input data for evaluation of the deviations.

Figures 12 and 13 show the single pitch deviations f_{pi} and the individual cumulative pitch deviations F_{pi} for gears A and B, respectively, when the left tooth side is considered and no filtering of the point clouds is applied. Table 3 illustrates the maximum single pitch deviation f_p and the total cumulative pitch deviation F_p either for the left tooth side (LS) or the right tooth side (RS). It is observed that filtering the point clouds lowers substantially the obtained class classification numbers in both gears. We recall that lower class classification numbers mean lower tolerances.

Table 4 shows the profile deviations and class tolerance classification related to this type of deviation for gears A and B. Lower class classification numbers are observed in both gears as a result of the filtering process. However, gear A gets a

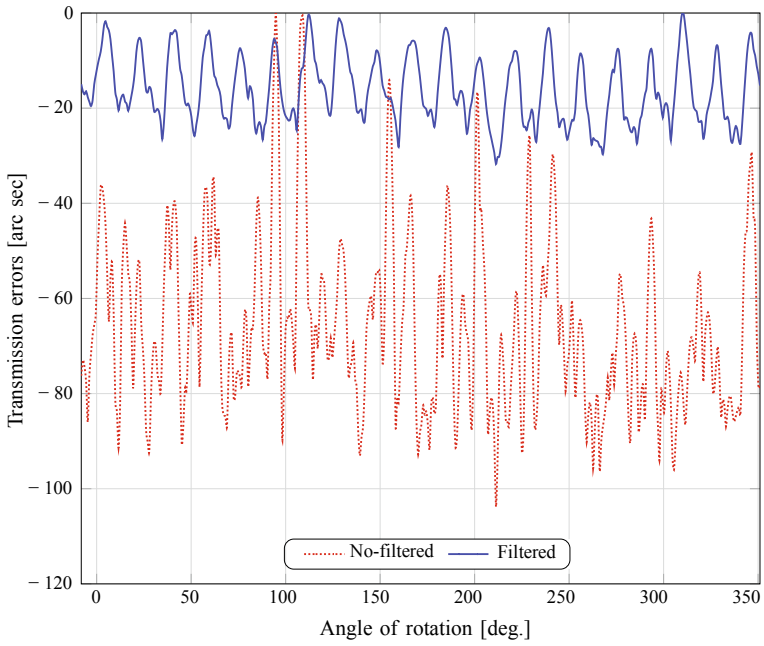


Fig. 10 Unloaded functions of transmission errors of the to-be-inspected gear A

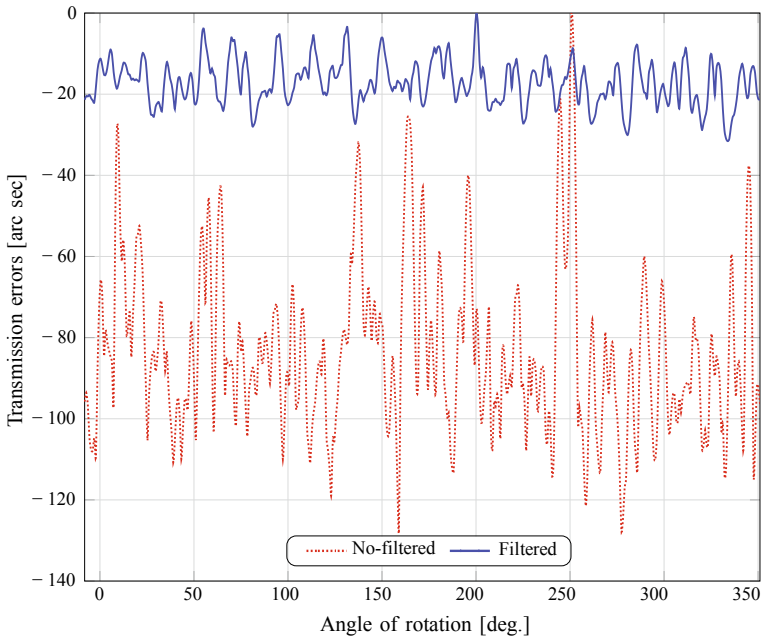


Fig. 11 Unloaded functions of transmission errors of the to-be-inspected gear B

Table 2 Variables for evaluation of the flank deviations of the to-be-inspected gears A and B

Variable [mm]	Gear A (non-filtered)	Gear A (filtered)	Gear B (non-filtered)	Gear B (filtered)
L_α	14.416	14.321	9.180	9.159
λ_α	0.481	0.477	0.306	0.305
L_β	26.845	26.845	26.845	26.845
λ_β	0.895	0.895	0.895	0.895
ρ_b	5.25	5.25	5.25	5.25

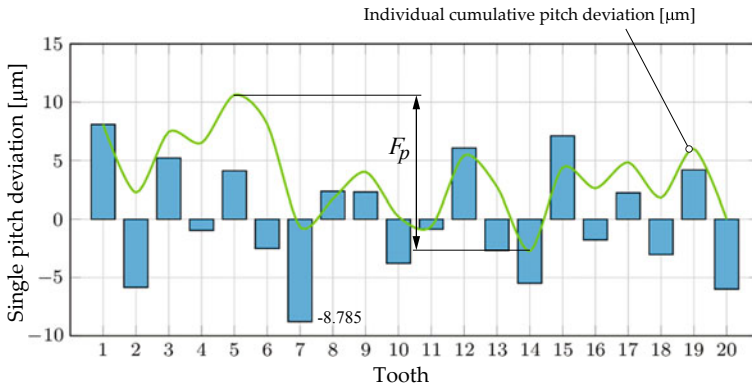


Fig. 12 Single and cumulative pitch deviations of the to-be-inspected gear A when no filtering is applied to the point clouds of the left tooth side

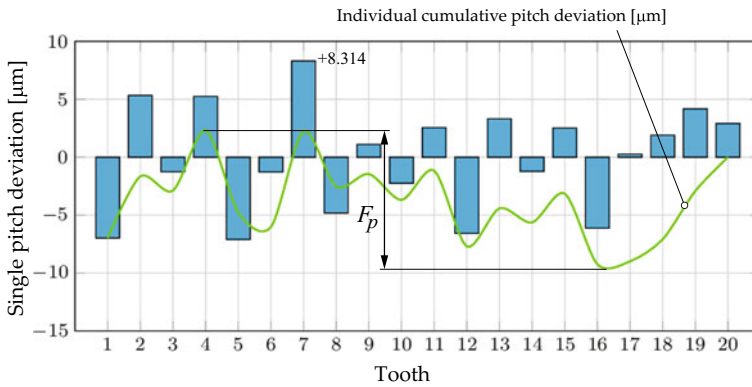


Fig. 13 Single and cumulative pitch deviations of the to-be-inspected gear B when no filtering is applied to the point clouds of the left tooth side

Table 3 Pitch deviations and class classification of the to-be-inspected gears A and B

Deviations/ Class	Gear A (non-filtered)		Gear B (non-filtered)		Gear A (filtered)		Gear B (filtered)	
	LS	RS	LS	RS	LS	RS	LS	RS
f_p [μm]	8.785	12.230	8.314	36.117	2.573	2.680	2.424	5.467
A_{f_p}	6	7	6	11	2	3	2	5
F_p [μm]	13.357	20.890	11.560	46.220	3.190	4.825	3.050	6.480
A_{F_p}	4	5	4	8	1	1	1	2
Class	7		11		3		5	

Table 4 Profile deviations and class classification of the to-be-inspected gears A and B

Deviations/ Class	Gear A (non-filtered)		Gear B (non-filtered)		Gear A (filtered)		Gear B (filtered)	
	LS	RS	LS	RS	LS	RS	LS	RS
F_α [μm]	27.013	57.123	35.943	56.190	15.682	16.714	13.666	10.491
A_{F_α}	8	11	9	10	7	7	6	6
f_{f_α} [μm]	17.426	43.123	23.046	43.169	7.288	8.805	6.511	4.999
$A_{f_{f_\alpha}}$	8	10	9	10	5	6	5	4
f_{H_α} [μm]	+34.098	-35.742	+54.903	+37.907	+16.149	+15.151	+5.638	+8.931
$A_{f_{H_\alpha}}$	10	11	11	11	8	8	5	7
Class	11		11		8		7	

Table 5 Helix deviations and class classification of the to-be-inspected gears A and B

Deviations/ Class	Gear A (non-filtered)		Gear B (non-filtered)		Gear A (filtered)		Gear B (filtered)	
	LS	RS	LS	RS	LS	RS	LS	RS
F_β [μm]	31.233	25.948	41.832	56.684	5.848	6.256	25.183	10.491
A_{F_β}	9	8	9	10	4	4	8	6
f_{f_β} [μm]	28.607	25.485	20.574	42.718	4.454	5.175	5.618	19.568
$A_{f_{f_\beta}}$	9	9	8	10	4	4	4	8
f_{H_β} [μm]	-13.8	-10.02	-13.964	-20.528	+6.765	-5.378	+4.269	-11.062
$A_{f_{H_\beta}}$	7	6	7	8	5	5	4	7
Class	9		10		5		8	

larger class classification number than gear B due to the fact that an involute profile has been considered as a reference profile instead of a crowned profile.

Table 5 shows the helix deviations and their corresponding class tolerance classification numbers for gears A and B. The filtering of the point clouds also lowers the class classification number for both gears. Gear B shows a larger class classification number than gear A due to the fact that a standard helix was considered in gear B as a reference helix instead of a lead crowned helix.

Table 6 Runout deviations and class classification of the to-be-inspected gears A and B

Deviations/Class	Gear A (non-filtered)	Gear B (non-filtered)	Gear A (filtered)	Gear B (filtered)
F_r [μm]	23.0	56.0	5.0	9.0
A_{F_r}	6	8	2	3

Table 7 Tooth thickness tolerances of the to-be-inspected gears A and B

Tolerance	Gear A (non-filtered)	Gear B (non-filtered)	Gear A (filtered)	Gear B (filtered)
T_n [μm]	25.0	48.0	5.0	6.0

Table 6 shows the runout deviations. The filtering process also lowers the class classification number related to runout deviations in both gears. The same occurs with the normal tooth thickness tolerance, T_n , as shown in Table 7.

9 Conclusions

The performed research work allows the following conclusions to be drawn:

1. Computational approaches to estimate the main gear flank deviations as defined in the ISO Standard 1328-1:2013 (pitch deviations, profile deviations, helix deviations, runout deviations, and normal tooth thickness variation) are proposed and applied to reconstructed helical gears from point clouds obtained with a non-contact metrology machine.
2. Results show that filtering the point clouds is necessary for a better estimation of the contact pattern and function of transmission errors of the reconstructed gears from point clouds when in mesh with a master gear. Preliminary results of the assessment of the gear class classification according to the ISO Standard 1328-1:2013 by virtual metrology have been obtained. However, this assessment requires further verification and comparison with results obtained with a contact metrology machine.

Acknowledgements The authors express their deep gratitude to the Spanish Ministry of Economy, Industry and Competitiveness (MINECO), the Spanish State Research Agency (AEI) and the European Fund for Regional Development (FEDER) for the financial support of research project DPI2017-84677-P.

References

1. Fuentes-Aznar, A., Gonzalez-Perez, I.: Integrating non-contact metrology in the process of analysis and simulation of gear drives. AGMA Fall Technical Meeting, paper 18FTM21, 1–15 (2018)
2. Gonzalez-Perez, I., Fuentes-Aznar, A.: Tooth contact analysis of cylindrical gears reconstructed from point clouds. *Mech. Mach. Sci.* **81**, 219–237 (2020)
3. Gonzalez-Perez, I., Guirao-Saura, P.L., Fuentes-Aznar, A.: Application of the bilateral filter for the reconstruction of spiral bevel gear tooth surfaces from point clouds. *J. Mech. Design* **143**, 053401-1–10 (2021)
4. International Standard ISO 1328-1: Cylindrical gears—ISO system of flank tolerance classification, Part 1: Definitions of allowable values of deviations relevant to flanks of gear teeth (2013)
5. Piegl, L., Tiller, W.: *The NURBS book*. Springer, Berlin (1995)
6. Samet, H.: *Foundations of Multidimensional and Metric Data Structures*. Elsevier, San Francisco (2006)
7. Han, X.F., Jin, J.S., Wang, M.J.: Guided 3D point cloud filtering. *Multimed Tools Appl.* **77**, 17397–17411 (2018)

Cylindrical Arc Gears: History, Achievements, and Problems



Vladimir N. Syzrantsev 

Abstract The article reflects the results of the study of geometry, contact and bending strength, as well as failure probability associated with contact and bending endurance of progressive gears, i.e. cylindrical arc teeth gears, achieved within the framework of national scientific schools (USSR and Russia). These gears in the conditions of machine unbraced drive bodies can significantly increase the durability of both contact and bending strength and endurance. Modern lines of study of cylindrical arc gears are shown.

Keywords Cylindrical gears · Arc teeth · Studies · Russia

1 Introduction

In Russian technical literature, reference is made to patents obtained abroad in the early twentieth century when describing the history of cylindrical arc (curvilinear in length, circular, arched) gears (Fig. 1). At the same time, Radzevich (USA) [73, 74] has found, apparently, the first ever patent for gears with a circular “tooth line” [67], Fig. 2.

In the USSR, and then in the Russian Federation, researchers began developing the geometry of cylindrical arc gears, ways of cutting with various tools and shaping motions in the second half of the twentieth century. Over the past seventy years, almost a couple of dozen methods of manufacturing cylindrical wheel arc teeth, original tools, machines for cutting arc teeth, various designs of gearboxes and drives based on these progressive meshing gears have been proposed [8–18, 20, 22–34, 37–39, 42, 68–70, 78, 80–82, 84–93]. This is not a complete list of defended technical solutions that facilitate manufacturing cylindrical arc gears. 25 candidate’s dissertations have been defended [3, 4, 6, 47, 49, 53–57, 59, 60, 62–64, 71, 72, 75, 97, 99, 102, 104, 106, 127, 128] as well as 6 doctoral theses [5, 50, 66, 98, 107, 121].

V. N. Syzrantsev (✉)

Tyumen Industrial University, Volodarskogo Street 38, 625000 Tyumen, Russia

e-mail: syzrantsevvn@tyuiu.ru



Fig. 1 Cylindrical arc gears

UNITED STATES PATENT OFFICE.

A. C. SEMPLE, OF CINCINNATI, OHIO.

RACK AND PINION.

Specification of Letters Patent No. 5,647, dated June 27, 1848.

To all whom it may concern:

Be it known that I, AMZI C. SEMPLE, of Cincinnati, in the county of Hamilton and State of Ohio, have invented a new and useful form of teeth or cogs to be used in the racks and pinions and otherwise for various purposes, by which a great increase of strength, as well as accuracy of motion, is secured over any other form now in use; and I do hereby declare that the following is a full, clear, and exact description of the construction and operation of the same, reference being had to the annexed drawings, in which my form of cogs or teeth are exhibited as applied to a press, Figure 1, in the drawings, making a part of this specification, and more particularly Figs. 4 and 7, which exhibit a diagonal form, and Figs. 6 and 8, which show the arched or curved form of 20 teeth or cogs, and my invention consists in constructing such teeth or cogs essentially in a curved or diagonal form as therein set

forth, by which it will be seen that the cogs or teeth meshing together when subjected to a heavy pressure incline, the center of the one to the center of that into which it works, thus securing a true and accurate motion, the base of each cog or tooth at the same time occupying a greater surface upon the rack or periphery of a wheel is rendered much stronger by such peculiar construction.

What I claim as my invention, and desire to secure by Letters Patent, is—

The form of the teeth or cogs, both in the rack and in the pinion meshing into the same; either diagonal as in Figs. 4 and 7 or arched or curved as in Figs. 6 and 8, whereby strength and accuracy of motion are the better secured as herein described.

A. C. SEMPLE.

Witnesses:
I. BIGELOW,
S. A. PETCH.

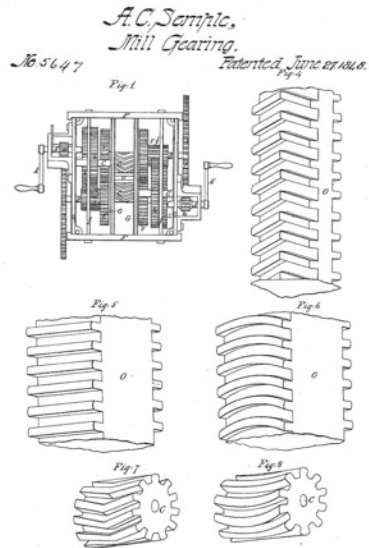


Fig. 2 The first patent for gears with a circular tooth shape

The development of this type of cylindrical gear results from the need to increase the load capacity and contact and bending endurance of gears in conditions of unbraced machine bodies and occurrence of unavoidable errors in the manufacture and assembly of gear elements.

Unlike other machine parts, the required performance of cylindrical gears is only provided by meeting a set of different criteria: bending strength of wheel and gear teeth, bending endurance of the teeth, contact strength and endurance of tooth flanks,

deep contact strength and wear of tooth flanks and avoidance of exceeding the noise and vibration characteristics specified in the technical documentation. At the same time, in real operating conditions of high-loaded, energy-saturated machines, when the external torque and actual twist angle of wheel teeth flanks (it depends on both manufacturing errors of wheels, shafts and body parts and their strain during the operation) change according to the laws of random variables, traditional cylindrical gears with straight, helical, double helical, barrel-shaped teeth do not provide the required load capacity and durability. Moreover, in the above-mentioned operating conditions, the transmission ratio is to be as close as possible to a constant value, a deviation from which increases the vibration of the gear, leads to additional dynamic load in meshing and, ultimately, loss of its performance. With the correct geometry of arc teeth, the cylindrical gear can increase the contact strength and bending endurance of the teeth by 1.5–4 times in real operating conditions.

As an example, we present test results of the cylindrical gear of a tractor on-board gearbox, which has the following parameters: the number of gear teeth is, the number of wheel teeth is, the module is mm and the tooth face is mm. The required spur gear life is 11,000 h. The calculation of the gear contact strength at the maximum amount of teeth misalignment in meshing during two minutes (the misalignment caused by the manufacturing accuracy of the part constituents comprised by the on-board gearbox was taken in account) showed that the gear durability is ensured. The result of the tests of on-board gearboxes on the closed-loop stand, showed that the actual gear life is 5600–6000 h. During the tests, using integral type strain gauges [109, 110, 115], the actual teeth misalignment in meshing was $7'$, caused not only by technological errors in the manufacture of parts, but also by strains caused by the cantilever load of the gearbox output shaft from the track tension. With this magnitude of misalignment, the calculated life of the spur gear corresponds to 6000 h. Note that at a twist angle of $8'$, the contact area in meshing of the studied gear, under the influence of load, does not extend to the entire wheel tooth face. This fact excludes a possibility of calculating the strength and durability of the cylindrical gear according to GOST 21354-75. To achieve the service life of the on-board gearbox required by the technical requirement specification, a cylindrical arc gear was installed in the gearbox (the calculated tool radius is 220 mm), which has geometric parameters similar to a spur gear.

The on-board gearbox with a cylindrical arc gear was tested on the stand for 11,000 h. The check of the gear that had worked out the required service life showed no signs of fatigue damage (pitting, wear) on the surfaces of the gear and wheel teeth.

In order for the transmission ratio in a cylindrical spur gear in any phase of meshing to be constant, the profile in any end section of the tooth is the same section of the involute; the gear is matched, and all its geometric and kinematic characteristics are calculated on the basis of the theory of gear tooth action in a plane. Depending on the forming method, arc teeth can be manufactured both involute-profiled in the middle section only [5, 50, 53, 59, 75, 99, 107], and involute-profiled in any end section of the arc tooth [6, 62, 71, 81, 100, 101, 108, 127]. In the absence of misalignment, an alignment error of the gear and wheel axes and gear and wheel displacement in the axial direction, the arc gear remains matched regardless of the teeth forming method applied and is described with models developed in the framework of the theory of

gear tooth action in a plane. A completely different situation occurs in arc teeth meshing in the presence of the above errors in the relative position of the gear and wheel axes or the displacement of the gear and wheel in the axial direction. In these conditions, meshing becomes spatial, generally mismatched, and its study is only possible on the basis of the methods developed in the theory of spatial gearing by meshing [7, 50, 61, 107].

Close to the described one, the problem of matching determination has already arisen for cylindrical involute helical gears, involute bevel gears, involute face gear pairs, when, within the framework of the theory of gear tooth action in a plane, it became impossible to prove matching of these gears, which have the spatial nature of meshing. The solution was obtained by Erikhov [50] based on the use of special methods developed by him within the theory of spatial gearing: two-parameter envelope and sequential envelope. An important consequence of the work [50] is the proof of the following. If the flanks of the wheel and gear teeth (including arc ones) are envelopes of families of generating surfaces which are an involute helicoid, then the gear is matched and not sensitive to position and assembly errors, if the gear and wheel teeth flanks are in correct contact.

2 Issues of Determining Geometric Parameters of Arc Teeth Flanks of Cylindrical Wheels

The beginning of the twentieth century was marked by the emergence of a number of companies that specialized in the production of machines and tools for cutting spiral bevel wheel teeth: Gleason (USA), Klingelnberg (Germany), Oerlikon (Switzerland). The experience of using these gears has shown that in order to obtain the required performance and load capacity of spiral bevel gears, it is necessary to localize the meshing contact both in the cross-sectional and longitudinal direction of the teeth. These gears are mismatched; the instant transmission ratio, equal to, only remains unchanged in the center of the pressure spot and alters during the meshing phase. The law of the transmission ratio cannot be of any type; the regularity of alterations in the meshing phase must be of such type which will compensate the geometric mismatch of the gear with the wheel and gear teeth contact and bending strains that occur when the gear is under load. Bevel gears with spiral teeth, the flank geometry of which is determined taking into account the maximum approximation to the constant law of the gear ratio when the gear is under load, in contrast to matched gears, are called approximate gears, and the problem of determining geometric parameters of the tooth flanks is the synthesis of gears.

The given problem is the most difficult in the theory of spatial gearing. Its solution requires the use of special mathematical tools, numerical methods for solving systems of transcendental equations, and methods for optimizing ravine functions, taking into account the restrictions of equations and inequations [61, 107]. In our country, F. L. Litvin, M. G. Segal, K. I. Gulyaev, K. M. Pismanik, M. L. Erikhov, V. I. Goldfarb,

D. T. Babichev, I. I. Dusev, G. I. Sheveleva, V. I. Medvedev, B. P. Timofeev, E. S. Trubachev, S. A. Lagutin, B. A. Lopatin, V. N. Syzrantsev, A. E. Volkov and their disciples and followers [7] were involved in the development of various approaches to solving problems of geometric synthesis of gears with spatial gearing (bevel, worm, spiroid), including semi-rolled bevel gears.

In the process of cutting spiral bevel gears, meshing (circular in shape for the Gleason method, in a cycloid form in the Oerlikon method, in the form of an involute in the Klingenberg method) of a [generating crown gear](#) and a blank is reproduced. At the same time, if we direct the radius of the generating crown gear to infinity, it turns into a rack; and reducing the face angle of the cut wheel to zero in the extreme case we get a spiral cylindrical gear. That is, a spiral cylindrical gear is essentially a special case of gear, both in terms of forming methods and problems inherent to spiral bevel gears.

A transition from cylindrical gears with gear tooth action in a plane (spur) to the gears with spatial gearing (with arc teeth and localized contact) has raised a number of issues, primarily associated with the peculiarities of choosing the wheel teeth flank geometry providing an increased lifetime of the gear.

Firstly, if the geometric parameters of the flanks of cylindrical wheel straight and helical teeth practically do not depend on the methods of their manufacture, then the processes of forming arc teeth, corresponding to various methods of their processing significantly affect both the magnitude and nature of changes in the geometric parameters of the active teeth flanks and kinematic gear indicators.

Secondly, in cylindrical spur and helical gears, regardless of the methods of forming their teeth, if there is a twist angle of the gear axes, the contact point moves to the tooth end. A different situation occurs in gears with a localized contact. Here, each method of teeth forming corresponds to meshing geometric and kinematic characteristics that define the position of the teeth contact points in the gear, the distribution of backlashes between the teeth flanks in the finite vicinity of this point and alteration of instant transmission ratio within one-pair and multiple contacts.

The third issue of localized-contact gears is calculation of the load distributed over the contact area. Here it is necessary to have such calculation methods that, along with bending-shear and contact strains of the teeth, would take into account the position of the initial contact point of the teeth flanks and their actual integrity, as well as the effect of “transfer” of the contact area onto one or both ends of the tooth.

Finally, the variation of the gear teeth contact conditions in cylindrical arc gears determined by a random nature of external factors (transmitted load) raises the problem of evaluating the probability of the gear failure-free operation both by contact and bending endurance of arc teeth.

3 Characteristics of Arc Teeth Cylindrical Gears Formed in Various Ways

The analysis of manufacturing methods for cylindrical wheel arc teeth shows that they are divided into the following groups, close to the methods of cutting spiral bevel gears, depending on the tools and shaping motions used. The first group of methods (analogous to the Gleason methods) includes a circular cutter head (Fig. 3), the generating surface of which is a hyperboloid [37], in a general way, and a straight circular cone [13, 18, 27, 32, 91] or a cylinder [16, 17, 22, 29, 30, 80, 87], in particular cases. The transition to cutting each subsequent tooth space is carried out with interruption of the cutting process—by the single indexing method. The second group of methods [9, 10, 15, 39] is based on the use of cutter heads similar to those proposed by Oerlikon (Fig. 4) for cutting cyclopoloid teeth of bevel wheels by the continuous generating method. The third group methods use such tools as [8, 20, 25, 26, 28, 33, 37] a spiral-disc milling cutter, Fig. 5 (spiral-disc grinding wheel or hone). The generating surfaces are involute, Archimedean, convolute helicoid, or spiral ones

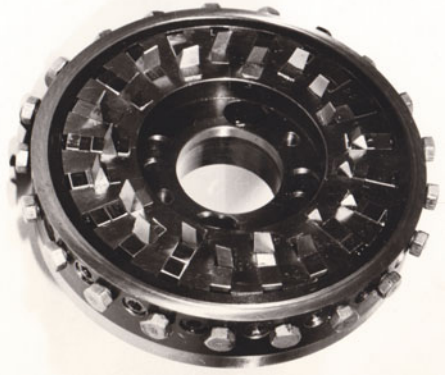
Fig. 3 Circular cutter head



Fig. 4 Oerlikon cutter head



Fig. 5 Spiral-disc milling cutter (sharpened)



of a more general type. Wheel teeth processing in this group of methods is carried out with continuous generation. These methods can be considered as a special case of tooth forming, using bevel spiral milling cutters developed by Klingelnberg.

When describing the groups of teeth cutting methods briefly discussed above, we note the following. The obvious advantage of the first group methods is tool simplicity. Technical solutions for cutter head manufacturing has been perfected during the production process of circular bevel gears. This is the only group of methods the tools of which are not correlated with the module of the cut wheels—the most important circumstance for manufacturing arc teeth gears. However, the discontinuity, which requires a creation of special tooth-cutting machines of complex kinematic structure, that are currently absent, and limited (as shown by the accumulated experience of cutting circular bevel gears) productivity of the process are constraining reasons for the development of the first group methods.

The second group methods use a more complex tool, in which the blades are arranged in groups so that their cutting edges form a series of repeated spirals (entries) on the tool. The continuity of the process allows increasing the productivity of tooth processing up to two times compared to the methods of the first group. At the same time, the methods of the second group do not allow finishing gear teeth, and their application also requires a serious modernization of existing machine designs, since they do not have the required shaping motions.

The spiral-disc milling cutters used in the third group of methods are quite similar to the tools of the second group methods by design features. The principal difference between these cutters is the location of the cutting edges on a spiral generating surface, which allows manufacturing spiral-disc tools for finishing operations. Spiral-disc milling cutters can be made with both sharpened [57] and relieved teeth [53, 106]. A serious advantage of the third group methods is a possibility of implementing the gear cutting process according to a one-parameter scheme, which not only provides high productivity of tooth processing, but also requires minimal modernization of gear milling machines, allows to dramatically reduce the length of kinematic chains of machines and increase their rigidity.

Among the third group methods, we choose using the tool the generating surface of which is an involute helicoid. During the process of cutting arc teeth of the gear pair with this tool, as shown in [107], the pair turns out to be matched regardless of assembly errors. There are no other options for manufacturing cylindrical arc gears insensitive to errors in the relative position of the gear pair teeth in meshing, among all known methods of forming arc teeth.

The disadvantage of the third group methods is toughening restrictions for some parameters of the tools (mainly by the value of the calculated radius), caused by cutting the gear teeth from the end sides. The tools of this group of methods, as well as hob cutters, can only cut the wheels of a specific module.

The fourth group is represented by one method [34], in which a shaver is used, which is the tool made in the form of a multiple-thread spiral line. This is a way to effectively finish arc teeth in the process of continuous generation. Its peculiarity is that there are all the prerequisites to implement the effect of “shaving cut” in the processing operation. And, finally, the fifth group of methods is represented by a tool in the form of a circular broach with blades of an involute profile (a cup grinding wheel sharpened along the involute), and processing is generating-free, in conditions of single indexing.

The introduction of cylindrical arc gears into a practical creation of reliable gear-boxes and drives of heavily loaded mechanisms and machines is connected with a comprehensive elaboration of technological processes of their production, creation of highly efficient tools and implementation of cutting teeth processes on universal CNC machines rather than on dedicated ones. The main scope of scientific research carried out over the past decades is related to the solution of numerous problems of technological support of cylindrical arc gear manufacture in the framework of arc teeth forming methods corresponding to the first group.

A research team at the State University of Tula is engaged in the development of various designs of circular blades, cutting technologies for cylindrical circular gears with the middle section involute profile of the tooth on CNC machines. These studies, initiated under the guidance of Prof. Koganov, are on their way and reflected in the works of his disciples and followers [4, 5, 19, 21, 36, 41, 56, 66, 72, 102, 128]. It should be noted that it was at this university where the study of semi-rolled cylindrical arc gears was first started [3] under the scientific leadership of Koganov and continued in the works [5, 72], which allows to implement transmission ratios in a gear pair up to ten while reducing the machine time of cutting gear teeth.

A particular variant of the first group methods for cutting arc teeth is a method that uses a circular cutter head with blades having a zero-profile angle. Initially, this method of cutting arc teeth was proposed in [100, 101] and further improved in [42, 79–82, 86–90, 92, 93]. The peculiarity of this method is that in any end section, the arc tooth profile is an involute [108]. According to the authors, this geometry is theoretically correct in comparison with other methods of forming arc teeth flanks. This is a big misconception. It is a result of considering the geometric characteristics of arc teeth meshing using the theory of gear tooth action in a plane, rather than spatial gearing, which includes the cylindrical arc gear. In this case, the theory of gear tooth action in a plane is only applicable if there are no errors in the relative position of

the wheels in the gear (twist angle, alignment error, and axial displacement of the wheels relative to each other). Only under these conditions, the active path of action (working line) in the gear is located in the middle section of the arc tooth and the gear is matched with both linear and point contact.

Arc teeth are 20–30% stronger than straight ones; that is why a cylindrical arc gear is more effective in bending strength and endurance than a spur gear. As for the contact strength and endurance, the effectiveness of the cylindrical arc gear is not so obvious. The value of contact stresses in a gear is determined in each meshing phase by the length of contact lines. In comparison with the spur gear, the contact lines in the arc gear (with linear contact) are longer by 3–5%, while in the helical gear, the length of contact lines, comparable to the arc gear, is provided at an angle of inclination of about 10° due to the overlap ratio. I.e., the contact strength of the arc gear will always be lower in the absence of teeth misalignment in meshing, compared to the helical gear with a tooth angle of inclination of more than 10° , and especially with the herringbone gear, in which a tooth angle is 25° or more. In addition, unlike spur and helical gears, in cylindrical arc gears during a linear contact in the areas adjacent to the teeth ends, there is a differential friction effect, which is the greater the larger the arc tooth longitudinal curvature, which also reduces the contact strength of the arc gear.

The situation changes dramatically when the required performance of cylindrical gears is to be ensured at their operation in unbraced bodies, when the resulting twist angle of teeth flanks is a random value and reaches $10'–30'$. In such conditions, rear-axle drives of locomotives, tractors, and drilling rig top drives are operated. As noted above, the angle of misalignment (γ') in meshing, which occurs during the operation of a tractor on-board gearbox, leads to a twofold decrease in durability of the spur gear, due to the edge contact and a significant increase in contact stresses at the tooth end. At a twist angle of $10'$ or more (such values have been recorded when operating locomotive gears), it is a big challenge to ensure the required performance of cylindrical gears with the teeth linear contact. It is in these operating conditions that the use of cylindrical arc gears is effective and allows ensuring the required durability of the gears.

There is a traditionally widespread opinion that the arc gear has the property of compensating the twist angle by self-adjustment of one of the gear pair elements (if it is possible to move them along the shaft). Indeed, in the presence of a twist angle, the contact point in middle section meshing, where the helix angle is zero, is shifted to one of the arc teeth ends. In the linear contact, as in the spur gear, the presence of a twist angle immediately leads to the edge contact. With a localized contact along the arc tooth length, the displacement of the contact point to the end of the tooth, where the helix angle is different from zero, depends on the localization value. Due to the arc tooth helix angle at the end, when the gear is loaded, an axial force occurs in meshing, which ensures self-adjustment of the gear or wheel. In the course of axial displacement, e.g. of the gear, the contact point moves along the arc tooth flank towards the middle section of the gear tooth. Since the maximum helix angle at the tooth end gradually decreases to zero in the middle section of the tooth, then as the gear shifts, the acting axial force decreases (to zero in the extreme case).

As a consequence of the above, as shown by experimental studies, the value of the twist angle achieved in the process of gear self-adjustment under a constant external load is not $<3'$. Further compensation of the twist angle becomes impossible due to a decrease in the axial force, which is insufficient to overcome the friction force in the coupling of the gear elements with the shaft. There are no available studies of the self-adjustment effect in conditions where position errors and external torque alter according to the laws of random variables.

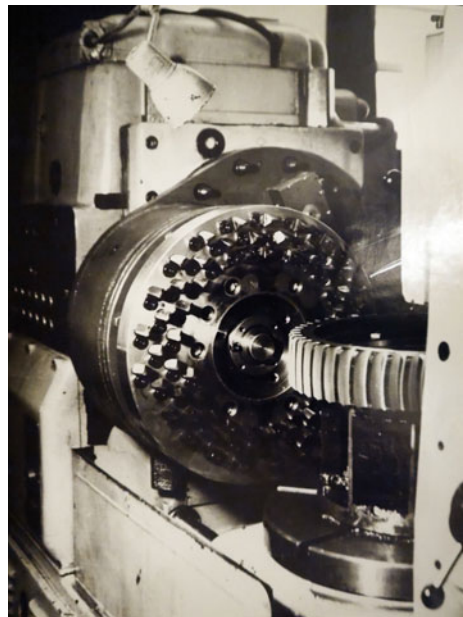
Regarding the gears, the arc teeth flanks of which have an involute profile in each end section [100, 101, 108], we can note the following facts. In the absence of gear and wheel axes misalignment, both with linear and point (localized along the length) contact, the gear is matched, the instantaneous transmission ratio (position function) is constant and the geometric and kinematic characteristics of the gear can be calculated on the basis of the theory of gear tooth action in a plane. If there is a twist angle, the contact of the gear and wheel active tooth flanks occurs rather at points where the normals to the tooth flanks coincide than in the end sections of the teeth. In this case, gear matching is disrupted and the position function not only becomes variable [127], but also takes the form in which it is only possible to provide a given transmission ratio at one contact (calculated) point of the tooth flank. A similar situation occurs in the synthesis of spiral bevel and hypoid gears geometry [61], in which the calculated point is located either in the middle of the active tooth flank, or with a slight offset to its inner end.

In a cylindrical arc gear [100, 101], the position of the calculated point depends on the value of the twist angle; and its coordinates can be determined only on the basis of the spatial gearing theory [50, 61, 107]. In bevel and hypoid gears, the reduction of the negative impact of gearing mismatching and the “transfer” of gears to the class of approximate gearing achieved by using in teeth cutting circular cutter heads, the blades of which are made with profile angles different from the nominal one (blade number corrections). A similar method [127] of modifying the arc teeth active flank is also applicable to gears with an involute teeth profile in their end sections. Since in these gears, the deviation of the blade profile angle from zero depends on the value of the expected twist angle [127], at which the gear will operate, then, it is necessary to have a set of blades with angles other than zero as in the manufacture of bevel and hypoid gears. Taking this circumstance into account, as well as the need to solve the synthesis problem by the methods of the theory of spatial gearing by meshing [7, 107, 111], i.e. determination of the optimal values of the cutter head profile angle and the value of contact localization in the longitudinal direction of the teeth, providing a minimum deviation of the transfer function from the nominal value with a given value of the twist angle and the required gear durability, we can state that arc gears with an involute profile in the end sections of the teeth have no advantages, in comparison with other methods of cutting arc teeth. Moreover, it is in these gears where the transfer function error at identical twist angles reaches a maximum value, compared to other ways of forming arc teeth; and to consider this gear the only theoretically correct one, which is stated in a number of advertising materials, is to mislead both the consumers and research workers.

Features of the geometry and processes of cutting arc teeth by the second method [9, 10, 15, 39] are considered in papers [76, 77].

A comprehensive study of gears, the arc teeth formation of which is carried out by spiral tools (the third group of methods), were carried out under the scientific guidance of Prof. Erikhov at the Kurgan Machine-Building Institute (now the State University of Kurgan) since the 1970s, and has been continued by Prof. Syzrantsev and their disciples [50, 53, 54, 57, 59, 60, 63, 64, 75, 97, 104, 106, 107, 127]. Within the framework of these studies, original designs of spiral-disc tools have been proposed and manufactured: sharpened and relieved spiral-disc milling cutters and spiral-disc hones [53, 57, 75, 106]. A theory of profiling relieved spiral-disc milling cutters has been developed [106]. Special slides for gear milling machines have been developed and manufactured (Fig. 6), which accomplish the process of cutting cylindrical arc teeth [53, 57, 75]. For the first time for cylindrical arc gears, based on the actual integrity of the contacting surfaces, the presence of the twist angle and the possibility of moving out of the contact area onto one or both ends of the tooth, a complex of theoretical and experimental works to determine the stress distribution in the contact area in arc teeth meshing, required for arc gear contact strength and endurance calculation has been implemented [51, 54, 64, 107]. To calculate the stress distribution over the contact area [1, 51, 54, 107], taking into account the teeth internal and contact strains in meshing, the mathematical apparatus of the boundary value problem theory has been used. The results of the calculation have been proved by agreement with the figures of the numerical calculation of the contact load according to the program [103] and experimental studies [2].

Fig. 6 Cutting a gear with a spiral-disc milling cutter



In the process of the arc gear operation, there have been obtained experimental data on alteration of its element position function when varying transmission ratios, twist angles and torque values, proving the adequacy of the developed mathematical models [64, 107]. These studies are unique; they have no analogues either in our country or abroad. Theoretical and experimental studies of arc teeth bending strength and endurance have been carried out [63, 97, 123]. Based on the mathematical apparatus of nonparametric statistics [107, 113, 114, 116, 117], some approaches [119, 120, 122, 124] have been proposed to estimate a probability of failure-free operation of arc teeth cylindrical gears with random external load. A synthesis method has been developed for gear geometric parameters to ensure their maximum durability in terms of contact endurance [107] with the random nature of a teeth misalignment angle in meshing and external load. For three main types of cylindrical arc gears, taking into account geometric features of their contact in meshing, engineering design methods by contact and bending strength and durability have been developed [118] for various conditions of their loading in operation.

Within the framework of this scientific school, theoretical and experimental studies of loading and geometry of other types of cylindrical arc gears as well have been carried out [59, 60, 104, 127].

4 Modern Lines of Research of Cylindrical Arc Gears

The analysis Currently, a number of creative teams are involved in the study of cylindrical arc gears in the Russian Federation. The State University of Tula, Ryazan Institute (branch of the Technical University of Moscow) and OOO “Gears of MGOU” have been performing research on working out new production technologies for cylindrical arc gears on four-axis CNC machines, providing modification of teeth flanks and on improving the designs of various types of circular cutter heads, including zero profile blades. At OOO “STC-Reductor” in St. Petersburg, a process of cutting cylindrical arc gears with circular cutter heads on CNC machines using the single indexing method has been mastered. The State University of Kurgan goes on improving cylindrical arc teeth roller pinion gear (system) [35, 40, 43, 83, 94, 95]. This type of gear is effective for ball mill drives, cement kilns and other low-speed but highly loaded drives operating in an atmosphere with a high content of abrasive particles. The dimensions of the elements of these gears reach several meters. The use of arc rollers here allows not only to compensate for the inevitable teeth misalignment in meshing, but also to significantly increase the maintainability of gears by replacing worn rollers with new ones.

The scientific research of arc teeth cylindrical gears, which began at the Kurgan Machine-Building Institute, is currently continued at the Industrial University of Tyumen [108, 115, 118–124]. The features of the work performed is as follows.

In meshing arc teeth, flank shaping of which is performed by circular cutter heads, the linear or point contact may be implemented. If the arc teeth are cut spirally with a disc tool, then a local-linear contact can be obtained in meshing. With this type of

contact, the bearing capacity of the gear is close to that with a linear contact, but the danger of edge contact in the presence of a twist angle is significantly reduced.

For a local-linear contact, the backlash function in meshing cannot be described using principal relative curvatures, which required development of special methods to estimate meshing loading [1, 7, 54, 64, 107]. When performing the work [6], it was found that in meshing of bevel arc gears cut with spiral-disk tools by the method of continuous generation, in each phase of meshing, the gear and wheel teeth flanks can correctly contact at two points spaced along the tooth length rather than at one. I.e., two contact lines are implemented in meshing and the load is distributed between the two contact areas. Based on the above, in work [104], a cylindrical arc gear cut by spiral-disc milling cutters and having two contact areas distributed along the length in meshing, has been theoretically and experimentally studied. The principal feature of this gear is that in the process of its loading, two axial forces directed against each other occur in meshing arc teeth. It is the equilibrium of these forces that ensures the self-adjustment of one of the gear elements (gear or wheel) in the presence of teeth misalignment in meshing. Essentially, this gear is similar to a gear with double helical teeth, but with localized contact in their meshing. If the generating surface of a spiral-disk tool is an involute helicoid, then the gear remains matched [50] even when the twist angle of the teeth in meshing is different from zero. Experimental studies of this gear have shown that at a twist angle of up to 30', the teeth always mesh in two areas due to self-adjustment of the gear.

For the first time, an adaptive arc gear allows self-adjustment of the pinion (gear) or wheel in the conditions of a random error field and external load [96], Fig. 7.

An adaptive cylindrical arc gear has a body which contains an input shaft with a mounted gear and an output shaft with a mounted wheel, which has a possibility of axial movement. On the input shaft, between the gear and bearings, distance

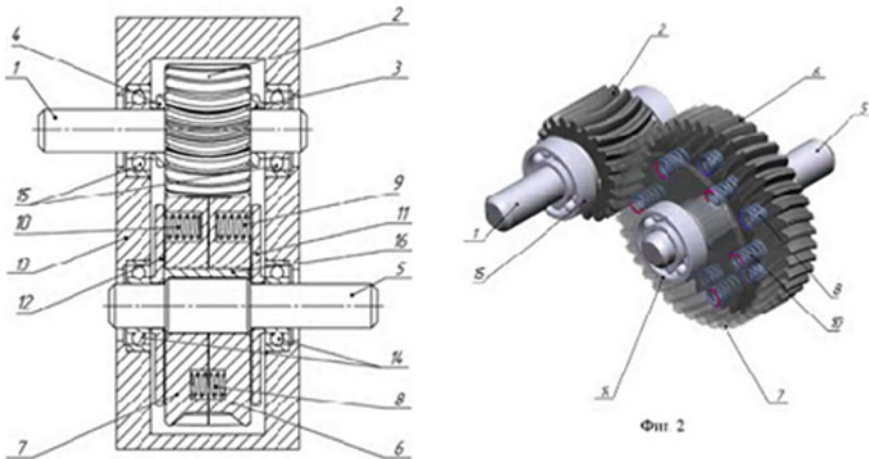


Fig. 7 Adaptive arc gear

sleeves are installed. The wheel is made of two half-wheels, between which an elastic element is installed. Between each half-wheel and the bearing, elastic elements and a bushing to prevent axial movement are installed. This gear can be manufactured in both generated and semi-rolled versions. Forming adaptive gear arc teeth is possible by any of the methods discussed above, including cutter heads on CNC machines. The principal feature of this gear is a presence of two contact points located outside the middle section of the arc tooth in each meshing phase. At a given value of semi-wheel displacement, determination of the contact point coordinates, calculation of their principal and principal relative curvatures and, the instant transmission ratio is only possible by methods of the theory of spatial gearing [7, 50, 61, 107]. In general, the gear is mismatched. To determine optimal geometric parameters of the adaptive gear, it is necessary to implement a solution of the synthesis problem, as it is performed for circular bevel gears. In order to reduce noise and vibration, the profile of the adaptive arc gear is to be modified in the contact area. To modify the arc tooth flank, the method considered in [112] can be used. For its implementation, a circular cutter head is used, the straight cutter edges of which are offset relative to the axis of the head rotation and have a corrected profile angle.

Figure 8 shows the working lines and the contact braking zones of the semi-rolled [119] adaptive arc gear with: $z_1 = 23$; $z_2 = 73$; $m_n = 10$ mm; $x_1 = 0.440$; $x_2 = 0.041$; $b_w = 120$ mm; $\alpha_0 = 20^\circ$; $a_w = 480$ mm. The calculated diameter of the cutter head when cutting the convex side of the wheel arc tooth is $R_{g2} = 215.0$ mm; the concave side of the gear arc tooth is $R_{g1} = 220.0$ mm; the axial displacement of the semi-wheels relative to each other is $\Delta S = 1.36$ mm.

Figure 9 shows the working lines and contact braking zones of the same gear with a higher integrity of the arc teeth flanks. The estimated diameter of the cutter head when cutting the convex side of the wheel arc tooth is $R_{g2} = 218.0$ mm; the concave side of the gear arc tooth is $R_{g1} = 220.0$ mm; the axial displacement of the semi-wheels relative to each other is $\Delta S = 0.55$ mm.

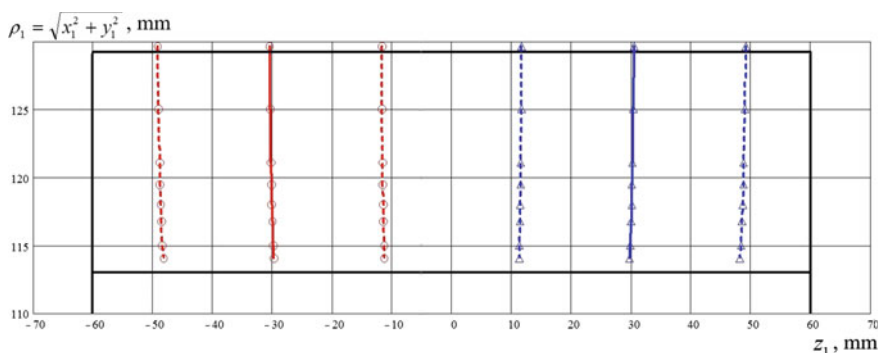


Fig. 8 Working lines (continuous curves) and boundaries of the contact braking zones (circles—left, triangles—right), $R_{g2} = 215.0$ mm; $R_{g1} = 220.0$ mm

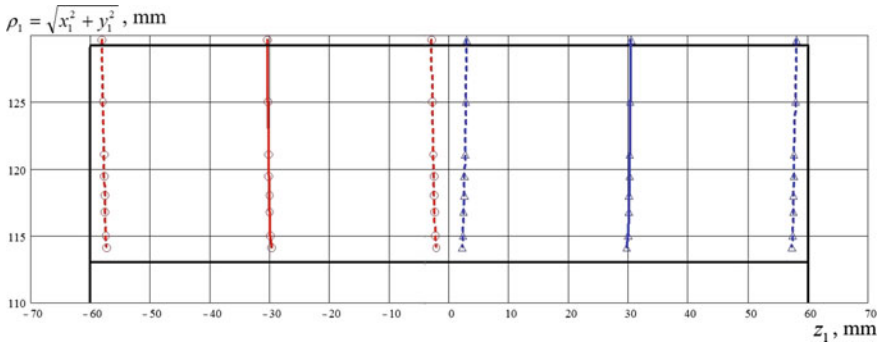


Fig. 9 Working lines (continuous curves) and boundaries of the contact braking zones (circles—left, triangles—right), $R_{g2} = 218.0$ mm; $R_{g1} = 220.0$ mm

Currently, the Industrial University of Tyumen is developing mathematical models for rolled and semi-rolled versions of the adaptive arc teeth gears to calculate: geometric characteristics of areas of contact, stress distribution throughout contact areas, stress estimation in the arc teeth roots, determination of contact and bending strength, and the probability of failure-free operation in conditions of a given gear duty.

Since the end of the previous century, Chinese scientists have been actively involved in the study of cylindrical arc gears [44, 48, 52, 58, 65, 105, 125, 126]. Their work is mainly devoted to the study of the gear geometry, separate issues of estimating the bending and contact strength of arc teeth, forming of which is performed with circular cutter heads. An exception is research papers [45, 46], which proposed and considered an original method of cutting arc teeth; but, in our opinion, this method has no prospects for industrial application.

References

1. Airapetov, E.L., Gorodnichij, V.P., Erikhov, M.L., Syzrantsev, V.N.: Arc teeth cylindrical gear loading. *J. Vestnik Mashinostroeniya* **2**, 20–22 (1986)
2. Airapetov, E.L., Gorodnichij, V.P., Erikhov, M.L., Syzrantsev, V.N.: Experimental study of arc teeth gears. *J. Vestnik Mashinostroeniya* **3**, 20–21 (1986)
3. Anan'ev, V.N.: Manufacture of cylindrical semi-rolled circular teeth gear pairs. Ph.D. Thesis, Tula, TPI (1989)
4. Bobkov, M.N.: Processing technology of gear pump spindle circular teeth. Ph.D. Thesis, Tula, TPI (1988)
5. Bobkov, M.N.: Theoretical aspects of manufacturing technology for circular teeth cylindrical wheels. D.Sc. Thesis, Tula, TGTU (1998)
6. Bochkova, D.E.: Forming circular teeth of a cylindrical wheel pair with a localized contact area. Ph.D. Thesis, Tula, TGTU (2019)
7. Babichev, D.T., Lagutin, S.A., Barmina, N.A.: Russian school of the theory and geometry of gearing. Part 2. Development of the Classical Theory of Gearing and Establishment of the Theory of Real Gearing in 1976–2000. *J. Mech. Mach. Sci.* **81**, 1–46 (2020)

8. Copyright certificate of the USSR SU No. 1939 A1. IPC B23F 9/08 Method of cutting spiral gears. Artem'ev, A.A. (1950) (in Russian)
9. Copyright certificate of the USSR SU No. 227066 A1. IPC B23F9/04 Method of cutting gears. Moshkovskij, G.I., Dogoda, M.I. (1968) (in Russian)
10. Copyright certificate of the USSR SU No. 252825 A1. IPC B23F 9/08 Method of continuous cutting of wheel arc teeth. Nalein, V.L. (1969) (in Russian)
11. Copyright certificate of the USSR SU No. 282897 A1. IPC B 23F 9/02, B23F 9/08 Method of processing circular teeth of cylindrical and screw gears. Erikhov, M.L. (1970) (in Russian)
12. Copyright certificate of the USSR SU No. 429909 A2. IPC B23F 9/02, B23F 9/08, B23F 9/10 Method of processing circular wheel teeth of cylindrical and screw gears. Drovovozov, G.P., Erikhov, M.L., Ratmanov, E.V. (1974) (in Russian)
13. Copyright certificate of the USSR SU No. 443732 A1. IPC B23F 9/10 Method of cutting circular symmetrical teeth. Malein V.L. (1974) (in Russian)
14. Copyright certificate of the USSR SU No. 521084 A1. IPC B23F 1/06, B23F 9/0 Method of cutting cylindrical wheel circular teeth. Korotkin, V.I., Zhuravlev, G.A. (1976) (in Russian)
15. Copyright certificate of the USSR SU No. 601093A1. IPC B23F9/04 Method of cutting gears. Dogoda, M.I., Gogolev, O.P., Terenik, V.D. (1978) (in Russian)
16. Copyright certificate of the USSR SU No. 785569 A1. IPC F16H 1/08 The cylindrical gear. Sidorenko, A.K. (1980) (in Russian)
17. Copyright certificate of the USSR SU No. 795773 A1. IPC B23F 9/10 Method of processing cylindrical wheel circular teeth. Sidorenko, A.K. (1981) (in Russian)
18. Copyright certificate of the USSR SU No. 1021530 A. IPC B23F 9/00 Method of manufacturing teeth wheels with a localized pressure spot. Koganov, I.A., Bobkov, M.N. (1981) (in Russian)
19. Copyright certificate of the USSR SU №1016095 A1. IPC B23F21/02 Method of grinding circular teeth wheels. Koganov, I.A., Bobkov, M.N., Anan'ev, V.N. (in Russian) (1983)
20. Copyright certificate of the USSR SU No. 1009660 A1. IPC B23F 21/04, B23F 21/22 The cutter head to cut circular teeth cylindrical wheels. Ionenko, I.D., Kolesnikov, V.N., Ratmanov, E.V., Syzrantsev, V.N. (1983) (in Russian)
21. Copyright certificate of the USSR SU No. 996117 A1. IPC B23F 21/22 The cutter head. Koganov, I.A., Bobkov, M.N., Anan'ev, V.N., Timofeev, B.S. (1983) (in Russian)
22. Copyright certificate of the USSR SU No. 1013148 A1. IPC B23F 9/10 Method of manufacturing the circular teeth rack. Sidorenko, A.K., Korgun, I.P. (1983) (in Russian)
23. Copyright certificate of the USSR SU No. 1052344 A1. IPC B23B 5/42 The relieved teeth lathe. Drovovozov, G.P., Ionenko, I.D., Ratmanov, E.V., Syzrantsev, V.N. (1983) (in Russian)
24. Copyright certificate of the USSR SU No. 1089391A1. IPC G01B 5/20 The device to measure the linear coordinate of the tooth longitudinal line. Gorodnichij, V.P., Ionenko, I.D., Ratmanov, E.V., Rozenberg, K.Yu., Syzrantsev, V.N. (1984) (in Russian)
25. Copyright certificate of the USSR SU No. 1151391 A2. IPC B 23 F 21/04 The cutter head to cut circular teeth cylindrical gear wheels. Erikhov, M.L., Ionenko, I.D., Ratmanov, E.V., Syzrantsev, V.N. (1985) (in Russian)
26. Copyright certificate of the USSR SU No. 1152731 A1. IPC B23F 21/04, B23F 21/2 The cutter head. Gel'man, A.A., Kolesnikov, V.N., Syzrantsev, V.N., Tropin, V.V. (1985) (in Russian)
27. Copyright certificate of the USSR SU No. 1158313 A1. IPC B23F 9/00 Method of cutting circular teeth cylindrical gear wheels. Koganov, I.A., Shejnin, G.M., Bobkov, M.N. (1985) (in Russian)
28. Copyright certificate of the USSR SU No. 1164011 A2. IPC B23F 21/04 The cutter head to cut circular teeth cylindrical gear wheels. Ionenko, I.D., Ratmanov, E.V., Syzrantsev, V.N. (1985) (in Russian)
29. Copyright certificate of the USSR SU No. 1166927 A1. IPC B23F 9/00 Method of manufacturing a mating couple of circular teeth gears. Sidorenko, A.K. (1985) (in Russian)
30. Copyright certificate of the USSR SU No. 1180191 A1. IPC B23F 9/04 Method of processing gears. Sidorenko, A.K., Tsivkovskij, A.G., Eskin, V.I. (1985) (in Russian)

31. Copyright certificate of the USSR SU No. 1195185 A1. IPC G01B 21/08 The gear-tooth micrometer. Drovovozov, G.P., Ionenko, I.D., Ratmanov, E.V., Syzrantsev, V.N. (1985) (in Russian)
32. Copyright certificate of the USSR SU No. 1266681 A1. IPC B23F 9/02 Method of processing the circular teeth cylindrical wheel. Koganov, I.A., Shejnin, G.M., Bobkov, M.N., Petrova, N.P. (1986) (in Russian)
33. Copyright certificate of the USSR SU No. 1268323 A1. IPC B23F 9/02 The cutter head to process circular teeth wheels. Gorodnichij, V.P., Ionenko, I.D., Milyutin, V.M., Ratmanov, E.V., Syzrantsev, V.N. (1986) (in Russian)
34. Copyright certificate of the USSR SU No. 1269928 A1. IPC B23F 9/00 Method of finishing cutting arc teeth gear wheels. Ratmanov, E.V., Syzrantsev, V.N. (1986) (in Russian)
35. Copyright certificate of the USSR SU No. 1265419 A1. IPC F16H 1/24 The screw-and-nut roller gear. Erikhov, M.L., Kostenko, S.G., Ol'shtynskij, P.V., Gorokhov, V.M. (1986) (in Russian)
36. Copyright certificate of the USSR SU No. 1261755 A1. IPC B23F 9/10 Method of processing circular teeth. Shejnin, G.M., Bobkov, M.N., Shejnin, B.G. (1986) (in Russian)
37. Copyright certificate of the USSR SU No. 1287998 A1. IPC B23F 21/00, B23F 21/22 Cutter head. Ratmanov, E.V., Rozenberg, K. Yu., Syzrantsev, V.N. (1987) (in Russian)
38. Copyright certificate of the USSR SU No. 1310609 A1. IPC G01B 5/14 The device to control discontinuous helical surfaces of objects. Ionenko, I.D., Ratmanov, E.V., Syzrantsev, V.N. (1987) (in Russian)
39. Copyright certificate of the USSR SU No. 1296327 A1. IPC B23F 9/02 Method of cutting gear wheel circular teeth in conditions of continuous generating. Sukhorukov, Yu.N., Belyanov, F.V., Shehekin, B.M., Matsej, R.A., Dobryninskij, A.G. (1987) (in Russian)
40. Copyright certificate of the USSR SU No. 1446390 A2. IPC F16H 1/24 The screw-and-nut roller gear. Erikhov, M.L., Kostenko, S.G., Ol'shtynskij, P.V., Gorokhov, V.M. (1988) (in Russian)
41. Copyright certificate of the USSR SU No. 1505694 A1. IPC B23 F21/00 The cutter head. Shejnin, G.M., Bobkov, M.N. (1989) (in Russian)
42. Copyright certificate of the USSR SU No. 1664479 A1. IPC B23F9/02 Method of finishing cutting involute profiles of cylindrical teeth gears. Belyaev, A.I., Mikhajlov, G.I., Sidorenko, A.K., Siritsyn, A.I. (1991) (in Russian)
43. Copyright certificate of the USSR SU No. 1753100 A1. IPC F16 H 1/28 The planetary gearboxes and method of its assembly. Erikhov, M.L., Kostenko, S.G., Fonotov, V.T. (1992) (in Russian)
44. Cai, X.W., Fang, Z.D., Su, J.Z.: Study on meshing characteristics of face gear drive with arcuate tooth based of manufacture on NC machine. *J. Aerosp. Power* **27**(1), 198–203 (2012)
45. Chang, Q., Hou, L., Li, B., Jia, B.: Modal analysis of cylindrical gears with arcuate tooth trace. *J. Periodica Polytechnica Mech. Eng.* **59**(1), 23–29 (2015)
46. Chang, Q.: Parallel translating mechanism process-oriented mathematical model and 3-D model for cylindrical gears with curvilinear shaped teeth. *Jordan J. Mech. Indus. Eng.* **10**, 171–177 (2016)
47. Drovovozov, G.P.: Study of geometrical and kinematic patterns of gearing formed with the generating wheel. Ph.D. Thesis, Kurgan, KMI (1980)
48. Dai, Y., Yukinori, A., Jiang, D.: Hobbing mechanism of cylindrical gear with arcuate tooth traces and experimental investigation. *J. China Mech. Eng.* **17**(7), 706–709 (2006)
49. Evstigneev, M.I.: Study of the cutting method of arc teeth cylindrical wheels. Ph.D. Thesis, Moscow (1948)
50. Erikhov, M.L.: Principles of systematics, methods of analysis and issues of synthesis of gearing patterns. D.Sc Thesis, Khabarovsk, KhPI (1972)
51. Erikhov, M.L., Sheveleva, G.I., Syzrantsev, V.N., Anosova, T.P.: Analysis of elastic interaction of gear tooth surfaces formed by spiral-disk tools. *J. Izvestiya VUZov. Mashinostroenie* **3**, 45–50 (1984)

52. Fang, Z.D., Cao, X.M., Shen, Y.B.: Tooth surface design and manufacture for arcuate tooth trace face-gear. *J. Aerosp. Power* **25**(1), 224–227 (2010)
53. Gubar SA: Study of contact geometry and development of methods for selecting parameters of arc teeth cylindrical gears. Ph.D. Thesis, Kurgan, KMI (1981)
54. Gorodnichij, V.P.: Study of loading and contact endurance of arc teeth cylindrical gears. Ph.D. Thesis, Kurgan, KMI (1983)
55. Golovachev M.I.: Calculation of arc teeth cylindrical gears strength. Ph.D. Thesis, Moscow, MVTU (1986)
56. Grunichev, A.V.: Technological aspects of designing circular teeth cylindrical gears and gear processing tools (on the example of gears of KAMAZ driving axles). Ph.D. Thesis, Tula, TGTU (1994)
57. Ionenko, I.D.: Development of a set of technological solutions for processing longitudinally modified cylindrical wheel teeth of with spiral disc cutters. Ph.D. Thesis, Kurgan, KMI (1988)
58. Jiang, Y.Q., Hou, L., Zhao, Y.: The equation of the contact line of the involute curvilinear-tooth cylindrical gear pump for the agricultural tractor. *Open Mech. Eng. J.* **8**, 879–884 (2014)
59. Kravchuk, A.A.: Theoretical and experimental studies of the arc teeth cylindrical transmission. Ph.D. Thesis, Khabarovsk, KhPI (1976)
60. Kostenko, S.G.: Synthesis of patterns, geometric calculation of meshing and experimental evaluation of the durability of arc screw-and-nut roller cylindrical gears. Ph.D. Thesis, Kurgan, KMI (1989)
61. Litvin, F.L.: Theory of gear meshing. Nauka, Moscow (1968)
62. Lipatov, S.I.: Development of a zero profile multi-cutter generating tool for high-performance arc wheel gear cutting on CNC machines. Ph.D. Thesis, Moscow, MGOU (2013)
63. Makhalov, A.G.: Study of bending endurance of cylindrical arc gears. Ph.D. Thesis, Kurgan, KMI (1983)
64. Milyutin, V.M.: Determination of the area of rational use of cylindrical gears based on a comparison of their loading taking into account geometrical and kinematic features. Ph.D. Thesis, Kurgan, KMI (1986)
65. Ma, Z., Wang, X.: Research on a highly durable and heavy-duty gearing. *J. Xi'an Jiaotong Univ.* **36**(3), 282–286 (2002)
66. Molikov, A.A.: Fundamentals of high-performance technology for manufacturing cylindrical gear wheels. D.Sc Thesis, Tula, TGTU (2009)
67. Patent US No. 5.647 United States of America. Rack and Pinion. Sempke A.M. (1848)
68. Patent US No. 3915060 United States of America. Method for cutting paired gears having arcuate tooth traces. Tamotsu K. (1975)
69. Patent No. 2641745 Federal Republic of Germany, B 23 F 9/10. Verfahren zur Herotellung eines otirn zahnradpaares Verzahnungmaxhine zur Durchföh-rung des Verfahrens stirn zahnradpaares hergestellt nach dem Verfahren. Kotthaus E. (1977)
70. Patent CN No. 201225383 (Y) China, F16H 1/08. Arc teeth cylindrical gear speed reducer. Song A. and others (2009)
71. Parshin, A.N.: Development of methods for meshing analysis and synthesis and manufacturing arc cylindrical gear wheels. Ph.D. Thesis, Moscow, MGOU (2008)
72. Polyakov, V.V.: Technology for processing circular teeth of the semi-rolled cylindrical gear. Ph.D. Thesis, Tula, TGTU (2013)
73. Radzevich, S.P.: Gear Cutting Tools: Science and Engineering. CRC Press, Florida (2017)
74. Radzevich, S.P.: Theory of Gearing: Kinematics, Geometry, and Synthesis. CRC Press, Florida (2018)
75. Ratmanov, E.V.: Analytical and experimental study of the meshing of cylindrical gears formed by spiral disk tools. Ph.D. Thesis, Kurgan, KMI (1977)
76. Reshetov, L.N., Dogoda, M.I., Klin, M.V.: Features of geometry and tooth cutting of cylindrical quasi-involute gears with a cycloidal line of contact. *J. Izvestiya VUZov. Mashinostroenie* **5**, 48–52 (1980)
77. Reshetov, L.N., Dogoda, M.I., Klin, M.V.: Revisiting certain issues of the geometry of cylindrical arc gears with cycloidal line of contact. *J. Izvestiya VUZov. Mashinostroenie* **4**, 49–53 (1980)

78. Russian Patent SU No. 1787077 A3, МКИ B23F9/00. Method of processing a pair of cylindrical arc gears. Voronin B.F. (1993) (in Russian)
79. Russian Patent RU No. 2005019 C1, IPC B23F21/22. Cutter head. Shirokikh, E.V., Siritsyn, A.I., Belyaev, A.I., Mikhajlov, G.I. (1993) (in Russian)
80. Russian Patent RU No. 2009798 C1, IPC B23F21/22. Cutter head. Shirokikh, E.V., Siritsyn, A.I., Mikhajlov, G.I., Grushichev, V.V., Lipatov, A.M. (1994) (in Russian)
81. Russian Patent RU No. 2049608 C1, IPC B23F9/02. Method of processing involute circular teeth of cylindrical wheels. Belyaev, A.I., Siritsyn, A.I., C Siritsyn, D.A., Lobanov, N.A. (1995) (in Russian)
82. Russian Patent SU No. 1831978 A3, IPC B23F9/02. Method of forming cylindrical gear arc teeth. Sidorenko, A.K., Lobanov, N.A., Korbakov, A.V., Kozlov, Y.A. (1995) (in Russian)
83. Russian Patent RU No. 2191302 C2, IPC F16H1/24. The screw-and-nut roller gear. Gear roller transmission. Tret'yakov, A.P., Votinov, V.A., Kostenko, S.G., Gerasimov, V.Y. (2002) (in Russian)
84. Russian Patent RU No. 2322329 C1, IPC B23F 9/08 Method of manufacturing cylindrical arc gears. Plakhtin, V.D., Davydov, A.P., Parshin, A.N. (2008) (in Russian)
85. Russian Patent RU No. 2322329 C1, IPC B23F 9/08 Method of processing cylindrical arc gears. Bobkov, M.N., Shejnin, G.M., Polyakov, V.V. (2009) (in Russian)
86. Russian Patent RU No. 2404030 C1, IPC B23F 9/00 Method of manufacturing cylindrical arc gears. Plakhtin, V.D., Pankov, I.G., Davydov, A.P., Margolit, R.B., Parshin, A.N., Lipatov, S.I. (2010) (in Russian)
87. Russian Patent RU No. 2430813 C2, IPC B23F 21/22 The cutter head to cut arc teeth of cylindrical gears. Margolit, R.B., Lipatov, S.I., Parshin, A.N., Davydov, A.P., Plakhtin, V.D., Pankov, I.G. (2011) (in Russian)
88. Russian Patent RU No. 2447975 C1, IPC B23F 9/08 Method of manufacturing cylindrical arc gears. Vinogradov, A.N., Davydov, A.P., Lipatov, S.I., Margolit, R.B., Pankov, I.G., Parshin, A.N., Khar'kov, M.A. (2012) (in Russian)
89. Russian Patent RU No. 2467838 C2, IPC B23F 9/08 Method of manufacturing cylindrical arc gears. Davydov, A.P., Lipatov, S.I., Margolit, R.B., Pankov, I.G., Parshin, A.N. (2012) (in Russian)
90. Russian Patent RU No. 2469230 C1, IPC F16H 55/08 F16H 1/08 The cylindrical arc gear. Davydov, A.P., Lipatov, S.I., Margolit, R.B., Pankov, I.G., Parshin, A.N. (2012) (in Russian)
91. Russian Patent RU No. 2510789 C2, IPC B23F 9/02 B23F 9/08 Method of processing a pair of cylindrical gears. Bochkova, D.E., Bobkov, M.N., Shejnin, G.M., Malikov, A.A. (2014) (in Russian)
92. Russian Patent RU No. 2551250 C1, IPC F16H 1/08 The cylindrical arc gear. Vinogradov, A.N., Davydov, A.P., Lipatov, S.I., Margolit, R.B., Pankov, I.G. (2015) (in Russian)
93. Russian Patent RU No. 2564791 C1, IPC F16H 1/06 F16H 1/20 Cylindrical arc gear reduction unit. (options). Vinogradov, A.N., Davydov, A.P., Lipatov, S.I., Margolit, R.B., Pankov, I.G. (2015) (in Russian)
94. Russian Patent RU No. 178007 U1 IPC F16H 1/24 The screw-and-nut roller gear. Kostenko, S.G. (2018) (in Russian)
95. Russian Patent RU No. 194541 U1, IPC F16H 1/24 The screw-and-nut roller gear. Kostenko, S.G., Piven', V.V. (2019) (in Russian)
96. Russian Patent RU No. 2721579 C1, IPC F16H 1/06 The adaptive cylindrical arc gear. Syzrantsev, V.N., Syzrantseva, K.V., Vibe, V.P., Denisov, Y.G. (2020) (in Russian)
97. Rozenberg, K.YU.: Development of procedure for strength calculation of cylindrical gears with arc teeth. Ph.D. Thesis, Kurgan, KMI (1984)
98. Sevryuk V.N.: The circular surface generalized analytical theory and its application to gear design. D.Sc Thesis, Voroshilovgrad (1972)
99. Shakhbazov, N.A.: Study of the geometry and formation of cylindrical wheel circular teeth. Ph.D. Thesis, Tbilisi (1974)
100. Sidorenko, A.K.: Gear «70-NKMZ». Mashinostroenie, Moscow (1984)
101. Sidorenko, A.K.: «90-VNIITI» tooth depth arc gear. Kolomna (1998)

102. Sidorkin, A.V.: Shaving and rolling circular teeth cylindrical gear wheels. Ph.D. Thesis, Tula, TGTU (2010)
103. Sheveleva, G.I.: Theory of generation and contact of moving bodies. Mosstankin, Moscow (1999)
104. Shtin, O.A. Evaluation of the performance of two-point contact cylindrical arc gears. Ph.D. Thesis, Kurgan, KMI (1993)
105. Su, J.Z., Fang, Z.D., Cao, X.M.: Tooth contact analysis of face gear drive with curvilinear shaped tooth by format cutting. *J. Aerosp. Power* **25**(6), 1427–1431 (2010)
106. Syzrantsev, V.N.: Theoretical basis for profiling spiral generating surface tools and study of the processing method of bevel wheel circular teeth. Ph.D. Thesis, Kurgan, KMI (1977)
107. Syzrantsev, V.N.: Synthesis of meshing cylindrical gears with a localized contact. D.Sc Thesis, Kurgan, KMI (1989)
108. Syzrantsev, V.N.: Study of the processing method for hardened cylindrical wheel arc teeth. *J. Izvestiya VUZov. Oil and Gas* **4**, 99–102 (2012)
109. Syzrantsev, V.N., Golofast, S.L.: Cyclic strains measurement and machine parts longevity forecasting according to integral strain gauges indications. Nauka, Novosibirsk (2004)
110. Syzrantsev, V.N., Golofast, S.L., Syzrantseva, K.V.: Diagnostics of Loading and Resource of Parts of Machines Transmissions and Carrying Systems According to Integral Strain Gauges Indications. Nauka, Novosibirsk (2004)
111. Syzrantsev, V.N., Gorodnichij, V.P.: Methods of synthesis of geometric parameters of localized contact cylindrical gears. *J. Vestnik Mashinostroeniya* **9**, 35–37 (1990)
112. Syzrantsev, V.N., Mockvina, EYu., Chernaya, L.A.: Method of profile modification of the tooth flank of the semi-rolled bevel gear. *J. Izvestiya VUZov. Mashinostroenie* **5**(722), 33–40 (2020)
113. Syzrantsev, V.N., Nevelev, Y.P., Golofast, S.L.: Calculation of Equipment Durability Based on the Methods of the Distribution-Free Statistics. Nauka, Novosibirsk (2008)
114. Syzrantsev, V.N., Novoselov, V.V., Sozonov, P.M., Golofast, S.L.: Evaluation of Safety and Strength Reliability of Main Pipelines Using Nonparametric Statistics. Nauka, Novosibirsk (2013)
115. Syzrantsev, V., Syzrantseva, K.: Determination of stresses in tooth roots of gears by Integral Strain Gauges. *J. Adv. Eng. Res.* **133**, 841–846 (2017)
116. Syzrantsev, V., Syzrantseva, K.: Processing of experimental data by means of nonparametric statistics. *IOP Conf. Ser.: J. Phys.: Conf. Ser.* **1059**, Art. No. 012019 (2018)
117. Syzrantsev, V., Syzrantseva, K.: Verification of recovery of distribution density function of the random variable by methods of nonparametric statistics. *IOP Conf. Ser.: Mater. Sci. Eng.* **481**(1), Art. No. 012004 (2019)
118. Syzrantsev, V.N., Syzrantseva, K.V.: Arc Cylindrical Gears: Geometry, Strength, Reliability. TIU, Tyumen (2020)
119. Syzrantsev, V., Syzrantseva, K., Kolbasin D.: Forming Surfaces of Semi-rolled Cylindrical Gearing Wheel and Gear Arc Teeth. *Lecture Notes in Mechanical Engineering* (2021)
120. Syzrantseva, K.V.: Prediction of gear failures using nonparametric statistics. *J. Vestnik Mashinostroeniya* **12**, 10–13 (2009)
121. Syzrantseva, K.V.: Improvement of the methodology to estimate loading and reliability of machine parts based on the features of their operational strain. D.Sc Thesis, Tyumen, TIU (2018)
122. Syzrantseva, K., Syzrantsev, V.: Reliability estimation of machine parts with complicated geometry on a base of methods of nonparametric statistics. *J. J. Eng. Appl. Sci.* **11**(2), 204–209 (2016)
123. Syzrantseva, K., Syzrantsev, V., Babichev, D.: Comparative analysis of stress–strain condition of cylindrical gears arc teeth and spurs. *Lect. Notes Mech. Eng. ICIE* **2019**, 101–108 (2020)
124. Syzrantseva, K.V., Syzrantsev, V.N., Kolbasin, D.S.: Comparative estimation of the failure probability of cylindrical arc and helical gears by tooth bending endurance. *AIP Conf. Proc.* **2176**(1), Art. No. 020010 (2019)

125. Tseng, R.T., Tsay, C.B.: Contact characteristics of cylindrical gears with curvilinear shaped teeth. *J. Mechan. Mach. Theory* **39**(9), 905–919 (2004)
126. Tseng, R.T., Tsay, C.B.: Mathematical model and surface deviation of cylindrical gears with curvilinear shaped teeth cut by hob cutter. *J. Mech. Des. Trans. ASME* **127**(5), 982–987 (2005)
127. Varshavskij, M.R.: Development of methods to estimate loading and durability of arc gears with a new geometry. Ph.D. Thesis, Kurgan, KMI (2002)
128. Vasin, V.A.: Design and technological support of the process of forming circular teeth of cylindrical wheels. Ph.D. Thesis, Tula, TGTU (2005)

Gear Tooth Edge Deburring and Chamfering in 5Axis CnC Manufacturing



Claude Gosselin

Abstract The intent of this chapter is (i) to review the major chamfering and deburring possibilities currently available on the market and (ii) to present how off-the-shelf tools can be used on a 5, 4+1 or 4 Axis CnC machine to do part or all of the chamfering for a given gear production. The installation of End Mill, Ball Mill, Conical Side Milling and Chamfer tools is presented with the issues to consider in terms of interference and collision risks.

Keywords Gears · Deburring · Chamfering · Cylindrical gear · Bevel gear

1 Introduction

Deburring and chamfering of gears is widely seen as a less than glamorous task. Indeed, what paper in the gear literature champions the “optimization” of deburring and chamfering?

Yet deburring is fundamental in gear quality since it allows removing cutting burrs that through harden at heat treatment and are then likely to be released in the lubricant and cause damage to the tooth meshing surfaces and bearings, all of which may eventually lead to the failure of the gearbox [2, 3]. Even if the parts are not heat treated, remaining cutting burrs released in the lubricant are likely to cause damage.

Beyond this fundamental point, burrs can cut the hands of the manipulating personnel. And in case of contact between a tooth edge and a hard object, a dent may appear rendering the part unacceptable.

While deburring is the process of removing remaining material burrs caused by the cutting process—for example Face Milling of spiral-bevel or Coniflex¹ straight-bevel gears—chamfering is the process of removing material along a tooth edge, at tooth tip, Toe or Heel, such as to eliminate sharp edges. Therefore, a chamfering operation of very small depth will do pretty much the same as a deburring operation.

¹Coniflex is a registered trademark of the Gleason Works, Rochester, NY.

C. Gosselin (✉)

Involute Simulation Softwares Inc., 1139 Ave des Laurentides, Quebec, QC G1S-3C2, Canada
e-mail: Hygears@hygears.com

Chamfering has many advantages in that it removes any remaining burrs, and therefore eliminates the need for a deburring operation, and at the same time provides a smooth entry for the tool used at hard finishing. Chamfering also reduces the risk of tip edge contact where high contact stresses are caused.

Chamfering can be performed using different tools such as Ball Mill, End Mill, Chamfer tools, disks and, in some cases, special tools. Ball Mill tools are sometimes the only possibility to chamfer, for example at tooth Toe or Heel, where the head of the machine cannot reach using other tools; however, Ball Mills will leave a double edge caused by their spherical form. End Mill tools can easily be used to chamfer the tip of the teeth, but are of a more limited use at Toe or Heel if the helix or spiral angle is large.

Disks can be used to chamfer at tooth tip; at Toe and Heel, they are cumbersome and when the tooth profile curvature is large, such as when the tooth number is low, it is more difficult to ensure a constant chamfer. On the other hand, Chamfer Tools, i.e. End Mill tools with a conical end, are well adapted to chamfer the tooth tips, the Toe edges (for bevel pinions with a small pitch cone angle) and the Heel edges (for bevel crown gears). Given that Chamfer Tools are available off-the-shelf in various dimensions and cone angles, they are an inexpensive response to a delicate issue.

This paper presents a general approach at the use of Ball Mill, End Mill, Disk and Chamfer tools for chamfering in a 5Axis CnC machine. The approach is based on the HyGEARS [1] software and is applied to spur, helical, straight and spiral bevel gears. Results show that End Mill and Chamfer tools provide excellent flexibility, involve only minimal cycle time and generally allow for even chamfering of both tooth flanks.

2 Review of [some] Existing Chamfering/Deburring Methods

The most basic deburring machine, and possibly the most widely used, is a pair of human hands holding the part and moving a small grinding tool along the gear tooth edges. This of course is a tedious job for anyone, beside being unhealthy because of the volatile grind residue. And the deburring quality is definitely a function of the worker's fatigue level, the worker's sight, and the size of the part: thus, consistency is far from guaranteed (Fig. 1).

Several manufacturers offer either dedicated machines for the deburring/chamfering of gear teeth, or machines incorporating a secondary process to clean up after the part has been generated. A good example is Gleason's spur and helical hobbing machines [4] producing clean parts with a secondary operation after tooth hobbing (Fig. 2).

Gleason also offers "chamfer rolling" where special tools for a given tooth geometry—face width, module, pressure angle—mesh with the soft cut part to remove any burr and chamfer the tooth ends in one operation.



Fig. 1 Manually chamfering a spiral bevel gear

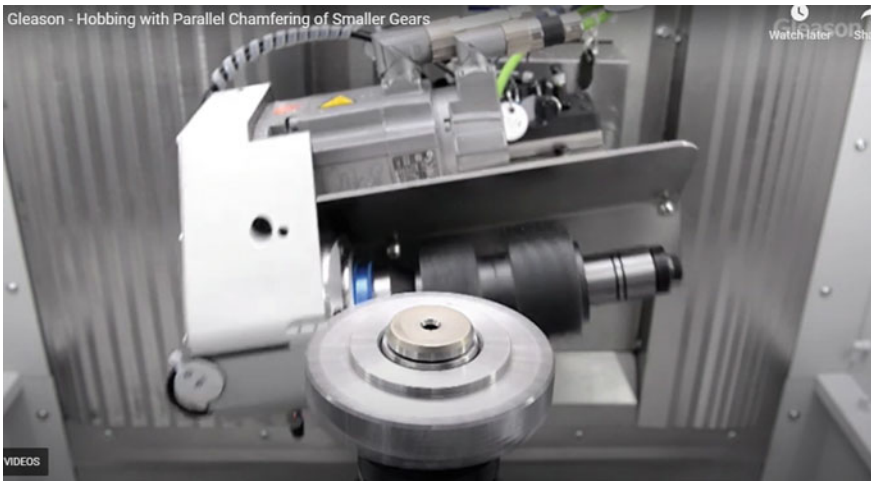


Fig. 2 Gleason secondary Toe and Heel chamfering of a cylindrical gear

Klingelberg also uses a secondary process [5] with a special tool to deburr the Toe and Heel of spiral bevel gears. The process takes place on the same machine after the teeth have been cut, which saves alignment time when the part is deburred on a different machine, and therefore ensures excellent quality. And as is shown in Fig. 3, both the Toe and Heel can be chamfered. This of course implies a special tool

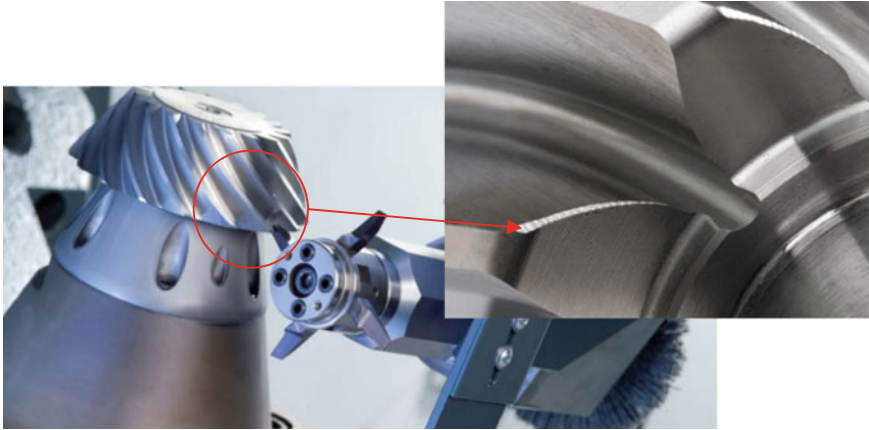


Fig. 3 Klingelnberg Toe and Heel chamfering of a spiral bevel pinion

and a Klingelnberg machine. Note however that the chamfer is not of constant size and tapers off before reaching the tooth fillet which is untouched.

There are also dedicated chamfering machines such as Liebherr's [6] where the work piece is moved from the hobbing machine to the deburring machine. A special tool then deburrs each tooth end and the tooth tips. Of course, two machines are required, which increases floor space, and there are handling steps adding to the overall cycle time; on the other hand, should one machine be down, the other machine can continue operating (Fig. 4).

An interesting approach by RedinMachine [7] uses an end-mill like tool to follow the Toe and Heel tooth edges, as shown in Fig. 5. The movement is continuous and the angle between the tool and work axes ensures a sufficient bevel at the tooth edge. The tool diameter is dictated by the width of the tooth gap at the root. The process can be used on spur, helical, straight and spiral bevel gears but there are limits as will be shown later on.

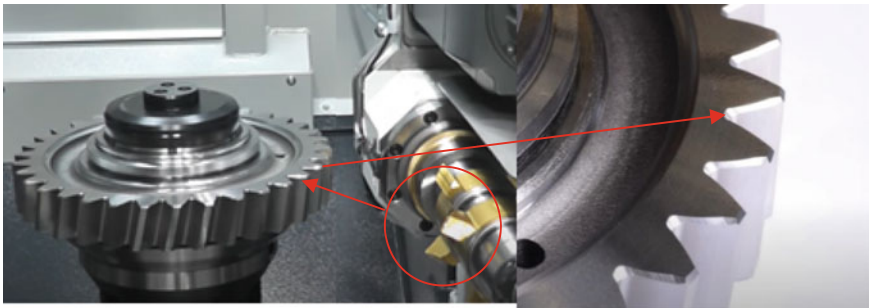
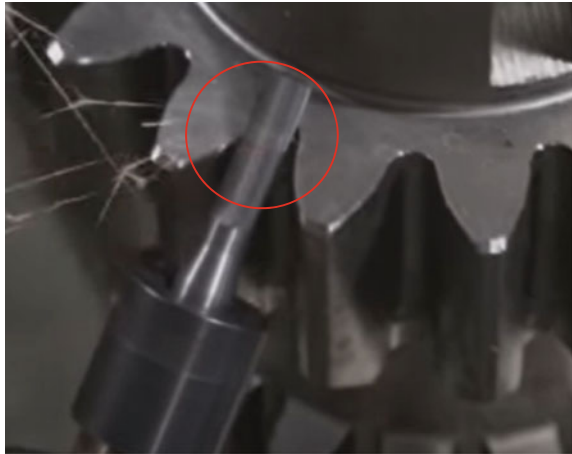


Fig. 4 Liebherr Toe and Heel chamfering of a helical gear

Fig. 5 RedinMachine End Mill chamfering of a spur pinion

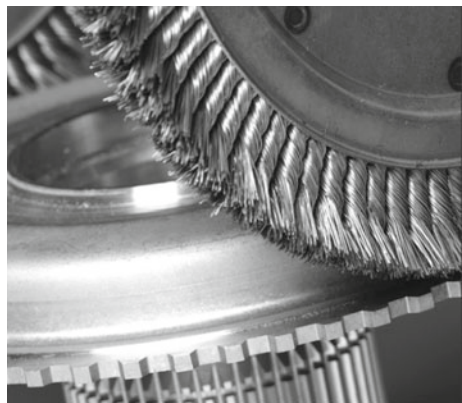


The above methods can all be considered “chamfering” methods since a cutting tool is used to both remove burrs and some material after the cutting process. This material removal when chamfering is beneficial for the life of the grinding tools when hard finishing as it ensures a smooth tool entry.

Another approach (Fig. 6) offered by Weiler Abrasives [8] uses wire brushes running either parallel or perpendicular to the tooth gap to remove the burrs at tooth tip or Toe and Heel. Of course, when the brush is parallel to the tooth gaps, the hardness and depth into the tooth gaps of the brush wires must be selected such as to avoid damaging the surface finish while removing the burrs.

Curtiss-Wright offers yet another approach using glass beads [9] in a shot peening-like operation which is well tailored to very small and delicate parts. Yet, in some cases burrs remain after the operation and a secondary hand operation may be required. Fig. 7 shows a 0.45 mm module straight bevel pinion where significant burrs can be seen after the teeth were cut. Glass bead peening was used to clean

Fig. 6 Brush deburring by Weiler Abrasives



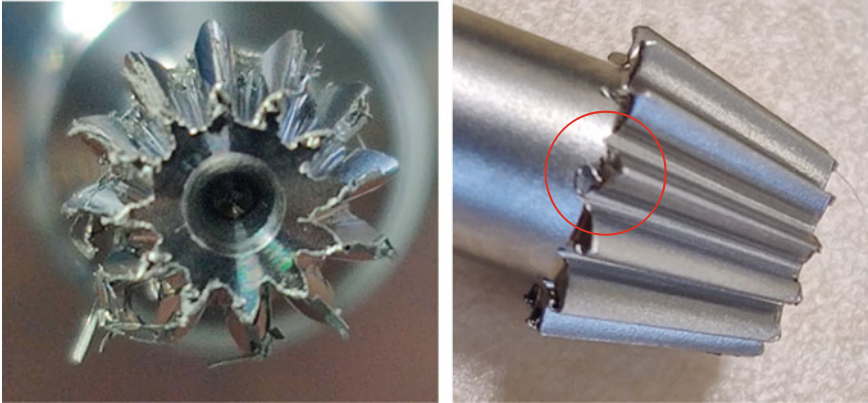


Fig. 7 Straight bevel pinion before and after glass bead deburring

the part and, although the result is spectacular, some burrs remain at Toe and Heel which must still be cleaned by hand. In addition, the surface finish of the part was altered by the peening action which may affect the behavior of the gearset if there is no finishing operation.

The above paragraphs intended to give a glimpse on the wide variety of methods that are available to chamfer and deburr gear teeth, but do not pretend to either cite all the manufacturers or all the methods.

However, one comment that springs out is that these methods generally require dedicated equipment; one can also say that these methods are not directly applicable to all of spur, helical, face, straight *and* spiral bevel gears.

Given the increased requirements for “clean” parts, given the fact that many manufacturers have a varied production in terms of gear types and sizes, and given that, increasingly, gear manufacturers are drawn to 5Axis CnC machines because of their flexibility, a more general approach to chamfering and deburring is required which is the focus of the next sections.

3 A General Approach to CnC Chamfering

In the following paragraphs, several definitions are made:

- the term “chamfering” is used in a general sense and can also describe deburring when the chamfer depth is very small;
- the gear manufacturer has a 5, 4+1 or a 4 Axis CnC machine available;
- standard “off-the-shelf” tools are used;
- the chamfering operations follow the tooth cutting operations, whether shaping, milling or face-milling on the same CnC machine such that no additional handling is required;

Fig. 8 End Mill tool**Fig. 9** Ball Mill tool**Fig. 10** Chamfer tool

- all the figures below are based on “AC” type CnC machines, i.e. Vertical Milling Centers. The paragraphs below also apply to “BC” type machines, i.e. Horizontal Turning Centers.

3.1 Off-the-Shelf Tools

In what follows, the considered off-the-shelf tools include:

- End-Mill tools; these are available in a wide range of diameters from many manufacturers, and are typically inexpensive (Fig. 8);
- Ball-Mill tools; these are also available in a wide range of sizes from many manufacturers, and are also inexpensive (Fig. 9);
- Chamfer tools; these are more specialized, but are easily found at low prices in different sizes; cone angles of 60 and 90° are common (Fig. 10);
- CoSIMT tools; CoSIMT is an acronym for Conical Side Milling Tool, and may refer to a disk-like slotting tool, or to tools such as Sandvik’s InvoMill² and CoroMill where a solid body is fitted with cutting blade inserts that are changed when worn out; the blade inserts can have parallel cutting edges, (left, Fig. 10) such as for a slotting tool, or non parallel cutting edges as used in the InvoMill tools (right, Fig. 11) for spiral bevel gears; while strictly not always off the shelf, these are available easily enough to be considered here;
- Wire-brush tools; these come from many manufacturers, in a large range of sizes and wire hardness (Fig. 12).

Given the variety in the shapes of these tools, the movements and the tooth edges that can be chamfered will be different. We will therefore look at each tool and see how it can be applied to different gear types. (Wire brushes are omitted in the following given their comparatively simple installation).

²Trade Marks, Sandvik Corp.

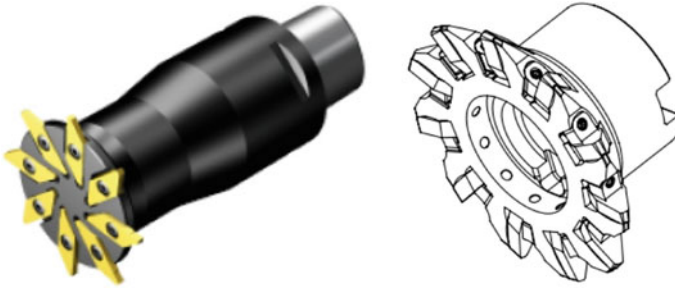


Fig. 11 Conical side milling Tool—CoSIMT

Fig. 12 Wire brush for deburring



3.2 End Mill Chamfering

Because of its shape the End Mill (EM) appears to be more limited for some gear geometries and tooth areas. However, given its typically low price and wide availability, it can also be a tool of choice.

Straight Bevel and Spur Gears

In this section, straight bevel and spur gears are treated together because of the similarity in shape.

EM tools can be used to access the Toe, Heel and Tip edges of spur and straight bevel gears, for both small and large pitch cone angles.

When chamfering the Toe or Heel edges, the EM tool must be angled relative to the tooth edge (left, Fig. 13) in order to create a beveled chamfer.

Beyond the coordinates of the local point, five unit vectors (right, Fig. 13) are required at any point along the tooth edge:

- \vec{T} : the local tangent vector,
- \vec{N} : the local normal vector,
- \vec{V}_o : $\vec{N} \times \vec{T}$,

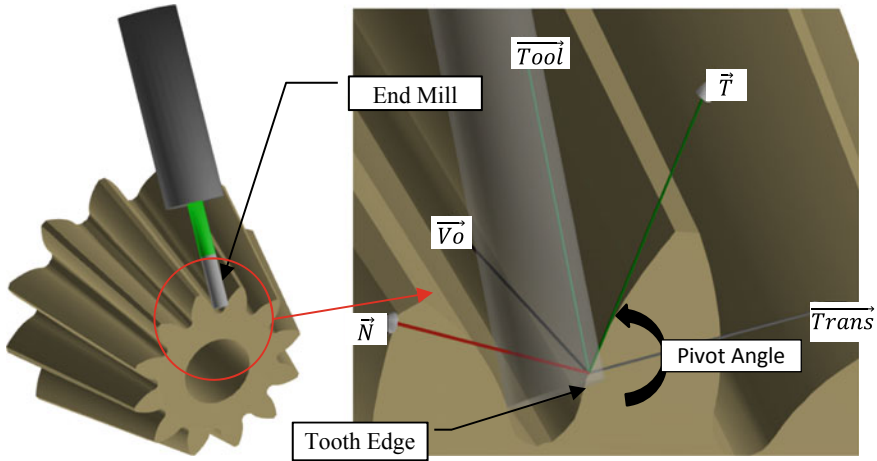


Fig. 13 Typical end mill installation for Toe/Heel chamfering—spur and straight bevel gears

\overrightarrow{Trans} : the axis about which the tool vector is pivoted,
 \overrightarrow{Tool} : the tool vector.

\overrightarrow{Vo} is obtained from the cross product of \vec{N} and \vec{T} . Vector \overrightarrow{Trans} is obtained by pivoting \vec{T} about \overrightarrow{Vo} of $\frac{\pi}{2}$ – the local pressure angle; then, pivoting \vec{T} about \overrightarrow{Trans} by the desired pivot angle gives vector \overrightarrow{Tool} . The pivot angle is a user input which depends in part on the length of the EM and the size of tool holder to avoid interference with the work.

However, depending on the pitch cone angle, the CnC machine’s turn-table tilt capability may be exceeded, as is the case for the straight bevel pinion (left, Fig. 14) when chamfering the Toe: the turntable angle reaches -140° for a 50° pivot angle, which is beyond the typical limit of -105° and the tool spindle collides with the turn table. Reducing the pivot angle to 25° brings the turn table angle to -112° which is amenable to most AC type machines.

On the other hand, chamfering the Heel would cause no issue (right, Fig. 14) as the turntable tilt is now -25° , well within the machine’s range.

The situation is likely to be different when the pitch cone angle of the work piece is large, as shown in Fig. 15 where both Toe and Heel chamfering can be performed since the turn table tilt remains within the machine’s limits.

Tip deburring can be addressed in 2 ways: using either the tip of the EM tool or its cutting edges.

When the EM’s cutting edges are used, large work piece rotation angles are to be expected when changing tooth flanks (left and center, Fig. 16) and therefore the operation should be split such that all the tips on one tooth flank are done and then all the tips on the opposite tooth flank are chamfered, which would improve cycle times.

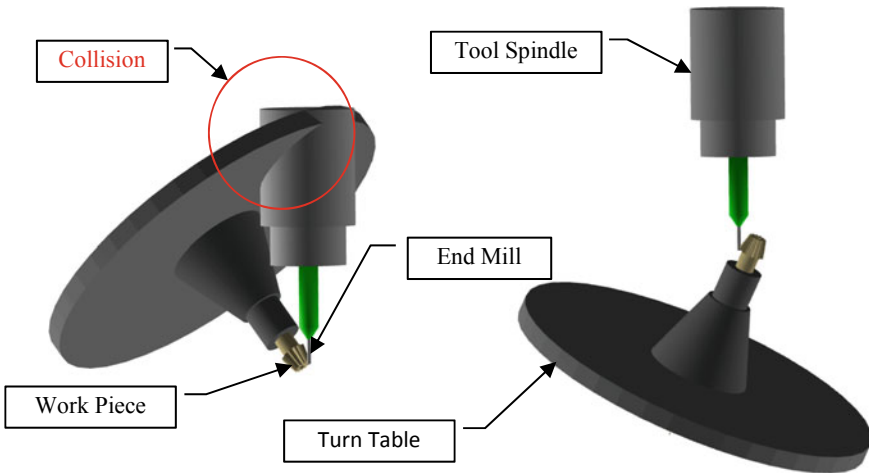


Fig. 14 “AC” type CnC machine limits for Toe/Heel chamfering—small pitch cone angle bevel gear

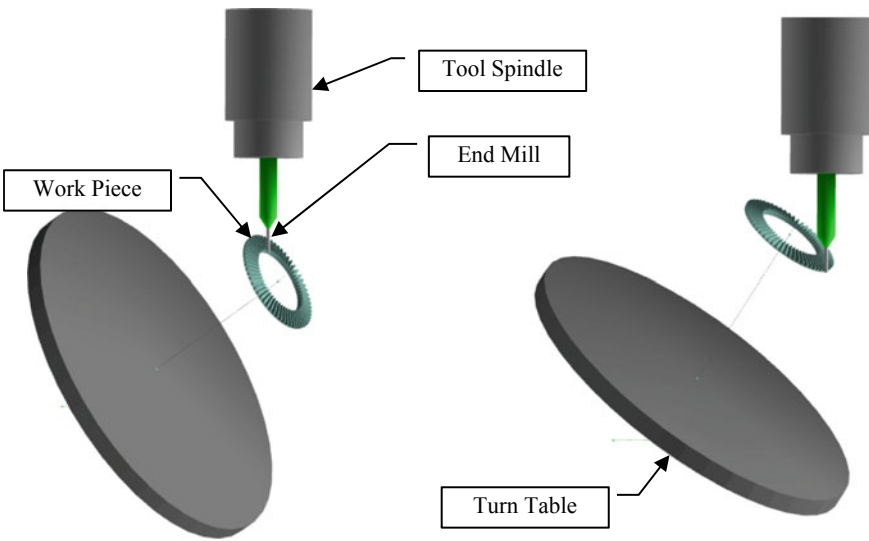


Fig. 15 “AC” type CnC machine limits for Toe/Heel chamfering—large pitch cone angle bevel gear

The same comments apply when the pitch cone angle of a straight bevel gear is large, as is shown in Fig. 17.

Tip chamfering can also be performed using the EM tool’s tip which, in most cases, is a better approach since the turn table tilt is less and there are no risks of tool

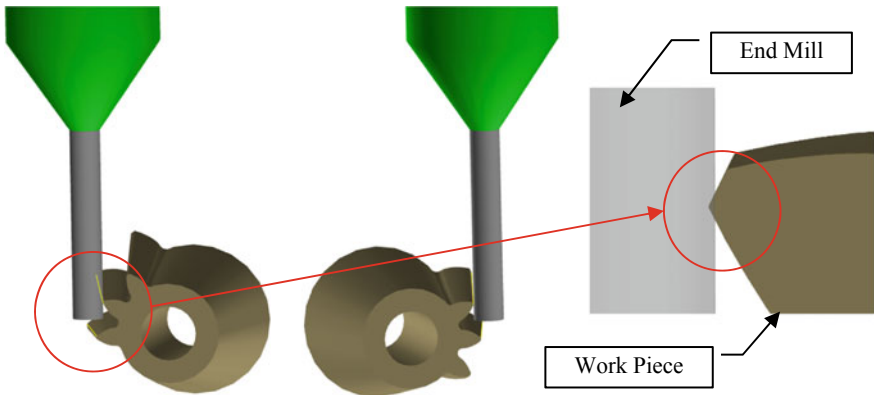


Fig. 16 Tip chamfering of a small pitch cone angle bevel gear—EM tool side is used

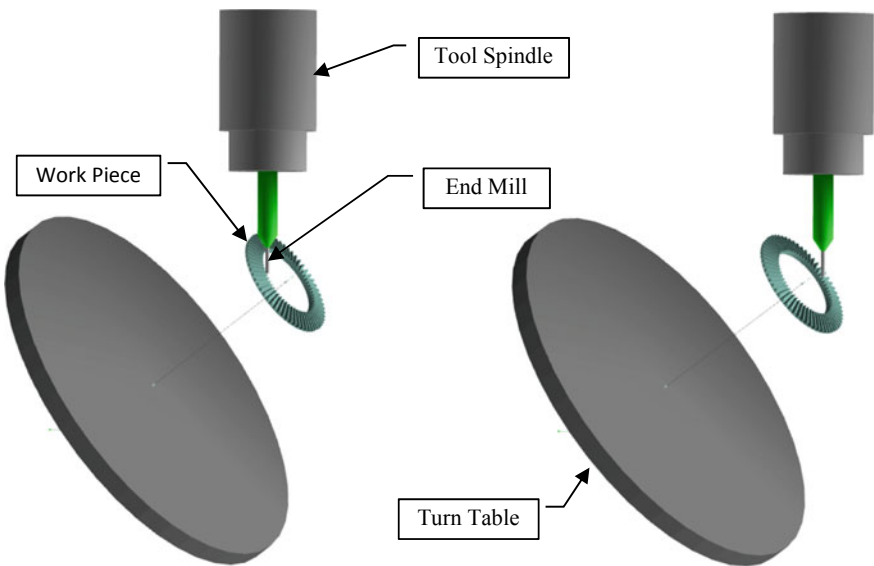


Fig. 17 Tip chamfering of a large pitch cone angle bevel gear—EM tool side is used

interference. However, the tool diameter becomes a limiting factor to avoid damaging the opposite tooth flank.

When chamfering the Tip edges, the EM tool must be tangent to the axial direction of the tip and angled to provide the desired chamfer (Fig. 18).

Again, five unit vectors (left, Fig. 18) are required at any point along the tooth Tip edge:

- \vec{T} : the local tangent vector,
- \vec{N} : the local normal vector,

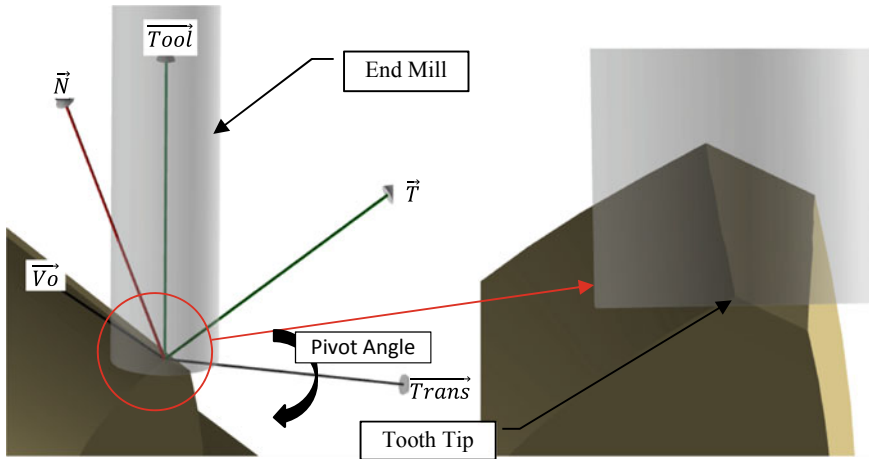


Fig. 18 Typical End Mill installation for Tip chamfering—Spur and straight bevel gears

\vec{Vo} : $\vec{N} \times \vec{T}$,
 \vec{Trans} : the axis about which the tool vector is pivoted,
 \vec{Tool} : the tool vector.

\vec{Vo} is obtained from the cross product of \vec{N} and \vec{T} . Vector \vec{Trans} is obtained by pivoting \vec{T} about \vec{Vo} of $\frac{\pi}{2}$ – the local pressure angle; pivoting \vec{T} about \vec{Vo} to bisect the Tip edge (right, Fig. 18), and about \vec{Trans} by the required pivot angle to ensure that the tool is perpendicular to the axial direction of the Tip edge yields vector \vec{Tool} (Fig. 19).

In the above, Toe and Heel chamfering are performed with neither rotation of the work piece—apart from indexing—nor change in turn table tilt which improves the predictability of the movements, especially when the work piece is large and heavy. This also implies that 4 and 4+1 axes machines can be used.

By contrast, Tip chamfering of bevel gear teeth requires a continuous reorientation of the tool axis in reference to the work piece axis and, therefore, a 5 Axis CnC machine is required.

Helical Gears

Helical gears are treated separately because the helix angle introduces peculiarities not found on spur and straight bevel gears. The same considerations apply to spiral bevel gears.

While Tip chamfering can be performed in the same way as for spur and straight bevel gears, i.e. either with the side of the tool or its tip end, the Toe and Heel tooth ends present different angles on each tooth flank, as described in Fig. 20 where flank L shows obtuse angle α_L and flank R shows acute angle α_R .

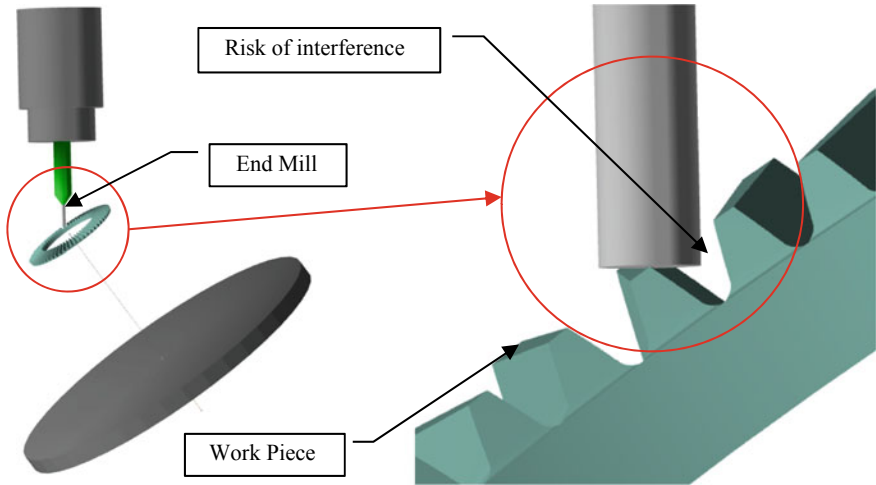


Fig. 19 Tip chamfering of a large pitch cone angle bevel gear—EM tool tip is used

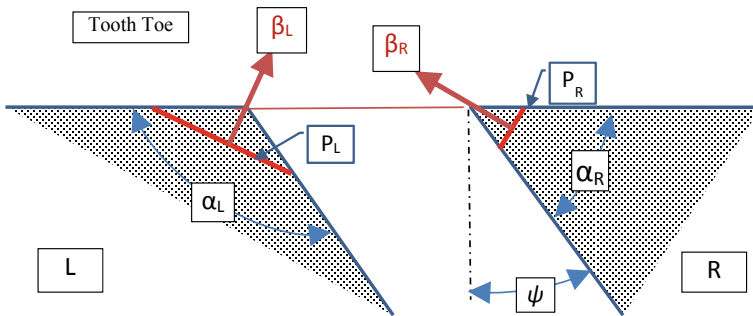


Fig. 20 Toe/Heel chamfer angles for helical and spiral bevel gears

Vectors β_L and β_R divide angles α_L and α_R in 2 equal halves. Lines P_L and P_R , perpendicular to vectors β_L and β_R , are at an equal depth from the tip point and clearly do not have the same lengths. This means that chamfering for equal depth will not produce equal chamfers on the L and R flanks.

While in itself this is not dramatic, in practice the appearance suffers and the effective face width is reduced on one tooth flank relative to the other.

In addition, the acute side, R in Fig. 20, presents a small pointed edge that is likely to through harden and be brittle, so easy to break if stressed.

Therefore, when chamfering the Toe and Heel tooth ends, it is good practice to adjust the chamfering depth of the obtuse angle to produce the same chamfer length as on the acute angle, or vice-versa.

Now, six unit vectors (right, Fig. 21) are required to orient the EM at any point along the tooth edge:

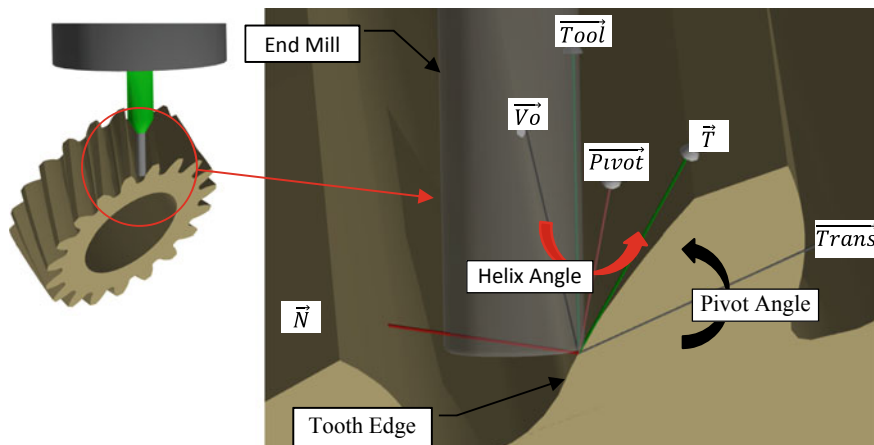


Fig. 21 End Mill installation for Toe/Heel chamfering—helical and spiral bevel gears

- \vec{T} : the local tangent vector,
- \vec{N} : the local normal vector,
- \vec{Vo} : $\vec{N} \times \vec{T}$,
- \vec{Tool} : the tool vector,
- \vec{Trans} : axis about which vector \vec{Tool} is rotated by the Pivot Angle,
- \vec{Pivot} : axis about which vector \vec{Tool} is rotated by the local helix/spiral angle.

\vec{Vo} is obtained from the cross product of \vec{N} and \vec{T} . Again, vector \vec{Trans} is obtained by pivoting \vec{T} about \vec{Vo} by $\frac{\pi}{2}$ —the local pressure angle; vector \vec{Pivot} is obtained from the cross product of \vec{Trans} and \vec{Vo} ; then, pivoting \vec{Pivot} about \vec{Trans} by the user inputted Pivot Angle gives vector \vec{Tool} which is then pivoted about axis \vec{Pivot} to account for the local helix/spiral angle.

We also see in Fig. 22 that one tooth end typically cannot be reached easily because of the risk of interference between the tool spindle and the turn table. Then, either the Pivot Angle must be reduced or an alternate solution is required, which is presented further in the text.

Spiral Bevel Gears

Spiral bevel gears have the most complex shapes in terms of tooth flank topography and blank. These gears therefore call for a general solution that is applicable whatever the local spiral angle, face width, generating process, module or pressure angle.

And again, End Mills can be used to chamfer some tooth edges, but now the options are more limited because the spiral angle can become quite significant at the Heel tooth edge for large offset hyoid pinions.

For example, consider tip chamfering with the cutting edge of the End Mill as shown in Fig. 23. While chamfering the convex flank causes no issue (left, Fig. 23),

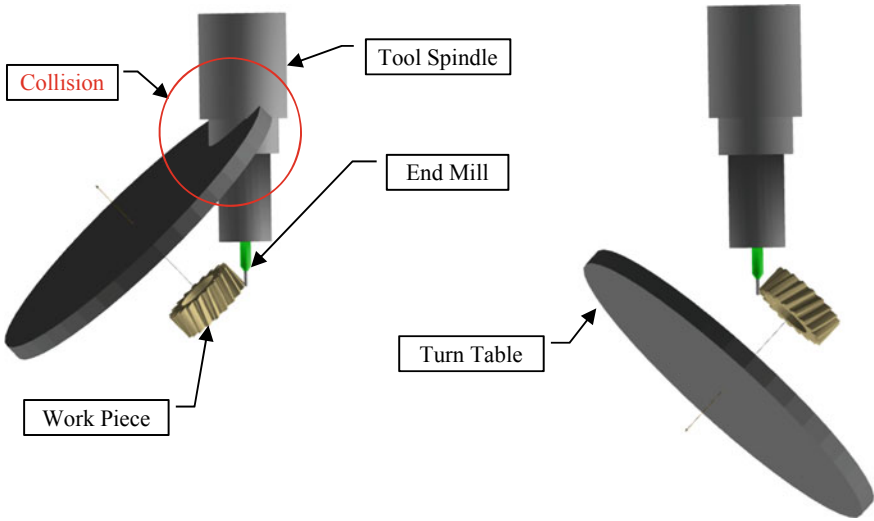


Fig. 22 Toe/Heel chamfer limits for helical gears

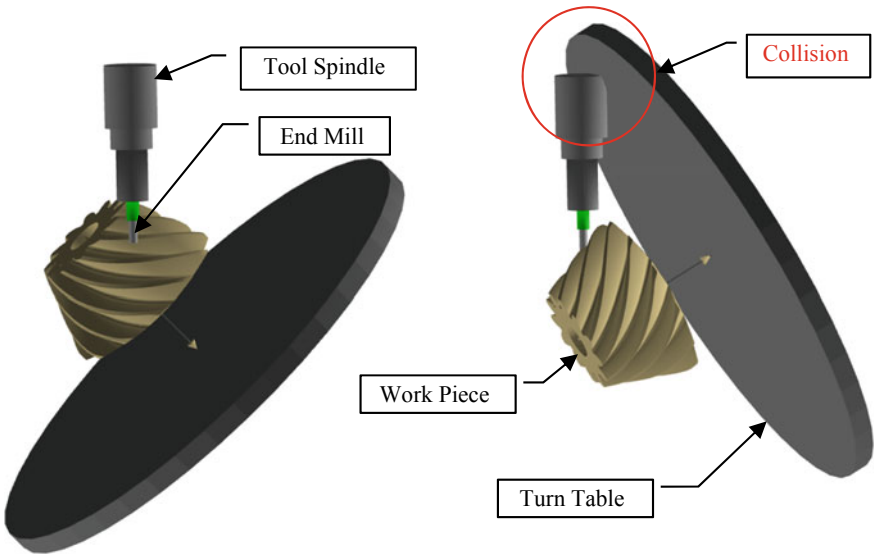


Fig. 23 Tip chamfering with EM cutting edge—spiral bevel pinion

chamfering the concave flank (right, Fig. 23) causes a collision risk between the tool spindle and the turn table.

This approach is therefore not acceptable and the EM tool tip is to be used which, as shown in Fig. 24, causes no issue on either flank.

Figure 25 shows the Tip edges of a small spiral bevel pinion chamfered using an

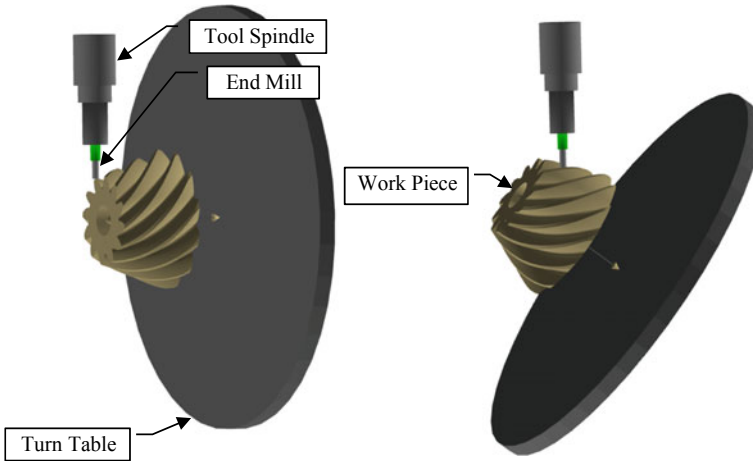


Fig. 24 Tip chamfering with EM tip end—spiral bevel pinion

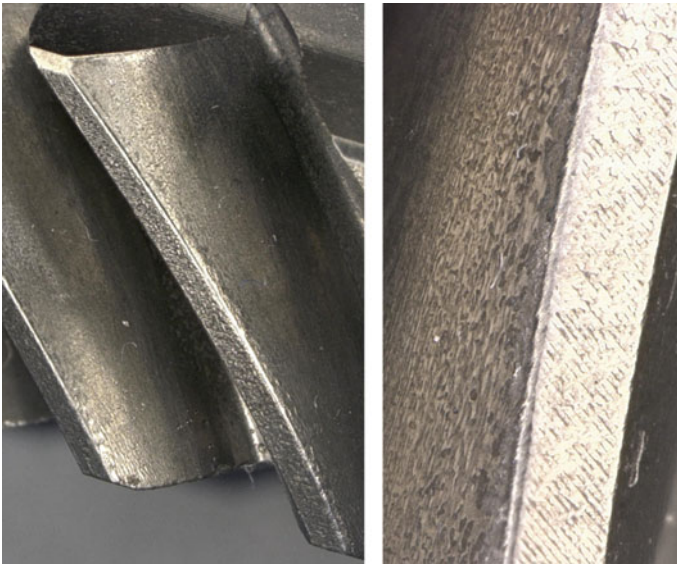


Fig. 25 Sample Tip chamfering with EM tip end—spiral bevel pinion

EM. The chamfers are almost small enough to confuse with deburring.

When chamfering tooth Toe and Heel edges, other considerations arise. For one, when chamfering the Toe of a pinion with a small pitch cone angle, again the turn table angle is likely to exceed the machine's limit and collide with the tool spindle (left, Fig. 26).

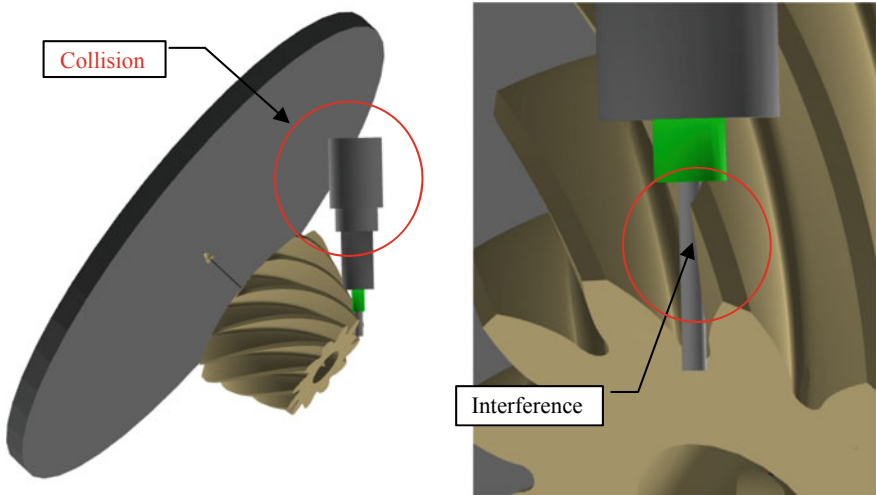


Fig. 26 Toe chamfering with EM—spiral bevel pinion

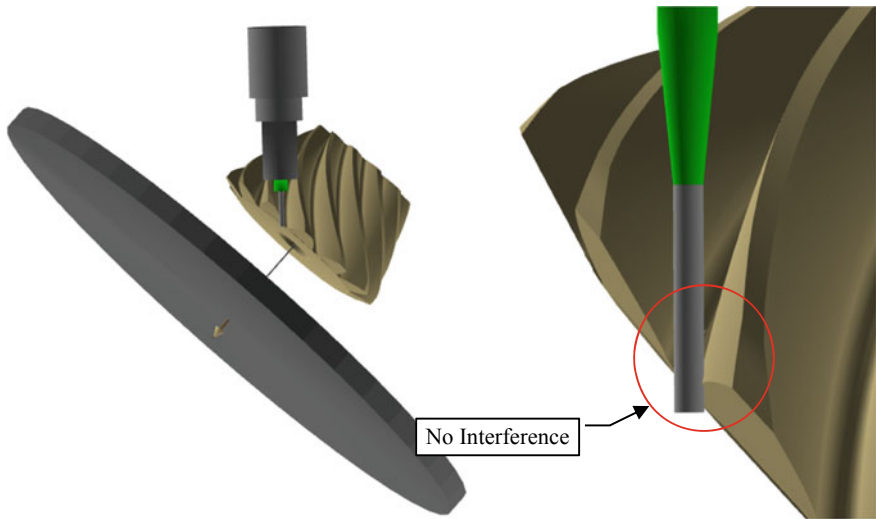


Fig. 27 Heel chamfering with EM—spiral bevel pinion

Beyond this, even a small diameter End Mill is likely to interfere with the concave tooth flank when chamfering the bottom of the tooth (right, Fig. 26) and therefore either the Pivot Angle must be reduced, or else this solution becomes unacceptable.

Tool spindle to turn table collision is not likely to occur at Heel (left, Fig. 27); and if the Pivot Angle is correctly chosen, tool interference with the tooth flank can be avoided (right, Fig. 27).

3.3 Ball Mill Chamfering

The Ball Mill tool (BM), thanks to its spherical end, can be fitted in places where an End Mill tool would not do an acceptable job.

Consider for example the spiral bevel pinion shown in Fig. 28, left. The Ball Mill tool can be plunged vertically along the Toe and Heel edges without any risk of tool spindle to turn table interference. And by carefully selecting the Ball Mill diameter, the fillet area can also be chamfered.

Five unit vectors (left, Fig. 29) are required to control the BM at any point along a tooth edge:

- \vec{T} : local tangent vector,
- \vec{N} : local normal vector,
- \vec{V}_o : $\vec{N} \times \vec{T}$,
- \vec{Tool} : the tool vector,
- \vec{Trans} : axis about which vector \vec{Tool} is rotated by the Pivot Angle.

\vec{V}_o is obtained from the cross product of \vec{N} and \vec{T} . Again, vector \vec{Trans} is obtained by pivoting \vec{T} about \vec{V}_o by $\frac{\pi}{2} +$ the local pressure angle; vector \vec{Tool} is obtained from the cross product of \vec{Trans} and \vec{V}_o ; vector \vec{Tool} can be pivoted parallel to itself about the local tooth edge point by the Chamfer Angle—left, Fig. 29—and about vector \vec{Trans} by the user inputted Pivot Angle.

However, there is a potential issue with this type of tool in that if the diameter of the spherical end is small, which is required to fit in the fillet area, a double lip

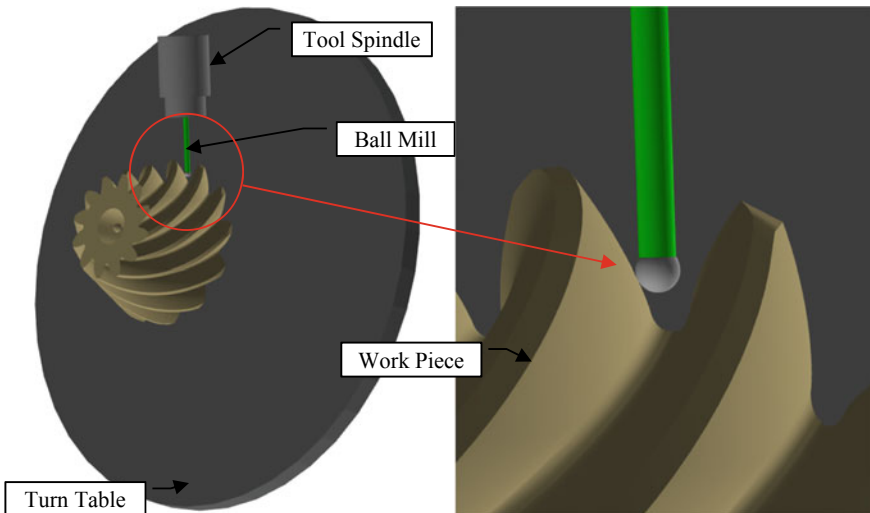


Fig. 28 Heel chamfering with BM—spiral bevel pinion

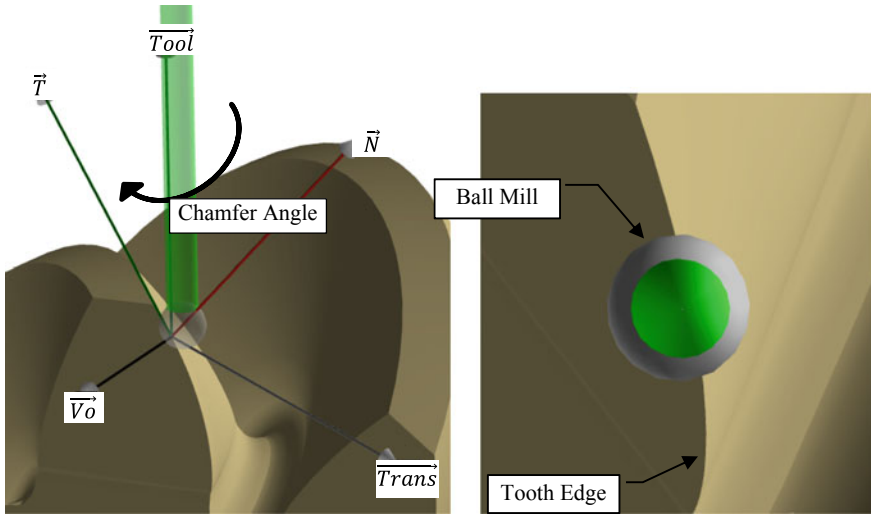


Fig. 29 End Mill installation for Toe/Heel chamfering—helical and spiral bevel gears

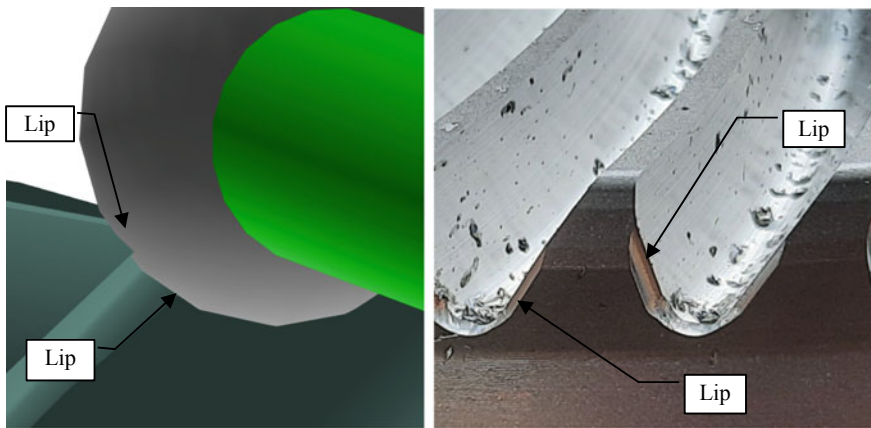


Fig. 30 Heel chamfering with BM—double lip edge created

is created where the tool enters and exits the tooth edge, as Fig. 30 shows. In many instances, this is unacceptable and either an alternative solution is required, or else the BM diameter is increased to minimize the double lip and the fillet area is not targeted.

3.4 Chamfer Tools

Chamfer Tools (CT) are widely available and come in varied sizes. They offer an interesting, and inexpensive, alternative to End Mill tools since they can be used along tooth tips and, at least, at one tooth end, Toe or Heel.

For example, the case of Fig. 30 would rather appear as shown in Fig. 31, left, with a result similar to what appears in Fig. 31, right: the quality of a CT tool chamfer is obvious.

Seven unit vectors (Fig. 32) are required to orient the CT at any point along the tooth edge:

- \vec{T} : the local tangent vector,
- \vec{N} : the local normal vector, pivoted about \vec{Pivot} such as to face the cutting edge of the Chamfer Tool,
- \vec{Vo} : $\vec{N} \times \vec{T}$,
- \vec{Tool} : the tool vector,
- \vec{Trans} : axis about which vector \vec{Tool} is rotated by the Pivot Angle,
- \vec{Pivot} : axis about which vector \vec{Tool} is rotated by the local spiral angle,
- $VnCone$: perpendicular to vector \vec{Tool} and the tooth edge and used to control the movement along the tool axis caused by Ds.

\vec{Vo} is obtained from the cross product of \vec{N} and \vec{T} . Again, vector \vec{Trans} is obtained by pivoting \vec{T} about \vec{Vo} by $\frac{\pi}{2}$ + the local pressure angle; vector \vec{Pivot} is obtained from the cross product of \vec{Trans} and \vec{Vo} ; then, pivoting \vec{Pivot} about \vec{Trans} by the user inputted Pivot Angle gives vector \vec{Tool} which is then pivoted about axis \vec{Pivot} to account for the local helix/spiral angle. Since the tool cannot be used on its tip, it

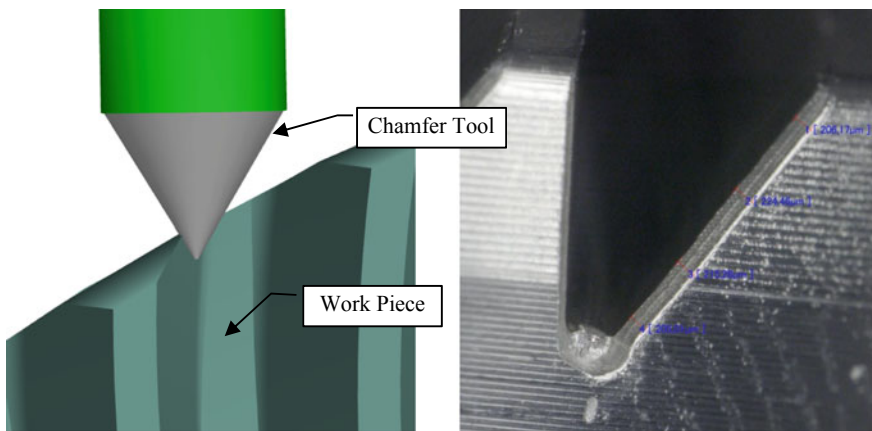


Fig. 31 Heel chamfering with Chamfer Tool—smooth chamfer edge

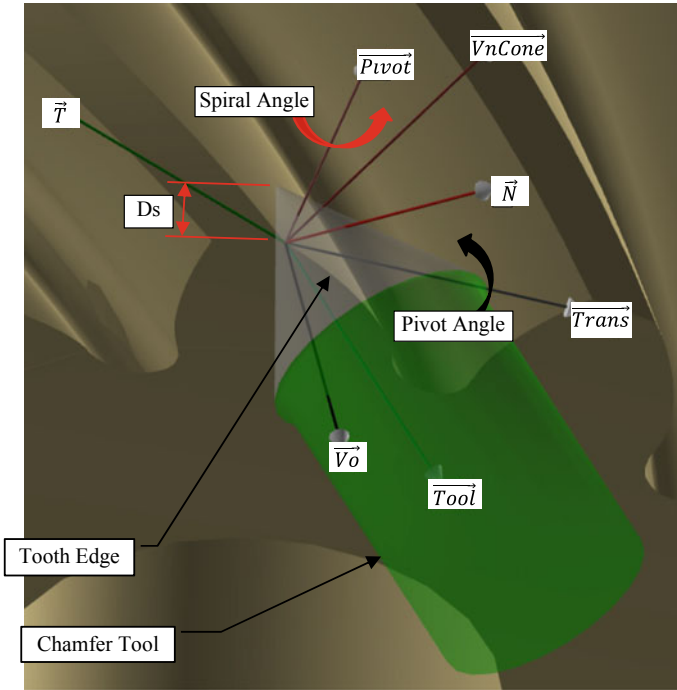


Fig. 32 Chamfer Tool installation for Toe/Heel chamfering—Spiral Bevel Gears

is moved by distance D_s along its cutting edge and vector \overrightarrow{VnCone} is used to guide the movement.

As can now readily be deduced, D_s , the tip diameter and the cone angle of the CT are prime variables in the chamfering operation.

Consider, for example, the CT at nearly the bottom of the 4.8 mm module pinion tooth (left, Fig. 33) where $D_s = 2$ mm, the tip diameter is 0.1 mm, and the cone angle is 60° : while still chamfering the convex Toe tooth edge, the CT is already gouging into the concave Toe tooth edge.

By reducing D_s to 1.5 mm (right, Fig. 33) gouging on the opposite tooth flank is avoided altogether. Therefore, the allowable amount of penetration D_s is a function of the current point on the tooth edge, the local spiral or helix angle, and the tip diameter and cone angle of the CT.

One disadvantage of the Chamfer Tool is that it must attack the Toe or Heel tooth edges from outside the part, which means that for bevel gears with a small pitch cone angle, the Toe end of the teeth can be chamfered, and for gears with a larger pitch cone angle, the Heel end of the tooth can be chamfered. At the opposite end, it is likely a collision will result between the turn table and the tool spindle unless some adjustments are made to the operation parameters.

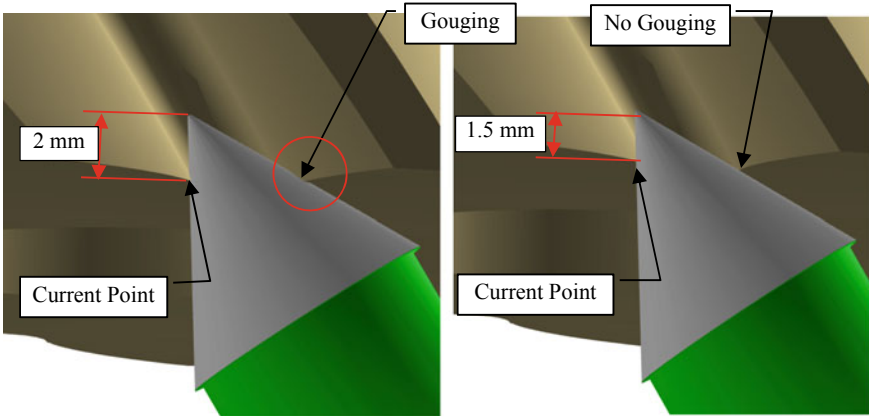


Fig. 33 Chamfer Tool gouging on the opposite tooth flank

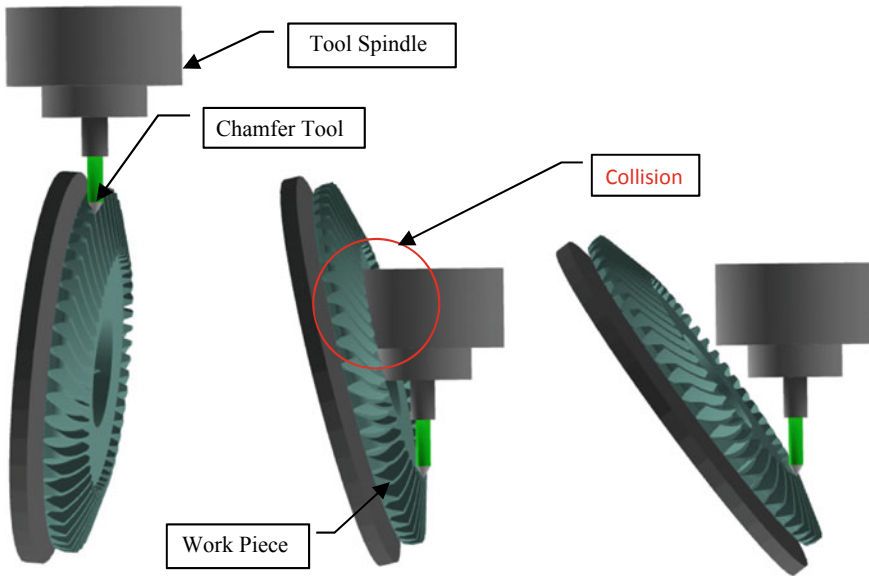


Fig. 34 Chamfering Toe and Heel—Large pitch cone angle spiral bevel gear

For example (left, Fig. 34) the Chamfer Tool is set up for the Heel on a spiral bevel gear with a large pitch cone angle; it is clear that using a tool holder long enough allows avoiding any collision between the machine's tool spindle and the turn table.

If the Toe end of the tooth is to be chamfered, the tool spindle clearly collides with the work and turn table (center, Fig. 34). The "Pivot Angle" controls the angle between the Chamfer Tool's axis and the tooth Toe or Heel edge; in both the left and middle Fig. 34, the Pivot Angle is set to 90°. If the Pivot Angle is now set to, say,

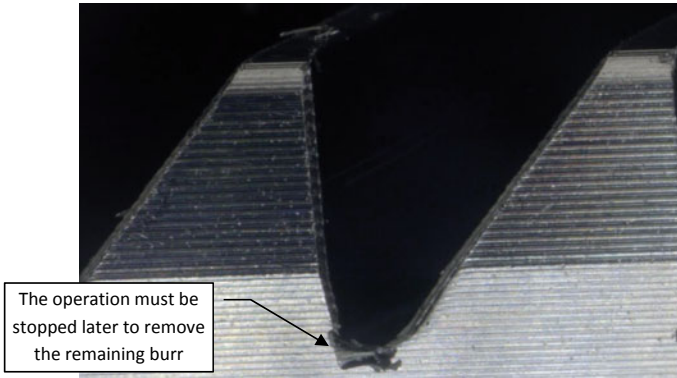


Fig. 35 Sample Heel chamfer—large pitch cone angle spiral bevel gear

65°, we rather get what appears in Fig. 34, right, and now, any risk of collision has disappeared and the chamfering operation can proceed.

Figure 35 shows a typical chamfer at the Heel of a large pitch cone angle spiral bevel gear. The teeth are non generated. The chamfers on each flank show comparable sizes. However, at the root, the CT movement needs to continue deeper since a burr has remained.

The main disadvantage of a non 90° Pivot Angle is that the bottom part of the Chamfer Tool may become parallel to the bottom of the tooth or, even worse, its cutting edge may make a negative angle with the tooth gap root. In such a case, the tool movement must be stopped before it reaches the bottom of the tooth gap and a small area is not chamfered or deburred. Fig. 36, left, shows the Chamfer Tool with a 65° Pivot Angle; there is still a positive angle between the cutting edge and the bottom of the tooth gap; by opposition, Fig. 36 right, the Pivot Angle is rather 45° and clearly the movement must be stopped before the tool reaches the bottom of the tooth gap to avoid damaging the tool and creating a dent in the root.

If the work piece has a small pitch cone angle, and this applies to cylindrical gears as well, then it is clear that while the Toe end of the tooth poses no issue, left Fig. 37, the Heel end cannot be chamfered with this tool because of collision risks between the tool spindle and the turn table, and also likely excessive turn table tilt—right Fig. 37, unless the work holding support is long enough to allow sufficient clearance; otherwise, one must resort to using either End Mill, a Ball Mill or a CoSIMT tool.

Of course, chamfering the tooth Tip causes no issue, either on the pinion or gear, as is shown in Figs. 38 and 39.

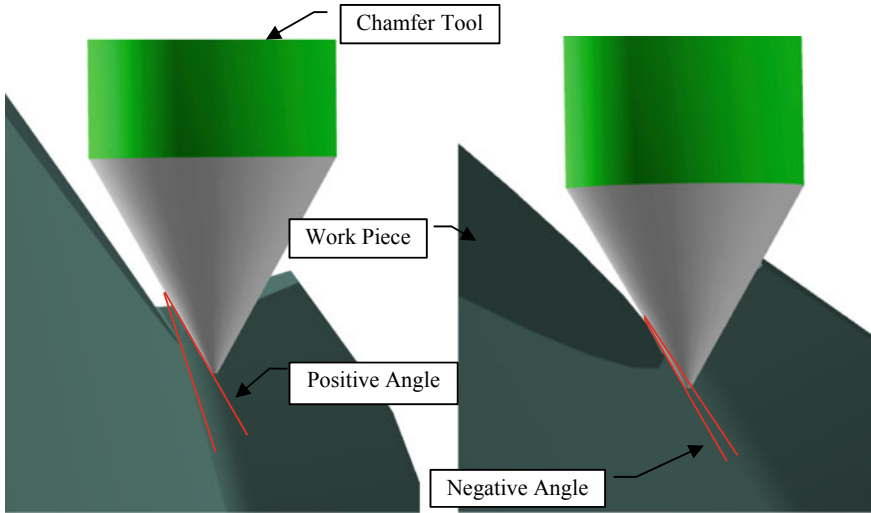


Fig. 36 Clearance angle—cutting edge to tooth root

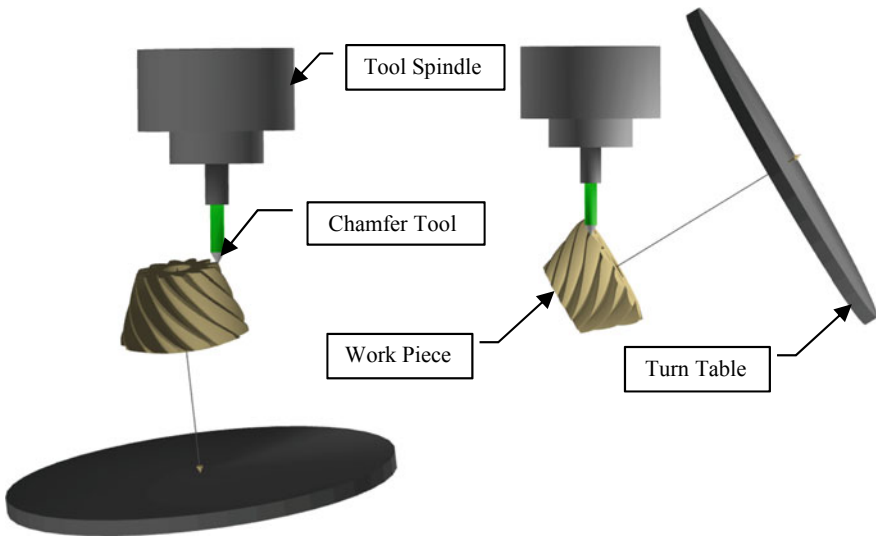


Fig. 37 Chamfering Toe and Heel—small pitch cone angle spiral bevel gear

3.5 CoSIMT Tools

A CoSIMT, or Conical Side Milling Tool, is a disk-shaped tool whose cutting edges can take different profiles: Involute, circular arc, or a more standard straight edge. In the latter case, the cutting edges may be parallel to, or make an angle with the radial

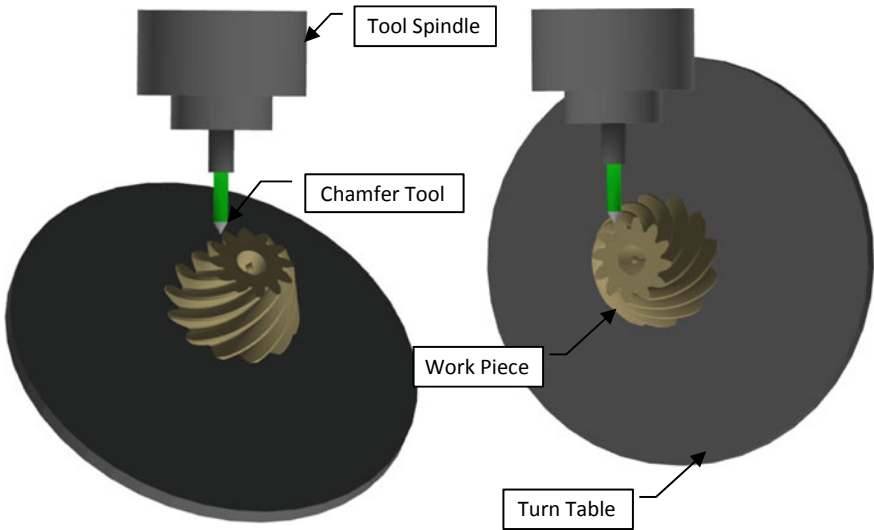


Fig. 38 Pinion Tip chamfering with Chamfer Tool

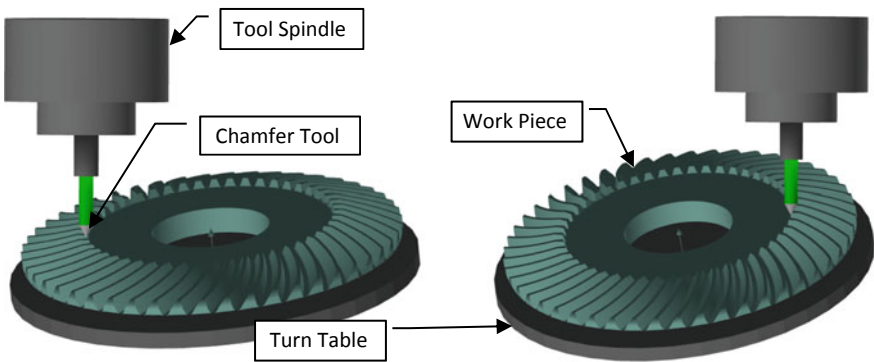


Fig. 39 Gear Tip chamfering with Chamfer Tool

direction. Such tools come in several base geometries, and tool manufacturers such as Sandvik, P. Horn, Iscar, Ingersoll Rand make disk bodies to different diameters on which blade inserts are screwed. The CoSIMT could also be a grinding disk.

These tools can be used to chamfer pretty much any gear type, given the blade angles are chosen correctly. For example, the tooth tips of a spur gear can be chamfered using a CoSIMT with 15° blade angles (left, Fig. 40) or 0° (right, Fig. 40) and both will give the same results.

The same comment applies to helical gears (left, Fig. 41), where the cutting edges are angled relative to the CoSIMT radius, and straight bevel gears (right, Fig. 41) where the cutting edges are parallel to the CoSIMT radius.

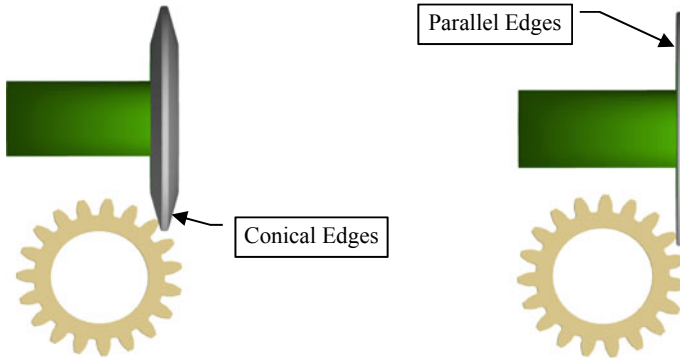


Fig. 40 Spur gear Tip chamfering with a CoSIMT

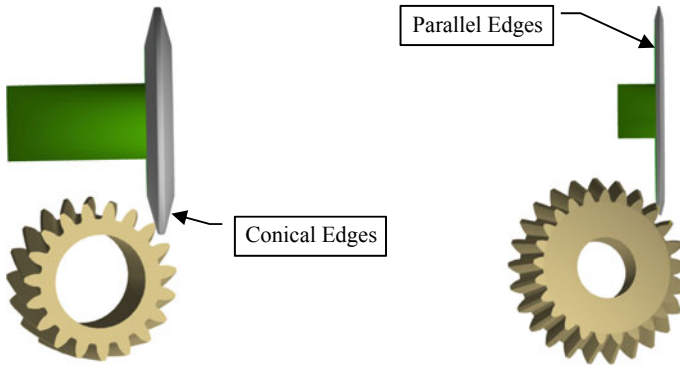


Fig. 41 Helical and straight bevel gear Tip chamfering with a CoSIMT

However, for spiral bevel gears, the CoSIMT *must* have a convex side that is used to chamfer the concave tooth tip, and normally a flat or concave side that is used to chamfer the convex tooth tip, although a convex blade will also work as Fig. 42 shows.

Four unit vectors (Fig. 43) are defined to orient the CoSIMT at any point along the tooth Tip edge of a spur or straight bevel gear:

- \vec{T} : the local tangent vector; the cutting edge slides along this vector such that the cutting blades work away from their tips;
- \vec{N} : the local normal vector,
- \vec{Vo} : unit vector along the tooth tip edge,
- \vec{Tool} : vector parallel to the tool axis.

\vec{Vo} is obtained from the local partial derivative along the tooth tip. Vector \vec{N} is pivoted about \vec{Vo} by half the difference between the local pressure angle and 90° to yield the

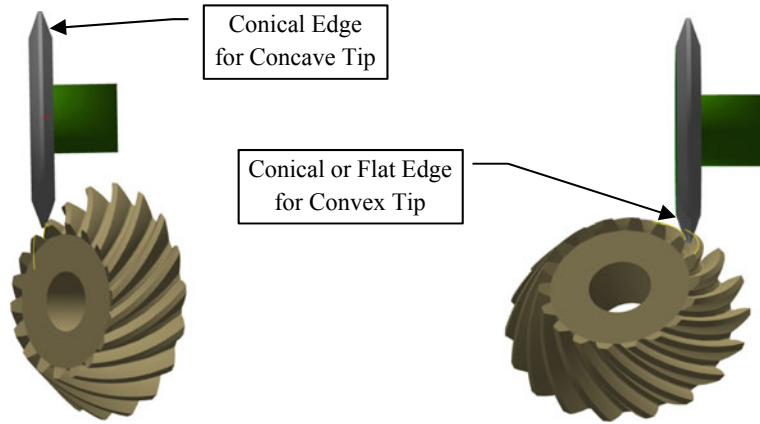


Fig. 42 Spiral bevel gear Tip chamfering with a CoSIMT

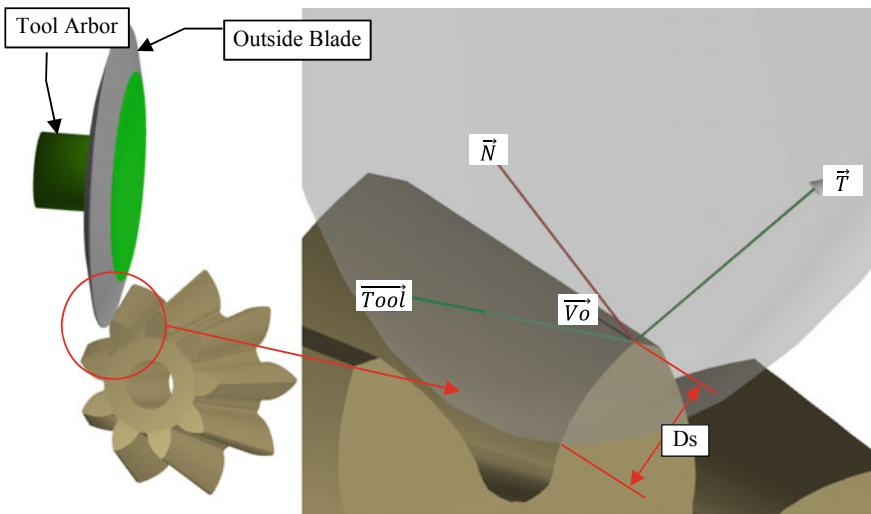


Fig. 43 CoSIMT Tool installation for Tip chamfering—spur and straight bevel gears

tool axis vector \vec{Tool} . To avoid working on the blade tips, the CoSIMT slides along vector \vec{T} by distance D_s .

A similar approach is used for Tip chamfering of spiral bevel gears with a CoSIMT, Fig. 44, although the tooth geometry is decidedly more complex.

Although the above show that it is relatively easy to chamfer tooth tips using a CoSIMT, the same cannot be said of Toe and Heel tooth edge chamfering. The main reason is tool size which must be limited in order not to damage the tooth flank behind the tooth Toe or Heel edge; this therefore limits the CoSIMT diameter and

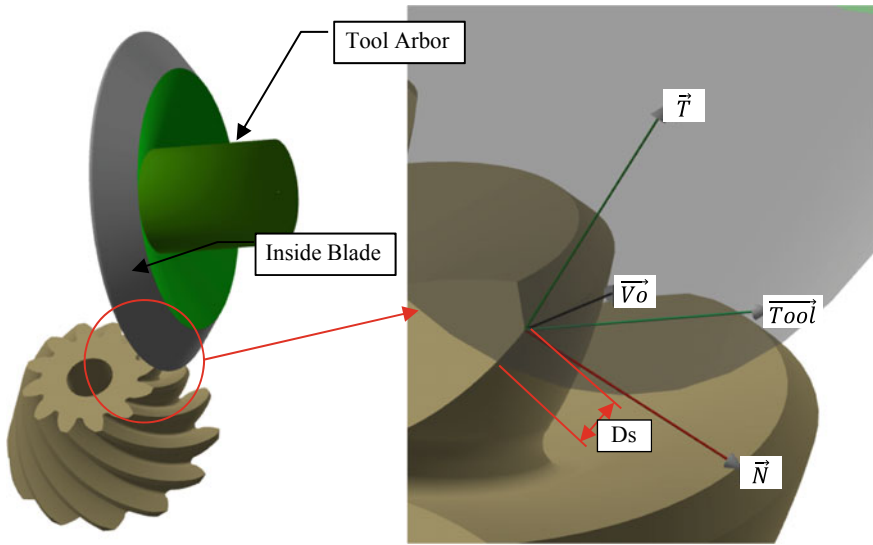


Fig. 44 CoSIMT Tool installation for Tip chamfering—spiral bevel gears

the chamfer angle. On the other hand, the sturdiness of CoSIMT tools ensure a long service life and makes them choice tools.

In addition, while chamfering the left tooth edge with the CoSiMT's outside blade—i.e. the blade on the opposite side of the arbor—causes no risk of interference between the tool's arbor and the work piece (left, Fig. 45), using the inside blade—the blade on the same side as the arbor—requires an elongated arbor (right, Fig. 45) to avoid interference and this is likely to lead to vibrations and uneven results.

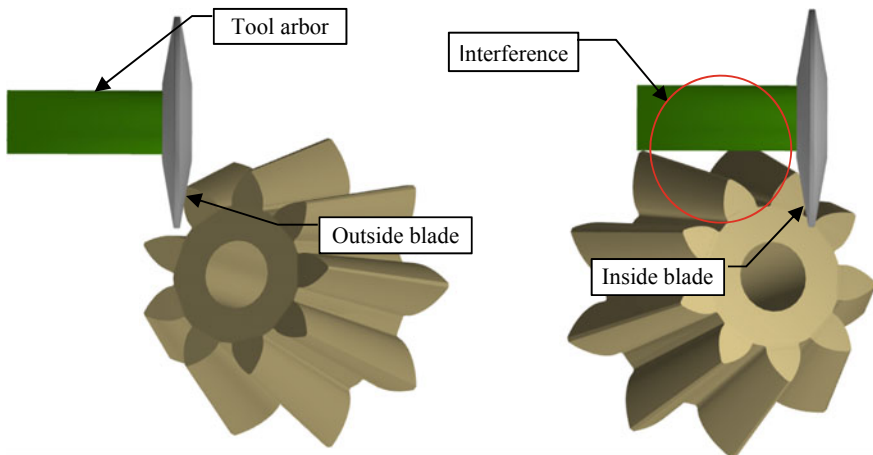


Fig. 45 CoSIMT Toe/Heel chamfering with different blades—straight bevel gears

This implies that, for practical reasons, the CoSIMT outside blade should be used to chamfer *both* the left and right tooth Toe and Heel edges, as shown in Fig. 46. This also implies that the process is not continuous: all the Toe/Heel edges on one tooth flank are done, and then all the edges of the other tooth flank. In practice, this does not involve excessive cycle time and is well worth given all the chamfering can be done using a single tool.

Five unit vectors (left, Fig. 47) are defined to orient the CoSIMT at any point along the Toe/Heel edge of a spur or straight bevel gear:

- \vec{T} : local tangent vector; the cutting edge slides of distance D_s along this vector such that cutting blades work away from their tips;
- \vec{N} : the local normal vector,

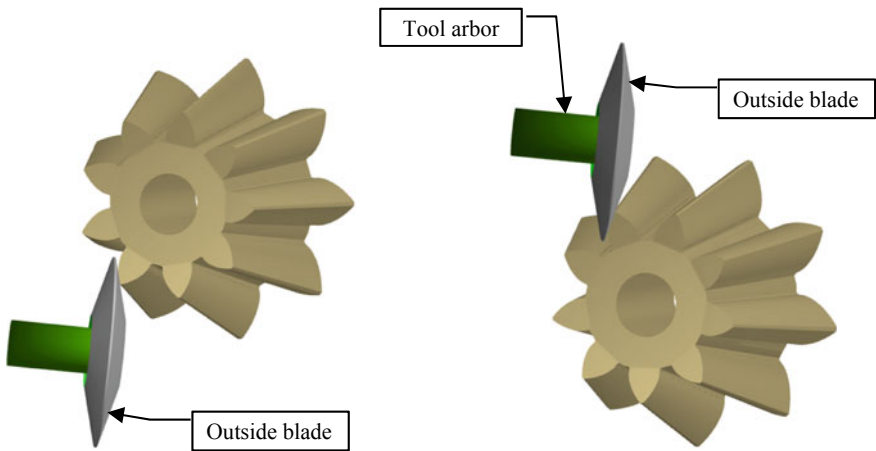


Fig. 46 CoSIMT Toe chamfering both tooth flanks using the outside blade—straight bevel gear

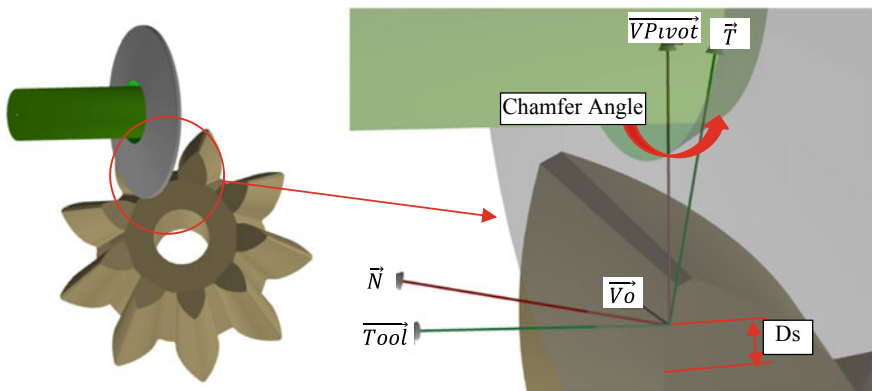


Fig. 47 CoSIMT Tool installation for Toe/Heel chamfering—straight bevel gears

- \vec{Vo} : $\vec{N} \times \vec{T}$,
- \vec{Tool} : vector parallel to the tool axis,
- \vec{Pivot} : axis about which vector \vec{Tool} is rotated by the desired chamfer angle.

\vec{Vo} is obtained from the cross product of \vec{N} and \vec{T} . To avoid working on the blade tips, the CoSIMT slides along vector \vec{T} by distance D_s ; this is therefore a “Moving Contact Point” that ensures even wear along the cutting edge of the tool and improves tool life.

In the case where the CoSIMT OD is too large, the tool can be pivoted out of the mesh around axis \vec{Tool} , as shown in Fig. 48.

Finally, by carefully selecting the CoSIMT tool dimensions, it is also possible to target the *root area* of the Toe and Heel edges.

Fig. 49 shows—in several different positions—a CoSIMT chamfering a straight bevel pinion tooth Toe edge: it is clear that the fillet and root areas of the tooth gap can be targeted by carefully selecting the CoSIMT dimensions, Chamfer Angle and Pivot Angle.

The same approach is used for spur, helical and spiral bevel gears and will therefore be omitted here.

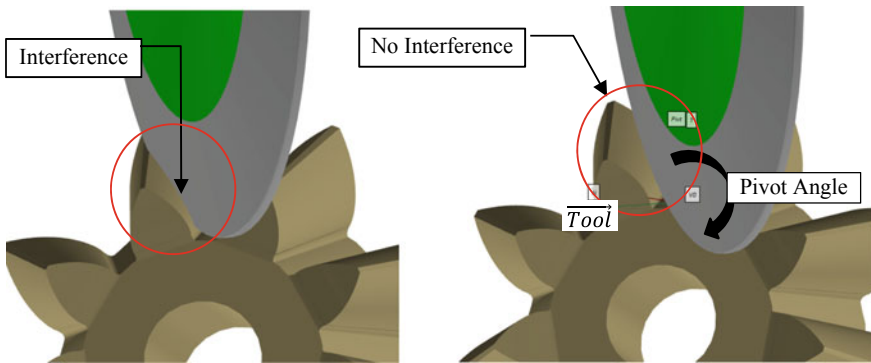


Fig. 48 CoSIMT pivot to avoid interference—Toe/Heel chamfering

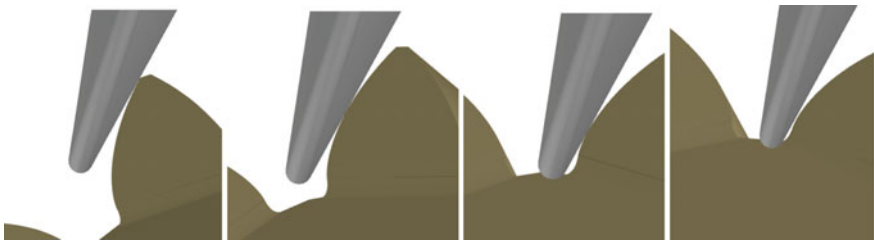


Fig. 49 CoSIMT chamfering at Toe: tooth flank and root

4 Conclusion

The intent of this chapter was to explore some of the deburring and chamfering options that are offered to gear manufacturers.

As was shown, most gear machine manufacturers already offer several possibilities, either integrated to their gear cutting machines or in separate embodiments. These solutions offer excellent results and cycle times, and are intended for mass production.

For small to medium volumes, and for a varying production in terms of gear types and sizes, such machines often are not economically viable, especially so that most require special tools matching the module, face width, pressure angle and helix angle of the parts to chamfer or deburr.

Given the increasing use of 5, 4+1 and 4 Axis CnC machines in the gear industry, where small to medium gear volumes are an everyday task, and where widely different gear types can be produced on the same machine, there is a need for different avenues allowing efficient chamfering—and thus deburring—of spur, helical, straight bevel and spiral bevel gears using off-the-shelf tools, which was the focus of this chapter.

The considered off-the-shelf tools include End Mills, Ball Mills, Chamfer Tools and Conical Side Milling Tools, i.e. CoSIMT.

In all cases, it is possible to chamfer either, or both, the Toe and Heel edges, and the Tip edges. In many instances, adjusting chamfer parameters such as the Pivot Angle allows chamfering every part of the tooth; this is especially true of End Mill and Ball Mill tools, although Ball Mill tools leave a double lip because of their spherical tip.

Overall, the CoSIMT tool may be the best all around chamfering tool in that, if its dimensions are well selected, it can access all edges of a gear tooth, be it spur, helical, straight or spiral bevel.

As was demonstrated in the above paragraphs, while deburring and chamfering is an unloved task, it is by far *not a trivial* task since the targeted geometries are complex and varied.

The methods presented in this paper are all integrated into the HyGEARS software, whose post-processor generates the G-Codes for any CnC machine and controller on the market. Therefore, an unused, or lightly used, 4, 4+1 or 5 Axis CnC machine could be put to good use chamfering parts.

References

1. www.HyGEARS.com
2. Horst, B.: A Basic Guide to Deburring and Chamfering Gears. Gear Technology, July August (1995)
3. McGuinn, J.: Chamfering/Deburring Still a Player—Now More than Ever. Gear Technology, September October (2018)
4. Klein, G.: The Evolution of Gear Chamfering, September October (2018)
5. Ribbeck, K.-M.: Deburring—The Underestimated Task, September October (2018)
6. www.Liebherr.com, Deburring and Chamfering Machine LD 180/280 C

7. www.redinmachine.com
8. Weiler, A.: Gear Deburring with Brushes. www.WeilerAbrasives.com
9. www.cwst.com/shot-peening-overview/glass-bead-peening

Worm-Type Gear with Steel Gearwheel



Evgenii S. Trubachev

Abstract The manuscript presents a study of a variety of a worm gear having a truncated gear rim as compared to the common worm gear. This gear has been originally invented by Egorov and Iofik and, as shown here, it has a number of favorable geometrical and kinematic, power, strength, layout, and manufacturing properties. It is offered to name it “QN-gear” and to use hardened steel as the material of its gear rim that sharply raises its strength. The quantitative and qualitative comparison with the nearest analogues—worm and spiroid gears has shown the perspective of applying such a gear design, first of all, for the case of low rotation speeds. Equations are obtained for calculation of the worm axial module and dependences for prevention of tooth undercutting and sharpening, which are, in fact, limitations at optimization design. Proposals are made to improve the performance and production characteristics of QN-gears with hardened steel gearwheel rims by gear optimization and contact localization. To improve the economic efficiency of gear production, it is proposed to produce gearwheels with curvilinear and asymmetric profiles by means of standard involute hobs and multi-cutter running heads. An example of a gearbox based on the steel QN-gear is given showing high load characteristics in testing.

Keywords Worm gear · Spiroid gear · Load capacity · Strength

1 Introduction

The problem of applying hardened steel to produce worm gearwheels [1] is one of promising and nowadays insufficiently used possibilities to improve the durability and economic performance of worm gears. The preventing property that forces to use antifriction materials enabling relatively fast running-in is the poor contact conditions in the pitch point of a cylindrical worm gear, because this point is always a regular node one [2]; the speed of its movement along the surface of the worm thread is equal to zero, the contact line is located extremely unfavorably, the angle between its

E. S. Trubachev (✉)

Institute of Mechanics Named After Professor V. I. Goldfarb, Kalashnikov Izhevsk State Technical University, Izhevsk, Russia
e-mail: truba@istu.ru

tangent and the vector \mathbf{v}_s of the relative speed is also almost equal to zero. A radical way to eliminate this disadvantage is known—to remove a part of the gearwheel rim adjacent to the pitch point. Perhaps, Grubin and Lytskhier were the first Russian (Soviet) researchers to propose this method [3]—see Fig. 1.

This idea was developed in gears, which were named by authors (Egorov and Iofik) as cylindrical worm ones [4, 5] having larger gearwheel diameters in comparison with the Grubin-Litskhier gearwheel—see Fig. 2.

The gear version in accordance with the scheme in Fig. 2a has exterior benefits: the total width of the gear rim is greater, respectively, the total length of contact lines is greater, and the load transmitted by their segments is lower. However, there still remain two other disadvantages in this version of the worm gear:

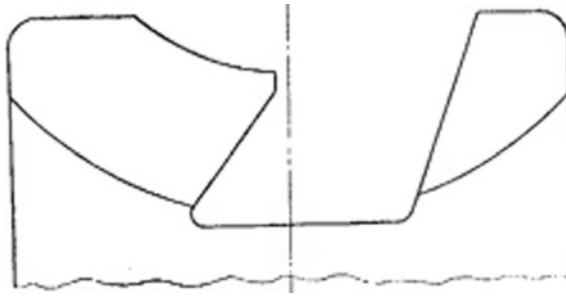
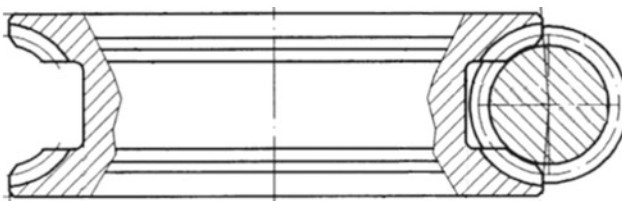
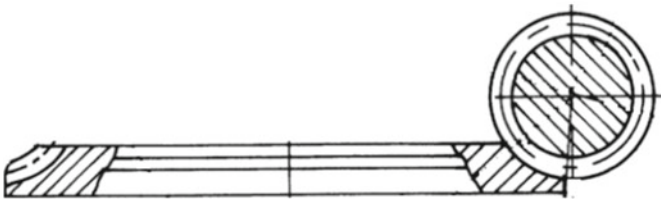


Fig. 1 The axial profile of the Grubin-Litskhier worm gearwheel



(a) gear in accordance with [4]



(b) gear in accordance with [5]

Fig. 2 Worm gears by Egorov and Iofik with the removed central part of the gearwheel rim

- the repeated contact of worm threads [6], which causes their higher heat load;
- the high sensitivity of the gear to the error of the gearwheel axial arrangement.

Probably, it is caused by the fact that at practical implementation of this gear in gearboxes for general purpose mechanical engineering [7] its gearwheel, like a gearwheel of a common worm gear, was made of bronze—the antifriction material that provides fast running-in.

In [8], a version of solving the problem of applying hardened steel for worm gears is presented for a non-orthogonal worm gear without the so-called meshing axes, and the result of practical implementation of this solution in a serially produced low-speed heavy-loaded gearbox for pipeline valves is shown. However, the non-orthogonal arrangement of axes is not a “great pleasure” for production. Therefore, the version for the scheme in Fig. 3b seems to become an effective solution to the above problem at the orthogonal arrangement of axes, because it provides:

- elimination of the repeated contact;
- possibility of a simple and easily controlled contact localization along the tooth length;
- lower sensitivity to the action of errors.

Exactly this version is a subject of consideration in this manuscript, particularly, the features of selecting gear parameters, obtained gear properties in comparison with its analogues, and results of practical cutting and testing. The presented results confirming and developing the initial conclusions made by authors of the gear are proving the gear originality and significant difference from its analogues. Therefore,

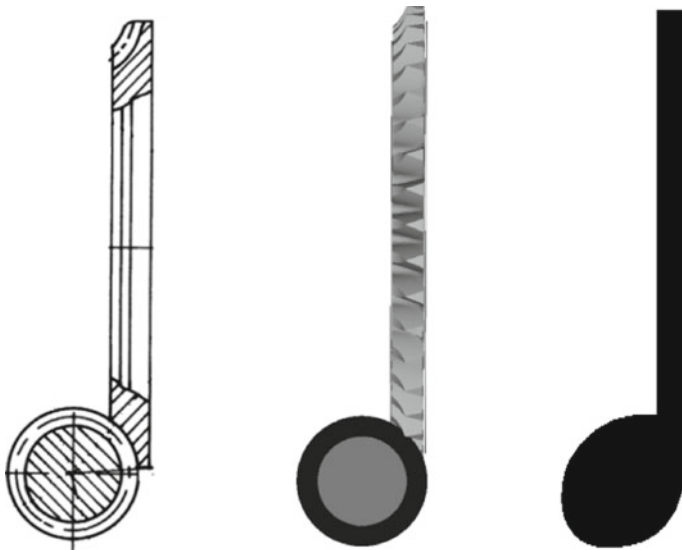


Fig. 3 QN-gear and the note “Quarter note”

it seems that the gear is worth giving its own name. Further in the manuscript the name “QN-gear” will be used for short (Quarter-note gear—see Fig. 3).

2 Some General Comments

The presence of the meshing axis in the meshing zone (in the orthogonal unshifted worm cylindrical gear it passes parallel to the gearwheel axis contacting the pitch cylinder of the worm) forces the contact lines to draw along teeth; this situation is fundamentally kept for almost any profile of the worm and gear ratio [9]. Figure 4a shows as an example the lines of the conjugated contact for an orthogonal Archimedean worm gear with the gear ratio equal to 40 and interaxial distance equal to 100 mm (the lines are extended beyond the meshing zone to demonstrate their shape evolution). It can be seen that as you move away from the middle plane of the gearwheel (plane $y = 0$), angles between the vector of relative velocity (it practically coincides with the circumferential direction of the worm) and the tangent to the contact line are increasing. This well-known fact is the main motive for removal of the central part of the gear rim. Having left, in fact, one third of the gear rim, Egorov and Iofik, developed the gearwheel for greater use of the meshing surface area with favorable properties—they moved the face of the gearwheel towards greater values of y coordinate, increased the maximum diameter, and introduced a negative shift of the worm (Fig. 4b). These techniques allow to increase the overlap factor and, as a consequence, to compensate the negative effect of the acquired reduction of the worm gearwheel face width. In accordance with the classification by Georgiev and Goldfarb [10], the worm gear is thus transferred to a higher class, and its gearing zone is shifted relative to the interaxial line along the gearwheel axis.

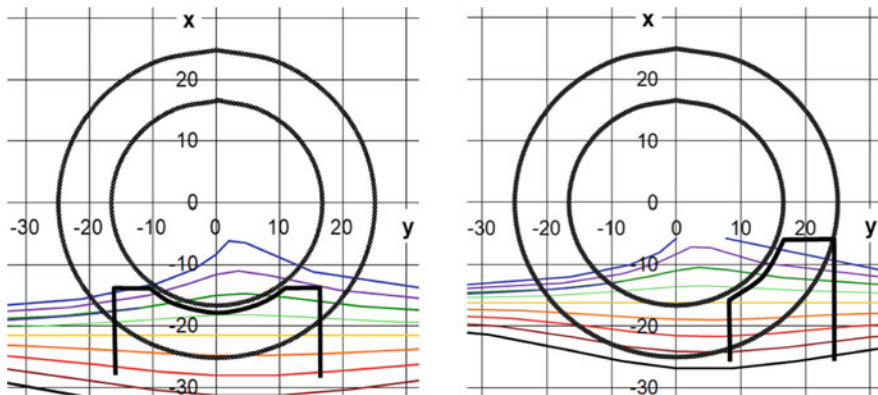


Fig. 4 Meshing surfaces of worm gears with Archimedes worms

3 Gear Scheme

As it is usually done [11, 12], it is reasonable to start the calculation of the QN-gear by choosing the gear scheme, i.e. by defining the pitch surfaces. The first question here is: which cylinder of the worm is reasonable to be chosen as the initial one? In the case of common worm cylindrical gears it is the pitch cylinder, and for spiroid ones it is the outer cylinder, because in this case:

- greater completeness of contact is provided (contact lines are stretched along the worm profile);
- conditions of tooth undercutting are adequately evaluated.

In the QN-gear the situation is almost the same: contact lines can be evaluated from Fig. 4; and undercutting, as it will be shown below, is one of the restrictions for parameter selection. Therefore, it is suggested to choose the outer cylinder with a diameter of d_{a1} as the worm initial cylinder in the QN-gear. The initial surface of the gearwheel in the orthogonal case will be a torus surface contacting with this cylinder and limited by two end faces, the position of which is set by the parameters B_2 and b_2 —see Fig. 5, while contacting of initial surfaces takes place in the plane $z = 0$ along the arc of the circumference $x^2 + y^2 = (0.5d_{a1})^2$.

Reasons for selecting the worm diameter of the QN-gear are almost the same as for a conventional worm cylindrical gear. The issue of optimal ratio of the gearwheel rim displacement from the interaxial line, the width and the largest diameter of the gearwheel rim remains open in many respects and may depend, for example, on the required ratio of tooth contact and bending strength. Based on the experience in gear

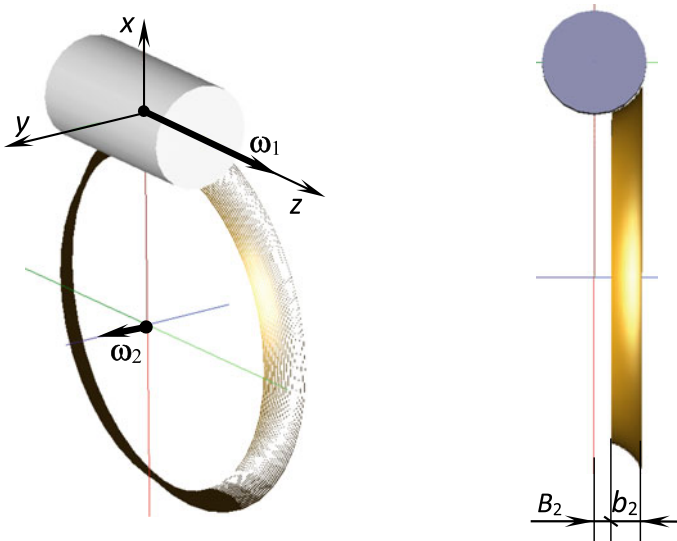


Fig. 5 Initial surfaces and scheme of QN-gear

design and testing, it is possible to accept:

$$B_2 = 0.15d_{a1}. \quad (1)$$

It allows providing the minimum angle between the tangent to a contact line and the vector of relative speed not $<11^\circ \dots 15^\circ$, and the average one—about $40^\circ \dots 45^\circ$, and it is well agreed with this recommendation in [4, 5] (0.2...0.4 from outer radius of the worm). For obvious reasons, the following inequalities should also be kept:

$$(B_2 + b_2) \rightarrow (\leq) 0.5d_{a1}, \quad (2)$$

$$d_{M2} \rightarrow (\leq) 2 \left[a_w - \sqrt{(0.5d_{a1})^2 - (B_2 + b_2)^2} \right] \quad (3)$$

Selection of the worm axial module m_x should be made from the condition of collinearity of the helical line and the relative velocity vector, in the general case it gives the expression [13]:

$$m_{x \text{ id}} = \frac{2}{z_{(1)}} \frac{(0.5d_{a1})^2(x + a_w) \sin \Sigma}{[(0.5d_{a1})^2(i - \cos \Sigma) - zy \sin \Sigma - xa_w \cos \Sigma]}, \quad (4)$$

where $z_{(1)}$ is the number of worm threads; a_w , Σ are the distance and angle between the axes; i is the gear ratio; x , y , z are the Cartesian coordinates of the point of contact of the pitch surfaces in the coordinate system shown in the Fig. 5.

In the orthogonal case:

$$m_{x \text{ id}} = \frac{2(x + a_w)}{z_{(2)}} \quad (5)$$

or—for the convenience of correlating the variable coordinate with the assigned parameters B_2 and b_2 and taking into account $x^2 + y^2 = (0.5d_{a1})^2$:

$$m_{x \text{ id}} = \frac{2 \left(a_w - \sqrt{(0.5d_{a1})^2 - y^2} \right)}{z_{(2)}} \quad (6)$$

As you can see, the value of $m_{x \text{ id}}$ depends on the selection of the point position on the line of the initial surfaces contact (x or y coordinates).

4 Restrictions of Parameter Selection—Tooth Undercut and Sharpening

The practice of calculations shows that the QN-gear is characterized by undercutting of the 1st type (Fig. 6) caused by the appearance of the so-called singular line of the enveloping surface in the meshing zone. It is the geometrical place of singular points of the enveloping surface. To predict and prevent this phenomenon at the stage of selecting parameters of the gear scheme, we use the method and algorithm thoroughly described in [14]. The main analytical expression here is a system of equations solved at points of the worm pitch surface:

$$\begin{cases} \mathbf{n}\mathbf{v}_s = F_m(x, y, z) = 0, \\ \mathbf{N}\mathbf{v}_2 = F_u(x, y, z) = 0. \end{cases} \quad (7)$$

Here, the first equation is the meshing equation ($\mathbf{n}(x, y, z, p_\gamma, \alpha_{lim})$ is the limiting contact normal, $p_\gamma = 0.5m_xz_{(1)}$ is the helical parameter of the worm, α_{lim} is the sought limiting axial angle of the worm profile), and the second one is the condition of intersection of the normal $\mathbf{N} = \{\partial F_m/\partial x, \partial F_m/\partial y, \partial F_m/\partial z\}$ to the meshing surface with the gearwheel axis (\mathbf{v}_2 is the speed of the contact point at joint motion with the gearwheel).

The solution (α_{lim}) for which the mentioned singular points and, consequently, the tooth undercut appear in the meshing is usually not single. The resulting set of solutions is used to select maximum and minimum values, and the profile angles of the right and left flanks of worm threads should be selected as their largest and smallest (taking into account the sign) values, respectively. The main factors that affect the values of angles α_{lim} are:

- removal of the gearwheel B_2 ;
- worm diameter d_{a1} ;
- worm axial module m_x ;
- gear ratio i .

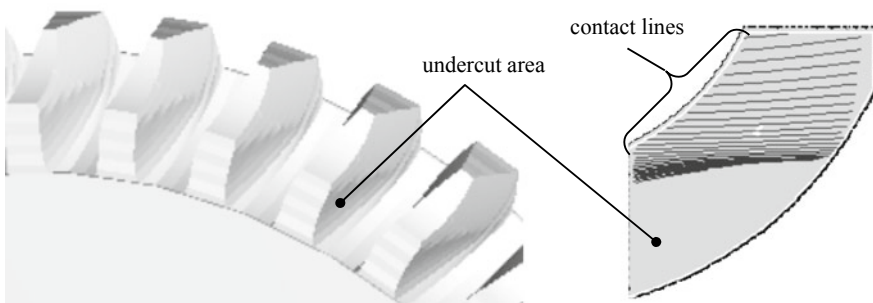


Fig. 6 Undercutting of gearwheel teeth in the QN-gear

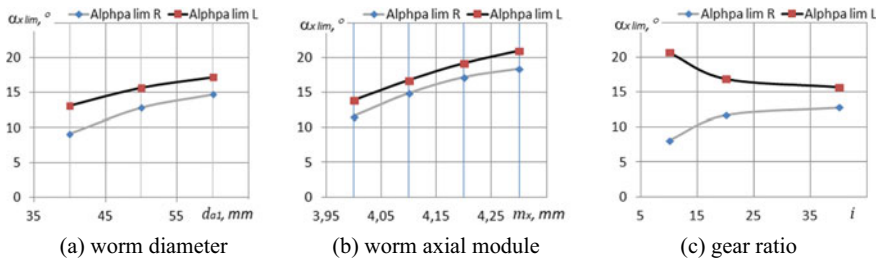


Fig. 7 Main factors of tooth undercutting in the QN-gear

Figure 7 shows the dependencies of limiting angles on the last three factors (B_2 , taken to be equal to $0.15d_{a1}$) for the orthogonal gear with the interaxial distance of 100 mm. Evidently, the risk of undercutting goes up with increasing the worm diameter, its axial module and decreasing the gear ratio, and it is higher for one of the flanks (the left one facing the positive values of z coordinate—for the coordinate system shown in Fig. 6). Considering this fact, one can recommend the introduction of an asymmetric worm thread profile to avoid undercutting if necessary, and the less the gear ratio is, the larger the asymmetry should be.

The second limitation is the tooth sharpening that occurs at the intersection of the torus and cylindrical sections of the tooth vertex edge. Of course, this sharpening can be eliminated by an additional chamfer on this tooth vertex, as it is shown in the original patent [4, 5]. However, this technique reduces the area of contact surfaces and the length of contact lines, so we will consider further how it can be done by choosing the gear parameters. The main influencing factors here are as follows:

- the thickness s_x of the worm thread;
- the axial module m_x of the worm;
- the largest diameter d_{M2} of the gearwheel.

Due to the obvious influence of the first of the factors, the main interest is to improve the gear by two latter ones. And here lies one of the main contradictions for the designing engineer: on the one hand, the gearwheel diameter should be increased to use the gear possibilities more completely—to increase the overlap factor and length of contact lines, and to reduce contact stresses. On the other hand, the risk of tooth sharpening is increased in this case (in Fig. 8b it can be recognized by the intersection of opposite flanks). The general thoughts here are as follows:

- to increase the diameter d_{M2} one should choose larger values m_x (larger values y in (6)), see Fig. 8c;
- this increases the risk of tooth undercutting (see Fig. 7b) which may require an increase in axial profile angles above the commonly accepted value of 20° ;
- there is some limit of the gear diameter d_{M2} in terms of increasing the gear performance.

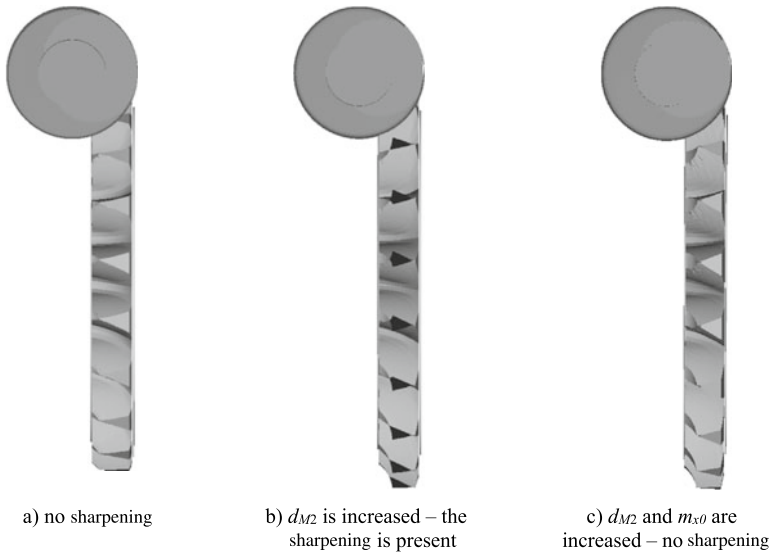


Fig. 8 Tooth undercutting sharpening in the QN-gear (please, replace the word "undercutting" with "sharpening")

In summary, one can recommend the range $d_{M2} = (1.8 \dots 1.9)a_w$ and the value $y = (0.30 \dots 0.43)d_{a1}$ to calculate the axial worm module by (6) which results in the expression:

$$m_x = \frac{2a_w - (0.5 \dots 0.8)d_{a1}}{z_{(2)}} \quad (8)$$

The values m_x obtained by this expression turn to be a little larger than worm modules for the common worm cylindrical gear with the same gear ratio, inter-axial distance and worm diameter, and they proximately correspond to the negative coefficients of its worm shift in the range $-0.5 \dots -2.5$. This increase of the module (reduction of the shift coefficient) leads to an increase in the risk of undercutting and reduction of contact stresses in the meshing.

5 Contact Localization

The manuscript's title focuses on the fact that it is reasonable to use a steel gearwheel subjected to thermal or chemical thermal hardening treatment in the QN-gear. This, to our opinion, is not obligatory, but gives a better implementation of the gear potential in terms of tooth strength and economy. In this regard, the issue of providing the

contact localization is more relevant than for common worm gears with gearwheels allowing for relatively fast running-in.

In conventional worm gears, the contact is usually localized in the central area of the tooth flank with adverse meshing conditions. For gears shown in Fig. 3a and b, the localized contact can only be achieved by cutting each of the half-rim individually (at least if the traditional method of forming by the generating worm is used): each rim should have the assigned design point and properly chosen number of machine-tool settings. In general, this results in at least two different sets and two gear machining operations. In this context, the QN-gear has the advantage: contact localization along both flanks can be achieved per one setting of the cutting tool. For this purpose, the method is applicable which has been first proposed in [15] and stated in detail in [16] and which involves the following basic steps:

- selection of design points on opposite tooth flanks;
- specifying a number of machine-tool setting parameters—the machine-tool interaxial angle, number of threads, axial module and the radii of the curvature of the generating worm profile;
- calculation of the remaining parameters—the machine-tool interaxial distance, diameter, angles and thicknesses of the generating worm profile—for conditions assigned at the design points [15, 17]:

$$\begin{aligned} \mathbf{nv}_{01} &= 0 \\ \tan \gamma &= -\frac{\mathbf{ne}_t}{\mathbf{nk}}, \\ \tan \alpha_x &= -\frac{\mathbf{ne}_r}{\mathbf{nk}}, \end{aligned} \quad (9)$$

where \mathbf{v}_{01} is the velocity of the generating worm relative to the operating worm in their joint virtual meshing at the design point, γ is the helix angle, \mathbf{e}_t , \mathbf{e}_r and \mathbf{k} are unit vectors of circumferential, radial and axial directions with respect to the axis of the generating worm.

Contact localization by the tooth height (profile) is provided mainly by the selection of the proper ratio of profile curvatures for the operating and generating worm, and by the length—by the selection of the module and the number of threads for the generating worm, and the machine-tool angle.

Similar to common worm gears, it is reasonable to provide contact localization in QN-gears by applying:

- a single- or double-thread hob (in particular, a standard involute hob) [18];
- an assembled running-in tool cutter head with 2, 3 or 4 carbide cutters [16]

The question still remains: What is the best place for contact localization—placing the design point in the middle of the tooth or shifting it to one of its face ends, apex or root? The answer to this question should take into account the asymmetry of the modification field (Fig. 11), gearwheel deformations during heat treatment and

under load in the gearbox, and the necessity to provide the preferable initial load concentration within the area of more favorable contact conditions.

6 Comparison of the QN-Gear with Classical Worm and Spiroid Gears

The QN-gear can be competitive within a wide range of operating conditions, but if we talk about the gear with a steel gearwheel, to our opinion, the most promising implementable application here is the case of low speeds and heavy loads. Figure 9

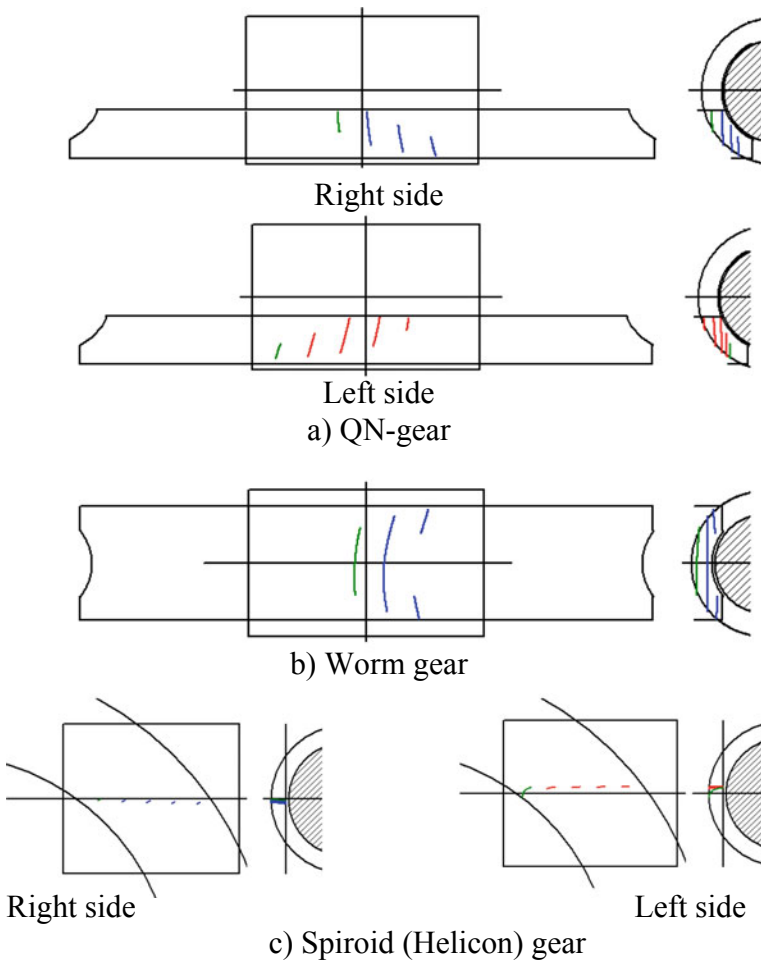


Fig. 9 Lines of conjugated contact in compared gears

and Table 1 show some results for such a gear as compared with analogues of the same dimension (plan view areas taken by gears are said to be equal)—classical worm cylindrical and spiroid gears. Calculations are made by means of the program complex “SPDIAL+” [12]. Pairs of assessments are given for the QN-gear and spiroid one: for right flanks—in numerator, for left flanks—in denominator.

The main conclusions of gear comparison are as follows:

1. Indicators that determine the gear resistance to scuffing.
 - 1.1 Contact stresses in the classical worm gear are lower than in the QN-gear and spiroid one (right flanks are meshing that are usually chosen as the main operating ones due to higher efficiency, lower forces that deform the structure and cause the stress concentration; see also [19]).
 - 1.2 Gears are comparable in the sliding speed: at a relatively large gear ratio, its main component—the worm speed—linearly depends on the diameter of the latter, and it is selected almost equal in all three gears.

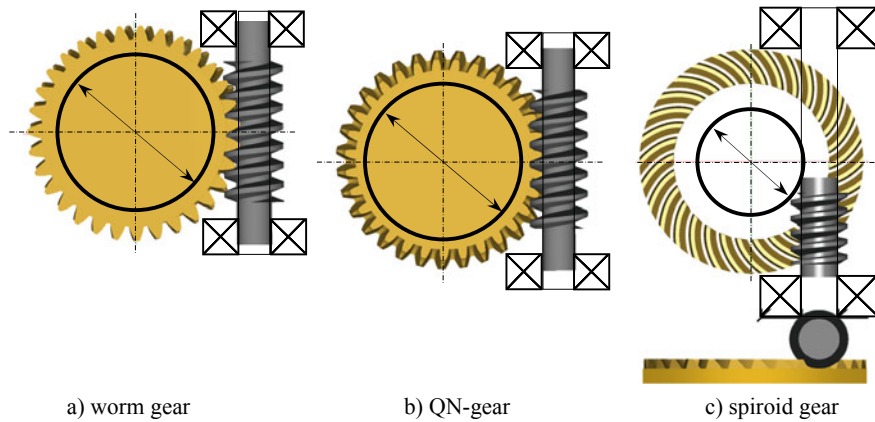


Fig. 10 To comparison of layout features of gears

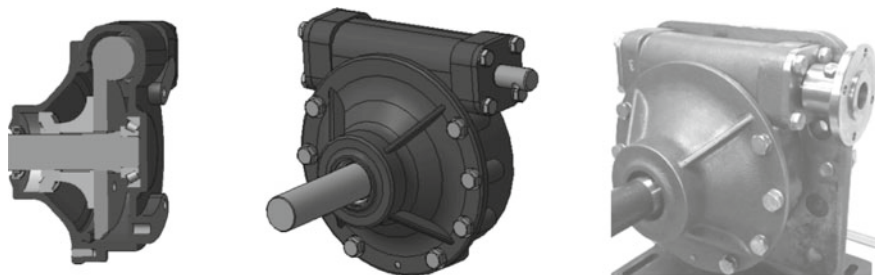


Fig. 11 The gearbox based on the QN-gear

Table 1 Main parameters and performance of compared gears

	QN-gear	Worm gear	Spiroid gear	
Frequency of worm rotation, rev/min	35			
Torque at the gearwheel, Nm	5000			
Gear ratio	50			
Interaxial distance, mm	105	110	60	
Maximum diameter of the gearwheel, mm	195	191	211	
Outer diameter of the worm, mm	50	50	48	
Axial module of the worm, mm	3.48	3.55	2.50	
Gearwheel face width, mm	16	38	30.5	
Overlap factor	4.2/4.7	2.75	5.7/5.8	
Total length of contact lines, mm	30.3/35 _{to} 6	55.9	25.3/29 _{to} 1	
Sliding speed, m/s	0.082	0.082	0.074	
Average angle between the tangent to the contact line and the vector of relative velocity, °	43/38	23	82/77	
Average speed of contact points displacement, m/s	Worm	0.051/0.050	0.031	0.078/0.076
	Gearwheel	0.0023/0.0018	0.0023	0.0047
Contact stresses, MPa (maximum in phases)	1600/1700	1150	1650/850	
Efficiency (friction coefficient 0.1)	0.420/0.425	0.428	0.402/0.370	
Axial force at the worm, H	57,000	56,300	72,000	
Axial force at the gearwheel, H	5800/21,300	9300	13,300/39,600	
Sensitivity to the error of the gearwheel axial position	Low	High	Low	
Possibility to adjust the backlash by the gearwheel axial displacement	Yes	No	Yes	

- 1.3 The QN-gear and the classical worm one have a higher efficiency (see also [18]), which determines less heat generation in the contact.
- 1.4 With regard to the arrangement of contact lines and velocities of contact point displacement along flanks (related parameters), the QN-gear actually takes an intermediate position between the classical worm gear and the spiroid one; in this case, contact points with these parameters equal to zero are excluded at meshing zones of the QN-gear and spiroid one.

Therefore, in the QN-gear there are objective reasons to obtain a higher resistance to tooth scuffing than in the classical worm one, and when added to the reduced sensitivity to the action of errors, it is the argument for applying the hardened steel as the QN gearwheel material.

2. Parameters that determine the tooth strength.
 - 2.1 Worm axial modules for the QN-gear and classical worm one are almost one and a half as much as that for the spiroid worm.
 - 2.2 The overlap factor of the QN-gear and the spiroid one are considerably higher than that of the worm gear.
 - 2.3 Forces acting in the meshing of the QN-gear and the classical worm one are more than a quarter less than those acting in the spiroid gear (see also [19]).

Therefore, there are objective reasons to obtain a higher resistance to tooth breakage in the QN-gear than in both other compared gears.

3. With regard to gear layout properties, the QN-gear also has an intermediate position between the classical worm and spiroid gears. Thus, the following is true for this gear (Fig. 10):
 - 3.1 Similar to the classic worm gear, there are better options for positioning a large central hole in the gearwheel than in the spiroid gear.
 - 3.2 Similar to the spiroid gearwheel, the QN-gearwheel is flatter than the classical worm gearwheel, which allows saving its cost, and, additionally, reducing the corresponding size of the casing.
 - 3.3 Worm bearings arranged on either side of the gearwheel can be placed closer to the meshing area than in the case of a spiroid gear, and their dimensions can be reduced due to lower meshing forces.
 - 3.4 Gearwheel bearings are also a little less loaded with axial forces than in the case of a spiroid gear.
4. The influence of the worm profile. An additional benefit can be obtained if the QN-gear worm profile is made asymmetrical and convex (i.e., the risk of undercutting is reduced). Table 1 shows the parameters of a symmetrical QN-gear with worm profile angles 18.2° , and contact stresses in meshing the left flanks are higher than in meshing of the right ones by 7% (1710 and 1600 MPa, respectively). If we make the profile asymmetrical and convex (profile angles are 23° and 20° , profile radii are 80 mm each), it is possible to equalize and reduce contact stresses to the value of 1580 MPa. Thus, along with the varying m_x, d_{M2}, B_2 the change of the worm thread profile for the QN-gear provides an effective tool for the gear optimization.

7 Example of Practical Implementation: Cutting and Testing Results

The QN-gear with the parameters listed in Table 1 was implemented in the low-speed (worm speed 35 rpm) gearbox¹ (Fig. 11) of the agricultural machine bogie

¹The design is made by eng. A. I. Shutkina.

drive. The worm and the gearwheel were made of 40X steel with volume hardening to the hardness of HRC 45–50. A grease with the addition of 10% mass fraction of lubricated graphite and 5% molybdenum disulfide (MoS_2) was used in the gearbox. The contact in the gear was localized, and the gearwheel was cut with a standard involute hob with a normal module of 3.5 mm. The actual contact pattern generally showed a good match with the calculated one (Fig. 12). After a short (20 revolutions of the gearwheel in each direction) running-in with a gradual increase in the load, the gear was subjected to peak torques 5000 Nm acting during one quarter revolution at a relative duty factor of 25% within 20 cycles. Then a long testing was carried out (the total time was about 1000 h) for the output torque smoothly varied within 1200...2400 Nm with the period of 8 h. The contact pattern increased during the test, taking up finally most of the active part of the tooth flank. In the steady heat mode, the gearbox heating reached $68^\circ\text{--}70^\circ$, with an average efficiency of 0.40–0.43 (the resulting test diagrams of the efficiency variation versus torque are shown in Fig. 13). Next, the gear was subjected to peak loads of 5300 Nm acting throughout

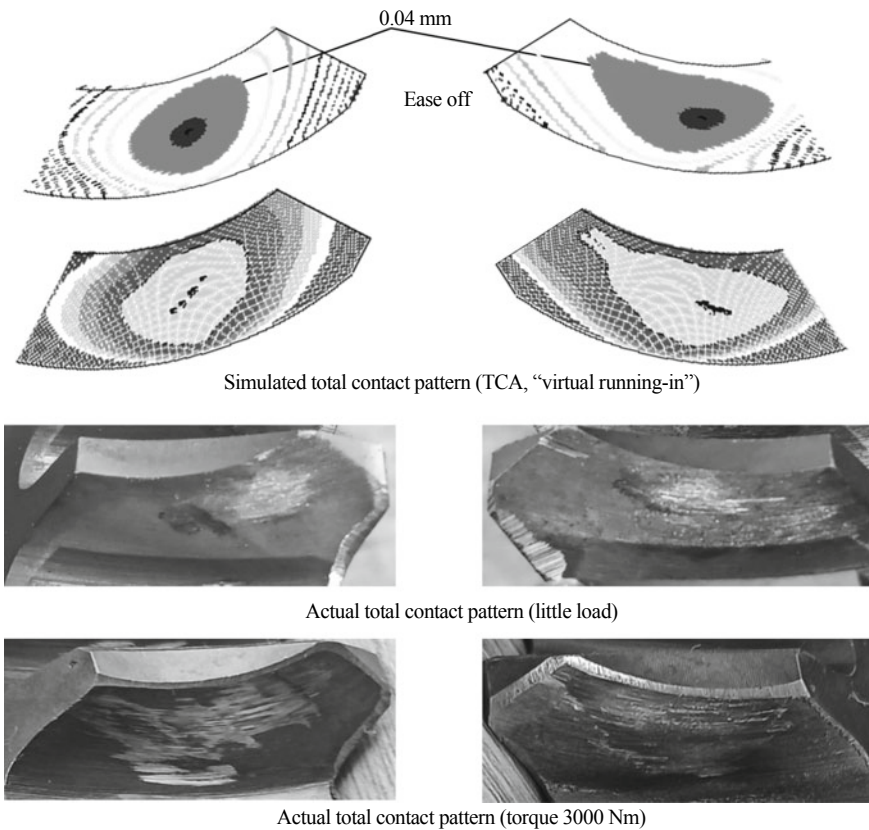


Fig. 12 Contact localization in the sample QN-gear

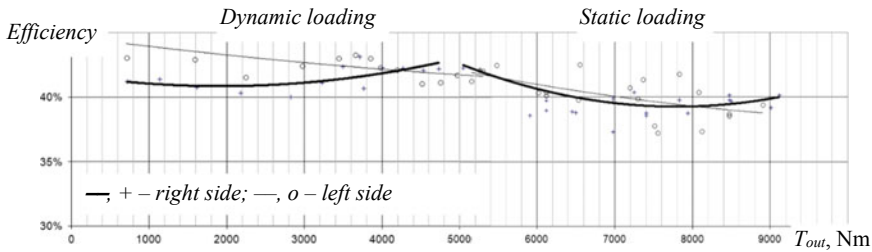


Fig. 13 Experimental values of efficiency for the gearbox with QN-gear

the gearwheel turning by 20° , with the total number of reversible loading of about 1000 cycles. No critical damage of the gear appeared. Finally, the gear was brought to failure at reversible static loading. The breakage occurred at 9000 Nm, and it was the gearbox shaft that fractured, mainly because of torsion stresses.

Of course, such a short first experience cannot be the basis for the calculated evaluation of the gear load capacity, but it has shown that the QN-gear with a steel gearwheel can become an effective alternative to the classical worm and spiroid ones. The obtained torques of 5300 Nm at short-term loading, and not <9000 Nm at static loading are not inferior (probably, surpass) to torques of the best samples of gearboxes for controlling the pipeline valves with similar dimensions [20–22].

8 Conclusion

The analysis made in the manuscript has shown the perspective application of a worm gear with a truncated gear rim made of hardened steel, which is proposed to be called “QN-gear”. The perspective concerns, at least, the case of low rotational speeds, although this gear can be considered as an alternative to the classic worm and spiroid ones in other cases, as it combines many favorable geometric and kinematic, force, strength, layout, and manufacturing properties.

The obtained dependences for calculation of the worm axial module and dependences for prevention of tooth undercutting and sharpening are, in fact, limitations at the optimization design. Besides, in comparison with the basic solution of Egorov and Iofik, the following improvements allowing to increase operational and manufacturing characteristics of the gear are offered:

- to apply the hardened steel for manufacturing of QN-gearwheels, which provides the increased tooth strength;
- to go beyond worms with ruled surfaces and, moreover, apply a curvilinear and asymmetrical profile for gear optimization;
- to use standard involute hobs or multi-cutter running heads for gearwheel cutting to localize contact and increase the gear production efficiency.

References

1. Sternberg, M., Langenbeck, K., Haas, A.: Studies of worm gears with a combination of steel-steel materials. In: *Gearing and Transmissions*, no. 1, pp. 30–39. Izhevsk (1997)
2. Korostelev, L.V.: Peculiarities of meshing at the pitch point of the worm gear. *Mashinovedeniye* **2**, 41–45 (1967)
3. Grubin, A.N., Litskhier, M. B.: Author's certificate N 88654 (USSR). Worm gearwheel. Application No. 400091, 1 July 1948
4. Egorov, I.M., Iofik, B.S.: Cylindrical worm gear: Pat. 2 132 983 RF, МПК F16H 1/16/N 98114477/28, publ. 10.07.1999
5. Egorov, I. M., Iofik, B. Sh.: Cylindrical worm gear: Pat. 2 136 987 RF, МПК F16H 1/16/ N 99103702/28, publ. 10.09.99
6. Parubets, V.I.: Repeated contact in cylindrical worm gear. *Vestnik Mashinostroeniya*. **N1**, 15–19 (1984)
7. <https://reduktor.ru/images/WEBstaty.pdf>. Accessed 1 Feb 2021
8. Trubachev, E.S., Kuznetsov, A.S., Puzanov, V.Y.: Non-orthogonal worm gearbox. In: *Proceedings of International Symposium. Theory and Practice of Gearing and Transmissions*, pp. 387–392, Russia. ISTU Publishing House, Izhevsk (2014)
9. Lagutin, S.A.: Analogs of axes of meshing in general type worm gearing. In: Goldfarb, V., Barmina, N. (eds.) *Theory and Practice of Gearing and Transmissions: In honor of Professor Faydor L. Litvin*, Springer International Publishing AG, Switzerland, vol. 34, pp. 145–158 (2015)
10. Georgiev, A.K., Goldfarb, V.I.: Aspects of geometrical theory and research results for spiroid gears with cylindrical worms. In: *Mechanics of Machines*, no. 31, pp. 70–80. Nauka, Moscow (1971)
11. Goldfarb, V.I.: Aspects of the problem of automation of gears and gearbox design. In: *Gearing and Transmissions*, no. 1, pp. 20–24. Izhevsk (1991)
12. Goldfarb, V.I., Lunin S.V., Trubachev, E.S.: Development and application of computer-aided design and tooth contact analysis of spiral-type gears with cylindrical worms. In: *Proceedings of AGMA Fall Technical Meeting*, pp. 1–11. St. Louis, USA (2002)
13. Goldfarb, V.I., Ezerskaya, S.I.: To the question of choosing the size of a helical parameter in the orthogonal spiroid gear with a cylindrical worm. *Izvestia vuzov. Mashinostroenie* **N2**, 184–186 (1975)
14. Trubachev, E.S.: Synthesis of conjugate spiroid gearing by conditions of undercutting elimination. In: *Vestnik Mashinostroeniya*, no. 9, pp. 7–11. Moscow (2004)
15. Trubachev, E.S.: Vector field of normal lines and its application to studying the geometry of spiroid gearing with a helicoidal worm. In: *University Proceedings “Problems of Design for Products of Mechanical Engineering and Information Engineering*, pp. 3–14. ISTU Publishing House, Izhevsk (1999)
16. Trubachev, E.S.: New possibilities of tooth cutting by running cutter heads. In: Goldfarb, V., Trubachev, E., Barmina, N. (eds.) *New Approaches to Gear Design and Production*, vol. 81, pp. 295–310. Springer International Publishing AG, Switzerland (2020)
17. Lagutin, S.A.: Local synthesis of general type worm gearing and its applications. In: *Proceedings of the 4th World Congress on Gearing and Power Transmissions*, vol. 1, pp. 501–506. Paris (1999)
18. Trubachev, E., Savelyeva, T., Pushkareva, T.: Practice of design and production of worm gears with localized contact. In: Goldfarb, V., Trubachev, E., Barmina, N. (eds.) *Advanced Gear Engineering*, vol. 51, pp. 327–344. Springer International Publishing AG, Switzerland (2018). ISBN: 978-3-3-319-60398-8, <https://doi.org/10.1007/978-3-319-60399-5>
19. Goldfarb, V., Trubachev, E., Pushkareva, T., Savelyeva, T.: Comparative investigation of worm and spiroid gears with cylindrical worms. In: Uhl, T. (eds.) *Advances in Mechanism and Machine Science*. IFToMM WC 2019. Mechanisms and Machine Science, vol. 73, pp. 925–935, Springer, Cham (2019). https://doi.org/10.1007/978-3-030-20131-9_92

20. Goldfarb, V.I., Glavatskikh, D.V., Trubachev, E.S., Kuznetsov, A.S., Lukin, E.V., Ivanov, D.E., Puzanov, V.Y.: Spiroid Gears for Pipeline Valves. Veche, Moscow (2011)
21. <https://www.rotork.com/en/products-and-services/gearboxes-and-valve-accessories/quarter-turn-gearboxes>. Accessed 1 Feb 2021
22. <https://www.auma.com/en/products/part-turn-gearboxes/>. Accessed 1 Feb 2021

Parametric Synthesis of Technological Systems for Gear Finishing



M. Storchak

Abstract Service properties of gears are formed at the stages of their finishing processes, such as gear grinding, shaving, gear honing, lapping, running-in, etc. Determining the optimal parameters and structure of the technological system that provide the specified gear properties is the task of synthesizing such a system. These task is multivariate and limited by the lack of general principles for their solution. The article proposes the synthesis principles of a technological system based on a systematic approach by representing the technological system as a generalized design object. The synthesis is implemented as a logical design scheme, which is interpreted by the morphological model. This model regulates the process of synthesis by information, optimization and algorithmic systems of a design object, regardless of the processing type. Developed objects of the information system: simulation models of the machining geometry, tooth profile shaping, the dynamic interaction of the technological system links and the model of the process technological characteristics, describe the relationships between real objects of the technological system. An optimization system was selected from the information system by which an algorithmic design system was developed. Using the developed method, a number of technological systems have been synthesized for the gears finishing.

Keywords Computer-aided engineering · Gear finishing · Technological system · Synthesis

1 Introduction

The main properties of technological systems (TS), which determine their technical and economic characteristics and the output parameters of the machined products, are laid down at the time of these systems synthesis (design).

The methodology of the system design requires that the process of synthesis itself is considered as a system [1, 2]. Belonging to such a system model is the logical

M. Storchak (✉)

Institute for Machine Tools, University of Stuttgart, Stuttgart, Germany

e-mail: michael.storchak@ifw.uni-stuttgart.de

scheme for the design of technological systems (LSD TS). Even the synthesis process of technological systems for the finishing of gears is considered here as a totality of logically arranged project procedures and operations, seen from the point of view of the methodology for the system design. The decomposition of the initial task with regard to the synthesis of technological systems is carried out according to particular principles. These principles are formulated by experts on a corresponding subject area of the planning task. The following principles are postulated in order to conduct the decomposition in the synthesis of technological systems for the finishing of gears [2, 3]:

- *Resulting from their viability, correlations between real physical objects of the technological system for the finishing of gears are described as models of machine engagement by means of abstract objects of the information system. An optimization system follows from these models in such a way that the function of its objects guarantees the synthesis:*

$$\forall_{\mathbb{M}} P \exists_{\mathbb{M}} P : \{(R \Leftrightarrow I_S) \subset O_S \Rightarrow (\Sigma \wedge \mathbb{X})\}, \tag{1}$$

where I_S and O_S are the corresponding information and optimization systems.

- *By choosing a rational structure of the technological system and optimizing independent parameters of machine engagement, it is possible to realize the synthesis of technological systems for the machining of gears as intersection of its sets in the range of possible optimal values, which are determined by the functioning of the optimization system and the boundary conditions:*

$$\forall_{\mathbb{M}} P \exists_{\mathbb{M}} P : \left\{ (R \wedge \mathbb{X}) \left[\left(\Sigma \xRightarrow{Q^d} \Sigma \right) \wedge opt(\mathbb{X} \cap \hat{\mathbb{Z}}) \right] \right\}, \tag{2}$$

where $\hat{\mathbb{Z}}$ is the set of the boundary conditions.

According to these demands, a decomposition of the original task is carried out with regard to the planning of technological systems for the finishing of gears. The following fundamental principles are postulated for carrying out the according level of decomposition [3]:

- *Serving as functional (sufficient) relations of the technological system are objects of an information system: models imitating the geometry of machine engagement, the formation of the tooth profiles of the gears to be cut, the dynamic interaction between members of the technological system, as well as a regression model regarding the formation of the technological characteristics in the finishing of gears:*

$$\forall_{\mathbb{M}} P \exists_{\mathbb{M}} P : \{ \min (R_{I_S}) \Leftrightarrow (D_G \wedge D_F \wedge D_D \wedge D_T) \} \tag{3}$$

where R_{I_S} are the relations of the information system; D_G, D_F, D_D, D_T are the corresponding models imitating the geometry of machine engagement, the formation of the tooth profiles of the gears to be cut and the dynamic interaction between the elements of the technological system as well as a regression models regarding the formation of the technological characteristics in the finishing of gears;

- *The local quality criteria reflecting the efficiency of the technological system are realized by means of objective functions. These objective functions are determined during the functioning of the imitation models. The local quality criteria reflecting the operating characteristics of the technological system are realized by means of regression models of the technological characteristics worked out in experimental tests:*

$$\forall_{\mathbb{M}} P \exists_{\mathbb{M}} P : \{ (\mathbb{R}_{I_S} \subset K_{ij}^E) \wedge (F_{I_S} \subset K_{ij}^D) \} \tag{4}$$

where F_{I_S} is the set of objective functions; K_{ij}^E, K_{ij}^D are the local quality criteria reflecting the efficiency and the operating characteristics of the gears to be cut.

As a result of previous developments, the information system I_S [2] was created, the objects of which: a simulation model of the machine gearing geometry [3], the tooth profile shaping [4], the dynamic interaction of TS links [5] and a full-scale model of the machining process technological characteristics [2], describe connections of TS real objects. In accordance with the developed synthesis method [3], it is necessary to select the optimization system O_S from I_S , on the basis of which the algorithmic system A_S should be developed, which provides software implementation of the design (synthesis) process. As a rule, optimization problems for complex objects, which include technological systems, are multi-criteria with contradictory objective functions [6]. In this regard, it is extremely difficult for a developer to choose a well-grounded solution (and it, of course, should be a compromise), since the well-known classical methods for finding extrema and newest search optimization methods are designed to solve single-criterion problems. The successful solution of a multicriteria problem, with contradictory and sometimes incompatible criteria, which takes place in our case, is based on the creation of an optimization system (2). In accordance with the postulated propositions (3) and (4) of the original TS synthesis problem decomposition, the main tasks of the optimization system are: determination of TS objects, the choice of the optimization method, and the choice of the convolution method of the local quality criteria vector. The creation of the O_S ensures the development of a general algorithm for the synthesis of TS, and the development of principles for choosing its structure will provide the synthesis of the desired TS.

2 Optimization System of Design Process

In accordance with the postulated proposition (1), the optimization system O_S should be separated from the information system I_S . The selection process provides for the identification of the optimization system objects. With regard to the consideration technological systems, O_S objects are: the vector of system quality criteria W_v , the vector of objective functions F_v , the vector of design parameters X_v and the vector of boundary conditions Z_v [2, 7]:

$$\forall_{\mathbb{M}} P \exists_{\mathbb{M}} P : \{O_S \subset Z_{O_S} \Rightarrow (W_v \wedge F_v \wedge X_v \wedge Z_v)\}, \quad (5)$$

where $v = 1, 2, 3, \dots, k, \dots$

Multiparameter optimization is performed in the presence of a local quality criteria $W_v(x)$ set, forming a vector of quality criteria W_v , and the set of local design parameters x is a vector of design parameters X_v . This vector changes in n -dimensional parameter space, which consists of points x with Cartesian coordinates $x(\alpha_1, \alpha_1, \dots, \alpha_n)$. Thus, each set $\alpha_1, \alpha_1, \dots, \alpha_n$ corresponds to a point x in the parameter space. The quality criteria vector is formulated by the developer on the basis of existing experience, well-known researches and expert opinions in the consideration area. This is how the following postulate can be formulated:

- *The quality criteria vector consists of local quality criteria reflecting the efficiency of synthesized technological system functioning and the service properties of the machined gears:*

$$\forall_{\mathbb{M}} P \exists_{\mathbb{M}} P : \{W_v \subset (K_v^{eff} \wedge K_v^{sp})\} \quad (6)$$

It should be noted here that the more local criteria the developer introduces, the more complete understanding of the synthesized system and the results of its functioning he can get [1, 7]. However, with an increase in the number of various local quality criteria, the efforts for synthesizing such a TS increase significantly. The multicriteria formulation of the problem is more close to the real system and less abstraction [1]. The choice of the quantity and internal content of quality criteria in the synthesis of technological systems is the most difficult and least orderly stage, which practically does not lend itself to automation in modern conditions. Therefore, the result of the synthesis is determined by the art and preparedness of the developer to solve such problems. The quality criterion can be determined by any characteristic of the system. When choosing it, there is only one limitation—the criterion must have a monotonic connection with the system characteristics. Based on the previously performed analysis [2, 8–11], operational and technological local quality criteria for the technological systems synthesis in the gears finishing are postulated. The following local quality criteria are proposed as operational ones: potential energy

of shape change W_1 , contact strength of machined gears W_2 , bending strength of machined gears W_3 . Technological local quality criteria are the following: productivity of finishing W_4 , tool life W_5 , error of the machined gear rim W_6 , generalized parameter of the surface layer quality of the machined gears teeth W_7 .

Technological local quality criteria W_4 , W_5 and W_7 are determined by the characteristics of previously developed models of the machine gearing geometry [3], the profile teeth shaping [4] and the dynamic interaction of TS links [5], as well as the regularities obtained as a result of experimental studies of the gearing error conversion W_6 and the surface layer quality W_7 in the finishing process [2]. These criteria are determined as a result of the developed models functioning and regression experimental dependencies. Optimization according to technological local criteria is a prerequisite for the synthesis of highly efficient technological systems that ensure their implementation in modern conditions. A sufficient condition for the TS synthesis is optimization according to the criteria of service (operational) properties. The most common operational criterion for the quality of a TS is the criterion reflecting the energy effect of the system on the surface layer bearing capacity of the machined gears teeth. The damage of the teeth surface layers is mainly of a fatigue (cyclic) nature, therefore, to determine the influence of the technological system parameters on the fatigue strength, it is necessary to use the corresponding fatigue strength criteria. However, despite a significant number of these criteria, there is still no generally accepted and reliable criterion. This is explained by the fact that verification of any strength criterion (especially fatigue) requires numerous experimental data, which are very laborious and time-consuming. In addition, the cyclic strength is significantly influenced by the loading pattern, the type of test material, the rigidity of the loading machine, etc. In this regard, the researchers get different results, which causes a mismatch of criteria. Therefore, most theories of fatigue strength are based on the corresponding provisions of the static strength theory. The commonality of the processes of static and fatigue (cyclic) destruction is confirmed by the presence of a correlation relationship between the characteristics of their strength. The assessment of fatigue strength from the limiting values of normal or tangential contact stresses can be considered only a first approximation, since it is valid only for a one-dimensional stress state. Whereas in the vicinity of the contact surface, the stress state of the tooth is essentially three-dimensional. Therefore, it is preferable to assess the strength of the gears teeth surface layer according to some of the most reliable theory of strength corresponding to the reduced equivalent stresses, taking into account the three-dimensional nature of the teeth stress-strain state. For this, the most applicable criterion for the specific potential energy of shaping [12]. This is explained by the fact that this theory, on the one hand, is free from restrictions associated with the scope of Hooke's law (i.e., it remains valid for inelastic bodies), and on the other hand, it makes it possible to establish the conditions for the onset of not only plastic deformations, but also damage. According to this criterion, a dangerous state occurs when the value of the specific potential energy of shaping U_S reaches a critical value [12]:

$$U_S = \sqrt{0.5 \cdot [(\sigma_1 - \sigma_2)^2 + (\sigma_1 - \sigma_3)^2 + (\sigma_2 - \sigma_3)^2]} \leq [U_S]_{cr} \quad (7)$$

where $\sigma_1, \sigma_2, \sigma_3$ are principal stresses.

To increase the limit of the cyclic strength of the teeth surface layer, it is necessary to reduce the acting equivalent stresses. In all likelihood, this can be achieved by changing the friction parameters of the contact surfaces of the mating gears teeth and the magnitude of residual stresses in the near-surface layers of the tooth profile. The solution of the contact problem of mating tooth profiles tangency [2] provides the determination of such initial stresses at which the resulting stress state of the tooth profile surface layer has the lowest potential energy of shaping. In this case, the bearing capacity of the gear teeth has the greatest strength. The Fig. 1 presents the numerical analysis of the shaping in the potential energy of the gear teeth surface layer as a local quality criterion TS. This figure shows the dependence of the dimensionless equivalent stress in the center of the tooth profiles contact area along their depth for various values of the dimensionless residual stresses and the friction coefficient. As can be seen from the above graphical dependencies, by introducing residual stresses (σ_{RS}) along the depth of the tooth surface layer, it is possible to significantly reduce the most dangerous depth stresses. In the absence of residual stresses in the surface layers of the teeth, these stresses reach their highest value at a relative depth of $y = 0.7 \cdot a$ (a—width of contact area). The friction coefficient (k_{FC}) also has a significant effect on the stress distribution, especially at shallow depths from the tooth profile surface.

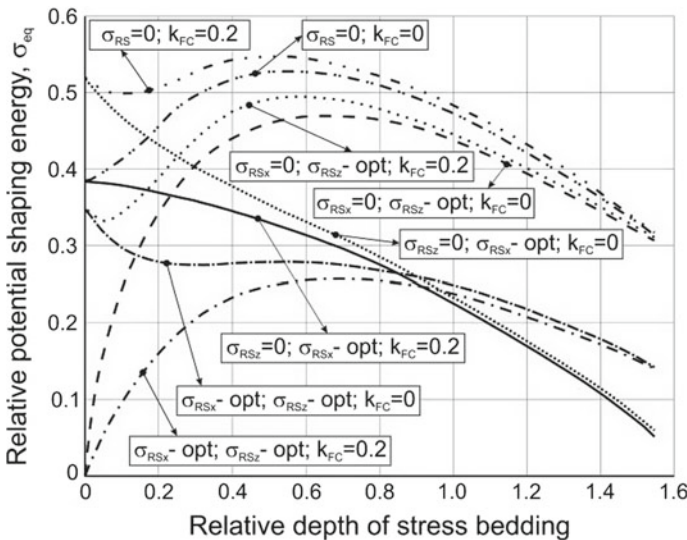


Fig. 1 Dependence of the shaping potential energy over the depth of the gears surface layer on the value of residual stresses and the friction coefficient between mating teeth

The most common failure cause of high-speed and high-stress gears is contact damage of the gear teeth working surfaces, sometimes called pitting [13]. This type of fracture is common in enclosed gears, which generate high contact stresses in the contact zone. The maximum permissible contact stress τ_{\max} is taken in most cases as a criterion for the endurance of the teeth surface layer of such gears [9, 11]. The magnitude of this stress depends on the position of the contact point on the engagement line. For gears with external engagement, this value is determined by the relationship [9, 13]:

$$\tau_{\max} = 0.142 \cdot \sqrt{\frac{F \cdot E \cdot A \cdot \sin \alpha}{\rho_1 \cdot \rho_2}} \leq [\tau_{\max}], \quad (8)$$

where F normal force acting in engagement, E Young's modulus, α pressure angle, ρ_1, ρ_2 profile curvature radii at the contact point respectively, $[\tau_{\max}]$ highest permissible contact stress.

Thus, the quantity τ_{\max} is proportional to the value of $\sqrt{\rho_1 \cdot \rho_2}$. If the influence of the engagement of adjacent teeth pairs of the mating gears on the contact conditions is not taken into account, then the value of τ_{\max} takes the greatest values at the beginning and end of the engagement phase. However, when external gearing of gears, the contact ratio is usually greater than 1. Consequently, the greatest shear stresses occur at the beginning and end of a one-pair engagement. This is consistent with experimental data [13]. With a criterion constraint, dependence (8) can be used as a local quality criterion for the operational properties of the machined gears.

One of the main reasons for the performance loss in heavy-loaded low-speed and medium-speed gears is tooth breakage as a result of insufficient bending strength of the teeth. This often happens in gearboxes and final drives of various machines and mechanisms [3, 11]. Obviously, the highest bending stresses σ_{\max} , in the gear tooth during its loading, can be used as a local performance criterion of quality TS. In this case, the criterion boundary condition is the condition $\sigma_{\max} \leq [\sigma_{\max}]$. As a result of numerical modeling of the stress state of gear teeth [2, 11], it was established:

- the greatest bending stresses occur in the area of the fillet curve of the active and adjacent teeth profile;
- the main influence on the stresses distribution in the tooth body is exerted by the shape and curvature radius of its fillet curve, as well as the profile shape and the ratio of its geometric dimensions;
- bending stresses can be controlled by changing the gears geometry, in particular the shape, radius of curvature and the geometric dimensions of the fillet curve.

The latter result makes it possible to use the developed model to determine the objective function of the corresponding local or generalized quality criterion for the operational properties of the machined gears. Naturally, the use of such quality criteria does not provide for a change in the geometric parameters of the active part of the gear tooth profile. This profile is the initial value for TS synthesis. Changes in the

shape, curvature and geometric dimensions of the fillet curve and modification curves are not the initial values for the TS synthesis and can be used as design parameters.

The proposed local criteria for the operational (service) properties of the machined gears are most expedient to use in the TS synthesis as criterion boundary conditions, since the gears operational properties are essentially determined by the technical requirements for the machined gears. The allocation of the objective functions vector is the central point in determining the optimization system. This vector is extracted from the information system during the functioning of its models (see Eq. 3). The methodology for identifying the vector of design parameters is given in [3]. One of the essential points in the definition of the optimization system is the identification of the boundary conditions vector [2, 3]. This makes it possible to select their real values from the area of design parameters optimal values and, thereby, to relate abstract optimal values with real TS. The boundary conditions vector that defines the set of constraints \hat{Z} is subdivided into a set of parametric Z_α , functional Z_f and criterion constraints Z_w :

$$\forall_{\mathbb{M}} P \exists_{\mathbb{M}} P : \{Z_v \Rightarrow \hat{Z} \subset (Z_\alpha \wedge Z_f \wedge Z_w)\}, \quad (9)$$

Parametric boundary conditions are specified in the form of inequalities:

$$\{\alpha_j^*\} \leq \{\alpha_j\} \leq \{\alpha_j^{**}\} \quad (10)$$

for $j = 1, 2, \dots, n$. Boundary conditions (10) are divided into constraints on the technological capabilities of tool manufacturing, on the technical implementation of the machining process, on the quality parameters of machining, etc. A set of parametric boundary conditions defines an n -dimensional parallelepiped P in the common parameter space. Thus, each point of the parallelepiped P corresponds to a certain state of the information system, the parameters of which satisfy the system of constraints and vice versa. Functional constraints are set by an inequalities system of the form:

$$\{c_i^*\} \leq \{f_i(X)\} \leq \{c_i^{**}\} \quad (11)$$

for $i = 1, 2, \dots, m$. This type of constraints is divided according to the number and content of information system models, according to their technical implementation, according to the conditions for the models functioning, etc. The system of functional constraints selects in the parallelepiped P a certain region G , consisting of vector X points of a parameters set and simultaneously satisfying the system of functional constraints (11). The most difficult stage of vector \hat{Z} identification is the determination of the vector of criteria constraints. This vector is defined as:

$$W_v(X) \leq W_v^{**} \quad (12)$$

for $v = 1, 2, \dots, k$; W_v —the worst acceptable value of the quality criterion.

Often, at the initial stage, the developer cannot determine the criteria constraints when synthesizing complex systems. This becomes possible after several iterative steps of solving the parametric optimization problem.

The introduction of several local quality criteria at the same time significantly complicates the optimization process. In these cases, it is necessary to apply the convolution of the local quality criteria vector by artificially transforming them into a single scalar compromise criterion. Determination and formulation of quality criteria for the developed models is the most difficult and crucial stage of TS synthesis. These criteria are usually compromise. When creating compromise criteria, there are no and, perhaps, cannot exist, pre-developed recommendations. That is why, the local quality criteria convolution and the determination of the individual criteria weight coefficients can be carried out only by a developer who is sufficiently aware of the synthesized TS content. The examples discussed below require the combination of several conflicting criteria. For example, increasing machining productivity while increasing the gears precision. There are various methods of quality criteria convolution into a single compromise scalar criterion [2, 14, 15]: additive, multiplicative, minimax, etc. By analyzing various convolution methods, two main synthesis methods of the considered TSs are determined: multiplicative and additive. The multiplicative method is used with conflicting technological local quality criteria, and the additive method is used with a significant number of local quality criteria reflecting both the technological and operational properties of the machined gears.

Determination of local quality criteria vectors W_v , objective functions F_v , design parameters X_v and constraints vector Z_v in accordance with propositional Eqs. (3)–(6) and (9) as objects allows the developer to assert about the creation of an optimization system O_S . Thus, the problem of multicriteria optimization is postulated [14, 15], which has the form:

$$\forall_{X \in \mathbb{G} \subset P \subset \mathbb{R}^n} X(\alpha_i) \quad \exists_{X \in \mathbb{G} \subset P \subset \mathbb{R}^n} X = (\alpha_1, \alpha_2, \dots, \alpha_n) \mapsto W_v(X) = \underset{\alpha \in \mathbb{G}}{extr} W_v(X), \tag{13}$$

where $P = \langle X \mid \alpha_j^* \leq \alpha_j \leq \alpha_j^{**}, j = \overline{1, n} \rangle$ —initial n -dimensional parallelepiped of design parameters; $\mathbb{G} = \langle X \mid f_i \leq 0, i = \overline{1, m} \rangle$ —existence area of system.

For the functioning of the optimization system, it is necessary to determine the optimization method. It is determined by the type of target and compromise functions, the number of design parameters, the technical capabilities of the developer, etc. Based on the well-known developments in this area, expert assessments and our own experience, it has been established that to solve the problem (13) in relation to determining the optimal values range of the technological systems parameters for finishing gear, it is most expedient to use the LP-search method [2, 14, 16]. The LP-search method is based on probing a multidimensional parallelepiped of the P -space of independent parameters by an LP_τ -sequence, any binary section of

which is a P_τ -mesh [16]. The test points selection in a multidimensional space is made using uniformly distributed LP_τ -sequences, which are distinguished by the best properties of uniformity and allow, with a minimum number of tests, to obtain a fairly complete picture of the models resource capabilities for each quality criterion. In this case, the test points have the property that their projections onto any coordinate axis in the parameter space are different and are located quasi-uniformly. The LP-search method provides a uniform overview of the entire parameter space with a relatively small number of tests. This provides an effective application of this method in the multicriteria systems synthesis, which include technological systems for gear finishing. The completed identification of the optimization system, including the choice of the optimization method and the method of local quality criteria convolution of the system, provide the transition to the development of the algorithmic system for TS design process.

3 Algorithmic System of the Design Process

The objects of the algorithmic system are the structural optimization algorithm A_Σ , the software-implemented parametric optimization (parametric synthesis) algorithm A_X , and the auxiliary software-implemented parametric optimization algorithms A_H :

$$\forall_{\mathbb{M}} P \exists_{\mathbb{M}} P : \{A_S \subset Z_{A_S} \Rightarrow (A_\Sigma \wedge A_X \wedge A_H)\}, \quad (14)$$

The result of structural synthesis from the view point of cutting processes is a technological process scheme, a scheme of an object and production means movement (in this case, a workpiece and a tool) with the necessary discontinuities in motion, a scheme of interaction between the main objects of the production process, and, finally, a scheme of a specific TS. The latter is hierarchically a subsystem to the mentioned objects. In terms of its internal content, this scheme is in a certain way independent, if the designed object is considered as a system. In this case, the result of the structural synthesis is the TS scheme for finishing the gears. It includes a kinematic scheme of the machining process, which determines the tool relative position in space and the gear being machined, the vectors of their movement including additional and setting ones, a set of tools, the type of connection between the movements of the tools and the gear, the processing method in the case of multi-tool settings using. Structural synthesis of technological systems for the gears finishing, like any other structural synthesis, operates with abstract mental concepts. Objects of structural synthesis are abstract, do not have a numerical equivalent, and therefore, structural synthesis, as a rule, cannot be automated. There are the following methods of structural synthesis [1, 2, 16]:

- exhaustive search of known solutions (combinatorial exhaustive search methods);
- combinatorial methods of partial enumeration (random sampling, heuristic methods in the dialogue mode);

- search for variants of structures in countable sets of unknown or unlimited cardinality;
- problematic methods of synthesis problems.

In principle, the structures number of technological systems for gears finishing is limited. Taking into account this circumstance and the absence of a numerical equivalent of the sought TS structure, for the structural synthesis enumeration methods were selected, in particular, the method of expert estimates and rank correlations of expert advice was used. In this case, well-known structures available in the data bank were used. Based on the available experience and on the analysis of the technological systems structures for gears finishing, the following structures are entered into the data bank:

- one-tool finishing, the kinematic scheme of which implements the engagement of the tool and the gear being machined as the engagement of a helical and/or hyperboloid gear pair;
- parallel and/or sequential two-tool machining with free rolling of the tool and gear, as well as rigid kinematic connection between them and between tools;
- combined grinding and surface plastic deformation.

These technological systems are the most optimal in their structure. The final conclusion about the optimality of this or that structure can be made only after parametric synthesis of these structures. A scheme of the structural choice organization of technological systems is shown in Fig. 2. When performing parametric synthesis,

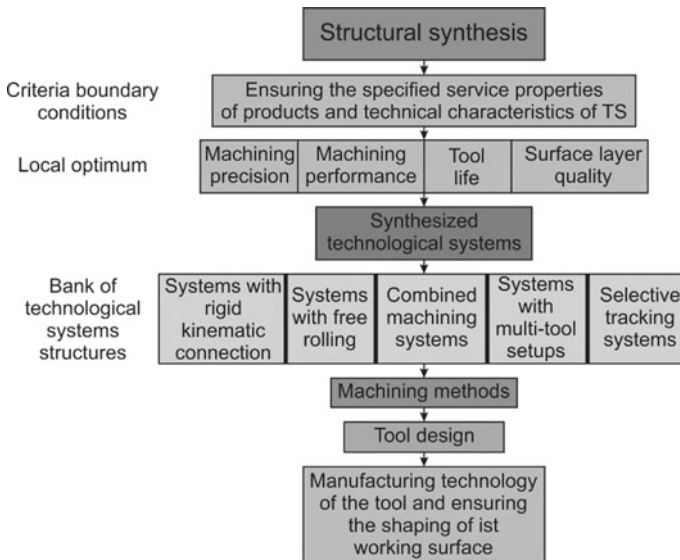


Fig. 2 Organization schema of the structural selection of technological systems for gears finishing

it is assumed that the structural optimization algorithm A_{Σ} has been developed and the structural synthesis has already been performed.

As a result, the processing scheme and all other necessary objects of the TS structure Σ are determined. The basis of the parametric optimization algorithm is the software implementation of the LP-search method as applied to the design of the required technological systems, aimed at solving the problem (13). As a rule, the solution to this problem involves several iterative processes for probing the entire region of the system's \mathbb{G} existence. This is due to the fact that with a fairly close coincidence of the model and the real system, i.e. with a significant number of quality criteria, the structure of the set \mathbb{G} turns out to be very complex and has discontinuities. In this case, the preliminary assignment of criterion constraints is very valuable, which makes it possible to determine the set \mathbf{D} of admissible points of the design parameters vector \mathbf{X} that satisfy boundary conditions (10)–(12). This achieves a set constraint and the best solution to problem (13) can be sought in the set \mathbf{D} , which is much more profitable.

By definition [16], the point of the design parameters vector is called optimal to Pareto if there is no other similar point, at which at least one of the quality criteria $W_v(\mathbf{X})$ took the best value while the values of all other criteria did not deteriorate. A set $\mathbb{P} \subset \mathbb{G}$ is called Pareto set if it consists optimal to Pareto points. The definition of the set \mathbb{P} is performed using the mathematical apparatus of the LP_{τ} -sequence, which has the best characteristics of uniformity among all known sequences. This allows 2^{20} points of the sequence to be calculated using only 20 guide points, and therefore significantly reduces the amount of computation. Any other choice of test points in multidimensional areas leads to unsatisfactory results due to the fundamental lack of multidimensional geometric intuition in human thinking. At the first stage of the LP-search, a test table is drawn up. Testing is understood as the calculation of the objective functions of the information system models at a certain value of the parameters that satisfy the selected LP_{τ} -sequence. For this, n initial points $\alpha_1, \alpha_2, \dots, \alpha_n$ are sequentially selected, uniformly distributed in the initial parallelepiped with coordinates $X_i = (\alpha_{i1}, \alpha_{i2}, \dots, \alpha_{in})$. When constructing them, the first n points of the LP_{τ} -sequence $Q_0, Q_1, \dots, Q_n, \dots$ are used, uniformly distributed in the n -dimensional unit cube K^n . Moreover, $n = 2^m$ is an integer power of 2. The Cartesian coordinates of the next point of the sequence $Q_i = (q_1, q_2, \dots, q_{in})$ are used to calculate the Cartesian coordinates of the points X_i belonging to the parallelepiped \mathbf{P} . When constructing points Q_i of an LP_{τ} -sequence, the following condition must be met: the sequence of points Q_i must be uniformly distributed to the cube K^n , and any binary section of this sequence containing at least $2^{\tau+1}$ points must be a P_{τ} -mesh. For this, equality must be satisfied:

$$\lim_{n \rightarrow \infty} \frac{S_n(P)}{n} = V_n, \quad (15)$$

where V_n volume of n -dimensional parallelepiped \mathbf{P} , points quantity Q_i with numbers $1 \leq i \leq n$ belonging to \mathbf{P} .

In the parametric synthesis of the sought TS, an ultrafast algorithm for constructing LP_{τ} -sequences [14] is used, which provides a significant acceleration of the optimization process. For this, the order of Q_i points is chosen such that each subsequent point is easily calculated from the previous one and so that the binary sections of the new sequence coincide with the binary sections of the initial sequence. The last condition guarantees the preservation of all basic and additional properties of uniformity. In addition, such an algorithm ensures that calculations are performed using only logical operations [14, 15]. For large n , this algorithm is much faster than standard algorithms using a random number generator. Using the developed program, it is possible to quickly and efficiently construct points of LP-sequences for probing the multidimensional hyper parallelepiped of the technological system parameters. The LP-search algorithm consists of three main stages [2, 16]:

- compilation of test tables with parameter values corresponding to the LP_{τ} -sequence conditions, according to which the current values of the system quality criteria are calculated;
- selection of criterion boundary conditions;
- checking the problem solvability and optimization itself.

At the first stage, the parameters space of the synthesized system is probed and at each point the system model, criteria for its quality are determined, and a test table is compiled, characterizing the capabilities of each criterion. The second stage is central to solving the entire synthesis problem. It requires the participation of a specialist who enters the quality criteria and criterion constraints in the interactive mode. A specialist can also change the system quality criteria and their limitations if the local optimum does not meet the technical requirements. At this stage, the test table is studied and the limits of change in the numerical values of the quality criteria are determined. At the third stage, an admissible set \mathbf{D} of possible solutions the problem (13) is determined when criterion constraints (12) are satisfied. When using trade-off criteria for the quality of the system, criterion constraints should also be compromise with a similar convolution. Quite often the set \mathbf{D} is empty. In this case, the algorithm returns to the second stage for additional probing, or, if this does not help, then for the introduction of other types of convolution or other initial approximation of quality criteria. When using unmatched quality criteria, the return of the algorithm requires a change in the criteria constraints, or the algorithm returns to the first stage and increases the number of sounding points n . The latter is highly undesirable, since it significantly increases the computation time, and when using compromise criteria, the problem may not be solved. Based on the above, an algorithm A_X has been developed for the software implementation of determining the optimal to Pareto parameters set \mathbf{X} . The block diagram of the algorithm is shown in Fig. 3.

The developed algorithmic system was tested in the synthesis of technological systems for gear honing of hardened gears. Based on the specific gears undergoing the finishing process, the TS structure was initially selected by the enumeration method—single-tool processing with diamond gear hons with an elastic connection of the gear rim with the tool hub. It is accepted that the quality criteria vector

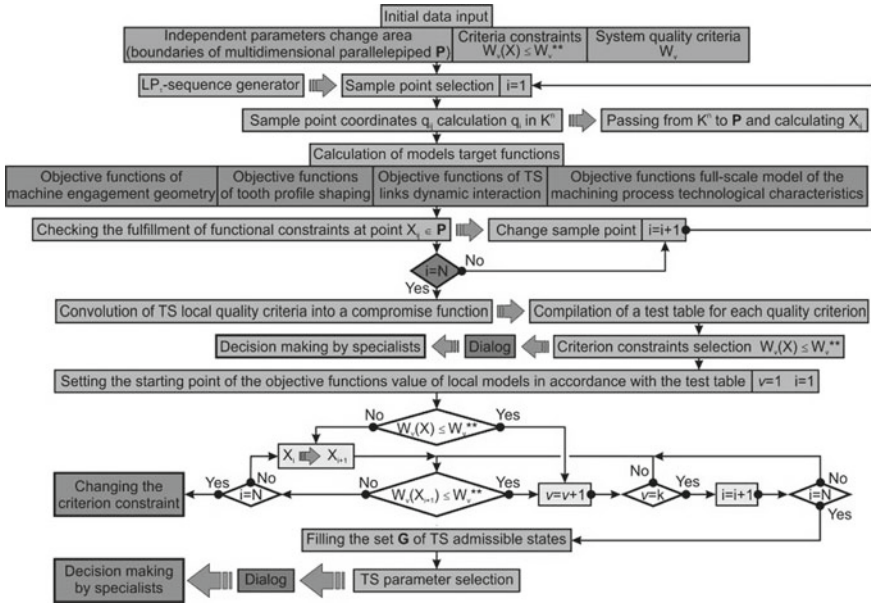


Fig. 3 Scheme of an algorithm for parametric optimization (synthesis) of technological systems for gears finishing

consists of two local criteria: the maximum processing productivity and the greatest tool life. The convolution of the selected criteria into one scalar function is carried out by the additive method with the weights introduced by the developer. The objective functions vector reflecting the introduced local quality criteria consists of the dependence of the working layer tool volume [3], the total length of the contact lines in the machine gearing of the tool-machined gear [4] and the vibration activity of the machining process [5]. The design parameters vector consists of the gear hone geometric and design parameters, machining modes, the parameters of the connection stiffness between the tool gear rim and the tool hub, etc. When determining the constraints vector, a boundary conditions criterion was introduced for the generalized quality parameter of the gears teeth surface layer.

Parametric constraints consist of constraints on the technological capabilities of tool manufacturing, constraints determined by the adopted equipment, and constraints due to the specifics of the finishing process. The specific values of these quantities are determined by the developer. In this case, functional boundary conditions define the lower bound of the used target functions. After determining all objects of the algorithmic system, the optimal values of the design parameters vector are calculated. The design parameters values determined by the developed software algorithm A_X are shown in Table 1.

where z_0 —teeth number of gear hone, $\beta_0, [^\circ]$ —inclination angle of the gear hone teeth line, $b_0, [mm]$ —tool rim width, $d_{a0}, [mm]$ —tool tooth tip diameter, $d_{10}, [mm]$ —initial diameter of gear hone, $m_0, [kg]$ —tool mass, $I_0, [kg \cdot m^2]$ —inertia moment of

Table 1 Optimum design parameters for the gear honing process

No.	z_0	β_0	b_0	d_{a0}	d_{10}	m_0	I_0	c_{ec}	h_{ec}	c_e	h_e	n_0
1	41	25	40	245	221	1.5	$8 \cdot 10^{-3}$	$2.4 \cdot 10^{-3}$	10	$0.43 \cdot 10^4$	8	400–500
2	43	15		235	210	2.0	$2 \cdot 10^{-3}$	$4.7 \cdot 10^{-3}$	16	$0.27 \cdot 10^4$	10	500–600

gear hone, c_{ec} , [N/m]—elastic connection stiffness between the tool gear rim and the tool hub, h_{ec} , [kg/sec]—damping coefficient of elastic connection between the tool gear rim and the tool hub, c_e , [N/m]—engagement stiffness, h_e , [kg/sec]—damping coefficient of engagement, n_0 , [sec⁻¹]—tool spindle speed;

$\beta_1 = 0^\circ$ —inclination angle of the machined gear teeth line, $b_1 = 30$ [mm]—width of machined gear rim, $d_{a1} = 127.2$ [mm]—tooth tip diameter of machined gear, $d_{a2} = 182.43$ [mm]—tooth tip diameter of the mating gear, $x_1 = 0$ —basic rack displacement coefficient of machined gear, $x_2 = 0.53$ —basic rack displacement coefficient of the mating gear.

Successful laboratory and industrial tests of the synthesized technological gear honing system [2] make it possible to recommend the developed synthesis method for other types of technological systems.

4 Synthesized Technological Systems

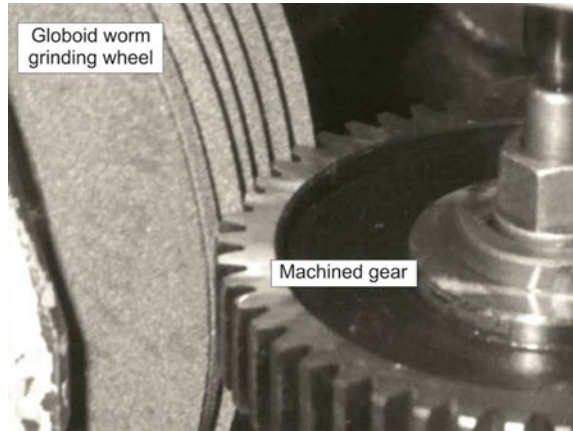
The developed software-implemented algorithm was used in the synthesis of various technological systems for gears finishing with a rigid kinematic connection between the tool and the gear being machined, with free rolling and combined processing. Below are some examples of synthesized technological systems.

4.1 Systems with a Rigid Kinematic Connection

The overwhelming majority of gear grinding systems are synthesized technological systems with a rigid kinematic connection. A significant increase in processing productivity while ensuring the required accuracy of the product is achieved by using worm gear grinding. A general view of the technological system of this processing process is shown in Fig. 4.

A significant increase in accuracy and a decrease in the complexity of machining gears is achieved when using a continuous process of gear grinding with a worm wheel, followed by finishing processing by the free rolling method, for example, gear shaving or gear honing. For this, the value of the removed allowance must be not less than the absolute value of the kinematic error of the gear being machined and not more than the sum of the reduced kinematic error and the radial runout of its gear rim. As a result of such gear grinding, the highest possible positioning accuracy

Fig. 4 Technological system of worm globoid grinding



of the same tooth profiles is achieved. After gear grinding, a free rolling finishing operation is performed. The teeth same profiles, the positioning accuracy of which was ensured in the previous operation, are used as an additional technological base. This is realized by force closure along the same tooth profiles.

The synthesized TS of gear grinding by continuous rolling provides the highest possible accuracy of the tooth profiles relative position of the gears being machined, however, the components of cyclic errors, for example, the errors of the tooth profile, remain significant. The smallest possible error in the teeth profile is provided by the methods of unit division, in which the production circle is the base circumference of the gear being machined. When grinding with this method, the conditions of tool contact with the machined gear for forward and reverse travel are different. This is due to the fact that with a forward stroke, cutting is carried out by the circle butt, and with the opposite, by its periphery. Due to the significantly different stiffness TS in these directions, there are both different cutting forces [17, 18] and significantly different thermal loads [19, 20] are arised. This results in significant and uneven tool wear. When synthesizing this TS, the quality criteria are a compromise criterion for tool wear under various cutting conditions at the entry and exit of the tool into the gear cavity. The cutting edge of the tool is formed by the intersection of two conical surfaces A and B, the axis of which coincides with the tool rotation axis—Fig. 5. The tip of the cutting edge is located on a straight line tangent to the base circle of the gear being machined. Depending on the specified machining conditions, various types of curves can be used as generators of the conical surfaces. During the relative movement of the tool from the tooth root to the tooth tip of the gear being machined, the cutting process is carried out by the edge A, and from the tooth tip to the tooth root—by the edge B.

The use of such a TS ensures the same cutting conditions during the entire engagement phase. However, the presence of tapered working surfaces located at an angle to the end of the tool leads to its displacement relative to the machined gear in the direction of the tool rotation axis. This creates an additional error in the tooth profile.

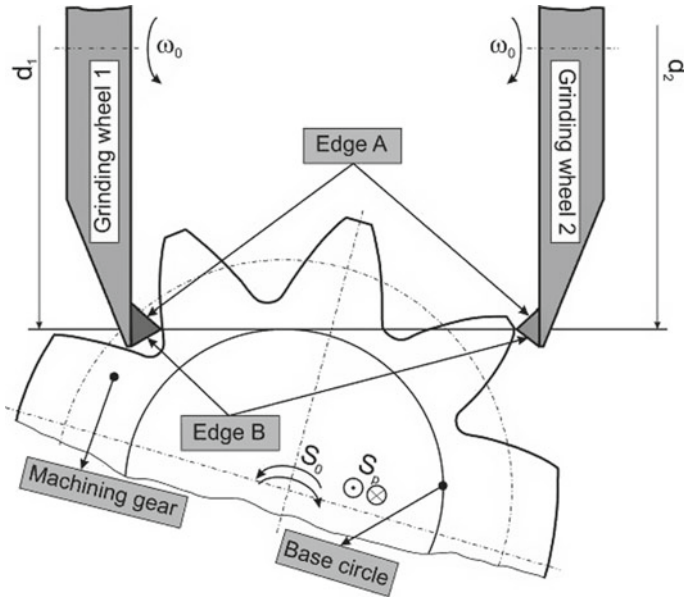


Fig. 5 Scheme of gear grinding by the zero method ensuring the same cutting conditions when the tools enter and exit the machined tooth slot

This error can be eliminated if the resultant cutting force was constant and directed perpendicular to the axis of tool rotation. To do this, it is necessary to change the direction of the cutting force vector during the period when the tool leaves the tooth cavity. To synthesize such a TS, a compromise condition for the constancy of the cutting force and the vector of its direction is used as a local quality criterion. For this, the cutting elements of the tool are limited by two concentric circles B and C with diameters d_1 and d_2 , the axes of which coincide with the axis of tool rotation—Fig. 6.

The half of the difference between these diameters should be between 0.5 and 3.5 of the selected depth of cut. The tool is set so that the line tangent to the base circle of the gear to be machined is located between the edges B and C—Fig. 6a.

During the movement of the tool from the tooth root to the tooth tip of the gear, cutting is carried out with the edge C, and during its movement from the tooth tip to the tooth root—with the edge B. In both cases, the cutting is performed with the periphery of the grinding wheel that provides the greatest tool rigidity. The linear size of the work items, which should be located between the mentioned edges, is relatively small. To implement such a tool, polycrystalline superhard materials are used, in particular, dense modifications of boron nitride—Fig. 6b.

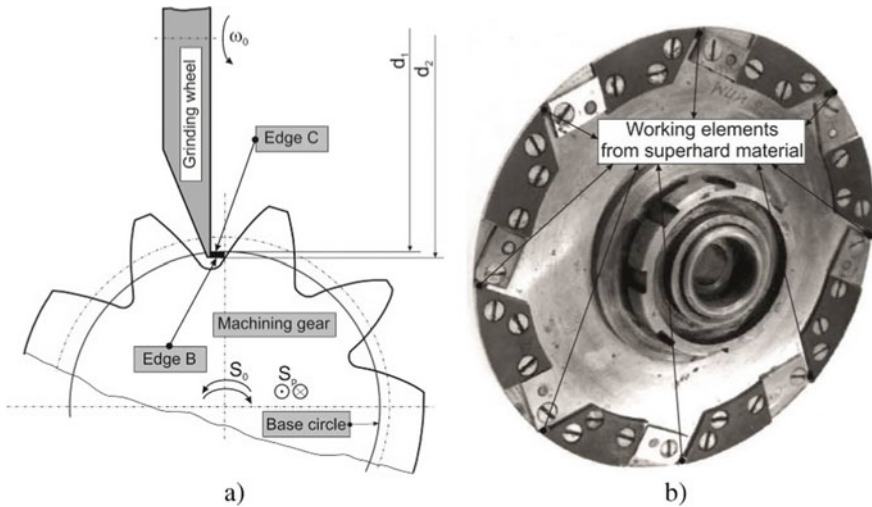


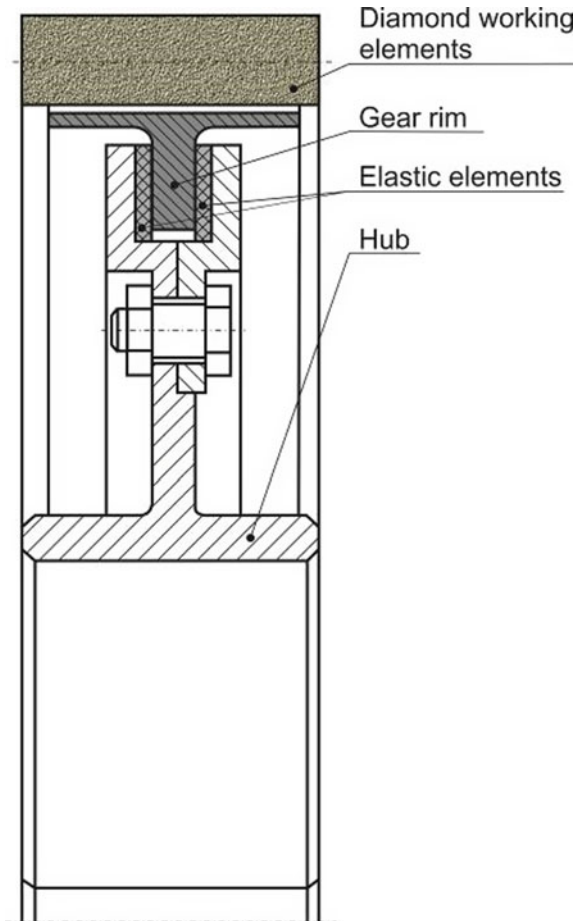
Fig. 6 Scheme of gear grinding (a) and tool (b) by the zero method with a constant direction of the resultant cutting force vector

4.2 Systems with Free Rolling

The synthesis of technological systems with free rolling was carried out on specific examples of the gear honing process. The results obtained are not limited only to this process and can be extended to other types of free rolling machining, such as gear shaving, final dimensional calibration, lapping, etc. As a result of the TS synthesis, the optimal geometric parameters of the working elements and the design dimensions of the diamond gear hones, as well as the requirements for the design features of the tool, were determined. On the basis of these recommendations, diamond gear hones with an elastic connection of the gear rim with the tool hub and glued working elements on a metal bond have been developed—Fig. 7.

These tools provide significant material removal for gear honing from 0.04 to 0.06 mm per tooth side of the machined gear. The use of a combined tool structure and glued diamond elements cause significant tool errors. Therefore, such gear hones are used mainly for machining gear with low accuracy degrees. For the gears machining of high accuracy degrees, diamond elastic gear hones on deeply vulcanized rubber bonds have been synthesized—Fig. 8. The gear rim of the tool is made of a rubber bond of substantially lower hardness than a bond of working elements. This ensures an elastic connection between the gear rim and the tool hub. Working diamond elements consist of two plates connected by a bridge and forming opposite profiles of gear hone teeth—Fig. 8b. This greatly simplifies the manufacturing technology of the tool and provides the possibility of applying a significant positive correction of the teeth profile. The latter contributes to an increase in the teeth strength, the efficiency of using superhard materials and a decrease in tool wear. Manufacturing the body

Fig. 7 Design of a diamond gear hone with an elastic connection of the gear rim with the hub and glued working elements on a metal bond



of the gear hone rim from a more elastic material provides a significant increase in the contact ratio in the engagement of the tool with the gear being machined. The applied rubber bond is easily dressed by means of gear grinding along the tooth profile. This makes it possible to use elastic diamond gear hones for machining gears of high accuracy degrees, including machining after gear grinding.

When machining gear of significant dimensions with a deep defect layer, large nicks and burrs, the efficiency of elastic diamond gear hones using is significantly reduced. This is due to the insufficient size of the removed allowance, ineffective removal of nicks and burrs, and insufficient reliability of the tool as a whole. The high cutting ability and strength of the diamond gear hones teeth on metal bonds ensures their effective use when processing gears with the specified properties. However, the desire to remove a significant amount of allowance along with a constant cutting ability compared to elastic tools leads to a significant increase in the cyclic errors

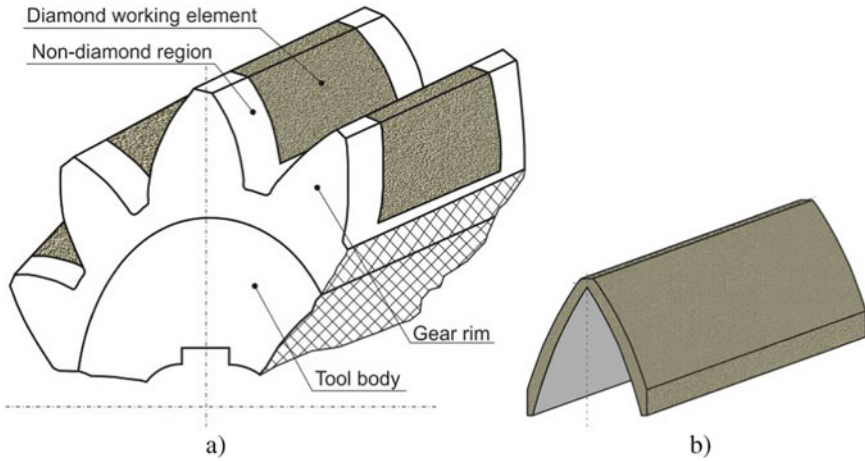


Fig. 8 Design of a diamond elastic toothed hon (a) and a working diamond element (b)

components of the machined gears teeth. Gears of high accuracy degrees are especially susceptible to this. To increase the efficiency of the use of diamond elastic gear hons, tool designs have been synthesized that combine the advantages of both diamond toothed hons with a metal bond and elastic toothed hons and are free from the above disadvantages. Such tools are called diamond combined gear hons—Fig. 9. The basic design of these tools is the design of elastic diamond toothed hons. The gear rim of diamond combined gear teeth consists of working elements with different abrasive ability and alternating both in the circumferential direction and along the width of the gear rim. Technologically, this is ensured by pressing one or more elements on a metal bond into each tooth of an elastic hone—Fig. 9a. Different

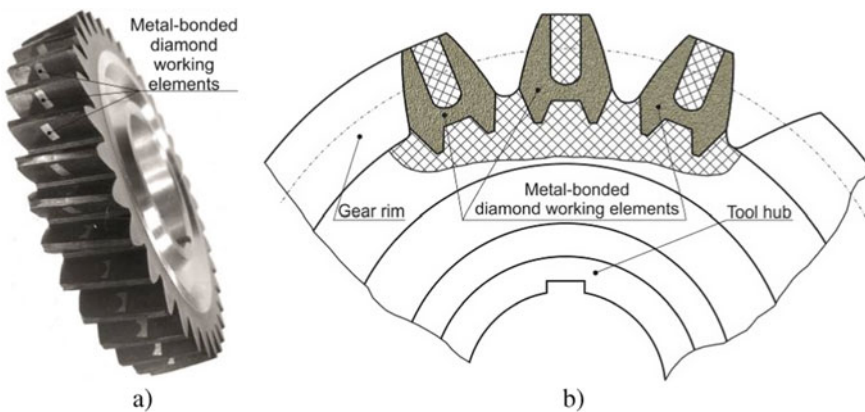


Fig. 9 General view (a) and design (b) of a combined gear hone with working diamond elements of a special shape

cutting ability of tool working elements is provided by their manufacture from a metal and rubber-containing bond—Fig. 9b. The ratio in the tool of the working elements number with different cutting ability, as well as the ratio of the cutting ability intensity of different bonds are determined by the required roughness of the machined surface, the specified amount of material removal, the size of nicks and burrs, etc.

Diamond working elements on a metal bond have a special shape that approaches the shape of ideal tool wear, inherent in the shape of wear of hyperboloidal engagement links [3, 21]. In addition, this shape ensures reliable holding of the working elements in the elastic hone teeth. The presence of working elements in the combined toothed hones simultaneously on the metal and rubber-containing bonds, located on the elastic base of the tool gear rim, provides high cutting ability and wear resistance of the tool with low roughness of the machined gear teeth profiles and effective removal of nicks and burrs.

5 Conclusions

In accordance with the decomposition scheme of the initial problem of the synthesis of technological systems for gears finishing [3], an optimization system of the synthesis process is separated from the information system and its objects are determined as elements of the optimization problem. On the basis of thus determined optimization system, an algorithmic system of the synthesis (design) process has been developed. The objects of the algorithmic system are the structural synthesis algorithm and the software implemented algorithm for multiparameter optimization of design parameters by the LP-search method. The structural design algorithm is based on the method of enumerating the data bank structures. To organize such a data bank, a structures set of technological systems for gear finishing is proposed.

On the example of the synthesis of technological systems for gear honing of hardened gears, the expediency of using the developed method is shown and a number of systems for the gears finishing by rigid kinematic connection of the tool with the machined gear and the systems with free rolling are synthesized. For the implementation of synthesized technological systems, methods of gears finishing and tools for their implementation are proposed.

References

1. Bertalanffy, L.V.: *General System Theory*, p. 289. George Brazillier, New York (1969)
2. Storchak, M.: *Technological Systems for Finishing Gears*, p. 448. Institute for Superhard Materials, Kiev (1994)
3. Storchak, M.: Optimization of Geometrical Engagement Parameters for Gear Honing. In: Radzevich, S.P. (ed.) *Advances in Gear Design and Manufacture*, pp. 35–64. CRC Press, Taylor & Francis Group (2019)

4. Storchak, M.: Simulation of the teeth profile shaping during the finishing of gears. In: *Mechanisms and Machine Science*, vol. 81, pp. 365–384. Springer (2020). https://doi.org/10.1007/978-3-030-34945-5_16
5. Storchak, M.: Dynamic model of the technological system for gears finishing. *Dudley, Handbook* (2021)
6. Le Riche, R.: *Global Optimization of Mechanical Systems*. Engineering Sciences, p. 113. Ecole Nationale Supérieure des Mines de Saint-Etienne (2008)
7. Banichuk, N.V.: *Problems and Methods of Optimal Structural Design*, p. 313. Plenum Press, New York (1983)
8. Krivosheya, A., Danilchenko, Ju., Storchak, M., Pasternak, S.: Design of shaping machine and tooling systems for gear manufacturing. In: *Theory and Practice of Gearing and Transmissions*, pp. 425–450. Springer (2016). https://doi.org/10.1007/978-3-319-19740-1_21
9. Babichev, D., Storchak, M.: Synthesis of cylindrical gears with optimum rolling fatigue strength. *Prod. Eng. Res. Dev.* **9**(1), 87–97 (2015). <https://doi.org/10.1007/s11740-014-0583-6>
10. Radzevich, S.P.: *Theory of Gearing. Kinetics, Geometry and Synthesis*, p. 685. Taylor & Francis Group (2013)
11. Babichev, D., Storchak, M.: Quality characteristics of gearing. In: *Advanced Gear Engineering*, pp. 73–90. Springer Netherlands (2018). https://doi.org/10.1007/978-3-319-60399-5_4
12. Timoshenko, S.: *Strength of Materials*, 2nd edn., p. 510 D. Van Nostrand Company Inc., New York (1940)
13. Geitner, M., Zornek, B., Tobie, T., Stahl, K.: Investigations on the pitting load capacity of internal spur and helical gears. *Forsch. Ingenieurwes.* **83**, 553–561 (2019). <https://doi.org/10.1007/s10010-019-00327-8>
14. Kreyszig, E.: *Advanced Engineering Mathematics*, 10th edn., p. 1283. Wiley (2011)
15. Kleene, S.C.: *Mathematical Logic*, p. 432. Dover (2001)
16. Sobol, I.M., Statnikov, R.B.: Choice of Optimal Parameters in Problems with Many Criteria, p 110. Moscow, Science (1981). (In Russian)
17. Kushner, V., Storchak, M.: Modelling the material resistance to cutting. *Int. J. Mech. Sci.* **126**, 44–54 (2017). <https://doi.org/10.1016/j.ijmecsci.2017.03.024>
18. Heisel, U., Kushner, V., Storchak, M.: Effect of machining conditions on specific tangential forces. *Produc. Eng.* **6**(6), 621–629 (2012). <https://doi.org/10.1007/s11740-012-0417-3>
19. Möhring, H.-C., Kushner, V., Storchak, M., Stehle, T.: Temperature calculation in cutting zones. *CIRP Ann. Manuf. Technol.* **67**(1), 61–64 (2018). <https://doi.org/10.1016/j.cirp.2018.03.009>
20. Heisel, U., Storchak, M., Krivoruchko, D.: Thermal effects in orthogonal cutting. *Produc. Eng. Res. Dev.* **7**(2–3), 203–211 (2013). <https://doi.org/10.1007/s11740-013-0451-9>
21. Litvin, F.L., Fuentes, A.: *Gear Geometry and Applied Theory*, 2nd edn., p. 800. Cambridge University Press, Cambridge (2004)

Gears in Russian University Courses on Mechanism and Machine Science



Eduard G. Krylov and Natalya A. Barmina

Abstract The paper provides a survey of a gear section in a typical Theory of Machines and Mechanisms (TMM) course taught in Russian Universities. This course is called Mechanism and Machine Science (MMS) in foreign universities. Aspects of teaching/learning the theory of gearing, delivering lab classes, and making a design project present the logics of the topic. All the mentioned issues are illustrated with examples and problems. Some recommendations are given to improve students' comprehension of the studied material and its mastering. It is shown that organizing and holding Students International Olympiads on Machine and Mechanism Science (SIOMMS) is important to keep students motivated towards studying gears. The paper also provides some perspectives, among which the harmonization of MMS study courses in different countries is considered as an important challenge for the mechanical engineering community in the nearest future. Such harmonization is necessary with regard to unification of concepts and notation, review of the content of foreign courses and their comparison with the Russian one, and studying the successful international engineering practice. If this work is successful, the gear graduates will be able to work freely in industrial enterprises operating in international markets, participate in the international scientific research, conferences, symposia and other events.

Keywords Gear · TMM · MMS · Teaching · Curriculum · Problems · Labs · Olympiads

E. G. Krylov
Kalashnikov Izhevsk State Technical University, Izhevsk, Russia
e-mail: 649526@mail.ru

N. A. Barmina (✉)
Institute of Mechanics, Kalashnikov Izhevsk State Technical University, Izhevsk, Russia
e-mail: barmina-nat@mail.ru

1 Introduction

In recent decades there has been a trend of increasing gear production; the European production of gears reached €13.4 billion in 2014 [1]. Gear mechanisms are used in almost all branches of engineering, including industry, construction, transport and many others. Therefore, a modern mechanical engineer must have general knowledge of the design, manufacture and operation of toothed mechanisms and their components.

In the curricula of technical universities, toothed mechanisms are represented in special courses and in the Theory of Machines and Mechanisms (TMM). This course is called Mechanism and Machine Science (MMS) in foreign universities.

Special study courses for future gear engineers deal with complex issues that require coordinated solution of many interrelated problems. These include choice of the gearbox structure and design, synthesis of the gear mechanism's acceptable geometry, assessment of the link quality, geometry optimization, and design of manufacturing processes, selection or design of tools, testing, repair, recycling and others [2]. The tasks listed refer to the Integrated Gear Design (IGD), which is based on complex advanced theoretical positions based on sophisticated mathematical methods and practical recommendations.

The theory of machines and mechanisms (hereinafter – MMS) as a training course has the generalized character. MMS presents the basic physical laws to develop approaches to real object modeling, considers math description of the models, and basic concepts characterizing the properties of object models, such as, for example, kinematic pairs. Mechanisms, including gears, are then classified, and their analysis and synthesis are considered. Thus, the MMS course can be seen as an introduction to the design of specific types of mechanisms (linkages, gears, cams and others). In addition to the noted main objectives of the course, it provides rich opportunities to develop qualities necessary for the modern engineer - qualities of an analyst, researcher, and designer [3].

This manuscript sets out the logic of the MMS course with regard to analysis and synthesis of toothed mechanisms, gives an overview of the content of the *Gears* section in the course, as well as the methods, ways, and peculiarities of students' education. Examples are given for the theoretical issues, labs, practical exercises and problems. It is shown how the section under discussion is presented at MMS student Olympiads.

2 Gears Section in the MMS Standard Academic Program

The MMS standard academic program [4] gives 68 contact hours for lectures, 34 h for labs and practical work, and a course design project. Unfortunately, in recent years, there has been a significant reduction in the total number of MMS hours, with a particularly sharp reduction in the number of contact hours. For example,

Table 1 General gear mechanism topics

No.	Topic
1	Fundamental law of toothed meshing
2	Spur gearing
3	Involute properties. Standard proportions of gear systems
4	Manufacture of gear teeth
5	Interference and undercutting. Radial shift
6	Fundamentals of meshing actions
7	Additional conditions at involute gearing synthesis
8	Internal gearing
9	Parallel-axes helical gears
10	Crossed-axes helical gears
11	Worms and worm gears
12	Epicyclic gear trains
13	Allowable number of planetary gearwheels
14	Structural synthesis of planetary gear trains
15	Synthesis of closed-circuit differential gear trains

following the recommendations of the Ministry of Higher Education and Science of the Russian Federation, the number of contact hours for all mechanical engineering academic programs in Kalashnikov Izhevsk State Technical University (ISTU) was reduced: 34 h for lectures, 17 for labs, and 4 h for the course design project.

In section «2.11. Synthesis of toothed mechanisms» of the standard academic program it is proposed to study the topics specified in Table 1.

Technical universities expand the content of these topics and make it more specific. Thus, Bauman Moscow State Technical University organizes the study of issues related to the synthesis of toothed mechanisms in the form of six large units [5], see Table 2.

The sequence of topics and subtopics listed in Table 2 corresponds to the logic of presentation of the theoretical material in classical textbooks of Artobolevsky [6] and Frolov [7]. International MMS textbooks have similar sections related to gear design [8, 9].

The theory of a higher kinematic pair is usually one of the first topics related to gears. Based on the analysis of the relative motion of the points A and B of the links forming the higher kinematic pair, the position of the instantaneous center P of relative rotation of the conjugate profiles 1 and 2 is found, see Fig. 1 [7]. This introduces the concept of a pitch point, which is fundamental to *Gears* section of the MMS course. In particular, the students are shown in the coming topics that the relative sliding velocity V_{BA} of the conjugate tooth profiles is proportional to the distance from the pitch point to the point of the profiles contact.

The analysis makes it possible to formulate the fundamental law of the in-plane toothed meshing.

Table 2 Study units

No.	Title of educational unit	Content
1	Fundamentals of the theory of the higher kinematic pair	Introduction to the theory of the higher pair, basic concepts and definitions. Mechanisms with higher kinematic pairs (KP) and their classification. Coupling and coupling transfer. Fundamental law of toothed meshing. The notion of centrodes and the pitch point. Conjugate profiles in higher KP. The sliding velocity of profiles in the higher KP. The center of rotation of the moving link. Pressure angle in mechanisms with higher KP. Gears and their classification. Involute gear. Involute of a circle and its parametric equations. Meshing of two involute gearwheels
2	Involute gearing (part I)	Standard proportions of an involute gearwheel. The thickness of the tooth of the gearwheel measured at any profile point. Methods of manufacture of involute gear teeth. Counterpart rack, basic rack tooth profile. Basic dimensions of a gearwheel. Types of gearwheels. Gearwheel undercutting and sharpening. Involute spur gearing and its parameters. Basic equations of the involute gearing
3	Involute gearing (part II)	Classification of gears. Blocking contours (diagrams) for the cutter shift choice. Indicators of an involute gearing quality. Contact ratio. Tooth shape ratio. Specific pressure ratio. Specific sliding coefficient. Optimal geometric synthesis of gears. CAD software for gear design. Helical gears, design of helical gearing. Overlap ratio (axial contact ratio) in helical gears
4	Novikov gears, bevel gears, worm gears	Novikov gears, bevel gears, worm gears, cycloidal gears
5	Kinematics of planetary gear trains	Simple and compound gear trains. Planetary gear trains. Graphical and analytical analysis of planetary gear trains using Willis's method (formula method)
6	Synthesis of typical planetary gear trains	Synthesis of typical planetary gear trains as a design problem. Selection of numbers of teeth according to method of matching multipliers. Condition of coaxiality, condition of neighborhood for planetary gears, condition of assembly of planetary gear trains. Examples of synthesis. Optimization and CAD software for synthesis of planetary gear trains

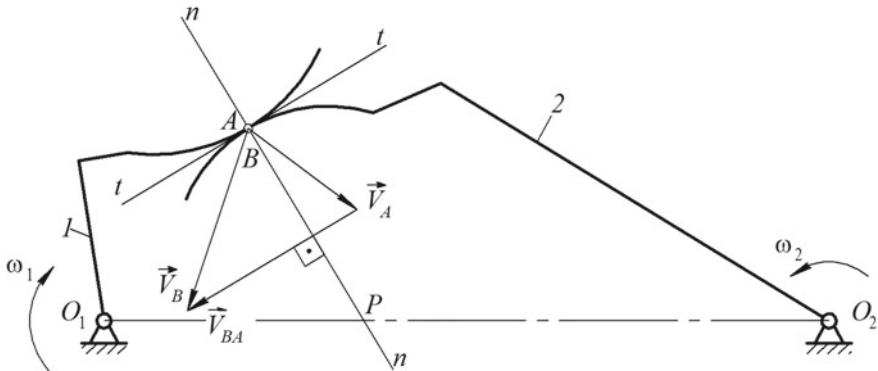


Fig. 1 Layout of rotating links forming a higher kinematic pair. Position of the pitch point. Velocity diagram

All MMS courses consider the geometry of involute gearing in detail. Students then learn the principles of gear tooth manufacturing by form cutters and generating (running-in) cutters. Animation, slides and video training are extremely useful. This makes it possible to illustrate the variety of tools used, as well as the relative movements of the gearwheel workpiece and the tool. The animation of movements of teeth and movement of the contact point along the pressure line facilitate understanding of the involute gear functioning.

It should be noted that, with rare exceptions, the MMS course is usually limited to considering the *external* meshing of involute gearwheels.

The phenomenon of tooth undercutting near the tooth root is closely related to tooth cutting. Students are explained the physical nature of this phenomenon, given formulas for the minimum tooth number to avoid undercutting, and are told about positive and negative shifts of the cutter tool.

Great attention is paid to the consideration of the gearing qualitative parameters influencing the smooth and silent operation of the gearbox, possible wear and strength of teeth. The MMS courses deal with the following qualitative parameters: contact ratio, specific sliding ratio, and specific pressure ratio. The concept of blocking contours (diagrams) for the selection of the cutter shift is given based on the provision of optimal quality parameters of gearing.

It is rather hard for students to master a large amount of complicated information on the geometry and kinematics of gears without solving problems and doing labs. One of the most recognized textbooks for this purpose is the collection of MMS problems by Artobolevsky and Edelstein [10].

The geometrical synthesis of an involute gearing requires knowledge of the basic parameters of conjugate profiles and understanding of their possible changes caused by the manufacturing process (cutter shift) and assembly (variation of the center distance) as well as the ability to calculate the qualitative indicators. Many textbooks provide recommendations for step-by-step calculation of corrected (cut with a shift) gearing [10–12], in particular those based on formulas suggested by Gavrilenko [13].

Second-year students (who are mainly taught MMS) find it rather difficult to deal with educational material containing a large number of geometrical parameters, formulas and drawings often overloaded with information. It is therefore very useful to give students a large number of easy-to-solve problems for every aspect of the geometrical synthesis of gearing. This provides the necessary practical skills to promote a better understanding of the topic.

Below are some examples of the problems of this sort.

Problem 1 Point A belongs to an involute and is located at the radius vector of $r_A = 50$ mm, the profile angle is $\alpha_A = 20^\circ$. What is the profile angle at point C lying on the same curve if the radius vector is $r_C = 70$ mm? Make a picture [14].

Problem 2 For a gearwheel cut by a standard rack cutter, the following is given: module $m = 5$ mm, diameter of the dedendum circle $d_f = 85$ mm, diameter of the pitch circle $d = 100$ mm. Determine the tooth thickness S measured along the pitch circle [14].

Problem 3 For the external meshing of two involute gears it is known: pressure angle $\alpha = 20^\circ$, module $m = 10$ mm, the number of teeth $z_1 = 20$, $z_2 = 30$. Both gears are cut without shift. Then, if the center distance increases by 5 mm relative to the designed one, what will the modified angle of pressure α^* and the new radii of pitch circles be [15]?

Problem 4 A pair of involute spur gearwheels should have the module $m = 12$ mm and tooth numbers $z_1 = 10$, $z_2 = 14$. Make a modification (shifting of a cutter) to avoid tooth undercutting and determine all sizes of both gearwheels [13].

The geometric proportions and manufacturing of crossed-helical, bevel, hypoid, and worm gears are considered in textbooks [7, 10, 13, 16, 17 etc.]. However, due to the limited contact time, these issues are often not discussed at classes.

In the kinematics section, the main issues are related to determining the gear ratio of gear trains (including those with planetary and differential stages—epicyclic gear trains), and finding absolute and relative angular speeds. These problems are not challenging for students. On the contrary, selecting the number of teeth by a given gear ratio requires a large number of mathematical operations, and presents considerable difficulties for students. It is recommended to solve such tasks using computer programs.

The problems of kinematics of gear trains with fixed axes are solved analytically or graphically (by velocity diagrams), see Fig. 2 [18]. For spatial gear trains vector diagrams are used, see Fig. 3 [18].

The next major topic is the kinematics of planetary and differential mechanisms. In Russian MMS courses the gear ratio is mainly found by Willis method (in international textbooks it is known as the formula method). Two modifications of the Willis formula are used for planetary mechanisms.

The first modification considers every gear stage provided the handle H is stopped: $\frac{\omega_a - \omega_H}{\omega_b - \omega_H} = \pm \frac{z_b}{z_a}$, where H is the handle, a and b are gearwheels, z is the tooth number.

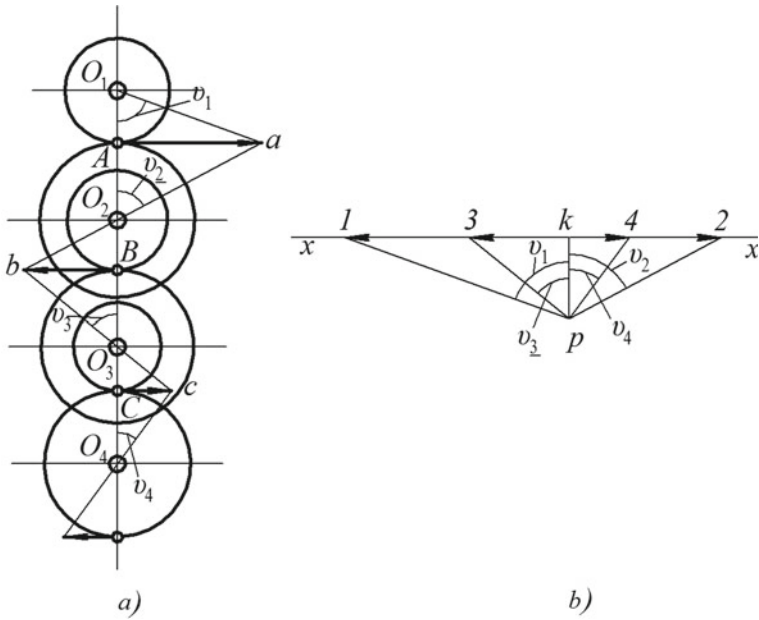


Fig. 2 Compound gear train: **a** linear velocities on the scheme, **b** angular velocity diagram

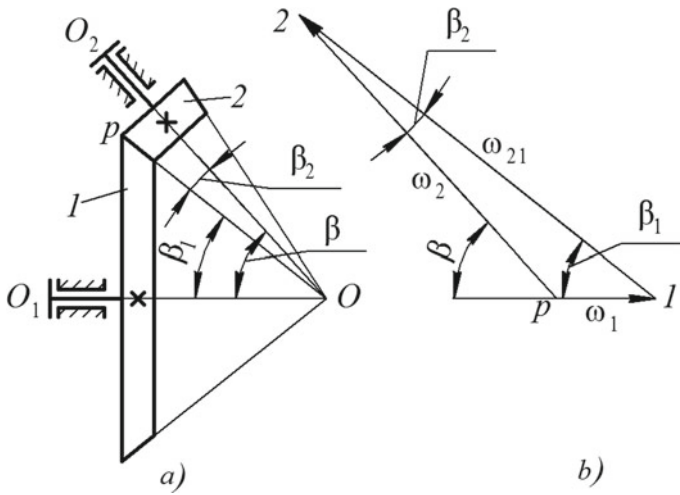


Fig. 3 Bevel gear train: **a** scheme, **b** vector diagram of angular velocities

Using the second modification, it is possible to determine the gear ratio of the whole mechanism according to the formula:

$$i_{aH}^b = 1 - i_{ab}^H.$$

In the latter formula, the upper index refers to an element that is fixed.

The gear ratio of the differential mechanism can be determined using the first modification of the Willis method.

The topic of determining the gear ratio of epicyclic mechanisms is widely presented in textbooks. Since in these mechanisms gearwheels can rotate around moving axes, it is important to teach students to distinguish absolute and relative angular speeds, and to determine them. Examples of angular velocity problems are given below [14].

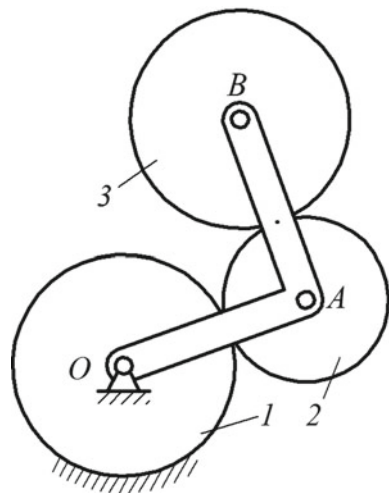
Problem 5 The handle OAB of a planetary mechanism (see Fig. 4) rotates with an angular speed $\omega_H = 15$ rad/s, while the central wheel 1 is stationary. Determine the angular velocities of gears 2 and 3 provided the number of teeth are $z_1 = z_3 = 30$, $z_2 = 20$.

Problem 6 Assuming that the gear ratio (with the stopped handle H_2) is $i_{56}^{H_2} = 4$, find the relative rotational speed n_{5H_2} (speed of the gearwheel 5 relative to the handle H_2), if the output shaft rotates with the speed $n_B = -20$ rpm, see Fig. 5.

Problem 7 In the gearbox having the total gear ratio $i_{AB} = 40$, the shaft A makes $n_A = 1500$ rpm (see Fig. 6). Find the angular speed of the gearwheel z_4 relative to A , if $|i_{47}| = 12$.

The problems of angular speeds and gear ratios of epicyclic mechanisms can also be solved graphically. An example is shown in Fig. 7 [18].

Fig. 4 Planetary mechanism



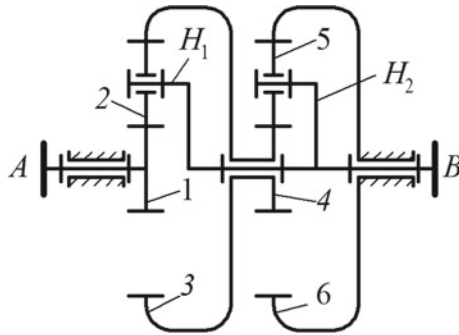


Fig. 5 Double-handle planetary mechanism

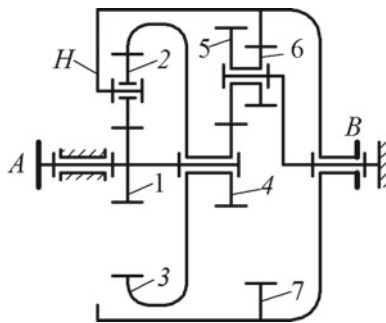


Fig. 6 To the problem 7

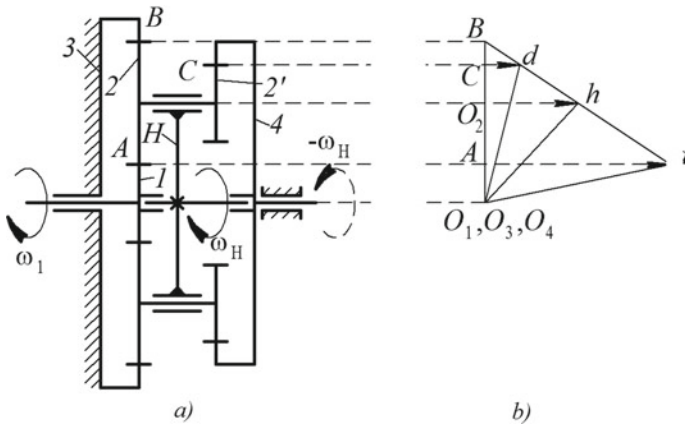


Fig. 7 Planetary gearbox: **a** scheme of mechanism; **b** angular velocity diagram

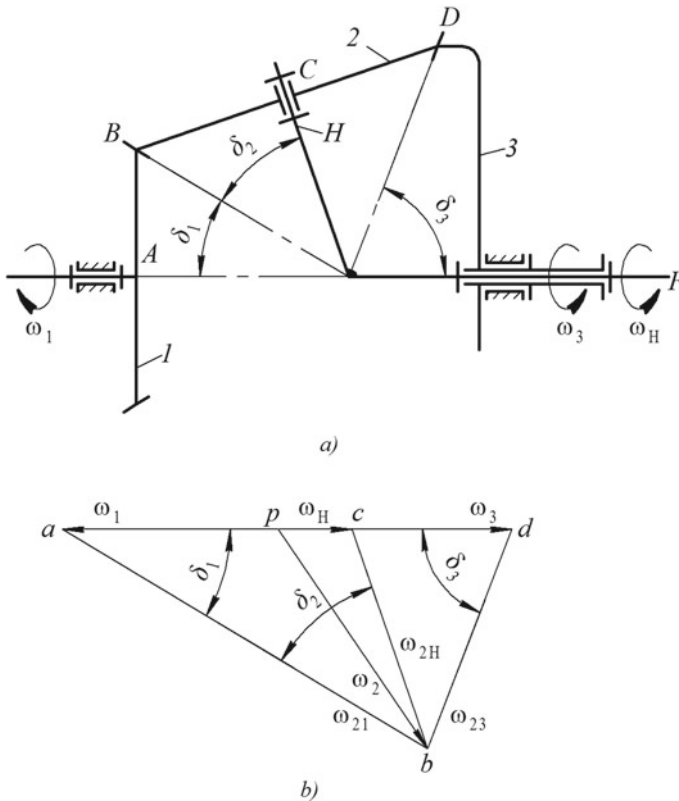


Fig. 8 Bevel planetary gearbox: **a** scheme of mechanism; **b** angular velocity diagram

Similar investigations are also carried out for crossed-axes planetary gearboxes [7, 13, 18]. Figure 8 shows the velocity diagram for a bevel gear differential with two degrees of freedom.

Some MMS study courses deal with the kinematics of biplanetary epicyclic gear trains with an additional gear-linkage group between the twin satellites, see Fig. 9 [19]. Such mechanisms are analyzed by both analytical and graphic methods [7, 18].

The topic “Synthesis of planetary gear trains” is presented in the MMS courses by the condition of coaxiality, condition of neighborhood for planetary gears, and condition of assembly of the planetary gear train. The example is given below.

Problem 8 For the combined gear train shown in Fig. 10 determine the number of teeth of all gearwheels. What is the maximum possible number of satellites 2 in this mechanism? The gear ratio is $i_{17} = 11$.

The efficiency of gears and gearboxes is given in most textbooks, but hardly discussed in the classes due to the lack of contact hours.

Today gear mechanisms, like many others, are designed using automated design (CAD) systems. And yet, the wide variety of gear mechanisms used in industry

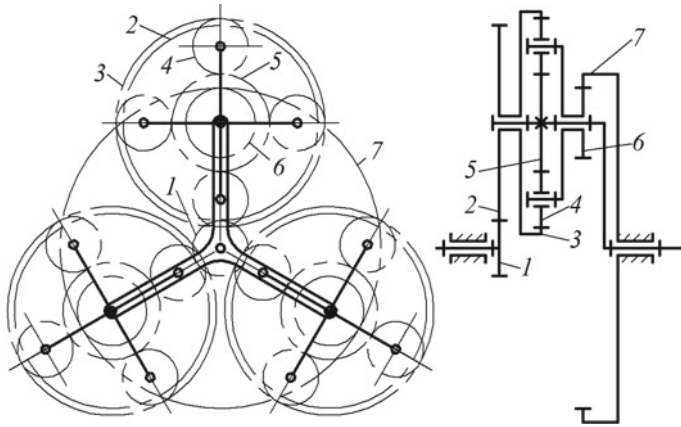
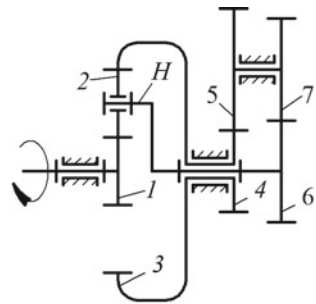


Fig. 9 Biplanetary gear train and its kinematic scheme

Fig. 10 Combined gear train



and transport along with rapidly changing approaches to the mathematical modeling make it difficult to create universal CAD systems for the synthesis and design of gears [1]. Therefore, it is particularly important to enable students in the course of their studies to master various types of software:

- to make robust calculation of traditional types of gear drives;
- to research the impact of various kinematic, structural, technological and operational parameters on different quality characteristics of the studied gear sets;
- to make optimization search.

Many Russian technical universities have developed computer programs for analysis and synthesis of involute gears [20–22]. For example, the Department of Applied Mechanics of the Tyumen Industrial University uses software developed mainly on the basis of MS Excel, using VBA (Visio Basic for Application) [23]. These computer programs are used for: design and comparative analysis of different types

of involute gears and gear trains; lab classes “Manufacturing of gears by a generating cutter”; demonstration at lectures; practical lessons on gear cutting; scientific research; calculations for industry; making diagrams and schemes for scientific papers and presentations, as well as for student books and many others [23].

The computer programs like these are developed in many technical universities. However, the issue of applying the gear software in the MMS course has not yet been raised in the most general way, linking the motivation of students to their acquisition of knowledge, skills, participation in quasi-professional and activities.

3 Gears in Labs and Design Projects

Because of the shortage in contact hours there are only three gear labs in MMS course at Kalashnikov Izhevsk State Technical University (ISTU), see Table 3. The first two are related to geometric analysis and synthesis of involute gears (Figs. 11 and 12). The third lab examines the kinematics of the planetary gear train.

Gear design is an important part of the MMS course project. The typical points of the design are as follows.

1. *Synthesis of a machine drive scheme.* In most cases, the drive of the machine consists of a serial connection of one or two pairs of fixed-axes gears, plus a planetary gear train. The total gear ratio of the drive is assigned, it is necessary to divide it up between the gears and to select the number of gearwheel teeth. The method of multipliers is used.

2. *Synthesis of involute spur gearing.* The basic geometric parameters, including the shift of a cutting rack, are calculated for two gearwheels being in an external meshing. The cutter shift should be selected using blocking contours (diagrams) according to the conditions of: no undercut of teeth or maximum contact strength or specified center distance or specified sliding of conjugate contours or maximum bending strength.

3. *Calculation of qualitative parameters of meshing.* For the gearing under design, the contact ratio and the specific sliding coefficient should be calculated.

4. *Drawing of the gearing.* At the Bauman Moscow State Technical University, most of the calculations for the design project are made using universal commercial software Excel, MathCad etc. In particular, these programs are used for the selection of the cutter shift and for the kinematic synthesis of the planetary gear train [24].

4 Gears in Student International Olympiads on Mechanism and Machine Science

The section of gears is usually one of the most difficult in the MMS study course. Therefore, motivation is of the utmost importance for students to successfully master it. Solving non-standard problems, performing creative tasks, competitions can make

Table 3 Gear labs

Lab	Title	Content	Method	Tools
1	Decoding geometric parameters of involute spur gearwheels by measuring the length of the common normal	Calculation of basic geometric parameters for a gearwheel with the absent marking (no information printed on the gearwheel). The shift of the cutter is among these parameters	Measurement of the length of the common normal	Gearwheel, slide gage, gear tooth caliper
2	Manufacturing of gears by generating cutters	Simulation of cutting of involute spur gearwheels by a generating cutting rack. Study of the effect of the cutter shift on tooth shape and dimensions	Calculation of the cutter shift in order to avoid the undercutting of teeth. Imitation of the tooth cutting method on the paper blank	Device for imitating the cutting of involute spur gearwheels by a rack cutter, paper blank
3	Kinematics of planetary gear trains	Drawing a kinematic diagram of the proposed mechanism; calculating its mobility, gear ratio, verifying the fulfillment of the condition of coaxiality, determining the maximum number of satellites from neighboring and assembly conditions	The method of motion reversion (Willis' method), formulas for conditions of coaxiality, neighborhood, assembly	Material models of planetary gear trains

a big contribution to the development of student motivation to study gears, and development of interest towards gearing science. One possible way to realize such opportunities is through student Olympiads. The All-Russian Student Olympiads on MMS have been held in Russia for the last 30 years. Following its mission of promotion of Mechanism and Machine Science among young people all over the world, the Executive Council of IFToMM in Guanajuato, Mexico, June 2009, has resumed establishing the regular Student International Olympiad on MMS (SIOMMS) [25, 26]. In 2011–2018 four International Olympiads were held [27].

Traditionally, two topics related to gears are included in the Olympic problem set: *geometry of toothed meshing* (SIOMMS2011, SIOMMS2013, SIOMMS2016), and *gear trains* (SIOMMS2011, SIOMMS2013, SIOMMS2016, SIOMMS2018). Below is the text of a typical contest problem [28].

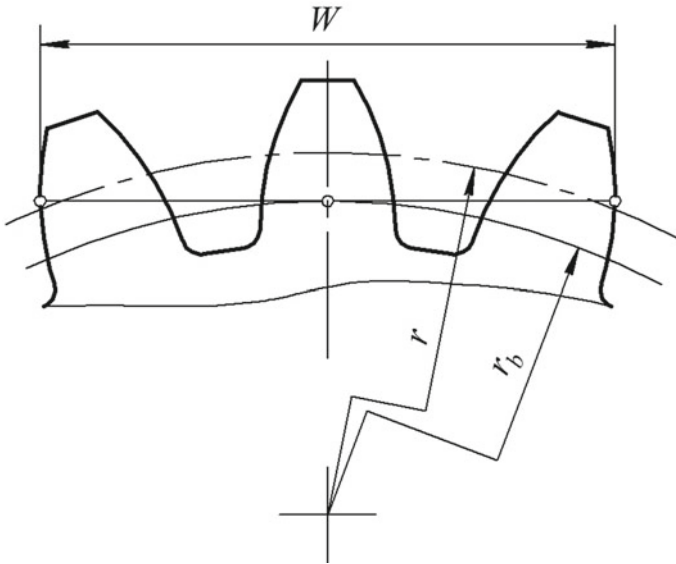


Fig. 11 Diagram for determining the length of the common normal (lab 1)

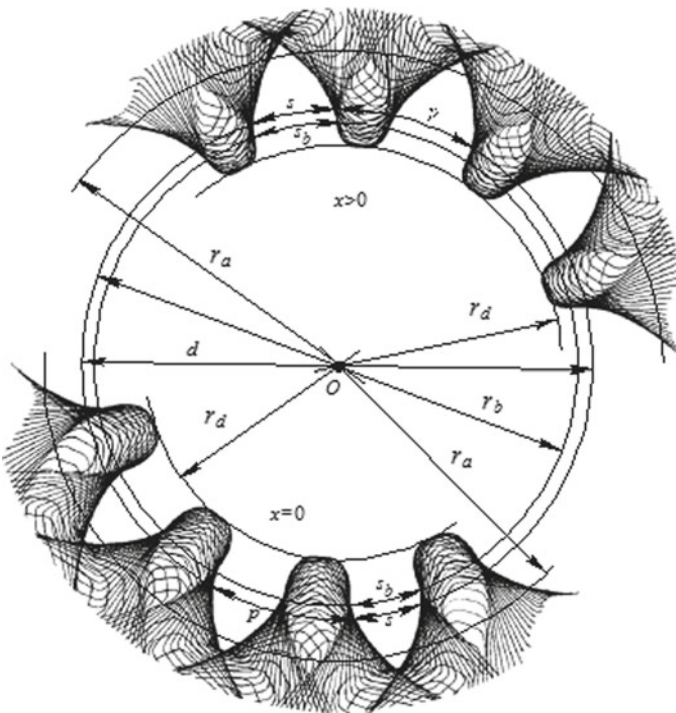
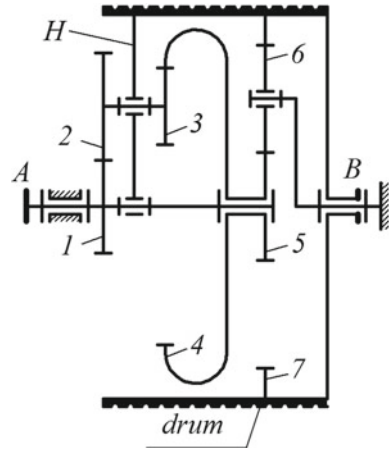


Fig. 12 Imitation of tooth cutting on a paper blank (lab 2)

Fig. 13 The gearbox of the Contest problem



Contest problem. A gearbox used to drive the drum in a hoisting mechanism (see Fig. 13) has been destroyed because of overloading. Since the drawings of gears were lost, the only information below is available about the gearbox:

- all mating gears are of the same module m ;
- gears 4, 5, 7 have tooth numbers $z_4 = 63$, $z_5 = 24$, $z_7 = 72$, respectively;
- gears 1 and 3 have an equal tooth number $z_1 = z_3$;
- all gears are cut with a standard tool (angle of pressure 20° , the length of addendum is equal to the module $h_a = m$; the radial clearance coefficient is $c^* = 0.25$, no shift).

Questions:

1. Calculate the mobility of the gearbox. Reveal idle degrees of freedom, if any.
2. Determine the number of teeth for all unknown gears provided the gear ratio of the mechanism is to be 22.

Usually, the gear ratios of combined gearboxes, with the exception of biplanetary epicyclic mechanisms, are relatively easy to solve by participants in the Olympics. Yet the selection of tooth numbers and especially the geometric study of meshing gearwheels cut with shift are much more difficult for students. It is natural that, under conditions of the limited time and stress, participants make mistakes even in simple calculations [28].

In any case, preparation and participation in the Olympiad give students a very strong motivation to study this challenging section of the MMS and contribute to its mastering by them. Some former members of Kalashnikov ISTU student teams in SIOMMS are working now at the Institute of Mechanics named after Professor V. I. Goldfarb, the leading scientific and production institution for spiroid gears in Russia. This demonstrates once again the usefulness of student Olympiads.

5 Conclusion

The gear section of the MMS course is usually studied in the second year of a technical university curriculum. It provides basic information, which is then used in the course of Machine Design, as well as in specialized gearing courses. Knowledge of the basics of gear mechanisms is absolutely necessary for a mechanical engineer specializing in any narrow field. The MMS course in the discussed aspect has great educational significance in the general professional sense for all mechanical engineers. This course can also be seen as an introduction section for future designers, process engineers, manufacturing engineers, and field engineers – all experts involved in the gear industry.

There are strong scientific and educational schools in Russian universities to provide high-level teaching of the toothed mechanism section. Scientific conferences are held regularly, and Russian scientists work successfully in the IFToMM Technical Committee for Gearing and Transmissions.

Harmonization of MMS study courses offered in different countries is an important task for the mechanical engineers community in the near future. Such harmonization is necessary with regard to the unification of concepts and notation, investigation of foreign courses material and comparison it with a native one, familiarization with successful international engineering practices. If this work is successful, the gear specialists will be able to work freely in industrial enterprises operating in international markets, participate in international scientific research, conferences, symposia and other events. IFToMM activity [26] objectively contributes to this process.

References

1. Abadjieva, E., Abadjiev, V., Karaivanov, D.: Bulgarian experience in applying and improving knowledge in the field of theory and application of modern gears. In: *Mechanisms and Machine Science* (Book Series), vol. 81, pp. 47–70 (2020). https://doi.org/10.1007/978-3-030-34945-5_2
2. Babichev, D.T., Lagutin, S.A., Barmina, N.A.: Russian school of the theory and geometry of gearing. Part 2. Development of the classical theory of gearing and establishment of the theory of real gearing in 1976–2000. In: *Mechanisms and Machine Science* (Book Series), vol. 81, pp. 1–46 (2020). https://doi.org/10.1007/978-3-030-34945-5_1
3. Balyakin, V., Krylov, E.: Cultural and educational significance of MMS competitions for future engineers. In: *Mechanisms and Machine Science* (Book Series), vol. 64, pp. 3–10 (2019). https://doi.org/10.1007/978-3-030-00108-7_5
4. Federal State Higher Education Standards Portal. <http://fgosvo.ru/ppd/11/11>. Accessed 25 Jan 2021. (in Russian)
5. http://m-umk.bmstu.ru/index_2. Accessed 21 Jan 2021
6. Artobolevsky, I.I.: *Mechanism and Machine Theory*, 4th edn. Science, Moscow (1988). (in Russian)
7. Frolov, K.V. (ed.): *Theory of Mechanisms and Machine Mechanics*, 5th edn. Publishing house of Bauman Moscow State Technical University, Moscow (2004). (in Russian)
8. Khurmi, R.S., Gupta J.K.: *Theory of Machines*, 14th edn. Chand & Co Ltd. (2005)

9. Uicker, J., Pennock, G., Shigley, J.: *Theory of Machines and Mechanisms*, 4th edn. Oxford University Press, New York, Oxford (2011)
10. Artobolevsky, I.I., Edelstein, B.V.: *Collection of Problems on the Theory of Mechanisms and Machines*. Science, Moscow (1988). (in Russian)
11. Matveyev, Y.A., Matveyeva, L.V.: *Theory of Mechanisms and Machines*. Alpha-M, Infra-M, Moscow (2009). (in Russian)
12. Gorbenko, V.T., Gorbenko, M.V.: *Theory of Machinery and Machines*. Course design. Tomsk Polytechnic University, Tomsk (2007). (in Russian)
13. Mashkov, A.A.: *Theory of Mechanisms and Machines*. High School, Minsk (1971). (in Russian)
14. Guryev, B.I., et al.: *Theory of Mechanisms and Machines*. Ufa State Aviation Technical University, Ufa (2008). (in Russian)
15. Gorbenko, M.V., Gorbenko, T.I.: *Collection of Problems and Exercises on the Theory of Mechanisms and Machines*. Tomsk Polytechnic University, Tomsk (2011). (in Russian)
16. Baranov, G.G.: *Course on Machinery and Machine Theory*. Publishing House: Mechanical Engineering, Moscow (1967). (in Russian)
17. Yermak, V.N.: *Theory of Mechanisms and Machines (Short Course)*. Kuzbas State Technical University, Kemerovo (2011). (in Russian)
18. Yudin, V.A., Petrokas, L.V.: *Theory of Mechanisms and Machines*, 2nd edn. Higher School, Moscow (1977). (in Russian)
19. Drewniak, J., Kądziołka, T., Zawisłak, S.: Kinematics of Bevel Biplanetary Gear. In: *Advanced Gear Engineering, Mechanisms and Machine Science (Book Series)*, vol. 51, pp. 289–303 (2018). https://doi.org/10.1007/978-3-319-60399-5_14
20. Egorova, O.V.: 3-D computer simulation in teaching of the discipline “Theory of mechanisms and machines”. *News of higher education institutions. Mech. Eng.* **7**(664), 79–86 (2015). <https://doi.org/10.18698/0536-1044-2015-7-79-86>. (in Russian)
21. Petrov, G.N.: Computer simulation of mechanical systems in “Model Vision”. *Sci. Tech. Bull. St. Petersburg State Polytech. Univ.* **1**(3), 75–76 (2004). (in Russian)
22. Babichev, D.T., Lebedev, S.Yu.: TIU experience in the use of computer-aided design methods in a study course Theory of mechanisms and machines. In: Balakin P.D. (ed.) *Third International Science and Technology Conference “Problems Of Engineering” 2019*, vol. 1, pp. 21–31. Publishing House: Omsk State Technical University (Omsk) (2019). (in Russian)
23. Babichev, D.T., Smovj, A.I., Krivošeja, A.V.: Synthesis of modern involute spur gears in the course “Applied Mechanics”. *Bull. Natl. Techn. Univ. KhPY. Probl. Mech. Drive* **35**(1144), 10–19 (2015). (in Russian)
24. Chernaya, L.A., Timofeyev, G.A.: *Theory of Machinery and Machines*. Course Design. Student Book. Publishing House: Bauman Moscow State Technical University, Moscow (2019). (in Russian)
25. Goldfarb, V., Krylov, E., Perminova, O., Barmina, N., Vasiliev, L.: Aspects of teaching “Advanced gears” for future mechanical engineers within “Bachelor of science” programs at technical universities. In: *Advanced Gear Engineering, Mechanisms and Machine Science (Book Series)*, vol. 51, pp. 271–287. Springer (2018). https://doi.org/10.1007/978-3-319-60399-5_13
26. Goldfarb, V.I., Krylov, E.G., Serova, T.S.: IFToMM contribution to attraction of youth to MMS development and promotion. *Mech. Mach. Theory* **100**, iii–vii (2016). <https://doi.org/10.1016/j.mechmachtheory.2016.02.008>
27. Krylov, E.G., Devyaterikov, S.A., Gubert, A.V., Egorova, O.V.: SIOMMS: evolution and development. *Mech. Mach. Theory* **153**, (2020). <https://doi.org/10.1016/j.mechmachtheory.2020.104029>
28. Goldfarb, V.I., Krylov, E.G., Elensky, A.V.: Analysis of the participant solutions of the first student international Olympiad on mechanism and machine science. *Mech. Mach. Theory* **70**, 293–297 (2013). <https://doi.org/10.1016/j.mechmachtheory.2013.08.003>

Geared Designs from the Past for Today Inspiration



Marco Ceccarelli  and Fernando Viadero Rueda 

Abstract This paper is a short-illustrated survey of past designs in gearing systems as a tribute to the memory of Prof. Veniamin Goldfarb, who included in his expertise on Gearing Technology also its History. The paper outlines main gear designs that can be considered milestones in the development of Gearing Technology up today. Design aspects and evolutions are discussed with illustrative examples to show main aspects of the evolution of design solutions and expertise in geared systems with indication of challenges and future trends for a successful development of the field and its application to modern machine technology.

Keywords Gearing technology · History of gears · History of MMS · History of IFToMM · Prof goldfarb

1 Introduction

Gear transmissions are mechanical systems used in various applications to transform and transmit power or motion.¹ The objective of gear transmissions is to allow the transmission of movement between shafts through the contact of different elements

¹Prof. Veniamin Goldfarb (1940–2019) was a worldwide reputed scientist of gearing systems with a successful activity of technological transfer also with a production of industrial products, at Institute of Mechanics of Kalashnikov Izhevsk State Technical University. He was also a leader in IFToMM—International Federation for the International Federation for the Promotion of Mechanism and Machine Science (MMS) as being Vice-President and Chair of Technical Committee for Gears with several international activities among which it is to note that he was the initiator of SIOMMS, the IFToMM Student Olympiad on MMS.

M. Ceccarelli (✉)

Department of Industrial Engineering, Laboratory of Robot Mechatronics, University of Rome Tor Vergata, 00133 Rome, Italy
e-mail: marco.ceccarelli@uniroma2.it

F. V. Rueda

Department of Structural and Mechanical Engineering, University of Cantabria, 39005 Santander, Spain
e-mail: viaderof@unican.es

called teeth. These transmissions are present in sectors such as automotive, energy, agriculture, manufacturing or aerospace. Gears have always been considered fundamental for machines and for the innovative development not only of mechanical transmissions but also of new machine solutions and their evolution. This importance is also recognized on a historical level as it is outlined in the history of engineering both in technical or specific monographs in the history of transmissions, for example [1–3], as in encyclopedic works on the history of machines and inventions, for example [4–6].

In the general treaties, however, a fundamental role of gear technology is not clearly recognized, so much so that even today in the research funding programs the issues relating to mechanical transmissions and particularly gears are not considered of priority but they tend to think that this technology is now so mature that it does not require further funding and can only be left to commercial industrial development for the design and application of gears. Historical development, however, indicates that gears have always had to support both the design of the machines and the materials used in them with innovative solutions as well as responding to the needs of greater functional and energy efficiency which today is even more stringent, especially when designed as linked to problems of sustainable energy and pollution that are due precisely to the intrinsic dissipative phenomena in power transmission.

Among the classic authors of research on gear drives are famous names such as Olivier, Willis, Giulio, Buckingham, Wildhaber, Dudley, or Musser, who contributed significantly to gear developments since the early days of Industrial Revolution up to today. However, in the last forty years and due, among other things, to the growing demand for quieter transmissions, with lower development and maintenance costs, it has led to a huge amount of researches and publications on gears whose wide variety in this paper is shortly described as per the future trends in the field of gear research.

In this work with an illustrative approach we want to outline this fundamental role and the evolution of concepts and solutions for gears that have led to a significant development in the technology of mechanical systems up to today's robotic and mechatronic systems in which a functionality can still be recognized essential due to mechanical transmissions when such systems perform mechanical functions with transmission of movement and force. The examination that is reported in this paper also wants to indicate how solutions of the past contain concepts and even solutions of current interest that can be used and further elaborated to obtain new solutions and also to update the successful designs of the past towards applications with increasingly higher structural and functional characteristics.

2 Gear Solutions and Applications

Gears have been fundamental since the first mechanical transmissions which led to the development of the first machines both in terms of efficiency and functionality. The solutions of antiquity remain mostly bibliographic sources with few archaeological findings which, however, surprisingly show technological levels that were unthinkable for those times until recently.

An emblematic example is shown in Fig. 1 regarding the Antikythera mechanism, dated of 2nd century B.C., for which studies of a few decades, [7, 8] have highlighted with the high technological levels in antiquity, being this mechanism recognized as a first digital computer based on the operation of trains of gears. In addition to the complexity of the assembly of the gear trains, Fig. 1a, the specific design of the tooth profiles is remarkable, resulting in triangular profiles, Fig. 1b of precise execution well suited to low speed operation as the typical one for the instrument for which they were designed. This example demonstrates that already in ancient times the design of gears not only had a wide use in machines as emphasized also in the first specific treatises such as that by Vitruvius, but they were considered fundamental for the design and operation of systems with high precision and efficiency.

The re-flourish of machines during the Renaissance, [9], also saw an intense design activity on mechanical transmissions with traditional structures and with solutions

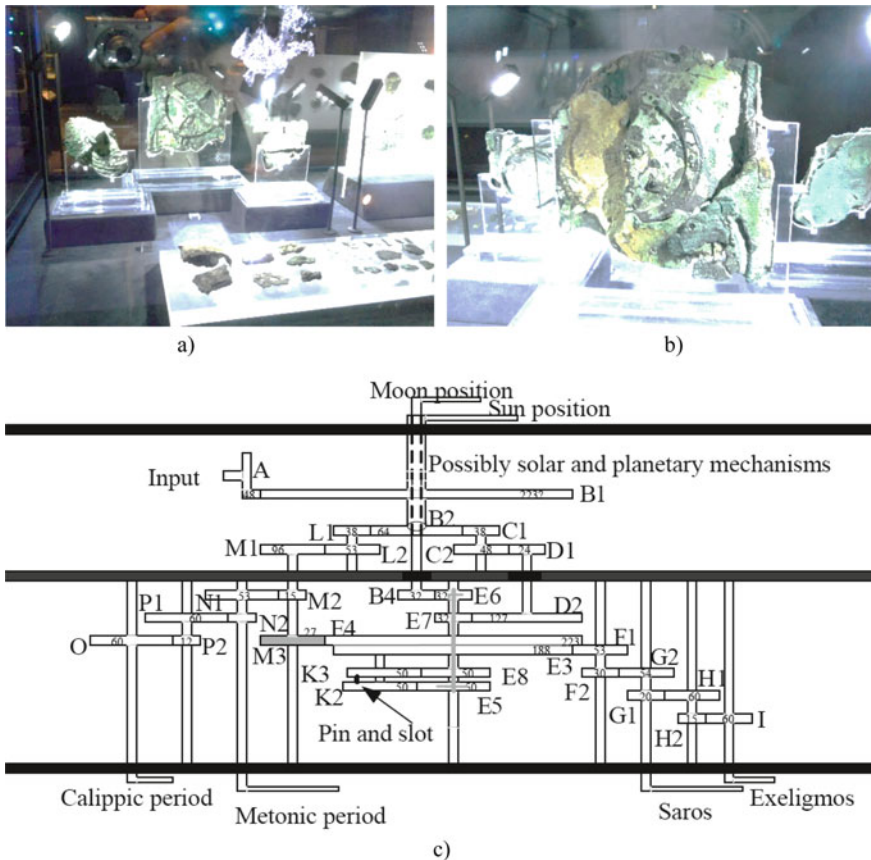


Fig. 1 Antikythera gearbox, an example of gears in Antiquity: **a** museum exposition of remains in Athens; **b** a detail of a geared sector; **c** a modern model [8]

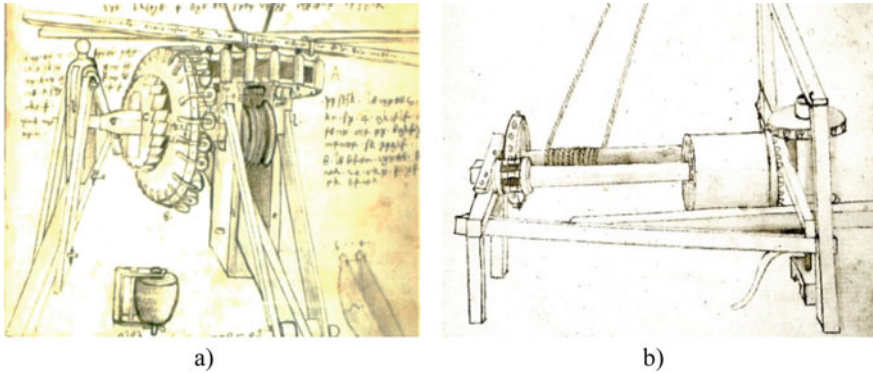


Fig. 2 Example of geared systems designed at the beginning of Renaissance in 13th century by Filippo Brunelleschi: **a** a composed gear train; **b** a powered capstan

made of new solutions in order to improve both the operating conditions and the efficiency of old and new machines. Emblematic examples are shown in Figs. 2 and 3. In particular, Fig. 2 shows examples of mechanical transmissions for weightlifting systems in traditional and innovative cranes with gear systems that are adapted to the specific needs and specific structures of the tower crane. Figure 2a shows the work of Filippo Brunelleschi for his cranes in the construction of the Duomo of Florence in the mid-13th century as the combination of a traditional pin wheel with an innovative roller toothed wheel with remarkable, concept of high modernity, in the such as the sturdiness of the pin gear wheel is combined with the high efficiency of the roller gear wheel to limit the effects of friction in power transmission. In Fig. 2b it should

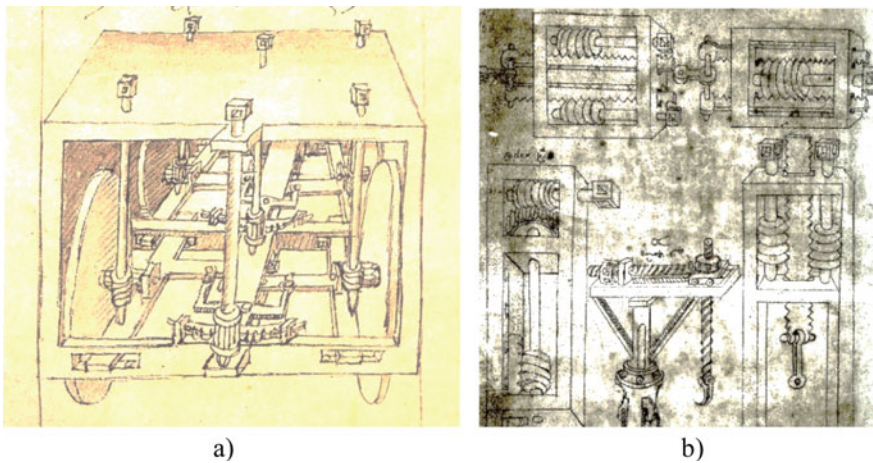


Fig. 3 Example of geared systems designed during Renaissance in: **a** steering vehicle by Francesco di Giorgio in 14th century; **b** a selection of geared solution by anonymous in 15th century

be noted how gear trains with toothed wheels of different nature are combined for the efficiency in the operation of a hoist whose functionality is not detailed to indicate the versatility of the proposed solution.

Figure 3 shows how the renewed interest in gear transmission systems has also produced innovative and widely practiced solutions. Figure 3a, [10], shows the application of gear sectors for the steering of vehicles of innovative design, as well as mechanical transmissions with orthogonal axes for the actuation of the wheels. This activity was also source and motivation of an identification of a community of experts, with anonymous and famous experts like the case of Francesco di Giorgio, [10].

In Fig. 3b practical solutions of transmissions for lifting loads by an anonymous engineer are reported as a result of a practice widespread at the end of the Renaissance. This interest in innovation and the dissemination of practical solutions can be recognized with the distinctive features of modern approaches which in the field of gears are concretized on the one hand in research activities and on the other in the industrial development of extensive production of solutions. This need for dissemination has given rise to manuals as in the case of Fig. 4 where we represent the first manual of 1588, [11], and a modern manual in 1961, [12], which report the centrality of gear solutions in the design of machines and mechanisms.

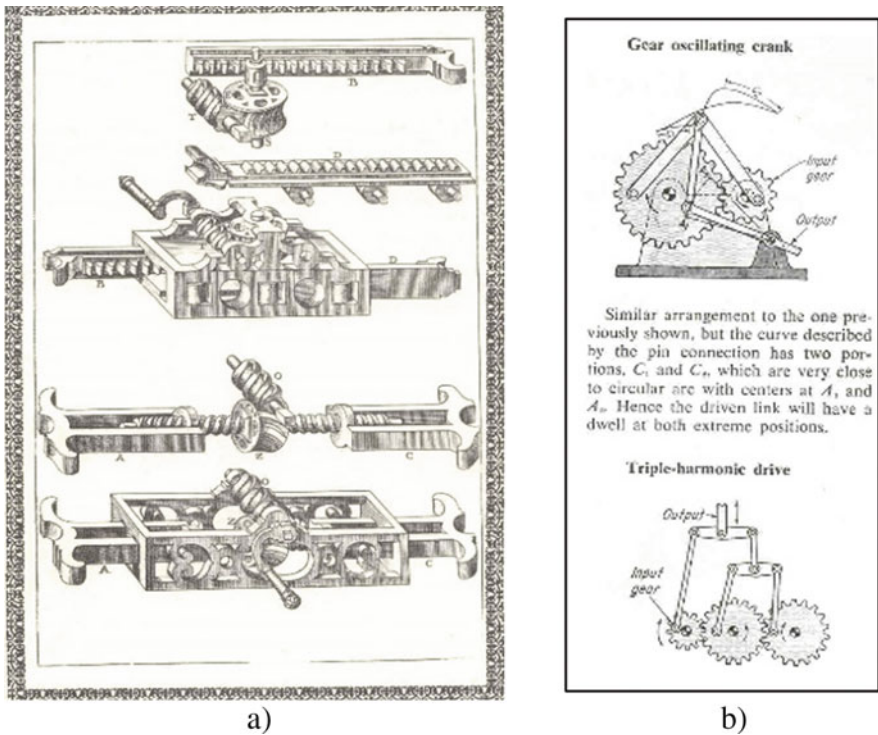


Fig. 4 Examples of collections of geared transmissions in: **a** first handbook of mechanical designs by Agostino Ramelli in 1588 [11]; **b** a modern handbook of machine design [12]

The explosive development of machines during the Industrial Revolution required and gave rise at the same time to considerable developments in the design and functionality of gears, leading to theoretical developments and manufacturing processes still valid today. Remarkable are, for example, the definition of involute profiles and various other geometric topologies as well as the notching manufacturing processes for mass production. The application of gears in all types of machines has been a source of functionality and robustness of the machines in a large variety of solutions that starting from structures for flat transmissions have also reached solutions with skewed transmission axes giving rise to the solutions shown according to the diagrams modern in Fig. 5. Furthermore, the ever-increasing need for high performance has also given rise to innovative gear inventions both in terms of train structures such as planetary solutions, as well as radically different solutions such as the harmonic drive in Fig. 6, [13]. The complexity and robustness of modern mechanical gear transmissions can be summarized by the gearbox represented in Fig. 7 with the high efficiency that can be obtained today, [14].

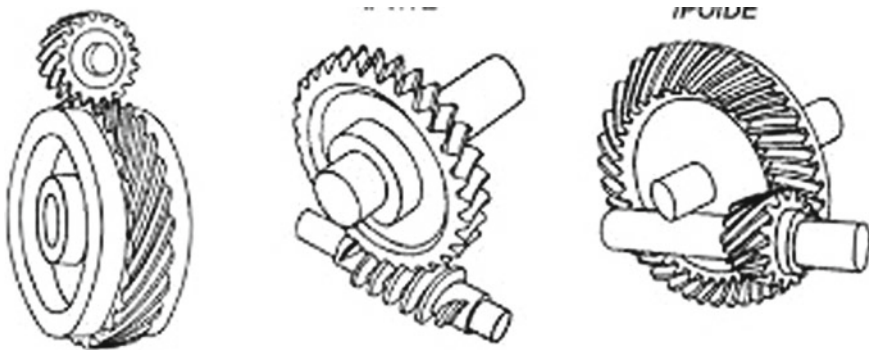


Fig. 5 Gear designs for power transmission between skew axes

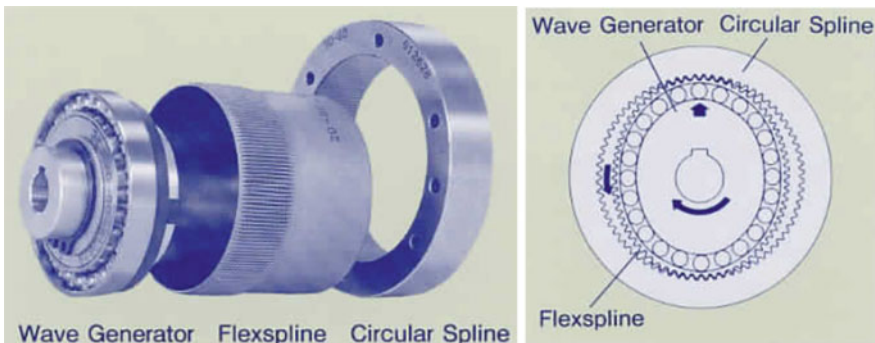


Fig. 6 The geared design of Harmonic Drive invented in 1960s [13]



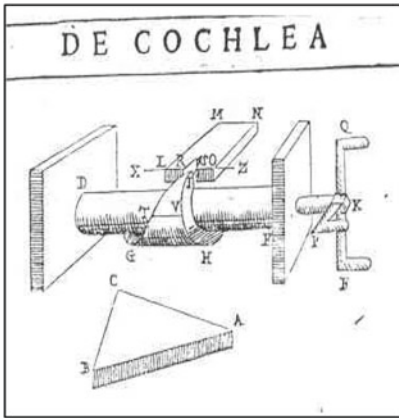
Fig. 7 A gearbox as gear train for transmission in modern vehicles

Such a significant activity with inventions by inventors and engineers can be recognized as produced by a worldwide disseminated community that today is expresses also in thematic technical-scientific committed like the IFToMM Technical Committee on Gears [15].

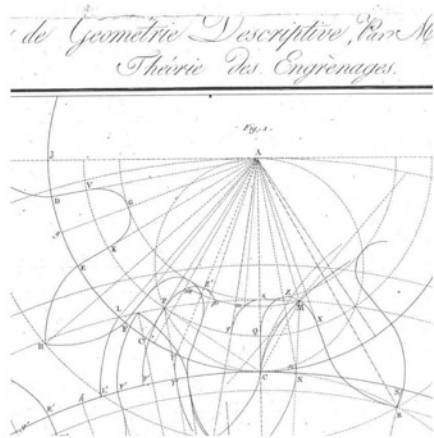
3 Modelling and Analysis

Together with the development of practical and constructive solutions, an interest was directed to a rationalization and a theory for designing the functionality of gears since the beginning of machine design. An emblematic example is a first study of mechanics in the functioning of the thread of a gear by Guidobaldo del Monte, recovering the concepts of Archimedes' mechanics in Fig. 8a [16]. The gear theory has been developing over the centuries as an application of descriptive and then analytical geometry with relevant developments not only on a theoretical but also practical level as in the example of the beginning of the 19th century shown in Fig. 8b [17], regarding the profile geometry and a study of the phenomenon of interference in involute profiles.

Figure 9 wants to summarize the further theoretical development for the design and characterization of complex gear systems using abstraction techniques and the mathematization of functionalities by reporting a current example that is relative to an epicycloid train with a representation in the form of a graph [18].



a)



b)

Fig. 8 Modelling and analysis of gear characteristics: **a** an early modern analysis of worm characteristics in geared system by Guidobaldo Del Monte in 1577, [16]; **(a)** a scheme of 19th century for operation analyse of gear profile under the risk of interference, [17]

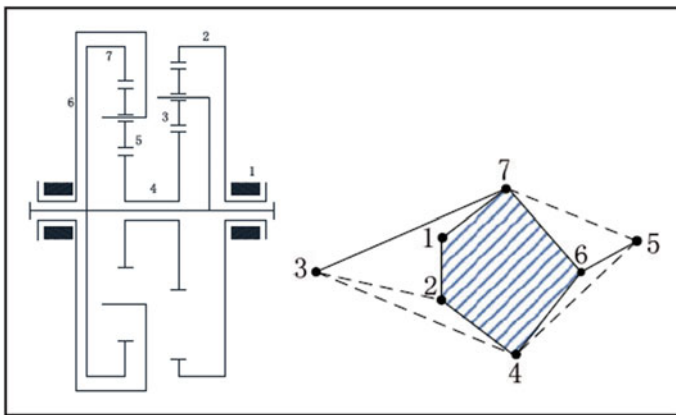


Fig. 9 A modern modelling for epicycloid gear characteristics using graph theory [18]

4 Modern Design Problems and Research Activities

Next some of the research lines in the field of gear transmission dynamics, which have been developing from the middle of the last century to the present, are presented

Özgülven and Houser [19] carried out a review of the dynamic models, establishing the following as ultimate objectives: bending and/or contact stresses in the teeth, determination of the loads acting on other elements (especially on the supports), emitted noise level, transmission efficiency, reliability, durability, tooth defects such as pitting

and scoring, natural system frequencies, vibratory movement and stability. Parey and Tandom [20], approached the simulation of the behavior of gear transmissions under fault conditions, in order to develop new maintenance strategies and procedures. To do this, they made a compilation of dynamic spur gear models that incorporate the existence of defects. Wang [21] also carried out a compilation work, focused on the non-linear aspects that characterize the dynamic behavior of gear drives. Among other aspects, he addressed the non-linearities due to variable stiffness, the presence of clearance and friction. However, as indicated in [19] it is difficult to group the different mathematical models used in the analysis of the dynamic behavior of gears given the wide variety of models proposed.

The study of the dynamic behavior of gear transmissions requires addressing different approaches related to the design and analysis of this type of elements, such as: description of the geometry of the wheels, location of contact points or areas, definition of contact forces or the formulation and resolution of dynamic equations.

Determining the geometry of the tooth profiles, as well as the development of tools and procedures for their manufacture and verification, is a fundamental aspect of gear drives. The procedure for the construction of tooth profiles that is widely accepted, using generation tools, is based on Litvin's proposal collected in various texts [22, 23], which have been evolving, incorporating new developments.

The determination of the contact points or areas between profiles can be carried out following a similar procedure to that used to obtain their geometry [24–26], in order to analyze the path or path of contact and define manufacturing settings that provide transmissions with low noise and vibration. At this point, we want to highlight the contributions of V. Goldfarb [27] on investigation of spiroid gears as well as on general issues of theory of gearing.

Regarding the study of contact efforts, different approaches must be distinguished depending on the objective pursued. Thus, on the one hand, there are those who intend to study local phenomena at the level of the contacts between teeth, such as the distribution of the load on the contact surface, the influence of the shape of the tooth on said distribution, or the tension level, with an approach it is of the quasi-static type [28, 29]. On the other hand, there are the more global approaches whose objective is to know the interaction between the different elements of the transmission and ultimately to study the dynamic behavior of the system as in [30–34].

Five different groups in the dynamic models of gear transmissions can be considered [19]: models with simple amplification factors, models with tooth flexibility, dynamic models, rotor-dynamic models and torsional models. The first proposal that considered the vibratory behavior of the transmissions has been attributed to Tuplin [35], who proposed a mass-spring model excited by means of a wedge that represented the possible shape errors of the profiles as in Fig. 10. However, this model does not consider a fundamental aspect such as the periodic nature of the excitement. Soon the need arose to incorporate this factor and the first formulations appeared that took into account the variable contact stiffness because of the oscillation in the number of pairs of teeth supporting the load as in Fig. 11.

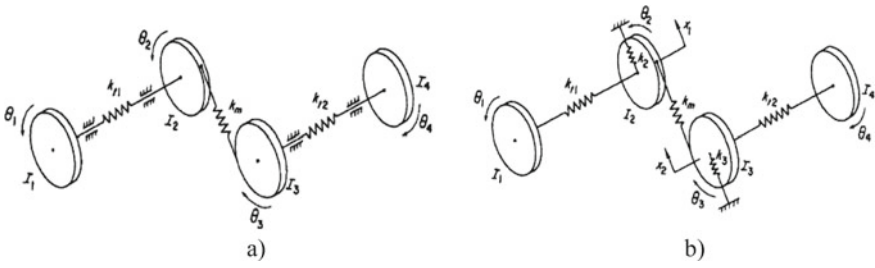


Fig. 10 Dynamical models of gears, [19]: **a** a rotational scheme; **b** a rotational-translational dynamic scheme

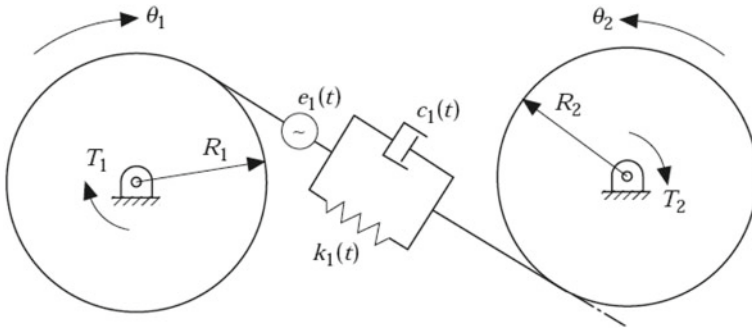


Fig. 11 A torsional model with contact in a single pair of teeth [32]

The main characteristic of this type of problem is the presence of a parametric excitation that arises as a consequence of the fluctuation in the contact stiffness, so the way to approach this aspect allows the different models developed to be classified more reasonably [36].

5 Conclusions

This paper presents a very brief account of the history but of the importance of gears with illustrative examples of design solutions and issues addressed for the development of the theory and practice of gears in machine applications. The work, even if limited in the analytical examination of the contributions and in the temporal developments, may be of interest to recognize ideas for professional practice and research activities as inspired by solutions and problems of the past.

References

1. Litvin F.L.: Developments of gear technology and theory of gearing. *J. Gearing Trans.* (2), 4–29 (1998)
2. Vullo, V.: *Gears. Volume 3: A Concise History.* Springer Series Solid and Structural Mechanics (2020). ISBN 978-3-030-40163-4
3. Dudley, D.W.: *The Evolution of the Gear Art.* Washington D.C, AGMA (1969)
4. Capocaccia, A. (Ed.): *History of Technique*, Turin, UTET (1973). (In Italian)
5. Bautista, Paz E., Ceccarelli, M., Echavarri, Otero J., Munoz Sanz, J.J.: *A brief illustrated history of machines and mechanisms*, Science and Engineering, Book series on History of Machines and Machine Science, vol. 10. Springer, Dordrecht (2010)
6. Singer, C., et al. (Eds.): *History of Technology*, Vol. 2. Boringhieri, Turin (2012)
7. Wright, M.T.: Epicyclic Gearing and the Antikythera mechanism. Part I, *Antiq. Horol.* **27**, 270–279 (2003)
8. Koetsier, T.: Phases in the unraveling of the secrets of the gear system of the Anti-kythera mechanism. In: Yan, H.S., Ceccarelli, M. (eds.) *International Symposium on History of Machines and Mechanisms*, pp. 269–294. Springer, Dordrecht (2009)
9. Ceccarelli, M.: Renaissance of Machines in Italy: from Brunelleschi to Galilei through Francesco di Giorgio and Leonardo. *Mech. Mach. Theory* **43**, 1530–1542 (2008)
10. Ceccarelli, M.: Contributions of Francesco di Giorgio in Mechanism Design, *Anales de Ingeniería Mecánica*, Año 21, UNED, Madrid, Septiembre, pp. 352–362 (2018)
11. Ramelli, A.: *Le Diverse et Artificiose Machine*, Paris (1588)
12. Chironis, F.: *Mechanisms, Linkages, and Mechanical Controls.* McGraw-Hill, New York (1961)
13. Musser, C.W.: US Patent No. 2,906,14 (1959)
14. Goldfarb, V., Trubachev, E., Barmina, N.: Innovations in design and production of spiroid gears in the XXI century. In: *Power Transmissions 2019-MATEC Web of Conferences*, vol. 287, p. 01002 (2019)
15. IFiOMM; IFotm webpage. www.iftomm.net. Accessed ob 3 Feb 2021
16. Del Monte, G.: *Mechanicorum Liber*, Apud Hieronymum Concordiam, Pisauri (1577)
17. Hachette, J.N.P.: *Traité Elementaire Des Machines*, Paris (1811)
18. Xue, Hui-Ling., Liu, Geng, Yang, Xiao-Hui: A review of graph theory application re-search in gears. *Proc. IMechE Part C: J. Mech. Eng. Sci.* **230**(10), 1697–1714 (2016)
19. Özgüven, H.N., Houser, D.R.: Mathematical models used in gear dynamics: a review. *J. Sound Vib.* **121**(3), 383–411 (1988)
20. Parey, A., Tandon, N.: Spur gear dynamic models including defects: a review. *Shock Vib Dig.* **35**(6), 465–478 (2003)
21. Wang, J., Li, R., Peng, X.: Survey of nonlinear vibration of gear transmission systems. *Appl. Mech. Rev.* **56**(3), 309–329 (2003)
22. Litvin, F.L.: *Theory of Gearing*, Nauka, Moscow, (in russian) (1960)
23. Litvin, F.L., Fuentes, A.: *Gear Geometry and Applied Theory*, 2nd edn. Cambridge University Press, UK (2004). ISBN 0-521-81517-7
24. Argyris, J., Fuentes, A., Litvin, F.L.: Computerized integrated approach for design and stress analysis of spiral bevel gears. *Comput. Methods Appl. Mech. Eng.* **191**(11–12), 1057–1095 (2002)
25. Zhang, J., Fang, Z., Cao, X., Deng, X.: The modified pitch cone design of the hypoid gear: manufacture, stress analysis and experimental test. *Mech. Mach. Theory* **42**(2), 147–158 (2007)
26. Seol, I.H., Litvin, F.L.: Computerized design, generation and simulation of meshing and contact of worm-gear drives with improved geometry. *Comput. Methods Appl. Mech. Eng.* **138**(1–4), 73–103 (1996)
27. Goldfarb, V.I., Isakova, N.V.: Variants of spiroid gearing from pitch realization point of view. *J. Gearing Transm* **1**, 25–34 (1995)
28. Vedmar, L.: *On the design of external involute helical gears.* Transactions of Machine Elements Division. Lund Technical University (1981)

29. Pedrero, J.I., Pleguezuelos, M., Artés, M., Antona, J.A.: Load distribution model along the line of contact for involute external gears. *Mech. Mach. Theory* **45**, 780–794 (2010)
30. Kahraman, A.: Effect of axial vibrations on the dynamics of a helical gear pair. *J. Vib. Acoust.* **115**(1), 33–39 (1993)
31. Theodossiades, S., Natsiavas, S.: On geared rotordynamic systems with oil journal bearings. *J. Sound Vib.* **243**(4), 721–745 (2001)
32. Amabili, M., Rivola, A.: Dynamic analysis of spur gear pairs: steady-state response and stability of the SDOF model with time-varying meshing damping. *Mech. Syst. Signal Process.* **11**(3), 375–390 (1997)
33. Vexel, P., Maatar, M.: A mathematical model for analyzing the influence of shape deviations and mounting errors on gear dynamic behaviour. *J. Sound Vib.* **191**(5), 629–660 (1996)
34. Fernandez, A., Viadero, F., Iglesias, M., Garcia, P., de-Juan, A., Sancibrian, R.: A model for the study of meshing stiffness in spur gear transmissions. *Mech. Mach. Theory* **61**, 30–58 (2013)
35. Tuplin, W.A.: Dynamic loads on gear teeth. *Mach.* (1953)
36. Kahraman, A., Singh, R.: Interactions between time-varying mesh stiffness and clearance nonlinearities in a geared system. *J. Sound Vib.* **146**(1), 135–156 (1991)

Theory of Adaptive Transmission



Konstantin Ivanov 

Abstract The adaptive transmission (AT) represents the gearing with constant meshing of toothed wheels and with a variable gear ratio. Animation model AT is placed on an author's site (<https://adaptation.kz>). The transmission has a simple design. It works without a control system. It corresponds to a modern line of creation of the independent self-controlling car. The transmission is created on the basis of an author's invention «Effect of Force Adaptation in Mechanics». The essence of the invention—a planetary kinematic chain with two degrees of freedom in which toothed wheels form the mobile closed contour adapted for a variable load. Definability of the motion is attained by introduction of the closing transmission jamming the closed contour and the hydrostatical converter (dashpot) which is wedging out the closed contour strictly definitely. The converter provides relative motion of links with the speed depending on loading (creates the constraint of speed and force). The principle of definability of motion of the kinematic chain with two degrees of freedom and with one input on the basis of interconnection of parameters of the hydrostatical converter and closing transmission is developed. In the paper the theory of force adaptation in a combination with the definability principle which allows creating the effective and reliable stepless self-controlled gearbox is presented.

Keywords Self-regulation · Adaptive transmission · Hydrostatical converter

1 Introduction. Adaptive Transmissions

The adaptive transmission (AT) is a mechanism that independently changes the gear ratio depending on the resistance to motion. The AT contains a kinematic chain with two degrees of freedom and an additional constraint that ensures the definability of the movement. Nowadays, the continuously varying transmission (CVT)—an automatic step transmission has become widespread [1]. But the stepped CVT is not an adaptive

Konstantin Ivanov (✉)

Almaty University of Power Engineering and Telecommunication, Almaty, Kazakhstan
e-mail: ivanovgreek@mail.ru

transmission as it requires the use of a control system. Self-regulation in CVT within one stage is provided by a hydrodynamic converter.

The author suggested using a self-braking transmission to create AT without a converter [2], but the design was not tested experimentally. Attempts by Crockett [3] and Volkov [4] to use a hydrodynamic converter in combination with constant-mesh transmission were unsuccessful—the transmission was not widely used due to its low control range. Harris patented the AT in the form of a planetary mechanism with two degrees of freedom and one input without a hydrodynamic converter [5]. However, a mechanism with two degrees of freedom cannot work reliably without an additional constraint.

The author developed the theory of force adaptation [6–9] based on the use of the principle of virtual work. It has been proven that a closed contour in a two-mobile kinematic chain creates an additional constraint and provides force adaptation to variable external load. The found regularities constituted the scientific discovery “Effect of force adaptation in mechanics”. However, the force adaptation determines only necessary adaptation condition that takes place in the motion mode with two degrees of freedom.

At the start in one-mobile mode of movement to overcome the starting resistance, it was proposed to use a scheme with an approximately dead position of the mechanism (two-row planetary gear with input and output carriers of the AT length), which creates a sufficient adaptation condition [10–12]. On the basis of this theory, a number of copyright patents were created [13–15]. However, the experiment showed that adaptation is possible only if there is sufficient internal friction in the mechanism [16].

The further researches have been directed on search of conditions of reliable start with transition to a two-mobile regime of motion. Earlier in the course of research of the circuit design of the mechanism some point theoretically connecting divided links (the centre of coincidence of speeds) [10, 11, 17] has been detected. Use of this point allows to keep relative mobility of links at superposition of restriction on their motion, or to create real constraint at conservation of number of a degree of freedom. With that end in view the initial kinematic chain with two degree of freedom is carried out in the form of the mechanism in a dead position. The additional mobile constraint is inducted into this mechanism in the form of the gearing with a pitch point in the centre of coincidence of speeds. This additional mobile constraint provides a continuous exit of the mechanism from a dead rule and allows to create the reliable self-controlled mechanism [17, 18]. However such way simply inducts redundant constraint which does not change power interacting.

The analysis of the force interaction of the parameters of the two-movable kinematic chain showed that the principle of virtual work does not guarantee equilibrium, since the reaction in the motionless instant center of speeds of some link remains unbalanced [19]. The author proposed to introduce an additional frictional force into the two-mobile chain, replacing the unbalanced reaction [19, 20].

To ensure the reliability of the mechanism, a power activation of the closed contour by adding real force constraint is required. However, this connection must keep the closed contour mobility. Consequently, the additional constraint must be a constraint of a fundamentally new type. It must impose a strictly defined limitation of movement

while maintaining the relative mobility of the links. It is advisable to develop a general principle of definability of the motion of the two-movable kinematic chain of the AT.

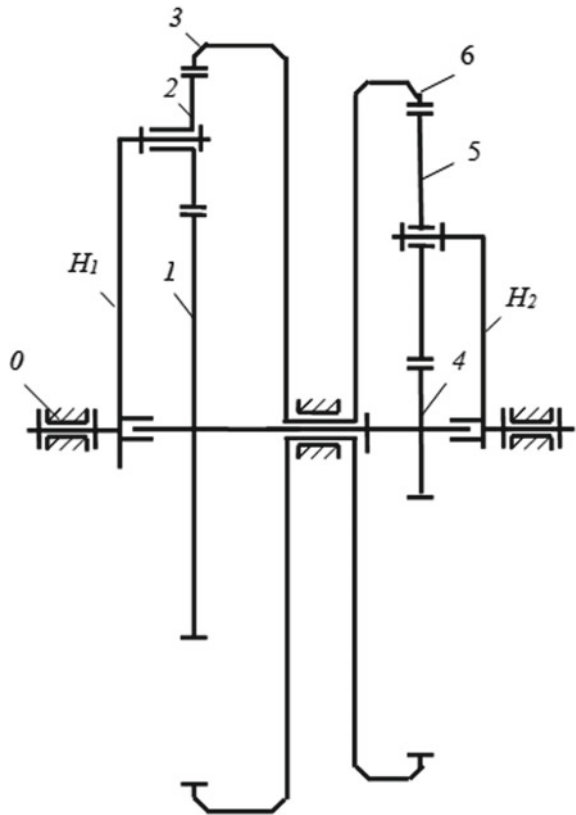
The paper presents the theoretical foundations for the creation of adaptive transmission in the form of the theory of force adaptation in combination with the principle of definability of motion.

2 Stages of Creating of Adaptive Transmission

The simplest adaptive transmission (see Fig. 1) is a two-movable gear mechanism with a closed contour. The mechanism contains the rack 0, input carrier H_1 , closed contour of gears 1-2-3-6-5-4 and output carrier H_2 . The closed contour contains the input satellite 2, block of sun wheels 1-4, block of ring wheels 3-6 and output satellite 5.

The basis for the creation of AT is the theory of force adaptation of a two-mobile mechanism with one input, using the effect of force adaptation [6...9]. This theory

Fig. 1 The simplest adaptive transmission



is based on performing a force analysis of a mechanism using the principle of virtual work. The performed strength analysis leads to obtaining the main condition of force adaptation

The effect of force adaptation has the following essence: for a given constant parameters of the input power M_{H1} , ω_{H1} and a given output moment of resistance M_{H2} , the output angular velocity ω_{H2} is inversely proportional to the variable output moment of resistance M_{H2} . This is a necessary adaptation condition, which theoretically determines the creation of an additional connection in a two-movable kinematic chain.

The interaction of kinematic and power parameters is carried out according to the principle of possible work using real displacements.

As a result of the force analysis, the equilibrium condition for external forces was obtained

$$M_{H1}\omega_{H1} + M_{H2}\omega_{H2} = 0. \quad (1)$$

Equation (1) analytically represents a connection between the parameters of the kinematic chain, additional to the conditions of statics.

The combination of two degrees of freedom with an additional constraint ensures that the output angular velocity depends on the external load. This property follows from Eq. (1) taking into account the negative sign of the output power

$$\omega_{H2} = M_{H1}\omega_{H1}/M_{H2}. \quad (2)$$

Equation (2) expresses the effect of force adaptation in mechanics—the output angular velocity is inversely proportional to the output moment of resistance at constant input power.

The following stages of the creation of the AT theory take place.

- (1) Development of the theory of force adaptation based on the use of a two-lift mechanism with a movable closed contour. The basis is the necessary condition for force adaptation—the presence of a closed contour.

A two movable gear mechanism with a closed contour, developed by the author [2], is an adaptive gear variator that implements the scientific discovery “The effect of force adaptation in mechanics” [6–8].

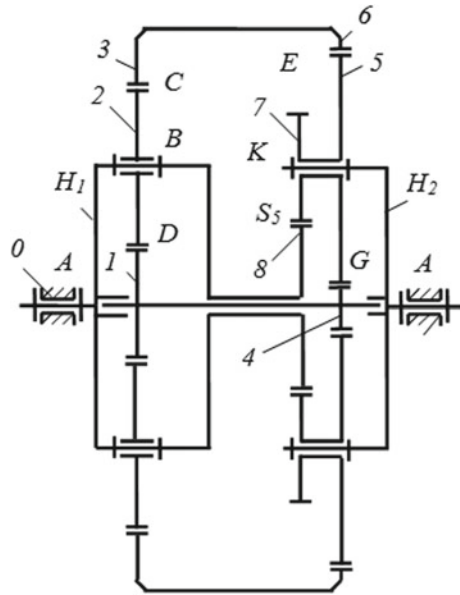
The definability of this mechanism must be provided with a closed contour.

The mechanism theoretically fulfills the necessary condition for force adaptation (Eq. 2).

However, the mechanism cannot provide reliable operation due to the presence of two degrees of freedom. It limits the ability to start movement (start) in the presence of starting resistance.

- (2) Development of a sufficient condition for force adaptation based on the use of redundant constraint. The basis is a gear mechanism with a closed contour and

Fig. 2 Adaptive transmission with a closed contour and redundant constraint



redundant constraint in the form of a dead position (Fig. 2). This redundant connection determines a sufficient condition for force adaptation.

For stage 2, theoretical and experimental studies were carried out [16, 17].

The structure of the mechanism is similar to the previous diagram (Fig. 1). The mechanism has a redundant connection in the form of a dead position created by the equality of the lengths of the input H_1 and output H_2 carriers $r_{H1} = r_{H2}$. As a result, the lines of action of external forces coincide. This leads to the creation of an additional connection and to jamming at the start. After the start, wedging is performed by an additional backup gear 8-7, which transfers the movement from the input carrier H_1 to the satellite 5.

A prototype of the mechanism has been developed (Fig. 3), a spatial image of the parts is presented (Fig. 4), and a test bench has been created to test the effect of force adaptation (Fig. 5).

The following devices are shown on the test bench: base (traction) motor 1, variator with adaptive transmission 2, auxiliary (braking) motor 3, dashboard 4, monitor 5.

Based on the data obtained, the traction characteristic of the variator was built (Fig. 6).

The effect of force adaptation takes place (Fig. 6): for given constant parameters of the input power M_{H1} , ω_{H1} and a given output torque of resistance $M_R = M_{H2}$ the output angular velocity $\omega_R = \omega_{H2}$ is inversely proportional to the variable output torque of resistance $M_R = M_{H2}$.

The analysis of the definability of movement showed that a closed contour imposes a connection only theoretically (based on the principle of virtual work). In this case, the effect of force adaptation is manifested only due to the presence of internal friction

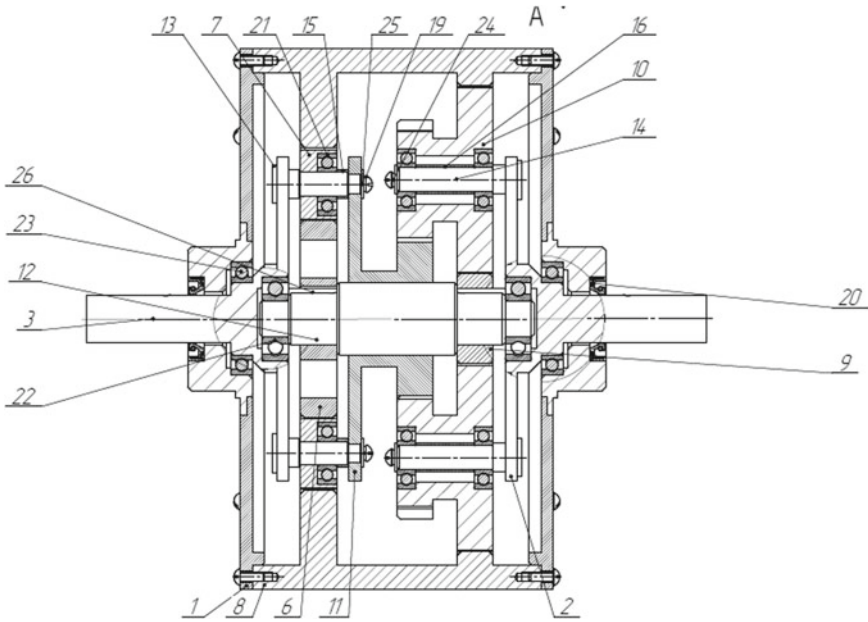


Fig. 3 Assembly drawing of adaptive transmission

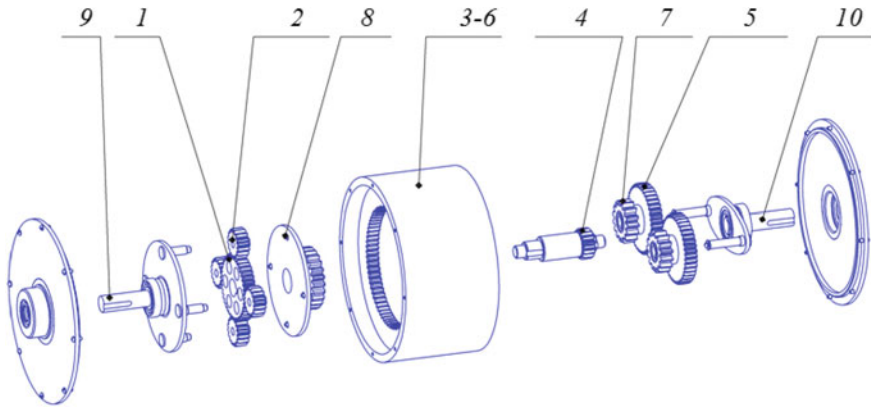


Fig. 4 Spatial image of adaptive transmission parts. 9—input carrier, 2—input satellite, 1—4—block of solar wheels, 8—toothed wheel of doubling transfer 8-7 with a disk affiliated to the carrier 9, 3-6—block ring wheels, 4—solar wheel with the shaft to which the solar wheel 1 is affiliated, 7—toothed wheel of doubling transfer 8-7, 5—output satellite in the block with a wheel 7 of doubling transfers, 10—output carrier

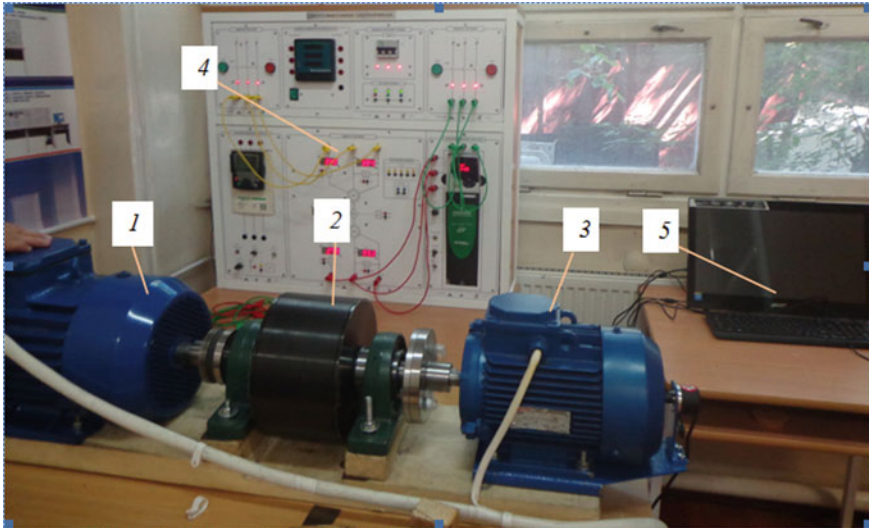
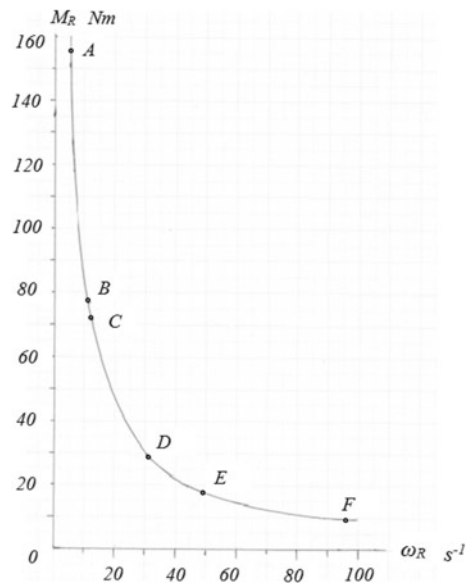


Fig. 5 Test bench of the adaptive transmission (toothed variator)

Fig. 6 Experimental traction characteristic of the adaptive transmission (toothed variator)



in the relative movement of the transmission links within narrowly limited limits. Obviously, to activate the closed contour, a real link must be added to it. However, this connection must keep the closed contour mobility. Consequently, the additional link must be a link of a fundamentally new type. It must impose a restriction on movement while maintaining the relative mobility of the links.

Conclusion: the mechanism fulfills the necessary and sufficient conditions for force adaptation in the form of a closed contour and additional redundant constraint. However, the definability of the movement takes place within limited limits.

3 Analysis of Determinability of Motion of Two-Mobile Chain

First, let us analyze the determinability of the movement of a lever two-movable kinematic chain with one input. The kinematic chain (Fig. 7) contains a rack 0, an input link 1, an intermediate link 2, and output links 3 and 4.

To the right of the mechanism is a plan of the linear speeds V_i $i = 1, 3, 4$ of the links of the mechanism. S —instantaneous center of speeds of link 2; $\omega_2 = V_1/SB$ —angular velocity of link 2. Linear dimensions of links $BC = BD$. External forces act on the mechanism: F_1 —input driving force, R_3, R_4 —output resistance forces. Forces and speeds are parallel to the axis Ox .

The mechanism has two degrees of freedom, which correspond to the translational and rotational motion of link 2.

Let us formulate the condition of equilibrium of the mechanism according to the principle of possible works.

$$F_1 V_1 - R_3 V_3 - R_4 V_4 = 0. \tag{3}$$

Equation (3) reflects the functional essence of the two moving mechanism: for the given constant parameters of the input power and the given resistance forces, the speeds of the two output links are unknown (to be determined).

The speeds of the points of the mechanism are related by the equation

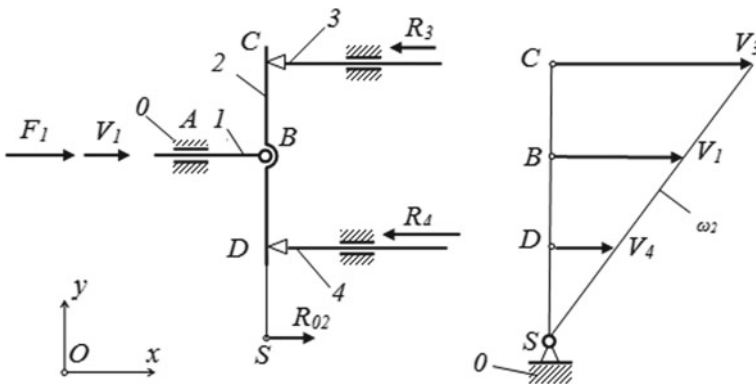


Fig. 7 Lever two movable kinematic chain

$$\frac{V_3 - V_1}{V_4 - V_1} = u_{34}^{(1)}. \quad (4)$$

Here $u_{34}^{(1)}$ —gear ratio from link 3 to link 4 with fixed link 1. $u_{34}^{(1)} = -BD/BC$.

The system of two Eqs. (3) and (4) determines the relationship of the parameters of the mechanism with two degrees of freedom and allows for the given parameters of the mechanism F_1, V_1, R_3, R_4 to determine two kinematic parameters—the speed of the two output links V_3, V_4 .

Solving the system of two Eqs. (3) and (4), we obtain

$$V_4 = V_1 \frac{F_1 + R_3(u_{34}^{(1)} - 1)}{R_3 u_{34}^{(1)} + R_4}, \quad (5)$$

$$V_3 = (1 - u_{34}^{(1)})V_1 + u_{34}^{(1)}V_4. \quad (6)$$

Thus, Eqs. (5) and (6) confirm the status of the principle of possible displacements as a necessary and sufficient condition for equilibrium [17].

However, contrary to this statement, there is no definability of motion in the two movable mechanism. If $R_3 = R_4$, then there is no torque on link 2 and the mechanism will go into a state with one degree of freedom.

If $R_3 \neq R_4$, then the more loaded output link will be motionless and the mechanism will also go into a state with one degree of freedom.

To resolve this contradiction, let us analyze the interaction of parameters in two moving mechanisms.

Equation (5) corresponds to the equilibrium equation of link 2 in the form of the sum of moments relative to the instantaneous center of velocities S , taking into account the substitutions $V_1 = \omega_2 \cdot SB$, $V_3 = \omega_2 \cdot SC$, $V_4 = \omega_2 \cdot SD$ and equality of external forces to the reactions at the points B, C, D : $F_1 = R_{12}$, $R_3 = R_{32}$, $R_4 = R_{42}$. After substituting these values and canceling ω_2 , we obtain the equation of moments about the point S

$$F_1 \cdot SB - R_3 \cdot SC - R_4 \cdot SD = 0. \quad (7)$$

Equation (7), corresponding to Eq. (3), is not a necessary and sufficient condition for the equilibrium of the statics for link 2. In addition to the Eq. of moments for the equilibrium of link 2 and the entire mechanism, the condition of equality of forces to zero should also be used $\sum F = 0$

$$F_1 - R_3 - R_4 + R_{02} = 0,$$

where R_{02} is the reaction at a fixed point S .

$$R_{02} = R_3 + R_4 - F_1. \quad (8)$$

Therefore, the equilibrium equation of the mechanism, according to the principle of possible displacements, must also take into account the force R_{02} . However, this force in Eq. (5) is excluded, since the velocity of the point of application S is zero.

Consider what happens if it turns out $R_4 > R_3$. To move the point D of application of greater force R_4 , it is necessary to fulfill the equilibrium condition $\sum M_C = 0$ (or $F_1 \cdot BC + R_{02} \cdot SC - R_4 \cdot DC = 0$) which includes the force R_{02} . However, in the absence of real support at the point S , the force R_{02} does not exist.

As a result, the point D of application of the greater force will be fixed.

In connection with this circumstance, an insoluble contradiction arises: on the one hand, in two moving mechanism, link 2 must have a fixed reference point with a reaction R_{02} , on the other hand, the addition of this connection will lead to the transition of the mechanism into a one-movable state.

It would seem that the presence of two inputs (links 3 and 4) and one output (link 1) would make the chain in question definable. However, changing the status of the links does not eliminate the need to have a real fixed point S of link 2 to achieve equilibrium.

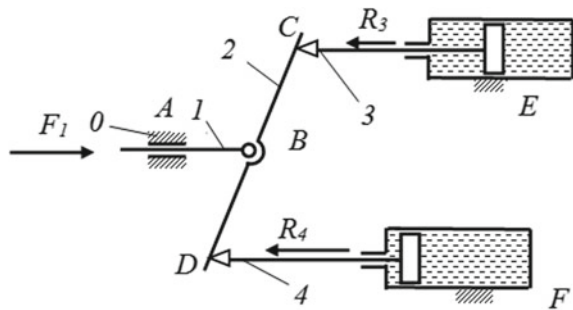
The analysis of the relationship between the parameters of the two-moving kinematic chain shows that the two-moving kinematic chain is a statically indeterminate system.

However, it is quite possible to create a fixed position of the free (not connected with the rack) link 2 by external forces. On Fig. 8, the input hydraulic cylinders set in motion the pistons and links 3 and 4. The positions of the pistons depend on the speed and determine the positions of the points C and D of link 2 in the absence of its connection with the rack. The displacements of the points of application of forces corresponding to time will be called forced. The motors create forced displacements.

Hence, the conclusion follows: the static indeterminacy of a two-moving kinematic chain causes an intermediate free link with an instantaneous center of velocities, which must have a fixed support. Quite definite forced displacements of the free link, not connected with the rack, can be provided only by forces that have an unambiguous fixed position of the points of application at any time.

The force of resistance can create forced displacement by means of a cataract (Fig. 9). The cataract contains a piston 1 with calibrated bypass holes and a hydraulic cylinder 2.

Fig. 8 Creation of a forced position of an uncontrollable chain by external compelling forces



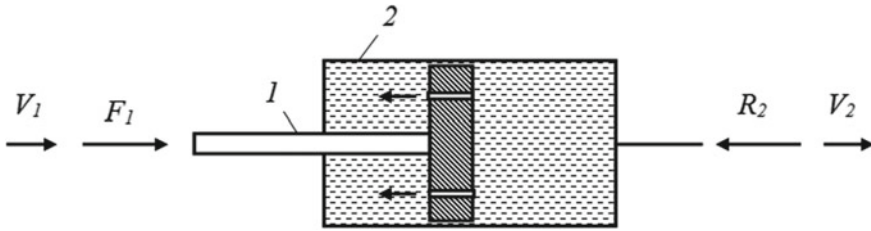


Fig. 9 Linear dashpot (cataract)

The principle of operation of a cataract is to create a forced relative movement of the links by passing a viscous fluid between the links using internal friction. The position of the point of application of the resistance force depends on the liquid flow rate through the bypass holes.

If in Fig. 8 the driving hydraulic cylinders 3 and 4 should be replaced with cataracts connected to the rack by translational kinematic pairs *E* and *F* then the resulting kinematic chain with an input link 1 and two output links in the form of cataracts will acquire a definite motion, since the output speeds of the cylinders depend on the resistance forces. In this case, the intermediate link 2 will be completely balanced, and the reaction will be at the instantaneous center of speeds $R_{02} = 0$.

Cataract works as follows.

The input force F_1 (Fig. 9) moves the piston 1 at a speed V_1 . The resistance force $R_2 > F_1$ prevents the movement of cylinder 2, which moves at a speed $V_2 < V_1$ due to the liquid bypass through the bypass holes. There is a relative movement of the links with speed $V_{12} = V_1 - V_2$ under the action of the force of the cataract $F_{12} = R_2 - F_1$. The relative velocity is related to the liquid flow through the bypass holes

$$V_{12} = v/A, \tag{9}$$

where *A* is the cross-sectional area of the cylinder,

v is the liquid flow rate through the bypass holes.

The fluid flow rate *v* is directly proportional to the pressure *p* generated by the forces.

Power of cataract

$$P_C = F_{12}V_{12}. \tag{10}$$

The power of the cataract is spent on overcoming the internal friction of the fluid and performs a useful function—creating a forced movement of the output link 2.

The characteristic of cataract is an experimental relationship $F_{12} = f(V_{12})$ and depends on the ratio of the cross-sectional area of the piston to the area of the bypass holes. Simplified $F_{12} = kV_{12}$ (*k* is the experimental coefficient).

The relationship between the parameters of movement of the cataract is determined by the principle of possible movements, taking into account the power of the cataract

$$F_1 V_1 - R_2 V_2 - F_{12} V_{12} = 0. \tag{11}$$

After substituting the values $V_{12} = V_1 - V_2$, $F_{12} = F_2 - F_1$ and transformations into Eq. (11) we obtain

$$V_2 = V_1 \frac{2F_1 - F_2}{F_1}. \tag{12}$$

From here we determine the limits of changes in the output force and output speed of the cataract $F_1 < F_2 < 2F_1$, $0 < V_2 < V_1$.

Gear ratio cataract $u_{12} = V_1/V_2$ or $u_{12} = F_1/(2F_1 - F_2)$. Here $1 < u_{12} < 2$.

Efficiency of cataract taking into account the loss factor $\varepsilon = F_{12} V_{12}/F_1 V_1$

$$\eta = 1 - F_{12} V_{12}/F_1 V_1. \tag{13}$$

Thus, the forced relative translational movement of the links is created by a cataract, which performs this action by spending energy.

Forced relative rotational movement of the links can be created in a similar way using a rotary cataract.

Rotational cataract (Fig. 10) contains an input shaft 1 with a rotating piston in the form of a blade having bypass openings, and an output shaft 2 with a cylinder also having blades that allow free rotation of the piston blade. The cylinder is filled with a viscous liquid.

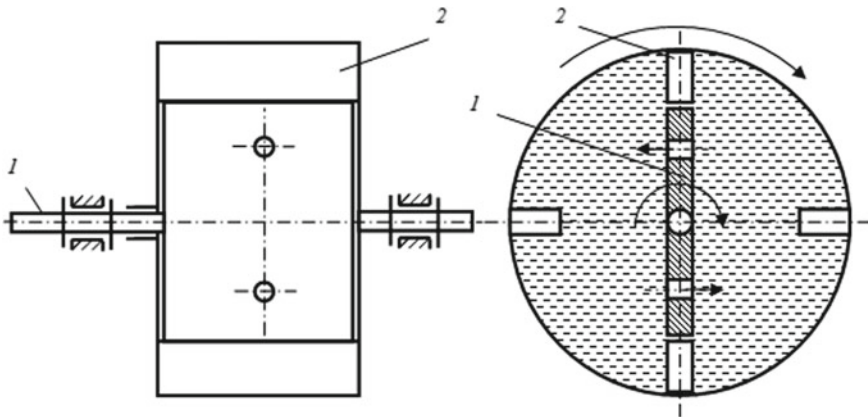


Fig. 10 Rotational dashpot (cataract)

The input shaft 1 of a rotating cataract with a driving moment M_1 rotates a piston with a blade, which carries with it a viscous liquid. A viscous liquid located between the blades of the cylinder carries with it the cylinder, on the shaft 2 of which there is a moment of resistance M_2 . Bypass holes in the piston blade provide a bypass of rotating fluid when the piston rotates relative to the cylinder. Rotating cataracts allow rotation of the input and output shafts at different angular velocities ω_1 and ω_2 . In the operating mode of movement, the moment of resistance to the movement of the cylinder M_2 exceeds the driving moment M_1 . The moment of cataract is $M_{12} = M_2 - M_1$. The input shaft with a driving moment M_1 provides a rotational movement of the output shaft 2 with an angular velocity $\omega_2 < \omega_1$ due to the liquid bypass through the bypass holes. Under the influence of the moment M_{12} the cataract moves links 1 and 2 with a relative angular velocity $\omega_{12} = \omega_1 - \omega_2$.

Power cataract

$$P_C = M_{12}\omega_{12} = (M_2 - M_1)(\omega_1 - \omega_2). \quad (14)$$

The characteristic of a cataract is determined by the capacity of the bypass holes (the ratio of the area of the blade of the rotating piston 1 to the area of the bypass holes), depending on the pressure. In a cataract with a given characteristic, the relative angular velocity corresponds to the applied external moments.

Rotational cataract provides a fixed position of the output shaft with a moment of resistance M_2 applied to it, depending on the fluid flow through the bypass holes. The fixed position of the output shaft 2 is determined by the angle of rotation φ_2 which depends on the speed of the cataract.

The relative angular velocity is related to the fluid flow rate through the bypass holes

$$\omega_{12} = v/rA, \quad (15)$$

where A is the area of the blade of the rotating piston,

v is the fluid consumption,

r is the radius of the location of the bypass holes.

The fluid flow rate v is directly proportional to the pressure p generated by the input and output torque.

The power of the cataract is spent on overcoming the internal friction of the fluid, but it performs a useful function—creating time-fixed movements of the output link.

The relationship between the parameters of movement of a cataract is determined by the principle of possible displacements, taking into account the power spent on internal friction

$$M_1\omega_1 - M_2\omega_2 - P_C = 0. \quad (16)$$

Here the moment of the cataract is equal to the moment of internal friction of the fluid, which ensures the overflow of the fluid through the bypass holes $M_{12} = M_f$.

Substituting the value P_k into Eq. (16), we obtain after transformations the dependence of the output angular velocity on the moment of resistance (adaptation equation for cataract)

$$\omega_2 = \omega_1(2M_1 - M_2)/M_1. \quad (17)$$

Equation (17) expresses the analytical relationship that a cataract with a given characteristic imposes on the variable parameters M_2 and ω_2 . With constant input power parameters M_1 , ω_1 the torque reference M_2 determines the value of the angular velocity ω_2 and the angular displacement of the output link 2, fixed in time.

From Eq. (17) implies:

When $M_2 = M_1$ we have $\omega_2 = \omega_1$. When $M_2 = 2M_1$ we have $\omega_2 = 0$.

Resistance torque range

$$M_1 \leq M_2 \leq 2M_1.$$

There is also a feedback

$$M_1 \leq M_2 \leq 2M_1. \quad (18)$$

Efficiency cataract $\eta = 1 - P_K/M_1\omega_1$. Or

$$\eta = 1 - \frac{(M_2 - M_1)(\omega_1 - \omega_2)}{M_1\omega_1}. \quad (19)$$

In the range of variation of the moment of resistance, the efficiency varies from 0 to 1.

Intermediate value at $M_2 = 2M_1$, $\omega_2 = 0.5\omega_1$, $\eta = 0.75$.

The use of a cataract, which imposes an additional connection on one of the speeds, in a system with two degrees of freedom leads to definability of motion without loss of properties associated with the presence of two degrees of freedom.

4 Principle of Determinability of Motion of Adaptive Transmission

The essence of the method of definiteness of movement: definiteness of the movement of two movable kinematic chain Self-adjusting transmission provides cataracts, which imposes an additional connection in the form of a function of the relative position of cataract links from speed. In this case, energy is consumed for the relative movement of the links (for the internal friction of the fluid).

In order to provide the specified range of Self-regulation, it is necessary to combine the force adaptation with the hydrostatic converter (cataract). The closed loop must provide force adaptation, and the hydrostatic transducer ensures motion definability. In this case, the range of self-regulation increases in the presence of small required relative displacements of cataract links by creating a stressed power state of a closed loop with the introduction of an additional redundant connection.

Structurally, the motion determinability method is implemented as follows. First, a jamming link is introduced into the movable closed loop, which imposes an additional connection. The wedge link is then replaced by a cataract, adding a functional degree of freedom (relative position dependent on speed).

The jamming link should be made in the form of a link that introduces an excess geometric connection, which turns into a real connection by minimally changing the corresponding geometric parameter. In this case, a small geometric deviation leads to the appearance of a large force on the wedge link. After replacing the wedge with cataract, the wedge force will self-adapt to the minimum relative speed of movement according to the characteristic of the cataract. Cataracts have a direct effect on the closed loop, which transmits movement to the output link of the transmission. Placing a cataract in a closed loop provides an indirect effect on the output link, which leads to a high control range with high **efficiency**.

5 Creation of Definable Adaptive Transmission

Definable adaptive transmission (Fig. 11a) contains the basic adaptive two-mobile kinematic chain in an aspect two-row planet gear H_1 -1-2-3-6-5-4- H_2 and additional force-speed constraint in the form of a rotational dashpot 9 with closing transmission 8-7. On Fig. 11b the plot of linear speeds of the gearbox is presented.

The blade 9 of the cataract in composition of AT (Fig. 11a) is connected with input carrier H_1 and the cylinder is connected with a wheel 8 of closing transmissions 8-7 passing motion on the satellite 5. This constraint becomes active and calls the forced power interacting in the closed contour if the pitch point P of wheels 8 and 7 does not coincide with point S_5 —the centre of coincidence of speeds of links H_1 and 5. Further for simplification we will use designation S instead of S_5 . (A dot line shows the wheel 8 creating passive constraint when point P coincides with point S . In this case, the peripheral speeds of the blade and cylinder coincide and the cataract does not work). An additional link in the form of a cataract with the 8-7 gear provides the definition of the movement of the two-way chain.

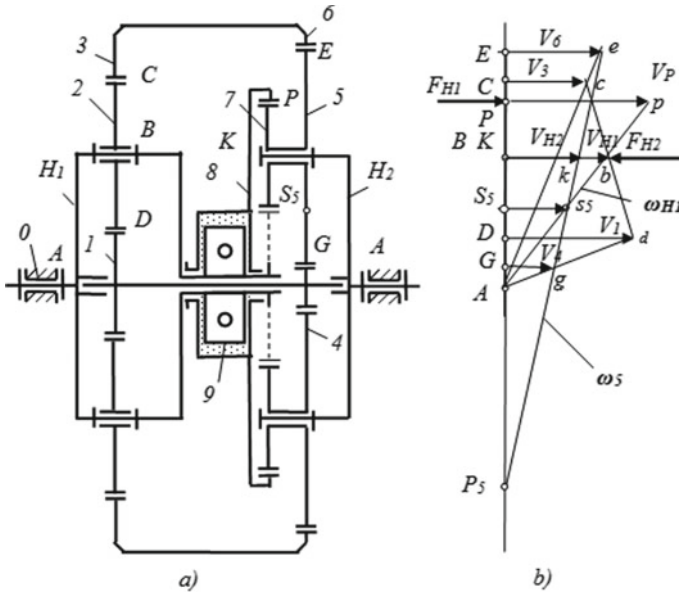


Fig. 11 Self-controlled gearbox SCG

6 Kinematic and Force Analysis of Basic Two-Mobile Kinematic Chain. Force Adaptation

The kinematic analysis of the basic two-mobile kinematic chain (Fig. 11a) is carried out by traditional way [6, 7 and 8] and consists in definition of all kinematic parameters.

The force analysis is based on use of the virtual work principle for the kinematic chain containing a mobile closed contour [6, 7 and 8]. Analytically constraint of parameters of the two-mobile kinematic chain containing a mobile closed contour is expressed by formulas

$$F_{H1}V_{H1} + F_{H2}V_{H2} = 0, \tag{20}$$

$$M_{H1}\omega_{H1} + M_{H2}\omega_{H2} = 0. \tag{21}$$

From here

$$\omega_{H2} = M_{H1}\omega_{H1}/M_{H2}. \tag{22}$$

Here F is the force, M is the moment, V is the linear speed, ω is the angular velocity. Indexes match to designations of links.

Equation 22 connects force and kinematic parameters and expresses the Effect of Force Adaptation: output angular velocity directly proportional to input power and inversely proportional to variable output moment of resistance.

The main feature of calculation of a two-mobile chain consists that constraint of external parameters in the form of the Eq. 22 provides definability of calculation on a condition of force adaptation. This equation allows to gain preliminary two initial kinematic parameters— ω_{H1} and ω_{H2} for mechanical system with two degree of freedom at the set parameters of input power and output moment of resistance. After that all kinematic and force parameters of SCG will be definable.

7 Principle of Motion Definability of Two-Mobile Kinematic Chain

The virtual work principle does not provide equilibrium of a two-mobile kinematic chain as an unbalanced reaction in the motionless instant centre of speeds of the link which has been not connected with a rack occurs [19]. Definability of motion can be attained if the mechanical system is completely counterbalanced. The principle of definability of motion characterizes an achievement of full equilibrium of mechanical system.

It is possible to present the equilibrium equation of basic planetary kinematic chain of AT (Eq. 20) in the form of an equilibrium equation of a link 5 by a virtual work principle. For this purpose superposed forces of the kinematic chain F_{H1} and F_{H2} should be carried on the output satellite 5. Force F_{H1} will be enclosed to a link 5 in the form of reactions $R_{65} = F_{H1}r_3/r_6$ and $R_{45} = F_{H1}r_1/r_4$. Force F_{H2} will be enclosed to a link 5 in the form of reaction $R_{H2-5} = F_{H2}$.

Then Eq. 20 of the basic kinematic chain equilibrium will become

$$R_{35}V_6 + R_{45}V_4 - R_{H2-5}V_{H2} = 0. \quad (23)$$

The Eq. 23 by a virtual work principle generally does not provide the equilibrium of a link 5 as the unbalanced reaction R_{05} will be enclosed in the instant centre of speeds P_5 of link 5. It is defined on a condition of equality of the link 5 sum forces to null: $R_{05} = R_{35} + R_{45} - R_{H2-5}$. Or

$$R_{05} = F_{H2} - F_{H1}. \quad (24)$$

The link 5 is rotated in relative motion round point S_5 together with force R_{05} in point P_5 . Such situation occurs on start, when the output carrier is motionless, and also in operating conditions.

On start, when the output carrier is motionless, the input force F_{H1} carried from the input carrier on a link 5 should overcome resistance of force F_{H2} . It would be possible in the presence of a real support in point P_5 with force R_{05} .

For an equilibration of the link 5 in the absence of a support it is necessary to inject into the kinematic chain additional constraint in the form of the closing transmission 8-7 connecting the carrier H_1 with the satellite 5. This constraint will appear passive if pitch point P coincides with point S .

Transmission 8-7 transfers force F_P to the satellite 5 in pitch point P from the carrier H_1 . Such constraint will appear active if pitch point P does not coincide with point S . But active constraint will chock the closed contour 1-2-3-6-5-4-1 and will eliminate force adaptation. To keep mobility in the closed contour, it is necessary to inject in completing a circuit the rotational dashpot 9 providing disconnecting and strictly certain relative mobility depending on carried force.

From condition of equilibrium $\sum M_{S5} = 0$ for link 5 we will gain the closing (jamming) force in the additional transmission, providing definability of motion of the kinematic chain of AT

$$F_P = F_{H2} \cdot KS/PS_5. \quad (25)$$

This force should be carried from input carrier H_1 to a link 5 through the converter—the rotational dashpot keeping two degree of freedom strictly definitely. The input moment of dashpot M_1 on the blade 1 (Fig. 10) is equal to the input moment on input carrier $M_1 = M_{H1}$ and output moment M_2 on the cylinder 2 (Fig. 10) is equal to the moment of force F_P overcoming resistance on output link 5— $M_2 = F_P r_8$.

Let's observe the dashpot interconnection of parameters (Fig. 10).

In the dashpot (cataract) the of resistance to cylinder motion M_2 exceeds driving moment M_1 . The dashpot moment $M_{12} = M_2 - M_1$. The input shaft with driving moment M_1 provides a rotary motion of the output shaft 2 with angular velocity $\omega_2 < \omega_1$ at the expense of liquid by-way through drain ports. Under the influence of the dashpot moment M_{12} the motion of links 1 and 2 with relative angular velocity $\omega_{12} = \omega_1 - \omega_2$ occurs.

Power of the dashpot

$$P_C = M_{12}\omega_{12} = (M_2 - M_1)(\omega_1 - \omega_2). \quad (26)$$

The dashpot characteristic is defined by carrying capacity of drain ports (the relation of the square of the blade of the rotated piston 1 to the square of drain ports) depending on the pressure. In the cataract with the set characteristic the relative angular velocity matches to the applied external moments. The rotational dashpot provides the position of the output shaft fixed on a time with moment of resistance M_2 applied to it which is depending on the liquid charge through drain ports.

Power of the dashpot is spent for overcoming of an internal friction of a liquid but carries out useful function—creation of the displacements of output link fixed on a time.

The interconnection of the dashpot parameters motion is defined by a virtual work principle taking into account the power of the dashpot spent for an internal friction

$$M_1\omega_1 - M_2\omega_2 - P_C = 0. \quad (27)$$

Let's substitute value P_k from the Eq. 26 into Eq. 27, we will gain after transformations the dependence of output angular velocity on a resistance moment (the equation of the dashpot adaptation)

$$\omega_2 = \omega_1(2M_1 - M_2)/M_1. \quad (28)$$

From here we define limits of change of the dashpot output parameters: $M_1 < M_2 < 2M_1, 0 < \omega_2 < \omega_1$.

Transmission ratio of dashpot $u_{12} = \omega_1/\omega_2$ or $u_{12} = M_1/(2M_1 - M_2)$. Here $1 < u_{12} < 2$.

8 Synthesis of AT

Synthesis of AT contains definition of parameters of the basic two-mobile kinematic chain on a condition of force adaptation [8, 11] and definition of parameters of the closing kinematic chain by a principle of definability of motion.

Definition of geometrical, kinematic and force parameters of the basic two-mobile kinematic chain on a condition of force adaptation is carried out by a technique stated in sources [8, 11] on the basis of use of the formula of force adaptation (Eq. 24) defining the constraint created by the closed contour.

The parameters of AT closing chain definition is carried out on a condition of the maximum tractive resistance overcoming on start at the motionless output carrier.

Statement of problem of the closing chain synthesis (Fig. 11).

The circuit design of the basic two-mobile kinematic chain providing force adaptation is given. The kinematic parameters (plot of linear speeds) and force parameters $M_{H1}, M_{H2} = M_{H2\max}, M_{H2\max} = 3M_{H1}$ are given.

It is necessary to define geometrics of closing transmission r_8, r_7 and parameters M_C, ω_C of the dashpot creating the force-speed constraint at breaking.

The solution:

1. We search out a position of the instant centre of relative turn of a link 5 concerning input carrier H_1 (a position of point S_5 or S) on the plot of linear speeds (Fig. 11b) as the point of intersection of angular velocities lines of these links.
2. We set a position of pitch point P of closing transmission 8-7 and define radiuses of wheels 7, 8: $r_7 = KP = KS, r_8 = r_{H2} + r_7$.
3. We define a wedging out force of dashpot F_P from equilibrium condition of link 5 $\sum M_{S5} = 0$: $F_P = F_{H2} \cdot KS/PS = M_{H2} \cdot KS/r_{H2}PS$.
If accept $KS = r_7, PS = 2r_7, M_{H2\max} = 3M_{H1}$ then

$$F_{P\max} = \frac{3M_{H1}}{2r_{H2}}. \quad (29)$$

4. We define the moment of dashpot placed between input carrier H_1 and a wheel 8

$$M_C = M_8 - M_{H1}. \quad (30)$$

Here $M_8 = F_P r_8$ —the output moment of the dashpot.

$$M_8 = \frac{M_{H2} r_8}{2r_{H2}}. \quad (31)$$

Or $M_8 = \frac{3M_{H1} r_8}{2r_{H2}}$.

The output moment of the dashpot cannot exceed maximum value $M_8 \leq 2M_{H1}$. From here we will gain geometrical restriction $r_8 \leq 4r_{H2}/3$ which for the observed circuit design is carried out.

5. We define angular velocity of the dashpot

$$\omega_C = \omega_{H1} - \omega_8. \quad (32)$$

Here $\omega_8 = \omega_7 u_{87}$, $\omega_7 = \omega_5$, u_{87} is the transmission ratio, ω_5 is the angular velocity of a wheel 5 at the motionless output carrier.

6. We define the maximum (starting) power of the dashpot.

$$P_C = M_C \omega_C. \quad (33)$$

Or $P_C = 0.16M_{H1}\omega_{H1\max}$.

7. We define a minimal transmission efficiency with account only the dashpot at the moment of start

$$\eta_{\min} = (M_{H1}\omega_{H1} - P_C)/M_{H1}\omega_{H1}. \quad (34)$$

Or $\eta_{\min} = (M_{H1}\omega_{H1} - P_C)/M_{H1}\omega_{H1} = 0.84$.

The maximal efficiency at $\omega_8 = \omega_{H1}$ has value $\eta_{\max} = 1$.

9 Force-Speed Interacting of AT Links in Operating Condition

In adaptive self-controlled transmission (Fig. 11a) interacting of links of basic two-mobile kinematic chain H_1 -1-2-3-6-5-4- H_2 , additional jamming transmission 8-7 and dashpot links (the piston is rigidly connected with carrier H_1 , the cylinder is rigidly connected with a wheel 8) occurs.

Constraint of links of basic two-mobile kinematic chain is presented by the Eq. 21.

Constraint of links of the dashpot is presented by the equation Eq. 27. In this equation it is necessary to execute the replacements connected with a notation of Fig. 11:

$$P_C = M_{H1-8}\omega_{H1-8} = (M_8 - M_{H1})(\omega_{H1} - \omega_8). \quad (35)$$

In closing transmission it is necessary to consider constraint of wheels 8-7 without efficiency

$$M_8 = M_7\omega_7/\omega_8 = M_5u_{78}. \quad (36)$$

Here M_5 is the moment on the output satellite 5,

u_{78} is the transmission ratio expressed through numbers of teeth of wheels, $u_{78} = z_8/z_7$.

Equations (21) and (35) define the interconnection of AT parameters.

The general equation of parameters interconnection by a virtual work principle looks like

$$M_{H1}\omega_{H1} - P_C = M_{H2}\omega_{H2}. \quad (37)$$

From here we define a basic formula of force adaptation

$$\omega_{H2} = (M_{H1}\omega_{H1} - P_C)/M_{H2}. \quad (38)$$

The formula (37) is a basis of calculation of self-controlled transmission with the dashpot.

The minimal efficiency of the mechanism taking into account losses only in a cataract makes about 90% and is defined by formula

$$\eta = (M_{H1}\omega_{H1} - P_C)/M_{H1}\omega_{H1}. \quad (39)$$

10 Bases Properties of AT

1. The adaptive transmission (or gear variator) represents the two-mobile two-row planetary train with constant catching of toothed wheels and with additional force-speed constraint.
2. AT works in the set control range independently (without control system).
3. Control range of AT depends on geometrics of the basic adaptive two-mobile kinematic chain (according to the theory of force adaptation) and from dashpot parameters (according to a definability principle). Theoretically at efficiency of the dashpot equal 0, 9 the range of change of a transmission ratio has limits from 1 to 5.

4. The dashpot unlike the fluid converter is the low-speed hydrostatical energy converter working in the conditions of statics equilibrium that defines its high reliability and efficiency.
5. AT is the low-speed transmission which is not requiring high-speed engines.
6. AT has doubtless advantages before CVT: simplicity of a design, absolute adequacy of work of not switched transmission, high reliability, an off-line operation in a wide control range.

11 Conclusion

The executed researches allow to formulate following general principles of creation of definable self-controlled mechanisms of AT:

- (1) The basis of the self-controlled mechanism is the kinematic chain with two degree of freedom, having one input, one output and the mobile closed contour placed between them.
- (2) The definability of motion of the mechanism is provided with forcing constraint of force and speed in an aspect of the dashpot with closing transmission into the mobile closed contour.

Force-speed constraint is the brand new constraint of force and speed (the moment and angular velocity). The closing additional transmission in combination with the dashpot can provide this constraint.

The stated material defines a technology of the brand new AT creation.

References

1. Lang, K.R.: Continuously Variable Transmissions. An Overview of CVT Research Past, Present, and Future, p. 11. 21 W. 732, USA. (2000)
2. Ivanov, K.S.: Transmission with automatically adjustable speed. The preliminary patent of republic Kazakhstan, p. 5. № 3208 from 15.03.1996 (1996)
3. Crockett, S.J.: Shiftless, continuously-aligning transmission, p. 9. Patent of USA 4,932,928, Cl. F16H 47/08, U.S. Cl. 475/51; 475/47.1990 (1990)
4. Volkov, I.V.: Way of automatic and continuous change of a twisting moment and speed of twirl of the output shaft depending on a tractive resistance and the device for its realization, p. 12. The invention description to the patent of Russia RU 2 234 626 from 27.03.2004 (2004)
5. Harries, J.: Power transmission system comprising two sets of epicyclic gears, p. 11. Patent of Great Britain GB2238090 (A) (1991)
6. Ivanov, K.S.: Discovery of the force adaptation effect. In: Proceedings of 11th World Congress in Mechanism and Machine Science, vol. 2, pp. 581–585. Tianjin, China (2004)
7. Ivanov, K.S.: Theoretical basis of gear stepless adjustable transmission. The theory of mechanisms and machines. The periodic scientifically-methodical journal. №2 (16), vol. 8, pp. 36–48. The St.-Petersburg state polytechnical university (2010)
8. Ivanov, K.S.: Theory of continuously variable transmission (CVT) with two degrees of freedom. paradox of mechanics. In: Proceedings of the American Society of Engineers

- Mechanics (ASME) International Mechanical Engineering Congress & Exposition (IMECE 2012), pp. 933–942. Houston, Texas, USA (2012)
9. Ivanov, K.S.: Paradox of mechanics—a basis of creation CVT. Transactions of 2-d IFToMM Asian Conference on MMS, pp. 245–264. Tokyo, Japan 7–10 Nov. 2012 (2012)
 10. Ivanov, K.: Optimal design of adaptive toothed variator (CVT). In: EngOpt 2018, Proceedings of the 6th International Conference on Engineering Optimization, pp. 1178–1192. Springer, Lisbon
 11. Ivanov, K.S.: Theoretical bases of creation of toothed variator. (1018). In: Transactions of EUCOMES 2018, pp. 244–255. Springer (2018)
 12. Ivanov, K., Ceccarelli, M., Ozhiken, A., Caffolla, D., Gonzalez Cruz, C.: Design and experiences of a planetary gear box for adaptive drives. In: Transactions of EUCOMES 2018, pp. 169–176. Springer (2018)
 13. Ivanov, K.S., Yaroslavtseva, E.K.: Way of automatic and continuous change of a twisting moment and speed of twirl of the output shaft depending on a tractive resistance and the device for its realisation, p. 10. The patent of Russia RU № 2398989. 10.09.2010 (2010)
 14. Ivanov, K.S., Almaty, K.Z.: Gebrauchsmusterinhaber. Bezeichnung-Einrichtung zur automatischen und kontinuierlichen Drehmoment- und Drehzahlveränderung einer Abtriebswelle je nach Fahrwiderstand. Urkunde über die Eintragung des Gebrauchsmusters Nr. 20 2012 101 273. 1. Tag der Eintragung 02.05.2012. Deutsches Patent und Markenamts. Bundesrepublik Deutschland (2012)
 15. Ivanov, K.S., Yaroslavceva, E.K.: Transmission and device for torque and output speed modification depending on driving resistance. International Application No.: PCT/IB2018/000007. Priority Data: 17152037.2–18.01.2017. World Intellectual Property Organization (WIPO), 26.07.2018 (2018)
 16. Ivanov, K.S.: Self-control gear variator. Creation and tests. Engineering industry: the network electronic scientific log., vol. 2, №3, pp. 1–9 (2017)
 17. Radzevich, S.P., Ivanov, K.S., et al.: Advances in gear design and manufacture, Chap. 7. Adaptive Gear Variators (CVTs), p. 360. CRC Press. Taylor & Francis Group (2019). 6000 Broken Sound Parkway NW, Suite 300. Boca Raton, FL 33487-2742. International Standard Book Number-13: 978-1-138-48473-3 (Hardback). (K. Ivanov: pp. 244–294)
 18. Ivanov, K.S., Yaroslavceva E.K.: Getriebe und Einrichtung zur Drehmoment- und Abtriebsdrehzahländerung je nach Fahrwiderstand. Urkunde über die Eintragung des Gebrauchsmusters Nr 21 2018 000 129. Bundesrepublik Deutschland, 21.08.2019 (2019). <http://depatisnet.dpm.a.de>
 19. Ivanov, K.S.: Prospects of creation of mechanisms with two degree of freedom. IFToMM World Congress on Mechanism and Machine Science. Advances in Mechanism and Machine Science. Springer Nature Switzerland AG (2019)
 20. Ivanov, K.S.: Self-control mechanisms. Monograph, p. 28. ISBN 978-601-7889-88-3. Printery “CES”. Almaty (2019)

Load State of Low-Speed Spiroid Gears



Andrey Kuznetsov and Alexander Sannikov

Abstract The problem of analyzing a heavy-loaded low-speed multi-pair spiroid gear with account of the influence of elastic and elastoplastic contact, bending and shearing interaction of spiroid gearwheel teeth and spiroid worm threads is considered. The main steps of the developed algorithm for calculating the load distribution and plastic strain of flanks taking into account the elastic and elastoplastic nature of the contact, multi-pair character of meshing, and macro- and micro-roughness of flanks of gear elements are briefly described. For the case of elastoplastic contact, zones of plastic contact on spiroid gear tooth flanks are determined, and the value of plastic strain is calculated. Flanks of spiroid gear teeth are presented in the algorithm as a set of areas (cells) with coordinates of centers calculated taking into account the analyzed factors influencing the load distribution in the spiroid gearing, such as manufacturing and (or) assembly errors, macro- and micro-roughness, and deformation of spiroid gear supports. The manuscript presents numerical results of studying real spiroid gears for gearboxes of pipeline valves (PV) having the elastic and elastoplastic character of contact, presented in the form of summary tables and diagrams of torque distribution, load concentration factors in contact areas and plastic strain areas, demonstrating the efficiency of the algorithm. Results of comparing the gearboxes of different generations are given that show the ways of applying this algorithm at the design stage and results of improving load characteristics of new generations of gearboxes. Numerical results of the algorithm operation correlate well with the operating experience and can be used to analyze the load-carrying capacity of spiroid gears.

Keywords Spiroid gear · Loaded contact · Elastoplastic contact · Plastic strain · Load-carrying capacity · Manual gearboxes

A. Kuznetsov · A. Sannikov (✉)
Scientific Department “Institute of Mechanics Named After Professor V. I. Goldfarb”,
Kalashnikov Izhevsk State Technical University, Izhevsk, Russia
e-mail: Alex1_87@mail.ru

A. Kuznetsov
e-mail: andrkuzn@istu.ru

1 Introduction

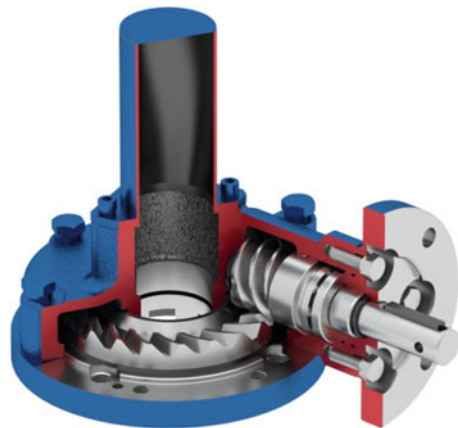
Analysis of load-carrying capacity is an integral and one of the most complex problems in gear design, since it allows for predicting the serviceability and reliability of a gear within the limits of a given service life at the design stage. This analysis becomes significantly more complicated when studying gears with the multi-pair contact and with complex spatial arrangement of flanks. A spiroid gear is related exactly to these gears; it got wide application in gearboxes for pipeline valves (PV)—see Fig. 1. These gearboxes are characterized by heavy loading mode and almost static mode at overloads, duty factor 25%, low frequency of input shaft rotation (usually below 100 rpm and almost always not more than 220 rpm), short operating life of several thousands of control cycles in the “OPEN-CLOSE” mode or dozens of thousands in the regulating mode. The experience of spiroid gear operation in gearboxes for pipeline valves has shown that at the very first cycles of operation a certain plastic strain appears on flanks (see Fig. 1) [1, 2] influencing the stress-strain state (SSS) of the gear and, as a consequence, its load-carrying capability. This influence should be taken into account at the stage of gear design, since it irreversibly breaks the initial tooth geometry and leads to redistribution of load transmitted by teeth.

A common method for the DM analysis is the finite element method (FEM), but it has a number of significant drawbacks:

- an increase in calculation errors when estimating stresses on relatively non-smoothly conjugated transition sections of teeth at their roots;
- a sharp increase in computational complexity for the case of the multi-pair contact, which is typical for spiroid gears.

These drawbacks are worsened by the necessity of evaluation in several meshing phases and choosing the most risky phase, as well as by the necessity of evaluation of many design solutions (many gears and their layout designs, many combinations of errors and strains) at the design stage.

Fig. 1 General view of multi-turn gearbox RZAM-S-500



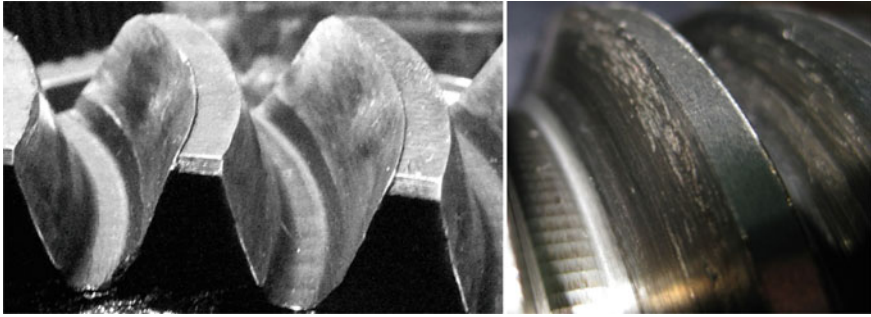


Fig. 2 Plastic strain on spiroid gearwheel teeth

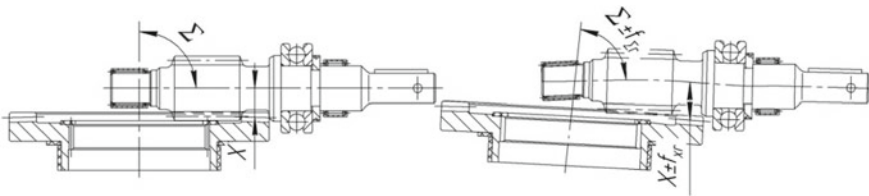


Fig. 3 To deformations of gear elements

The problem is mainly solved by methods proposed and developed in works of Zablonkii [3], Sheveleva [4], Airapetov [5], and others, that are reduced to solving a system of linear equations of simultaneous displacement of contacting surface points and equilibrium of loaded elements. Assumption of an elastic tooth contact model is not always justified in the case of heavy-loaded spiroid gears. This disadvantage is eliminated in the algorithm proposed in works [6–8]. This manuscript presents the results of applying the proposed algorithm at the analysis of the load state of heavy-loaded spiroid gears taking into account manufacturing and assembly errors, as well as at the design of gearboxes for pipeline valves (Fig. 2).

2 Algorithm for Analysis of Elastically and Plastically Loaded Multi-Pair Contact

Let us mention that in this manuscript the study will be conducted primarily to determine the load distribution after the first operating cycles, when tooth wear is a negligible running-in factor and during the action of peak loads. This assumption is based on the practice of testing and operating the PV gears and gearboxes. Wear on contact surfaces is possible further and is not a dominant factor in gear operation when properly designed, manufactured and operated. The tooth geometry obtained

by elastoplastic loading simulations can be used as initial information for calculating the evolution of contact surfaces with regard to wear.

The algorithm itself is described in detail in [6–8]; below we present only a summary of its main steps and the incorporated assumptions. The loaded gear under study is a discretely loaded system in which the condition of joint displacement of cells of flanks of worm threads and gearwheel teeth and the condition of force equilibrium are described by the following system of equations:

$$\begin{cases} w_{km} + S_{0km} - \Delta_{\varphi 2km} = 0 \\ \sum_D F_{k'm'} \tilde{r}_{2k'm'} - T_2 = 0 \end{cases} \quad (1)$$

where w_{km} is the elastoplastic displacement; S_{0km} is the initial (before calculating the load distribution) clearance between km th cells of flanks, $\Delta_{\varphi 2km}$ is the relative displacement of km th cells as a result of mutual approach for the elements at gear loading, $\tilde{r}_{2k'm'}$ is the arm of the resultant force $F_{k'm'}$ applied in the $k'm$ 'th cell relative to the gearwheel axis, T_2 is the assigned torque at the spiroid gearwheel.

The number of equations of the system (1) is not known beforehand and is specified during calculation. Also during calculation all sought parameters are specified: the contact area D , the value $\Delta_{\varphi 2}$ of approaching the links and the value of discretely applied forces.

In a little simplified form the algorithm consists of the following steps:

- (1) input (calculation) of initial data: initial clearances S_{0km} , physical and mechanical properties of materials of elements, the torque T_2 ;
- (2) input and calculation of data for the first approximation: approach of elements, the set of loaded interfered cells (of the area D), forces in these cells;
- (3) extraction of elastoplastically strained cells in the area D by the excess of contact pressure above the specified limit; calculation of plastic displacement in these cells which is proportional to this excess;
- (4) correction of forces in elastoplastically strained cells from the condition that the pressure is equal to the limiting one; correction of forces in other loaded cells by the condition of force equilibrium;(the next algorithm steps refer to both the first and all following iterations)
- (5) calculation of the elastic displacement in each cell as a linear combination of displacements from all discretely applied forces;
- (6) calculation of clearances/interferences (hereinafter—discontinuities ξ) formed between teeth after taking into account elastic and plastic displacements at the assigned approach; correction of the approach value depending on the average discontinuity ξ_{cp} ;
- (7) correction of plastic displacements according to the value of average discontinuity ξ_{cp} ; herewith, a part of elastoplastically loaded cells, in which the plastic displacement became negative, returns to the number of elastically loaded cells;

- (8) correction of the contact area D ; those cells are added, in which the value of discontinuity turned out to be negative (the calculated interference of surfaces occurred, the cell came into contact and started transmitting the torque);
- (9) correction of forces in every elastically loaded cell depending on the value of its discontinuity; in this case, if the calculated value of force turned out to be less than zero, the cell is excluded from the contact area, and if the force causes the pressure greater than the limiting one, the cell passes to the number of elastoplastically loaded cells; correction of forces in those cells from the condition of equality of the pressure to the limiting one;
- (10) correction of forces in elastically loaded cells to provide the equilibrium condition (the last equation of the system (1));
- (11) determination of the total strain area based on the set of strain areas in all the design phases of meshing;
- (12) checking the termination condition of the algorithm for the selected criterion of the calculation accuracy and performing the stress-strain state (SSS) analysis.

One of the main assumptions made in the algorithm is that the increments of plastic strain and the value of exceeding the allowable contact stress (pressure) are proportional, the deformations are directed along the normal to the surface and are caused by a normal force, the influence of the oil layer in meshing is not considered [9]. As shown in [8], such assumptions do not have a significant impact on the result of the algorithm operation and the obtained data are quite reliable.

The algorithm can be used to estimate load distribution under short-term action of the maximum torque, when the valve internal diameter is blocked, and the resistance to rotation of the locking element in its seals and shaft supports is due to one-sided medium pressure in the valve. In addition, the peak torque is possible in pipeline valves when the locking element is initiated after long standing with little or no lubrication of rubbing contact surfaces, often with elements of their corrosion or adhesion, or during abnormal loading situations of the valve with a gearbox. The peak torque is the most risky, it is the most probable instant of gear failure and causes the greatest plastic strain of teeth. Exactly the case of this torque action is under the study discussed below (Tables 1, 2, 3, 4, 5 and 6).

3 Effect of Manufacturing and Assembly Errors on the Load State of Spiroid Gears

Tables 3, 4, 5, 6 and 7 and Figs. 4, 5, 6 and 7 show the results of numerical studying the following factors affecting the gear load state:

- manufacturing and assembly errors;
- strain of structural elements.

To take them into account we have chosen the following errors:

Table 1 Parameters and performance characteristics of the studied gears

Parameter	RZA-S-4000	RZA-S-2000
	Value	
Interaxial distance, mm	70	60
Worm axial module, mm	2.249	2.275
Number of gearwheel teeth/worm threads	1/65	1/46
External diameter of spiroid worm, mm	47	45
External/internal diameters of the gearwheel, mm	213/160	138/175
Addendum/dedendum factors	1/1.2	1/1.2
Theoretical overlap factor	5.8	3.4
Profile angles for right/left flanks	9.81°/29.93°	11.76°/28.78°
Maximum torque at the output shaft, Nm	4000	2000
Peak torque at the output shaft, Nm	8000	4000
Material for gear elements/surface hardness	Steel 40X/45...50 HRC	

Table 2 Sets of errors involved in the study

Number of the set	Errors, mcm					
	f_{ar}	$f_{\Sigma r}$	f_{px}	f_{fr}	H_o/i	f_{xr}
0	–	–	–	–	–	–
1	450	–	–	–	–	–
2	–450	–	–	–	–	–
3	–	200	–	–	–	–
4	–	–200	–	–	–	–
5	–	–	120	–	–	–
6	–	–	–120	–	–	–
7	–	–	–	30	–	–
8	–	–	–	–30	–	–
9	–	–	–	–	100/6	–
10	–	–	–	–	–	340
11	–	–	–	–	–	–340
12	450	200	120	30	100/6	340
13	–450	–200	–120	–30	100/6	–340
14	450	200	120	30	–	340
15	–450	–200	–120	–30	–	–340

Table 3 Load concentration factor in the gear of the gearbox RZA-S-4000

Phase	K_f in phases for different sets of errors at elastic character of the contact															
	N0	N1	N2	N3	N4	N5	N6	N7	N8	N9	N10	N11	N12	N13	N14	N15
0	1.14	1.14	1.16	1.35	1.29	1.44	1.53	1.15	1.14	1.2	1.15	1.14	1.18	1.29	1.62	1.31
1	1.17	1.17	1.19	1.39	1.30	1.45	1.60	1.17	1.17	1.19	1.18	1.16	1.41	1.33	1.94	1.35
2	1.25	1.25	1.26	1.44	1.42	1.54	1.68	1.25	1.25	1.21	1.25	1.24	1.81	1.37	2.08	1.40
3	1.22	1.23	1.23	1.42	1.40	1.54	1.68	1.22	1.22	1.19	1.23	1.22	1.84	1.38	1.37	1.38
4	1.18	1.20	1.19	1.40	1.37	1.52	1.64	1.18	1.18	1.24	1.18	1.18	1.37	1.32	1.34	1.36
5	1.15	1.16	1.17	1.39	1.35	1.52	1.61	1.16	1.16	1.27	1.16	1.15	1.35	1.31	1.31	1.34
Phase	K_f in phases for different sets of errors at elastoplastic character of the contact															
0	1.15	1.14	1.17	1.33	1.29	1.41	1.52	1.15	1.15	1.16	1.15	1.14	1.24	1.28	1.17	1.31
1	1.18	1.17	1.20	1.36	1.31	1.42	1.59	1.18	1.18	1.17	1.19	1.17	1.26	1.31	1.30	1.34
2	1.25	1.25	1.27	1.42	1.41	1.50	1.66	1.25	1.25	1.21	1.25	1.24	1.36	1.36	1.37	1.38
3	1.22	1.23	1.24	1.41	1.39	1.50	1.65	1.22	1.22	1.19	1.23	1.22	1.41	1.37	1.37	1.38
4	1.18	1.19	1.19	1.37	1.36	1.48	1.62	1.18	1.18	1.24	1.18	1.18	1.39	1.33	1.33	1.35
5	1.16	1.16	1.17	1.34	1.34	1.47	1.58	1.16	1.16	1.20	1.16	1.15	1.31	1.32	1.32	1.33

Table 4 Calculation results for the gear of the gearbox RZA-S-4000

Phase	Maximum ΔT_{2j} for different meshing phases at different sets of errors, %															
	N0	N1	N2	N3	N4	N5	N6	N7	N8	N9	N10	N11	N12	N13	N14	N15
0	5	5	6	2	9	14	1	4	7	12	5	6	40	21	31	1
1	9	9	9	3	13	18	3	8	10	15	8	10	517	35	65	4
2	1	1	6	4	2	5	4	1	2	10	1	1	891	7	62	2
3	1	1	2	5	2	6	8	3	2	9	7	2	580	8	63	7
4	1	1	1	6	2	11	5	1	2	6	3	1	10	3	8	4
5	1	1	1	7	4	12	4	0	2	6	2	2	7	10	7	2
Area	<i>w_p in contact areas for the phase with the maximum variation of the torque in the area at different sets of errors, mcm</i>															
0	19.6	19.4	18.4	23.1	37.2	51.9	0.0	16.3	25.6	7.1	38.3	24.5	83.6	4.5	54.8	0.7
1	3.3	3.0	4.3	24.1	5.2	18.3	0.0	1.4	8.6	34.3	23.7	4.7	65.4	31.2	31.1	3.7
2	3.8	3.1	4.9	28.0	3.9	13.1	0.4	1.5	9.8	35.4	24.0	5.4	64.5	37.9	29.1	6.2
3	3.3	1.9	4.6	31.7	1.2	5.4	5.7	0.9	9.6	28.3	23.6	4.8	75.8	33.7	62.3	8.2
4	1.5	0.3	3.5	35.3	0.0	0.0	10.5	0.0	7.7	24.9	22.7	2.9	80.9	34.9	64.2	11.2
5	2.4	0.0	2.0	60.9	0.0	0.0	12.2	0.0	4.7	25.4	21.3	1.1	110.9	38.6	97.9	10.9
6	0.0	0.0	0.0	42.4	0.0	0.0	22.8	0.0	1.0	19.1	18.3	0.0	0.0	33.3	113.7	25.2

Table 5 Load transmission concentration factor in the gear of the gearbox RZA-S-2000

Phase	K_f in phases for different sets of errors at elastic character of the contact															
	N0	N1	N2	N3	N4	N5	N6	N7	N8	N9	N10	N11	N12	N13	N14	N15
0	1.10	1.12	1.11	1.26	1.22	1.29	1.37	1.10	1.09	1.10	1.09	1.10	3.17	1.15	3.20	1.14
1	1.11	1.11	1.13	1.34	1.22	1.28	1.46	1.11	1.10	1.13	1.11	1.10	3.18	1.13	3.20	1.17
2	1.16	1.13	1.18	1.42	1.22	1.31	1.53	1.17	1.15	1.19	1.16	1.15	3.25	1.18	3.18	1.22
3	1.17	1.16	1.18	1.42	1.23	1.36	1.47	1.17	1.17	1.23	1.18	1.16	3.30	1.27	3.30	1.22
4	1.14	1.14	1.14	1.35	1.21	1.38	1.38	1.14	1.15	1.28	1.15	1.14	1.34	1.22	2.00	1.19
5	1.13	1.16	1.11	1.27	1.24	1.43	1.29	1.14	1.13	1.12	1.13	1.14	3.05	1.10	1.34	1.16
Area	K_f in phases for different sets of errors at elastoplastic character of the contact															
0	1.10	1.12	1.11	1.25	1.21	1.27	1.37	1.10	1.09	1.08	1.09	1.10	1.04	1.11	1.30	1.14
1	1.11	1.11	1.13	1.33	1.21	1.28	1.46	1.11	1.10	1.09	1.11	1.10	1.26	1.14	1.27	1.16
2	1.16	1.14	1.18	1.40	1.23	1.33	1.52	1.17	1.16	1.16	1.17	1.15	1.15	1.23	0.86	1.23
3	1.18	1.17	1.18	1.38	1.24	1.38	1.48	1.17	1.18	1.19	1.18	1.17	1.40	1.22	2.05	1.23
4	1.15	1.15	1.14	1.31	1.22	1.38	1.39	1.15	1.15	1.17	1.15	1.14	1.42	1.24	1.38	1.19
5	1.13	1.15	1.11	1.24	1.24	1.40	1.29	1.13	1.13	1.12	1.13	1.14	1.39	1.11	1.22	1.16

Table 6 Calculation results for the gear of the gearbox RZA-S-2000

Phase	Maximum ΔTz_j for different meshing phases at different sets of errors, %															
	N0	N1	N2	N3	N4	N5	N6	N7	N8	N9	N10	N11	N12	N13	N14	N15
0	0	0	0	1	1	1	0	0	0	7	1	0	1020	6	819	0
1	0	0	0	2	0	2	0	0	0	9	1	0	1664	6	2396	0
2	2	2	8	3	3	9	4	7	2	9	3	2	2717	28	3679	4
3	7	6	7	5	9	34	8	5	8	18	8	8	1665	16	5389	8
4	7	8	6	12	12	18	11	6	8	15	8	8	139	22	149	3
5	0	1	0	5	1	3	0	0	0	5	1	0	616	3	29	1
Area	<i>w_p in contact areas for the phase with the maximum change of the torque in the area at different sets of errors, mcm</i>															
0	10.8	13.1	8.6	28.3	25.0	41.0	0.0	10.6	17.9	4.7	41.2	13.4	85.3	6.6	91.2	12.5
1	2.7	3.1	2.4	30.6	5.4	7.7	0.0	2.3	3.6	28.3	26.0	2.9	119.2	32.3	118.5	1.4
2	2.8	2.7	2.3	37.6	3.4	2.2	1.9	1.7	3.6	32.0	26.3	3.0	120.4	18.0	119.2	3.2
3	0.6	0.6	0.5	42.9	0.0	0.0	3.7	0.0	0.8	28.2	24.4	0.6	121.0	27.0	117.8	2.2
4	5.7	5.3	0.0	41.7	0.6	0.0	17.6	0.0	3.4	0.0	4.0	6.0	0.0	0.0	120.9	27.3

Table 7 Basic parameters for the first group of gearboxes

Parameter	RS1-60	RZA-S-2000
	Value	
Interaxial distance, mm	60	60
Worm axial module, mm	2.75	2.748
Number of gearwheel teeth/worm threads	46/1	46/1
External diameter of spiroid worm, mm	42	42
External/internal diameters of the gearwheel, mm	200/145	175/138
Addendum/dedendum factors	1/1.2	1/1.2
Profile angles for right/left flanks	10°/30°	11.76°/27.87°
Maximum torque at the output shaft, Nm	1500	2000
Peak torque at the output shaft, Nm	2469	4000
Material for gear elements/surface hardness	Steel 40X/45...50 HRC	
f_{ar} , mcm	50	
f_{px} , mcm	100	
f_{Σ} , mcm	50	
f_x , mcm	-10	

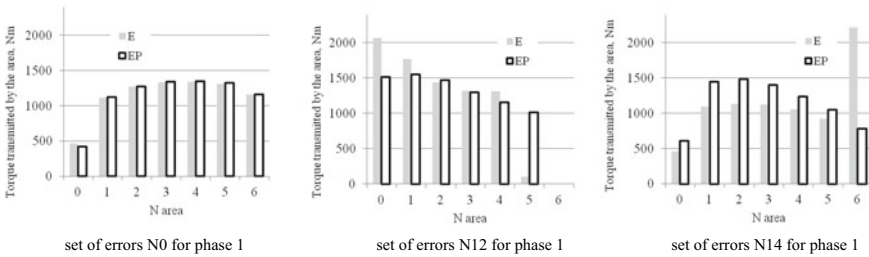


Fig. 4 Distribution of torque over contact areas for the gear of the gearbox RZA-S-4000

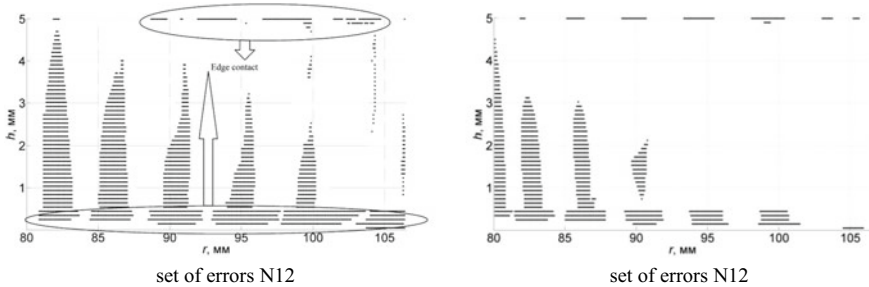


Fig. 5 Plastic strain distribution over the gearwheel tooth flank for the gearbox RZA-S-4000 in phase N2

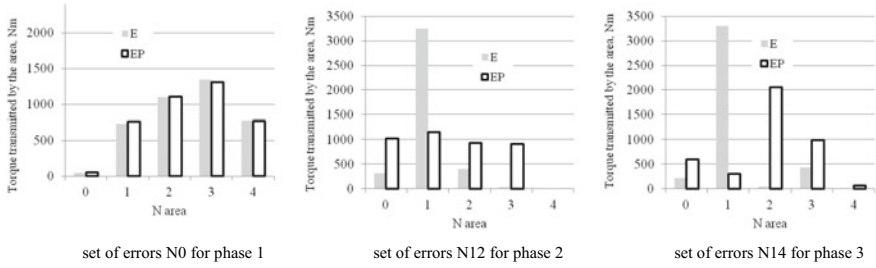


Fig. 6 Torque distribution over contact areas in the gear of the gearbox RZA-S-2000

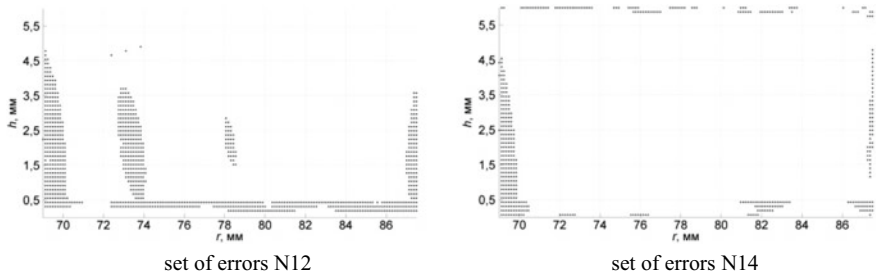


Fig. 7 Plastic strain distribution over the gearwheel tooth flank for the gearbox RZA-S-2000 in phase N2

- interaxial angle error ($f_{\Sigma r}$, Fig. 3);
- error of the interaxial distance (f_{ar});
- pitch error of the worm (f_{px} , for the single-thread gears it is actually the accumulated error of the helical line);
- profile error of worm thread flanks (ff_r);
- faceting (H_0);
- error of the gearwheel axial position (f_{xr}) (Fig. 3).

When simulating the DM, the error of interaxial angle includes two components: the manufacturing error itself and the misalignment of positions of the worm shaft and the gearwheel rim due to deformations of structural elements (Fig. 3).

The first part of the study includes the analysis of influence of errors taken separately. Values of the selected errors are presented in Table 2 and correspond to the limit deviations for the 12th degree of accuracy (RF Standard classification) of the studied gears. The second part discusses combinations of errors which (according to the calculations results in the first part) have the greatest influence on load concentration in unfavorable zones:

- for interaction of transient zones at roots of teeth and threads;
- for interaction of two edges of teeth and threads including the apical and face edges.

Each of these cases can lead to breakage or a defect contributing to breakage: in the first case it is the chippage at the apex, in the second case it is the bending breakage.

The evaluation was performed for 6 meshing phases (combinations of positions of instantaneous contact areas) with the worst one selected with respect to the following factors:

- factor of load concentration on teeth and threads for the whole phase (K_f), calculated as the ratio of the maximum torque transmitted by the instantaneous contact area (T_{2j}) to the average torque (T_{2av}) calculated by the condition of uniform load distribution:

$$K_f = \frac{\max\{T_{2j}\}}{T_{2av}}, j = \overline{0, N_j}, \quad (2)$$

where $\max\{T_{2j}\}$ is the maximum torque for all areas in the considered meshing phase, Nm;

N_j is the number of instantaneous contact areas in the considered meshing phase;

$$T_{2av} = \frac{T_2}{N_j}, \quad (3)$$

- redistribution of the torque (ΔT_{2j}) in instantaneous contact areas caused by the appearance of plastic strain on flanks of the tooth and thread calculated according to the formula

$$\Delta T_{2j} = \left(\frac{T_{2jE} - T_{2jEP}}{T_{2jE}} \right) 100\%, \quad (4)$$

where T_{2jE} is the calculated torque transmitted by the j th instantaneous area when considering the elastic character of the contact, Nm;

T_{2jEP} is the calculated torque transmitted by the j th instantaneous area when considering the elastoplastic character of the contact, Nm;

- values of plastic displacement (w_p) on flanks of the tooth and thread.

Basing on researches by A. V. Kirichek [10] and the recommendations presented in [11], the allowable value of w_p for steel 40X worms and gearwheels subjected to volume hardening to 45... 50 HRC, will be taken 30... 50 mcm.

The research was carried out by “SPDIAL+” CAD system. Spiroid gears for two representatives of a number of quarter-turn gearboxes for pipeline valves (models RZA-S-4000 and RZA-S-2000) were chosen as study objects. On the one hand,

dimension proportions of these gearboxes elements are similar. On the other hand, gears differ significantly in the overlap ratio (the number of tooth pairs in simultaneous meshing)—by almost 1.6 times. Parameters of the gearboxes are presented in Table 1.

As mentioned above, the load concentration on teeth and threads was the **first** to be evaluated by the concentration factor (K_f) (see Tables 3 and 5). Values of torque and concentration factors in tooth pairs with the most noticeable change of these values when taking into account the elastoplastic character of contact rather than the elastic one are shown there in bold type for clarity.

Redistribution of torque over the instantaneous contact areas caused by plastic strain of the gearwheel tooth and worm thread flanks was the second to be evaluated. Because of the large number of data in Tables 4 and 6, diagrams (see Figs. 4 and 6) present the detailed results only for the meshing phase with the maximum torque redistribution. In diagrams, the letter “E” represents the test data for the elastic contact and letters “EP” are for the elastoplastic contact. Figures 5 and 7 also show the distribution of plastic strain centers on the development view of the spiroid gearwheel tooth flanks, where black points indicate the centers of plastic strain in the considered phase and at the specified set of errors; r is the spiroid wheel radius, h is the spiroid gearwheel tooth height (O is the root). The maximum change in the torque at the area and its consequent plastic strain are shown there in bold type for clarity. Additionally, the cells in which plastic strain exceeded our assigned allowable value of $30\ \mu\text{m}$ are framed in these tables.

Summarizing the results of the above calculations, the following conclusions can be made:

- (1) redistribution of torque on instantaneous contact areas, caused by plastic strain of teeth is the most noticeable in gears containing errors, especially at such unfavorable combinations, when the contact comes out on tooth edges. In particular, these are errors of the interaxial angle and gearwheel axial position (sets of errors N12, N14) or when the load is concentrated in one area, as for the case of the pitch error (set of errors N5) and the interaxial angle error (set of errors N4);
- (2) appearance of plastic strain on tooth flanks at peak loads strengthens the advantage of the spiroid gear—its relatively low sensitivity to manufacturing and assembly errors. In particular, even at the assigned low level of accuracy (12th degree of accuracy) and unfavorable combination of errors described in the previous paragraph, the contact pattern has an acceptable shape and location;
- (3) the character of torque distribution between instantaneous contact areas and, consequently, the degree of load concentration is mainly influenced by the worm axial pitch error and the interaxial angle error, and their influence is intensified with an increase of the overlap factor (load concentration for RZA-S-4000 gearbox is higher than that for RZA-S-2000);
- (4) unfavorable edge contact at the tops and roots of gearwheel teeth and worm threads is caused by a combination of the positive error in the axial position of the gearwheel (the gearwheel is close to the worm) and the interaxial angle

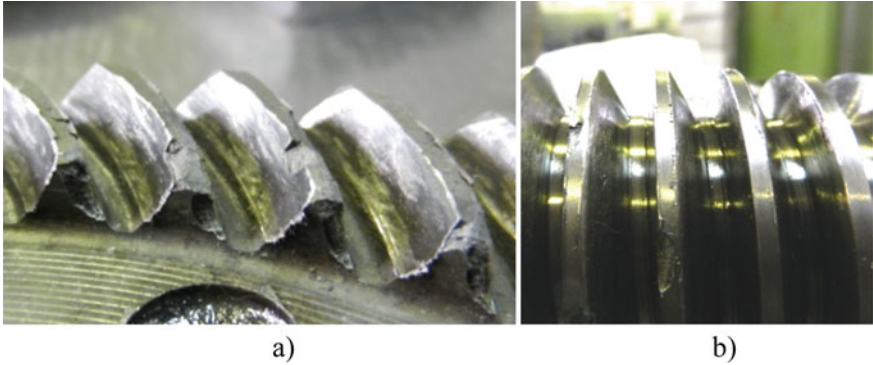


Fig. 8 Chippage on **a** gearwheel teeth, **b** worm threads

- error. Here, the sign of the latter depends on the initial position of the contact pattern (its displacement to the heel or toe of the tooth);
- (5) plastic strain of top edges enables load leveling, but it can be the reason of their chipping (Fig. 8). In order to reduce the load concentration on tooth edges we propose:
 - to limit the approach of the spiroid gearwheel to the worm (while assigning appropriate requirements to the axial position of the gearwheel and the meshing adjustment);
 - to provide contact localization that compensates the appearance of a systematic error or structural deformation that lead to the edge contact;
 - to increase the radial clearance in the gear (this measure requires checking that the tooth bending strength is retained);
 - (6) faceting on the tooth flank of the gearwheel does not lead to an increase in the load concentration in meshing as a whole; in combination with other errors, faceting promotes more uniform load distribution between tooth pairs and exclusion (or reduction) of the edge contact at the tooth toe and heel; the highest level of faceting should be limited after assessing the plastic strain and its comparison with the allowable value.

4 Comparison of Gear Load State for Different Generations of Gearboxes

One of the trends of the advanced mechanical engineering is to make products more compact [2]. Reducing the size itself usually leads to the producing cost reduction and, consequently, to an increase in competitiveness. It is highly desirable, but, of course, it is not always possible: there are factors that limit the possibility of reduction. In case of low-speed heavy-loaded gears, one of the main factors is the loss of tooth

strength due to the reduction of their size and increase in the load acting on teeth. It is possible to quantitatively estimate the possibility of reducing the size and/or changing the ratio of gear parameters just by applying the developed method and software. The second aspect is to determine the load allowable for each gear dimension size. In this work, we considered an allowable level of contact load state of gears (bending strength of teeth was not considered), at which:

- plastic strain of contact surfaces does not progress with the increasing number of loading cycles, i.e. plastic strain in a short period of operation leads to a certain established form of contact surfaces;
- plastic strain does not exceed a certain assigned value determined by plastic properties of tooth materials.

Two pairs of quarter-turn and multi-turn gearboxes analogous to those of generation 1 and 3 (developed in 2000–2005 and 2010–2016) were selected for the evaluation.

Torques transmitted by instantaneous contact areas, the factor of load distribution over instant contact areas in the considered meshing phase (K_{ff}) (5) and the plastic strain in these areas at the action of the maximum and peak torque with and without errors (results will be marked with “err” in the text) were calculated for each gearbox. To determine the magnitude of errors, a sample of serial products was taken and the average value of each error was determined. The following errors were chosen as simulated ones: f_{ar} , f_{xr} , $f_{\Sigma r}$, f_x , their values will be given below for each group of gearboxes.

$$K_{ff} = \frac{T_{2j}}{T_{2av}}, \quad (5)$$

The first group of gearboxes are quarter-turn ones designed to control ball valves and butterfly valves. Gearboxes RS1-60 and RZA-S-2000 were chosen, their geometrical characteristics are given in Table 8, and their layout design is shown in Fig. 9. The main differences of RSA-S-2000 gearbox from the comparable predecessor RS1-60 are as follows:

- the reduced gearwheel diameter: from 200 mm to 175 mm (1.14 times);
- the reduced facewidth of the gearwheel: from 27.5 mm to 18.5 mm (1.49 times);
- contact localization by the tooth height is introduced.

Calculation results are presented in Table 9, and diagrams are shown in Fig. 10.

In all considered cases (both gears and both levels of their loading) the calculation gave a limited zone of plastic strain of teeth (of course, when it was present). This gives grounds to predict: the process of plastic strain of contact surfaces in gears will not progress.

The change in the size of the 3rd generation gearboxes resulted in:

- a reduction of the overlap factor;
- a slight decrease in the arm of the force action in the meshing.

Table 8 Simulation results for the first group of gearboxes

N area	RS1-60				RZA-S-2000			
	Torque transmitted by the area, Nm							
	At $T_2 = 2000$ Nm		At $T_2 = 4000$ Nm		At $T_2 = 2000$ Nm		At $T_2 = 4000$ Nm	
	–	err	–	err	–	err	–	err
0	3	104	53	57	–	–	–	–
1	395	785	781	744	486	476	958	897
2	442	613	879	852	562	555	1128	1106
3	439	362	871	876	535	540	1093	1121
4	434	135	855	891	417	426	820	876
5	288	0	561	580	–	–	–	–
–	K_{ff}							
0	0	0.3	0.1	0.1	–	–	–	–
1	1.0	2.0	1.0	0.9	1.0	1.0	1.0	0.9
2	1.1	1.5	1.1	1.1	1.1	1.1	1.1	1.1
3	1.1	0.9	1.1	1.1	1.1	1.1	1.1	1.1
4	1.1	0.3	1.1	1.1	0.8	0.9	0.8	0.9
5	0.7	0.0	0.7	0.7	–	–	–	–
–	Value of plastic strain in the area, mcm							
0	0.00	9.90	9.74	9.12	0.00	0.00	–	–
1	1.75	8.39	7.85	7.44	0.00	0.00	5.61	2.82
2	2.69	5.76	10.28	12.16	0.00	0.00	6.12	3.35
3	3.73	1.72	11.83	14.1	0.00	0.00	2.6	2.11
4	3.83	0.00	12.87	15.62	0.00	0.00	0.00	2.52
5	0.00	0.00	8.28	10.12	–	–	–	–

As can be seen from the presented data, all this led to the fact that the torque transmitted by individual instant contact areas increased, but the load concentration did not occur. The growth was almost uniform for all most loaded areas, which are concentrated in the central (stronger) part of the tooth. At the peak load, the plastic displacement of tooth flanks is on average 1.3...2 times less due to the introduced profile contact localization, which helps to eliminate the edge contact at the tops and roots, where the plastic strain was concentrated for the 1st generation gearbox. The values of the maximum plastic displacement 15.62 μm for the 1st generation gearboxes and 6.12 μm for the 3rd generation gearbox do not exceed the allowable value taken above (30 μm).

Typical tests of the 3rd generation gearboxes showed their operability during the whole specified service life under the action of the mentioned (peak, maximum and nominal) rated loads.

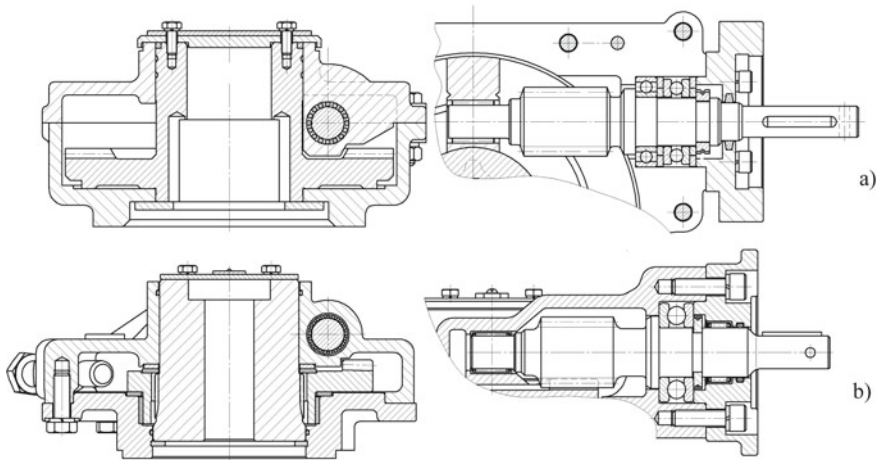


Fig. 9 Section view of the gearbox **a** RS1-60 and **b** RZA-S-2000

Table 9 Basic parameters for the second group of gearboxes

Parameter	RZAM-S-2500 (generation 1)	RZAM-S-2500 (generation 3)
	Value	
Interaxial distance, mm	77	65
Worm axial module, mm	5.04	4.005
Number of gearwheel teeth/worm threads	35/2	37/2
External diameter of spiroid worm, mm	55	59,5
External/internal diameters of the gearwheel, mm	250/190	224/170
Addendum/dedendum factors	0.8/1.0	0.8/1.0
Profile angles for right/left flanks	8.82°/24.37°	10.56°/27.38°
Maximum torque at the output shaft, Nm	2500	
Peak torque at the output shaft, Nm	5000	
Material for gear elements/surface hardness	Steel 40X/45...50 HRC	
f_{ar} , mcm	60	
f_{px} , mcm	-30	
f_{Σ} , mcm	-80	
f_x , mcm	20	

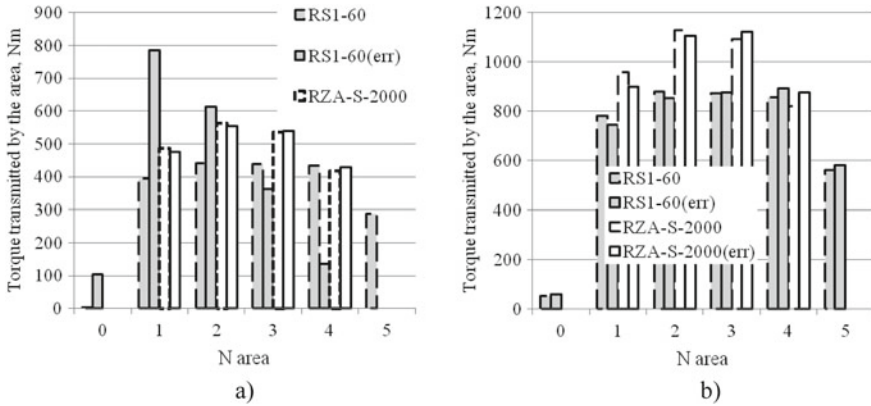


Fig. 10 Torque distribution over instant contact areas in the gear of the first group of gearboxes at **a** $T_2 = 2000$ Nm and **b** $T_2 = 4000$ Nm

The second group of gearboxes are multi-turn ones intended to control gate and wedge gate valves, which are characterized by higher duration of one operating cycle—from 5 to 60 minutes.

Therefore, multi-turn gearboxes have a slightly lower load-carrying capacity than quarter-turn ones at similar weight and size characteristics. To estimate the load-carrying capacity, RZAM-S-2500 (generation 1) and RZAM-S-2500 (generation 3) gearboxes were chosen; their geometrical characteristics are presented in Table 10, and their design layouts are shown in Fig. 11. The main differences of RZAM-S-2500 (generation 3) gearbox are:

- the reduced gearwheel diameter: from 250 mm to 224 mm (1.11 times);
- the reduced interaxial distance: from 77 mm to 65 mm (1.18 times);
- the increased worm outer diameter: from 55 mm to 59.5 mm (1.11 times).

Calculation results are presented in Table 11, and diagrams are shown in Fig. 12.

Similar to the case of quarter-turn gearboxes, one can say that the process of plastic strain of contact surfaces in gears will not progress.

When reducing the size of the 3rd generation gearboxes, the overlap factor was decreased; nevertheless, a more balanced contact localization allowed for achieving the uniform torque distribution over instant contact areas. It led to reduction of the value of plastic displacement as compared to the 1st generation gearboxes. This torque distribution caused a 70% decrease in plastic displacement, with the values of the largest calculated plastic displacement being 19 μm for the 1st generation gearboxes and 6 μm for the 3rd generation ones, which also do not exceed the allowable value (30 μm).

Typical tests of the 3rd generation gearboxes showed their operability during the whole specified service life under the mentioned (peak, maximum and nominal) rated loads.

Table 10 Simulation results for the second group of gearboxes

N area	RZAM-S-2500 (generation 1)				RZAM-S-2500 (generation 3)			
	Torque transmitted by the area, Nm							
	At $T_2 = 2500$ Nm		At $T_2 = 5000$ Nm		At $T_2 = 2500$ Nm		At $T_2 = 5000$ Nm	
	–	err	–	err	–	err	–	err
0	496	0	1015	0	565	0	1014	0
1	981	958	1926	1652	727	994	1473	1819
2	971	924	1893	1833	703	886	1521	1763
3	52	618	167	1515	505	619	991	1417
–	K_{ff}							
0	0.8	0.0	0.8	0.0	0.9	0.0	0.8	0.0
1	1.6	1.5	1.5	1.3	1.2	1.6	1.2	1.5
2	1.6	1.5	1.5	1.5	1.1	1.4	1.2	1.4
3	0.1	1.0	0.1	1.2	0.8	1.0	0.8	1.1
–	Value of plastic strain in the area, mcm							
0	0.00	0.00	6.47	0.00	6.1	8.11	5.64	0.00
1	0.00	8.54	8.61	18.89	0.00	0.00	1.07	4.12
2	0.00	4.31	9.39	16.05	0.00	0.00	0.85	3.20
3	0.00	0.00	15.12	7.84	0.00	0.00	4.39	1.16

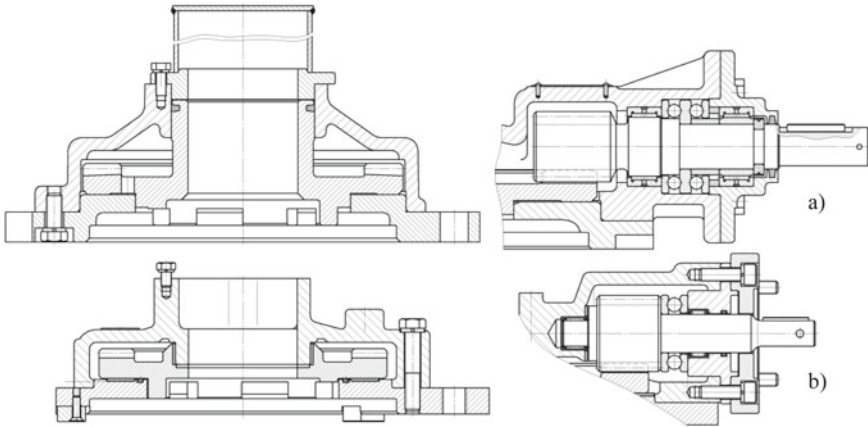


Fig. 11 Section view of the gearbox **a** RS1-60 (PS 28) and **b** RZA-S-2000 (PS 142)

Table 11 Results of manual gearbox simulation

N area	RRZA-S-3500			
	Torque transmitted by the area, Nm			
	N phase			
	3	3err	4	4err
0	381	390	149	160
1	941	959	893	913
2	1034	1038	1009	1013
3	976	966	961	952
4	169	147	487	463
–	K_{ff}			
0	0.54	0.56	0.21	0.23
1	1.34	1.37	1.28	1.30
2	1.48	1.48	1.44	1.45
3	1.39	1.38	1.37	1.36
4	0.24	0.21	0.70	0.66
–	Plastic strain in the area, mcm			
0	11.71	12.73	7.75	9.35
1	1.37	1.55	1.24	1.54
2	1.16	32.20	1.27	32.77
3	0.00	23.07	0.00	23.43
4	2.56	0.82	3.83	3.46

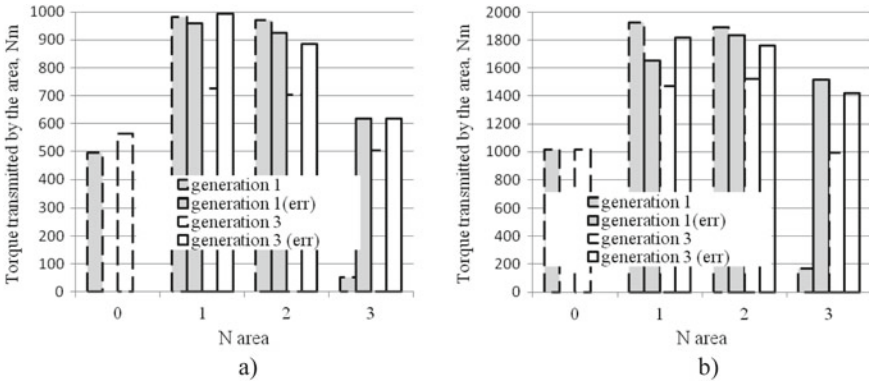


Fig. 12 Torque distribution over instant contact areas in the gear of the second group of gearboxes at **a** $T_2 = 2500$ Nm and **b** $T_2 = 5000$ Nm

5 Load State of 3rd Generation of Manual Gearboxes

In recent years, there has been a clear trend towards a separate gearbox layout version for pipeline valve gearboxes—exclusively for manual operation. These gearboxes are characterized by:

- an increased maximum torque;
- a shorter, often unrated service life;
- a smoother application of torque at the input shaft;
- a lower rotation speed, not more than 10...30 rpm.

In particular, global manufacturers such as AUMA [12], Rotork [13], Pro-Gear [14], based on their general gearbox range, have developed individual ranges exclusively for manual operation with the increased torque while maintaining the original gear dimensions. In response to this trend, a new range of manual quarter-turn spiroid gearboxes was developed based on the 3rd generation of gearboxes. While retaining the basic gear parameters, the design of the gearbox has been slightly modified:

- the worm radial bearing supports were replaced with sliding bearings, which increased the static load; it also allowed to develop the worm journal parts in the cross-section, which increased the worm bending strength;
- the scheme of gearwheel bearing supports has been changed: the radial load is taken by radial supports which are holes in the casing and base; the axial load is transmitted to the base along the whole area of its contact with the spiroid gearwheel, which allows to eliminate such a negative factor as the deflection of the spiroid gearwheel.

These changes made it possible to strengthen the gearbox layout design while retaining its original overall dimensions.

These layout changes were largely technical and did not pose any particular problem. The main problem was assessing the possibility of heavier loading of the main elements of gearboxes—spiroid gears. For this purpose, two series of calculations were performed to determine the maximum torque while designing the range of manually controlled gearboxes:

- In the first series, using the described above algorithm, the maximum torque was determined by contact loading, at which the value of plastic strain does not exceed the allowable value, and the area of plastic strain does not progress;
- In the second one, the maximum torque by bending loading was determined in the ANSYS system [15–19]. In this case, the surfaces imported into the system took into account the plastic strain which occurred after running-in and which was calculated during the first series of calculations. We took the value of 1100 MPa calculated according to Russian Standard GOST 21354 as the allowable bending stress.

At the peak torque the same level of loading is assumed for the gearboxes of both ranges, that leads to failure (risk of failure) of gearbox elements. The purpose of

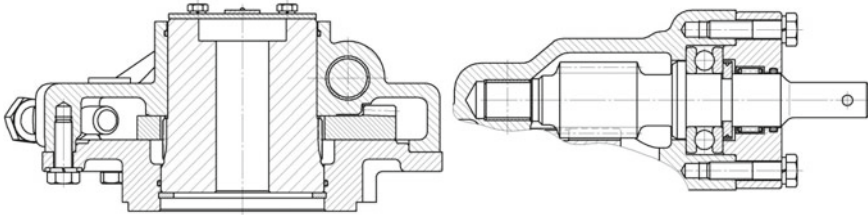


Fig. 13 Section view of the gearbox RRZA-S-3500

the calculation was to establish/verify the acceptability of increasing the maximum torque of the gear. At simulation of the first series of calculations, two states were considered—without the influence of errors and with their influence. In particular, for RZA-S-3500 model gearbox it was the mentioned above RZA-S-2000. We will also use this gearbox to demonstrate the example of the performed calculations. The layout of the designed gearbox is shown in Fig. 13, the results of the first series of calculations are summarized in Table 11, and the second series is shown in Fig. 14 and summarized in Table 12.

The torque increase resulted in a slight increase in load concentration at the tooth center. The maximum load concentration factor was 1.48 which can be explained by smaller bending compliance at the central part of the tooth, as it was previously demonstrated in [6].

The table shows that bending and shearing stresses do not exceed allowable values with the safety factor of 1.8. Typical tests of the gearbox model RRZA-S-3500 showed its operability during the whole specified service life under the action of rated loads, and a specially performed “crash-test” of the gearbox showed that the

Fig. 14 Graphic representation of ANSYS calculation results

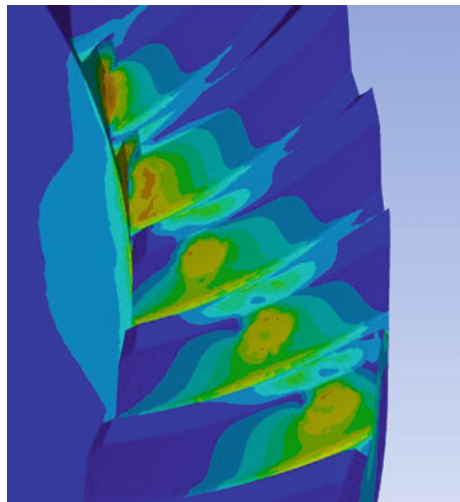
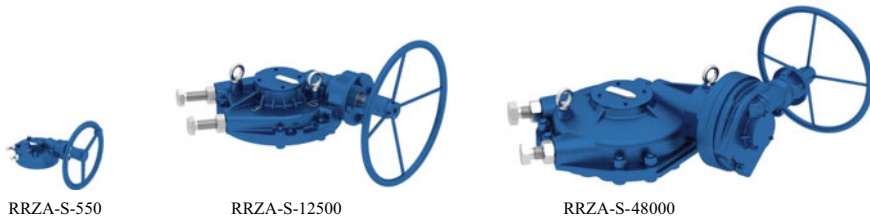


Table 12 Results of calculation by ANSYS

N area	Maximum bending and shearing stress at the tooth root, MPa
0	600
1	520
2	498
3	553
4	180

**Fig. 15** General view of manual quarter-turn spiroid gearboxes

meshing retains its strength even under the statically applied torque of 6050 Nm (the worm cover fastening proved to be the weakest element of the gearbox as a whole).

Similar calculations for other representatives of the gearbox range for manual control gave similar results. The main technical characteristics of the designed new range of manual control gearboxes (Fig. 15) and the value of maximum plastic strain calculated at the highest torque are shown in Table 13.

6 Conclusion

The presented calculation algorithm for analyzing the load distribution in the multi-pair spiroid gearing will make it possible to evaluate the elastoplastic contact area, the value of plastic strain of tooth flanks, and to specify the values of loads acting on individual teeth. The calculation results should become the basis for evaluating the strength of a multi-pair heavy-loaded gear by the conditions of allowable contact surface strain and the strength of worm threads and gearwheel teeth under the action of maximum and peak loads.

Table 13 Technical specification of the designed series of manual gearboxes


Parameter	RRZA-S-550	RRZA-S-1200	RRZA-S-1900	RRZA-S-3500	RRZA-S-6500	RRZA-S-12500	RRZA-S-18000	RRZA-S-25000	RRZA-S-36000	RRZA-S-48000
Model of the gearbox analog	RZA-S-300	RZA-S-600	RZA-S-1000	RZA-S-2000	RZA-S-4000	RZA-S-8000	RZA-S-11200	RZA-S-16000	RZA-S-20000	RZA-S-32000
Interaxial distance, mm	30.5	40	50	60	70	90	93	110	122	130
External diameter of spiroid worm, mm	25	28	37	42	47	61	62	73	75	85
External diameter of spiroid worm, mm	90	117	147	175	213	268	300	330	350	400
Maximum torque at the output shaft, Nm	600	1200	1900	3500	6500	12500	18000	25000	36000	48000
Peak torque at the output shaft, Nm	900	2000	2500	4000	8000	16000	25000	32000	48000	60000
Mass, kg	5	9	12	18	28	55	70	93	105	135
Maximum value of plastic strain calculated at the maximum torque, mcm	29.87	31.50	30.62	32.77	34.12	38.98	29.56	31.23	40.27	45.64

References

1. Goldfarb, V.I., Glavatskikh, D.V., Trubachev, E.S., Kuznetsov, A.S., Lukin, E.V., Ivanov, D.E., Puzanov, V.Yu.: Spiroid Gears for Pipeline Valves. Veche, Moscow (2011)
2. Goldfarb, V.I., Trubachev, E.S., Kuznetsov, A.S.: Comparative analysis of generations of the spiroid gearboxes for pipeline valves drives. *Armaturostroeniye* **N1**(94), 80–87 (2015)
3. Zablonskiy, K.I., Popel, O.E., Telis, I.Ya.: Determination of load distribution between teeth in globoid gearing. *Izvestiya vuzov, Mashinostroeniye* **7** (1971)
4. Sheveleva, G.: Solution of the contact problem by method of consequent loading. *Izvestiya vuzov, Mashinostroeniye* **9**, 10–15 (1986)
5. Goldfarb, V.I., Airapetov, E.L., Novoselov, V.Yu.: Calculated model of bending deformation of a spiroid gearwheel tooth. In: Proceedings of the XXXVIII International Machine Parts Department Conference, pp. 26–29. Slovakia, Bratislava (1997)
6. Trubachev, E., Kuznetsov, A., Sannikov, A.: Model of loaded contact in multi-pair gears. In: *Advanced Gear Engineering, Mechanisms and Machine Science* **51**, Springer International Publishing AG Switzerland, pp. 45–72, <https://doi.org/10.1007/978-3-319-60399-5> (2018)
7. Kuznetsov, A., Sannikov, A.: Method of calculation of elasto-plastically heavy-loaded low-speed spiroid gear. *Bulletin of Kalashnikov ISTU, N2*(20), pp. 60–64. ISTU Publishing House, Izhevsk (2017)
8. Sannikov, A.M.: Validation of the model of elastoplastic contact of spiroid gears. *Izvestiya vuzov, Mashinostroeniye* **4**, 23–33 (2020)
9. Tretyakov, E.M.: Method for contact strength calculation of solids by limiting contact loads. *Herald of the Bauman Moscow State Technical University. Mechanical Engineering* **4**, pp. 98–124 (2012)
10. Kirichek, A.V.: Providing the quality of non-coaxial screw mechanisms by strain hardening of their mating parts. DSc Thesis. Vladimir (1999)
11. Gear manufacturing. Reference book. B.A. Taits ed., 3rd ed. Moscow, Mashinostroeniye (1990)
12. <https://www.auma.com/en/products/multi-turn-gearboxes>. Accessed 5 Jan 2020
13. <https://www.rotork.com/en/products-and-services>. Accessed 5 Jan 2020
14. <http://www.pro-gear.su/products/>. Accessed 5 Jan 2020
15. Volkov, A.E., Sheveleva, G.I., Medvedev, V.I.: Calculating the contact pressures in bevel gear drives with different tooth models. *J. Mach. Manuf. Reliab.* **2**, 63–66 (2003)
16. Karatushin, S.I., Pleshanova, Y., Bilyuk, N.A., Bokuchava, P.N.: Verification power calculation for teeth of the gearbox planetary stage by ANSYS. *Izvestiya vuzov, Mashinostroeniye* **12**, 77–84 (2015)
17. Hohn, B., Steingrover, K., Lutz, M.: Determination and optimization of the contact pattern of worm gears. *Proc. Int. Conf. Gears VDI* **1**, 341–352 (2002)
18. Fuentes, A., Ruiz-Orzaez, R., Gonzalez-Perez, I.: Compensation of errors of alignment caused by shaft deflections in spiral bevel gear drives. In: *Theory and Practice of Gearing and Transmissions. Mechanisms and Machine Science*, vol. 34, pp. 301–320. Springer, Springer International Publishing AG Switzerland, ISBN 978-3-319-19740-1 (2016)
19. Houser, D.: The effect of manufacturing microgeometry variations on the load distribution factor and on gear contact and root stresses. *Gear Technol.* **6**, 51 (2009)

Uncertainties in Modeling the Lifetime-and-Functional Properties of Gear Trains and Transmissions and Ways to Reduce Them



V. B. Algin , M. A. Kananovich, S. M. Paddubka, U. M. Sarachan, S. V. Shil'ko, and V. E. Starzhinsky

Abstract Typical cases of problem situations associated with uncertainties in modeling properties of gears and transmissions of cars, tractors and other similar technically complicated items are considered. Such items work in a changing environment, consist of many heterogeneous non-standard components and are controlled by the operator. Typical uncertainties include: isomorphism, incorrect schematization, lack of detailed data about the item, variation of the environment, the presence of a variety of calculation (modeling) methods, etc. Ways of resolving problem situations associated with uncertainties are developed. Reducing the uncertainty in modeling the individual lifetime of an item can be achieved through digitalization (diagnostic data, recognition of item state). When uncertainty is unavoidable, it is recommended to create a decision-making space that is convenient for stakeholders to analyze and assess the degree of risk resulting from their decisions. It is shown that situations in decision-making can be significantly enhance by introducing an indicator that successfully describes a set of basic properties of an item. The main provisions of the article are accompanied with examples from the authors' own practice. The considered approaches are methodologically typical for many complex mechanical and combined items based on mechanical systems.

Keywords Gear train · Transmission · Uncertainty · Modeling · Operation conditions · Functional properties · Reliability · Solution space

V. B. Algin (✉) · S. M. Paddubka
The State Scientific Institution "The Joint Institute of Mechanical Engineering of the National Academy of Sciences of Belarus", Minsk, Belarus

M. A. Kananovich
LLC "Sababa Labs+K", Minsk, Belarus

U. M. Sarachan
LLC "Sababa Labs", Minsk, Belarus

S. V. Shil'ko · V. E. Starzhinsky
The State Scientific Institution "V.A. Belyi Metal-Polymer Research Institute of National Academy of Sciences of Belarus", Gomel, Belarus

1 Introduction

Any activity is associated with uncertainty. Even more uncertainty arises when modeling activities. Scientific research is a search for patterns that are formulated using intuitive basic concepts/terms. Basic concepts are not strictly defined, they are introduced, otherwise a closed circle is created when concepts are expressed through each other. Moreover, the basic concepts themselves always contain uncertainty.

The simplest definition of uncertainty is given in [1], where it is noted that many specialists in decision theory, statistics and other quantitative fields have defined uncertainty, risk, and their measurement as: Uncertainty is the lack of certainty, a state of limited knowledge where it is impossible to exactly describe the existing state, a future outcome, or more than one possible outcome. The problem of uncertainty attracts many authors and it is studied from various points of view.

The book [2] is about understanding uncertainty, about handling it and, above all, about helping you to live comfortably with uncertainty so that you can better cope with it in your everyday life.

In [3], sources of uncertainty and a method to propagate uncertainty throughout a project analysis are investigated. Propagating uncertainty allows the impact of adding information about an input parameter to carry through to the result. A probabilistic model that explicitly includes probability distributions for parameters can indicate the degree of uncertainty reduction to be expected by obtaining more information.

Many types of uncertainty affect the design and operation of complex systems [4]. Uncertainty is not always a negative to be mitigated; robust, versatile and flexible systems not only mitigate uncertainties, they can also create additional value for users. A framework to aid in the understanding of uncertainties and techniques for mitigating and even taking positive advantage of them is presented. Current and developing methods for dealing with uncertainties are projected onto the framework to understand their relative roles and interactions [4].

The problems of quantifying uncertainty in computational science and engineering are presented in the proceedings of the UNCECOMP 2019 conference [5]. The aim of the conference is to reflect the recent research progress in the field of analysis and design of engineering systems under uncertainty, with emphasis in multi-scale simulations. Some characteristic papers from these proceedings are considered below.

In [6], a hybrid surrogate modeling approach is proposed for the uncertainty quantification of nonlinear stochastic dynamical systems in the time domain. The model is constructed using a nonlinear system identification tool, the Nonlinear Auto Regressive with eXogenous (NARX) input model, and the Kriging approach for uncertainty propagation.

In [7], two types of uncertainty (aleatory and epistemic) are distinguished. Aleatory uncertainty arises from the natural variability in dynamical environments and material properties, errors in manufacturing processes or inconsistencies in the realisation of systems. Aleatory uncertainty cannot be reduced by empirical effort. Epistemic uncertainty is caused by measurement imperfections or lack of perfect

knowledge of a system. This could be due to not knowing the full specification of a system in the early phases of engineering design.

Imperfect scientific understanding of the underlying physics involved, would cause uncertainty in the future performance of a system even after the design specifications have been decided. If uncertainties are small they can often be neglected or swept away by looking at the worst-case scenarios. However, in situations where the uncertainty is large, or would affect an engineering decision, this approach is suboptimal or impossible. Instead, a comprehensive strategy of accounting for the two kinds of uncertainty is needed that can propagate imprecise and variable numerical information through calculations. Paper [7] describes a software tool, named puffin, that takes existing code and converts into uncertainty aware code in the same language making use of intrusive uncertainty propagation techniques. It can work either automatically or with user specification of the uncertainties involved in the system.

In [8] it is indicated that when developing a mathematical model to simulate the fatigue damage of steel members, many sources of uncertainty are identified. First, the model input parameters have a wide range of variability. Furthermore, additional uncertainty arises by the simplification of mathematical models adopted, as well as, field measurement errors and varying application conditions. The material response to applied stress is considered complicated since there are several factors that can alter the endurance limit. These factors include: surface finish, size, type of loading, temperature, corrosive, and other aggressive environments, mean stresses, residual stresses, and stress concentrations. Also, fatigue data must be obtained from specimens and used in design for structural safety as mentioned in design codes. However, this information is not often available. Therefore, study [8] presents a structural health monitoring approach to overcome the limitation and inaccurate estimation of damage quantification models. The suggested framework relies on fatigue damage prediction models incorporated with real time damage records. All sources of uncertainty are incorporated in the health monitoring scheme to guarantee an optimal statistical identification of the state damage. The accuracy and robustness of the presented scheme will be assessed through a set of controlled experiments and numerical simulation of real case scenario.

In fact, the work [8] is based on digitalization, that is, the use of a digital twin (DT), which is currently the most effective tool for reducing uncertainty by obtaining data on the operating conditions and loading modes of a particular item.

In [9], a DT approach was developed for performing mission optimization under uncertainty aimed at ensuring system safety with respect to fatigue cracking. This is achieved by designing mission load profiles for the mechanical component such that the damage growth in the component is minimized, while the component performs the desired work. The proposed approach has three components: damage diagnosis, damage prognosis, and mission optimization. All of them are affected by uncertainty regarding system properties, operational parameters, loading and environment, as well as uncertainties in sensor data and prediction models. Therefore, the proposed methodology includes the quantification of the uncertainty in diagnosis, prognosis, and optimization, considering both aleatory and epistemic uncertainty sources.

Under considering DT for the topic of gears and transmissions, it should be noted the following studies:

- simulation of the tooth root strength under consideration of material quality, finishing process and size effects [10],
- improved tooth contact analysis by using virtual gear twins [11],
- standardized gear unit model and creating an industry-wide standard for simple data exchange in transmission development under the name REXS (Reusable Engineering EXchange Standard) [12],
- Digital Twin of gear measuring center [13],
- combining gear designing with manufacturing process [14].

The analysis of publications leads to the conclusion that models and methods associated with the problem of uncertainty are very individual and difficult to transfer from one object to another.

The aim of this study is to systematize typical cases of problem situations associated with uncertainty in modeling basic properties of gear trains and transmissions and to substantiate approaches and methods for resolving these problem situations.

The properties of gears and transmissions are realized when they function as part of machines. Therefore, it is necessary to consider the operating conditions of machines and the actions of their operators, which are largely uncertain in nature.

2 Examples of Uncertainties in the Life Cycle of Gears and Transmissions

2.1 A Plurality of Representations of the Same Object

Isomorphism is a plurality of representations of the same object that endowed with structure. A typical example is the problem of isomorphism in the synthesis of the structure of gear transmission systems.

A practical task is to describe the set of structures for the subsequent synthesizing diagrams (schemes) of planetary gearboxes. The main idea is to transfer the isomorphism problem from the “graph” sphere to the area of constructing matrices of a certain kind. The number of inputs of the link V_i into planetary mechanisms is called the degree of the link $\deg V_i$ (a link can enter one or more mechanisms). All variants of the distribution of the $\deg V_i$ should be described in advance. Usually, these variants are few.

When constructing a matrix of incidents for describing structure, several rules (conditions) are used. The basic rule that ensures the construction of the original canonical matrix is as follows: it is necessary to use parts (links) with the lowest numbers for each structure. Additional ones are: (1) integrity (except for individual cases when the initial structure is represented by several fragments), (2) no blocking,

A	V1	V2	V3	V4	V5	V6
U1	1	1	1			
U2	1	1		1		
U3			1		1	1

B	V1	V2	V3	V4	V5	V6
U1	1	1		1		
U2	1	1	1			
U3			1	1	1	

Fig. 1 Canonical matrix **A** (left) and non-canonical one **B** (right) describing the same structure

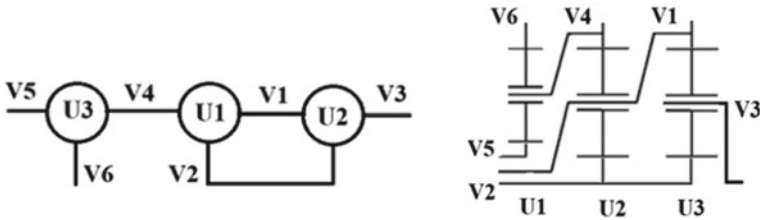


Fig. 2 Structure (left) and diagram (right) corresponding to the matrices in Fig. 1

Variant 1	Variant 2	Variant 3
1 1 0 1 0 0 0	1 1 1 0 0 0 0	1 1 1 0 0 0 0
1 1 0 0 1 0 0	1 1 0 1 0 0 0	1 1 0 1 0 0 0
1 0 1 0 0 1 0	1 0 1 0 1 0 0	1 1 0 0 1 0 0
1 0 1 0 0 0 1	0 1 0 0 0 1 1	0 0 1 0 0 1 1

Fig. 3 Variants of the computer construction of canonical matrices for four mechanisms containing seven links with the different distribution of degrees by links: variant 1 (distribution 4-2-2-1-1-1-1), variants 2 and 3 (distribution 3-3-2-1-1-1-1)

(3) variety: using all different options for selecting parts (links) with different status of $degV_i$ [15].

Figure 1 shows matrices **A** and **B** describing the structure of the planetary block of three three-link mechanisms U1–U3 and six links V1–V6. Figure 2 shows the structure and diagram corresponding to the matrices in Fig. 1. Figure 3 shows examples of computer construction of canonical matrices [16].

2.2 Schematization of Gears and Transmissions to Simulate Their Dynamics

Ulf Grenander notes: “The search for regularity is a dominant theme in man’s attempt to understand the world around him. Any such attempt is based on an assumption, tacitly made or explicit, that phenomena in nature and in the man-made world

are governed by laws that result in order and structure” [17]. Below this idea is concretized in relation to the considered objects of mechanics.

A mechanical system with elementary mechanical components (the concentrated masses and the massless joining links) is essential idealization which imposes certain restrictions on possible combinations of joints for mentioned items.

Typical errors in schematization are: (1) drawing up equations without a calculated mechanical system; (2) arbitrary connection of components of mechanical systems.

Before modeling, it is necessary to move from a real-world object to its model, which includes components idealized within a certain scientific discipline. Without such a transition, a situation is possible when the composed equations may not correspond to any object considered in a given scientific discipline, which means that these equations do not make sense.

However, the use of the accepted idealized components is not a sufficient condition for correct modeling. Typical examples of errors that arise with an arbitrary connection of force, inertial and elastic components are analyzed in [16, 18]. Some examples of such errors are in Fig. 4. It is shown that regardless of the software package in which the simulation is performed, the program hangs due to uncertainty in the choice of parameters in the course of calculations, although the initial model of the object is formed by the program, and it proceeds to dynamic calculation.

With this in mind, it is proposed to form mechanical systems according to certain rules and with certain restrictions, which are caused by mechanical systems with concentrated parameters and the use of a computer as a discrete computing device. For this, the concept of a “regular mechanical system (RMS)” has been developed.

The RMS concept considers that mechanical system consists of the concentrated masses (inertial components) and massless (non-inertial) devices-connectors: shafts, clutches, brakes, gears, motionless links, and other devices imposing kinematic connections for masses. Masses can be in contact interaction. For devices-connectors the direct connecting (not through inertial component) is prohibited. External force (torque) can effect only on the masses.

This is a principle of regularity, which is used for the representation of a real object. Its violation can lead to wrong schematizations and errors in calculations or impossibility of mathematical model realization by the computer.

A general view of a regular mechanical system is shown in Fig. 5. Other provisions of the RMS concept and examples of the use of regular mechanical systems in practical calculations of the dynamics of multi-mass systems (Multibody Dynamics), including those with a variable structure, are given in [16, 18–20].

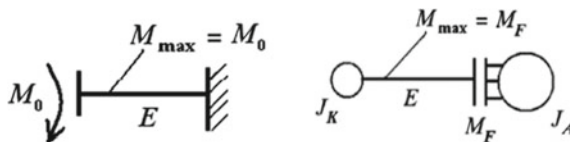
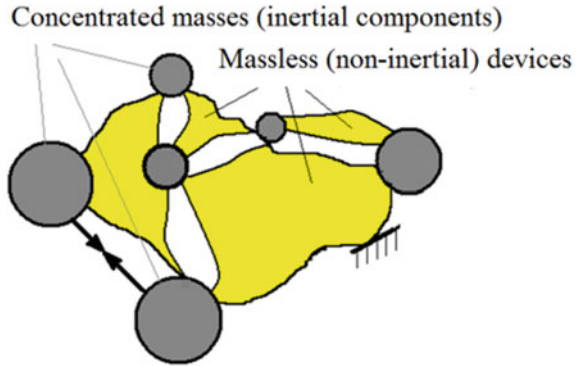


Fig. 4 Incorrect mechanical models: application of a torque to a massless elastic link (left), model with a massless friction clutch (right)

Fig. 5 General representation of regular mechanical system



2.3 Environment Variation

A common way to determine the reliability indicators of items is to monitor them in operation. However, for highly reliable products, this is long time consuming. A shorter way is to determine the load modes of their main elements, and then carry out probabilistic calculations in which the variation of load modes for these elements is reproduced.

The problem of structuring and reflection in the calculations of the load modes of transmissions of mobile machines is most deeply considered in the works of the scientific school of Corresponding Member of the Belarussian Academy of Sciences Igor Tsitovich [21].

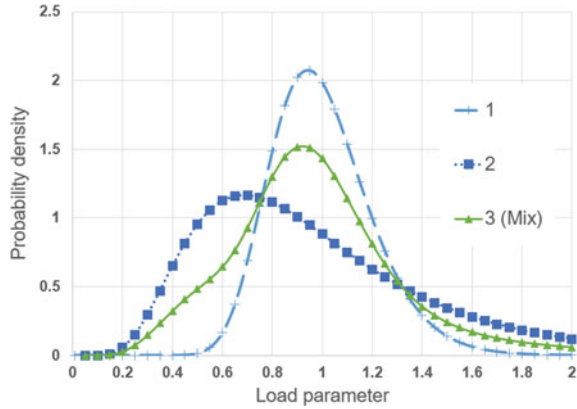
There are known proposals for the use in the calculations of generalized data obtained by “mixing” the load distribution curves for individual conditions (taking into account their shares) into a generalized curve. However, such proposals are wrong. The approach of the scientific school of Igor Tsitovich is that in the calculations it is necessary to take into account the variety of load modes and the generalized curve cannot correctly replace the variation.

An illustrative example demonstrating the fallacy of mixing load curves. Figure 6 shows the load curves for a transmission part obtained in two typical operating conditions 1 and 2, with a relative duration of α_1 and α_2 , while $\alpha_1 + \alpha_2 = 1$. The averaged curve 3 is obtained by mixing curves 1 and 2 under the condition $\alpha_1 = \alpha_2 = 0.5$. In practice, the durations α_1 and α_2 vary from machine to machine. An estimate is given below to show that the measure of damage caused by the variation of α_1 and α_2 is significantly different from the measure of damage obtained on the average curve 3.

To assess the damage measure of a part, you can use the formula

$$D = (p_i)^m \Delta f_i \tag{1}$$

Fig. 6 Load curves 1 and 2 for typical conditions and curve 3 as a result of their averaging



This formula is specific to the measure of damage caused by the accumulation of fatigue damage. In this formula: m is an exponent of stress-cycle diagram of a typical part; p_i is load, Δf_i is the duration (number of loading cycles of the part) at the considered load p_i .

The measure of damage caused by the action of curves 1 and 2 is

$$D_{12} = \alpha_1 D_1 + \alpha_2 D_2 \tag{2}$$

The values of D_{12} calculated for the variable duration of α_1 (and $\alpha_2 = 1 - \alpha_1$, respectively) and the case $m = 3$ (contact fatigue) are given in Table 1. Besides the damage measures from the considered curves at typical values of m are shown in Table 2.

From the presented data, it can be seen that the use of the averaged curve leads to significant errors, especially if the gamma percentage resource is estimated at high gamma values. The use of variation of loading conditions in probabilistic calculations is considered below for a more general case: variation of operation conditions.

Table 1 Total damage measures for different contribution of the curves for $m = 3$

α_1	0	0.1	0.2	0.3	0.4	0.5	0.6	0.7	0.8	0.9	1.0
D_{12}	1.36	1.34	1.31	1.29	1.27	1.24	1.22	1.20	1.17	1.15	1.13

Table 2 Damage measures from the considered curves for typical m

m	Curve 1	Curve 2	Curve 3 (mix)
3	1.13	1.36	1.24
6	1.81	4.38	3.09
9	4.08	20.89	12.49

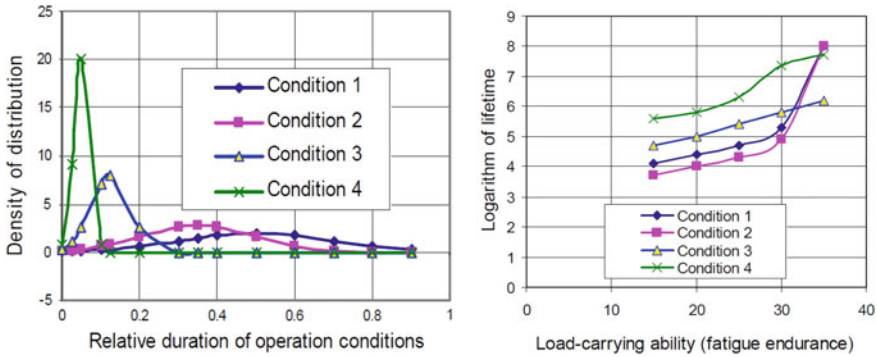


Fig. 7 Representation of operation conditions (left) and Lifetime-strength curves (right)

Reliability calculation with taking into account the operation conditions as common factor. In the widespread practice of probabilistic calculations of systems, distributions of the lifetimes of elements are used as initial information, and load indicators are not taken into account. In calculating the lifetimes of mechanical components based on the characteristics of their loads and load-carrying ability, the load indicators are considered as independent, which is incorrect. This is especially important when calculating transmission planetary trains, reducers and driving axles, for which the load level of all elements is determined by the input torque. And the input torques differ according to the operating conditions. This problem is considered in [22, 23].

Loading concepts are different for different elements of the machine. But all loads are caused by operation conditions. The operation conditions are probabilistically described in terms of relative durations for generally accepted typical conditions (see Fig. 7, left). To assess loaded systems, in the general case, the calculation can be carried out using data on lifetimes of their elements for certain operation conditions. For this, lifetime-strength curves of the elements are used (Fig. 7, right). These curves should be previously obtained by deterministic calculations of mechanics of machines.

The relative durations of operation conditions α_k and the load-carrying ability of elements are random variables. Using a method of statistical modeling (Monte-Carlo), in each cycle of modeling the durations of the operation conditions α_k ($k = 1, 2, \dots, K$) and load-carrying abilities of elements are reproduced. Then using lifetime-strength curves the lifetimes of elements can be found at these conditions.

This forms the distributions of the lifetimes for the elements and the system as a whole under all conditions at the end of the simulation. To obtain the condition $\sum \alpha_k = 1$ in each cycle, the special correction is used. When the statistical modeling is carried out, the characteristics of the initial and corrected values, related to the total sum, are different. Therefore, closeness of parameters of distributions α_k to the given values is provided by means of a special computational procedure that performed before the main procedure [16, 18].

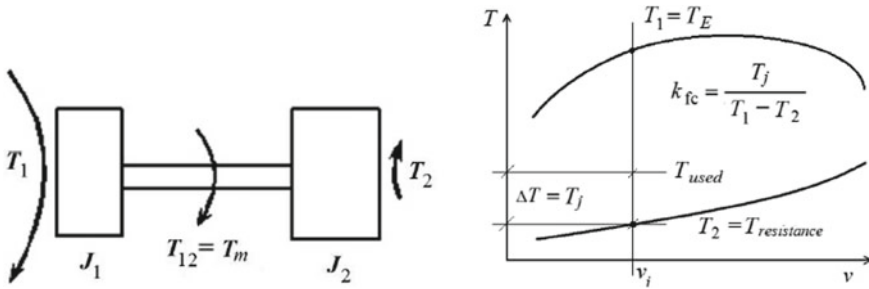


Fig. 8 Dual-mass (J_1 – J_2) diagram of a machine unit with applied torques (left) and graphical interpretation of the free traction coefficient k_{fc} (right)

Driving style. In modern sources, driving style is evaluated mainly in terms of energy efficiency. At the same time, driving style is one of the most significant factors in assessing load and lifetime.

It is proposed to evaluate the driving style by the free traction coefficient k_{fc} [16, 18]. This is the fraction of free traction that the driver uses to accelerate the vehicle (see Fig. 8).

In the figure, T_1 is the torque coming from the engine, T_2 is the torque from the drag forces, T_{12} is the torque that loads the transmission, T_j is the torque that is used to accelerate the vehicle.

It makes sense to distinguish three main driving styles: Quiet ($k_{fc} = 0.25$), Active ($k_{fc} = 0.5$), and Sporting ($k_{fc} = 0.75$). These k_{fc} values refer to the lowest transmission gear. Top gear is mainly used to maintain an acceptable driving speed. Therefore, for the top gear, it can be assumed that the k_{fc} has lower values: 0.05 (Quiet style), 0.1 (Active style), and 0.5 (Sporting style). Intermediate values of the k_{fc} are used for intermediate gears.

Some calculations have been performed and their results are presented below. The design object was Sport Utility Vehicle (SUV). This SUV, like SsangYong Rexton, has gross weight 2550 kg, a maximum capacity of the engine 165 hp/4000 rpm. Road condition is “Country” with an average rolling resistance coefficient $f_0 = 0.025$. The values of the free coefficient k_{fc} are given in Table 3.

Results of lifetime calculations in relation to groups of parts (gears, bearings) of the input shaft (1 Input) and of the output shaft (2 Output) of the gearbox are in Fig. 9.

Table 3 Distribution of k_{fc} by gears (gear ratios) from first to V (top) gear and driving style for the SUV

Driver style	I (4.315)	II (2.475)	III (1.536)	IV (1.000)	V (0.807)
Quiet	0.25	0.145	0.092	0.061	0.05
Active	0.50	0.290	0.183	0.122	0.10
Sporting	0.75	0.619	0.552	0.514	0.50

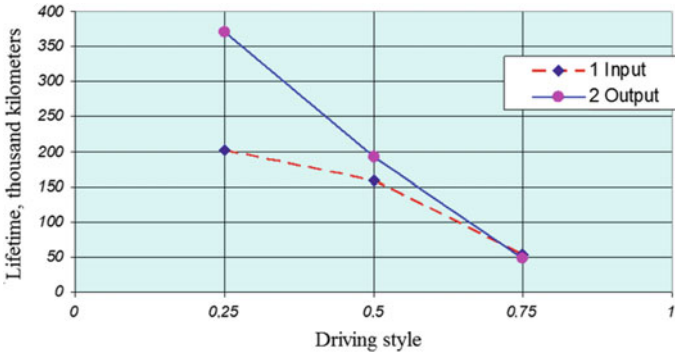


Fig. 9 Lifetime vs. driving style

These results show that that lifetimes of transmission parts in the sporting driving style is 4–7 times less than in the quiet one. Thus, driving style is an important factor when lifetime calculating and designing a vehicle transmission.

2.4 Lack of Detailed Data on Unit Design

A modern vehicle contains many units supplied by third parties. The supplier indicates the characteristics of this unite in the catalogs of its products, but does not provide the data required to estimate the lifetime. In such cases, a comparative lifetime assessment technique based on the use of available data can be applied. The main idea is to assess the damage measures of the unit when it is installed on the vehicle under study and vehicles-analogs that already use this unit.

It is known from the practice of operation that the gearbox ZF6S-850R has sufficient lifetime when it works in vehicles DAF FAN LF 55 and MAN TGL 8.180. The forward gear ratios of this gearbox $U_1 \dots U_6$ are known: 6.72; 3.68; 2.15; 1.41; 1.0; 0.79.

It is necessary to evaluate the gearbox lifetime when the gearbox ZF6S-850R will be used in the vehicle MAZ-447131.

Basic parameters of the vehicle MAZ-447131 and vehicles-analogs with gearbox ZF 6S-850R are presented in Table 4. For a detailed description of the parameters, see [24]. Additional data on vehicles and their loading modes are given in [25].

The total damage per km Q is determined by taking into account the damaging effect of the torque at the gearbox output by summing the damages ($\sum Q_i$) at six forward gears ($i = 1 \dots 6$). In general, Q is an integral estimate that may not always be associated with a particular transmission part. As a rule, the limiting elements are transmission parts (gears, bearings), the loading of which is determined by the torque acting on the gearbox output shaft. The limiting state for such parts is the accumulation of contact fatigue damage. The exponent of stress-cycle diagram for

Table 4 The basic parameters of the investigated vehicle and vehicles-analogs with gearbox ZF 6S—850R

Parameter	MAZ-447131 (haul car-van)	DAF FAN LF 55 (haul car-van)	MAN TGL 8.180 (dump truck)
Maximum engine torque, Nm	700	820	700
Gross weight, kg	19450	24500	18700
Rolling radius of a tire, m	0.38	0.45	0.38
Axle ratio	3.90	4.56	4.11
Number of loading cycles per km on gears $N_1 \dots N_6$, 1/km	$2.53 \dots 1.27 \times 10^2$	$2.16 \dots 1.08 \times 10^2$	$2.53 \dots 1.27 \times 10^2$
Relative runs on gears $\xi_1 \dots \xi_6$	0.006...0.300	0.006...0.300	0.006...0.300
Calculated torques on gears $M_{p1} \dots M_{p6}$, Nm	4230...498	4960...583	4230...498
Run factors on gears $K_{p1} \dots K_{p6}$	0.175...0.32	0.17...0.38	0.20...0.35
Total damage measure $Q = \sum Q_i$, (Nm) ³ /km	4.21×10^9	6.56×10^9	4.80×10^9
Relative damage measure, %	100	156	114

such parts $m = 3$. In considered case, the resulted damage measure is analogous to the damage measure for a bearing of output shaft of the gearbox.

Taking into account that the considered damage measure is inversely proportional to the lifetime, it can be assumed that the lifetimes of gearboxes on the vehicles under consideration will be in the same inverse relationship, and the considered gearbox ZF 6S-850R is suitable for operation at the MAZ-447131.

3 Main Types of Uncertainties in the Life Cycle of Gears and Transmissions. Methods and Approaches to Overcome Them

Based on the above examples and other data, the following types of uncertainties in the life cycle of gears and transmissions can be distinguished:

- Isomorphism (see Sect. 2.1),
- Fuzzy rules for object schematization (see Sect. 2.2),
- Environment variation (see Sect. 2.3),
- Lack of item data (see Sect. 2.4),

- Variety of calculation methods,
- Lack of an indicator that integrally reflects the various properties of the item.

The variety of calculation methods leads to epistemological uncertainty when there are different approaches and methods for modeling the same object or process. Thus, in [26], a description of nine high-cycle fatigue models is given for calculating the components of mechanical systems. And among them, five models belong to the linear version, three models are based on the revised version, and one model takes into account the endurance limit reduction.

An important condition for analysis and decision-making is to bring all calculation (modeling) methods to a single form of results presentation. In [26], for this, the lifetime form was used for all the indicated options, although many of them in their original form worked with effective and working stresses and other indicators not related to the lifetime.

The uncertainty of the environment can be partially eliminated through *digitalization*.

With unavoidable meaningful uncertainty, it is proposed to use the representation of the *decision-making space* in a form convenient for analyzing by the interested responsible parties.

3.1 Digitalization

Individualization of an item and its information model (Digital twin) from stage “making and assemblage” is presented in Fig. 10. Individualization takes place is due to the supplied components; used equipment and personnel (stage of making and assemblage); operation conditions, the operator and the maintenance (operation stage) [27, 28].

The current level of development of sensors and computer facilities also allows recognizing the state of the environment and transferring data for management systems and forecasting models that use data from the environment. In this case, the environment model also refers to the item digital twin.

When installing the sensors, the principle of minimum multiplicity should be adhering. Sensors, even in the minimum number, should reflect the force and speed constituents of the unit operation modes. In the ideal case, a one sensor can be used to obtain a load (force) spectrum, by which the load processes of all the limiting components are reconstructed.

Since it is not always possible to install a sensor to generate a signal about the loading the limiting element, the task of reconstructing local loads of limiting elements arises. To solve it, models that allow to reconstruct the stresses (or other loads) of the limiting elements from the signals of existing sensors, should be developed and used.

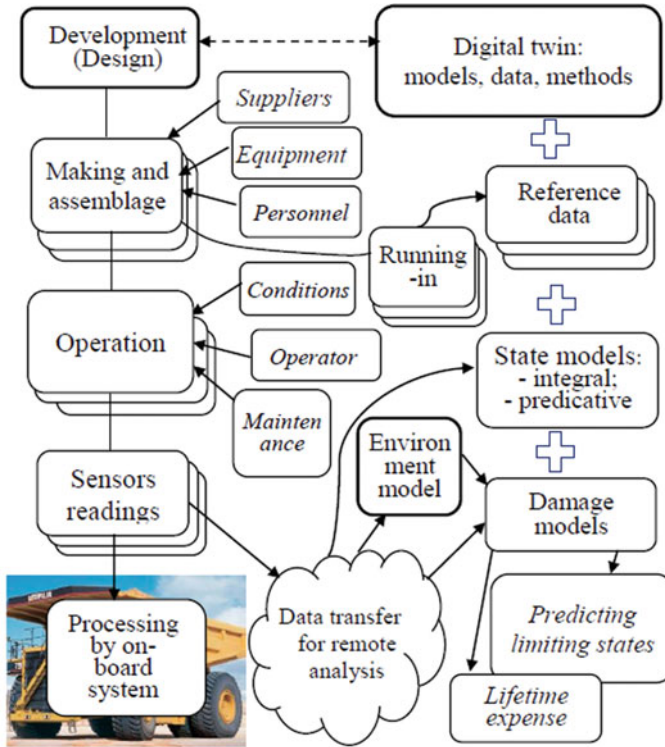


Fig. 10 Individualization of an item and its information model (Digital twin) from stage “making and assemblage”

It is rational to use the data on the loading in the form of general power flows, and individualize the loads for the limiting components to conduct when considering their limiting states.

The feature of the developed diagnostic method is using conceptual modeling the oscillating process for the gear drive and the propagation of vibrations in the transmission [27, 28]. It is advisable to applicate together integral diagnostic models and predictive ones based on damage accumulation (Fig. 10, block “State models”). Such a “two-coordinate” approach (from two points of view) ensures a higher veracity of the individual lifetime forecast.

The main variable individual component of any transmission unit is the level of its internal dynamic loading. Changes in this level are due to the peculiarities of the manufacture of the unit and the operating conditions of the machine, which includes the transmission unit. The most sensitive components to changes in the internal dynamic load of the unit are gears and bearings. The greatest damage to the clutches is associated with short-term transient processes, which requires individual monitoring of the modes of these processes.

3.2 *Visible Representation of the Decision-Making Space*

Representation of the entire space of possible solutions in a form convenient for responsible persons allows taking into account the probabilistic nature of the problem and assessing the risk of decision-making. This approach is an alternative to approaches based on the search for optimal solutions, in which a rigid fixation of constraints on parameters, which in reality vary significantly, is inevitable.

Typical representations of the solution space are:

- (1) probabilistic representation of a one-dimensional indicator/criterion,
- (2) clustering (for a small number of interrelated indicators),
- (3) introduction of an indicator that can integrity and reliably reflect the analysed properties of a complex item.

An example of using the first form is described in [29, 30], where a method is given for determining and representing energy consumption by an electric bus in the form of energy consumption distribution along the route, taking into account operational, weather and other conditions. factors.

An example of using clustering is given in [31]. Based on the results of the simulation of transient transmission processes, the areas of the diagram with the characteristic values of the parameters are identified and visually presented. These are the maximum dynamic torques on the input and output shafts, specific work and power of the clutch when it is engaged.

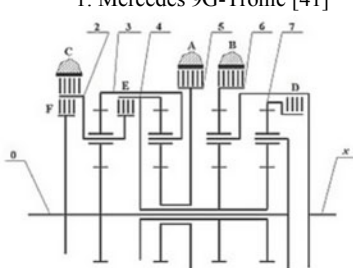
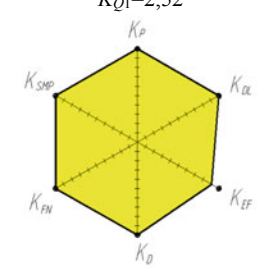
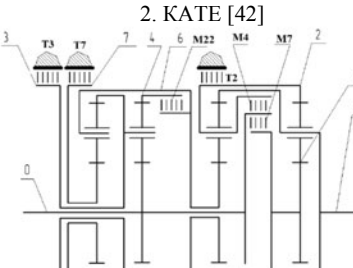
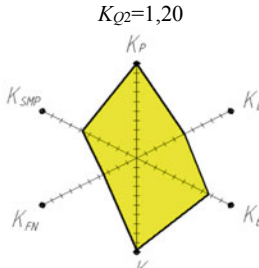
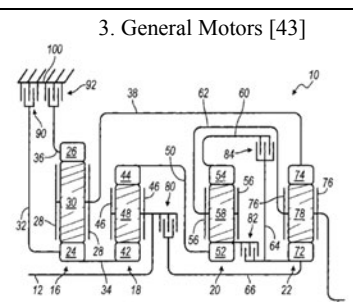
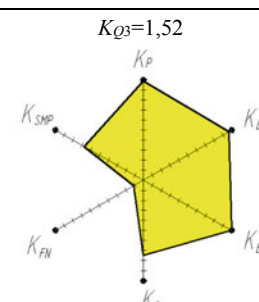
The ways of introducing indicators to reflect the properties of a complex object are considered below.

Introduction of a multidimensional indicator to reflect the heterogeneous properties of the product by an example a radar chart [16, 32]. The perfection of mechanical systems is determined on the basis of a set of indicators characterizing the basic their technical properties. These key features include: functionality (quality of set of gear ratios K_{FN} and range K_D), energy efficiency K_{EF} , weight and size (compactness K_P and design complexity K_{SMP}) and durability K_{DL} . All these indicators are formed as a result of calculations under the kinematic diagram. They are then normalized by dividing by the best values for the transmissions under consideration. The obtained values are used to build a radar chart and form a general indicator (Table 5).

The construction of a radar chart is accompanied not only by the image of the “radar”, but also by a general quantitative assessment of the transmission in the form of a complex quality indicator K_Q . This indicator is equal to the area of the formed polygon.

From presented results follows that the transmission 9G-Tronic has best value of K_Q . This fact confirms the high reputation of this transmission and as well as the reliability of the developed methodology.

Table 5 Assessment of gear transmissions: [41] = EP 3011190, [42] = RU 2549344, [43] = US 7699741

Transmission	Ratios	Evaluation
<p>1. Mercedes 9G-Tronic [41]</p> 	<p>5,503 3,333 2,315 1,661 1,211 1,0 0,865 0,717 0,601 -4,932</p>	<p>$K_{Q1}=2,52$</p> 
<p>2. KATE [42]</p> 	<p>5,85 2,95 2,0 1,5 1,2 1,0 0,85 0,74 0,65 -5,7</p>	<p>$K_{Q2}=1,20$</p> 
<p>3. General Motors [43]</p> 	<p>4,60 3,067 2,013 1,600 1,244 1,0 0,848 0,667 -3,653</p>	<p>$K_{Q3}=1,52$</p> 

Implementation of an indicator that reflects the homogeneous properties of parts of an item by example lifetime expense. The concept of the term “consumption of lifetime” for the single component is obvious, as well as the understanding of its additional term “residual life”. The assessment of the state of life for a complex object, consisting of several components, is ambiguous. And besides, some components can be replaced or repaired.

To eliminate this uncertainty and evaluate this property, the term “lifetime expense” for a technically complicated item (TCI) is introduced, as well as a new indicator. This indicator has the value of the life potential of the TCI and is determined as follows

$$K_A = \xi_1 K_{P1} + \xi_2 K_{P2} + \dots + \xi_n K_{Pn} \tag{3}$$

where K_{P_i} = lifetime expense of the i th main part of the TCI (presented as relative value); ξ_i = the weight factor that determines the contribution of the main part to the total lifetime expense of the TCI. It is proposed to consider ξ_i as the relative mass of the main part (the fraction of this part mass in the total mass of n parts that determine the TCI lifetime) [25, 28].

The next fundamental point is lifetime expense of the main part:

$$K_P = 1 - (1 - K_L)(1 - K_T) \tag{4}$$

where K_L = lifetime expense by lifelength (mileage, operating time); K_T = lifetime expense by time (age); K_L relates to damage processes under loads during working; K_T relates to damage processes under time (ageing processes).

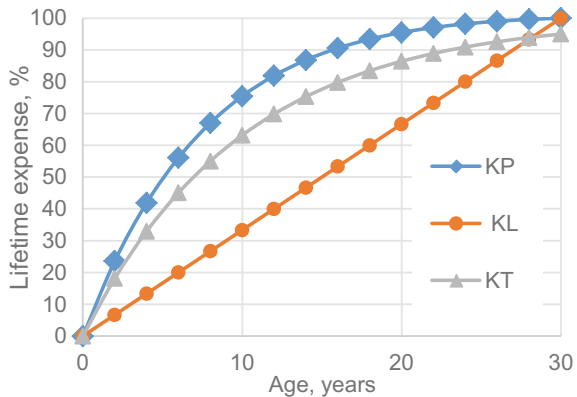
The values of K_L and K_T are determined at the time of monitoring/evaluating the technical condition of the TCI. Usually, the processes responsible for K_L and K_T can be considered as independent. Then, K_L can be interpreted as the probability of failure in the running hours (under the influence of loads in the duty cycle), and K_T as the probability of failure in age (time). Then K_P is the probability of failure of the main part of the TCI under the combined action of loads and age at the considered time.

The developed methodology is realized in the State standard of the Republic of Belarus [33].

Formulas for typical calculations of the lifetime expense of transmission and other units of mobile technics as well as examples of calculations are given in [25, 33].

Figure 11 shows the graphs of $K_L = K_L$, $K_T = K_T$, and $K_P = K_P$. It is estimated that 100% lifetime expense by age occurs over 30 years. The same period corresponds to 100% lifetime expense by lifelength (mileage). This case is illustrative; in real practice, the full expenditure of the lifetime in mileage and age, as a rule, is not simultaneously achieved.

Fig. 11 Lifetime expense KP for linear law KL and exponential KT [25]



4 Conclusions

For the first time, main types of uncertainties in the life cycle of gears and transmissions are presented, as well as the methods and approaches to reduced them.

A specific type of uncertainty for planetary transmissions is isomorphism in structure description. To overcome this the canonical matrices are proposed, the construction of which ensures the unambiguous representation of transmission structures for the subsequent synthesis of their kinematic diagrams (schemes).

Uncertainty in schematizing the transmission as a mechanical system is more general. Overcoming it is based on the use of the concept of a regular mechanical system. This concept takes into account the features of modeling the transmission as a mechanical system with concentrated parameters and using a computer as a discrete calculating device.

It is also quite common when there is no detailed data for the lifetime calculation of gears and other transmission elements. A comparative assessment method is proposed based on calculating the damage measure to the transmission during its operation on the vehicle under consideration and similar vehicles. In this case, damage measures are calculated using the available data from the vehicle specifications.

Variation of load conditions in the operation of the same type of items is inevitable. It is shown that to mix load modes related to a set of transmissions of the same type into a generalized curve is incorrect. Variation of load modes should be presented when performing probabilistic calculations of lifetimes for transmission parts.

Reducing uncertainty in modeling an individual lifetime of a technical item can be achieved through digitalization (diagnostic data, recognition of item state). In some cases, uncertainties are inevitable. In such situations, it is recommended to create a decision-making space that is convenient for stakeholders to consider and assess the degree of risk resulting from their decision.

A typical situation is the probabilistic presentation of the indicator, while the decision-maker must choose the probability corresponding to the calculated (design) value of the indicator.

With a small number of considered indicators, clustering can be used with the selection of characteristic areas in which the values of interrelated parameters are grouped.

Uncertainty in decision-making can be significantly reduced due to the successful introduction of an indicator that generally describes the totality of object properties. For example, for a comprehensive description of heterogeneous properties, a radar chart can be used with a quantitative indicator determined on its basis to describe various properties.

Homogeneous indicators related to item parts of different significances can be reduced to a single indicator taking into account the weight factors of the parts. This is shown by the example of estimating the lifetime expense of an item consisting of several parts with different lifetime expenses.

The considered approaches are methodologically typical for many complex mechanical and combined items based on mechanical systems.

References

1. Uncertainty, <https://en.wikipedia.org/wiki/Uncertainty>. Accessed 28 Oct 2020
2. Lindley, D.V.: *Understanding Uncertainty*. Wiley, Inc (2006)
3. Understanding Uncertainty, <https://www.researchgate.net/publication/298599367>. Accessed 28 Oct 2020
4. McManus, H., Hastings, D.: Current and developing methods for dealing with uncertainties are projected onto the framework to understand their relative roles and interactions. In: Fifteenth Annual International Symposium of the International Council On Systems Engineering (INCOSE), pp. 1–20. Rochester, NY (2005)
5. UNCECOMP 2019 Homepage, <https://2019.uncecomp.org>. Accessed 28 Oct 2020
6. Bhattacharyya, B., Jacquelin, E., Brizard, D.: Uncertainty quantification of nonlinear stochastic dynamic problem using a Kriging-NARX surrogate model. In: Papadrakakis, M., Papadopoulos, V., Stefanou, G. (eds.) UNCECOMP 2019: Uncertainty Quantification in Computational Sciences and Engineering, pp. 34–46. Greece (2019)
7. Gray, N., De Angelis, M. and Ferson, S.: Computing with uncertainty: introducing puffin the automatic uncertainty compiler. In: Papadrakakis, M., Papadopoulos, V., Stefanou, G. (eds.) UNCECOMP 2019: Uncertainty Quantification in Computational Sciences and Engineering, pp. 487–497. Greece (2019)
8. Wehbi, N.A., Slika W.G.: A health monitoring framework for optimal service life predictions of steel structures under fatigue loading. In: Papadrakakis, M., Papadopoulos, V., Stefanou, G. (eds.) UNCECOMP 2019: Uncertainty Quantification in Computational Sciences and Engineering, pp. 653–662. Greece (2019)
9. Karve, P.M., Guo, Y., Kapusuzoglu, B., Mahadevan, S., Haile, M.A.: Digital twin approach for damage-tolerant mission planning under uncertainty. *Eng. Fract. Mech.* **225**, 1–28 (2020)
10. Meis, J.-A., Teklote, F., Borowski, M.: Simulation of the tooth root strength under consideration of material quality, finishing process and size effects. In: International Conference on Gears, pp. 161–171. VDI Verlag GmbH, Garching/Munich (2019)
11. Schlecht, B., Schulze, T.: Improved tooth contact analysis by using virtual gear twins—how helpful is AI for finding best gear design? In: International Conference on Gears, pp. 203–215. VDI Verlag GmbH, Garching/Munich (2019)
12. Keuthen, M.: REXS—Standardized gear unit model. In: International Conference on Gears, pp. 701–712. VDI Verlag GmbH, Garching/Munich (2019)
13. Yin, P.L., Wang, J.H., Lu, C.X.: Digital twin of gear measuring center (DTGMC). In: International Conference on Gears, pp. 1521–1531. VDI Verlag GmbH, Garching/Munich (2019)
14. Kissling, U., Stolz, U., Türich, A.: Combining gear design with manufacturing process decisions. In: International Conference on Gears, pp. 1532–1544. VDI Verlag GmbH, Garching/Munich (2019)
15. Algin, V.: Algorithm for obtaining structures of planetary gearboxes. Development and application of computer techniques and tools for automated information processing, pp. 63–64. Minsk (1974) (in Russian)
16. Algin, V., Paddubka, S.: *Lifetime Mechanics of Vehicle Transmissions*. Belaruskaya Navuka, Minsk (2019). (in Russian)
17. Grenander, U.: *Regular Structures: Lectures in Pattern Theory*. Volume III. Springer, New York, Heidelberg, Berlin (1981)
18. Algin, V.: From Newton’s mechanics to dynamics of regular mechanical systems with variable states and power flows. In: 14th IFToMM World Congress, pp. 130–139. Taipei (2015)
19. Algin, V., Ivanov, V.: Kinematic and dynamic computation of vehicle transmission based on regular constructs. In: Merlet, J.-P., Dahan, M. (eds.) 12th IFToMM World Congress Proceedings, paper A14, 6 p. Besançon (2007)
20. Algin, V., Ivanov, V.: Application of regular rotational and translational constructs to vehicle dynamics problems. In: Brennan, M.J. (ed.) 7th European Conference on Structural Dynamics Proceedings, paper E16, 12 p. University of Southampton, Southampton (2008)

21. Paddubka, S., Algin, V., Starzhinsky, V., Shil'ko, S.: Development of mechanism and machine science in belarus by an example of gears and gear transmissions. In: IOP Conference Series: Materials Science and Engineering 393 012043, pp. 1–9 (2018)
22. Algin, V., Kim, H.-E.: Reliability and lifetime of mechanical units in operation and test. *Key Eng. Mater.* **326–328**, 549–552 (2006)
23. Algin, V.: Approaches and techniques for calculating real reliability of machine as a system of different dependent components and complicated logic of limiting states. In: 13th World Congress in Mechanism and Machine Science, 6 p. Mexico (2011)
24. Algin, V.: calculated modes for assessing operation properties and dependability of vehicles. In: Uhl T. (ed.) *Advances in Mechanism and Machine Science*. 15th IFToMM World Congress on Mechanism and Machine Science Proceedings, pp. 3749–3758. Springer (2019)
25. Algin, V.B.: *Calculation of Mobile Technics: Kinematics, Dynamics*. Lifetime, Belaruskaya Navuka, Minsk (2014). (in Russian)
26. Algin, V.B.: *Dynamics. Reliability and Lifetime Design of Transmissions of Mobile Machines*, Navuka i Tekhnika, Minsk (1995). (in Russian)
27. Algin, V., Ishin, M., Paddubka, S.: Models and approaches in design and diagnostics of vehicles planetary transmissions. IOP Conference Series: Materials Science and Engineering 393 012042, pp. 1–10 (2018)
28. Algin, V., Ishin, M., Paddubka, S., Starzhinsky, V., Shil'ko, S., Rackov, M., and Čavić, M.: Development of information model of power transmissions in the light of industry 4.0. *Int. Sci. J. "Mathem. Modelin."* **4**(2), 54–63 (2020)
29. Algin, V. Calculated modes for assessing operation properties and dependability of vehicles. In: Uhl, T. (ed.) *Advances in Mechanism and Machine Science*. IFToMM WC 2019. Mechanisms and Machine Science, vol. 73, pp. 3749–3758. Springer, Cham (2019)
30. Algin, V.: Justification of calculated cases for the assessment of the basic properties of land vehicles. In.: Beer, M. and Zio, E. (eds.) 29th European Safety and Reliability Conference (ESREL) Proceedings, pp. 3510–3517. Hannover (2019)
31. Belabenko, D., Algin, V.: Classification and visual representation of results of estimation of transmission loading at gearshift process. In.: *Topical Issues of Mechanical Engineering* 8, pp. 60–63. JIME NASB, Minsk (2019)
32. Algin, V., Ishin, N., Starzhinsky, V., Shil'ko, S., Rackov, Čavić, M.: Development of digital twins for gears and transmissions based on lifetime mechanics and composites mechanics. In.: *Topical Issues of Mechanical Engineering* 8, pp. 172–184. JIME NASB, Minsk (2019)
33. State standard of the Republic of Belarus STB 2578–2020. Dependability in technics. Estimation of lifetime expense for technically complicated items. Gosstandart, Minsk (2020)

Minimization of Contact Pressure in the Straight Bevel Gear with Saving of Its Size



A. E. Volkov, S. S. Biryukov, and S. A. Lagutin

Abstract The article focuses on straight bevel gears with localized contact. The problem of minimization of contact pressures without changing the size of the bevel gear is solved. The contact pressures are calculated by solving the contact problem of elasticity theory using the Hertz solution. The degree of contact, and, hence, the amount of contact pressure depends on the choice of synthesis parameter values. The synthesis parameters determine the position of the center of the bearing contact and its size. Optimal synthesis parameter values are calculated by solving a constrained optimization problem. The target function to be minimized is the maximum contact pressure. Absence of edge contact is a constraint. To solve the constrained optimization problem a heuristic algorithm is developed. A numerical example is given.

Keywords Constrained optimization problem · Contact pressure · Straight bevel gear

1 Introduction

It is well known that for a real gear transmission the strict conjugation of the active flanks is a disadvantage rather than an advantage. To compensate unavoidable manufacturing errors, as well as force and temperature deformations of the links, the gearing has to be designed as approximate. This is done by introducing an intentional transmission error function [1–3].

The approximate gearing is automatically created, if relative movements between the generating gear and the workpiece are different in the cutting pinion and gear. This is the case, for example, for the bevel and hypoid spiral gears. The problems of

A. E. Volkov (✉) · S. S. Biryukov

Federal State Budgetary Educational Institution of Higher Education, Moscow State University of Technology STANKIN, Vadkovsky per., 3A, Moscow, Russia

S. S. Biryukov

e-mail: bserg1234@mail.ru

S. A. Lagutin

JS Co Electrostal Heavy Engineering Works, Krasnay ul., 19, Elektrostal, Russia

analysis and synthesis of such gears are thoroughly studied in works of M. Baxter, F. Litvin, M. Segal, G. Sheveleva and many other authors [4–13].

In straight bevel gears as well as in spur and worm gears, the identity of the working and machine meshing allows theoretically strict meshing of the active surfaces. Therefore, the meshing approximation has to be introduced artificially by modifying one of the active surfaces relative to another [14]. Usually, longitudinal and profile modifications of the surfaces are used. The longitudinal modification of the surface should prevent the possibility of edge contact for any allowable manufacturing and assembly errors. The profile modification has to compensate for pitch errors and maintain the tooth-to-tooth accuracy within the limits allowed by the norms of the respective standard.

Usually, the tooth meshing algorithm under no load is used to determine the shape and location of the contact area. This is done interactively so that the contact area does not extend over the tooth edges. The calculation of the contact characteristics, namely the shape and position of the contact area at a given load, the maximum contact pressure and the distribution of pressure over the contact zone, is done as the last step in the gear design in order to verify the performance of the gear, but is not included in the optimization algorithm. This leads to orienting in the calculation process on the calculated contact pressure. If the contact pressure exceeds the allowable value, the design has to be changed.

This paper deals with straight bevel gears with localized contact. A technique for minimizing the contact pressure without changing the size of a spur bevel gear is proposed. Contact pressures are calculated by solving the contact problem of elasticity theory using the Hertz solution. The problem of finding a minimum of maximum contact pressure under condition of no edge contact is stated and solved in this paper. To solve the problem of conditional optimization, a heuristic algorithm has been developed.

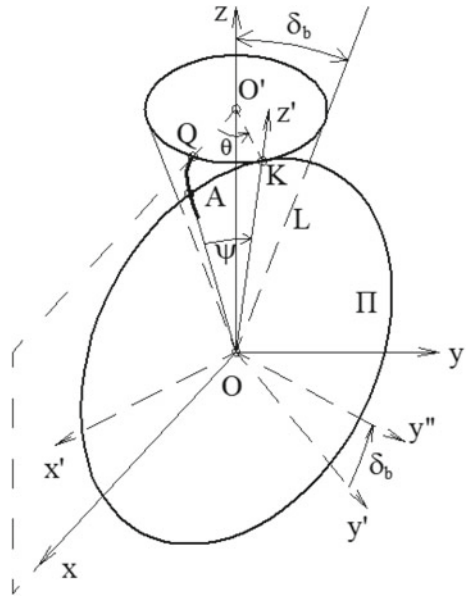
2 Synthesis of Straight Bevel Gear Flanks

2.1 Conical Involute Surface

Kinematically accurate meshing and linear tooth contact in a straight bevel gear is ensured by the use of gears with conical involute flanks. Detailed derivation of equations of such surfaces is given in Kolchin [15]. Main results of the derivation are given below.

We connect with each of the elements of the gear pair its own reference system $Oxyz$, the origin O of which is located at the apex of pitch cone, z axis is directed along its axis, and return points Q of spherical involutes QA are located in Oxz plane (see Fig. 1).

Fig. 1 The conical involute surface plotting scheme



In this reference system the coordinates $x_i(L_i, \varphi_i)$, $y_i(L_i, \varphi_i)$, $z_i(L_i, \varphi_i)$ of points of conical involute surface are determined by two parameters: cone distance L_i and angle φ_i

$$\begin{aligned} x_i &= x_i(L_i, \varphi_i) = L_i(\sin \varphi_i \sin \psi_i + \cos \varphi_i \cos \psi_i \sin \delta_{bi}); \\ y_i &= y_i(L_i, \varphi_i) = L_i(-\cos \varphi_i \sin \psi_i + \sin \varphi_i \cos \psi_i \sin \delta_{bi}); \\ z_i &= z_i(L_i, \varphi_i) = L_i \cos \psi_i \cos \delta_{bi}. \end{aligned} \tag{1}$$

Here the bottom index $i = 1$ refers to gear, $i = 2$ to pinion. The angles δ_{bi} of base cones are calculated through the angles δ_{pi} of pitch cones and pressure angle α

$$\delta_{bi} = \arcsin(\cos \alpha \sin \delta_{pi}). \tag{2}$$

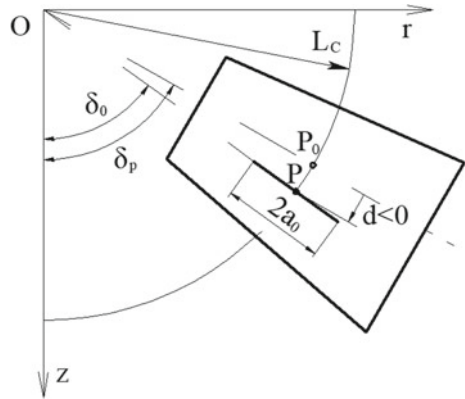
The parameter ψ_i is related to parameter φ_i with the dependence

$$\psi_i = \varphi_i \sin \delta_{bi}. \tag{3}$$

2.2 Modified Conical Involute Surface

The flanks of the meshing teeth defined by Eqs. (1), (2) and (3) ensure a constant gear ratio during meshing, but they do not produce a localized contact. Without

Fig. 2 The synthesis parameters



localization, the bearing contact can, in the presence of unavoidable errors, extend to the edges of the teeth. This can lead to an abrupt concentration of contact pressures on the edges and facilitate rapid wear and tooth breakage. In order to localize the contact, we introduce profile and longitudinal crowning of the flanks into the gear teeth from the surface, defined by Eqs. (1), (2) and (3) at $i = 1$. The crowning is determined by the synthesis parameters.

In Medvedev et al. [16] the following synthesis parameters of the modified active flanks are introduced (Fig. 2):

- L_c – radius of the sphere, on which the center of bearing contact located;
- d – distance from the center of the bearing contact to the pitch cone generatrix;
- a_0 – half of the width of the contact area;
- C – profile modification factor.

The modified gear tooth active flank is determined as follows. The radius-vector of each point of the modified gear flank is obtained by rotating the radius-vector of the corresponding point of involute flank around the rotation axis of the gear by an angle [16]

$$\Delta\theta_m = \Delta\theta_L(L_c, a_0) + \Delta\theta_P(C, d)$$

Here $\Delta\theta_L$ is the rotation angle of radius-vector of point, corresponding to the longitudinal modification of the active flank; $\Delta\theta_P$ is the rotation angle of radius-vector of point, corresponding to the profile modification.

The choice of synthesis parameter values is an important technological task, that cannot be solved without simulating the operation of the gearing under load.

The modified active surface of a gear tooth is defined by relations

$$x_1^* = x_1 \cos \Delta\theta_m - y_1 \sin \Delta\theta_m; \quad y_1^* = x_1 \sin \Delta\theta_m + y_1 \cos \Delta\theta_m; \quad z_1^* = z_1 \quad (4)$$

The pinion surface is not modified, hence

$$x_2^* = x_2; \quad y_2^* = y_2; \quad z_2^* = z_2 \tag{5}$$

The Eqs. (4) and (5) define the active flanks of the gear teeth to be manufactured.

3 The Mathematical Model of Tooth Contact in Gears

The performance of the gear is verified by calculating the contact characteristics of the teeth. The contact analysis in gears is carried out using the Hertz solutions of the problem of contact between two bodies bounded by surfaces of the second order [17]. The calculated parameters are the maximum contact pressures over meshing phase (Fig. 4); the bearing contact under load (Fig. 5), the transmission error curve.

The contact problem of elasticity theory is solved at each phase θ_1 of meshing.

The input is the following parameters:

- tooth surfaces of meshing gears written as Eqs. (4) and (5);
- Young’s modules E_1 and E_2 of gear teeth material;
- Poisson’s coefficients ν_1 and ν_2 ;
- torque M_0 on the gear shaft.

3.1 The Calculation of Contact Pressure Using the Hertz Solution

In a nutshell, the algorithm for determination of contact pressure is as follows:

1. For a given meshing phase θ_1 the parameters of contact points C of surfaces φ_1 and φ_2 as well as the angle θ_2 of pinion rotation to the moment of contact are determined. The calculation of the contact point parameters is described in detail in Medvedev et al. [16].
2. Representation of the backlash δt between the surfaces at the moment of their touching at point C as a quadratic form of coordinates u, v

$$\delta t = k_{uu}u^2 + k_{vv}v^2$$

This step of the algorithm is presented in detail in Sheveleva [8].

3. Determination of the ratio of the semi-axes of the instantaneous contact ellipse. The ratio $\mu = b/a$ of the minor semi-axis of the instantaneous contact ellipse to its major semi-axis is calculated from equation [18]

$$J_2(\mu)k_{uu} - J_1(\mu)k_{vv} = 0,$$

where

$$J_1(\mu_i) = \int_0^{\pi/2} \frac{\cos^2 \lambda \cdot d\lambda}{(\sin^2 \lambda + \mu_i \cos^2 \lambda)^{1/2}};$$

$$J_2(\mu_i) = \int_0^{\pi/2} \frac{\cos^2 \lambda \cdot d\lambda}{(\sin^2 \lambda + \mu_i \cos^2 \lambda)^{3/2}}$$

3.2 The Mathematical Model of Two-Pair Contact

The determination of the number of pairs of teeth in contact at a given meshing phase. The solution of the contact problem of the elasticity theory in gears, taking into account multi-pair contact, has been given in the works of many scientists [19–24].

Experience in applying the Hertz solution to the two-tooth contact problem in bevel gear shows [25], that usually the maximum contact pressure occurs on the border between the single-pair and two-pair contact. Therefore, it is crucially important to determine the boundaries of the single-pair contact. For this purpose, it is necessary to obtain the distribution of the transmitted torque in the area of the two-pair contact.

In order to calculate the contact pressures for two-pair contact, it is necessary to establish how the transmitted torque is distributed over the two pairs of teeth.

The torque distribution problem for each meshing phase can be represented as the problem of determining the forces on each of the springs (Fig. 3) compressed by the two plates. Each of the springs simulates the teeth pair contact. One of the plates is stationary; the other can rotate around the O-axis. In the initial position, the plate A touches the spring 1.

In order to make the plate touch spring 2 it is necessary to compress spring 1 by an amount of Δ . Let's assume that the given torque M_0 is the torque with relative to the O-axis, that is applied on the movable plate. Under the action of this torque the movable plate A has moved to the position B.

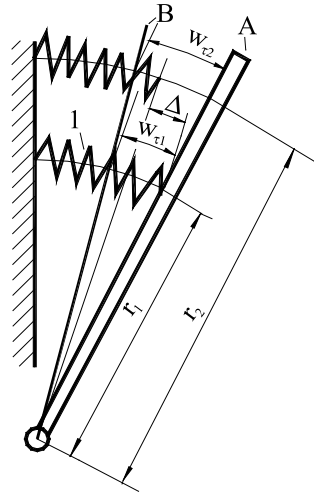
In equilibrium position the sum of torques M_1 and M_2 , compressing spring 1 and spring 2, and torque M_0 relative to the axis O should become zero

$$M_1 + M_2 - M_0 = 0 \quad (6)$$

The torques M_1 and M_2 are related to the spring compression by relations

$$M_1 = C_1 w_{\tau 1}^{3/2}; \quad M_2 = C_2 [(w_{\tau 1} - \Delta) r_2 / r_1]^{3/2} \quad (7)$$

Fig. 3 Two-pair contact calculation scheme



Here C_1 and C_2 are spring stiffness that correspond to the two pairs of simultaneously contacting teeth.

The Eq. (6) with respect to (7) is an equation relative to elastic convergence w_{t1} on an arc of circle of radius r_1 .

The relationship between the elastic convergence w_{t1} in the circumferential direction of the considered teeth pair and some contact characteristics is described by the following relations [24]:

$$P = \gamma w_{ti}^{3/2}; a = \chi P^{1/3}; b = \mu a; M_1 = C_1 w_{ti}^{3/2}.$$

Here P is the normal force on the tooth contact zone; M_1 is the torque transmitted by the considered tooth pair. The values of coefficients γ, χ, μ, C_1 depend on the rotation angle θ_1 of the gear. Calculation of these coefficients is given in [24].

Finally, the maximum contact pressure at the considered meshing phase θ_1 in the Hertz solution is determined by the formula

$$\sigma_H(\theta_1) = \sigma_H(L_c, d, a_0, C, \theta_1) = \frac{3P}{2S}.$$

The normal force P between the teeth depends on the magnitude of the transmitted torque and is calculated for each meshing phase. The area S of the instantaneous contact ellipse also depends on the meshing phase and the curvature of the contacting tooth flanks at that moment. Since the flank shape of one of the gears is determined by the synthesis parameters, the maximum contact pressure also depends on the synthesis parameters.

By solving the contact problem on each meshing phase, we obtain the maximum contact pressure function $\sigma_H(\theta_1)$ of the meshing phase (Fig. 4). We also determine the largest value of maximum contact pressures

Fig. 4 The maximum contact pressure of the meshing phase

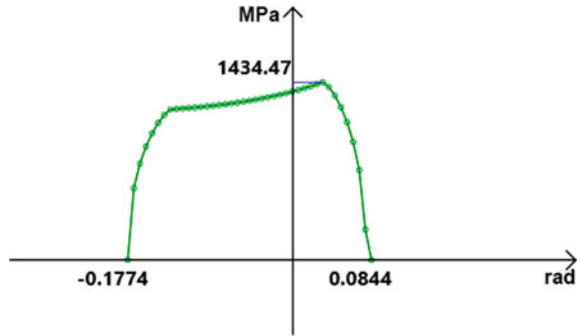
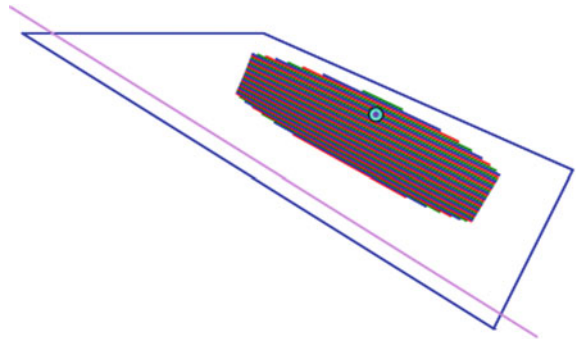


Fig. 5 The bearing contact on the gear flank



$$\sigma_{H \max} = \max_{\theta_1} \sigma_H(\theta_1).$$

Figure 5 shows the contour of the flank in the form of a trapezium, and the bearing contact inside the trapezium. Also, the point location on the flank where contact pressure equals $\sigma_{H\max}$ is calculated (the point in Fig. 5 is near the upper boundary of the bearing contact).

4 Reduction of Contact Pressures in the Straight Bevel Gear with the Same Overall Dimensions

4.1 Constrained Optimization Problem Statement

In the paper the problem of minimization of $\sigma_{H\max}$ by selection of values of synthesis parameters under constraint of edge contact absence is stated. In this case the size of the gear remains the same. The similar problem for spiral bevel gears was solved in [26].

The values of the synthesis parameters are determined by solving the constrained optimization problem. The objective function is the maximum contact pressure of the synthesis parameters. The constraint is the absence of edge contact. To accomplish this condition, the distances from the bearing contact to the tooth edges must be positive.

The maximum contact pressure depends on four synthesis parameters: L_c , d , a_0 , C . A study of the effect of synthesis parameters on the objective function shows that two parameters, L_c and a_0 , decrease the value of the objective function monotonically when increasing. These two parameters affect the bearing contact and the position of the bearing contact center across the tooth width.

The bearing contact width value is selected based on the restrictions on the bearing contact established in GOST 1758–81 [27]. The required bearing contact width is achieved by varying the parameter a_0 . By varying the parameter L_c , the specified distances from the bearing contact to the inner and outer ends of the gear tooth can be achieved.

By varying the remaining two parameters— d and C —the contact pressures in the gear are minimized at fixed values of the parameters L_c and a_0 .

To solve the optimization problem, we use heuristic algorithm, which essentially is as follows. At each stage of the solution the values of parameters L_c , a_0 are sequentially searched and then values of parameters d and C are selected.

4.2 Algorithm for Selection of Parameters d and C

Let’s consider in detail one of the steps of the algorithm. It is assumed that the values of L_c and a_0 are chosen and fixed. Then we need to find the minimum of the function

$$f(d, C) = \sigma_{H \max}$$

with the constraints

$$g_i(d, C) \geq 0, i = 1 \dots n; \tag{8}$$

where n is the number of constraints. The point (d', C') , for which the constraints (8) are satisfied, is chosen as the initial estimate.

At each iteration, 12 candidates are considered to continue the search for a solution. For this purpose, the values of the function $f(d_k, C_k)$ at the points are calculated:

$$\begin{cases} d_k = d' + \Delta d * \cos \phi_k \\ C_k = C' + \Delta C * \sin \phi_k \end{cases}, \tag{9}$$

where Δd and ΔC are the increments of parameters d and C ; ϕ_k is the angle determined at the current iteration by the formula

$$\phi_k = \frac{\pi}{6} * (k - 1), k = 1 \dots 12.$$

Among the points calculated by the formula (9), those are selected that satisfy the constraints (8). For them, the value of the objective function $f(d_k, C_k)$ is calculated and compared with the value at the point of initial approximation $f(d', C')$. Finally, the point is chosen with the lowest value of $f(d_k, C_k)$ at the given iteration, for which the following condition is satisfied

$$f(d_k, C_k) < f(d', C'). \quad (10)$$

It becomes the initial estimate at the next iteration:

$$d' = d_k, C' = C_k.$$

In case the point that satisfies constraints (8) and condition (10) is not found on the iteration, the steps Δd and ΔC are reduced by half, and the iteration is repeated. The search stops when at least one of the conditions $\Delta d < \varepsilon$, or $\Delta C < \varepsilon$, is fulfilled, where ε is some given value.

Thus, the point (d', C') is an intermediate solution to the constrained optimization problem at the considered stage of solution. At this stage, the dimensions and position of the bearing contact in relation to the tooth edges are checked. The values of parameters L_c and a_0 are corrected if necessary. Next the parameters d and C are selected according to the algorithm described above.

The problem of constrained optimization is considered to be solved if each change of the synthesis parameters results in either an increase of contact pressure or an edge contact.

As a result of iterative selection of synthesis parameter values the gear with localized contact is obtained. The shape of tooth flanks is determined using Eqs. (1), (4) and (5). This shape is used in construction of 3D gear models.

5 Numerical Example

Consider a straight bevel gear with number of teeth $z_1 = 15$; $z_2 = 30$; outer module 5 mm; face width 25 mm; pressure angle 20° . Nominal torque on the shaft of driving gear is 160 Nm. The strength characteristics of the gear material are $E = 210,000$ MPa; $\nu = 0.3$.

The following initial values of synthesis parameters are chosen: $L_c = 71.36$ mm; $d = -0.9$ mm; $a_0 = 8$ mm; $C = 0.02$. At these values there is no edge contact (Fig. 5), and objective function is $f(d, C) = 1434$ MPa (Fig. 4).

Fig. 6 Positions of an optimum bearing contact on gear tooth

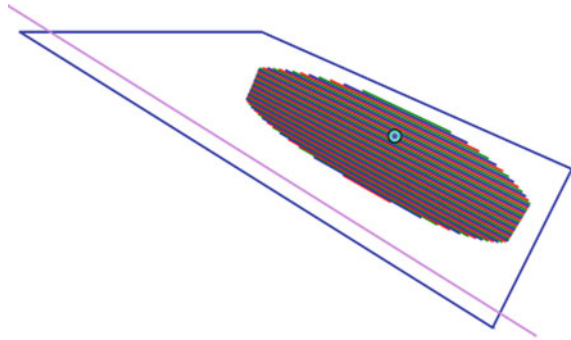
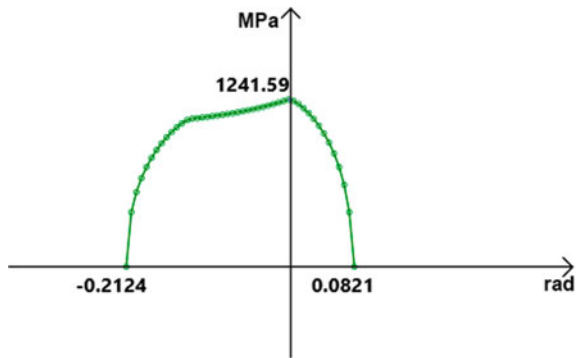


Fig. 7 The maximum contact pressure of the phase of meshing, obtained as a result of the solution of constrained optimization problem



As a result of solution of optimization problem, the following values of synthesis parameters were obtained: $L_c = 73.11$ mm; $a_0 = 9.28$ mm; $d = -1.24$ mm; $C = 0.0094$. The value of the objective function is $f(d, C) = 1242$ MPa. Figure 6 shows the optimum bearing contact obtained by solving the constrained optimization problem. According to the requirements of contact norms GOST 1758–81 [27] the bearing contact occupies about 70% of tooth width. There is no edge contact. The maximum contact pressure of the meshing phase is shown in Fig. 7. Thus, as a result of using heuristic algorithm the pressure in gear is reduced by 13.4%.

6 Conclusion

For the successful operation of straight bevel gears, contact localization is necessary just as for spiral bevel gears. However, in this case it is achieved by significantly different methods. These methods include building 3D models of straight bevel gears whose active tooth flanks are conical involute surfaces, followed by longitudinal and profile crowning of one of the surfaces from the conical involute surface and then determination of the contact pressures during meshing of one teeth pair. The crowning

parameters, which determine the position of the center of the localized bearing contact and its size, are derived from the solution of the constrained optimization problem. The objective function is the maximum contact pressure obtained from the Hertz solution. The problem solution constraint is the prevention of tooth edge contact. The implementation in metal of the described contact localization method requires machining of at least one of the gears on a multi-axis CNC machine.

Thus, the presented algorithm for solving the problem of constraint optimization allows minimizing contact pressures while maintaining the size of the straight bevel gear.

References

1. Segal', M.: Errors impact on contact conditions of spatial gear. *Mashinovedenie* **5**, 49–54 (1975). (in Russian)
2. Litvin, F.: *Development of Gear Technology and Theory of Gearing*, p. 124. NASA Reference Publication 1406, ARL-TR-1500 (1998)
3. Lagutin, S., Verhovski, A., Dolotov, S.: Technological design of worm gears with a localized contact. In: *Proceedings of 2nd International Conference "Power Transmissions 2006"*, Novi Sad, Serbia, pp. 177–182 (2006)
4. Baxter, M.: Basic geometry and tooth contact of hypoid gears. *Ind. Math.* **11** (Part 2), 19–42 (1961)
5. Litvin, F.: *Theory of Gearing*, p. 584. Nauka, Moscow (1968). (in Russian)
6. Lopato, G., Kabatov, N., Segal', M.: *Spiral Bevel and Hypoid Gears*, p. 423. Mashinostroenie, Moscow (1977). (in Russian)
7. Zhang, Y., Fang, Z.: Analysis of transmission errors under load of helical gears with modified tooth surfaces. *J. Mech. Des.* **119**(3), 1206 (1997)
8. Sheveleva, G.: *Theory of Generation and Contact of Moving Bodies*, p. 494. Stankin, Moscow (1999). (in Russian)
9. Syzrantsev, V., Ratmanov, E., Kotlikova, V.: Evaluation of the possibility of bevel and hypoid pairs manufacturing under severe technological constraints. *Tekhnika Mashinostroeniya* **2**, 52–56 (2001). (in Russian)
10. Medvedev, V., Volkov, A.: Synthesis of spiral bevel gear transmissions with a small shaft angle. *J. Mech. Des.* **129**(9), 949–959 (2007)
11. Shih, Y., Fong, Z.: Flank correction for spiral bevel and hypoid gears on a six-axis CNC hypoid gear generator. *J. Mech. Des.* **130**(6), 062604–1–11 (2008)
12. Simon, V.: Generation of hypoid gears on CNC hypoid generator. *J. Mech. Des.* **133**(12), 121003–1–9 (2011)
13. Cao, X., Deng, X., Nie, S.: Topological structure design of high order transmission error tooth surface of aviation spiral bevel gear based on conjugate tooth surface modification. *J. Aerospace Power* **30**(1), 195–200 (2015)
14. Lagutin, S.: Predesigned function of transmission errors for double modified helical gearing. In: *Proceedings of 9th National Congress of Theoretical and Applied Mechanics*, Varna, Bulgaria, vol. 1, pp. 253–261 (2001)
15. Kolchin, N.: Analytical calculation of planar and spatial gearings (with attachment to cutting tool profiling and calculation of meshing errors). *Mashgiz, M-L*, pp. 19–95 (1949). (in Russian)
16. Medvedev, V., Volkov, A., Biryukov, S.: Automation of technological preproduction of straight bevel gears. In: *New Approaches to Gear Design and Production, Mechanisms and Machine Science*, vol. 81, pp. 133–155. Springer Nature Switzerland AG (2020)

17. Medvedev, V., Sheveleva, G.: Synthesis of spiral bevel gear for permissible contact pressures. In: Proceedings of All-Russian Scientific and Practical Conference with International Participation "Gearbox Construction in Russia: Status, Problems, Prospects", St. Petersburg, pp. 59–61 (2002). (in Russian)
18. Rabotnov, Y.: Mechanics of Deformed Solids, p. 744. Nauka, Moscow (1979). (in Russian)
19. Sheveleva, G.: Determining the contact pressure in gear drives. Problemy Mashinostroeniya I Nadezhnosti Mashin **5**, 45–52 (1999)
20. Volkov, A.: Analysis of heavily-loaded gearing with account for simultaneous operation of three pairs of teeth. J. Mach. Manuf. Reliab. **6**, 84–91 (2000)
21. Litvin, F., Fuentes, A.: Gear Geometry and Applied Theory, p. 800. University press, Cambridge (2004)
22. Trubachev, E.: Synthesis of multipair loaded spiroid gear. In: Proceedings of International Symposium "Theory and Practice of Gears", IzhSTU n.a. M.T. Kalashnikov, Izhevsk, pp. 359–366 (2014). (in Russian)
23. Trubachev, E., Savelyeva, T., Pushkareva, T.: Practice of design and production of worm gears with localized contact. In: "Advanced Gear Engineering", Mechanisms and Machine Science, vol. 51, pp. 327–344. Springer International Publishing AG Switzerland (2018)
24. Medvedev, V., Volkov, A., Volosova, M., Zubelevich, O.: Mathematical model and algorithm for contact stress analysis of gears with multi-pair contact. Mech. Mach. Theory **86**, 156–171 (2015)
25. Medvedev, V., Matveenkov, D., Volkov, A.: Synthesis of contact-optimal spiral bevel gears. Russ. Eng. Res. **35**(1), 51–56 (2015)
26. Medvedev, V., Matveenkov, D., Volkov, A.: Reduction of contact and bending stresses in the bevel gear teeth while maintaining the same overall dimensions. In: Advanced in Mechanical Engineering, Lecture Notes in Mechanical Engineering, vol. 51, pp. 35–52. Springer Nature Switzerland AG (2019)
27. GOST 1758–81. Basic norms of interchangeability. Bevel and hypoid gears. Tolerances. 41, Izdatel'stvo Standartov, Moscow (1981). (in Russian)

Conic Linear Helicoids: Part 1. Synthesis and Analysis of the Basic Geometric Characteristics



Valentin Abadjiev  and Emilia Abadjieva 

Abstract An object of the current study is special surfaces with adequate and important applications in the synthesis and design of engineering devices. To the mentioned surfaces belong cylindrical, conic, and plane ones. The authors of this work put an accent on the synthesis and concrete analytical studies of the essential for engineering practice geometric characteristics of the most common type of conic helical surfaces—conic linear helicoids. Geometric results are obtained from the realized researches, and their application in the creation of different types of drives is clarified. In particular, researches show how conic helical surfaces serve as a technical basis for the creation of algorithms for the synthesis of spatial gear transmissions (Spiroid and Helicon gears of the convolute, involute and Archimedean type) (Spiroid and Helicon are trademarks registered by the Illinois Tool Works, Chicago, Ill.).

Keywords Conic linear helicoids · Synthesis and analysis · Mathematical modelling · Basic geometric characteristics

1 Introduction

Helical surfaces are one of the surfaces (after the cylindrical, conic, and plane ones) that are most widely used in engineering practice. In the most common case, they have two main applications in the industry:

- for the construction of active tooth surfaces in different types of gear mechanisms and as elements of the working bodies of numerous technological and transport mechanical systems (screw pumps, mixers of concrete-mixers, screw conveyor, press, etc.) [1–6],
- as basic elements of the cutting tools, different in their designation (hobs, twist drills, shavers with helical flutes, etc.) [7–10].

V. Abadjiev · E. Abadjieva (✉)

Institute of Mechanics-Bulgarian Academy of Sciences, Sofia, Bulgaria

V. Abadjiev

e-mail: abadjiev@imbm.bas.bg

There is a big number of specialized literature dealing with the geometry of so-called ***cylindrical linear helical surfaces***. They are surfaces generated by ***generatrix straight line***, when it realizes a helical motion relative to an axis, with a constant axial pitch [11–14]. Typical for the cylindrical helical surface is that when the helical motion of the generatrix line is realized, all its points form a helix with the same pitch, located on coaxial circle cylinders. Because of this, the helical surfaces are called also ***cylindrical*** ones. Depending on the geometric character of the generatrix line, the helical line, generated by it, can be rectilinear or with curvilinear generatrix (part of a circle, ellipse, parabola, etc.). In the first case here and hereafter we will assume the helical surface to be called ***linear*** (instead of rectilinear for simplicity), and in the other cases, we will use the name of the geometric shape of the generatrix line—circular, elliptical, parabolic, etc. In the most common case, the second type of helical surfaces should be called ***curvilinear***.

The linear helical surfaces are widely applied as active surfaces of the hob's teeth in the worm gears and gears of helical gear pairs with parallel and crossed axes [15, 16]. At the same time, they are the main constructive element of the teeth of the tools, applied in the elaboration of the wormgears and helical gear sets, as well as in the modular cutters, which are used for hobbing using the method of enveloping of the straight and helical gears.

In the current stage of the development of gear manufacturing, from the curvilinear tooth surfaces, the curvilinear helical surfaces have found the widest application concerning the appearance and the introduction in the industrial practice of gears of type Novikov [11].

Also, curvilinear helical surfaces represent the transition surfaces between the active tooth surfaces and the corresponding cylindrical surfaces at the bases of the teeth of the respective cylindrical gear pairs with helical teeth. The curvilinear helical surfaces have an application in the synthesis and the design of the root surfaces [1, 17] included in the elements of specialized cutting instruments.

In the scientific literature, one can find information about helical surfaces with an axial parameter that varies following a preliminary given law [13].

The present study is devoted to the synthesis of helical surfaces generated by a straight line, which in the most general case performs two helical motions [18]. The first helical motion consists of rotational motion around a constant axis and a translational motion parallel to this axis. The axis, in this case, will be called the ***longitudinal helical axis***, and the helical motion—***longitudinal axial helical motion*** or only ***axial helical motion***. The second helical motion also consists of rotation with respect to a helical axis and crossed translational motion, perpendicular to the helical axis. The crossed translational displacement, in the most common case, has a directrix, which is an orthogonal crossed axis of the longitudinal helical line. This helical motion is called a ***crossed helical motion***. In the described case, a helical surface is generated, depending on two helical parameters: ***axial and cross one (a parameter of cross displacement)***. It should be noted here, in the most common case, parts of these linear helical are used as flanks of the gears' teeth when these teeth are limited by co-axial conic rotational surfaces having a geometry different than a cylindrical surface.

In the concrete case, we will consider only linear helical surfaces with two helical parameters, for which the cross helical parameter is a constant one or varies according to a law which ensures that the shape of the co-axial surfaces is rotational cones or surfaces, which optimal approximation is realized with rotational cones. This is the reason that these linear surfaces are called *conic linear helical surfaces or conic linear helicoids*.

2 Synthesis of Conic Convolute Helical Surfaces

Generation of Conic Convolute Helicoids

The linear helicoids are widely applicable as active tooth surfaces of the spatial gear mechanisms with crossed-axes, both in the conditions of work-meshing and in the instrumental-gearing. Such choice of the active tooth surfaces for these gear mechanisms, especially when their synthesis is realized by the second principle of T. Olivier, is determined by the manufacturability, and in many cases, which include the manufacture of classic cylindrical worm gears, Spiroid and Helicon ones—they are the dominant alternative. The reason is that in these gear sets one of the gear coincides in geometry and basic dimensions with the instrument used to generate the other conjugate gear.

It is known that from a constructive and technological viewpoint, when implementing worm, Spiroid, and Helicon gears (especially in small production series) it is appropriate to use Archimedean helicoids, as their tooth flanks. For example, the studied and manufactured in the USA, Spiroid, and Helicon gear set [19–26], as well as a large part of the analogs created outside the USA, is equipped with the above-mentioned type of tooth surfaces [1, 25, 26].

The most common implementation of this type of helicoids is by turning on a lathe with a turning lathe tool in such a way that both of its cutting edges lie in a plane containing the geometric axis of the elaborated gear (longitudinal helical axis). When the gear sets of the considered group of spatial gear transmissions have small gear ratios (i.e. when a large number of helicoids has to be generated on the gear) the generation of the flanks is realized with worsening conditions of cutting because of the large helical angles of the helical lines (the longitudinal lines of the teeth) of the corresponding helicoids (i.e. the active tooth surfaces). This technological problem is solved by situating the plane containing the cutting edges of the instrument perpendicularly or close to perpendicularly to the helical line, which defines the longitudinal orientation of the synthesized helical teeth. In this case, the generation of *conic convolute helicoids* is achieved [1, 17, 27].

In Figs. 1, 2, and 3 three possible cases of generation of right-hand oriented conic convolute helicoids $\Sigma_1^{(j)}$ ($j = 1, 2$), that are determined by different possible geometric characteristics of the helical teeth (threads) [18, 28, 29] of the concrete gear, are shown. The process of generation of these helical surfaces is considered in the fixed coordinate system $S_p^{(j)}(O_p^{(j)}, x_p^{(j)}, y_p^{(j)}, z_p^{(j)})$ and consists of the following.

Fig. 1 Generation of conic convolute helicoids of I type

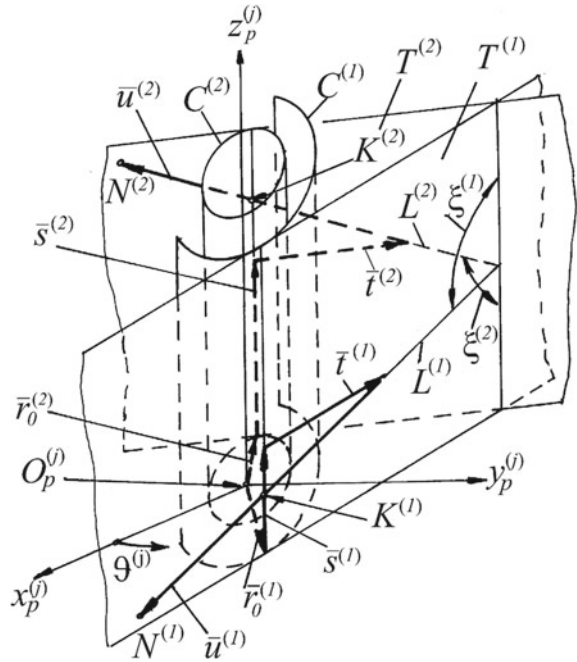


Fig. 2 Generation of the conic convolute helicoid of II type

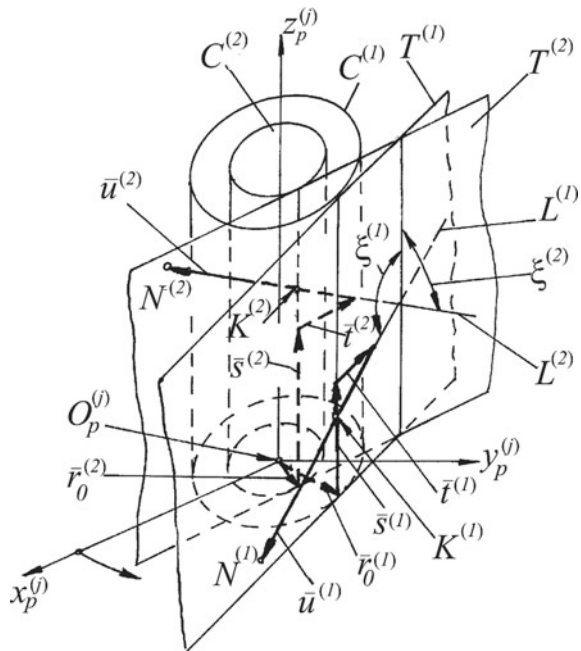
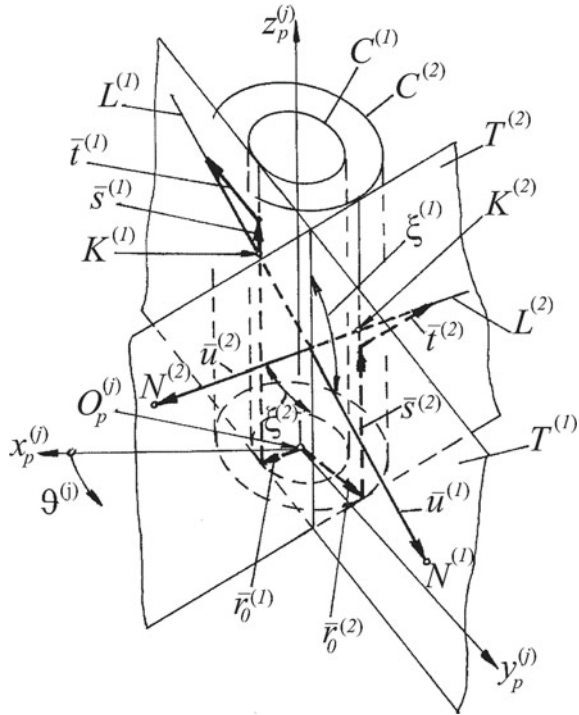


Fig. 3 Generation of the conic convolute helicoid of III type



The generatrix line $L^{(j)}$ doesn't cross the axis $O_p^{(j)} z_p^{(j)}$, which coincides with the geometric axis of the gear and forms with it an angle $0, 5\pi < \xi^{(j)} < \pi$. At the same time, the line $L^{(j)}$ lies in a plane $T^{(j)}$, which is tangential to the directed circle cylinder $C^{(j)}$. The generation of the conic convolute helicoid $\Sigma_1^{(j)}$ by the line $L^{(j)}$ is realized by its following motions [1, 18, 30]: an axial helical motion with a longitudinal axis $O_p^{(j)} z_p^{(j)}$ with a parameter $p_s^{(j)} = \text{constant}$; cross helical motion in the plane $T^{(j)}$, which is perpendicular to the axis $O_p^{(j)} z_p^{(j)}$ with a parameter $p_t^{(j)}$. We will remind one more time that the value of the $p_t^{(j)}$ is related to the conic form of the gear. The three cases of a generation of conic helicoids $\Sigma_1^{(j)}$ ($j = 1, 2$), illustrated in Figs. 1, 2, and 3, are determined by different geometric characteristics of the helical teeth of the conic gear. Here is the place to mention that $\Sigma_1^{(j)}$ ($j = 1$) is a conic convolute helical surface, which is oriented towards the positive direction of the axis $O_p^{(1)} z_p^{(1)}$ and $\Sigma_1^{(j)}$ ($j = 2$) is the helicoid oriented towards the negative direction of the $O_p^{(2)} z_p^{(2)}$. As it has already been said, parts of the $\Sigma_1^{(1)}$ and $\Sigma_1^{(2)}$ are used as work-surfaces of the helical teeth of the gear.

According to Figs. 1, 2, and 3, the vector equation of conic convolute helical surface $\Sigma_1^{(1)}$ is of the type [30]:

$$\bar{\rho}_1^{(j)} = \bar{r}_0^{(j)} + \bar{s}^{(j)} + \bar{t}^{(j)} + \bar{u}^{(j)}, \tag{1}$$

where

- $\bar{\rho}_1^{(j)}$ is the radius-vector of the point $N^{(j)}$ from the conic convolute helicoid $\Sigma_1^{(j)}$;
- $\bar{r}_0^{(j)}$ radius of the directed cylinder $C^{(j)}$;
- $\vartheta^{(j)}, u^{(j)}$ coordinates of the helical surface $\Sigma_1^{(j)}$;
- $s^{(j)} = p_s^{(j)} \vartheta^{(j)}$ axial displacement of the generatrix line $L^{(j)}$;
- $t^{(j)} = p_t^{(j)} \vartheta^{(j)}$ crossed (tangential to the directed cylinder $C^{(j)}$) displacement of the generatrix line $L^{(j)}$.

When (1) is projected in the coordinate system $S_p^{(j)}$, the following is obtained:

- for the case shown in Fig. 1:

$$\begin{aligned} x_p^{(j)} &= r_0^{(j)} \cos \vartheta^{(j)} \pm (u^{(j)} \sin \xi^{(j)} - p_t^{(j)} \vartheta^{(j)}) \sin \vartheta^{(j)}, \\ y_p^{(j)} &= r_0^{(j)} \sin \vartheta^{(j)} \mp (u^{(j)} \sin \xi^{(j)} - p_t^{(j)} \vartheta^{(j)}) \cos \vartheta^{(j)}, \\ z_p^{(j)} &= p_s^{(j)} \vartheta^{(j)} \pm u^{(j)} \cos \xi^{(j)}; \end{aligned} \tag{2}$$

- for the case shown in Fig. 2:

$$\begin{aligned} x_p^{(j)} &= r_0^{(j)} \cos \vartheta^{(j)} + (u^{(j)} \sin \xi^{(j)} - p_t^{(j)} \vartheta^{(j)}) \sin \vartheta^{(j)}, \\ y_p^{(j)} &= r_0^{(j)} \sin \vartheta^{(j)} - (u^{(j)} \sin \xi^{(j)} - p_t^{(j)} \vartheta^{(j)}) \cos \vartheta^{(j)}, \\ z_p^{(j)} &= p_s^{(j)} \vartheta^{(j)} \pm u^{(j)} \cos \xi^{(j)}; \end{aligned} \tag{3}$$

- for the case shown in Fig. 3:

$$\begin{aligned} x_p^{(j)} &= r_0^{(j)} \cos \vartheta^{(j)} \mp (u^{(j)} \sin \xi^{(j)} - p_t^{(j)} \vartheta^{(j)}) \sin \vartheta^{(j)}, \\ y_p^{(j)} &= r_0^{(j)} \sin \vartheta^{(j)} \pm (u^{(j)} \sin \xi^{(j)} - p_t^{(j)} \vartheta^{(j)}) \cos \vartheta^{(j)}, \\ z_p^{(j)} &= p_s^{(j)} \vartheta^{(j)} \pm u^{(j)} \cos \xi^{(j)}. \end{aligned} \tag{4}$$

In the equation systems (2), (3), and (4) the upper signs and $j = 1$ refer for the $\Sigma_1^{(1)}$, while the lower signs and $j = 2$ —for the $\Sigma_1^{(2)}$.

When substitute

$$R_0^{(j)} = u^{(j)} - \frac{p_t^{(j)} \vartheta^{(j)}}{\sin \xi^{(j)}} \text{ and } p^{(j)} = p_s^{(j)} \pm p_t^{(j)} \cot \xi^{(j)}, \tag{5}$$

in the (2), (3), and (4), they obtain the following expression:

- for the case shown in Fig. 1:

$$\begin{aligned}
 x_p^{(j)} &= r_0^{(j)} \cos \vartheta^{(j)} \pm R_0^{(j)} \sin \xi^{(j)} \sin \vartheta^{(j)}, \\
 y_p^{(j)} &= r_0^{(j)} \sin \vartheta^{(j)} \mp R_0^{(j)} \sin \xi^{(j)} \cos \vartheta^{(j)}, \\
 z_p^{(j)} &= p^{(j)} \vartheta^{(j)} \pm R_0^{(j)} \cos \xi^{(j)};
 \end{aligned}
 \tag{6}$$

- for the case shown in Fig. 2:

$$\begin{aligned}
 x_p^{(j)} &= r_0^{(j)} \cos \vartheta^{(j)} + R_0^{(j)} \sin \xi^{(j)} \sin \vartheta^{(j)}, \\
 y_p^{(j)} &= r_0^{(j)} \sin \vartheta^{(j)} - R_0^{(j)} \sin \xi^{(j)} \cos \vartheta^{(j)}, \\
 z_p^{(j)} &= p^{(j)} \vartheta^{(j)} \pm R_0^{(j)} \cos \xi^{(j)};
 \end{aligned}
 \tag{7}$$

- for the case shown in Fig. 3:

$$\begin{aligned}
 x_p^{(j)} &= r_0^{(j)} \cos \vartheta^{(j)} \mp R_0^{(j)} \sin \xi^{(j)} \sin \vartheta^{(j)}, \\
 y_p^{(j)} &= r_0^{(j)} \sin \vartheta^{(j)} \pm R_0^{(j)} \sin \xi^{(j)} \cos \vartheta^{(j)}, \\
 z_p^{(j)} &= p^{(j)} \vartheta^{(j)} \pm R_0^{(j)} \cos \xi^{(j)}.
 \end{aligned}
 \tag{8}$$

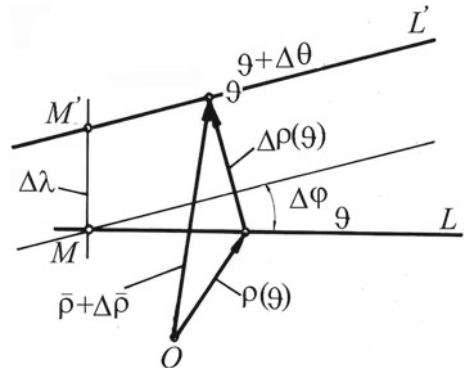
Equations (6), (7), and (8) represent the conic convolute helical surface $\Sigma_1^{(j)}$, as a cylindrical one with a helical parameter $p^{(j)}$ and coordinates $\vartheta^{(j)}$ and $R_0^{(j)}$. The coordinate $R_0^{(j)}$ is with accounting origin–point $K^{(j)}$ (the point of intersection of $L^{(j)}$ with the generatrix of the directed cylinder $C^{(j)}$, along which the cylinder tangents to the plane $T^{(j)}$). The point $K^{(j)}$ should be treated as a point of the directed helical line $\bar{\rho}_0^{(j)} = \bar{\rho}_0^{(j)}(\vartheta^{(j)})$ on the cylinder $C^{(j)}$.

3 Basic Geometric Characteristics of the Conic Convolute Surface

Parameter of Distribution

It is known [13, 14] that a basic characteristic of the surfaces with straight-line generatrix is their parameter of distribution. When generating surfaces of such type, the straight-line generatrix passes from its initial position towards another one, infinitesimal close to it by a rotation with some angle and some translation. These two

Fig. 4 Transition of the generatrix straight-line L in the infinitely closed position L'



displacements are infinitely small but their ratio has a limit which is called a parameter of distribution. In accordance with Fig. 4 [14], when the generatrix L , characterized with the parameter ϑ , passes into a position L' , characterized with an infinitely close value $\vartheta + \Delta\vartheta$, then the same line (L') rotates with an angle $\Delta\varphi$ and displaces from the previous position by $\Delta\lambda = MM'$. These two values are infinitely small but their ratio has a limit called a parameter of distribution [14]:

$$h = \lim_{\Delta\vartheta \rightarrow 0} \frac{\Delta\lambda}{\Delta\vartheta} \tag{9}$$

In order to determine the parameter of distribution $h^{(j)}$ of the conic convolute helical surface $\Sigma_1^{(j)}$, we represent the vector Eq. (1) in the form:

$$\bar{\rho}_1^{(j)} = \bar{\rho}_0^{(j)}(\vartheta^{(j)}) + R_0^{(j)}\bar{l}^{(j)}, \tag{10}$$

where

- $\bar{\rho}_0^{(j)}(\vartheta^{(j)})\{\chi_1^{(j)}, \chi_2^{(j)}, \chi_3^{(j)}\}$ is an equation of the directed helical line on the directed cylinder $C^{(j)}$;
- $\chi_1^{(j)}, \chi_2^{(j)}, \chi_3^{(j)}$ projections of the vector $\bar{\rho}_0^{(j)}$ in the coordinate system $S_p^{(j)}$;
- $\bar{l}^{(j)}\{l_1^{(j)}, l_2^{(j)}, l_3^{(j)}\}$ directed unit vector of the generatrix line $L^{(j)}$;
- $l_1^{(j)}, l_2^{(j)}, l_3^{(j)}$ projection of the vector $\bar{l}^{(j)}$ in the coordinate system $S_p^{(j)}$.

For the cases illustrated in Figs. 1, 2, and 3, we have:

- for Fig. 1:

$$\begin{aligned} \chi_1^{(j)} &= r_0^{(j)} \cos \vartheta^{(j)}, & \chi_2^{(j)} &= r_0^{(j)} \sin \vartheta^{(j)}, & \chi_3^{(j)} &= p^{(j)} \cdot \vartheta^{(j)}, \\ l_1^{(j)} &= \pm \sin \xi^{(j)} \sin \vartheta^{(j)}, & l_2^{(j)} &= \mp \sin \xi^{(j)} \cos \vartheta^{(j)}, & l_3^{(j)} &= \pm \cos \xi^{(j)}; \end{aligned} \tag{11}$$

- for Fig. 2:

$$\begin{aligned} \chi_1^{(j)} &= r_0^{(j)} \cos \vartheta^{(j)}, & \chi_2^{(j)} &= r_0^{(j)} \sin \vartheta^{(j)}, & \chi_3^{(j)} &= p^{(j)} \cdot \vartheta^{(j)}, \\ l_1^{(j)} &= \sin \xi^{(j)} \sin \vartheta^{(j)}, & l_2^{(j)} &= -\sin \xi^{(j)} \cos \vartheta^{(j)}, & l_3^{(j)} &= \pm \cos \xi^{(j)}; \end{aligned} \tag{12}$$

- for Fig. 3:

$$\begin{aligned} \chi_1^{(j)} &= r_0^{(j)} \cos \vartheta^{(j)}, & \chi_2^{(j)} &= r_0^{(j)} \sin \vartheta^{(j)}, & \chi_3^{(j)} &= p^{(j)} \cdot \vartheta^{(j)}, \\ l_1^{(j)} &= \mp \sin \xi^{(j)} \sin \vartheta^{(j)}, & l_2^{(j)} &= \pm \sin \xi^{(j)} \cos \vartheta^{(j)}, & l_3^{(j)} &= \pm \cos \xi^{(j)}; \end{aligned} \tag{13}$$

Then after application of the (9), the parameter of distribution for the studied conic convolute helical surface is [13]:

$$h^{(j)} = \frac{[d\bar{\rho}_0^{(j)}, \bar{l}^{(j)}, d\bar{l}^{(j)}]}{(d\bar{l}^{(j)})^2} = \frac{\begin{vmatrix} d\chi_1^{(j)} & l_1^{(j)} & dl_1^{(j)} \\ d\chi_2^{(j)} & l_2^{(j)} & dl_2^{(j)} \\ d\chi_3^{(j)} & l_3^{(j)} & dl_3^{(j)} \end{vmatrix}}{(dl_1^{(j)})^2 + (dl_2^{(j)})^2 + (dl_3^{(j)})^2}. \tag{14}$$

For the cases illustrated on Figs. 1, 2, and 3, then $h^{(j)}$ obtains the following expressions:

- for Fig. 1:

$$h^{(j)} = p^{(j)} + r_0^{(j)} \cot \xi^{(j)}; \tag{15}$$

- for Fig. 2:

$$h^{(j)} = p^{(j)} \pm r_0^{(j)} \cot \xi^{(j)}; \tag{16}$$

- for Fig. 3:

$$h^{(j)} = p^{(j)} - r_0^{(j)} \cot \xi^{(j)}. \tag{17}$$

Cross Section of the Conic Convolute Helicoid

The equation of the crossed section of the conic convolute helical surfaces (shown on Figs. 1, 2, and 3) with the plane $O_p^{(j)} x_p^{(j)} y_p^{(j)}$, i.e. when $z_p^{(j)} = 0$, has the following parametric form:

$$\rho_p^{(j)} = \sqrt{(r_0^{(j)})^2 + \left(\frac{p^{(j)}\vartheta^{(j)}}{\cot\xi^{(j)}}\right)^2}. \tag{18}$$

In Descartes coordinates, when $z_p^{(j)} = C_{z_p}^{(j)} = \text{constant}$, the cross-section of the three types pairs of conic convolute helicoids $\Sigma_1^{(j)}$ ($j = 1, 2$) is described by the following equations' systems:

- for Fig. 1:

$$\begin{aligned} x_p^{(j)} &= r_0^{(j)} \cos\vartheta^{(j)} + [\tan\xi^{(j)} \left(\frac{C_{z_p}^{(j)}}{\vartheta^{(j)}} - p_s^{(j)}\right) \mp p_t^{(j)}] \vartheta^{(j)} \sin\vartheta^{(j)}, \\ y_p^{(j)} &= r_0^{(j)} \sin\vartheta^{(j)} - [\tan\xi^{(j)} \left(\frac{C_{z_p}^{(j)}}{\vartheta^{(j)}} - p_s^{(j)}\right) \mp p_t^{(j)}] \vartheta^{(j)} \cos\vartheta^{(j)}; \end{aligned} \tag{19}$$

- for Fig. 2:

$$\begin{aligned} x_p^{(j)} &= r_0^{(j)} \cos\vartheta^{(j)} \pm [\tan\xi^{(j)} \left(\frac{C_{z_p}^{(j)}}{\vartheta^{(j)}} - p_s^{(j)}\right) \mp p_t^{(j)}] \vartheta^{(j)} \sin\vartheta^{(j)}, \\ y_p^{(j)} &= r_0^{(j)} \sin\vartheta^{(j)} \mp [\tan\xi^{(j)} \left(\frac{C_{z_p}^{(j)}}{\vartheta^{(j)}} - p_s^{(j)}\right) \mp p_t^{(j)}] \vartheta^{(j)} \cos\vartheta^{(j)}; \end{aligned} \tag{20}$$

- for Fig. 3:

$$\begin{aligned} x_p^{(j)} &= r_0^{(j)} \cos\vartheta^{(j)} - [\tan\xi^{(j)} \left(\frac{C_{z_p}^{(j)}}{\vartheta^{(j)}} - p_s^{(j)}\right) \mp p_t^{(j)}] \vartheta^{(j)} \sin\vartheta^{(j)}, \\ y_p^{(j)} &= r_0^{(j)} \sin\vartheta^{(j)} + [\tan\xi^{(j)} \left(\frac{C_{z_p}^{(j)}}{\vartheta^{(j)}} - p_s^{(j)}\right) \mp p_t^{(j)}] \vartheta^{(j)} \cos\vartheta^{(j)}. \end{aligned} \tag{21}$$

Equations (19)–(21) can be represented in the form:

$$\begin{aligned} x_p^{(j)} &= r_0^{(j)} \cos \vartheta^{(j)} + b^{(j)} \vartheta^{(j)} \sin \vartheta^{(j)}, \\ y_p^{(j)} &= r_0^{(j)} \sin \vartheta^{(j)} - b^{(j)} \vartheta^{(j)} \cos \vartheta^{(j)}; \end{aligned} \tag{22}$$

$$\begin{aligned} x_p^{(j)} &= r_0^{(j)} \cos \vartheta^{(j)} \pm b^{(j)} \vartheta^{(j)} \sin \vartheta^{(j)}, \\ y_p^{(j)} &= r_0^{(j)} \sin \vartheta^{(j)} \mp b^{(j)} \vartheta^{(j)} \cos \vartheta^{(j)}; \end{aligned} \tag{23}$$

$$\begin{aligned} x_p^{(j)} &= r_0^{(j)} \cos \vartheta^{(j)} - b^{(j)} \vartheta^{(j)} \sin \vartheta^{(j)}, \\ y_p^{(j)} &= r_0^{(j)} \sin \vartheta^{(j)} + b^{(j)} \vartheta^{(j)} \cos \vartheta^{(j)}. \end{aligned} \tag{24}$$

where $b^{(j)} = \tan \xi^{(j)} \left(\frac{C_{z_p}^{(j)}}{\vartheta^{(j)}} - p_s^{(j)} \right) \mp p_t^{(j)}$.

The character of the cross-section of the conic convolute helicoid can be clarified when the circular vector functions $\bar{l}^{(j)} = \bar{l}^{(j)}(\vartheta^{(j)})$ and $\bar{g}^{(j)} = \bar{g}^{(j)}(\vartheta^{(j)})$ [9] are introduced, such that the condition

$$\bar{l}^{(j)} = \bar{i}_p^{(j)} \cos \vartheta^{(j)} + \bar{j}_p^{(j)} \sin \vartheta^{(j)}, \quad \bar{g}^{(j)} = -\bar{i}_p^{(j)} \sin \vartheta^{(j)} + \bar{j}_p^{(j)} \cos \vartheta^{(j)}. \tag{25}$$

is fulfilled.

Because of $d\bar{l}^{(j)} / d\vartheta^{(j)} = \bar{g}^{(j)}(\vartheta^{(j)})$, then the direction of the vector $\bar{g}^{(j)}(\vartheta^{(j)})$ is determined by the counterclockwise rotation, determined by the positive direction of the axis $O_p^{(j)} z_p^{(j)}$ and it is tangent to the directed circle (defined by the directed cylinder $C^{(j)}$). Expressing with $\bar{r}_p^{(j)} = x_p^{(j)} \bar{i}_p^{(j)} + y_p^{(j)} \bar{j}_p^{(j)}$, for the cross-section of the conic convolute surface $\Sigma_1^{(j)}$ (in accordance with Eqs. (22), (23) and (24)) we can write:

$$\bar{r}_p^{(j)} = r_0^{(j)} \bar{l}^{(j)}(\vartheta^{(j)}) - b^{(j)} \vartheta^{(j)} \bar{g}^{(j)}(\vartheta^{(j)}), \tag{26}$$

$$\bar{r}_p^{(j)} = r_0^{(j)} \bar{l}^{(j)}(\vartheta^{(j)}) \mp b^{(j)} \vartheta^{(j)} \bar{g}^{(j)}(\vartheta^{(j)}), \tag{27}$$

$$\bar{r}_p^{(j)} = r_0^{(j)} \bar{l}^{(j)}(\vartheta^{(j)}) + b^{(j)} \vartheta^{(j)} \bar{g}^{(j)}(\vartheta^{(j)}), \tag{28}$$

Let us illustrate the cross-section of the $\Sigma_1^{(j)}$ in the coordinate plane $O_p^{(j)} x_p^{(j)} y_p^{(j)}$, i.e. for the case $C_{z_p}^{(j)} = 0$, when $b^{(j)} = -\frac{p_t^{(j)}}{\cos \xi^{(j)}} > 0$.

The above condition and the vector Eqs. (26), (27), and (28) determine the type/form of the cross-section of the type three pairs conic convolute helicoids $\Sigma_1^{(j)}$ ($j = 1, 2$) are shown in Figs. 5, 6, and 7 respectively.

Axial Section and an Axial Angle of $\Sigma_1^{(j)}$

Fig. 5 Cross-sections of the conic convolute helicoids $\Sigma_1^{(j)}$ ($j = 1, 2$) of I type: $CS^{(j)}$ —line of the crossed section of $\Sigma_1^{(j)}$

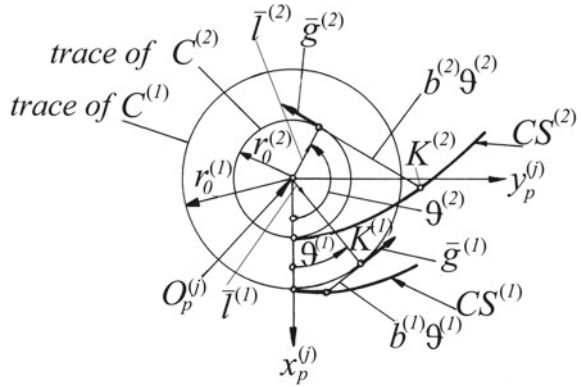


Fig. 6 Cross-sections of the conic convolute helicoids $\Sigma_1^{(j)}$ ($j = 1, 2$) of II type: $CS^{(j)}$ —line of the crossed section of $\Sigma_1^{(j)}$

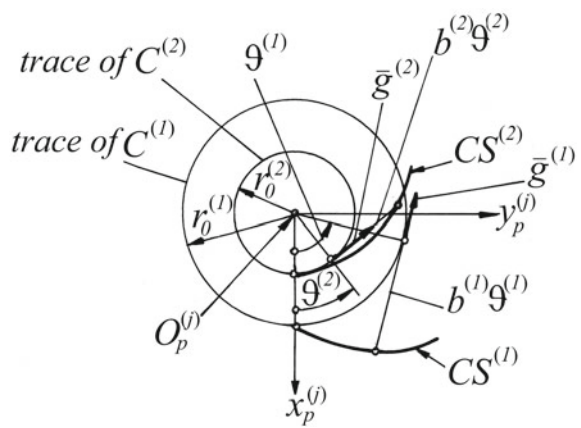
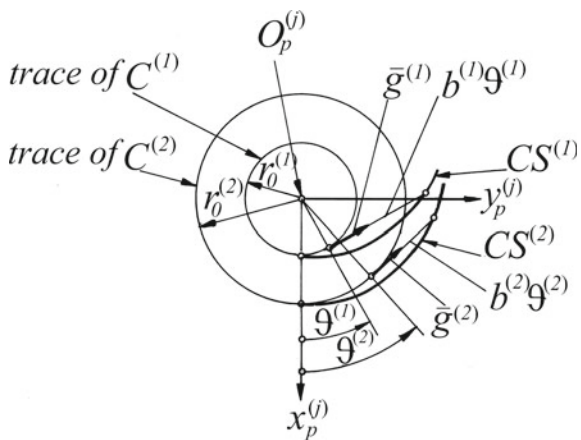


Fig. 7 Cross-sections of the conic convolute helicoids $\Sigma_1^{(j)}$ ($j = 1, 2$) of III type: $CS^{(j)}$ —line of the crossed section of $\Sigma_1^{(j)}$



A. Conic convolute helicoid $\Sigma^{(j)}$, described by the equations' systems (2) and illustrated in Fig. 1

When we substitute $y_p^{(j)} = 0$ in (2), then we obtain:

$$\begin{aligned} x_p^{(j)} &= \frac{r_0^{(j)}}{\cos\vartheta^{(j)}} = r_0^{(j)} \sec\vartheta^{(j)}, \quad z_p^{(j)} = -p^{(j)} \operatorname{conv}(\vartheta^{(j)}, k^{(j)}), \\ k^{(j)} &= -\frac{r_0^{(j)}}{p^{(j)}} \cdot \operatorname{cot}\xi^{(j)} > 0, \quad \operatorname{conv}(\vartheta^{(j)}, k^{(j)}) = k^{(j)} \tan\vartheta^{(j)} - \vartheta^{(j)}. \end{aligned} \tag{29}$$

Following [13], to clarify the character of the axial section of the studied conic convolute helicoid we will first determine the derivatives:

$$\begin{aligned} \frac{dx_p^{(j)}}{d\vartheta^{(j)}} &= r_0^{(j)} \frac{\sin\vartheta^{(j)}}{\cos^2\vartheta^{(j)}}, \quad \frac{dz_p^{(j)}}{d\vartheta^{(j)}} = -p^{(j)} \frac{k^{(j)} - \cos^2\vartheta^{(j)}}{\cos^2\vartheta^{(j)}}, \\ \frac{dz_p^{(j)}}{dx_p^{(j)}} &= -\frac{p^{(j)} k^{(j)} - \cos^2\vartheta^{(j)}}{r_0^{(j)} \sin\vartheta^{(j)}}, \\ \frac{d^2z_p^{(j)}}{dx_p^{(j)2}} &= -\frac{p^{(j)} \cos^3\vartheta^{(j)}(1 - k^{(j)} + \sin^2\vartheta^{(j)})}{(r_0^{(j)})^2 \sin^3\vartheta^{(j)}}. \end{aligned} \tag{30}$$

According to the fact, that in the most common case, the axial section $\Sigma_1^{(j)}$ is non-symmetric, then we realize the study when $\vartheta^{(1)} \in [0, \pi/2)$ and $\vartheta^{(2)} \in (-\pi/2, 0]$.

When $\vartheta^{(j)} = 0$, $x_p^{(j)} = r_0^{(j)}$ and $z_p^{(j)} = 0$, then this point corresponds to the tip of the curve “axial section”. When $\vartheta^{(j)}$ varies from 0 to $\pm\pi/2$, then $x_p^{(j)}$ augments from $r_0^{(j)}$ to $+\infty$, and $z_p^{(j)}$ is changed to $\pm\infty$. Hence, the function of the axial section (29) has asymptotes of the type:

$$\begin{aligned} z_p^{(j)} &= A^{(j)} x_p^{(j)} + B^{(j)}, \\ A^{(j)} &= \lim_{x_p^{(j)} \rightarrow \infty} \frac{z_p^{(j)}(x_p^{(j)})}{x_p^{(j)}} = \pm \operatorname{cot}\xi^{(j)}, \\ B^{(j)} &= \lim_{x_p^{(j)} \rightarrow \infty} [z_p^{(j)} - A^{(j)} x_p^{(j)}] = \pm p^{(j)} \frac{\pi}{2}. \end{aligned} \tag{31}$$

Then the equations of the asymptotes of the curves representing the axial section of $\Sigma_1^{(j)}$ are

$$z_p^{(j)} = \pm \operatorname{cot}\xi^{(j)} x_p^{(j)} \pm p^{(j)} \frac{\pi}{2}, \quad (j = 1, 2), \tag{32}$$

Here the upper signs correspond to $j = 1$ while the lower ones—to $j = 2$. If we introduce the angle $\delta^{(j)} = \xi^{(j)} - \frac{\pi}{2}$, then the Eq. (32) becomes

$$z_p^{(j)} = \mp \tan \delta^{(j)} x_p^{(j)} \pm p^{(j)} \frac{\pi}{2}. \tag{33}$$

The points of intersection of the asymptotes with the coordinate axis $O_p^{(j)} z_p^{(j)}$ determine from (33) and have applicatas:

$$z_p^{(j)} = \pm p^{(j)} \frac{\pi}{2}, \tag{34}$$

and the points of intersection of the asymptotes with the axis $O_p^{(j)} x_p^{(j)}$ have abscissas defined by equality

$$x_p^{(j)} = \frac{p^{(j)}}{\tan \delta^{(j)}} \cdot \frac{\pi}{2} = \frac{r_0^{(j)} \pi}{2k^{(j)}} \tag{35}$$

The points of the inflection of the curve with the axial section, we obtain from the condition:

$$\frac{d^2 z_p^{(j)}}{d x_p^{(j)2}} = 0. \tag{36}$$

Taking into account (30), the condition (36) is fulfilled, if $\cos^3 \vartheta^{(j)} (1 - k^{(j)} + \sin^2 \vartheta^{(j)}) = 0$, i.e. when

$$\vartheta^{(j)} = \pm \frac{\pi}{2} \text{ and } \vartheta^{(j)} = \pm \arcsin \sqrt{k^{(j)} - 1}. \tag{37}$$

If the first equation in (37) is realized, then the inflection points of the curve of the axial section will be in $\pm \infty$. When the second condition from (37) is fulfilled then the inflection points of the curve of the axial section will exist when,

$$1 < k^{(j)} < 2. \tag{38}$$

Let's analyze the curves of the axial section of the conic convolute helicoid $\Sigma_1^{(j)}$ as for the case defined by the condition (38), and outside of the defined interval, i.e. when $0 < k^{(j)} < 1$ and $k^{(j)} \geq 2$.

Case $k^{(j)} = \frac{\pi}{2}$. According to (37) and (38), for this case, points of inflection will exist on the curves of the axial section and they correspond to $\vartheta^{(j)} = \pm \arcsin \sqrt{\frac{\pi}{2} - 1}$ ($j = 1, 2$). From equality (35) it follows that through the tips of the curves of the axial section $\Sigma_1^{(j)}$ ($j = 1, 2$), pass their asymptotes. This case of the axial section is illustrated in Fig. 8.

Case $1 < k^{(j)} < \frac{\pi}{2}$. When we apply the above considerations it can easily be seen that the curves of the axial section $\Sigma_1^{(j)}$ have the form illustrated in Fig. 9.

Fig. 8 Curves of the axial section of the conic convolute helicoids $\Sigma_1^{(j)}$ ($j = 1, 2$) for the case $k^{(j)} = \frac{\pi}{2}$

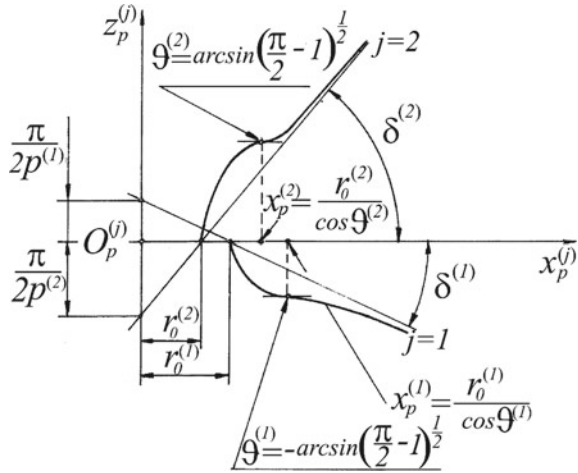
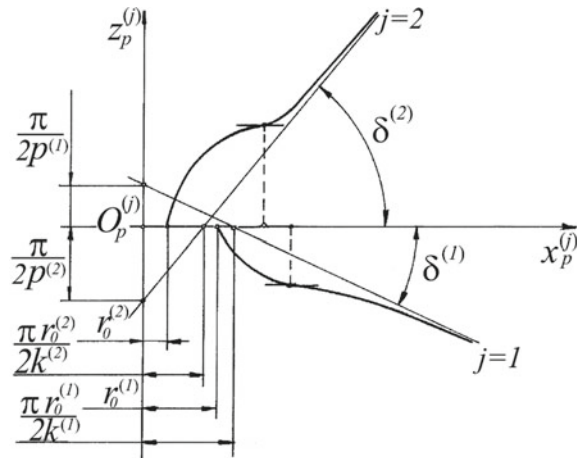


Fig. 9 Curves of the axial section of the conic convolute helicoids $\Sigma_1^{(j)}$ ($j = 1, 2$) for the case $1 < k^{(j)} < \frac{\pi}{2}$

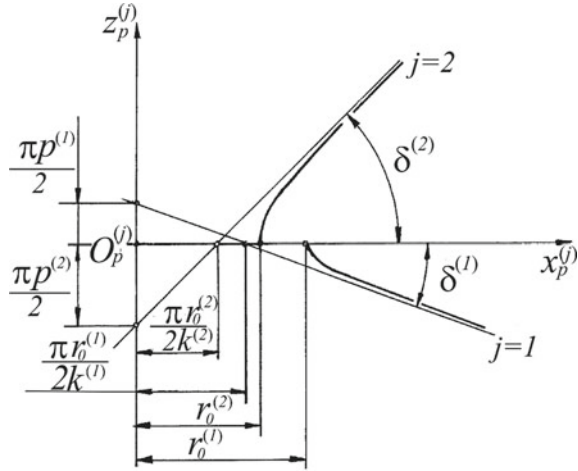


Case $k^{(j)} \geq 2$. Following (37) and (38), points of inflection do not exist on the curves of the axial section of the conic convolute helicoid $\Sigma_1^{(j)}$. The analytical condition corresponding to it, is

$$\frac{r_0^{(j)}}{p^{(j)}} \tan \delta^{(j)} \geq 2 \tag{39}$$

or $h^{(j)} - p^{(j)} \geq 0$. The form of the curves of the axial section, in this case, is shown in Fig. 10.

Fig. 10 Curves of the axial section of the conic convolute helicoids $\Sigma_1^{(j)}$ ($j = 1, 2$) for the case $k^{(j)} \geq 2$



Case $0 < k^{(j)} < 1$. Analyzing the last two equalities of (30) we establish that the curves of the axial section of $\Sigma_1^{(j)}$ have extremum when

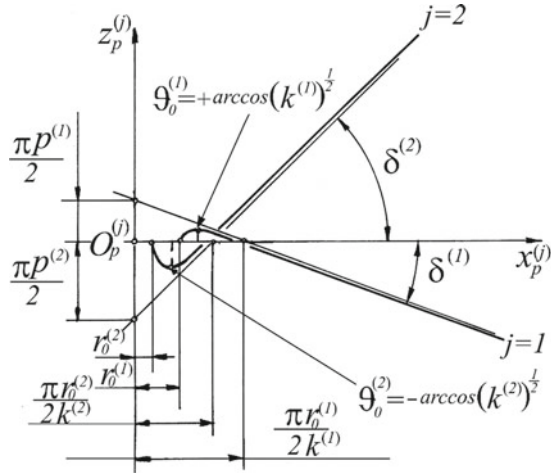
$$\vartheta^{(j)} = \vartheta_0^{(j)} = \pm \arccos \sqrt{k^{(j)}}. \tag{40}$$

From the last equality of (30) it can be seen that if $\vartheta^{(j)} = \vartheta_0^{(1)}$, then $\frac{d^2 z_p^{(1)}}{dx_p^{(1)2}} < 0$, i.e. the curve of the axial section of the conic convolute helicoid $\Sigma_1^{(1)}$ has maximum in a point determined by condition (40), while if $\vartheta^{(j)} = \vartheta_0^{(2)}$, then $\frac{d^2 z_p^{(2)}}{dx_p^{(2)2}} > 0$, i.e. the curve of the axial section of $\Sigma_1^{(2)}$, has a minimum in the point determined by the condition (40). Each one of the theoretical curves of the axial section of the linear convolute helicoid $\Sigma_1^{(j)}$, considered in the whole interval of $\vartheta^{(j)}$ (i.e. when $\vartheta^{(j)} \in [0, \pi/2)$ and $\vartheta^{(j)} \in (-\pi/2, 0]$ ($j = 1, 2$)) is symmetric with respect to the axis $O_p^{(j)} x_p^{(j)}$ and has an ordinary node, for the $\vartheta^{(j)} = \vartheta_1^{(j)}$ ($j = 1, 2$) that has the following coordinates:

$$\begin{aligned} x_p^{(j)} &= \frac{r_0^{(j)}}{k^{(j)}} \cdot \frac{\vartheta_1^{(j)}}{\sin \vartheta_1^{(j)}}, \\ z_p^{(j)} &= 0. \end{aligned} \tag{41}$$

In this case, the asymptotes of the axial section $\Sigma_1^{(j)}$, defined by the Eqs. (32) and (33), cross the axis $O_p^{(j)} x_p^{(j)}$ ($j = 1, 2$) at points determined by the expression (35). Comparing (35) and (41) it can be concluded that abscissas of the points of intersection between the curves of the axial section of the conic convolute helicoid $\Sigma_1^{(j)}$ with the axes $O_p^{(j)} x_p^{(j)}$ ($j = 1, 2$) are smaller than the abscissas of the points

Fig. 11 Curves of the axial section of the conic convolute helicoids $\Sigma_1^{(j)}$ ($j = 1, 2$) for the case $0 < k^{(j)} < 1$



of intersection with the abscissas with the same axis, since $1 > \frac{\sin\vartheta^{(j)}}{\vartheta^{(j)}} \geq \frac{2}{\pi}$, when $\vartheta^{(j)} \in [-\frac{\pi}{2}, 0)$ and $\vartheta^{(j)} \in (0, \frac{\pi}{2}]$.

The realized analysis for the character of the curve of the axial section of $\Sigma_1^{(j)}$ for the case $0 < k^{(j)} < 1$ is illustrated in Fig. 11. Here it should be specially mentioned that the case $k^{(j)} = 1$ transforms the **conic convolute helicoid into conic involute helicoid**, which case will be discussed separately.

The axial angle in an arbitrary point of the axial section of the studied conic helicoid is obtained from the equations' systems (30) [1]:

$$\begin{aligned} \tan\alpha_s^{(j)} &= \left| \frac{dz_p^{(j)}}{dx_p^{(j)}} \right| = \left| -\frac{p^{(j)}}{r_0^{(j)}} \cdot \frac{k^{(j)} - \cos^2\vartheta^{(j)}}{\sqrt{1 - \cos^2\vartheta^{(j)}}} \right|, \\ k^{(j)} &= -\frac{r_0^{(j)}}{p^{(j)}} \cot\xi^{(j)}, \quad \cos\vartheta^{(j)} = \frac{r_0^{(j)}}{x_p^{(j)}}. \end{aligned} \tag{42}$$

or

$$\alpha_s^{(j)} = \arctan \left| \frac{p^{(j)} \frac{r_0^{(j)}}{x_p^{(j)}} + x_p^{(j)} \cot\xi^{(j)}}{\sqrt{x_p^{(j)2} - r_0^{(j)2}}} \right|, \quad (j = 1, 2) \tag{43}$$

Substituting $x_p^{(j)} = r_p^{(j)}$ in (43), we receive the axial angle of $\Sigma_1^{(j)}$ in the point of an arbitrary conic surface co-axial of the outer surface of the conic gear, which has convolute helical teeth of the studied type.

B. Conic convolute helicoid $\Sigma_1^{(j)}$ described with a system of Eq. (3) and illustrated in Fig. 2

From the system (3), after a substitution of $y_p^{(j)} = 0$, we receive:

$$\begin{aligned} x_p^{(j)} &= r_0^{(j)} \sec \vartheta^{(j)}, \\ z_p^{(j)} &= -p^{(j)} \operatorname{conv}(\vartheta^{(j)}, k^{(j)}), \\ k^{(j)} &= \mp \frac{r_0^{(j)}}{p^{(j)}} \cot \xi^{(j)}. \end{aligned} \tag{44}$$

From the system (44) it can be seen, that for $j = 1 - k^{(1)} > 0$, and when $j = 2 - k^{(2)} < 0$. Hence, the character of the axial section of the $\Sigma_1^{(j)}$ we study only for the case $j = 2$, i.e. when $k^{(2)} < 0$. The cases $j = 1$ are identical for the studied in paragraph A. As it can be seen from Fig. 2, here $\vartheta^{(j)} > 0$.

When $\vartheta^{(2)} = 0$, $x_p^{(2)} = r_0^{(2)}$ and $z_p^{(2)} = 0$, and when $\vartheta^{(2)} = \pi/2$, $x_p^{(2)} = +\infty$ and $z_p^{(2)} = +\infty$. The asymptote of the curvature of the cross-section of the conic linear helicoid $\Sigma_1^{(2)}$ has the form:

$$\begin{aligned} z_p^{(2)} &= A^{(2)} x_p^{(2)} + B^{(2)}, \\ A^{(2)} &= -\cot \xi^{(2)}, \quad B^{(2)} = \frac{p^{(2)}\pi}{2}, \end{aligned} \tag{45}$$

i.e.

$$z_p^{(2)} = -\cot \xi^{(2)} x_p^{(2)} + \frac{p^{(2)}\pi}{2}, \tag{46}$$

or

$$z_p^{(2)} = \tan \delta^{(2)} x_p^{(2)} + \frac{p^{(2)}\pi}{2}. \tag{47}$$

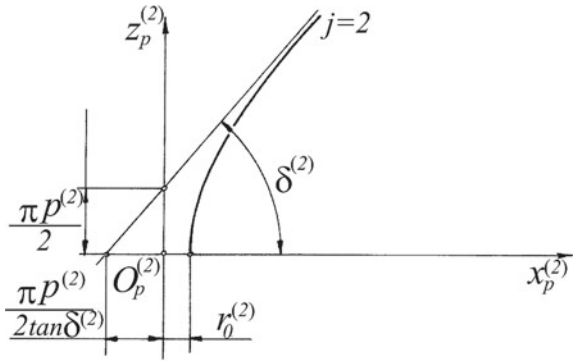
The intersection point of the asymptote (47) with the axis $O_p^{(2)} z_p^{(2)}$, is obtained from (44), after substituting of $x_p^{(2)} = 0$ and it has applicatas $z_p^{(2)} = \frac{p^{(2)}\pi}{2}$. Analogically we determine the point of intersection of the same asymptote with the axis $O_p^{(2)} x_p^{(2)}$ and it has the abscissa $x_p^{(2)} = -\frac{p^{(2)}\pi}{2 \tan \delta^{(2)}}$.

Then, the graphic form of the axial section of the conic convolute helicoid $\Sigma_1^{(2)}$ is shown in Fig. 12.

The axial angle of $\Sigma_1^{(j)}$ in an arbitrary point of the axial section is

$$\alpha_s^{(j)} = \arctan \left| \frac{p^{(j)} \pm x_p^{(j)} \cot \xi^{(j)}}{\sqrt{x_p^{(j)2} - r_0^{(j)2}}} \right|. \tag{48}$$

Fig. 12 Curve of the axial section of the conic convolute helicoid $\Sigma_1^{(2)}$ when $k^{(2)} < 0$



The upper sign in the Eq. (48) refers to the helicoid $\Sigma_1^{(1)}$, and the bellow sign—for $\Sigma_1^{(2)}$.

C. Conic convolute helicoid $\Sigma_1^{(j)}$, described by the equations’ systems (4) and illustrated in Fig. 3

From the system of Eq. (4), after substituting $y_p^{(j)} = 0$, we receive

$$\begin{aligned}
 x_p^{(j)} &= r_0^{(j)} \sec\vartheta^{(j)}, \quad z_p^{(j)} = -p^{(j)} \operatorname{conv}(\vartheta^{(j)}, k^{(j)}), \\
 k^{(j)} &= \frac{r_0^{(j)}}{p^{(j)}} \cot\xi^{(j)} < 0.
 \end{aligned}
 \tag{49}$$

Analogously to the realized study up to now, the curves of the axial section of the pairs of conic convolute helicoids $\Sigma_1^{(j)}$ ($j = 1, 2$) we study when $\vartheta^{(1)} \in (-\frac{\pi}{2}, 0]$ and $\vartheta^{(2)} \in [0, \frac{\pi}{2})$. From (49) it is obvious, that for $\vartheta^{(j)} = 0$, $x_p^{(j)} = r_0^{(j)}$ and $z_p^{(j)} = 0$, and for $\vartheta^{(j)} = \mp\pi/2$, $x_p^{(j)} = \infty$ and $z_p^{(j)} = \mp\infty$.

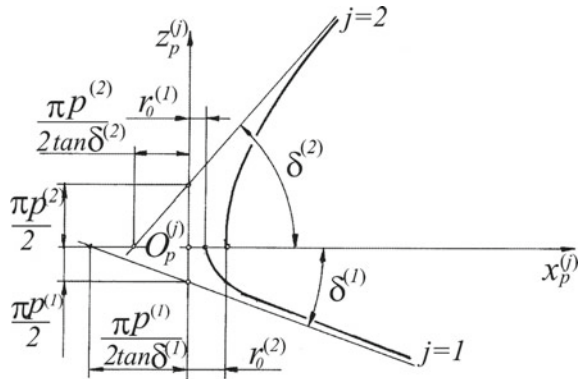
Asymptotes of the curves of the cross-section of the conic convolute helicoids are sought from the form (32) and (33), and it is not difficult to establish that they are described by equations:

$$z_p^{(j)} = \pm \cot\xi^{(j)} x_p^{(j)} \mp \frac{p^{(j)}\pi}{2}, \tag{50}$$

$$z_p^{(j)} = \mp \tan\delta^{(j)} x_p^{(j)} \mp \frac{p^{(j)}\pi}{2}. \tag{51}$$

The form of the axial section of $\Sigma_1^{(1)}$ for the studied case is illustrated in Fig. 13. The axial angle of the profile is determined by the expression

Fig. 13 Curves of the axial section of the conic convolute helicoids $\Sigma_1^{(j)}$ ($j = 1, 2$) for the case $k^{(j)} < 0$



$$\alpha_s^{(j)} = \arctan \left| \frac{p^{(j)} \frac{r_0^{(j)}}{x_p^{(j)}} - x_p^{(j)} \cot \xi^{(j)}}{\sqrt{x_p^{(j)2} - r_0^{(j)2}}} \right|. \tag{52}$$

4 Conclusion

A synthesis of three types of conic convolute helicoids is realized. The obtained equations show a theoretical possibility, depending on the basic geometrical characteristics of the designed conic convolute worm/pinion, to be generated the flanks of its helical teeth as parts of the studied pairs of conic convolute helicoids.

The derived analytical dependencies of the cross-section and the axial section, as well as the realized studies of the graphic images of these sections, precede the process of constructing algorithms for computer synthesis and design of these conic helical surfaces.

All of the obtained mathematical relations, treating the synthesis and design of the most common type of linear helicoid—conic convolute are basic for obtaining the corresponding ones for the pairs of conic involute and conic Archimedean helicoids.

The derived equations of the conic convolute helicoids, as well as the analytical descriptions of their cross-sections and axial sections, are important geometrical characteristics of the active tooth surfaces of the conic worms (respectively of the conic hobs). They are related to the technological synthesis of gear pairs with the application of these new types of helical surfaces, operating in the condition of work and/or instrumental meshing. Last but not least, it should be noted that the obtained analytical dependencies can be used in the organization of the procedures for measurement and control of parameters of these surfaces in the process of their manufacture.

References

1. Abadjiev, V.: On the synthesis and analysis of spiroid gears. Ph.D. Thesis. Institute of Mechanics, Bulgarian Academy of Sciences, Sofia (1984). (in Bulgarian)
2. Kovtushenko, A., Lagutin, S., Yantsin, Yu.: Worm-gears in drives of metallurgical equipment. *J. Probl. Mech. Eng. Mach. Reliab.* **5**, 41–48 (1994). (Moscow)
3. Lagutin, S.: Spatial gearing and synthesis of worm-gears with localized contact. In: Proceedings of the International Conference “Theory and Practice of Gears”, Izhevsk, pp. 185–192 (1998)
4. Long, V., Georgiev, A., Ivaykin, V., Alekseev, A.: Rotating device with spiroid gears designed for multi-operation CNC machine. In: Issues of Design, Manufacturing Technology and Implementation of Spiroid Gears and Reductors (Materials of a Scientific-Technical Seminar), Publishing House “Udmurtia”, Izhevsk, pp. 22–24 (1984)
5. Matveev, V., Georgiev, A., Yuminova, V.: Comparison of technical indicators of spiroid, worm and cylindrical gears, applied into crane with manual driving. In: Improvement of Calculation Methods, Design and Production Technology of Spiroid, Hypoid and Worm-Gears, and Reductors. Abstracts of the Republican Scientific Conference, Ustinov, pp. 33–34 (1986)
6. Stefanov, D., Abadjiev, V.: Electromechanical system for driving of mobile platforms. In: First International Conference on Technology and Robotics TEHRO’88, Duni, pp. 242–247 (1988)
7. Kirov, V.: Worm-hobs for generation of the spiroid gears. The dissertation of Ph.D. Thesis, Rousse University “Angel Kanchev” Ruse (1995). (in Bulgarian)
8. Kirov, V.: Experimental generation of the spiroid gears of type helicon. In: Jubilee Scientific Conference of VTU “Angel Kanchev”, vol. XXXV, series 1, Ruse, pp. 116–122 (1994). (in Bulgarian)
9. Lashnev, S., Yulikov, M.: Calculation and Design of Metal-Cutting Tools with an IBM Application. Mashinostroenie, Moscow (1975)
10. Long, V., Georgiev, A.: On the question of choosing the cutting regime, when multi-teeth spiroid worm gears are generated with a face cutting head. In: Improvement of Calculation Methods, Design and Production Technology of Spiroid, Hypoid and Worm Gears, and Reductors. Abstracts of the republican scientific and technical conference, Ustinov, pp. 5–7 (1986)
11. Litvin, F.: Theory of Gearing. Nauka, Moscow (1968). (in Russian)
12. Litvin, F.: Theory of gearing. AVSCOM Technical Report 88-C-035, NASA Reference Publication 1212, US Government Printing Office, Washington (1989)
13. Lyukshin, V.: The Theory of Helical Surfaces in the Design of Cutting Tools. Mashinostroenie Publishing House, Moscow (1968)
14. Rashevsky, P.: Course of Differential Geometry. State Publishing House of Technical and Theoretical Literature, Moscow (1956)
15. Dudley, D.: Gear Handbook. The Design, Manufacture, and Application of the Gears, McGraw-Hill Book Company, Inc., New York-Toronto, London (1962)
16. Phillips, J.: General Spatial Involute Gearing. Printed in Germany, Springer, Berlin (2003)
17. Abadjiev, V.: On the geometry of the convolute spiroid helicoid. In: 4th National Congress of Theoretical and Applied Mechanics, Varna, Book 1, pp. 158–163. Publishing House of the Bulgarian Academy of Sciences, Sofia (1981)
18. Abadjiev, V., Okhotsimsky, D., Platonov, A.: Research on the spatial gears and applications, keldysh institute of applied mathematics. Russian Academy of Sciences, Preprint No 89, Moscow (1997)
19. Minkov, K., Abadjiev, V.: Spiroid gears-geometric, technological, and operational features. *Mech. Eng.* **11**, pp. 495–498 (1980). (Sofia)
20. Bohle, F.: Spiroid gears. A new development in gears of the skew-axis type. *Machinery* **62**(2), 155–161 (1955). (Chicago)
21. Nelson, W.: Spiroid gearing. Part 1–basic design practices. *Mach. Design*, 136–144 (1961)
22. Nelson, W.: Spiroid gearing. Part 2–durability, strength, and efficiency. *Mach. Design*, 93–100 (1961)

23. Nelson, W.: Spiroid gearing. Part 3—materials, mounting detail, lubrication. *Mach. Design*, 165–171 (1961)
24. Saari, O.: The Mathematical Background of Spiroid Gears, No 7. *Industrial Mathematical Series*, Detroit (1956)
25. Schagerl, D.: Helicon-und Spiroid-Getriebe mit trapezformigem Schneckenprofil. Teil 1, *Industrie-Anzeiger* 91. Jg. Nr 52, 24–26, Munchen (1969)
26. Schagerl, D.: Helicon-und Spiroid-Getriebe mit trapezformigem Schneckenprofil. Teil 2, *Industrie-Anzeiger* 91. Jg. Nr 80, 1953–1957, Munchen (1969)
27. Abadjiev, V., Petrova D.: Registration of undercutting contact points in the generation of surfaces according to the second principle of T. Olivier. In: *Theoretical and Applied Mechanics*, Book 4, pp.11–14. Publishing House of BAS, Sofia (1985)
28. BDS 8540-84, 1985. Gear sets. Common terms. Definitions and symbols. Institute of Standardization, Sofia (1985)
29. Abadjiev, V.: Mathematical modelling for synthesis of spatial gears. *Proc. Inst. Mech. Eng. Part E: J. Process Mech. Eng.* **216**, pp. 31–46 (2002)
30. Abadjiev, V., Abadjieva, E.: On the conic convolute helicoids generation for active flanks of the spiroid pinion threads. *J. Theor. Appl. Mech.* **32**(2), 13–18 (2002). (Sofia)

Conic Linear Helicoids: Part 2. Applications in the Synthesis and Design of Spatial Motions Transformers



Emilia Abadjieva  and Valentin Abadjiev 

Abstract The current work presents authors' researches over the years oriented in the elaboration of geometric and analytical processes, dedicated to the synthesis and design of special spatial gear mechanisms. These mechanisms are applicable for quantitative and qualitative motions' transformation of one of the movable links depending on the implemented technological requirements. Based on the performed vector analysis of spatial motions transformation of type rotation into translation, a kinematic theory of this transformation is constructed. Using this kinematic theory the basic geometric-kinematic characteristics of spatial rack mechanisms, applicable to their synthesis are introduced. This study is dedicated to the synthesis of spatial rack mechanisms when the rotating link has linear (conic and cylindrical) helicoids. Based on a worked-out mathematical model, a surface of action/mesh region is synthesized respectively, of a transmission which geometric elements of the joints firmly connected with the rotating link are linear helicoids (conic and cylindrical ones). The surface of action/region of mesh are obtained analytically and are studied, and visualized for conic and cylindrical spatial rack drives.

Keywords Synthesis · Design · Geometric basic characteristics · Computer programs · Spatial rack drives

1 Introduction

The current work is dedicated to the, used by authors, principles of creation of spatial mechanical motions transformers. Over the years, the authors have devoted part of their theoretical researches to the synthesis and design of spatial motion transformers with two types of applications:

E. Abadjieva (✉) · V. Abadjiev
Institute of Mechanics-Bulgarian Academy of Sciences, Acad. G. Bontchev St., bl. 4. 1113, Sofia,
Bulgaria

V. Abadjiev
e-mail: abadjiev@imbm.bas.bg

- Spatial gear mechanisms realizing the change of rotation motions between shafts with crossed axes;
- Three-links spatial closed mechanical system, in which at a given rotational motion of one of the movable links, relative to the fixed link of the system, the other realizes a unique rectilinear translation, as the transformation of the given rotation into a rectilinear translation is realized by a set high kinematic joints, formed by the movable links (the velocities of rotation and translation of the links have an arbitrary placement in space).

The second group of the spatial mechanical systems is known in the techniques as spatial rack drives. These mechanisms are the object of the realized further researches.

2 Kinematic Theory of Spatial Rack Meshing

2.1 Mathematical Model of the Kinematic Contact at Rack Meshing

The study is consistent with the kinematic scheme of a spatial rack mechanism, given in Fig. 1. The motions transformation, realized by the rack mechanism, is characterized by the following conditions:

$$\begin{aligned} \omega_1 &= \text{constant}, \quad V_2 = \text{constant}, \\ \delta_r &= \angle(\bar{\omega}_1, \bar{V}_2) = \pi - \Sigma_r = \text{constant}, \\ j_{12} &= \frac{\omega_1}{V_2} = \frac{1}{j_{21}} = \text{constant}, \end{aligned} \quad (1)$$

where ω_1 is value of the angular velocity vector $\bar{\omega}_1$ of the rotating link $i = 1$; V_2 —value of the translation velocity vector \bar{V}_2 of link $i = 2$; δ_r —crossed angle between the motions transformation vectors; Σ_r —angle between the motion directions of rack mechanism; j_{12} , j_{21} —velocity ratio of motion transformation of type $(R \leftrightarrow T)$.

The transformation of motions of type rotation into translation and vice versa $(R \leftrightarrow T)$ is realized by high kinematic joints $(\Sigma_1 : \Sigma_2)$ which elements Σ_1 and Σ_2 at any moment have conjugate instantaneous contact points P (the points of tangential contact P can belong to the conjugate instantaneous contact line). It has to be mentioned that for the rack mechanism in every moment of motions transformation more than one high kinematic joint $(\Sigma_1 : \Sigma_2)$ takes part in the process of transformation. When a rotation with angular velocity $\bar{\omega}_1$ is applied to the link $i = 1$, the second motion link $i = 2$ obtains a translation velocity \bar{V}_2 . According to (1) the condition $V_2 = j_{21}\omega_1$ is accomplished for the value of \bar{V}_2 . Hence, the joints $(\Sigma_1 : \Sigma_2)$ shown in Fig. 1 are kinematically conjugated, and the rack mechanism, respectively. The study is realized by the right-hand coordinate systems $S(O, x, y, z)$, $S_0(O_0, x_0, y_0, z_0)$ and $S_i(O_i, x_i, y_i, z_i)$ ($i = 1, 2$) (see Fig. 1). $S(O, x, y, z)$ and $S_0(O_0, x_0, y_0, z_0)$ are fixed

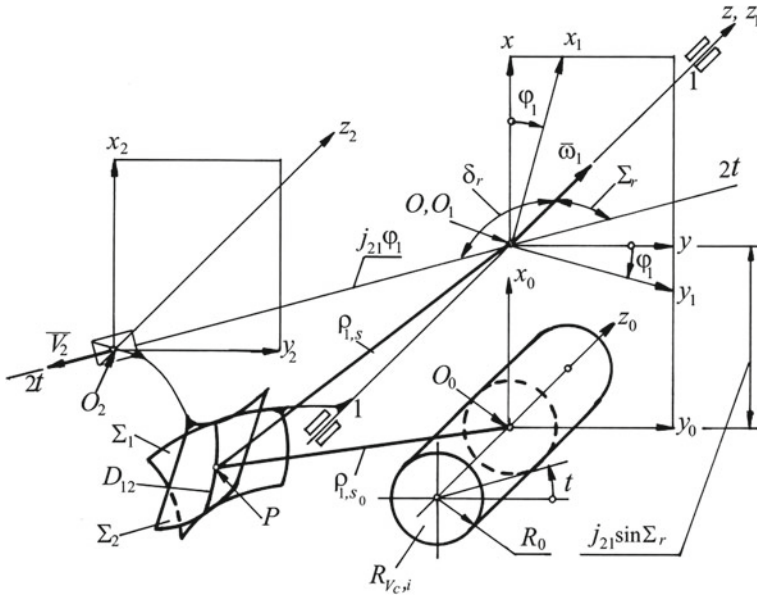


Fig. 1 Kinematic scheme of motion transformation of type $(R \leftrightarrow T)$

coordinate systems and $S_1(O_2, x_1, y_1, z_1)$ and $S_2(O_2, x_2, y_2, z_2)$ are connected with the motion links of the rack mechanism.

Let the elements Σ_1 and Σ_2 of high kinematic joints $(\Sigma_1:\Sigma_2)$, shown in Fig. 1 are defined parametrically in the fixed coordinate system S :

$$\begin{aligned} \bar{\rho}_{1,s} &= \bar{\rho}_{1,s}(u_1, \vartheta_1, \varphi_1), \quad \bar{\rho}_{2,s} = \bar{\rho}_{2,s}(u_2, \vartheta_2, j_{21}\varphi_1), \\ \bar{n}_{1,s} &= \bar{n}_{1,s}(u_1, \vartheta_1, \varphi_1), \quad \bar{n}_{2,s} = \bar{n}_{2,s}(u_2, \vartheta_2, j_{21}\varphi_1), \end{aligned} \tag{2}$$

where $\bar{\rho}_{i,s}$ is a radius-vector of the contact point P , as a point of Σ_i ; $\bar{n}_{i,s}$ —normal vector to the Σ_i in the same point; u_i, ϑ_i —independent parameters, determining the position of the point P .

For Σ_1 and Σ_2 the following conditions are fulfilled, because Σ_1 and Σ_2 are elements of high kinematic joints, which take part in a process of motion transformation:

$$\begin{aligned} \bar{\rho}_{1,s}(u_1, \vartheta_1, \varphi_1) &= \bar{\rho}_{2,s}(u_2, \vartheta_2, j_{21}\varphi_1), \\ \bar{n}_{1,s}(u_1, \vartheta_1, \varphi_1) &= \bar{n}_{2,s}(u_2, \vartheta_2, j_{21}\varphi_1), \end{aligned} \tag{3}$$

$$\begin{aligned} \dot{\bar{\rho}}_{1,s}(u_1, \vartheta_1, \varphi_1) &= \dot{\bar{\rho}}_{2,s}(u_2, \vartheta_2, j_{21}\varphi_1), \\ \dot{\bar{n}}_{1,s}(u_1, \vartheta_1, \varphi_1) &= \dot{\bar{n}}_{2,s}(u_2, \vartheta_2, j_{21}\varphi_1). \end{aligned} \tag{4}$$

where $\dot{\bar{\rho}}_{i,s}$ is an absolute velocity vector of the contact point P , as a point from Σ_i ; $\dot{\bar{n}}_{i,s}$ —an absolute velocity vector of the top of the normal vector $\bar{n}_{i,s}$ in the contact point P , as a point from Σ_i .

The first vector equation from (4), we can write as [9]:

$$\bar{V}_{12} = \bar{V}_1 - \bar{V}_2 = \bar{V}_{r,2} - \bar{V}_{r,1}. \tag{5}$$

Here \bar{V}_{12} is the relative (sliding) velocity vector of the contact point P ; \bar{V}_1 —transference velocity vector of P , joined to the surface Σ_i ; $\bar{V}_{r,i}$ —relative velocity vector of a point P , when P moves on the surface Σ_i .

The vector Eqs. (5) show that the coplanar vectors \bar{V}_{12} , \bar{V}_1 and \bar{V}_2 define a plane T_m , which determines the transference motion of the contact point P . \bar{V}_{12} , $\bar{V}_{r,1}$ and $\bar{V}_{r,2}$ are contained in a tangential plane T_n of Σ_1 and Σ_2 in the contact point P . The plane T_n defines the relative motion of P .

The displacement of sliding velocities \bar{V}_{12} in common contact points P of the geometrical elements Σ_1 and Σ_2 of the joints ($\Sigma_1:\Sigma_2$) is important for the kinematic conjugation of high kinematic joints.

2.2 Vector Analysis of the Relative (Sliding) Velocity

The study is based on the vector analysis of the vector function of the sliding velocity vector \bar{V}_{12} of the contact point P of the conjugate surfaces Σ_1 and Σ_2 of the rack mechanism (the contact point P can belong to the contact line D_{12}), which is illustrated in Fig. 1 [1, 2]:

$$\bar{V}_{12} = \bar{V}_{12}(x, y, z) = \bar{V}_1 - \bar{V}_2 = \bar{\omega}_1 \times \bar{\rho}_{1,s} - \bar{V}_2. \tag{6}$$

According to the condition of transformation (1), and the given in Fig. 1 symbols, for the function (6), which is written in a coordinate system $S(O, x, y, z)$, we obtain:

$$\begin{aligned} \bar{V}_{12} &= \bar{V}_{12}(x, y, z) = V_{12,x}\bar{i} + V_{12,y}\bar{j} + V_{12,z}\bar{k}, \\ V_{12,x} &= -y, \quad V_{12,y} = x + j_{21} \sin \Sigma_r, \quad V_{12,z} = j_{21} \cos \Sigma_r, \end{aligned} \tag{7}$$

where $V_{12,x}$, $V_{12,y}$, $V_{12,z}$ are coordinates of \bar{V}_{12} in the coordinate system $S(O, x, y, z)$; $\bar{i}, \bar{j}, \bar{k}$ —are unit vectors of the axes of the coordinate system $S(O, x, y, z)$.

In Eq. (7) without disturbing the community of arguments is accepted $\omega_1 = 1$ rad/s and therefore $V_2 = j_{21}$ m/s. The vector analysis of the vector function (7) is realized by defining its scalar and vector field.

Scalar field of the relative velocity \bar{V}_{12} of the conjugate tooth surfaces Σ_1 and Σ_2 in their common contact points P is a scalar function of the following type:

$$V_{12} = V_{12}(x, y, z) = \sqrt{V_{12,x}^2 + V_{12,y}^2 + V_{12,z}^2}, \tag{8}$$

with its definition area.

Hence the surfaces of type

$$V_{12}(x, y, z) = V_c, \quad V_c = \text{constant}, \tag{9}$$

are *surfaces of level* of the studied scalar field and they define it geometrically.

It is easy to determine their canonical type in the static coordinate system $S_0(O_0, x_0, y_0, z_0)$ from (7), (8), and (9):

$$\begin{aligned} x_0^2 + y_0^2 &= R_0^2, \quad z_0 = H, \quad H \in (-\infty, +\infty), \\ x_0 &= x + j_{21} \sin \Sigma_r, \quad y_0 = y, \quad z_0 = z, \\ R_0 &= \sqrt{V_c^2 - (j_{21} \cos \Sigma_r)^2}. \end{aligned} \tag{10}$$

Equation (10) shows that the surfaces of level of the defined scalar field $V_{12} = V_{12}(x_0, y_0, z_0)$ represent a family of coaxial cylinders with a family parameter V_c . These cylinders are called *kinematic cylinders of level* [1]. The axis of the family coaxial cylinders is O_0z_0 of the coordinate system $S_0(O_0, x_0, y_0, z_0)$, which in the fixed coordinate system $S(O, x, y, z)$ has the following equations:

$$x = -j_{21} \sin \Sigma_r, \quad y = 0, \quad z = H, \quad H \in (-\infty, +\infty). \tag{11}$$

According to Eq. (10) the surfaces of level of the studied scalar field will exist if the parameter V_c is chosen so that it fulfills the condition:

$$V_c \geq j_{21} \cos \Sigma_r. \tag{12}$$

The parameter V_c multiplied with ω_1^{-1} , defines the module of the sliding velocity vector \overline{V}_{12} . Every point, belonging to a concrete kinematic cylinder of level is characterized by this parameter V_c . The velocity ratio j_{21} is realized by every point of the cylinders of level. When in (12) the equality is fulfilled, then the Eq. (10) is transformed into a system of Eqs. (11), which describe the *zero kinematic cylinder of level* [1]. It contains those points from the static space, which are characterized by the smallest values of relative velocity motion. The locus of these points is the axis O_0z_0 of $S_0(O_0, x_0, y_0, z_0)$.

A computer program is created. It is oriented to the synthesis and visualization of the basic elements of the scalar and vector field of the sliding velocity of the rack mechanisms. The kinematic surfaces of level of the rack transmissions with concrete basic kinematic and geometric parameters are illustrated in Fig. 2.

The kinematic cylinders of level shown in Fig. 2 are $R_{V_{c,1}}$ corresponding with $V_{c,1} = 23$ mm/rad, $R_{V_{c,2}}$ corresponding with $V_{c,2} = 22$ mm/rad, $R_{V_{c,3}}$ corresponding with $V_{c,3} = 21$ mm/rad by $\Sigma_r = 60^\circ$ and $j_{21} = 42$ mm/rad.

Vector field of the relative velocity vector \overline{V}_{12} is that part of three-dimensional space:

$$\overline{V}_{12} = \overline{V}_{12}(x, y, z). \tag{13}$$

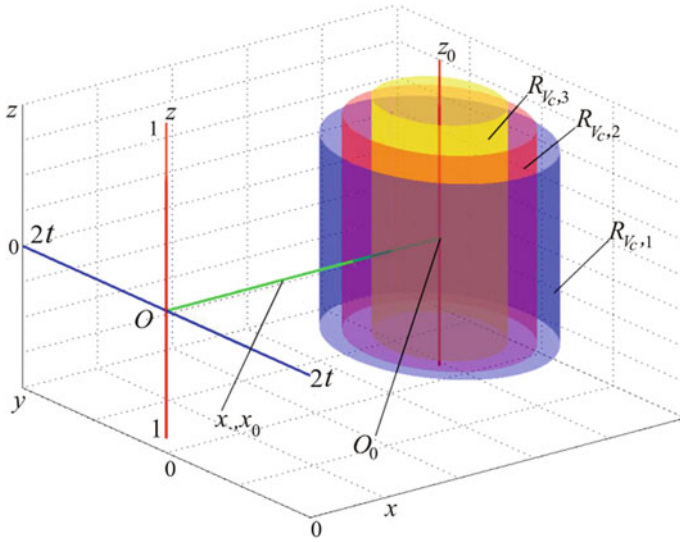


Fig. 2 Set of kinematic surfaces of level (kinematic cylinders of level)

The vector \bar{V}_{12} is defined in every point of the vector field. Let (13), respectively (7) is presented in the coordinate system $S_0(O_0, x_0, y_0, z_0)$:

$$\begin{aligned} \bar{V}_{12,z_0} &= V_{12,x_0}\bar{i}_0 + V_{12,y_0}\bar{j}_0 + V_{12,z_0}\bar{k}_0, \\ V_{12,x_0} &= -y_0, \quad V_{12,y_0} = x_0, \quad V_{12,z_0} = j_{21} \cos \Sigma_r, \end{aligned} \tag{14}$$

where $V_{12,x_0}, V_{12,y_0}, V_{12,z_0}$ are Cartesian coordinates of the vector \bar{V}_{12} in S_0 ; $\bar{i}_0, \bar{j}_0, \bar{k}_0$ —unit vectors of the axes of the coordinate system $S_0(O_0, x_0, y_0, z_0)$.

It is known [3] that every vector field is characterized by its own *vector lines*. The vector lines of the vector function (14) represent curves. The tangential lines in every point $P(x_0, y_0, z_0)$ to these curves coincide with the direction of the vector \bar{V}_{12} at the same point. They are defined by the following system of differential equations:

$$\frac{dx_0}{V_{12,x_0}} = \frac{dy_0}{V_{12,y_0}} = \frac{dz_0}{V_{12,z_0}}. \tag{15}$$

From the first and the third equation of (15) we obtain respectively:

$$x_0^2 + y_0^2 = R_0^2 = \text{constant}, \quad z_0 + p_{z_0} \cdot t = C_0 = \text{constant}, \tag{16}$$

where $p_{z_0} = j_{21} \cos \Sigma_r, \quad t = \arcsin x_0/R_0$.

Obviously, the vector lines of the vector field of the function $\bar{V}_{12} = \bar{V}_{12}(x_0, y_0, z_0)$ are a family of helical lines. They are obtained as intersections of the family of coaxial

cylinders with radius R_0 with a family of conoids with a helical parameter p_{z_0} . The following is fulfilled for p_{z_0} :

$$p_{z_0} = \frac{V_{12,z_0}}{\omega_{12}} = \frac{V_{12,z_0}}{\omega_1} = V_{12,z_0}, \tag{17}$$

because of the fact that for the examined mechanical system $\bar{\omega}_2 = \bar{0}$, and $\omega_1 = 1$ rad/s.

The conoids are called *kinematic conoids* [1]. The helical lines described by systems (16) and (17) are named *kinematic relative helices*. They are characterized by parameters $R_0, p_{z_0}, C_{0(i)}$ ($i = 1, 2$). It is evident when the kinematic relative helices are defined, then a relative helical motion of surfaces Σ_1 and Σ_2 is defined, which arises in the process of transformational motion ($R \leftrightarrow T$).

When in the Eqs. (16) is substituted $R_0 = 0$, they describe the equation of the axis O_0z_0 .

According to the values of the Cartesian coordinates of the sliding velocity \bar{V}_{12} in $S_0(O_0, x_0, y_0, z_0)$ from (14), for the value of sliding velocity, we can write

$$V_{12,s_0} = \sqrt{x_0^2 + y_0^2 + (j_{21} \cos \Sigma_r)^2}. \tag{18}$$

It is evident from (18) that the sliding velocity vector \bar{V}_{12} value in an arbitrary point from the axis O_0z_0 has minimal value:

$$V_{12,\min} = V_{12,z_0} = p_{z_0} = j_{21} \cos \Sigma_r. \tag{19}$$

For this reason, the axis O_0z_0 is called a *minimal kinematic relative helix*.

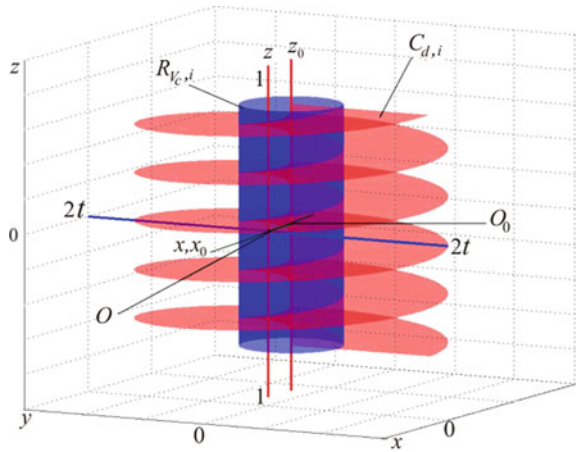
According to (17) and (19), if $\Sigma_r \in (-\pi/2, \pi/2)$ $p_{z_0} > 0$, therefore Eqs. (16) describe all the right-oriented kinematic relative helices, and when $\Sigma_r \in (\pi/2, 3\pi/2)$ $p_{z_0} < 0$, (16) and (17) define all the left-oriented kinematic relative helices. The kinematic surfaces of level and kinematic relative helical lines of the rack transmissions with concrete basic kinematic and geometric parameters are illustrated in Fig. 3.

The kinematic cylinder of level $R_{V_c,i}$ and kinematic conoid $C_{d,i}$, when $j_{21} = 42$ mm/rad and $V_c = 44$ mm/rad and $\Sigma_r = 60^\circ$ are shown in Fig. 3.

2.3 Normalized Kinematic Relative Helices

The value of the sliding velocity vector is a characteristic that takes part in the construction of important quality criteria, which is applied to mechanical transformers' synthesis by using high kinematic joints. This requires normalizing the module of the sliding velocity vector [1, 4, 6]. The study applies a method, which is based on the symbiosis between the vector and scalar fields of the function

Fig. 3 Kinematic scheme of the relative helix generation of the vector function $\bar{V}_{12} = \bar{V}_{12}(x, y, z)$



$\bar{V}_{12} = \bar{V}_{12}(x_0, y_0, z_0)$. It is realized when in (16) is substituted:

$$R_0 = \sqrt{V_c^2 - j_{21}^2 \cos^2 \Sigma_r} = \sqrt{V_c^2 - p_{z_0}^2}. \tag{20}$$

Then the normalized kinematic relative helices are described by the following sets of equations:

$$\begin{aligned} x_0^2 + y_0^2 &= (V_c^2 - p_{z_0}^2), & z_0 + p_{z_0} \cdot t_0 &= C_o, \\ p_{z_0} &= j_{21} \cos \Sigma_r, & t_0 &= \arcsin \frac{x_0}{R_0}. \end{aligned} \tag{21}$$

2.4 Synthesis of Kinematic Pitch Surfaces

Kinematic pitch surfaces, are surfaces that are treated as envelopes of the normalized relative helices of the vector function $\bar{V}_{12} = \bar{V}_{12}(x_0, y_0, z_0)$ by their relative motion toward the typical axes of the transformation of the type $(R \leftrightarrow T)$. But the sets of normalized relative helices are placed on concretely defined kinematic cylinders of level. In other words, the kinematic pitch surfaces should be treated as envelopes of the corresponding kinematic cylinders of level. These surfaces are firmly connected with the coordinate systems $S_i(O_i, x_i, y_i, z_i) (i = 1, 2)$.

Here we will present the set of Eqs. (10) in the form:

$$\begin{aligned} x_0 &= R_0 \sin t, & y_0 &= R_0 \cos t, & z_0 &= H, \\ H &\in (-\infty, +\infty), & t &= \arcsin \frac{x_0}{R_0}. \end{aligned} \tag{22}$$

Let us write the canonical form (22) of kinematical cylinders of level in the coordinate systems $S_i(O_i, x_i, y_i, z_i) (i = 1, 2)$ (see Fig. 3). For this purpose we use the following matrix equalities:

$$\|x_1 \ y_1 \ z_1 \ t_1\|^T = M_{S_1S_0} \|x_0 \ y_0 \ z_0 \ t_0\|^T, \tag{23}$$

where $M_{S_1S_0} = \begin{vmatrix} \cos \varphi_1 & \sin \varphi_1 & 0 & -j_{21} \sin \Sigma_r \cos \varphi_1 \\ -\sin \varphi_1 & \cos \varphi_1 & 0 & +j_{21} \sin \Sigma_r \sin \varphi_1 \\ 0 & 0 & 1 & 0 \\ 0 & 0 & 0 & 1 \end{vmatrix},$

and

$$\|x_2 \ y_2 \ z_2 \ t_2\|^T = M_{S_2S_0} \|x_0 \ y_0 \ z_0 \ t_0\|^T, \tag{24}$$

where $M_{S_2S_0} = \begin{vmatrix} 1 & 0 & 0 & -j_{21} \sin \Sigma_r \\ 0 & 1 & 0 & j_{21} \sin \Sigma_r \varphi_1 \\ 0 & 0 & 1 & j_{21} \cos \Sigma_r \varphi_1 \\ 0 & 0 & 0 & 1 \end{vmatrix}.$

By solving (23) and (24), we obtain respectively:

$$\begin{aligned} x_1 &= R_0 \sin(t + \varphi_1) - j_{21} \sin \Sigma_r \cos \varphi_1, \\ y_1 &= R_0 \cos(t + \varphi_1) + j_{21} \sin \Sigma_r \sin \varphi_1, \\ z_1 &= H, \quad H \in (-\infty, +\infty), \end{aligned} \tag{25}$$

and

$$\begin{aligned} x_2 &= R_0 \sin t - j_{21} \sin \Sigma_r, \\ y_2 &= R_0 \cos t + j_{21} \sin \Sigma_r \varphi_1, \\ z_2 &= H + j_{21} \cos \Sigma_r \varphi_1, \quad H \in (-\infty, +\infty). \end{aligned} \tag{26}$$

The sets of Eqs. (25) and (26) describe families of enveloped kinematic surfaces of level. Their envelopes are treated as a locus of the contact lines of enveloped and enveloping surfaces, which are written in the coordinate systems $S_i(O_i, x_i, y_i, z_i) (i = 1, 2)$. They are obtained when is added the following condition to (29) and (30):

$$\bar{e}_{0,S_i} \bar{V}_{i,S_i} = 0, \quad i = (1, 2), \tag{27}$$

where \bar{e}_0 is the unit vector to the arbitrary kinematic cylinder of level in its arbitrary point $P_0(x_0, y_0, z_0)$; \bar{V}_i —transference velocity vectors ($i = 1$ —rotational and $i = 2$ —translational) of an arbitrary point P_0 of an arbitrary kinematic cylinder of level; $S_i, i = (1, 2)$ —coordinate systems, connected with movable links $i = 1,$

realizing rotation with an angular velocity $\bar{\omega}_1$ and $i = 2$, realizing translation with velocity \bar{V}_2 .

For the cases $i = 1$ and $i = 2$ of the Eq. (27), the following equations of the relations between the parameters of the family of surfaces of level:

$$j_{21} \sin \Sigma_r \cos t = 0, \quad j_{21} \cos \Sigma_r \cos t = 0. \tag{28}$$

The solution of (28) is

$$t = \pi/2 + n\pi, \quad n = 0, 1, 2, 3, 4, \dots \tag{29}$$

Hence the kinematic pitch surfaces of rack mechanisms are two pairs of the rotational pitch cylinders (30) contacting with corresponding pitch plane (31):

$$\begin{aligned} x_1^2 + y_1^2 &= (R_0 - j_{21} \sin \Sigma_r)^2, \quad z_1 = H, \\ x_2 &= R_0 - j_{21} \sin \Sigma_r, \\ \cot \Sigma_r y_2 - z_2 + H &= 0, \quad H \in (-\infty, +\infty). \end{aligned} \tag{30}$$

$$\begin{aligned} x_1^2 + y_1^2 &= (R_0 + j_{21} \sin \Sigma_r)^2, \quad z_1 = H, \\ x_2 &= -(R_0 + j_{21} \sin \Sigma_r), \\ \cot \Sigma_r y_2 - z_2 + H &= 0, \quad H \in (-\infty, +\infty). \end{aligned} \tag{31}$$

It is evident from (30) and (31) that when $R_0 = 0$ the axoids of rack mechanisms are obtained. These axoids are a cylinder and a plane, which are tangential to the zero kinematic surface of level O_0z_0 .

The kinematic pitch cylinders are visualized, when the created computer program is used. They are defined for the concrete case of motion transformation by the first two equations from the system (30) (see Fig. 4) and (31) (see Fig. 5).

Fig. 4 Kinematic pitch cylinder I_1 with radius $|R_0 - j_{21} \sin \Sigma_r| : R_{V_{c,i}}$ —kinematic cylinder of level; $S_{c,i}$ —normalized relative helix

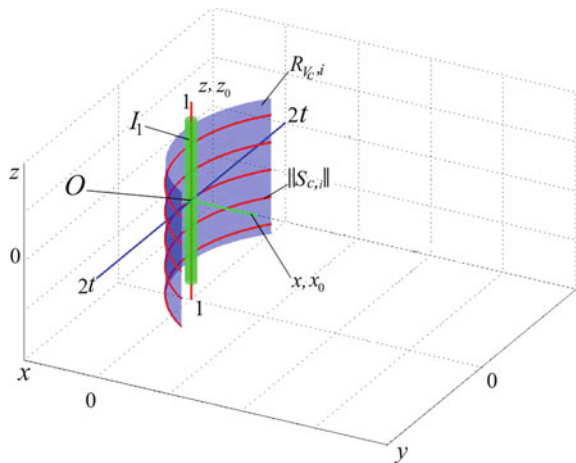
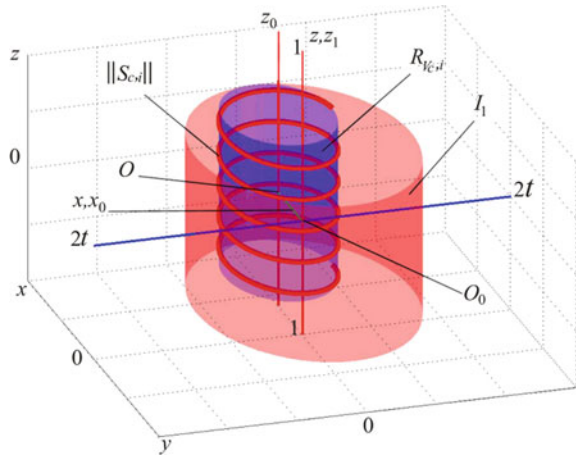


Fig. 5 Kinematic pitch cylinder I_1 with radius $|R_0 + j_{21} \sin \Sigma_r| : R_{V_{c,i}}$ —kinematic cylinder of level; $S_{c,i}$ —normalized relative helix



The shown in Figs. 4 and 5 are transformations of type $(R \leftrightarrow T)$, when $j_{21} = 42 \text{ mm/rad}$, $V_c = 44 \text{ mm/rad}$ and $\Sigma_r = 60^\circ$.

3 Mathematical Modelling of Spatial Rack Drives

3.1 Synthesis of Spatial Rack Drives, Which Rotating Link Has Conic Linear Helicoids

When synthesizing spatial rack mechanisms with a linear contact it is necessary to control their quality in the whole mesh region. Such approaches to synthesis' problems require an adequate mathematical model. The kinematic scheme of such mechanism is shown in Fig. 6. A mathematical model based on a mesh region is not universal one.

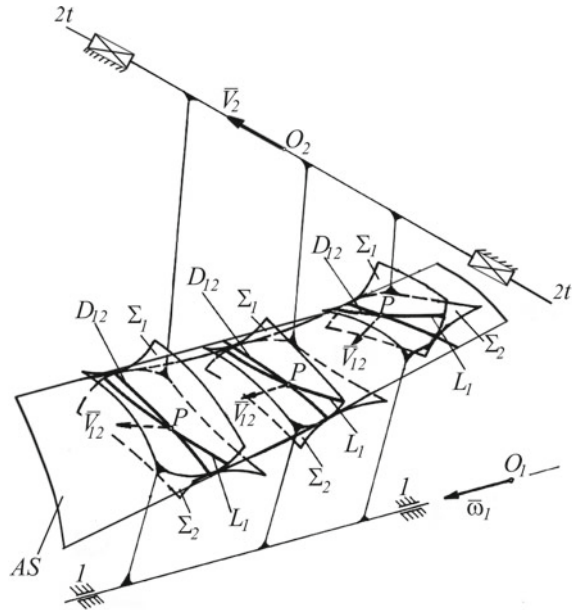
The reason is that the specific geometrical and kinematic characteristics of the mesh region depend on its position in space and the geometrical characteristics of the tool surface Σ_j generating the flanks $\Sigma_i (i = 1, 2)$.

This mathematical model is based on the second Olivier's principle and the link, performing rotation, and having surfaces Σ_1 , is chosen as a generating link. Generated surfaces Σ_2 belong to link 2, which realizes rectilinear translation.

The synthesis of spatial rack drives based on the second Olivier's principle, involves solving two main tasks:

- Synthesis of the tooth surfaces Σ_1 of the rotating movable link, which are identical to the instrumental surfaces Σ_j . Solving this mathematical problem provides the technology of manufacturing the rotating link of the rack drive.

Fig. 6 Kinematic scheme of spatial rack drive with linear contact between tooth surfaces Σ_1 and Σ_2 synthesized using a mesh region (MR): Σ_i —surface of the flank of links ($i = 1, 2$); $\bar{\omega}_1$ —rotation velocity of link $i = 1$; \bar{V}_2 —velocity of rectilinear translation of link $i = 2$; AS—action surface; D_{12} —contact line; L_1 —a longitudinal line of Σ_1



- Synthesis of the mesh region and definition of the dimensions and location of the mesh region on the surface of action. This task realizes the generation of active tooth surfaces Σ_2 of the movable link of rack mechanisms, which perform motion translation.

The synthesis of these types of mechanical transmissions, in accordance with the second Olivier’s principle, leads to solving two main tasks: synthesis of the active tooth surfaces of the base (instrumental) movable link—conic worm and synthesis of the surface of action/mesh region of the studied mechanism. The active tooth surfaces of the basic link are conic linear helicoids.

3.1.1 Synthesis of the Surface of Action/ Mesh Region of the Conic Rack Drives

The action surface, considered as a locus of the lines of the tooth contact in the fixed space, defines conjugate tooth surfaces of the second movable link—tooth rack. Based on the realized study and the developed algorithms for synthesis of three types of spatial rack drives—cylindrical with cylindrical linear rotating helicoids, face (with face linear rotating helicoids), and with conic (with conic linear rotating helicoids) are written three computer programs with analogical (typified) structure and organization of the calculated process. The developed programs illustrate the cases of the spatial conic, cylindrical, and face rack drives synthesis.

The offered here study is consistent with shown in Fig. 7 symbols.

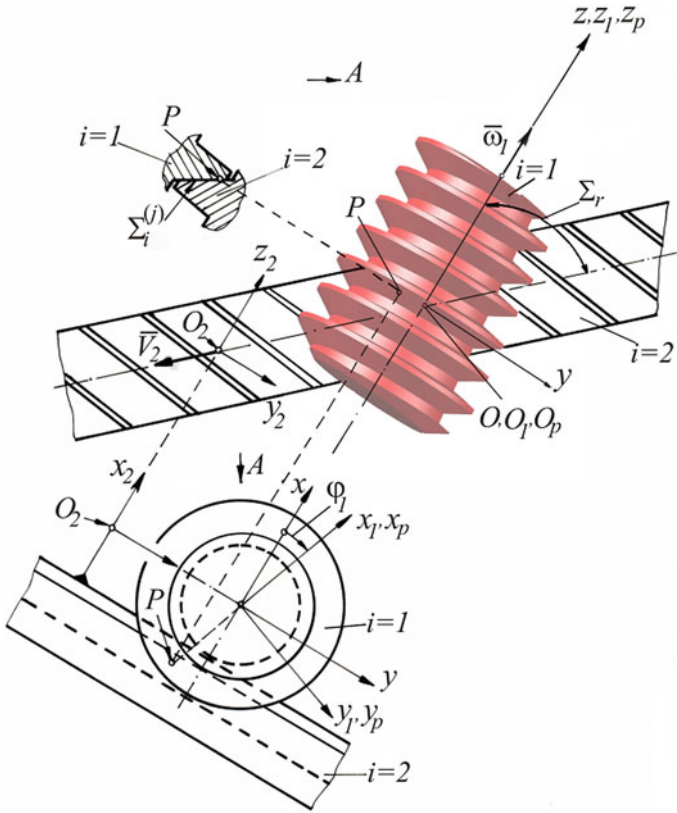


Fig. 7 Geometric-kinematic scheme of spatial rack drive having rotating linear conic helicoids

Conic convolute rack mechanism. The Eqs. (6) from the “Conic Linear Helicoids: Part 1. Synthesis and Analysis of the Basic Geometric Characteristics” (which is Part 1 of this study) of the linear helicoid $\Sigma_1^{(j)}$ are presented as:

$$\begin{aligned} x_p^{(j)} &= r_0^{(j)} \cos \vartheta^{(j)} \pm U^{(j)} \sin \vartheta^{(j)}, \\ y_p^{(j)} &= r_0^{(j)} \sin \vartheta^{(j)} \mp U^{(j)} \cos \vartheta^{(j)}, \\ z_p^{(j)} &= p^{(j)} \vartheta^{(j)} \pm U^{(j)} \cot \xi^{(j)}, \end{aligned} \tag{32}$$

where $U^{(j)} = R_0^{(j)} \sin \xi^{(j)} = u^{(j)} \sin \xi^{(j)} - p_i^{(j)} \vartheta^{(j)}$, $p^{(j)} = p_s^{(j)} \pm p_i^{(j)} \cot \xi^{(j)}$.

The set of Eqs. (32) describes the conic convolute helicoid as a cylindrical one with helical parameter $p^{(j)}$.

The normal vector in an arbitrary point of $\Sigma_1^{(j)}$ is described by equations system:

$$\begin{aligned}
 n_{1,x_p}^{(j)} &= \mp h^{(j)} \sin \xi^{(j)} \cos \vartheta^{(j)} - U^{(j)} \cos \xi^{(j)} \sin \vartheta^{(j)}, \\
 n_{1,y_p}^{(j)} &= \mp h^{(j)} \sin \xi^{(j)} \sin \vartheta^{(j)} + U^{(j)} \cos \xi^{(j)} \cos \vartheta^{(j)}, \\
 n_{1,z_p}^{(j)} &= U^{(j)} \sin \xi^{(j)}.
 \end{aligned}
 \tag{33}$$

It is known [5–7] that conic helicoids $\Sigma^{(j)}$ ($j = 1, 2$) are cylindrical helical surfaces with constant helical parameter $p^{(j)} = p_s^{(j)} \pm p_t^{(j)} \cot \xi^{(j)} = \text{constant}$.

Hence, for these surfaces is valid the equation of meshing [5, 7]:

$$\tan \Delta = \frac{n_{1,y}}{n_{1,z}} = \frac{p + j_{21} \cos \delta_r}{j_{21} \sin \delta_r} = \text{constant}.
 \tag{34}$$

Then the action surface of the conic convolute helicoid is described by using the Eqs. (32) and (33) (written in the fixed coordinate system $S(O, x, y, z)$) and the analytical type (34) of equation of meshing (see Fig. 8), i.e.

$$\begin{aligned}
 x^{(j)} &= r_0^{(j)} \cos \theta^{(j)} \pm U^{(j)} \sin \theta^{(j)}, \\
 y^{(j)} &= r_0^{(j)} \sin \theta^{(j)} \mp U^{(j)} \cos \theta^{(j)}, \\
 z^{(j)} &= p^{(j)} \vartheta^{(j)} \pm U^{(j)} \cot \xi^{(j)}, \\
 \frac{\mp h^{(j)} \sin \xi^{(j)} \sin \theta^{(j)} + U^{(j)} \cos \xi^{(j)} \cos \theta^{(j)}}{U^{(j)} \sin \xi^{(j)}} &= \frac{p^{(j)} - j_{21} \cos \Sigma_r}{j_{21} \sin \Sigma_r}.
 \end{aligned}
 \tag{35}$$

where $\theta^{(j)} = \vartheta^{(j)} + \varphi_1$, $U^{(j)} = u^{(j)} \sin \xi^{(j)} - p_t^{(j)} \vartheta^{(j)} \neq 0$, $p^{(j)} = p_s^{(j)} \pm p_t^{(j)} \cot \xi^{(j)}$, $h^{(j)} = p^{(j)} + r_0^{(j)} \cot \xi^{(j)}$.

The conjugated with $\Sigma_1^{(j)}$ ($j = 1, 2$) tooth surfaces $\Sigma_2^{(j)}$ ($j = 1, 2$) of the tooth rack $i = 2$ are obtained from the system (35), after writing it in the fixed coordinate system $S_2(O_2, x_2, y_2, z_2)$, firmly connected with link $i = 2$:

$$\begin{aligned}
 x_2^{(j)} &= r_0^{(j)} \cos \theta^{(j)} \pm U^{(j)} \sin \theta^{(j)}, \\
 y_2^{(j)} &= r_0^{(j)} \sin \theta^{(j)} \mp U^{(j)} \cos \theta^{(j)} + j_{21} \varphi_1 \sin \Sigma_r, \\
 z_2^{(j)} &= p^{(j)} \vartheta^{(j)} \pm U^{(j)} \cot \xi^{(j)} + j_{21} \varphi_1 \cos \Sigma_r, \\
 \frac{\mp h^{(j)} \sin \theta^{(j)} + U^{(j)} \cot \xi^{(j)} \cos \theta^{(j)}}{U^{(j)}} &= \frac{p^{(j)} - j_{21} \cos \Sigma_r}{j_{21} \sin \Sigma_r}.
 \end{aligned}
 \tag{36}$$

Conic Archimedean rack mechanism. The analytical representation of the action surface of the conic Archimedean rack drive (see Fig. 9) is obtained from the equation systems (35) after a substitution $r_0^{(j)} = 0$, whence $h^{(j)} = p^{(j)}$, i.e.

$$\begin{aligned}
 x^{(j)} &= \pm U^{(j)} \sin \theta^{(j)}, \\
 y^{(j)} &= \mp U^{(j)} \cos \theta^{(j)}, \\
 z^{(j)} &= p^{(j)} \vartheta^{(j)} \pm U^{(j)} \cot \xi^{(j)}, \\
 \frac{\pm p^{(j)} \sin \theta^{(j)} + U^{(j)} \cot \xi^{(j)} \cos \theta^{(j)}}{U^{(j)}} &= \frac{p^{(j)} - j_{21} \cos \Sigma_r}{j_{21} \sin \Sigma_r}.
 \end{aligned}
 \tag{37}$$

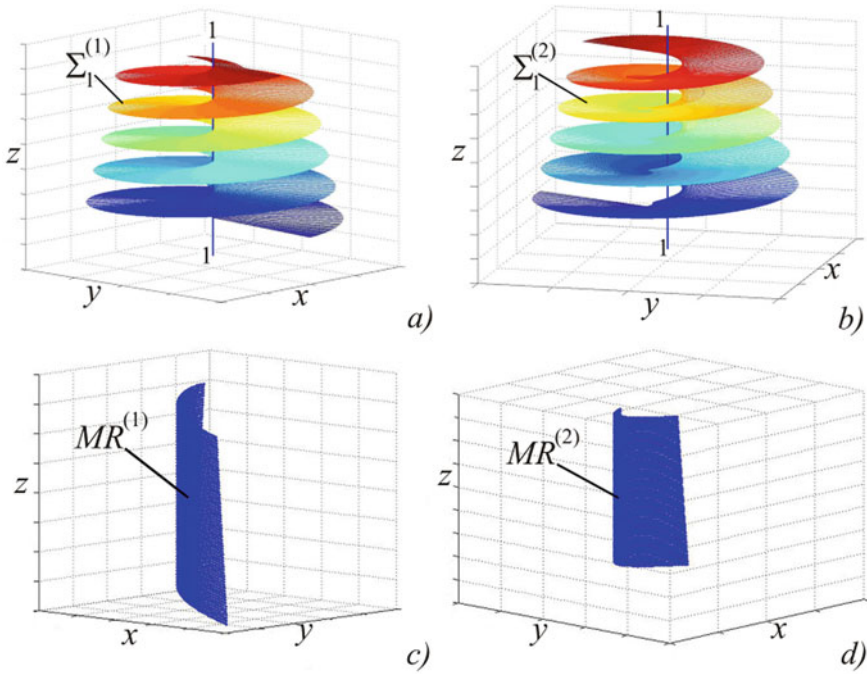


Fig. 8 Spatial conic convolute mechanism with velocity ratio $j_{21} = 2, 29$; number of the teeth $z_1 = 1$: **a** conic convolute worm $\Sigma_1^{(1)} \Rightarrow \xi^{(1)} = 98^\circ, r_0^{(1)} = 0.08 \text{ mm}; u^{(1)} \in [0, 10], \vartheta^{(1)} \in [0, 5\pi]$; **b** $\Sigma_1^{(2)} \Rightarrow \xi^{(2)} = 120^\circ, r_0^{(2)} = 0.94 \text{ mm}; u^{(2)} \in [0, 10], \vartheta^{(2)} \in [0, 5\pi]$; **c** region of mesh $MR^{(1)}$; **d** $MR^{(2)}$

Active tooth surfaces $\Sigma_2^{(j)}$ ($j = 1, 2$) of the tooth rack of the Archimedean rack mechanism are obtained from the system (37) with applying already mentioned substitutions:

$$\begin{aligned}
 x_2^{(j)} &= \pm U^{(j)} \sin \theta^{(j)}, \\
 y_2^{(j)} &= \mp U^{(j)} \cos \theta^{(j)} + j_{21} \varphi_1 \sin \Sigma_r, \\
 z_2^{(j)} &= p^{(j)} \vartheta^{(j)} \pm U^{(j)} \cot \xi^{(j)} + j_{21} \varphi_1 \cos \Sigma_r, \\
 \frac{\mp p^{(j)} \sin \theta^{(j)} + U^{(j)} \cot \xi^{(j)} \cos \theta^{(j)}}{U^{(j)}} &= \frac{p^{(j)} - j_{21} \cos \Sigma_r}{j_{21} \sin \Sigma_r}.
 \end{aligned}
 \tag{38}$$

Conic involute rack mechanism. From equations systems (35) after substituting $h^{(j)} = 0$, we obtain the analytical form of action surfaces (see Fig. 10) of the studied involute rack mechanism.

$$\begin{aligned}
 x^{(j)} &= r_0^{(j)} \cos \theta^{(j)} \pm U^{(j)} \sin \theta^{(j)}, \\
 y^{(j)} &= r_0^{(j)} \sin \theta^{(j)} \mp U^{(j)} \cos \theta^{(j)}, \\
 z^{(j)} &= p^{(j)} \vartheta^{(j)} \pm U^{(j)} \cot \xi^{(j)}, \\
 \cot \xi^{(j)} \cos \theta^{(j)} &= \frac{p^{(j)} - j_{21} \cos \Sigma_r}{j_{21} \sin \Sigma_r}.
 \end{aligned}
 \tag{39}$$

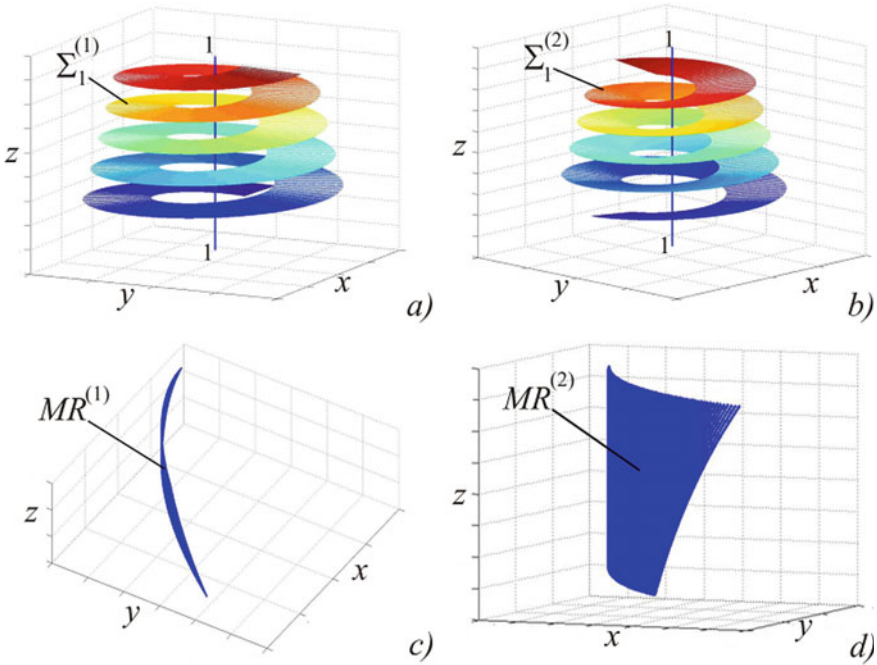


Fig. 9 Spatial conic Archimedean drive with velocity ratio $j_{21} = 2, 29$; number of the teeth $z_1 = 1$: **a** conic Archimedean right-handed worm $\Sigma_1^{(1)} \Rightarrow \xi^{(1)} = 98^\circ, u^{(1)} \in [5, 10], \vartheta^{(1)} \in [\pi/2, 10\pi]$; **b** conic Archimedean right-handed worm $\Sigma_1^{(2)} \Rightarrow \xi^{(2)} = 120^\circ, u^{(2)} \in [5, 10], \vartheta^{(2)} \in [\pi/2, 10\pi]$; **c** mesh region $MR^{(1)}$; **d** mesh region $MR^{(2)}$

Bellow (39) is written in the fixed coordinate system, connected with the link $i = 2$. Thus, the active tooth surfaces $\Sigma_2^{(j)}$ ($j = 1, 2$) of the spatial involute conic rack drive are obtained:

$$\begin{aligned}
 x_2^{(j)} &= r_0^{(j)} \cos \theta^{(j)} \pm U^{(j)} \sin \theta^{(j)}, \\
 y_2^{(j)} &= r_0^{(j)} \sin \theta^{(j)} \mp U^{(j)} \cos \theta^{(j)} + j_{21} \varphi_1 \sin \Sigma_r, \\
 z_2^{(j)} &= p^{(j)} \vartheta^{(j)} \pm U^{(j)} \cot \xi^{(j)} + j_{21} \varphi_1 \cos \Sigma_r \\
 \cot \xi^{(j)} \cos \theta^{(j)} &= \frac{p^{(j)} - j_{21} \cos \Sigma_r}{j_{21} \sin \Sigma_r}.
 \end{aligned}
 \tag{40}$$

3.1.2 Analysis of the Geometry of the Action Surfaces of the Conic Linear Rack Mechanisms

Here, the upper indexes “ j ” will be omitted when this analysis is performed. The analytical type of the action surfaces of the spatial conic convolute rack mechanism is described by the equation systems (35). Using the third equation of the same

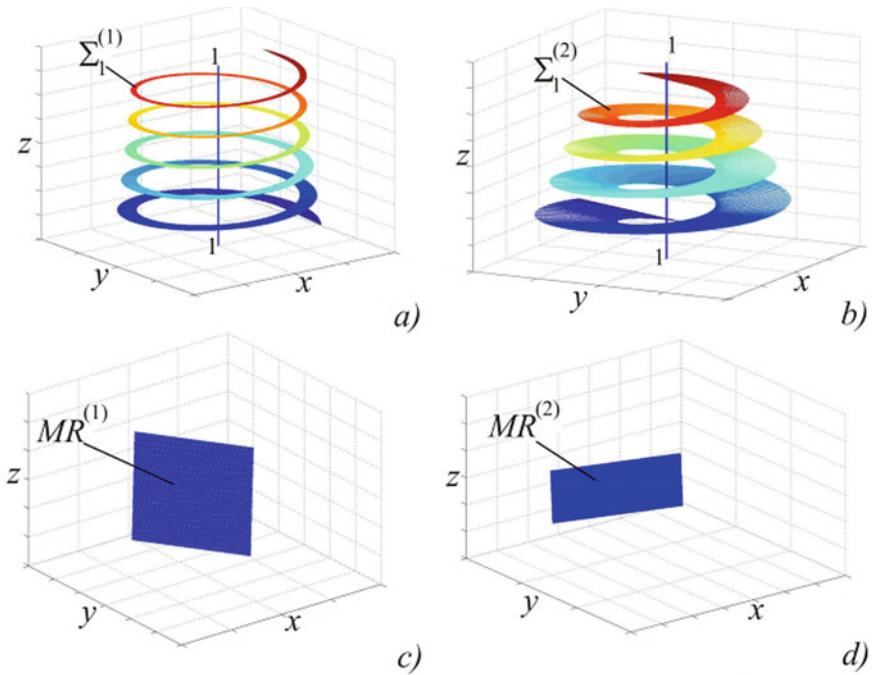


Fig. 10 Spatial conic involute mechanism with velocity ratio $j_{21} = 2, 29$; number of the teeth $z_1 = 1$: **a** conic involute right-handed worm $\Sigma_1^{(1)} \Rightarrow \xi^{(1)} = 98^\circ, r_0^{(1)} = 12, 93 \text{ mm}, u^{(1)} \in [0, 10], \vartheta^{(1)} \in [0, 10\pi]$; **b** conic involute right-handed worm $\Sigma_1^{(2)} \Rightarrow \xi^{(2)} = 120^\circ, r_0^{(2)} = 3, 44 \text{ mm}, u^{(2)} \in [0, 10], \vartheta^{(2)} \in [0, 10\pi]$; **c** mesh region $MR^{(1)}$; **d** mesh region $MR^{(2)}$

system, for the curvilinear coordinate ϑ of the conic convolute helicoid Σ_1 we can write:

$$\vartheta = \frac{z \mp u \cos \xi}{p \mp p_t \cot \xi} = f_1(z, u). \tag{41}$$

Here we will remind that in (35) are performed the substitutions $\theta = \vartheta + \varphi_1, U = u \sin \xi - p_t \vartheta \neq 0$. Let from the first equation of (35) we define:

$$U = \pm \frac{u - r_0 \cos \theta}{\sin \theta}, \tag{42}$$

and the obtained Eq. (42) substitutes in other two equations. Then:

$$y = r_0 \sin \theta - (x - r_0 \cos \theta) \cot \theta, \tag{43}$$

$$\frac{\mp h \sin^2 \theta \pm (x - r_0 \cos \theta) \cos \theta \cot \xi}{x - r_0 \cos \theta} = A,$$

where $A = \frac{p-j_{21} \cos \Sigma_r}{j_{21} \sin \Sigma_r} = \text{constant}$.

Let multiply both sides of the first equation of (43) with $\sin \theta$ and the obtained result is reduced to the quadratic equation regarding to $\cos \theta$, i.e.:

$$(x^2 + y^2) \cos^2 \theta - 2r_0x \cos \theta + r_0^2 - y^2 = 0. \tag{44}$$

The solution of (44) is of the type:

$$(\cos \theta)_{1,2} = \frac{r_0x \pm y\sqrt{x^2 + y^2 - r_0^2}}{x^2 + y^2}. \tag{45}$$

From (45) it follows:

$$\begin{aligned} (\cos \theta)_{1,2} &= f_2(x, y), \\ (\sin \theta)_{1,2} &= \sqrt{1 - [f_2(x, y)]^2} = f_3(x, y). \end{aligned} \tag{46}$$

Substituting (46) in the second equality of (43) we obtain the following equation:

$$F(x, y) = 0, \tag{47}$$

which is the analytical description of the action surface in the most common case of spatial conic linear rack mechanism—the convolute one. The equality (47) shows that the action surface of these type rack mechanisms is a cylindrical surface with generatrices, parallel to the z -coordinate axis Oz of the fixed coordinate system $S(O, x, y, z)$.

The conic Archimedean and involute rack drives are special cases of the conic convolute rack mechanism. Their action surfaces are described analytically by the system (35), after substituting $r_0 = 0$ (for the Archimedean rack drive) and $h = 0$ (for involute rack mechanism). Hence, in the most common case their action surfaces/mesh regions have characteristics, similar to those characteristics of the conic rack drive. In other words, the conic, Archimedean, and involute rack mechanisms have action surfaces that are related (from a geometric viewpoint) to the cylindrical (by form) action surfaces of the conic convolute rack drive.

For the case of rack mechanism, which rotating link has conic Archimedean helicoids, the equalities (45) and (46) are:

$$\begin{aligned} (\cos \theta)_{1,2} &= \pm \frac{y\sqrt{x^2+y^2}}{x^2+y^2} = f_2(x, y), \\ (\sin \theta)_{1,2} &= \sqrt{1 - [f_2(x, y)]^2} = f_3(x, y). \end{aligned} \tag{48}$$

Then the mesh region is:

$$F(x, y) \equiv \frac{pf_3(x, y) \pm xf_2(x, y) \cot \xi}{x} - A = 0. \tag{49}$$

The spatial conic rack drive has an action surface, for which the parameter of meshing is $h = 0$, when the rotating link of the conic rack mechanism is equipped with conic involute helicoids. For this case the action surface is described by the equation systems (39). There the equation of meshing is of the form:

$$\cos \theta_1 = \cos(\vartheta + \varphi_1) = \frac{p - j_{21} \cos \Sigma_r}{j_{21} \sin \Sigma_r} \tan \xi = A \tan \xi = \text{constant}. \quad (50)$$

From (50) follows that when the parameter of meshing $\varphi_1 = \text{constant}$ has a fixed value, the curvilinear coordinate ϑ keeps the constant value for all points from a single contact line, i.e. the contact line of this type conic linear rack mechanisms is a straight line. Thus, if the contact lines of the cylindrical action surface, representing its directrices, are transformed into a straight line, then the action surfaces from cylindrical ones are transformed into a plane.

3.2 Synthesis of Rack Mechanisms with a Rotating Link Having Cylindrical Linear Helicoids

The synthesis of spatial rack drives having cylindrical linear helicoids is analogous to the synthesis of the conic rack mechanisms. Therefore, all obtained equations and analytical relations, that treat rack mechanisms with conic linear helicoids, are transformed into those relating to the rack transmissions equipped with cylindrical helical surfaces, if $p_r^{(j)} = 0$ ($p_s^{(j)} \neq 0$) is substituted there. Their synthesis is illustrated graphically (Figs. 11, 12 and 13) using the above mentioned typified computer program.

4 Computer Programs for Visualization of Spatial Rack Mechanisms' Synthesis

4.1 Aspects of the Computer Programming of Gear Sets

The wide variety of gear transmissions, applied as transformers in quantitative and qualitative aspects of motions for different branches of technology, and the permanent tendency of researchers to create new and improved gearings and also the different and changing approaches to their mathematical modeling determine the difficulties in designing universal CAD systems with such a purpose. Because of that, the extremely dynamic development of modern technical computing devices and software applications should be noted. For realizing the scientific research in the field of

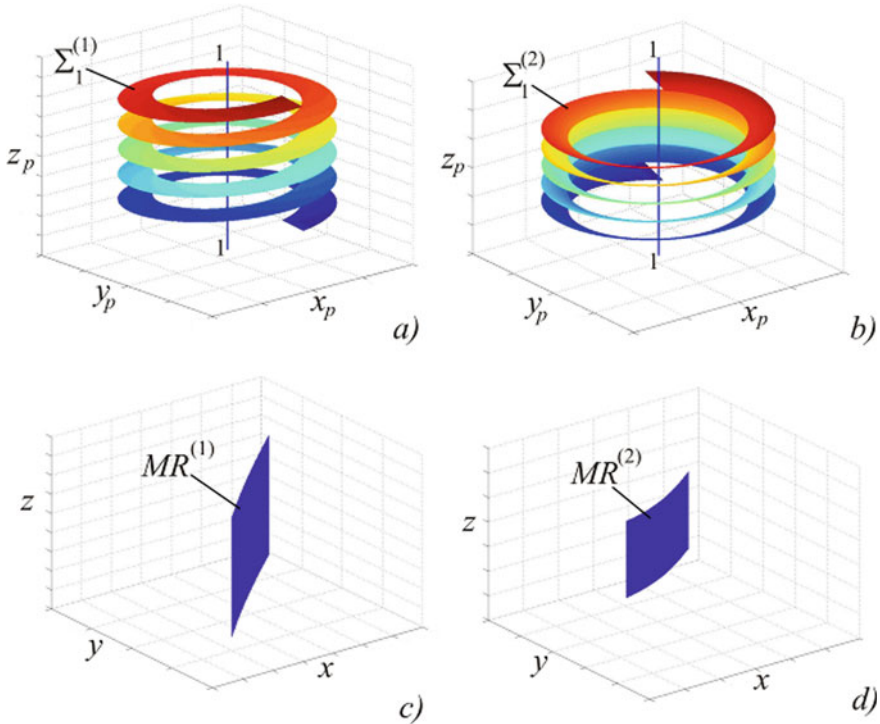


Fig. 11 Spatial cylindrical convolute rack mechanisms with velocity ratio $j_{21} = 2,29$; number of teeth ($z_1 = 1$): **a** cylindrical convolute right-handed helicoid $\Sigma_1^{(1)} \Rightarrow \xi^{(1)} = 98^\circ, r_0^{(1)} = 4, 15$ mm; $u^{(1)} \in [24, 03 - 35, 34], \vartheta^{(1)} \in [0 - 10\pi]$; **b** cylindrical convolute right-handed helicoid $\Sigma_1^{(2)} \Rightarrow \xi^{(2)} = 120^\circ, r_0^{(2)} = 17, 68$ mm; $u^{(2)} \in [24, 03 - 35, 34], \vartheta^{(2)} \in [0 - 10\pi]$; **c** region of mesh $MR^{(1)}$; **d** $MR^{(2)}$

gearing theory and also to ensure adequate scientific service for this type of mechanical transmissions, the computer synthesis has been developed, forming three types of software applications [1]:

First type. The programs of this type help to study the influence of various kinematical, dynamical, strength, design, technological, operational, and other parameters on various quality characteristics of the studied gear mechanisms. Essentially this type of software is not subjected to a specific strategy, related to CAD system construction. The developed mathematical models, algorithms, and computer programs are designed to establish the influence of actually existing parameters on the quality characteristics of specific gearings. Programs, created for these purposes can be used as modules, representing elements of criteria systems for determining the quality of gear mechanisms.

The above mentioned program is applied to study the vector field of sliding velocity in contact points of mesh region of spatial rack mechanisms and to define their kinematic pitch configurations belong to this type software.

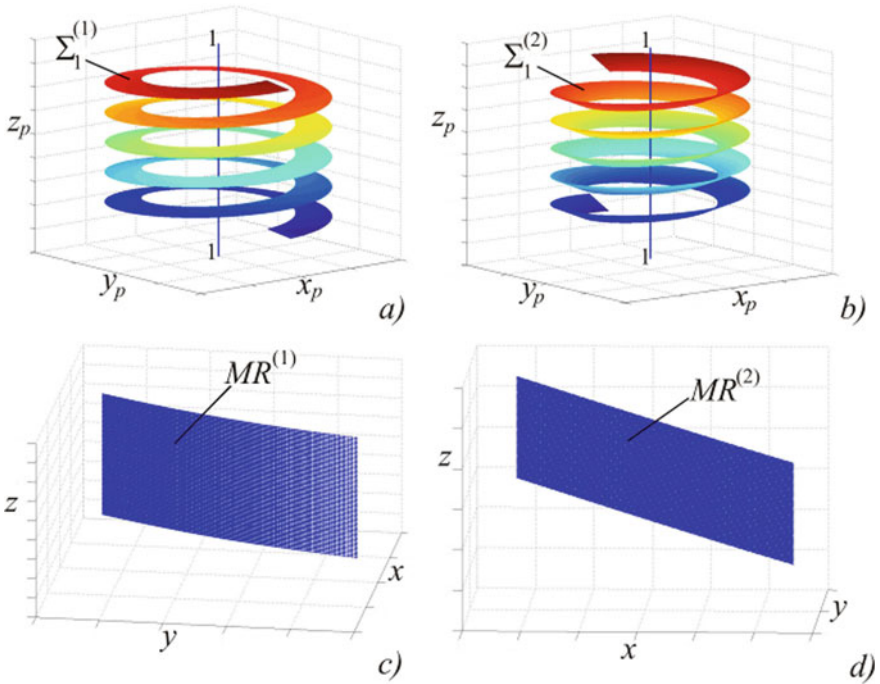


Fig. 12 Spatial cylindrical Archimedean drive with velocity ratio $j_{21} = 2,29$; number of the teeth $z_1 = 1$: **a** cylindrical Archimedean right-handed helicoid $\Sigma_1^{(1)} \Rightarrow \xi^{(1)} = 98^\circ, u^{(1)} \in [24, 03 - 35, 34], \vartheta^{(1)} \in [0, 10\pi]$; **b** cylindrical Archimedean right-handed helicoid $\Sigma_1^{(2)} \Rightarrow \xi^{(2)} = 120^\circ, u^{(2)} \in [24, 03 - 35, 34], \vartheta^{(2)} \in [0, 10\pi]$; **c** mesh region $MR^{(1)}$; **d** mesh region $MR^{(2)}$

Second type. This group includes computer programs organized on the basis of algorithms, contained in specialized standardization documents, company methods (standards and manuals) [8, 9, etc.]. The programs belonging here are designed on algorithms for geometric and strength calculation of the traditional types of gear mechanisms, conic and hypoid gears, plane rack mechanisms, etc. Algorithms, used in these cases usually do not optimize design but ensure the technological and instrumental requirements for gear pairs manufacturing, and also perform strength control of the geometrical and technologically synthesized gears.

Third type. Programs that belong to this category are those based on mathematical models developed on specific scientific researches. Modern gear mechanisms, including even classical gear drives that are treated from the point of view of current scientific (engineering) research, require the design of new mathematical approaches to their geometrical, technological, and strength synthesis. In this case, the optimization process can be realized by applying the “method of directed search” [1]. This way, the number of calculated variants of the synthesized gear mechanism is reduced. The essence of this method is:

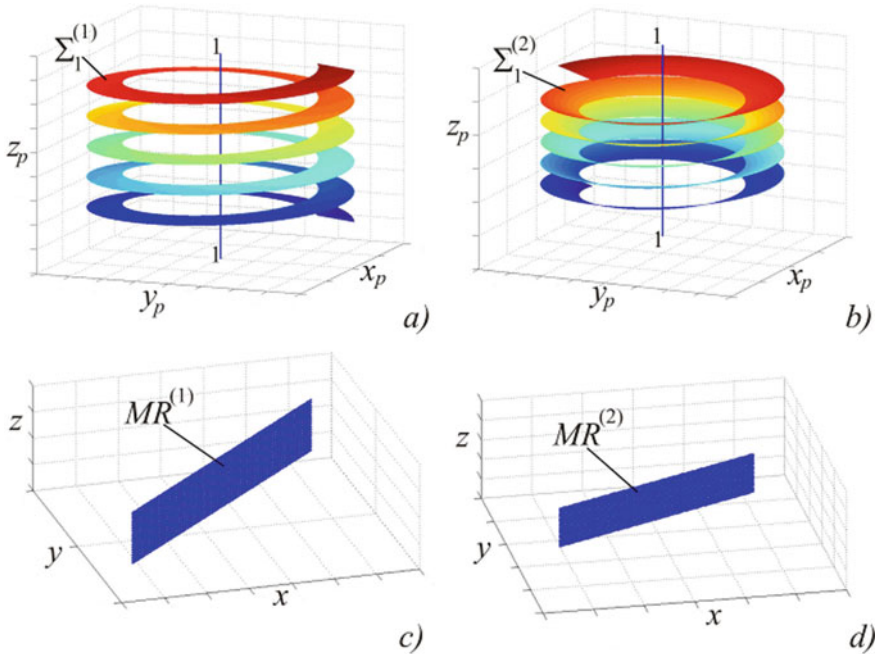


Fig.13 Spatial cylindrical involute drive with velocity ratio $j_{21} = 2,29$; number of the teeth $z_1 = 1$: **a** cylindrical involute right-handed helicoid $\Sigma_1^{(1)} \Rightarrow \xi^{(1)} = 98^\circ$, $r_0^{(1)} = 14,23$ mm; $u^{(1)} \in [24,03 - 35,34]$, $\vartheta^{(1)} \in [0, 10\pi]$; **b** cylindrical involute right-handed helicoid $\Sigma_1^{(2)} \Rightarrow \xi^{(2)} = 120^\circ$, $r_0^{(2)} = 3,46$ mm; $u^{(2)} \in [24,03 - 35,34]$, $\vartheta^{(2)} \in [0, 10\pi]$; **c** mesh region $MR^{(1)}$; **d** mesh region $MR^{(2)}$

- The input parameters, including those, that are unchangeable during the optimization process, are defined.
- The type of the variable parameters and the way of their variation is determined.
- The process of variation of the defined input variables is performed until the input optimization criteria are satisfied.
- The optimal variant of the synthesized gear set is chosen, for which there is an optimal satisfaction of the additional conditions, input to the mathematical model.

Hence, the process of optimization synthesis in the third type of software is based on adequate procedures, by which the needed solution is obtained through changing some parameters.

4.2 Computer Programs for Visualization of the Synthesis of Spatial Rack Drives

On the basis of this study and the defined algorithms for synthesis of three types of spatial rack mechanisms—cylindrical (with cylindrical linear and curvilinear rotating helicoids), face (with linear rotating helicoids), and conic ones (with conic linear rotating helicoids) three computer programs with similar (typified) structure and organization of their calculation process are written. We briefly present this product here.

The program described below should be considered as a symbiosis between the first and third types of software. It has the characteristics of the “directed search” method for synthesis but also this program realizes the visual study of the character of the geometry of active geometric elements $\Sigma_i^{(j)}$ ($i = 1, 2$), ($j = 1, 2$) of the kinematic joints $\Sigma_1^{(j)} : \Sigma_2^{(j)}$, by which the defined law for the transformation of type ($R \leftrightarrow T$) is realized. The program is written in MATLAB. It contains a description and declaration of input parameters and equation systems. From solving these systems, the basic characteristics of the spatial rack mechanisms are obtained. The content of the programs is illustrated in Figs. 14, 15, and 16.

The input parameters of the programs are:

- **Geometric parameters**
 - shaft angle Σ_r [grad] (for face rack mechanisms $\Sigma_r = 90^\circ$);

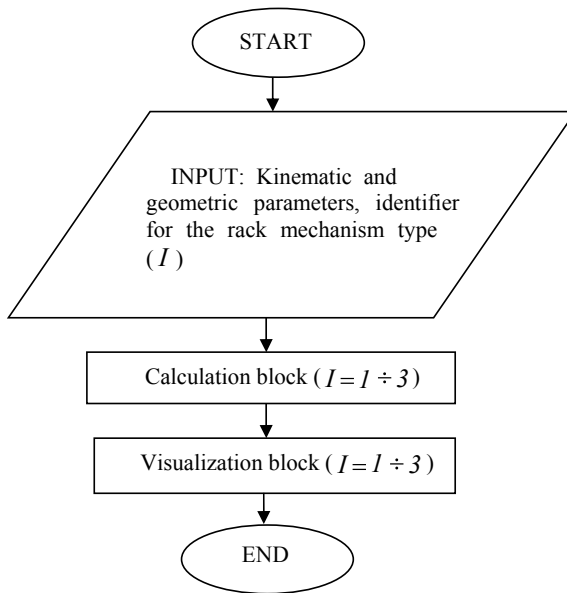


Fig. 14 Common block-scheme

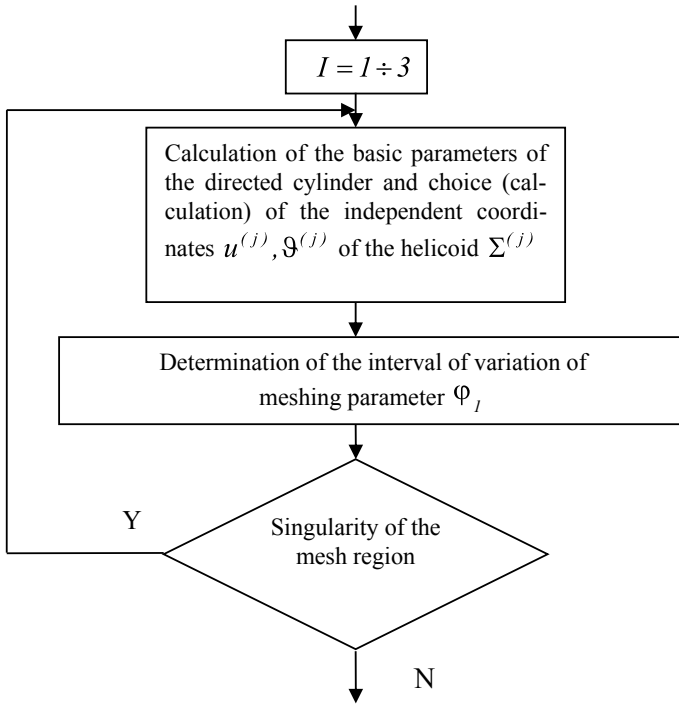


Fig. 15 Calculation block: $u^{(j)}, v^{(j)}$ —independent coordinates of the linear $\Sigma^{(j)}$ ($j = 1$ for the low-side helicoids, $j = 2$ for the high-side helicoids)

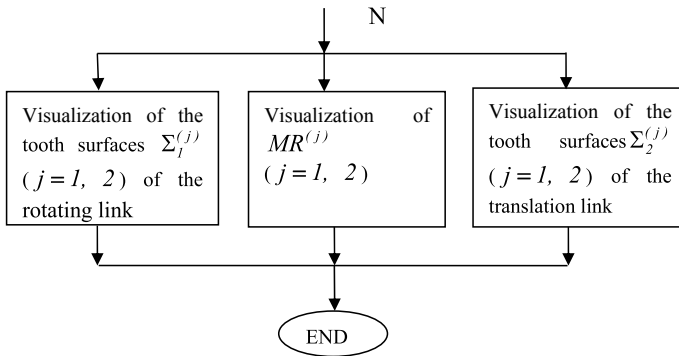


Fig. 16 Visualization block: $MR^{(j)}$ ($j = 1, 2$)—mesh regions of the synthesized rack mechanism

- crossed angle δ_r [grad];
- radius of the pitch circle of the rotating link— r_1 [mm];
- an obtuse angle between linear generatrix of the helicoid and axis of the rotating link $\xi^{(j)}$ [deg];

- tooth module m [mm];
- axial helical parameter p_s [mm/rad] (for cylindrical rack drive);
- crossed tangential parameter p_t [mm/rad] (for face rack drive);
- number of helicoids $\Sigma_1^{(j)}$ of the rotating link $i = 1$;
- Kinematic parameters
 - velocity ratio j_{12}/j_{21} [mm/rad]/ [mm/rad];
 - parameter of meshing φ_1 [deg];
- Identifier
 - for the convolute rack mechanism (cylindrical, face, conic)— $I = 1$;
 - for Archimedean rack mechanism (cylindrical, face, conic)— $I = 2$;
 - for involute rack mechanism (cylindrical, face, conic)— $I = 3$;

Diagrammatically, the calculation block of the program is organized in accordance with Fig. 15, and the visualization block is shown in Fig. 16.

The studied rack drives can be synthesized and visualized by using the described computer programs and AutoCAD [10]. Three specific representatives of the studied mechanical motion transformers are illustrated in Figs. 17, 18, 19.

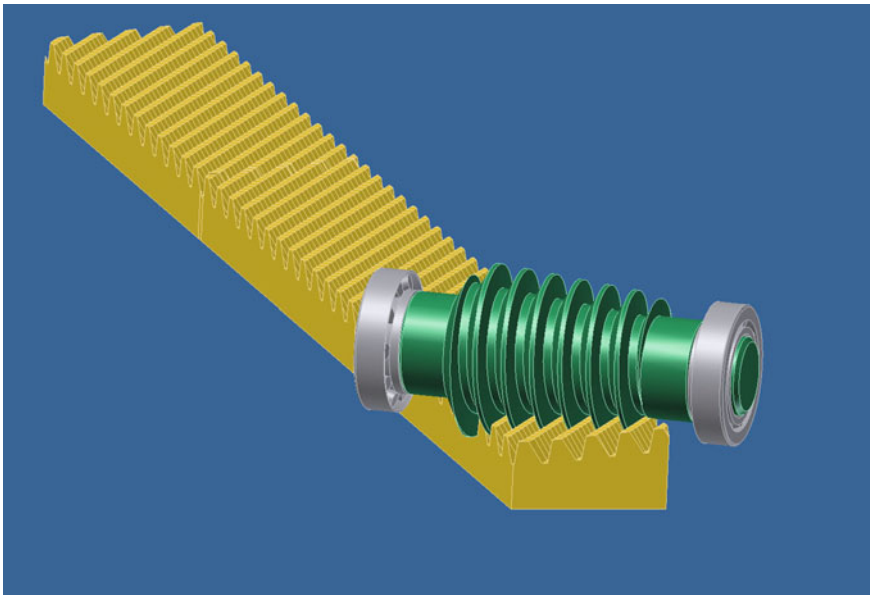


Fig. 17 Archimedean conic rack mechanism

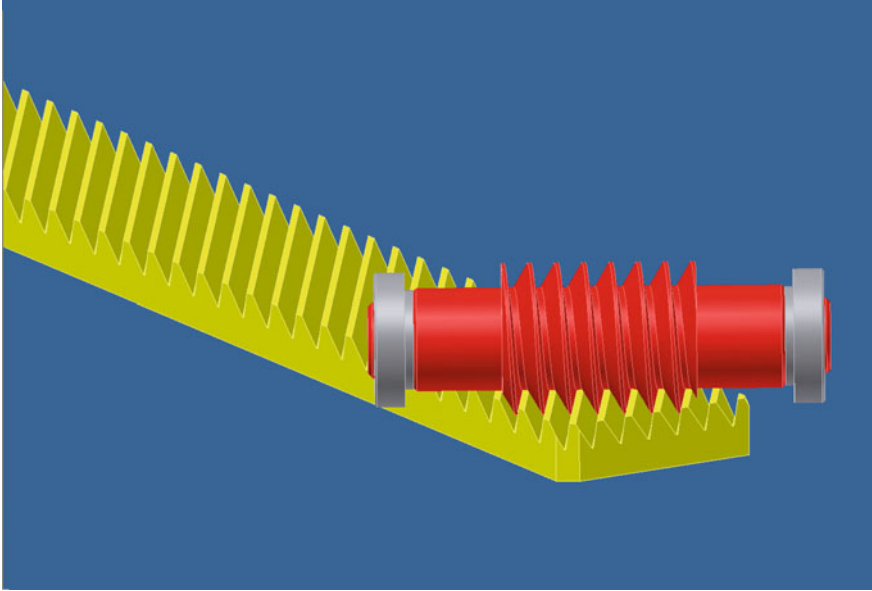


Fig. 18 Archimedean cylindrical rack mechanism

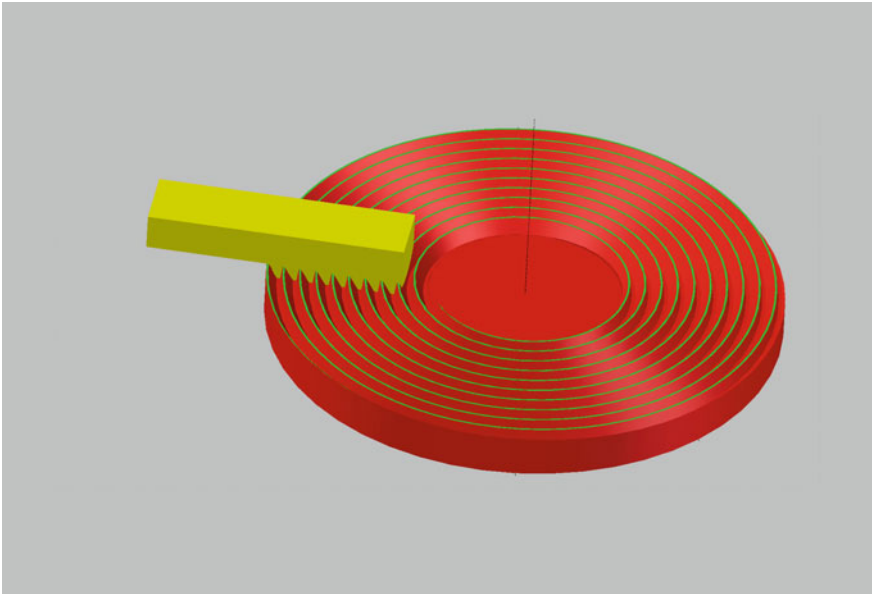


Fig. 19 Archimedean face rack mechanism

5 Conclusion

This article contains the basis of the kinematic theory of rack mechanisms. The kinematic-geometric essence of the basic constructive elements of the mathematical models for the synthesis of these gear mechanisms is defined in this context. In this study, they are called kinematic pitch surfaces and they are treated as essence and terminology of a special direction of the spatial meshing theory. All the mentioned pitch configurations are of great significance for defining those basic characteristics such as structure and geometry of gear set, longitudinal, and cross-orientation of the active tooth surfaces, module values of the teeth, coefficient of efficiency, a loading capacity of the gear mechanism, etc.

The current work is dedicated to the synthesis of spatial rack mechanisms having rotating linear helicoids—conic and cylindrical ones.

Typical for the studied type transmissions is the non-orthogonal crossed placement of the rotation axis of one of the movable link to the directrix of the velocity of the rectilinear translation of the second movable link. This is a premise for the presence of more free parameters. When we search adequate combination among them, it allows us to control the exploitation characteristics of the rack drives in their synthesis. On the base of the elaborated models and algorithms, a typified computer program for analysis, synthesis, and visualization of the basic geometric elements of the spatial rack drives is developed. It visualizes the basic elements of spatial rack drives when the rotating link has conic and cylindrical helicoids of the type: convolute Archimedean and involute.

Reference

1. Abadjiev, V.: Gearing Theory and Technical Applications of Hyperboloid Mechanisms. D.Sc. Thesis, Bulgarian Academy of Sciences, Institute of Mechanics (2007)
2. Saari, O.: The Mathematical Background of Spiroid Gears, Industrial Mathematical Series, No 7, 131–144, Detroit (1956)
3. Rashevsky, P.: Course of Differential Geometry. Ed. State Publishing House of Technical and Theoretical Literature, Moscow (1956)
4. Abadjiev, V., Abadjieva, E.: Sliding velocity vectors field in a case of spatial rack Mechanisms. J Theoret Appl Mech Sofia 30(1), 22–28 (2000)
5. Abadjieva, E.: Mathematical Models of the Kinematic Processes in Spatial Rack Mechanisms and their Application, Ph.D. Thesis, Institute of Mechanics (2010)
6. Abadjieva, E.: Spatial Rack Drives. Mathematical Modelling for Synthesis. VDM Verlag Dr. Müller e.K., (2011)
7. Kovatchev, G., Abadjiev, V.: On the synthesis of spatial rack mechanisms. In: Proceedings 6-th National Congress of Theory and Application Mechanica, Varna, 1, pp. 35–38, (1990)
8. Dudley, D.: Gear Handbook. Manufacture and Application of Gears. Mc Craw-Hill Book Company, New York, The Design (1962)
9. Dudley, D., J. Sprengrers, D. Schroder, H. Yamashina. Gear Motor Handbook, Spriger, Berlin Heidelberg (1995)
10. AutoCAD Inventor Professional Suite (2010)

Automation of Engineering Design and Configuration of Medium Complexity Products by Example of Spiroid Gearboxes



Olga V. Malina

Abstract The paper presents theoretical foundations of formalization and optimization of two basic traditional approaches to designing low-formalized objects of medium and high complexity: “bottom-up” when there is only technical specification as input data and “top-down”, when the process of structural synthesis is reduced to modification of existing layout designs. Unlike traditional approaches to the design with their logic based on subject algorithms, it is proposed to use enumeration algorithms as a synthesis apparatus. It allows to create a program system of structural synthesis invariant to the design object due to the fact that formalized knowledge of the subject domain is transformed from the process-forming one into data used by the system to check the correctness of the obtained results. The main information units of the proposed approach of structural synthesis implementation are the data of the domain classifier that unites sets of classification features of the design and their possible values, and also a set of restrictions stated as forbidden figures. The concept of configuration as the process of changing the prototype in order to obtain a new quality is introduced. It is shown that the task of configuration can arise in different statements both at the stage of development (when designing a new gearbox) and at the stage of operation (in the process of repair). The key issue of the configuration problem is outlined and an approach to the solution of this problem, which is also based on enumeration algorithms, is proposed.

Keywords Automation of design engineering · Structural synthesis · Classifier · Engineering design and configuration · Empirical and functional forbidden figures

1 Introduction

Designing mechanical engineering objects of medium or high complexity is a creative process due to the lack of knowledge about the unambiguous sequence of operations leading to finding the desired structure of the future product. Technical creativity

O. V. Malina (✉)

Kalashnikov Izhevsk State Technical University, Izhevsk, Russia

e-mail: malina_0705@mail.ru

in this interpretation is the process of finding a new technical solution that meets the requirements of the technical assignment based on knowledge, experience and intuition in the absence of direct end-to-end algorithms of the layout design synthesis.

Analysis of the design process of spiroid gearboxes [1–8] and already existing layout designs allows us to make the following observations which will have a significant impact on the development of the model of the automated structural synthesis process.

1. The design process begins with the problem statement, which stipulates critical values of consumer characteristics of the future gearbox. Such characteristics may be, for example, load capacity, dimensions and layout, operating conditions, operating mode, price, etc.
2. Specifications of the set of parameters specified by the customer may differ significantly from each other.
3. One and the same gearbox can be structurally suitable for different applications.
4. Implementation of a single problem statement can be a multitude of layout solutions.
5. There is no end-to-end algorithm that unambiguously describes the process of structural synthesis of a future layout design that meets the technical specification requirements.
6. The time of the gearbox layout development and its design quality largely depends on the experience and qualifications of the designing engineer.

Obviously, the design problem is a multi-criteria problem, in the absence of end-to-end solution algorithms and the presence of fuzzy restrictions.

It is also obvious that the designer's knowledge, experience, and intuition play a significant role in the design process implementation. Although today the scope of the design knowledge which is present in drawing albums, reference books, software products implementing the formalized engineering calculations, three-dimensional modeling, documenting and solving other engineering problems is quite large. Nevertheless, the design remains a process in which the subjective influence of a particular developer remains significant and sometimes even determinative.

2 Basic Concepts of the Task of Structural Synthesis Automation

Automation of the design process in terms of structural synthesis is primarily an attempt to provide a specific developer with the accumulated and formalized experience in the design of mechanical engineering products, in particular, spiroid gearboxes.

The solution of the automation problem forced researchers to look at the design process, data and knowledge involved in this process in a completely different way.

Traditional criteria and parameters were combined into a set of attributes describing the class of objects to be designed [9]; impossible combinations of values

of these attributes were formalized as forbidden figures [10–23]. The design process began to be considered as determination of values of all attributes describing the class of objects for a given instance, and development of a design corresponding to a specific technical specification—the additional definition of those attributes whose values are not defined by a technical specification [24]. The basic algorithm of the synthesis process was not the algorithms of the subject domain, but the enumeration algorithms for the set of features, while the subject algorithms perform the role of restrictions—forbidden figures—to be added in the synthesis process. And the main tasks demanding research and solution were, firstly, the generation of the qualitative set of features describing the class of designed objects, secondly, the synthesis of the set of forbidden figures, and, thirdly, the development of optimization methods which allow to realize the enumeration process for the sets described above.

The set of features of the subject domain is arranged in the form of a classifier [25–34].

The classifier has a faceted-hierarchical structure. The hierarchical method divides an object into functional elements, the facet method describes each functional element. Methods for creating such a classifier are described in detail in [35, 36]. A fragment of the classifier for a spiroid gearbox is shown in Table 1.

On the one hand, a classifier is such a set of features and their values, which allows to uniquely identify any layout version by a finite set of characteristics (linguistically, a characteristic is a feature plus value) defined for a given class of objects. On the other hand, it is the formalized knowledge about the class of objects - data for enumeration in the synthesis process.

Forbidden figures are the formalized restrictions of the subject domain imposed on the enumeration process. Structurally they can be either empirical or functional. An empirical forbidden figure is an impossible feature value or an impossible combination of feature values of the classifier. A functional forbidden figure is a certain formalized mathematical relation of the subject domain, cutting off impossible combinations of feature values. For example, the mathematical expression $Z = X + Y$ can be considered a forbidden figure because for the set of features $X = \{1, 2, 3\}$ $Y = \{5, 6\}$ and $Z = \{6, 7, 8, 9\}$ the sets $\{(1, 5, 7), (1, 5, 8), (1, 5, 9), (2, 5, 6), (2, 5, 8), (2, 5, 9), (3, 5, 6), (3, 5, 7), (3, 5, 9)\}, (1, 6, 6), (1, 6, 8), (1, 6, 9), (2, 6, 6), (2, 6, 7), (2, 6, 9)\}, (3, 6, 6), (3, 6, 7), (3, 6, 8)\}$ are forbidden.

Besides, empirical forbidden figures can be atomic and composite.

Atomic forbidden figures appear when imposing the technical requirements results in specification of the value of some attribute, making the other values of this attribute impossible—that is, forbidden ones.

Classification of forbidden figures is a tool of the structural synthesis process optimization.

In spite of the fundamentally different apparatus of implementing the automated process of structural synthesis, the proposed approach allows to fulfill both design ideologies familiar to the designing engineer:

- “bottom-up”—without a prototype;
- “top-down”—by changing the prototype.

Table 1 Fragment of the classifier for spiroid gearboxes

Functional apex	Feature		Value	
Gearbox	Gear ratio	p1	60	a11
			40	a12
			65	a13
			Other	...
	Overall dimension	p2	100	a21
			150	a22
Other			...	
Bearing support 1	Number of bearings	p3	2	a31
			Other	...
Bearing 1	Type of bearing	p4	N	a41
			B	a42
			Other	...
Bearing 2	Type of bearing	p5	M	a51
			C	a52
			Other	...
Bearing support 2	Number of bearings	p6	1	a61
			Other	...
Gearwheel unit	Presence of the 3rd bearing support	p7	Yes	a71
			No	a72
Bearing support 3	Number of bearings	p8	1	a81
			Other	...
			NILL	a82
	Presence of the bearing support	p16	Yes	a161
			No	a162
Shaft and gearwheel assembly	Method of gearwheel and shaft coupling	p9	Press fit	a91
			By the key	a92
			Other	...
	Presence of the key	p10	Yes	a101
			No	a102
Shaft of the gearwheel unit	Length	p11	L	a111
			Other	a112
Gearwheel	Gearwheel type	p12	Solid	a121
			Assembled	a122
Gearwheel hub	Diameter	p13	D1	a131
			D2	a132
			NILL	a133

(continued)

Table 1 (continued)

Functional apex	Feature		Value	
			Other	...
Assembled gearwheel hub	Diameter	p14	D3	a141
			NILL	a142
			Other	...
Assembled gearwheel	Presence of screws	p15	Yes	a151
			No	a152

3 “Bottom-Up Design”: Basic Approach

Optimization of the “bottom-up” structural synthesis process was considered in detail in [37]. It was shown that optimization of a computational process that implements structural synthesis by enumeration for a set of features depends on a number of factors:

- how much one can minimize the number of intermediate variants after multiplication by the next feature in the synthesis process, in particular, due to the performed earlier analysis of intermediate variants by forbidden figures;
- how much it is possible to minimize the computational load at forbidden figures analysis, taking into account that the main resources are spent on exclusion of functional forbidden figures.

To achieve the feasibility of the “bottom-up” structural synthesis, it was proposed to:

- alternate the stages of synthesis (additional multiplication by some set of features) and analysis (elimination of intermediate structures containing forbidden figures already obtained at this step) [38];
- to order the features for multiplication at synthesis [39], which will allow to control the rate of increasing the number of intermediate variants;
- to classify functional forbidden figures and generating functional relations by the level of computational complexity and to obtain new relations with lower computational complexity, which contributes to minimizing the computational complexity in analyzing intermediate variants for forbidden figures.
- to prevent the possibility of generating forbidden variants instead of analyzing the set of variants for forbidden figures [40].

The “bottom-up” synthesis algorithm can be represented in this case as a sequence of steps:

1. For each computational relation $P_n = f_1(P_1, P_2, \dots, P_{n-1})$ participating in the synthesis process, it is necessary to generate a maximally complete family of $F = \{P_n = f_1(P_1, P_2, \dots, P_{n-1}), P_1 = f_2(P_2, \dots, P_n), P_2 = f_3(P_1, P_2, \dots, P_n), P_{n-1} = f_n(P_1, P_2, \dots, P_{n-2}, P_n)\}$

2. To select the functional relation for which the power of features with the assigned values is maximum, and the most effective function is selected from the family of functions. At first the features—arguments are multiplied, and then the calculation is carried out to obtain the value of the feature—the value of the function. In turn, the order of multiplication of features-arguments is determined by the set of forbidden figures with the participation of these features and is carried out in accordance with the following algorithm:
 - (a) to find the set of forbidden figures Z_{ij} for each pair of features (P_i, P_j) for which it is possible to perform analysis for the intermediate variants obtained by multiplication of these features.
 - (b) to choose the first pair of multiplied features (P_a, P_b) such that $|Z_{ab}| = \max(|Z_{ij}|)$.
 - (c) to find the set of forbidden figures Z_{abk} for each disordered feature P_k .
 - (d) to choose the next feature P_c for multiplication among the disordered features such that $|Z_{abc}| = \max(|Z_{abk}|)$.
 - (e) if all features are ordered, then the desired order of multiplication is found, otherwise repeat from the item c) by selecting the most efficient one from the family of considered functions.
3. To repeat steps 2–3 for all functional relation generating functionally forbidden figures within the class of synthesized objects, with the order of multiplication of families of functions depending both on the number of features of the new family of functions whose values are specified in the previous step and on the number of empirical component forbidden figures that include feature values belonging to different functional relations.
4. Next, the set of intermediate variants is multiplied by features that are not part of the functional forbidden figures, the order of multiplication of features being determined by the power of the set of empirical forbidden figures built on the set of sequentially multiplied features. Variants potentially containing these forbidden figures are not generated.
5. The resulting set of intermediate variants is multiplied by features whose values do not participate in forbidden figures.

It is obvious that at structural synthesis implementing the “bottom-up” ideology the set of features participating in the process is defined before the beginning of synthesis, even if we synthesize the structure of only some part of it with the help of the developed object model. For example, having a model of a class of spiroid gearboxes, we can design a worm unit by separating a subgraph with the root vertex “Worm unit” from the model, which will show us all the features describing this structural unit of the gearbox.

4 “Top-Down” Design: Configuration Tasks

In practice, the ideology of “top-down” design is implemented much more often. Moreover, the problem in this statement is solved not only at the design stage when creating products, but often at the stage of operation during repair or upgrade.

The task of modifying an existing design will hereinafter be referred to as the configuration task, and the process of evaluating a change in a prototype and obtaining an updated structure will be referred to as configuration.

In order to formulate possible statements of the configuration problem, let us recall once again that in the proposed ideology a particular design is a set of characteristics, the number of which is determined by the set of features of the classifier of a given class of objects, and each characteristic is a feature and its value.

Let us consider the possible statements of the configuration process problem.

1. The system answers the question whether the given layout design corresponds to the new requirements of the specification.
2. The system answers the question what should be changed to make the prototype conform to the new requirements of the specification.
3. The system answers the question if it is possible to replace some part and keep the whole layout design operable.
4. The system answers the question what else is to be changed to retain the design operable after replacing a certain part.

The solution of a problem in the first statement is in fact an examination of the existing structure for its conformity with the new specification requirements.

A change in the specification can be as follows:

- A. changing the value of some design parameter specified in the prototype specification;
- B. supplementing the prototype’s specification with the value of additional parameters or introducing new criteria.

In spite of the principally different changes of the specification, the solution of the configuration problem in this statement will be the same, because the prototype that we are modifying is a set of features. The replacement of some feature’s value by another one will require checking for forbidden figures, which include the value of the new characteristic feature.

Implementation of this check is as follows:

1. From the set of empirical forbidden figures a subset $Z_{a_i^j} = \{z_{a_i^j}\}$ is selected consisting of figures which include the new value a_i^j of the feature being changed $P_j = \{a_k^j\}$.
2. The set of characteristic values $A = \{a_k\}$, describing the modified layout design (i.e., $a_i^j \in A$) is intersected sequentially with each forbidden figure. If the design layout contains at least one forbidden figure ($\exists z_{a_i^j}$ for which $z_{a_i^j} \cap A = z_{a_i^j}$) then the modification is impossible.

3. An analysis is performed to find out if the feature P_j whose value has been changed as part of the modification of at least one functionally forbidden figure z_{P_j} .
4. If no, then the analysis process ends; if yes, then arguments are substituted into the functional relation and the function value is calculated, and then the resulting set (arguments + function value) is intersected with the set describing the layout design. If the obtained specified set is a subset of the set describing the layout design, then the analysis of the following functional relation is performed, otherwise the modification is considered impossible.

The second statement of the problem means that if the modification performed by the user is recognized as impossible, the system must propose further changes to the layout design to make modification implementable.

There are two fundamentally different approaches to solving the problem in this statement.

1. The system actually solves the “bottom-up” synthesis problem, obtains a set of layout design versions, and then calculates the degree of identity of each newly obtained version with respect to the originally modified layout design.
2. The system solves the problem in the first statement, determines which new forbidden figures have emerged as a result of the modification and tries to annul them.

The advantage of the first statement is the presence of the developed, tested and giving good results method of synthesis by optimized enumeration.

The disadvantage is the unreasonable use of the whole set of features in the framework of object modification.

When considering the “bottom-up” ideology of structural synthesis, the starting points of implementation of the enumerative synthesis algorithm were the features, the set of which was defined when creating the model, before the synthesis. Meanwhile, when solving the problem in the mentioned statement, the problem of defining the set of those features, which should participate in the analysis when modifying the object structure, comes first.

To determine the specified set of features, the methodological basis of the approach is that the set of features involved in the synthesis will be determined by the set of forbidden figures arising in the process of modification.

Let us consider the simplest version of the implementation of this approach.

So, we have a prototype $A_p = \{a_k\}$, which is mathematically described as a set of values of characteristics, and each characteristic contains the value of an individual characteristic related to the classifier of this object.

We are given the task to replace one characteristic of this object (initially $a_i^j \notin A_p$). Obviously, changing a characteristic is the inclusion of another value of the same characteristic in the description of the synthesis object (the field of which $a_i^j \in A_m$, where A_m is the description of the modified version).

Obviously, the performed manipulation can lead to forbidden figures.

To describe this approach, let us introduce several concepts that will allow us to simplify process understanding.

A modified characteristic is a new value a_i^j of some feature P_j that must be included in the description of the structure. The value of the modified characteristic is a fixed (by the user) value of some feature.

The set of features of future synthesis P^{fs} is the set of attributes from the object classifier, the values of which can undergo changes in the description of structure due to modification of a certain characteristic, i.e. with fixation of a new value of the feature by a user within the existing structure.

Thus, implementation of this approach will contain the following steps:

- I. The value of the modified characteristic gets the status of the active key ($sw = a_i^j$).
- II. A subset of forbidden figures is selected from the set of forbidden figures $Z_{sw} = \{z_{sw}\}$ that meet one of the following conditions:
 1. The forbidden figure contains the value of the active key ($\forall z_{sw}, z_{sw} \cap sw = sw$).
 2. All the features whose values are included in the forbidden figure are present either in the description of the modified structure as characteristics or in the set of features of the future synthesis ($z_{sw} \cap (A_m \cup P^{fs} - sw) = z_{sw}$).
- III. The modified variant is checked for the presence of each forbidden figure included in the selected subset. The check is performed as follows:
 1. If all the features whose values are included in the forbidden figure being checked are present in the structure description of the object as some of their values, and the intersection of the structure description and the forbidden figure does not equal the forbidden figure, then this forbidden figure is absent in the description ($z_{sw} \cap A_m \neq z_{sw} \wedge (z_{sw} \cap P^{fs} = \emptyset) = 1$).
 2. The remaining forbidden figures are checked again for the formation of the set of features of the future synthesis:
 If all features whose values are included in the forbidden figure being checked are present in the set of feature values obtained by combining the set of feature values describing the structure and the set of future synthesis features, then the features, whose set of values is obtained by crossing the description of the object and the forbidden figure, are added to the set of future synthesis features, and the feature values obtained from the last crossing are excluded from the structure description (1. $A_z = A_m \cap z_{sw}$; 2. $\forall a_k^n \in A_z$ such a value of P_n is found that $a_k^n \in P_n$; 3. $P^{fs} = P^{fs} \cup \{P_n\}$; 4. $A_m = A_m + \{P_n\}$).
 When this step is performed for the first time, the features with the original modified value are excluded from the set of future synthesis features.
 3. Forbidden figures, which have already participated in the analysis, are marked, which allows to avoid the repeated analysis of their presence in the description of the object.

- IV Further, the next value of the feature placed in the set of features of the future synthesis acts as an active key.
- V The process comes to an end in the case when there is no single feature value in the set of the future synthesis that would not serve as an active key.

As a result of the above iterative process, we get a set of features, the multiplication of which will allow us to look for the correct modification of the changeable structure.

Obviously, the synthesis process in this case can be implemented according to the “bottom-up” synthesis ideology, but on the truncated set of features, which significantly optimizes the process.

If the resulting set contains a sufficient number of versions, the designing engineer has the right to state the target function to find the “best version”. Thus, the following objectives can be set as the specified target function:

- a version that has undergone the minimum number of changes;
- a version in which a part of the structure (a given subset of characteristics) has remained unchanged;
- maximum or minimum of some critical parameters, etc.

The result of structural synthesis may also be an empty set. Such a situation occurs when the designing engineer has chosen impossible combinations of initial data at the design and all versions have been found to be forbidden as a result of the analysis.

The advantage of the proposed method of synthesis is that it, on the one hand, allows to avoid multiple traversals of dynamically changing tree models whose structure is modified with each modification of the synthesis object, on the other hand, using the best features of the “bottom-up” synthesis algorithm, limits the set of features involved in the enumeration.

The third formulation of the problem is the need to obtain an answer to the question of replacing one part (sub-unit, unit) by another. In fact, the solution of the configuration problem in this statement is reduced to the solution of the first problem with some additions and is presented in the following steps.

1. The subset consisting of figures with new values of all changeable features is selected from the set of empirical forbidden figures provided that the forbidden figure does not consist only of values of features which have been modified as a result of replacement of a part of structure (part, unit, sub-unit). The addition of the first step described above in comparison with the analogous step in the first statement of the problem is a consequence of the fact that the part to be replaced as the part to which the replacement is made is a correct, free of forbidden figure set of features. The exclusion of the above mentioned subset of forbidden figures from the analysis reduces the analysis time, and hence the configuration as a whole.
2. The set of characteristics describing the modified layout design intersects sequentially with every forbidden figure. If the layout design contains at least one forbidden figure the modification is impossible.

3. The analysis is performed to find out, whether a feature, the value of which has been changed within modification, is an element of at least one functionally forbidden figure, which contains other features besides the modified ones.
4. If no, then the analysis process is finished; if yes, then the arguments are substituted into the functional relation and the function value is calculated, and then the resulting set (arguments + function value) is intersected with the set describing the construction. If the obtained set is a subset of the set describing the layout design, then the analysis of the following functional relation is performed, otherwise the modification is impossible.

Actually the solution of the problem in the fourth statement is reduced to a more complicated version of the second problem solution.

5 Conclusion

Configuration as a methodological approach to creating new structures of complex objects by changing the prototype is the direction familiar to the real design and at the same time promising in terms of formalizing the development of automation systems of structural synthesis.

Automation of the problem of configuration by using enumerative algorithms as the apparatus of synthesis makes the system-configurator a software product that can configure the structures of the most diverse objects, if the classifier of knowledge as well as the set of functional and empirical prohibited shapes are correctly stated.

The considered algorithms to solve the problems of configuration can be optimized, but even in this version they already allow to speak about the first approximation to solving the problem of the configuration process automation.

References

1. Kuznetsov, A. S., Lukin, E. V., Sannikov, A. M., Savelyeva, T. V.: Problems and methods of designing spiroid gearboxes for pipeline valves. In: *Intelligent Systems in Manufacturing*, vol. 1, pp. 47–52. ISTU Publishing House, Izhevsk (2014)
2. Kuznetsov, A. S., Lukin, E. V.: To the question of optimizing design of spiroid gearboxes for pipeline valves. In: *Intelligent Systems in Manufacturing*, vol. 2, pp. 121–126. ISTU Publishing House, Izhevsk (2011)
3. Goldfarb, V.I., Glavatskikh, D.V., Trubachev, E.S., Kuznetsov, A.S., Lukin, E.V., Ivanov, D.E., Puzanov, V.Yu.: *Spiroid Gears for Pipeline Valves*. Veche, Moscow (2011)
4. Goldfarb, V.I., Anferov, V.N., Glavatskikh, D.V., Trubachev, E.S.: *Spiroid Gearboxes for Operation in Extreme Conditions*. ISTU Publishing House, Izhevsk (2014)
5. Goldfarb, V. I., Trubachev, E. S., Kuznetsov, A. S.: Prospects and practice of spiroid gear application in drives of pipeline valves. In: *Proceedings of Tula State University. Technical Sciences*, pp. 61–74 (2011)

6. Kornilov, A. A., Ivanov, D. E.: Some results of experimental and calculation assessment of strength for complex parts of gearboxes for pipeline valves. In: *Intelligent Systems in Manufacturing*, vol. 2, pp. 111–116. ISTU Publishing House, Izhevsk (2011)
7. Goldfarb, V. I., Anferov, V. N., Sergeeva, I. V.: Variants of designs of spiroid gearboxes with rotaprint lubrication of gearing. In: *Intelligent Systems in Manufacturing*, vol. 2 (18), pp. 100–107. ISTU Publishing House, Izhevsk (2011)
8. Goldfarb, V.I.: Innovative development of theory and practice of spiroid gears and gearboxes. *Innovations* **N4**(198), 115–120 (2015)
9. Malina, O. V.: Features of the process of structural synthesis of automated gearbox design systems. In: *Proceedings of an International Conference “Theory and practice of gearboxes”*. ISTU Publishing House, Izhevsk, pp. 457–462 (1996)
10. Gorbatov, V. A., Yuzvishin, I. N.: Basic system multi-profile techniques on the eve of XXIst century. In: *Academia Collection of Scientific Works “Problems of Characterization Analysis and Logical Control”*. MHGU, Moscow, pp. 21–23 (1999)
11. Gorbatov, V. A.: Intellectualization of informatization technologies. In: *Proceedings of the World Congress ITS-93 Informational Communications, Networks, Systems and Technologies*. Moscow, pp. 1–5 (1993)
12. Gorbatov, V. A.: Characterization. Calculating Semantics. Artificial Intelligence. In: *Proc. of 13th All-Union Symposium “Logic Control with Computers”*. Moscow, pp. 3–7 (1990)
13. Gorbatov, V.A.: *Theory of Synthesis of Control Automata*. Tekhnika, Sofia (1973)
14. Gorbatov, V.A.: *Theory of Partially Ordered Systems*. Soviet Radio, Moscow (1976)
15. Gorbatov, V.A., Demyanov, V.F., Kuliev, G.B., et al.: *Automation of Complex Logic Structures Design*. Energia, Moscow (1978)
16. Gorbatov, V.A., Ostankov, B.L., Frolov, S.A.: *Regular Structures for Automated Control*. Engineering, Moscow (1980)
17. Gorbatov, V.A.: *Semantic Theory of Automata Design*. Energia, Moscow (1979)
18. Gorbatov, V.A.: *Computer Control Schemes and Graphs*. Energia, Moscow (1971)
19. Gorbatov, V.A., Kafarov, V.V., Pavlov, P.G.: *Logical Control of Technological Processes*. Energia, Moscow (1978)
20. Gorbatov, V. A.: Logic control: decade results and prospects. In: *Theses of reports of the 10th All-Union symposium “Logic control by means of computer”*. Moscow-Ustinov, pp. 3–7 (1987)
21. Gorbatov, V.A., Pavlov, P.G., Chetverikov, V.N.: *Logic Control of Information Processes*. Energoatomizdat, Moscow (1984)
22. Gorbatov, V. A.: Problems of creating integrated FMS-CAD/CAM systems. In: *Proceedings of the Coordination Meeting “Mathematical support of CAD and FMS in Mechanical Engineering”*. Izhevsk, pp. 3–10 (1984)
23. Malina, O. V.: The comparative characteristic of sets of forbidden figures of objects of different nature. In: *Proceedings of symposium “Information mathematics in informatology”*. ISTU Publishing House, Izhevsk, pp. 36–39 (1997)
24. Malina, O.V., Urzhumov, N.A.: Conceptual Approach to Development of Structural Synthesis Systems. *Inf. Math.* **1**(6), 184–187 (2007)
25. Mikoni, C. V.: On Class, Classification, and Systematization. In: *Ontology of design*, N1, vol. 6, pp. 67–80 (2016)
26. Mikoni, C. V.: Role and place of classifications in system analysis. In: *Proceedings of the 4th International Conference “System Analysis and Information Technologies”*, vol. 2, pp. 39–42. Abzakovo, Chelyabinsk (2011)
27. Gilchrist, A.: Research in information science. *Brit. Librarianship and Inf. Sci.*, 1966–1970. London, pp. 320–341 (1972)
28. Arntz, H.: Universality of classification. In: *Proc. 4 Int. Study Conf. Cl. Res*, vol. 2, Frankfurt, pp. (31–40) (1983)
29. Coates, E. J.: Subject searching of large scale information stores embracing all fields of knowledge: classification and concept matching. In: *Study Conf. Classif. Res. “Knowledge Organ. Inf. Retrieval”*, FID, London, N 716, pp. 17–22 (1997)

30. Pokrovskiy, M. P.: Scientific aspects of the classification problem. In: Yearbook-2007, Ekaterinburg, pp. 395–401 (2008)
31. Mai, J.-E.: The modernity of classification. *J. Doc.* **67**(4), 710–730 (2011)
32. Phillips, R.L., Ormsby, R.: Industry classification schemes. *J. Bus. and Finan. Librarianship* **21**(1), 1–25 (2016)
33. Pando, D.A., Almeida, C.C.: Knowledge organization in the context of postmodern from the theory of classification perspective. *Knowl. Organ* **43**(2), 113–117 (2016)
34. Eremin, L. N.: Classification and coding as a means of improving the efficiency of information technology. http://www.fakit.ru/main_dsp.php?top_id=6196. Accessed 21 Jan 2021
35. Malina, O. V., Moiseev, A. S., Malina, E. A.: Knowledge area classifier as an information model of structural synthesis system. Problems of its creation and extension. In: *Vestnik of South Ural State University. Series “Computer technologies, management, radioelectronics”*, vol. 20, N 4, pp. 5–13 (2020)
36. Malina, O. V.: Problems of developing the model of class of objects in intelligent CAD of gearbox systems. In: Goldfarb, V., Barmina, N., Trubachev, E. (eds.) *Advanced Gear Engineering, Mechanisms and Machine Science*, vol. 51, pp. 393–418. Springer (2018)
37. Malina, O., Valeev, O.: Aspects of optimization of the process of computer-aided design of complex objects. In: Goldfarb, V., Barmina, N., Trubachev, E. (eds.) *Advanced Gear Engineering, Mechanisms and Machine Science*, vol. 51, Springer, pp. 447–464 (2018)
38. Malina, O. V., Urzhumov, N. A.: Optimization of the process of structural synthesis of objects of medium complexity. In: *Vestnik IzhGTU*, vol. 1(33), pp. 144–150. ISTU Publishing House, Izhevsk (2007)
39. Malina, O. V., Valeev, O. F.: Approaches to minimizing the computer resources required to implement the process of structural synthesis of objects built on discrete structures. In: *Intelligent Systems in Manufacturing*, vol. 1 (18), pp. 29–34. ISTU Publishing House, Izhevsk (2013)
40. Malina, O.V., Valeev, O.F.: Model of the process of structural synthesis of objects built on discrete structures and features of its implementation. *Bullet. Kalashnikov Izhevsk State Tech. Univ.* **2**(57), 24–26 (2013)

Meshing Limit Line of Normal Arc-Toothed Cylindrical Worm Drive



Qingxiang Meng, Yaping Zhao, and Gongfa Li

Abstract The main purpose of this article is to establish the theory for determining the meshing limit line of the normal arc-toothed cylindrical worm drive. According to the meshing theory for gearing, the vector equations of the worm helicoid and the worm gear tooth surface, the unit normal vector of the worm helicoid, the meshing function, the meshing limit function of the worm drive, and so on are all acquired. The meshing limit points are determined by solving the nonlinear equation set, in which the iteration needs to be performed for determining the meshing limit point on the worm gear addendum while the iteration needs not to be performed for determining other meshing limit points. The numerical outcomes reflect that the meshing limit line divides the worm helicoid into the meshing zone and non-meshing zone, and the working length of the worm cannot reach half of its total thread length. The conjugate line of meshing limit line is roughly located in the middle of the worm gear tooth surface. The meshing limit line of the worm drive cannot be eliminated via adjusting the designing and operating parameters, and therefore the existence of the meshing limit line is an inherent feature for the normal arc-toothed cylindrical worm drive.

Keywords Meshing limit line · Worm drive · Normal arc helicoid · Meshing function · Working length

Q. Meng · Y. Zhao (✉)

School of Mechanical Engineering and Automation, Northeastern University, Shenyang 110819, People's Republic of China
e-mail: zhyp_neu@163.com

Y. Zhao

Provincial Key Laboratory of Dynamics and Reliability of Mechanical Equipment, Northeastern University, Shenyang 110819, People's Republic of China

G. Li

The Key Laboratory of Metallurgical Equipment and Control of Ministry of Education, Wuhan University of Science and Technology, Wuhan 430081, People's Republic of China

1 Introduction

The normal arc-toothed cylindrical worm drive is composed of a normal arc-toothed cylindrical worm and a worm gear. The so-called normal arc-toothed cylindrical worm is turned by a turning tool having the circular arc cutting edge, and the cutting edge is located in the normal section of the worm during turning it [1, 2]. Therefore, the tooth profile of the worm in its normal section is a standard circular arc and the worm helicoid is a normal circular helicoid. The worm gear is machined by a cylindrical hob whose generating surface is the same as the normal arc helicoid of the worm, and thus the cutting meshing of the worm gear is the same as the working meshing between the worm and the worm gear.

According to the formation principle of the worm drive, the worm gear tooth surface is the enveloped surface of the family of the hob generating surfaces. Due to the same shape between the generating surface of the hob and the normal circular helicoid of the worm, the worm gear tooth surface can also be regarded as the enveloped surface of the family of the normal circular helicoids. For an envelope process, the generating surface and the enveloped surface contact with each other along a curve at every instant, i.e. along an instantaneous contact line. Generally, the instantaneous contact lines have an enveloping line on the generating surface, namely, the meshing limit line or the second type of limit line [3]. Thus, the meshing limit line can divide the generating surface into two parts: the meshing zone and the non-meshing zone. For the normal arc-toothed cylindrical worm drive, the position of the meshing limit line on the worm helicoid will determine the working length of the worm. Furthermore, the conjugate line of meshing limit line can divide the worm gear tooth surface into two sub-meshing zones and the meshing performance in the neighborhood of the conjugate line generally is poor [4]. As a result, it can be seen that determining the meshing limit line for the normal arc-toothed cylindrical worm drive is of great significance for its geometric design.

The determination of the meshing limit line can be performed via connecting some meshing limit points which are determined by solving the nonlinear equation sets. The nonlinear equation set generally is composed of the meshing equation, the meshing limit equation, and a complementary equation. The complementary equation can be the location equation of the meshing limit point or the boundary equation of the member. Based on this method, the authors determined the meshing limit lines for some kinds of worm drives [5–7] and investigated the characteristics of the meshing limit line. The solving of the preceding equations was by means of the elimination method and geometric drawing to judge the existence of its solution and to determine the nice initial value for its iteration. However, if the parameters of the meshing limit point can be figured out without the help of the iteration, i.e. can be figured out from the algebraic formula, the determinations of the meshing limit points will be greatly simplified.

In this paper, the geometric model is established for the normal arc-toothed cylindrical worm drive. Some important formulas are obtained for the worm drive, for example, the vector equations of the worm helicoid and worm gear tooth surface, the

unit normal vector of the worm helicoid, the meshing function, the and meshing limit function of the worm drive. The nonlinear equation sets to determine the meshing limit line are built. The meshing limit points are determined from the algebraic formula and without the help of iteration except the meshing limit point on the worm gear addendum. Finally, the numerical results are provided for verification.

2 Generation of Normal Arc-Toothed Cylindrical Worm Drive

2.1 Generation of Worm Helicoid

The worm helicoid, i.e. the normal circular helicoid, is lathed by a lathe tool with the circular arc cutting edge and the cutting edge is located in the normal section of the worm as shown in Fig. 1. In this paper, the turning direction of the discussed worm is right-hand, and the helical angle of the worm at its reference cylinder is denoted by the symbol β . As shown in Fig. 1, a coordinate system $\sigma_1 \{O_1; \vec{i}_1, \vec{j}_1, \vec{k}_1\}$ is established for the worm, in which the coordinate origin O_1 is coincident with the middle point of the worm thread length and the vector \vec{k}_1 is coincident with the axis of the worm. At the initial position, the unit vectors \vec{j}_1 and $\vec{m}_1(0, 90^\circ - \beta)$ expand the normal section of the normal circular helicoid [3], and in this section, the radius of the circular arc cutting edge is denoted by the symbol ρ and its center O_c is on the axis \vec{j}_1 . The distance between the two points O_1 and O_c along the axis \vec{j}_1 is equal to the operating center distance a_c of the lathe tool.

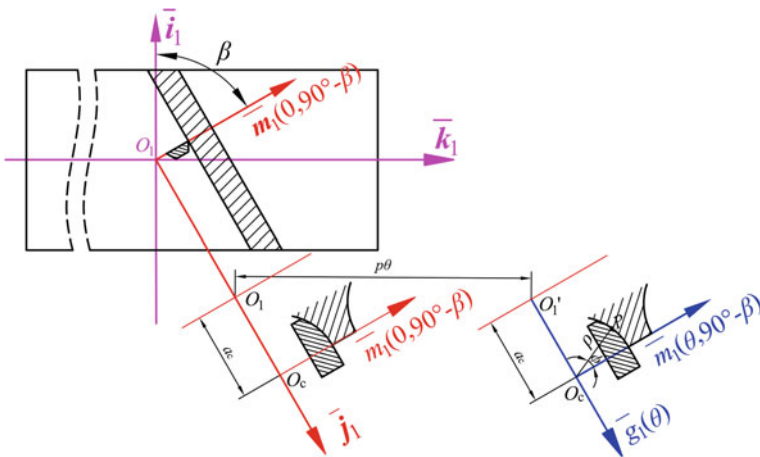


Fig. 1 Relative location and motion between worm and lathe tool

The worm rough is fixed while the lathe tool makes the helical motion during the generation of the normal circular helicoid. At the current location, the rotating angle of the worm around the axis \vec{k}_1 is denoted by the symbol θ and the moving distance of the lathe tool is met $\overrightarrow{O_1 O'_1} = p\theta\vec{k}_1$. Here, p is the helix parameter of the worm. At the current location, the unit vectors $\vec{g}_1(\theta)$ and $\vec{m}_1(\theta, 90 - \beta)$ expand the normal section of the normal circular helicoid, and the center O_c of circular arc cutting edge turns to the axis $\vec{g}_1(\theta)$, and $\overrightarrow{O'_1 O_c} = a_c\vec{g}_1(\theta)$. The point P is an arbitrary point of the circular arc tooth profile in the normal section of the normal circular helicoid, and the angle between $\vec{m}_1(\theta, 90 - \beta)$ and $\overrightarrow{O_c P}$ is denoted by the symbol ϕ . Based on this, the vector equation of the normal circular helicoid can be expressed in σ_1 by means of the two curvilinear coordinates θ and ϕ as below

$$\begin{aligned} (\vec{r}_1)_1 &= (\overrightarrow{O_1 P})_1 = (\overrightarrow{O_1 O'_1})_1 + (\overrightarrow{O'_1 P})_1 \\ &= p\theta\vec{k}_1 + (a_c - \rho \sin \phi)\vec{g}_1(\theta) + \rho \cos \phi\vec{m}_1(\theta, 90^\circ - \beta) \\ &= x_1\vec{i}_1 + y_1\vec{j}_1 + z_1\vec{k}_1 \end{aligned} \quad (1)$$

where $x_1 = \rho \cos \beta \cos \phi \cos \theta + (\rho \sin \phi - a_c) \sin \theta$, $y_1 = \rho \cos \beta \cos \phi \sin \theta - (\rho \sin \phi - a_c) \cos \theta$, and $z_1 = p\theta + \rho \sin \beta \cos \phi$.

The unit normal vector of the normal circular helicoid can be obtained based on the method in differential geometry [8] as follows

$$(\vec{n}_1)_1 = \frac{\frac{\partial(\vec{r}_1)_1}{\partial\theta} \times \frac{\partial(\vec{r}_1)_1}{\partial\phi}}{\left| \frac{\partial(\vec{r}_1)_1}{\partial\theta} \times \frac{\partial(\vec{r}_1)_1}{\partial\phi} \right|} = \frac{n_c}{D_0}\vec{e}_1(\theta) + \frac{n_g}{D_0}\vec{g}_1(\theta) + \frac{n_k}{D_0}\vec{k}_1 \quad (2)$$

in which the two symbols $\frac{\partial(\vec{r}_1)_1}{\partial\theta}$ and $\frac{\partial(\vec{r}_1)_1}{\partial\phi}$ are the two first-order partial derivatives of \vec{r}_1 in regard to θ and ϕ ; $D_0 = \sqrt{(\rho^2 \sin^2 \beta - C_1^2) \sin^2 \phi - 2C_2 \rho \sin \beta \sin \phi + a_c^2 + p^2}$, $C_1 = a_c \cos \beta - p \sin \beta$, $C_2 = a_c \sin \beta + p \cos \beta$, $n_c = (p - \rho \sin \beta \cos \beta \sin \phi) \cos \phi$, $n_g = (\rho \sin \beta_1 \sin \phi - C_2) \sin \phi$, and $n_k = (a_c - \rho \sin^2 \beta_1 \sin \phi) \cos \phi$.

2.2 Generation of Worm Gear Tooth Surface

During the generation of the worm gear tooth surface, two static coordinate systems $\sigma_{o1} \{O_1; \vec{i}_{o1}, \vec{j}_{o1}, \vec{k}_{o1}\}$ and $\sigma_{o2} \{O_2; \vec{i}_{o2}, \vec{j}_{o2}, \vec{k}_{o2}\}$ are respectively used to denote the initial positions of the worm and worm gear as shown in Fig. 2. The unit vector \vec{k}_{o2} is along the axial line of the worm gear and the origin O_2 is coincident with the middle point of worm gear tooth width. The two vectors \vec{k}_{o1} and \vec{k}_{o2} are perpendicular to each other. The two vectors \vec{i}_{o1} and \vec{i}_{o2} are coincident and are along the common

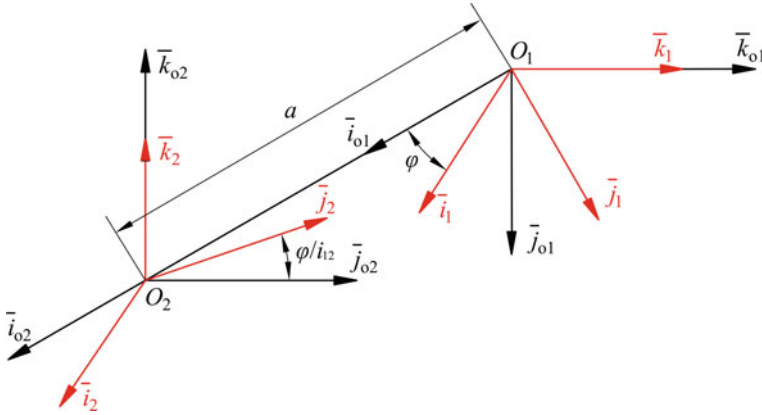


Fig. 2 Coordinate systems used in generation of worm gear tooth surface

perpendicular line of \vec{k}_{o1} and \vec{k}_{o2} . The distance between the two points O_1 and O_2 is equal to the center distance a of the worm pair. The two rotating coordinate systems $\sigma_1 \{O_1; \vec{i}_1, \vec{j}_1, \vec{k}_1\}$ and $\sigma_2 \{O_2; \vec{i}_2, \vec{j}_2, \vec{k}_2\}$ are respectively used to denote the current positions of the worm and worm gear. When the rotating angle between σ_{o1} and σ_1 is equal to angle φ , the rotating angle between σ_{o2} and σ_2 will be equal to φ/i_{12} , in which the symbol i_{12} is the transmission ratio of the worm drive.

When the worm rotates around \vec{k}_{o1} by the angle φ , a family $\{\Sigma_1\}$ of normal circular helicoids will be formed and denoted in σ_{o1} as

$$(\vec{r}_1)_{o1} = R[\vec{k}_{o1}, \varphi](\vec{r}_1)_1 = x_{o1}\vec{i}_{o1} + y_{o1}\vec{j}_{o1} + z_1\vec{k}_{o1} \tag{3}$$

where $x_{o1} = \rho \cos \beta \cos \phi \cos(\theta + \varphi) + (\rho \sin \phi - a_c) \sin(\theta + \varphi)$ and $y_{o1} = \rho \cos \beta \cos \phi \sin(\theta + \varphi) - (\rho \sin \phi - a_c) \cos(\theta + \varphi)$. The symbol $R[\vec{k}_{o1}, \varphi]$ is the rotation transformation matrix [3], and its expression is $R[\vec{k}_{o1}, \varphi] =$

$$\begin{bmatrix} \cos \varphi & -\sin \varphi & 0 \\ \sin \varphi & \cos \varphi & 0 \\ 0 & 0 & 1 \end{bmatrix}.$$

By using the rotation transformation matrix $R[\vec{k}_{o1}, \varphi]$, the unit normal vector of $\{\Sigma_1\}$ can also be obtained and denoted in σ_{o1} as

$$(\vec{n}_1)_{o1} = R[\vec{k}_{o1}, \varphi](\vec{n}_1)_1 = \frac{n_x}{D_0}\vec{i}_{o1} + \frac{n_y}{D_0}\vec{j}_{o1} + \frac{n_k}{D_0}\vec{k}_{o1} \tag{4}$$

where $n_x = n_e \cos(\theta + \varphi) - n_g \sin(\theta + \varphi)$ and $n_y = n_e \sin(\theta + \varphi) - n_g \cos(\theta + \varphi)$.

Without loss of generality, it can be assumed that the worm rotates around the axis \vec{k}_{o1} with the angular velocity $|\vec{\omega}_1| = 1 \text{ rad/s}$ during the generation. Thus, the

angular velocity of the worm gear is met $|\vec{\omega}_2| = 1/i_{12}$ rad/s. The relative angular velocity vector of the worm drive can be achieved in σ_{o1} as

$$(\vec{\omega}_{12})_{o1} = (\vec{\omega}_1)_{o1} - (\vec{\omega}_2)_{o1} = (\vec{\omega}_1)_{o1} - R[\vec{i}_{o1}, 90^\circ](\vec{\omega}_2)_{o2} = \frac{1}{i_{12}}\vec{j}_{o1} + \vec{k}_{o1} \quad (5)$$

in which $R[\vec{i}_{o1}, 90^\circ] = \begin{bmatrix} 1 & 0 & 0 \\ 0 & 0 & -1 \\ 0 & 1 & 0 \end{bmatrix}$.

In σ_{o1} , the relative velocity vector [3] of the worm drive can be obtained as

$$\begin{aligned} (\vec{V}_{12})_{o1} &= (\vec{\omega}_{12})_{o1} \times (\vec{r}_1)_{o1} - (\vec{\omega}_2)_{o1} \times (\overrightarrow{O_2O_1})_{o1} + \frac{d(\overrightarrow{O_2O_1})_{o1}}{d\varphi} \\ &= V_{12}^{(x)}\vec{i}_{o1} + V_{12}^{(y)}\vec{j}_{o1} + V_{12}^{(z)}\vec{k}_{o1} \end{aligned} \quad (6)$$

where $\frac{d(\overrightarrow{O_2O_1})_{o1}}{d\varphi} = 0$, $V_{12}^{(x)} = \frac{z_1}{i_{12}} \cos \varphi - y_1$, $V_{12}^{(y)} = x_1 - \frac{z_1}{i_{12}} \sin \varphi$, and $V_{12}^{(z)} = \frac{1}{i_{12}}(a - x_{o1})$.

By means of Eqs. (4) and (6), the meshing function of the worm drive can be acquired according to the definition in the gear meshing theory [3] as

$$\Phi(\theta, \phi, \varphi) = (\vec{V}_{12})_{o1} \cdot (\vec{n}_1)_{o1} = \frac{1}{i_{12}D_0}[A \sin(\theta + \varphi) + B \cos(\theta + \varphi) + C] \quad (7)$$

where $A = -n_g z_1 - n_k(\rho \sin \phi - a_c)$, $B = n_e z_1 - n_k \rho \cos \beta \cos \phi$, and $C = n_k(a - i_{12}p)$.

The vector equation of the worm gear tooth surface can be obtained from Eq. (3) after letting $\Phi = 0$ in Eq. (7) and can be denoted in σ_2 as below

$$\begin{aligned} (\vec{r}_2)_2 &= R[\vec{k}_2, -\varphi_2] \left\{ R[\vec{i}_{o2}, -90^\circ] \left[(\vec{r}_1)_{o1} + (\overrightarrow{O_2O_1})_{o1} \right] \right\} \\ &= x_2\vec{i}_2 + y_2\vec{j}_2 - y_{o1}\vec{k}_2, \quad \Phi(\theta, \phi, \varphi) = 0 \end{aligned} \quad (8)$$

where $x_2 = (x_{o1} - a) \cos \varphi_2 + z_1 \sin \varphi_2$ and $y_2 = -(x_{o1} - a) \sin \varphi_2 + z_1 \cos \varphi_2$.

According to the definition of the meshing limit function [3], the meshing limit function of the worm drive can be ciphered out from Eq. (7) as

$$\Phi_\varphi(\theta, \phi, \varphi) = \frac{\partial \Phi}{\partial \varphi} = \frac{1}{i_{12}D_0}[A \cos(\theta + \varphi) - B \sin(\theta + \varphi)]. \quad (9)$$

3 Computing Method of Meshing Limit Line of Worm Pair

Generally, the meshing limit line of a cylindrical worm pair is from the worm addendum to the worm gear addendum along the worm tooth depth [5, 6]. From Eqs. (7) and (9), the parameters of the meshing points on the limit line should satisfy the following equations

$$\begin{cases} A \sin(\theta + \varphi) + B \cos(\theta + \varphi) + C = 0 \\ A \cos(\theta + \varphi) - B \sin(\theta + \varphi) = 0 \end{cases} \quad (10)$$

The trigonometric functions $\sin(\theta + \varphi)$ and $\cos(\theta + \varphi)$ can be denoted by the components A , B , and C as below

$$\sin(\theta + \varphi) = -\frac{A}{C}, \quad \cos(\theta + \varphi) = -\frac{B}{C} \quad (11)$$

Taking the quadratic sum between $\sin(\theta + \varphi)$ and $\cos(\theta + \varphi)$ in Eq. (11) results in

$$A^2 + B^2 - C^2 = 0. \quad (12)$$

After substituting the expressions of the components A , B , and C into Eq. (12), this equation can be regarded as a quadratic equation with the unknown z_1 as follows

$$\left(n_e^2 + n_g^2\right)z_1^2 - 2B_z z_1 + C_z = 0, \quad (13)$$

where $B_z = n_k[\rho n_e \cos \beta \cos \phi - n_g(\rho \sin \phi - a_c)]$ and $C_z = n_k^2[\rho^2 \cos^2 \beta \cos^2 \phi + (\rho \sin \phi - a_c)^2] - C^2$.

The solution of Eq. (13) can be obtained as

$$z_1(\phi) = \frac{\hat{z}_1}{n_e^2 + n_g^2}, \quad (14)$$

where $\hat{z}_1 = B_z \pm \sqrt{B_z^2 - C_z(n_e^2 + n_g^2)}$. According to the numerical simulation, the symbol \pm in \hat{z}_1 should take $+$ to ensure the results are reasonable.

Equation (14) is equivalent to Eq. (10) and can be used to determine the meshing limit points.

For the meshing limit point on the worm addendum, the value of ϕ can be firsthand computed out from the equation of worm addendum $f_w = \sqrt{x_{o1}^2 + y_{o1}^2} - r_{a1} = 0$ without the help of the iteration as below

$$\phi_w = \arcsin \frac{a_c - \sqrt{a_c^2 \cos^2 \beta - (\rho^2 \cos^2 \beta - r_{a1}^2) \sin^2 \beta}}{\rho \sin^2 \beta}, \tag{15}$$

in which the symbol r_{a1} is the radius of the worm addendum circle.

Then the θ value of the meshing limit point on the worm addendum can be obtained from Eq. (14) after replacing the variable ϕ in Eq. (14) with ϕ_w in Eq. (15) as below

$$\theta_w = \frac{1}{p} \left(\frac{\hat{z}_1}{n_c^2 + n_g^2} - \rho \sin \beta \cos \phi_w \right). \tag{16}$$

Finally, the φ value of the meshing limit point on the worm addendum can be obtained from Eq. (11) by mean of Eqs. (15) and (16). Based on this, such a meshing limit point can be determined.

For the meshing limit point on the worm gear addendum, its determination should be realized via solving a unary nonlinear equation iteratively. Substituting Eq. (14) into the components A and B of Eq. (7), and then substituting the obtained results into Eq. (11) lead up to

$$\begin{aligned} A(\phi) &= \frac{A_\phi}{n_c^2 + n_g^2}, \quad B(\phi) = \frac{B_\phi}{n_c^2 + n_g^2} \\ \sin(\theta + \varphi) &= \frac{-A_\phi}{C(n_c^2 + n_g^2)}, \quad \cos(\theta + \varphi) = \frac{-B_\phi}{C(n_c^2 + n_g^2)} \end{aligned} \tag{17}$$

where $A_\phi = -n_g \hat{z}_1 - n_k (n_c^2 + n_g^2) (\rho \sin \phi - a_c)$ and $B_\phi = n_c \hat{z}_1 - n_k \rho \cos \beta \cos \phi (n_c^2 + n_g^2)$.

The components x_{o1} and y_{o1} in Eq. (3) can be denoted by the variable ϕ after substituting the last two expressions of Eq. (17) into Eq. (3), and the results are

$$x_{o1}(\phi) = -\frac{\hat{x}_{o1}}{C(n_c^2 + n_g^2)}, \quad y_{o1}(\phi) = -\frac{\hat{y}_{o1}}{C(n_c^2 + n_g^2)}, \tag{18}$$

where $\hat{x}_{o1} = \rho \cos \beta \cos \phi B_\phi + (\rho \sin \phi - a_c) A_\phi$ and $\hat{y}_{o1} = \rho \cos \beta \cos \phi A_\phi - (\rho \sin \phi - a_c) B_\phi$.

Substituting Eq. (18) into the equation of worm gear addendum leads up to a nonlinear equation with the unknown ϕ to determine the meshing limit point on the worm gear addendum as follows

$$f_g(\phi) = \sqrt{\left[\hat{x}_{o1} + a_c(n_e^2 + n_g^2)\right]^2 + C^2\hat{z}_1^2} + \sqrt{C^2r_{g2}^2(n_e^2 + n_g^2)^2 - \hat{y}_{o1}^2 - a|C|(n_e^2 + n_g^2)} = 0 \tag{19}$$

in which the symbol r_{g2} is the throat form radius of worm gear.

After obtaining the values of ϕ , θ , and φ from Eqs. (19), (14), and (11), respectively, the meshing limit point on the worm gear addendum can be determined.

Moreover, the parameters of the meshing limit points between the worm addendum and the worm gear addendum can be obtained from Eqs. (15) and (11) without the help of the iteration after the value of ϕ is given according to its obtained value range. Then the meshing limit line can be determined for the worm drive by means of the interpolation method.

4 Numerical Example

The design parameters of the normal arc-toothed cylindrical worm drive discussed in this paper and the operating parameters of the lathe tool are provided in Table 1.

Table 1 Parameters of worm drive

Description	Symbol and unit	Value
Transmission ratio of worm drive	i_{12}	33/4
Center distance of worm drive	a (mm)	160
Number of worm threads	Z_1	4
Modulus of worm	m (mm)	7
Tooth number of worm gear	Z_2	33
Helix parameter of worm	$p = mZ_1/2$ (mm)	14
Reference radius of worm	r_1 (mm)	38
Pressure angle of worm	α_n (°)	23
Reference helix angle of worm	$\beta = \arctan(2r_1/mZ_1)$ (°)	69.7751
Modification coefficient of worm gear	$\xi = (a - r_1)/m - Z_2/2$	0.9286
Tip radius of worm	$r_{a1} = r_1 + m$ (mm)	45
Reference radius of worm gear	$r_2 = mZ_2/2$ (mm)	115.5
Throat radius of worm gear	$r_{a2} = r_2 + m(1 + \xi)$ (mm)	129
Throat form radius of worm gear	$r_{g2} = a - r_{a2}$ (mm)	31
Radius of the circular arc cutting edge	$\rho = 8m$ (mm)	56
Operating center distance of lathe tool	$a_c = r_1 + \rho \sin \alpha_n$ (mm)	59.8809

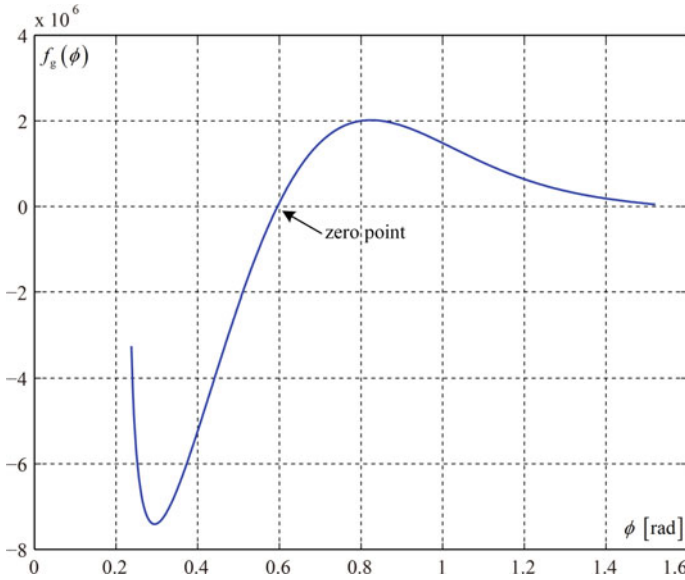


Fig. 3 Curve of $f_g(\phi)$

According to the parameters of the worm drive listed in Table 1, the values of the angles ϕ , θ , and φ are respectively computed from Eqs. (15), (16), and (11) for the meshing limit point F_1 on the worm addendum.

In order to determine the meshing limit point F_7 on the worm gear addendum, i.e. the intersection point between the meshing limit line and the worm gear addendum, Eq. (19) should be firstly solved iteratively. The curve of the function $f_g(\phi)$ in Eq. (19) is drawn in Fig. 3 to judge the existence of solution of the equation $f_g(\phi) = 0$ and to seek the iterative initial value. The interval of the angle ϕ in Fig. 3 is set as $[0, \pi/2]$ according to its definition. Figure 3 reflects that an intersection point exists between the curve of $f_g(\phi)$ and the abscissa axis, i.e. the function $f_g(\phi)$ has a zero point over the given interval. The value $\phi = 0.6$ rad which is near the zero point of $f_g(\phi)$ can be utilized as the initial value to solve Eq. (19) iteratively. Based on this, the solution of the equation $f_g(\phi) = 0$ can be obtained, and then the values of θ and φ can be figured out from (14) and (11), respectively. The numerical results of the preceding two meshing limit points are all listed in Table 2.

From Table 2, the interval of the angle ϕ from the meshing limit point on the worm addendum to the meshing limit point on the worm gear addendum is equal to $[19.5558^\circ, 34.1196^\circ]$. After giving the angle ϕ some values in its interval, the values of θ and φ can be respectively figured out from Eqs. (14) and (11) for the meshing limit points F_2 - F_6 between the preceding two endpoints. The numerical results of these meshing points are also provided in Table 2.

According to the numerical results in Table 2, all the meshing limit points are drawn in the axial sections of the worm and the worm gear as shown in Figs. 4

and 5, respectively. The meshing limit line on the worm helicoid and its conjugate line on the worm gear tooth surface are acquired via connecting these meshing limit points by means of the interpolation method. Moreover, the line DF_1E in Fig. 5 is the conjugate line of the worm addendum on the worm gear tooth surface.

Figure 4 displays that the meshing limit line of the normal arc-toothed cylindrical worm drive is roughly located in the middle of the worm helicoid along the worm axis. The worm helicoid is divided into the meshing zone and non-meshing zone by the meshing limit line as shown in Fig. 4 so that the whole thread length of the worm cannot be used in the meshing of the worm drive. The right side of the limit line is the meshing zone due to the positive value of the function $A^2 + B^2 - C^2$ in this side. In Fig. 4, the length between the two points F_1 and D along the worm axis is the working length of the worm and obviously, the ratio of the working length of the worm to its whole thread length is less than 1/2. The conjugate line of meshing limit line is roughly located in the middle of the worm gear tooth surface and divides the meshing zone into two sub-meshing zones as shown in Fig. 5.

Table 2 Parameters of meshing limit points

Point	Parameter						
	ϕ (°)	θ (°)	φ (°)	z_1 (mm)	$\sqrt{x_{o1}^2 + y_{o1}^2}$ (mm)	$-y_{o1}$ (mm)	$\sqrt{x_2^2 + y_2^2}$ (mm)
F_1	19.5558	-210.8656	145.5859	-2.0081	45	-0.6318	115.0220
F_2	21.9831	-177.0141	109.4738	5.4740	42.8591	1.7222	117.3033
F_3	24.4104	-152.0025	82.8943	10.7087	40.7486	3.3690	119.8702
F_4	26.8377	-132.4765	62.2256	14.5172	38.6715	4.5672	122.4627
F_5	29.2650	-116.6444	45.5351	17.3389	36.6309	5.4549	124.9861
F_6	31.6923	-103.4395	31.6726	19.4364	34.6297	6.1148	127.4058
F_7	34.1196	-92.1788	19.9017	20.9786	32.6706	6.6000	129.7107

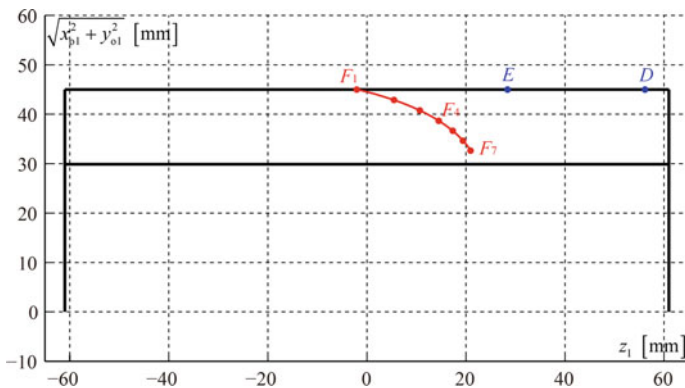


Fig. 4 Meshing limit line in worm axial section

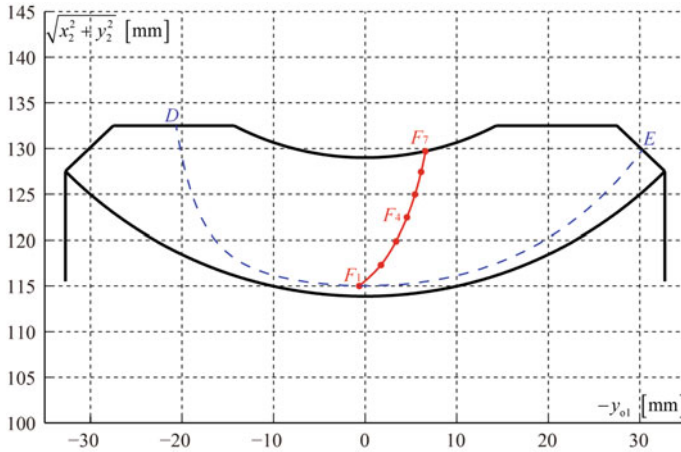


Fig. 5 Conjugate line of meshing limit line in worm gear axial section

In addition, a large number of numerical examples indicate that the meshing limit line of the normal arc-toothed cylindrical worm drive cannot be removed from the tooth surfaces. Thus, the existence of the meshing limit line is an inherent feature for the normal arc-toothed cylindrical worm drive.

5 Conclusions

The theory for determining the meshing limit line of the normal arc-toothed cylindrical worm drive is established. The vector equations of the worm helicoid and the worm gear tooth surface, the unit normal vector of the worm helicoid, the meshing function, the meshing limit function of the worm drive, and so on are all obtained.

The meshing limit point on the worm gear addendum is determined by solving a nonlinear equation iteratively which is acquired by means of the elimination method. The iteration is not needed to perform in the determination of other meshing limit points, and therefore the corresponding computer program can be simpler.

The numerical example is implemented and the obtained results reflect that the worm helicoid is divided into the meshing zone and non-meshing zone by the meshing limit line, and the working length of the worm cannot reach half of its total thread length. The conjugate line of meshing limit line is roughly located in the middle of the worm gear tooth surface and divides it into two sub-meshing zones. The existence of the meshing limit line is an inherent feature for the arc-toothed cylindrical worm drive since the meshing limit line cannot be eliminated via adjusting the designing and operating parameters.

Acknowledgements This study was funded by the National Natural Science Foundation of China (52075083) and the Open Fund of the Key Laboratory for Metallurgical Equipment and Control of Ministry of Education in Wuhan University of Science and Technology (MECOF2020B03 and 2018B05).

References

1. Yang, L.: Circular Arc Tooth Cylindrical Worm Drive. Shanxi People's Publishing House, Taiyuan (1984)
2. Meng, Q., Zhao, Y., Cui, J., et al.: Meshing characteristic of arc-toothed cylindrical worm pair and cutting geometric condition of its worm. *ASME J. Mech. Des.* **143**(6) (2021)
3. Dong, X.: Foundation of Meshing Theory for Gear Drives. China Machine Press, Beijing (1989)
4. Wu, H., et al.: Design of Worm Drive, vol. 1. Mechanical Industry Press, Beijing (1986)
5. Zhao, Y., Sun, X.: On meshing limit line of ZC1 worm pair. In: European Conference on Mechanism Science 2018, Aachen, Germany, pp. 292–298 (2018)
6. Zhao, Y., Mu, S., et al.: Meshing limit line of involute worm drive. *Mech. Mach. Sci.* **73**, 1129–1138 (2019)
7. Meng, Q., Zhao, Y., Yang, Z.: Meshing limit line of the conical surface enveloping conical worm pair. *Proc. Inst. Mech. Eng. Part C J. Mech. Eng. Sci.* **234**(2), 693–703 (2020)
8. Kristopher, T.: Differential Geometry of Curves and Surfaces. Springer, Switzerland (2016)

Improving the Efficiency of Gear Milling of Cylindrical Gears with Worm Cutters When Using Pulse Feed



M. M. Kane

Abstract The urgency of the problem of improving the efficiency of gear milling of cylindrical gears with worm cutters is shown. Cylindrical gears are among the most common, complex and critical machine parts. Gear milling of cylindrical gears with worm cutters is used for gear cutting approximately 90% of cylindrical gears. This method is characterized by low productivity and durability of worm cutters (the cost and complexity of this operation reach 60% of the values of these indicators in the manufacture of gears in General). This operation makes a great contribution to the formation of quality parameters of finished gears. The author shows that the share of this operation in the dispersion of quality indicators of teeth of finished gears reaches 49%. A cheap and effective way to improve the tooth-cutting process under consideration is to improve the cutting conditions during its implementation. To solve this problem, the author proposed a method for gear milling cylindrical gears with worm cutters with pulse feed. In this method, the axial feed of the cutter or workpiece does not occur continuously, but in pulses. This impulse is produced during the re-conjugating of the hob teeth with the workpiece when the cutter is rotated by a number of teeth that is not a multiple of the number of hob teeth. This allows you to reduce the specific cutting forces, the temperature in the cutting zone, and increase the rigidity of the workpiece-hob system when cutting. The author's experimental studies of the proposed method have shown that its application can reduce the average wear of the milling teeth by 1.43 times, the maximum possible wear of the milling teeth by 1.64 times, the intensity (speed) of wear of the milling teeth by 1.79 times, and increase the accuracy of the teeth by an average of 1.2 times. While maintaining the stability of worm mills in comparison with continuous feed gear milling, this method allows you to intensify the gear milling modes by about 1.6 times and increase the productivity of gear milling by about 1.5 times. The method can also be used for processing slots, grooves, and other surfaces with disc cutters.

Keywords Gear milling of cylindrical gears with worm cutters · Pulse feed of the cutter or workpiece · Improvement of cutting conditions · Improving gear milling performance · Worm mill durability · Gear tooth accuracy

M. M. Kane (✉)
Belorussian National Technical University, Minsk, Belarus
e-mail: kane_08@mail.ru

1 Introduction

Cylindrical gears are among the most mass-produced, complex and critical machine parts. Cutting the teeth of these gears for about 90% of standard sizes is performed on gear milling machines with continuous feeding of the workpiece or tool with worm cutters. The main disadvantages of this process are the low processing performance and durability of worm cutters. For this reason, the cost and labor intensity of this operation reaches 60% of the values of these indicators for the entire gear manufacturing process. The accuracy of finished cylindrical gears is largely formed by the operation of their gear cutting. Our research has shown that for gears that have passed after gear cutting operations of shewing, chemical-heat treatment, gear honing or gear rolling, the contribution of the gear cutting operation to the dispersion of the quality parameters of the finished gears reaches 49%. The above confirms the urgency of improving the productivity and accuracy of the gear milling process of cylindrical gears with worm cutters.

2 Description of the Method of Gear Milling of Cylindrical Gears with Worm Cutters with Pulse Feed

2.1 Kinematics of the Process

To achieve these goals, we proposed to improve the cutting conditions when gear cutting cylindrical gears with worm cutters by using pulse feed. In accordance with the proposed method [1], the axial feed of the workpiece or cutter during gear cutting occurs not at a constant speed, but in pulses. The pulse of the axial feed of the workpiece 2 or the cutter 1 (Fig. 1) occurs at the moment of re-conjugating of the adjacent teeth of the cutter with the workpiece, i.e. at the moment when one tooth (for example, tooth 3) completely (its vertex is at point α) or mostly (vertex at point α') has finished cutting, and the next tooth has not yet started it (the vertex of tooth 4 is at point b or b' outside the workpiece). This method can be used when cutting teeth or splines with worm or disk modular cutters, preferably with associated milling.

The proposed method of cutting the teeth of cylindrical gears can significantly improve the cutting conditions in comparison with existing methods. This is explained by the following:

1. After each feed pulse, the maximum thickness of the chip is removed by a new cutter tooth, since the feed pulse occurs when the cutter is rotated by the number of teeth K , not a multiple of the number of worm cutter teeth z_0 . This allows you to increase the thickness of the chips removed by each tooth, reduce the temperature of the worm cutter and the workpiece, and evenly distribute the load between the cutter teeth, since they all perform the same work. When cutting with a constant feed, the teeth of the cutter in its cross-section teeth of the

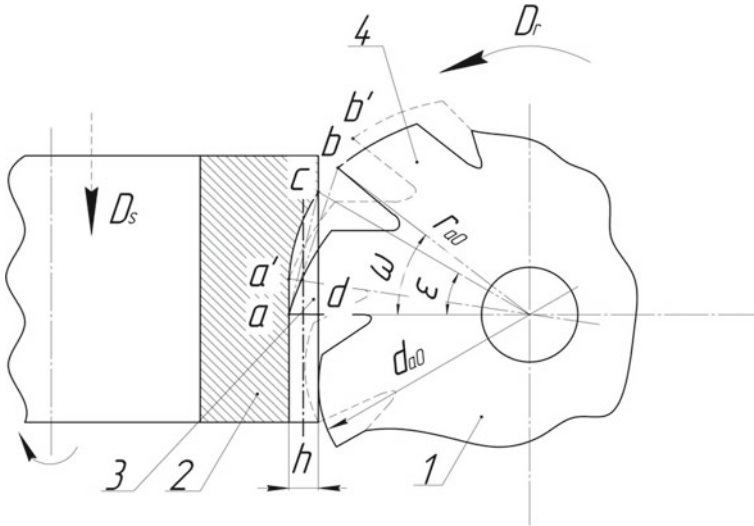


Fig. 1 Diagram of milling cylindrical gear wheels with a pulse feed

worm cutter are loaded unevenly. The first tooth that starts cutting removes the maximum thickness of the chips. The remaining teeth clean the treated surface and, with a small chip thickness, often do not cut, but rumple the treated surface. This increases the cutting forces and temperature, and causes uneven wear of the worm cutter teeth [2]. The experimental implementation of the proposed method for gear milling with a worm cutter showed that the workpieces were practically not heated, while with the traditional cutting scheme their temperature reached 50 °C;

2. No relative axial movement of the cutter and the workpiece during the cutting process allows to increase the rigidity of the system workpiece-tool by about 40% compared to traditional cutting scheme (as many times as it is known, the stiffness of any system in the more static stiffness of the system in dynamic condition). Increasing the rigidity of the technological system allows you to reduce system deformations and vibrations during cutting, improve the accuracy of processing and the quality of the treated tooth surfaces.
3. Increasing the chip thickness, as is known from the experience of milling with a passing feed and using a progressive cutting scheme for various processing methods, helps to reduce the specific cutting force and leads to increased tool life.
4. Cutting with variable feed, as shown by studies for various types of processing [3], reduces the intensity of tool wear and increases processing productivity.
5. The use of this method makes it easier to automate the control of the minute feed rate by changing the K value.

2.2 Interrelations of Characteristics of Gear Milling Modes of Cylindrical Gears with Pulse Feed

The main characteristics of the proposed method are:

1. The number of pulses of feed of the workpiece or tool in a minute

$$n_{imp} = \frac{n_0 z_0}{K}, \text{ min}^{-1} \quad (1)$$

where n_0 is the frequency of rotation of the cutter, min^{-1} ; z_0 is the number of strips of worm cutter or teeth of the disc cutter; K is an integer, not a multiple of z_0 .

2. The value of the feed pulse l , mm

$$l = S_0 \frac{n}{n_{imp}} = S_0 \frac{K}{z z_0 i}, \text{ mm} \quad (2)$$

where S_0 is the feed per revolution of the workpiece, mm/turn; n is the frequency of rotation of the workpiece, turn/min; z is the number of teeth of the gear being cut; i is the number of threads of the worm mill π

3. The valid duration of the impulse feed from condition its realization at the time of re-conjugating adjacent teeth of the worm cutter with the workpiece, i.e. on the site of bc (Fig. 1)

$$t_{imp} = \frac{L}{v_r 1000}, \text{ min} \quad (3)$$

where L is the path length of the top of tooth 4 (Fig. 1) mills, on which the pulse of the feed happens, mm; v_r —rotation speed of cutter, m/min.

The value of L (the length of the arc bc in Fig. 1) can be found with sufficient accuracy as the difference between the chords ab and ac (Fig. 1) according to the formula:

$$L = ab - ac = \sqrt{2r_{a0}h} - 2r_{a0}\sin\left(\frac{\pi}{z_0}\right), \text{ mm} \quad (4)$$

4. The speed pulse feed, m/min

$$V_s = \frac{L}{t_{imp.act} 1000}, \text{ m/min} \quad (5)$$

where $t_{imp.act}$ —actual duration of the feed pulse

5. Minute feed of the workpiece or worm cutter

$$S_{min} = ln_{imp} = ln_0 \frac{z_0}{K}, \text{ mm/min} \quad (6)$$

The use of pulse gear milling for the specified dimensions of the gear being processed and the cutter used is possible if one of the following conditions is met: $L > 0$ or $\omega > \varepsilon$ (Fig. 1). Calculations have shown that the proposed method can be implemented when cutting the teeth of cylindrical gears with a module $m = 3 \dots 5$ mm, with an outer diameter $d_{a0} = 80 \dots 150$ mm when using standard worm cutters

3 Experimental Study of the Gear Milling Process Cylindrical Gears with Pulse Feed

3.1 Conditions and Methods of Experimental Research

We performed an experimental study of this method on a modernized gear milling semi-automatic mod. 5B312 of Vitebsk Machine Tool Plant “VISTAN”, Belarus at the Minsk Gear Plant when processing det. 130-1701112 ($m = 4.25$ mm, $z = 45$, $h = 7.896$ mm) using a worm mill that had $z_0 = 10$, $r_{a0} = 50$ mm. The following processing modes were adopted: $n_0 = 100 \text{ min}^{-1}$, $v_r = 30$ m/min, $K = 3$, $n_{imp} = 333$ imp/min, $S_0 = 4$ mm/turn. In these modes, the following parameters of the pulse-fed gear cutting process took place: $t_{imp} = 0.0058$ s, $l = 0.026$ mm, $v_s = 0.43$ m/min, $L = 2.9$ mm. The values of S_{min} for the accepted modes by changing K can be in the range of 3... 26 mm/min. Analysis of these data shows the following:

1. The speed of the pulse feed movement is many times (about 72 times) less than the speed of the main cutting movement. Therefore, the impulse of the feed movement without deterioration of the cutting conditions can occur ahead of time, i.e. until one tooth of the cutter comes to the point α . This will only slightly reduce the instantaneous cutting speed. In Fig. this position of the cutter is shown as a dotted line. In this case, the cutting force acting on the tooth 3 should be reduced to the maximum permissible in terms of the necessary increase in the resistance of the cutter when using this method. The value of this force is determined experimentally. Using this phenomenon allows you to significantly increase the value of L and expand the scope of this method for these conditions ($S_{min} = 8.9$ mm/min). This indicates a wider range of changes

in the cutting modes of the proposed method compared to the traditional one and the expansion of the capabilities of the new method to increase the productivity of the gear cutting process.

2. The Maximum value of S_{\min} , which can be achieved when using pulsed gear milling at $n_0 = 100$ turn/min, $z = 45$, $S_0 = 0.4$ mm/turn is 26 mm/min, which is approximately 3 times more than traditional gear milling for the same conditions ($n_0 = 100$ turn/min, $z_0 = 45$, $S_{\min} = 8.9$ mm/min).

The durability of the cutting tool is a comprehensive indicator of the effectiveness of the processing method, the tool's performance. Therefore, when studying new processing methods and tool designs, first of all, their impact on tool life is evaluated. Depending on the tasks and conditions of the study, different characteristics of the resistance of worm cutters when cutting cylindrical gears are used.

1. The Average amount of wear of the cutter teeth when processing one wheel \bar{u}_n , as the ratio of the average wear of the cutter teeth to the number of n wheels cut by it.
2. The working time of the cutter until one of its teeth wears out to a certain limit value.
3. Maximum wear on one of the cutter teeth.
4. The total length of the processed teeth $L = zb$ (where z is the number of teeth of the cut wheel, b is the height of the wheel tooth) before the cutter teeth wear by a given amount.
5. The Average wear of the cutter teeth per unit length of one tooth of the cut wheels \bar{u}_{nzb} , defined as the ratio of the average wear of the cutter teeth to the product of nzb (the designations $n.z.b$ are given above).
6. Average wear of the cutter teeth depending on the processing time or the number of parts processed.

In our research, the tool durability characteristics were mainly taken as 1 and 5 of the above indicators, since they are the most versatile and suitable for comparative durability tests. When using the indicator \bar{u}_{nzb} as a characteristic of tool durability, studies can be carried out when processing gears with different numbers of teeth and different tooth heights.

The study was performed using experimental planning methods. As shown in [2, 4] and others, when gear milling cylindrical gears with a worm cutter, there is a linear character relationships of cutting modes S and V with the durability of the cutters. Assuming that this nature of these relationships will continue with pulse-fed gear milling, we conducted research using a first-order plan based on the scheme of a complete factor experiment (CFE). The number of experiments in the experiment plan was increased to 9, so that the graphs of paired relationships $y = f(S)$ and $y = f(v)$ (here y is an indicator of mill durability) it was possible to build not on two, but on three results of experiments. This increases the accuracy of determining the type of relationships specified.

The dependence $y = f(S, v)$ was described by the expression:

$$y = b_0 + b_1x_1 + b_2x_2 \quad (7)$$

Paired dependencies $y = f(S)$ and $y = f(v)$ were calculated as:

$$y = b_0 + b_1x \quad (8)$$

The dependence of the form (8), where the time of operation of the cutter or cutting path was taken as x , was also used to estimate the wear intensity. The characteristic of the wear intensity in this case is the value of the coefficient b_1 .

In order to exclude the influence of the quality of worm cutters on the results of experiments, all gears were processed with two cutters. Each cutter was used to cut from 10 to 25 gears at a single installation until a reliably determined wear of 0.5–0.7 mm was achieved.

A one-piece worm mill made of P6M5 steel (proportions, %, C = 0.8 – 0.9; W = 5.5 – 6.5; Cr = 3.8 – 4.4; V = 1.7 – 2.1; Mo = 5.0 – 5.5 by GOST 19265-73) with a diameter of 100 mm, $m = 4.25$ mm, with 10 rails and 7 working turns was used. The tests were carried out when processing gears made of 25XГМ steel (proportions, %, C = 0.23 – 0.29; Si = 0.17-0.37; Mn = 0.9 – 1.2; Cr = 0.9 – 1.2; Mo = 0.2 – 0.3 by GOST 4543-2016) $m = 4.25$ mm, $z = 45$, $b = 31$ mm (ring gear width) with a spline hole.

When studying the effect of S and v on the resistance of worm cutters during gear milling with pulse feed, the values of S varied within 5–8 mm/min, and the values of v -within 31.4–50.24 m/min. The pulse of the axial feed of the workpiece was produced after each rotation of the cutter on 7 teeth.

The adequacy of the obtained dependencies to experimental data was evaluated using the Fisher criterion.

Milling of teeth with a continuous feed of the workpiece was performed on the same machine as processing with a pulse feed of the workpiece, usually with the same cutter, but with a different position, i.e. with a different turn of the cutter. In both cases, the same number of wheels were processed. 8 series of experiments with pulse feed and 5 series of experiments with continuous feed were performed. The average values \bar{u} of wear of the worm cutter teeth when processing the same number of N gears by each of the compared methods, the coefficient b_1 depending on the type (8) $\bar{u} = f(L)$, where L is the length of the cutting path when processing N gears, the value of the maximum possible wear of the cutter teeth under these conditions $u_{\max} = 6\sigma$, where σ is the average square deviation of the mill wear values determined when processing N gears by this method. The ratio $u_{\max} = 6\sigma$ was assumed based on the assumption of the normal distribution of the values of wear of the cutter teeth over the period of its durability [5, 6].

3.2 Research Result

First, we studied the effect of cutting modes S and v on the resistance of worm cutters during gear milling with pulse feed. The following dependencies were obtained:

$$\bar{u}_n = 0.0237 + 0.0075v + 0.005S$$

$$\bar{u}_{nzb} = 0.0170 + 0.0054v + 0.0031S$$

The main results of this study are shown in Fig. 2. The following notation is accepted here: $u_1 = \bar{u}_n, u_2 = \bar{u}_{nzb}$. u_1 values are shown as solid lines, and u_2 values are shown as dashed lines.

Comparison of the resistance of worm cutters during gear milling with pulsed and continuous feeds is desirable for optimal cutting conditions. We have optimized the modes of gear milling with pulse feed. It is established that for the considered

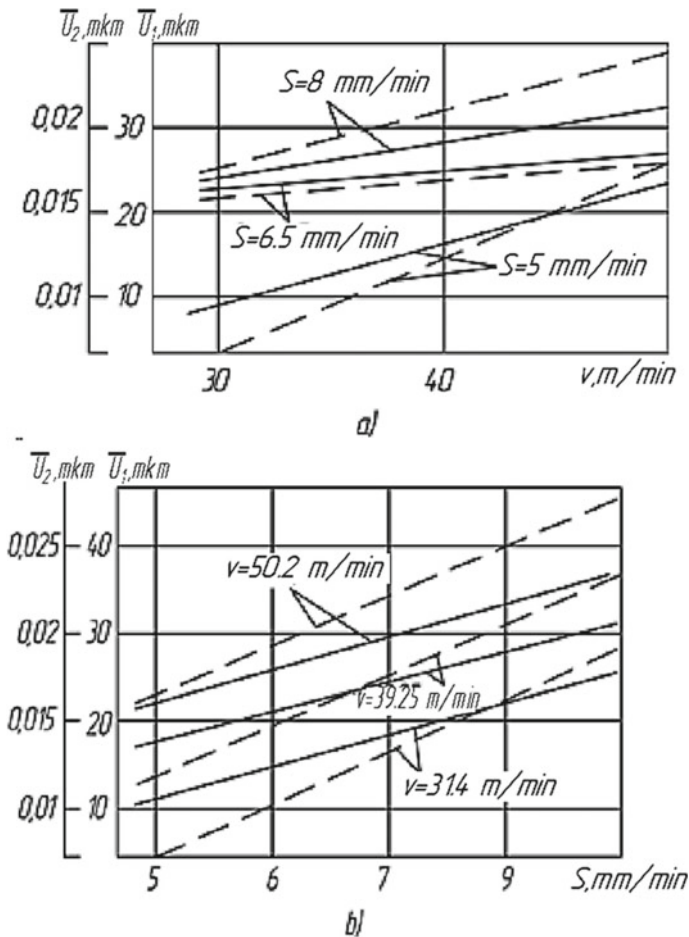
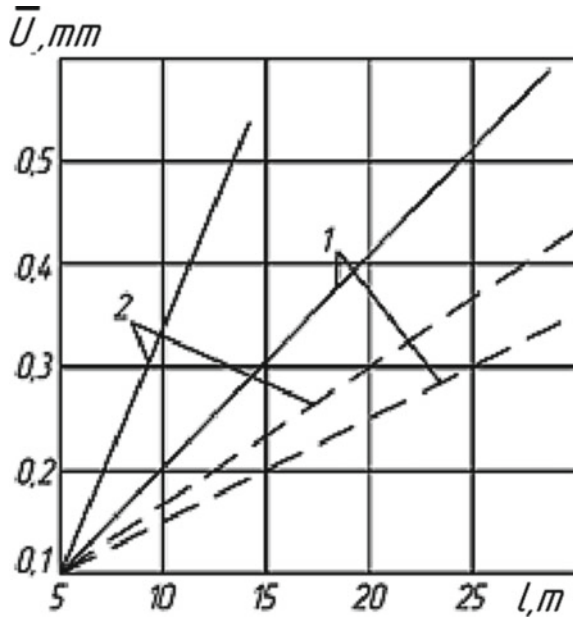


Fig. 2 The Dependencies of the wear characteristics of the teeth of the worm cutter on the speed V (a) and the feed S (b) when gear cutting with a pulse feed of the workpiece

Fig. 3 The Dependencies of the average wear \bar{u} of the teeth of the worm cutter on the cutting path L when processing with continuous (solid lines) and pulsed (dashed lines) feed of the workpiece; 1 and 2-the results of two experiments



processing conditions, the optimal values are $v = 30 - 35$ m/min, $S = 5.5 - 6.5$ mm/min. It was decided to conduct comparative resistance tests for the considered processing methods at the cutting modes: $v = 31.4$ m/min, $S = 6.5$ mm/min. At the specified modes, the considered gear is currently being processed in production conditions.

The main results of comparative studies of the resistance of worm cutters during gear milling of cylindrical gears with continuous and pulsed feeds are shown in Fig. 3.

The average values of the wear characteristics of the teeth of worm cutters when working with continuous and pulsed feed were $\bar{u} = 0.489$ and 0.343 mm, $b_1 = 0.0226$ and 0.0126 , $\sigma = 0.185$ and 0.113 mm, respectively.

Further research has shown that gear milling with pulse feed can significantly improve the accuracy of the wheels: during gear milling by an average of 20%, with subsequent shaving by an average of 35%.

Thus, the study showed:

- Dependencies of resistance factors of hobs from gear milling of cylindrical gears in the gear industry with continuous and pulse flows are linear with sufficient accuracy described by the polynomial of the first degree.
- Gear milling with pulse feed reduces the average wear of the teeth of the worm cutter by 1.43 times, the maximum possible wear of the teeth-by 1.64 times and the wear rate of the teeth of the cutter-by 1.79 times compared to gear milling with continuous feed of the workpiece.

- While maintaining the requirements for the quality of gears and the durability of worm mills, the proposed method allows you to intensify the gear milling modes of cylindrical gears by about 1.6 times and increase the productivity of this process by 1.5 times. This indicates the effectiveness of this method and the prospects of its application.

4 Conclusions

1. Analysis of the process of gear milling of cylindrical gears with a worm cutter with pulse feed shows that it allows, in comparison with gear milling with continuous feed, to improve cutting conditions by reducing the specific cutting forces, the temperature in the cutting zone, a more uniform load on the cutter teeth, increasing the rigidity of the technological system during cutting, reducing its deformations and vibrations. The use of this method also makes it easier to automate the control of cutting modes. All this helps to increase tool life, increase productivity and accuracy of processing.
2. Experimental studies of this process have confirmed its effectiveness: the average wear of the worm cutter teeth has been reduced by 1.4 times, the maximum possible wear by 1.6 times, the wear rate of the teeth by 1.8 times, and the accuracy of the teeth has been increased by 1.2 times. By intensifying the gear milling modes with a worm cutter, its productivity can be increased by 1.5 times.
3. The Method can be implemented on existing gear milling machines with numerical control after a small upgrade.

References

1. Patent No 1255315 of USSR, MKI B 23 F 5/20. The method of milling cylindrical gear wheels (in Russian)
2. Medveditskov, S.N.: High-performance gear cutting with milling cutters. Mashinostroenie, Moscow (1981). (in Russian)
3. Poduraev, V.N.: Automatically regulated and combined cutting processes. Mashinostroenie, Moscow (1977). (in Russian)
4. Sabirov, M.A.: Investigation of optimal cutting issues in gear milling of cylindrical gear wheels with worm cutters. Dissertation for the degree program scientist. Degree of candidate of technical Sciences. Ufa (1975) (in Russian)
5. Katsev, P.G.: Statistical methods of research of cutting tools. Ed 2-e reprocessing. Mashinostroenie, Moscow (1974) (in Russian)
6. Starzhinsky, V.E., Kane, M.M (eds.): Production technology and methods for ensuring the quality of gears and drive gears. Saint-Petersburg. Profession (2007) (in Russian)

Advanced Lifetime Tests of Plastic Gears with E- and S-Geometry



Gorazd Hlebanja, Matija Hriberšek, Miha Erjavec, and Simon Kulovec

Abstract Plastic gears became inevitable in many industries, numerous material pairs are available to fit any design needs. Material data bases and data sheets information is insufficient in this context, so on-site testing is necessary. Many applications use steel pinions and plastic gear, e.g., in speed reducers, where the pinion can be rather small, and they can run dry. Therefore, a combination alloy steel/POM became of interest and S-N diagrams were determined experimentally on testing rigs in company's lab, which are presented briefly. Yet another consideration is improved gear geometry; S-gears are proposed in this paper due to their experimentally proven qualities. Some information on this gear type is provided. Lifetime tests for this material combination and both gear types are shown in a diagram. It was also shown that the process temperatures never exceed permanent temperature limit of POM. Optical observations show several developed failure mechanisms. However, to assess quantitative wear levels a 3D measuring microscope is used.

Keywords S-gears · E-gears · Wear characterization · Fatigue · Lifetime tests

1 Introduction

Plastic gears are becoming crucial not only in consumer industries but also in quality demanding industries, e.g., in precision or medical devices, and even in power applications. It is almost unnecessary naming their qualities (like low mass and inertia,

G. Hlebanja (✉)

University of Novo Mesto, Na Loko 2, Novo Mesto, Slovenia

e-mail: gorazd.hlebanja@siol.net

G. Hlebanja · M. Hriberšek · M. Erjavec · S. Kulovec

Podkrižnik d.o.o., Lesarska c. 10, Nazarje, Slovenia

e-mail: matija.hribersek@podkrižnik.si

M. Erjavec

e-mail: miha.erjavec@podkrižnik.si

S. Kulovec

e-mail: simon.kulovec@podkrižnik.si

vibration dampening, running without external lubrication, etc.). However, their problems are thermal stability, precision of moulded parts, lower load, etc. On the other side, new materials with improved characteristics are emerging with increased rate. So, to design such gear pairs optimally, their fatigue data are becoming vital, whereas such data are unknown without experimental support. To summarize, there is a lack of reliable data in this context, even similar materials can differ, and various additives even enlarge this difference. So, a possibility to test gear pairs, made of potential material combination, on site can be the advantage for a company since it makes possible faster and independent evaluation and optimal material combination for each application. It is necessary to assess materials in terms of their mechanical, thermal and tribological properties. Despite many data can be extracted from material data sheets, the fatigue life of a gear pair depends on geometry, loading conditions, materials, working temperature, etc., which all originate from a particular application and its scenario. Such data are essential in plastic gear design.

The paper presents experimental results of lifetime tests under prescribed load conditions for selected combinations of thermoplastic gear pairs. Tests were repeated several times to gain statistically relevant result. Testbenches used in this context enabled controlled rotational speed and torque, whereas the spot temperature was monitored by a thermal camera.

The material combination of interest was alloy steel driving gear and driven POM (H) gear. Tests were produced for both, the involute and S-gear geometry. Results of this material combination shows an obvious advantage of S-gears in terms of durability. Data were imported in the KissSoft gear design software (for involute gears). This enabled the determination of Wöhler curves for these material combinations for root/flank areas. E-gears suffered a high temperature rise for the material combination steel and POM at high loads, which is due to highly deformed plastic gear teeth. A tip relief was proposed for E-gears for the next cycle of testing. Also, a 3D scanning topography was used to evaluate wear of tested gears.

2 Properties of the S-Gears

Many papers discussed various aspects of S-gears: the way they are defined [1], possibilities to design and produce various gear types (e.g., helical, crossed, worm gears, planetary gears, etc.) [2], radii of curvature, contact pressure, relative and sliding velocities, oil thickness, (initial) pressure angles, contact stress, etc. [3–5], thermal properties [6]. How do S-gears differ from the involute gears was also discussed in these papers. Important properties of S-gears can be summarized below:

1. Two parameters defining the rack flank curve can be used to modify gear tooth shape to improve its design, e.g., to acquire proper pressure angle, increase tooth root thickness, etc.
2. Cylindrical spur S-gears can operate with a low number of teeth down to 6 or even 4.

3. S-gears exhibit convex-concave contact in the vicinities of the meshing start and end zones.
4. S-gears feature comparatively higher radii of curvature, which implies lower contact pressure.
5. S-gears develop higher contact oil film thickness, which is due to higher relative velocities in the contact.
6. S-gears exhibit relatively longer dedendum part of a pinion tooth flank (comparing to the involute gear) which is meshing with a gear addendum. Difference between the pinion dedendum length and the gear addendum length indicates amount of sliding. And less sliding implies less frictional work and less developed heat, which is of special importance for plastic gears.

As stated in [1], S-gears are defined through the rack profile $y(x)$, where a coordinate system origin lies in the kinematic pole C:

$$y(x) = \begin{cases} a_p m \left(1 - \left(1 - \frac{x}{m}\right)^n\right), & x \geq 0 \\ -a_p m \left(1 - \left(1 + \frac{x}{m}\right)^n\right), & x < 0 \end{cases} \quad (1)$$

and $\lim_{x \rightarrow 0^+} y'(x) = \lim_{x \rightarrow 0^-} y'(x)$. x, y are Cartesian coordinates of the rack profile, m is module in mm, whereas factors a_p and n , namely the height factor and the exponent act as form factors, which affect the tooth shape properties. And the module acts as a scaling factor. The definition of the rack in Eq. (1) is necessary due to the half symmetry of the profile. The rack tooth can be regarded as a cutting tool.

The trigonometric procedure defining the path of contact and gears of an arbitrary number of teeth was described in detail in [1]. This procedure is valid for external as well as for internal gears. So, for an arbitrary point P on the rack tooth flank a unique point U on the path of contact is defined, provided that the normal to the rack profile curve in U passes through C. Similarly, a single point on a flank of a gear with an arbitrary defined number of teeth is produced. The transformations from the rack profile flank through the path of contact to gear flanks are bijective, that is they always give the same rack flank in the reverse direction. These transformations could also have been represented by object translations and rotations in appropriate coordinate systems, of course by employing the basic law of gearing.

As already stated, the gear flank and tooth shape influencing factors are a_p and n , however, one of them can be replaced by the initial pressure angle α_{w0} . Two gear pairs are shown here to illustrate the tooth shape variability in Fig. 1, both with $z_p = 10$ and $z_w = 30$. The first gear pair is with $\alpha_w = 22^\circ$ and $a_p = 1.3$ and the second one with $\alpha_w = 18^\circ$ and $a_p = 1.5$. All gears were designed with the module $m = 50$ mm and since the module acts only as a scaling factor, its size is of no importance in this context. Both rack profiles do not differ much, apart from the inclination and corresponding pressure angles. But the derived paths of contact apparently differ in their length and curvature in the meshing starting and end zones, as it can be observed in Fig. 1. The active parts of both paths of contact delimited by gear tip circles are designated as $\widetilde{A_1E_1}$ and $\widetilde{A_2E_2}$. So, for the higher pressure angle, the path of contact shortens and becomes more curved and inversely (longer and less curved path of

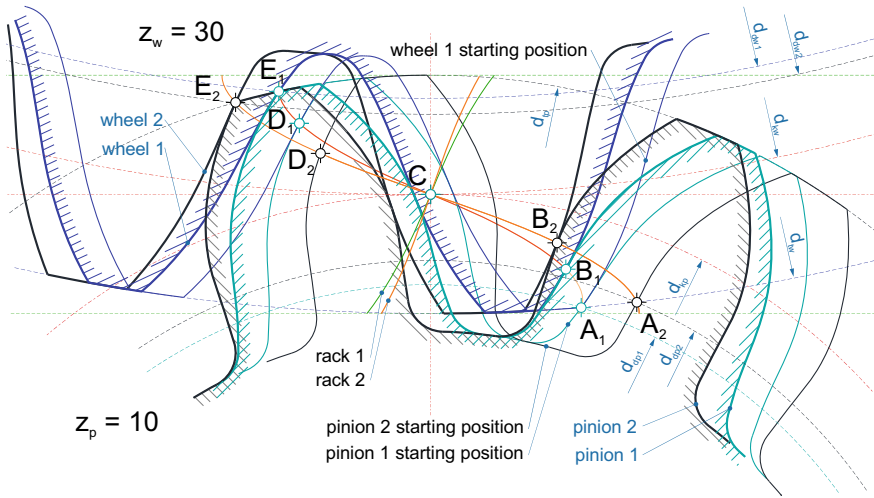


Fig. 1 Gear pair forms with pinion $z_p = 10$ and wheel $z_w = 30$. The generating rack 1 with (initial) pressure angle $\alpha_w = 22^\circ$ and rack 2 with $\alpha_w = 18^\circ$

contact) for lower pressure angles. The tooth root becomes stronger and tooth tip thinner for the larger pressure angle and inversely for smaller pressure angles. The active length of the path of contact \widetilde{AE} , the length \widetilde{AD} which corresponds to the base pitch and the contact ratio are collected in Table 1.

The mating gear teeth flanks start meshing with the pinion dedendum tip and the gear addendum root and proceed from the meshing start to the kinematic pole C and to the pinion addendum and the gear dedendum from C towards the meshing end point. The contact is propagating on the path of contact by rolling and sliding. The active size of the pinion dedendum is smaller than that of the gear addendum. This implies amount of sliding of the addendum on the shorter pinion dedendum, which can be deduced from Fig. 2, which represents the racks, the paths of contact, and the mating flanks of the S- and the E-gear pair. Amount of sliding also implies thermal impact. In general, the dedendum-addendum size difference depends on module, number of teeth, pressure angle. For S-gears the said difference also depends on forming factors—the height and the exponent. The size difference in the case of S-gears is comparatively more convenient, so less sliding is produced along the contact propagation compared to the involute case. The starting pressure angle for the S-gears is 18° and that of the E-gears 20° , and both gears with the same number of teeth, $z = 20$. As Fig. 2 implies:

Table 1 Path of contact characteristics for the S-gear pairs ($z_p = 10, z_w = 30, m = 50$ mm)

Initial pressure angle α_{w0}	18	22
Active length, $l_{\widetilde{AE}}$ [mm]	190.7	162.92
Base pitch, $l_{\widetilde{AD}}$ [mm]	148.2	144.5
Contact ratio, ε [I]	1.29	1.13

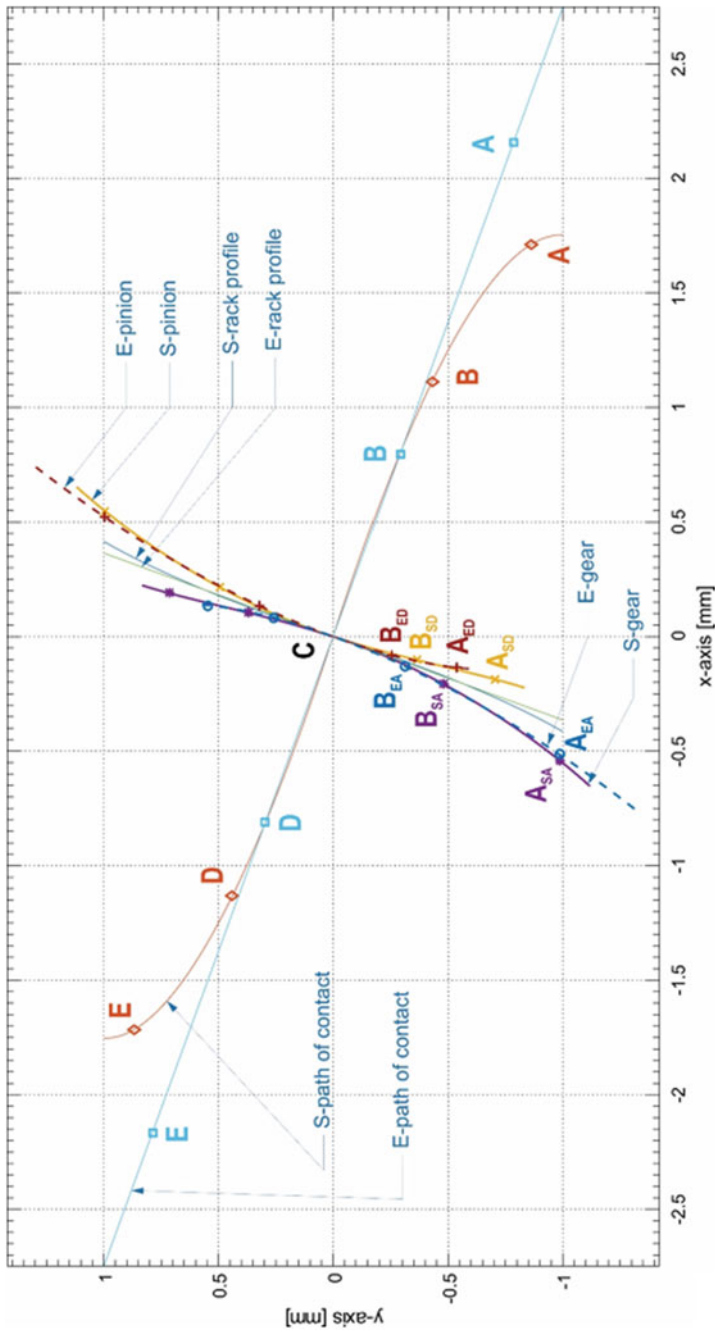


Fig. 2 Comparison of the E and S paths of contact, rack profiles and mating pinion and gear flanks, $m = 1$ mm, $z_p = z_w = 20$, $\alpha_{wE} = 20^\circ$, and $\alpha_{wS} = 18^\circ$

$$\Delta l_E = l(\widetilde{\mathbf{A}_{EA}\mathbf{B}_{EA}}) - l(\widetilde{\mathbf{A}_{ED}\mathbf{B}_{ED}}) > \Delta l_S = l(\widetilde{\mathbf{A}_{SA}\mathbf{B}_{SA}}) - l(\widetilde{\mathbf{A}_{SD}\mathbf{B}_{SD}}) \quad (2)$$

Near the meshing start point, involute gears feature small radii of curvature of the driving pinion and rather high radii of curvature of the driven gear, which implies high sliding velocities in this area. This phenomenon can be observed also in Fig. 2, whereas it becomes distinct when the numbers of teeth are notably apart.

The normal force F_N is transmitted through the contact, which causes the force of friction F_{fr} oriented tangentially to the contact and the corresponding power of friction, $P_{fr} = \mu F_N v_g$. The power of friction generated in the contact representing losses transforms to the heat flow, distributed to both involved flanks. A greater part of the heat is therefore distributed to the slower driving gear and the rest to the longer contacting area of the driven gear. The friction force grows to high levels already at the meshing start, which negatively influences (braking) the contact point velocity along the path of contact and induces negative sliding on the driving gear flank.

Based on the S-gear rack profile, the path of contact, the pinion and inner or outer gear can be calculated by a program. The same program was improved to enable calculation of power, work, flank pressure, contact width, velocities, and flash temperatures. All the parameters can be represented along the path of contact or the active flank profile. Power of friction is therefore given by:

$$P_{fr} = \mu \cdot F_N \cdot v_g = (\mu \cdot F_t / \cos \alpha_w) \cdot v_g \quad (3)$$

The work of friction along the active contact from the meshing start in A in time $t_A = 0$ to the meshing end in E (t_E) is given by:

$$A_{fr} = \sum_{t_A}^{t_E} P_{fri} \cdot \Delta t_i \quad (4)$$

So, the frictional work in a single pinion rotation is $z_p \cdot A_{fr}$, and multiplied by the rotational frequency frictional work accomplished in a minute $\nu \cdot z_p \cdot A_{fr}$. The average frictional power is then $P_{frav} = \nu \cdot z_p \cdot A_{fr}/60$. Table 2 collects data for torque 1.5 Nm for both, E- and S-spur gear pairs with $m = 1$ mm, $z_p = z_w = 20$, $\alpha_{wE} = 20^\circ$, $\alpha_{wS} = 18^\circ$, and $b = 6$ mm and steel/POM material combination. Values for E-gears are higher for 25%.

Table 2 Frictional work and average frictional power for S- and E- gear pair ($z_p = z_w = 20$, $m = 1$ mm, $T = 1.5$ Nm, $\nu = 1400 \text{ min}^{-1}$, $P_t = 219.9$ W)

	S-gears	E-gears
Work in a single contact [J]	0.0135	0.0169
Work in a single rotation [J]	0.2697	0.3389
Work in a minute [J]	377.6	474.5
Average frictional power [W]	6.294	7.909

3 Experimental Arrangement and Tested Gears

Material combinations for gear pairs to be tested are based on existing and potential applications. Due to importance of optimal material selection the company decided to develop and produce own testbenches. The necessity to acquire comparable results which could be input for plastic gear design software, a testbench according to VDI 2736, Part 4 [7] was designed and manufactured. This device is already in trial operation. Nevertheless, smaller devices proved to be useful and were used in this set of experiments. Based on test duration and rotational speed of the selected thermoplastic gears, lifetime cycles were calculated and imported together with flank/root temperature into KISSsoft Software, module Plastics Manager [8]. Based on the processed input data in Plastics Manager, Wohler Curves (S-N) for a selected material combination were obtained. After each experimental lifetime test, the wear characterization has been performed according VDI 2736, Part 2 [9] with Alicona device and evaluation of the gear failure mode. Wear was as well evaluated during testing to acquire wear development data along gear tooth flank.

3.1 Gear Geometry

Small spur S- and E-gears of module 1 mm, width 6 mm, both gears with 20 teeth, were used in these tests. Figure 3 shows their geometrical features. The pinion material in this experimental series was 42CrMo4 QT, alloy steel. Plastic gears were made of acetal homopolymer POM H. Technical data of gears are presented in Table 3. The pressure angle for S-gear in this case amounts to 26.8° in the meshing start point, decreases to 20° in C, and gradually increases to 26.8° for an ideal contact (Fig. 2).

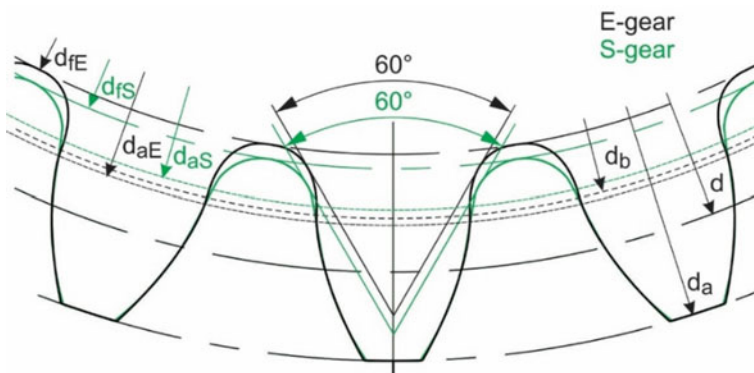


Fig. 3 Comparison of actual E and S gears provided for testing

Table 3 Basic data on S and E gears

Gear type	E-gears	S-gears
Pressure angle α [°]	20	18
Tip diameter, d_a [mm]	22	22
Reference diameter, d [mm]	20	20
Root diameter, d_f [mm]	17.4	17.7
Base diameter, d_b [mm]	18.79	–
Dedendum limit, d_{act} [mm]	18.95	18.59
Critical section s_{fn} [mm]	1,88	1,96

Table 4 Roughness and quality data of metal gears

Gear type	E-gear		S-gear	
	Left	Right	Left	Right
Arithmetic mean deviation R_a [μm]	0,16	0,255	0,187	0,206
Maximum height of the profile, R_z [μm]	1,08	2,27	1,28	1,36
Profile Q (DIN 3961/62)	6	4	5	7
Lead Q (DIN 3961/62)	5	5	7	6
Cumulative pitch F_p (DIN 3961/62)	4	4	1	1

As Fig. 3 and Table 3 disclose, E-gears (for these data) have smaller root, a bit thinner tooth and a bit thicker tip. It is also important that the active dedendum side of S-gears is larger.

Since metal gear surface roughness influences wear, corresponding data, inclusive gear quality according to DIN 3961/62 are presented in Table 4.

Manufacturing means of plastic gears can be injection moulding or cutting. Cut gears are of industrial interest for smaller lots and when a more precise tooth flank shape is prescribed or if alternative gear tooth flanks are of interest. Comparing cut and moulded gears of the same module and number of teeth by measurements of the quality Q according to DIN 3961/62 discloses at least for two grades higher Q of cut gears. Measuring gears on Wenzel GearTec coordinate measurement machine in our case showed the difference of two quality grades in favour of cut gears [10]. So, the quality of cut plastic gears is $Q = 8 \dots 9$ and that of moulded $Q = 10 \dots 11$, which also depends on a cutting tool. Basic disks made of POM without fillers are injection moulded, using an axial sprue enabling higher material flow to gain quality uniform physical characteristics. Disks are then cut by a HSS cutting hob on the CNC Koepfer machine tool as to enable effective manufacturing.

3.2 Experimental Arrangement

Testing results presented in this paper are based on experiments performed on two small testing rigs, which were used to acquire gear durability data. The testing rig is illustrated in Fig. 4. It consists of a framework on which two 4 poles asynchronous squirrel cage electro-motors ($P = 0.37$ kW and $M = 1.8$ Nm) are mounted. On the motor rear side two fans are mounted to remove redundant heat. Two small gears are mounted in such a way to precisely adapt centre distance. Power transmission from the motors to the shafts is by belts. Motors are controlled by two frequency inverters which acquire proper rotational frequency and load. The testing rig was calibrated based on laser measurement of shaft deformations with prescribed excitation frequency differences between both inverters. Based on shaft torsional deformation, torque, which is controlled based on current measurement, was calculated. A PLC based counter measures experiment duration time. The testing rig stops when gear failure appears. This is conditioned by nominal current drop for 5%.

It is important to have possibility of measuring contact temperature by a fast thermal camera, so the testing device was designed in such a way to enable frontal view. So, measurements of spot temperatures and temperature field of meshing gears were provided by a thermal camera Optris Xi80. Spot temperature was acquired during entire loading cycle of the lifetime tests, which was facilitated by Optris PIX Connect software.

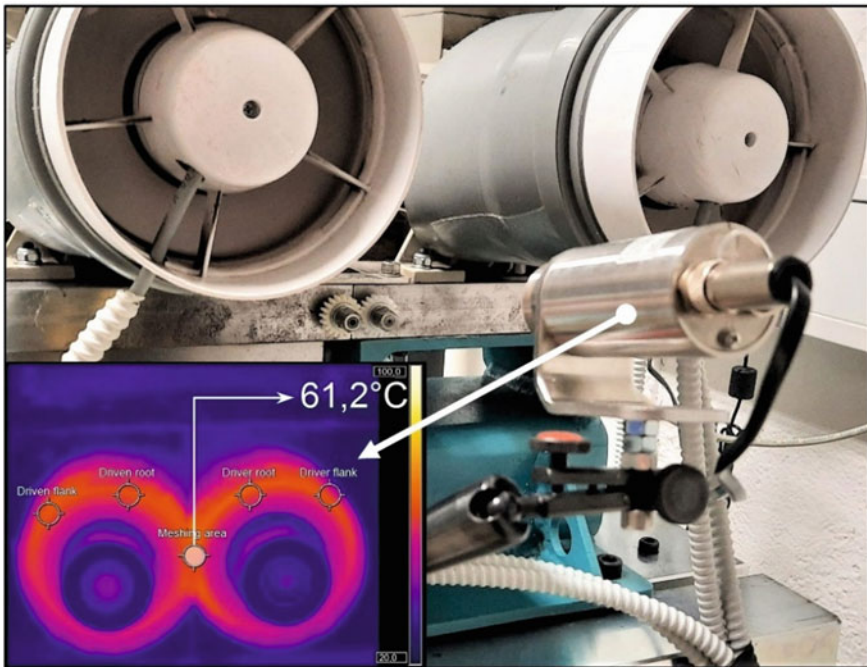


Fig. 4 Testing rig with the thermal camera focusing on a gear pair

4 Experimental Results

Lifetime gear tests were performed under standard environmental conditions with a temperature of 23 °C and a relative humidity of 50%. The experiments were performed at three different load levels, i.e., torques (1.5; 1.3; 1.1 Nm) at the same rotational frequency of the driving and driven gear, which was 1400 rpm. The selection of torques was furthermore based on the preliminary lifetime testing of different types of polymer gears reported in [11]. A computer program for temperature visualization was used to represent the average temperature in the meshing zone during testing. At the end of the test, an evaluation of the average temperature at which a gear failure occurred, was completed.

4.1 Lifetime Tests—Wöhler Diagrams

Many material pairs were submitted lately to lifetime tests, mostly based on acetal and nylon materials, with and without fillers [11, 12]. As already stated, this experimental set is focused on alloy steel (42CrMo4 quenched and tempered) driver, and acetal driven gear.

Wöhler diagrams, plotted based on achieved numbers of cycles in three load levels with three repetitions, are presented in Fig. 5. Results show better performance of

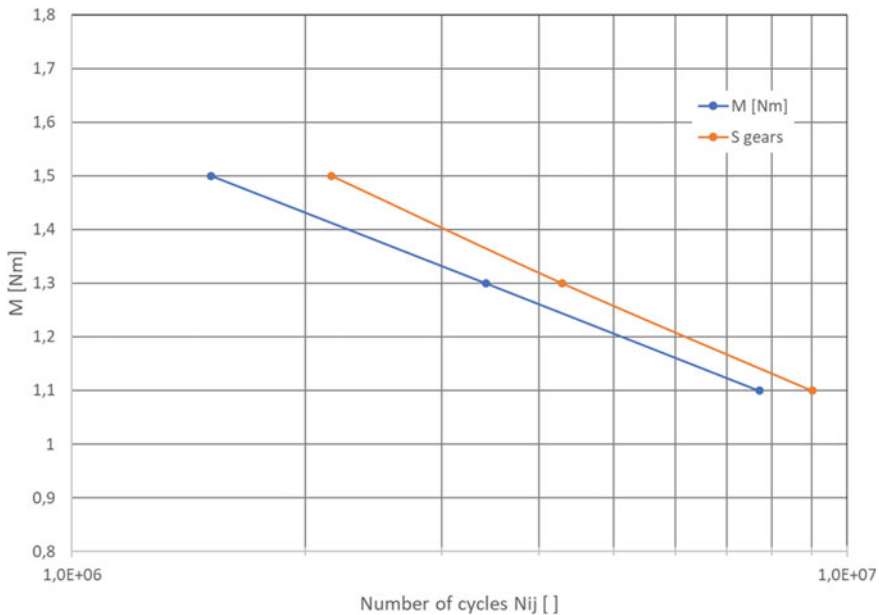


Fig. 5 Comparison of lifetime tests for alloy steel/POM E and S gears

S-gears, which is based on already discussed S-gear properties. This is especially notable with highly loaded gears. Similar results were gained in several attempts, various material combinations and in different labs, e.g., [13, 14]. In the research [13] it was also discovered that S-gears (POM/POM) have better thermal performance with lower loads, below 1 Nm.

An important aim of performing durability tests of thermoplastic gears is exportation of acquired temperature data (tooth flank and root) and lifetime test data, material mechanical and thermal properties, and temperature dependent modulus of elasticity into the program system KISSsoft plastic manager and build the material base, which then aids in building an advanced model to search an optimal solution for a particular application.

4.2 Thermal Measurements

Thermal camera was used to monitor and record spot temperatures of the loaded gear pair in operation. The available Optris Xi80 camera acquires the highest temperature in a 2×2 mm spot. The meshing zone, the driver flank and root, and the driven flank and root spot temperatures were observed in this research. This is diagrammatically presented for the involute gear pair with load 1,5 Nm in Fig. 6.

The courses of temperatures clearly distinguish between the metal driver and driven plastic gear. Temperatures are significantly higher for the plastic gear. The temperature-time (number of cycles) dependency consists of three main sections, which are: (a) running-in area where thermoplastic driven gear fits to steel gear in

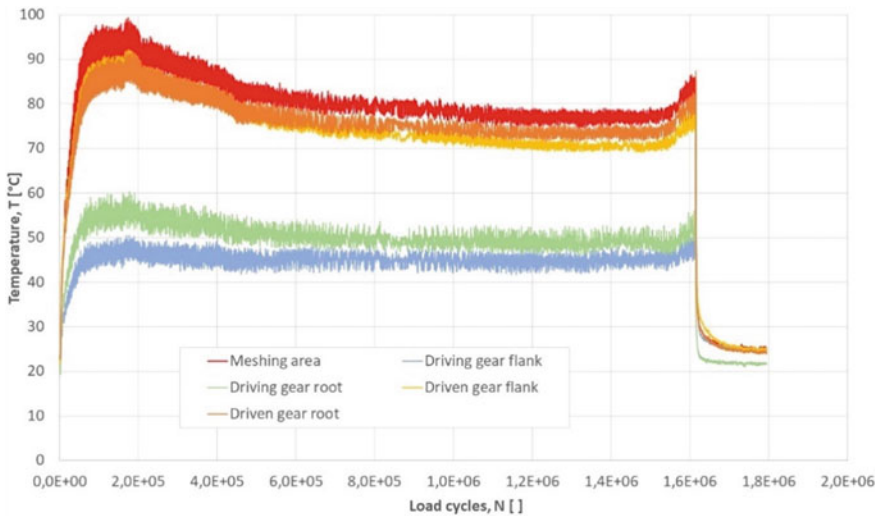


Fig. 6 Temperature-number of cycles (time) profiles for the E-gear pair loaded by 1.5 Nm

terms of tooth flanks; (b) a phase of a quasi-stationary operating at stable temperature; (c) a phase of increasing gear wear that, in combination with fatigue, causes failure of the thermoplastic gear. These phases are clearly distinguished in Fig. 6, which, beside meshing spot, also shows temperature diagrams of flank and root spots for both, the driver, and the driven gear.

Thermal behaviour of steel/POM gear pairs was discussed in [15] and it was observed that E-gear pair at 1.5 Nm exhibits an extraordinary temperature peak during running-in phase. This phenomenon can be attributed to the unmodified involute tooth tip profile and plastic gear tooth deformation due to a high load [16], whereas the steel gear can be regarded as a rigid body in this context. So, a driven gear suffers an additional impact at a meshing start point A and the temperature rise. The consequence is rather high initial wear of a driven plastic gear. The solution of this problem can be tip relief. No such trend during running-in phase was observed at lower load levels for E-gears. S-gears do not exhibit such temperature rise at all.

In the next phase, relatively stationary conditions prevail. For E gears the initially high temperature drops and prevails until the final phase. Uniform wear occurs in this phase for both gear types, thermal camera snapshots are shown in Fig. 7. The last phase of the lifetime test shows significant changes of the gears. This is due to the increased wear above the critical limit in connection with the fatigue of the material, which causes degradation of the bonds between the molecules in the material and the subsequent teeth failure. Process temperatures do not increase up to the constant working limit, which is for POM between 90 and 100 °C [17].

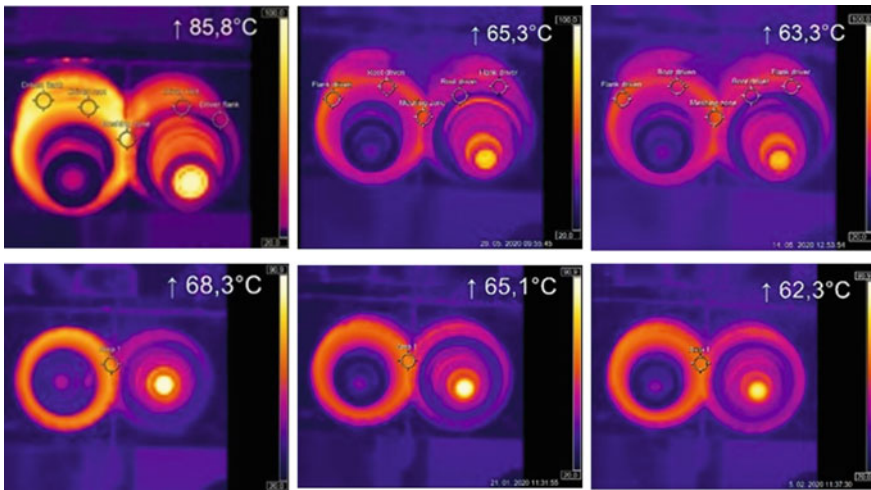


Fig. 7 Thermal camera snapshots for the meshing 42CrMo4/POM gear pairs in a stable region, $T = 1,5 \text{ Nm}$ (left); $T = 1,3 \text{ Nm}$ (centre); $T = 1,1 \text{ Nm}$ (right); E-gear (above), S-gear (below)

4.3 Optical Observation

The purpose of optical observations is to detect forms of gear failure in provided experiments. VDI 2736, Part 1 describes thermal overheating, root fracture, flank fracture, pitting, wear, and deformation as damage forms of plastic gears [17]. Worn gears exhibit at least some of the above-mentioned failure forms. And it is reasonable to expect to some extent different prevailing failure forms depending on load of gears with the same material combination.

The worn involute and S-gear after being loaded by 1.5 Nm until failure were examined optically to observe visible signs of damage. So, several photos were taken from the gear front, back, and face side. Some of the remaining teeth have rather long root and flank cracks, which are always near the pitch circle, which can be detected from the front side (seen by an observer when mounted on the testing rig). Some flank wear and flexural deformation appear as well. Tooth tips are also worn. And there are signs of thermal damage of flanks. From the back side, almost all teeth have rather long flank cracks, which initially proceed in the circumferential direction and then change the direction towards the opposite root. Some of root cracks spread over the entire face width. Figure 8 shows damage forms of the worn E-gear after its failure.

Damage forms of the S-gear run under the same conditions as E-gear pair are represented in Fig. 9. The front view shows regular, rather long cracks in the pitch circle zone or slightly below. Lower wear and flexural deformation, and some thermal damage are also present. Only several short root cracks can be observed from the rear side.

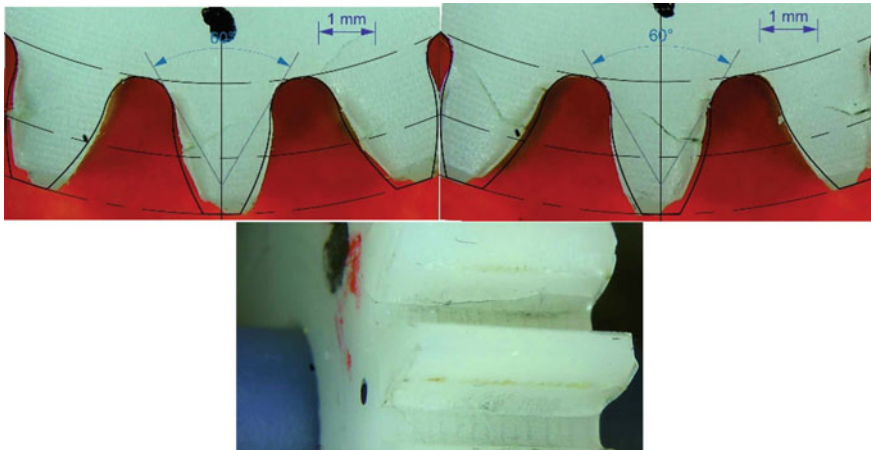


Fig. 8 Failure modes of the E-gear after experiment with load 1.5 Nm. (front—left, back—right, face side—below)

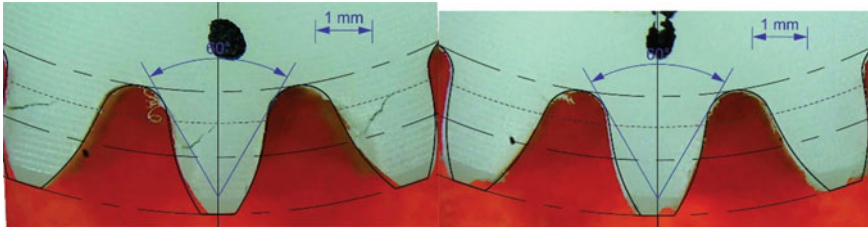


Fig. 9 Failure modes of the S-gear after experiment with load 1.5 Nm. (front—left, back—right)

4.4 Wear Measurement

It is necessary to access wear data quantitatively, and if possible, to access wear rate along the gear tooth flank. The basic idea is to detect a shape of a new plastic gear teeth shape and compare this reference shape to the worn gear teeth shapes. This can be done in successive manner as a process proceeds. Such an analysis is facilitated by an optical 3D measurement microscope, Alicona Infinite Focus SL. The Alicona 3D microscope is also used for precise measurements of cutting tools wear [18].

Some preliminary results for POM gears of both gear types are presented in Fig. 10 for the E-gear and in Fig. 11 for the S-gear. Two samples were scanned, both gears were loaded by torque of 1.1 Nm. The S-gear failed after 7.851×10^6 cycles and the E-gear after 7,780,156 cycles. Comparison of the new and the worn profile for both gear types shows severe wear. It appears as if fatigue is principal with higher loads and wear with lower loads.

So, wear development of the same gear pair during several stages from the new to the failed polymer gear is of interest. This can be processed for various loads from 1.5 down to 1.0 Nm or even lower. This is time consuming and a task to be accomplished later this year together with wear analysis according to VDI 2736. First results for the POM gears of both gear types loaded by 1.5 Nm, after 0.58×10^6 cycles are presented in Fig. 12. So, amount of wear for e.g., tip circle, pitch circle, active dedendum limit, etc. could be easily deducted. Some more wear is produced in E-gear pair in this case.

5 Conclusion

The presented chapter deals with testing and comparing E- and S-gears. S-gears are defined with a half parabolic function of the rack flank, which then defines a single path of contact which then defines external and internal gear geometry with any number of teeth. The height parameter a_p and the exponent n (form parameters) or the initial pressure angle α_w in C facilitate shaping of the gear, which was demonstrated in the chapter. Thermal properties of S-gears, i.e., their advantage over E-gears is in the fact that the former mesh with less sliding and more rolling, so S-gears reveal less frictional force and frictional losses or heat.

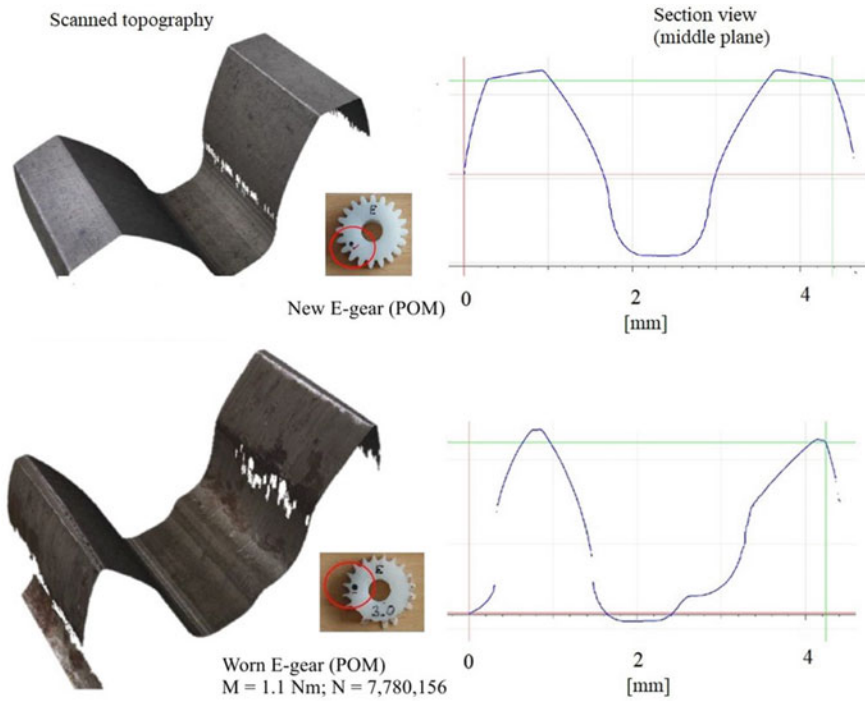


Fig. 10 E-gear teeth profile of the new (above) and worn gear (below)

The basic aim of durability tests, thermal and wear behaviour of gears made of various polymer materials and materials with fillers (fibres, stabilizers, lubricants, etc.) is to create a knowledge base which would facilitate proper material selection for demanding applications. As well it is necessary to improve knowledge on differences between E- and S-gear behaviour in applications.

The examined gear pairs were a combination of an alloy steel driving gear and a driven POM gear (POM contained some heat resistant additives). The tests with loads of 1.5, 1.3 and 1.1 Nm were repeated at least three times. They were conducted on small testbenches with thermal camera coverage and data logging. The testbench automatics registered failure time. There was a clear distinction between the S- and E-gears in favour of the former. Also, thermal characterization of S- and E-gears, based on continuous thermal records of the meshing, root, and flank areas of both gears, always shows lower temperatures of S-gears.

Regarding failure mechanisms, qualitative optical observations show fatigue cracks and fractures in root and flank area, flexural deformation, and wear. So, a tool for quantitative assessment was used, i.e., a precise 3D measurement microscope. 3D scanning is off-line, so the testing process is interrupted. First results are presented in the paper and show less wear of the S-gears, which could be attributed to lesser friction. The systematic research of wear started recently to improve the

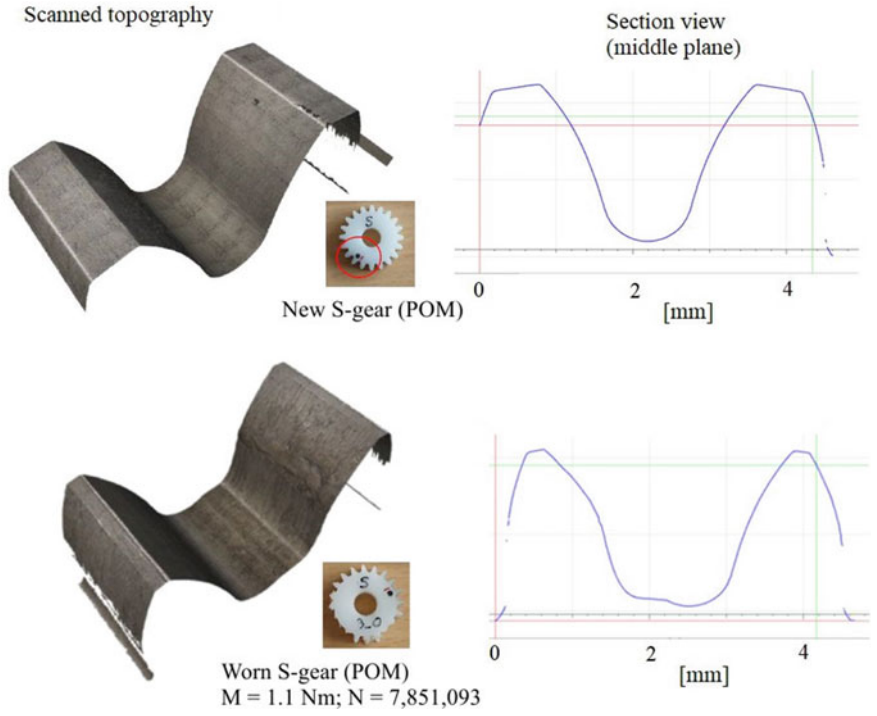


Fig. 11 S-gear teeth profile of the new (above) and worn gear (below)

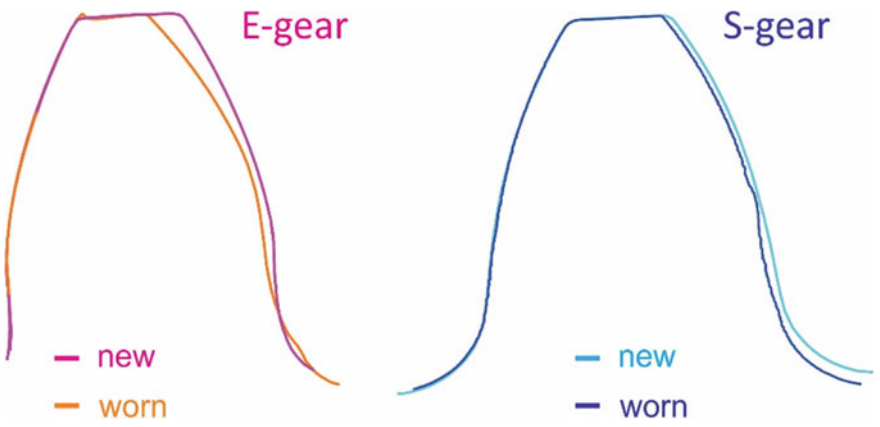


Fig. 12 S-gear teeth profile of the new (above) and worn gear (below)

understanding of the wear mechanisms and influences, e.g., gear geometry, load, number of cycles, etc.

The basic aim of durability tests, thermal and wear behaviour of gears made of various polymer materials and materials with fillers (fibres, stabilizers, lubricants, etc.) is to create a knowledge base which would facilitate proper material selection for demanding applications. As well it is necessary to improve knowledge on differences between E- and S-gear behaviour in applications.

Acknowledgements The investment is co-financed by the Republic of Slovenia and the European Union under the European Regional Development Fund, no. SME 2/17-3/2017 and C3330-18-952014.



EUROPEAN UNION
EUROPEAN REGIONAL
DEVELOPMENT FUND



REPUBLIC OF SLOVENIA
MINISTRY OF ECONOMIC DEVELOPMENT AND
TECHNOLOGY

References

1. Hlebanja, J., Hlebanja, G.: Spur gears with a curved path of contact for small gearing dimensions. In: International Conference on Gears, Garching near Munich, Germany, 4.-6.10.2010: Europe invites the world, (VDI-Berichte, ISSN 0083-5560, 2108). Düsseldorf: VDI-Verlag, pp. 1281–1294 (2010)
2. Hlebanja, J., Hlebanja, G.: Anwendbarkeit der S-Verzahnung im Getriebebau: Nichtevoventische Verzahnungen weiterentwickelt. Antriebstechnik, ISSN 0722-8546, 2005, 44(2), 34–38 (2010)
3. Hlebanja, G.: Specially shaped spur gears: a step towards use in miniature mechatronic applications. In: Miltenović, V. (ed.) Proceedings, The 7th International Scientific Conference Research and Development of Mechanical Elements and Systems—IRMES 2011, 27.-28.4.2011, Zlatibor, Mechanical Engineering Faculty, pp. 475–480 (2011)
4. Hlebanja, G., Hlebanja, J.: Recent development of non-involute cylindrical gears. In: Dobre, G., Vladu, M.R. (eds.) Power Transmissions: Proceedings of the 4th International Conference, Sinaia, Romania, June 20–23, 2012, (Mechanisms and machine science, ISSN 2211-0984, ISSN 2211-0992, vol. 13, pp. 83–98). Dordrecht [etc.]: Springer. cop. 2013 (2012)
5. Hlebanja, G., Hlebanja, J.: Influence of axis distance variation on rotation transmission in S-gears: example on heavy duty gears. In: International Conference on Gears, 7–9.10.2013, Garching (near Munich), pp. 669–679. Germany: Europe invites the world, (VDI-Berichte, ISSN 0083-5560, 2199). Düsseldorf: VDI-Verlag. cop. 2013 (2013)
6. Hlebanja, G., Kulovec, S., Zorko, D., Hlebanja, J., Duhovnik, J.: Influence of the tooth flank shape on thermal load of the gear. In: Europe invites the world, International Conference on Gears, International Conference on Gear Production, International Conference on High Performance Plastic Gears, Technische Universität München, Garching, Sept. 13–15, (VDI-Berichte, ISSN 0083-5560, 2294.2). Düsseldorf: VDI. 2017, pp. 1583–1592 (2017)
7. VDI 2736: Part 4. Thermoplastic gear Wheels: Determination of Strength Parameters on Gears. VDI-Richtlinien. Düsseldorf (2016)
8. Pogačnik, A.: Web demo 27.09.2018 – Plastic gear calculation. KissSoft (2018). https://old.kisssoft.ag/english/webdemos/downloads/plastic-gears/WebDemo_EN.pdf

9. VDI 2736: Part 2. Thermoplastic gear Wheels: Cylindrical gears Calculation of the load-carrying capacity. VDI-Richtlinien. Düsseldorf (2014)
10. Hlebanja, G., Kulovec, S., Hlebanja, J., Duhovnik, J.: On endurance of the S-shaped plastic gears. In: Simonovski, P., Rizov, T. (eds.) Proceedings: Balkan Association on Power Transmission Conference 2016: Faculty of Mechanical Engineering, Skopje, pp. 79–86 (2016)
11. Hlebanja, G., Hriberšek, M., Erjavec, M., Kulovec, S.: Durability investigation of plastic gears. In: Power transmissions 2019, 6th International BAPT Conference Power Transmissions 2019, Varna, Bulgaria, June 19–22, 2019, vol. 287, pp. 1–9 (MATEC web of conferences, ISSN 2261-236X). [Paris]: EDP Sciences (2019)
12. Hlebanja, G., Hriberšek, M., Erjavec, M., Kulovec, S.: Experimental determination of plastic gear durability. In: Marjanović Zulim, N. (ed.) IRMES 2019 Kragujevac, 5–7 September 2019, Kragujevac, (IOP Conference Series. Materials Science and Engineering (Online), ISSN 1757-899X, vol. 659, no. 1). [Kragujevac: Faculty of Engineering, 2019], vol. 659, no. 1, f. 1–11, <https://iopscience.iop.org/article/10.1088/1757-899X/659/1/012066> (2019). <https://doi.org/10.1088/1757-899X/659/1/012066>
13. Zorko, D., Kulovec, S., Tavčar, J., Duhovnik, J.: Different teeth profile shapes of polymer gears and comparison of their performance. *J. Adv. Mech. Design Syst. Manuf.* **11**(6), 1–10 (2017). <https://doi.org/10.1299/jamdsm.2017jamdsm0083>
14. Trobentar, B., Kulovec, S., Hlebanja, G., Glodež, S.: Experimental failure analysis of S-polymer gears. In: *Engineering Failure Analysis*, vol. 111 (104496), pp. 1–8. ISSN 1350-6307, April 2020. <https://doi.org/10.1016/j.engfailanal.2020.104496>
15. Hlebanja, G., et al.: Theory and Applications Based on S-gear Geometry, pp. xxx–xxx In: Radzevich, S.P., (ed.), *Recent Advances in Gearing: Scientific Theory and Applications*, 450 pages. Springer Nature, 2021. (in press, 2021)
16. Nieman, G., Winter, H.: *Maschinenelemente, Band II: Getriebe allgemein, Zahn-radgetriebe Grundlagen, Stirnrad Getriebe*. ISBN 3-540-11149-2. Springer Verlag, Berlin, Heidelberg, New York (1989)
17. VDI 2736: Part 1. Thermoplastic gear Wheels: materials, material selection, production methods, production tolerances, form design. VDI-Richtlinien. Düsseldorf (2016)
18. Grguraš, D., Kern, M., Pušavec, F.: Cutting performance of solid ceramic and carbide end milling tools in machining of nickel based alloy Inconel 718 and stainless steel 316L. In: *Advances in production engineering & management*, vol. 14, no. 1, pp. 27–38. ISSN 1854-6250, March 2019, http://apem-journal.org/Archives/2019/APEM14-1_027-038.pdf (2019). <https://doi.org/10.14743/apem2019.1.309>